AD_____
(Leave blank)

Award Number: W81XWH-06-1-0590
(Enter Army Award number assigned to research, i.e., DAMD17-00-1-0296)

TITLE: a New Therapeutic Paradigm for Breast Cancer Exploiting Low Dose Estrogen-Induced Apoptosis
(Enter title of award)

PRINCIPAL INVESTIGATOR: Virgil Craig Jordan, Ph.D.
(Enter the name and degree of Principal Investigator and any Associates)

CONTRACTING ORGANIZATION:
(Enter the Name, City, State and Zip Code of the Contracting Organization)
Georgetown University
Washington, DC 20057

REPORT DATE: June 2011
(Enter month and year, i.e., January 2001)

TYPE OF REPORT: Annual
(Enter type of report, i.e., annual, midterm, annual summary, final)

PREPARED FOR: U.S. Army Medical Research and Materiel Command
Fort Detrick, Maryland 21702-5012

DISTRIBUTION STATEMENT:

Approved for public release; distribution unlimited

The views, opinions and/or findings contained in this report are those of the author(s) and should not be construed as an official Department of the Army position, policy or decision unless so designated by other documentation.

REPORT DOCUMENTATION PAGE

Form Approved
OMB No. 0704-0188

Public reporting burden for this collection of information is estimated to average 1 hour per response, including the time for reviewing instructions, searching existing data sources, gathering and maintaining the data needed, and completing and reviewing this collection of information. Send comments regarding this burden estimate or any other aspect of this collection of information, including suggestions for reducing this burden to Department of Defense, Washington Headquarters Services, Directorate for Information Operations and Reports (0704-0188), 1215 Jefferson Davis Highway, Suite 1204, Arlington, VA 22202-4302. Respondents should be aware that notwithstanding any other provision of law, no person shall be subject to any penalty for failing to comply with a collection of information if it does not display a currently valid OMB control number. **PLEASE DO NOT RETURN YOUR FORM TO THE ABOVE ADDRESS.**

1. REPORT DATE *(DD-MM-YYYY)*	**2. REPORT TYPE**	**3. DATES COVERED** *(From - To)*
1 June 2011	Annual	19/02/2010 – 18/05/2011

4. TITLE AND SUBTITLE
A New Therapeutic Paradigm for Breast Cancer Exploiting Low Dose Estrogen-Induced Apoptosis

5a. CONTRACT NUMBER

5b. GRANT NUMBER
W81XWH-06-1-0590

5c. PROGRAM ELEMENT NUMBER

6. AUTHOR(S)
Virgil Craig Jordan, Ph.D.

e-mail: vcj2@georgetown.edu

5d. PROJECT NUMBER

5e. TASK NUMBER

5f. WORK UNIT NUMBER

7. PERFORMING ORGANIZATION NAME(S) AND ADDRESS(ES)
Georgetown University
Washington, DC 20057-0004

8. PERFORMING ORGANIZATION REPORT NUMBER

9. SPONSORING / MONITORING AGENCY NAME(S) AND ADDRESS(ES)
U.S. Army Medical Research
And Materiel Command
Fort Detrick, MD 21702-5012

10. SPONSOR/MONITOR'S ACRONYM(S)

11. SPONSOR/MONITOR'S REPORT NUMBER(S)

12. DISTRIBUTION / AVAILABILITY STATEMENT
Approved for public release; distribution unlimited

13. SUPPLEMENTARY NOTES

14. ABSTRACT

The purpose of the CoE is to discover the molecular mechanisms and the modulation of estrogen-induced apoptosis. The laboratory research project is focused on genomics and proteomics with a current focus on molecular interrogation to decipher mechanisms that may be applied to aid patient treatment. In parallel, but not supported by the CoE, is a pilot clinical study of estrogen-induced apoptosis in patients with metastatic breast cancer, that have had repeated cycles of successful antihormone therapy, but have subsequently failed and relapsed. The clinical study was originally at the Fox Chase Cancer Center (FCCC), but the coordinating center is now in the process of being moved to the Lombardi Comprehensive Cancer Center (LCCC). Patient materials are currently being transferred and our resources are being marshaled to allow us to adapt to the disruption of our time table, due to the requirement of moving the grant from FCCC to LCCC. Despite the challenge of re-establishing the molecular pharmacology laboratory of the Principal Investigator (PI), considerable momentum has now been achieved in all areas originally designated in the grant, e.g. a description of the time dependent changes in estrogen-responsive growth and apoptosis in model cell lines, an evaluation and description of the early proteomic pathways associated with estrogen-induced apoptosis dependent on the estrogen receptor (ER) co-activator AIB1 (SRC-3), the critical importance of the shape of the ER complex, c-Src activity to initiate apoptosis and the genomic spectrum of our endocrine resistant cell lines to define cell sensitivity to estrogen-induced apoptosis.

15. SUBJECT TERMS
Gene expression microarrays, proteomics, c-Src inhibitor PP2, estrogen receptor complex conformation, estrogen-induced apoptosis, high throughput RNA interference

16. SECURITY CLASSIFICATION OF:			**17. LIMITATION OF ABSTRACT**	**18. NUMBER OF PAGES**	**19a. NAME OF RESPONSIBLE PERSON**
a. REPORT	**b. ABSTRACT**	**c. THIS PAGE**			V.C. Jordan, OBE, PhD, DSc
Unclassified	Unlimited	Unclassified		480	**19b. TELEPHONE NUMBER** *(include area code)* (202)687-2897

Table of Contents

Introduction…… 3

Body…… 4

Task 1 (*LCCC – Isaacs, Swaby/Daly*)
Work Accomplished…… 4

Task 2
Task 2a (*FCCC - Jordan/Ariazi*)
Work Accomplished…… 5

Task 2b-1 (*GU - Jordan/Fan)*
Introduction…….. 6
Body (Work Accomplished)……..... 7

Task 2b-2 (*GU - Jordan/Sengupta)*
Introduction…….. 20
Body (Work Accomplished)……..... 20

Task 2b-3 (*FCCC - Jordan/Lewis-Wambi)*
Work Accomplished…… 32

Task 3
Task 3 (*GU - Riegel/Wellstein*)
Introduction…… 36
Body (Work Accomplished)……... 39

Task 4
Tasks 4a & 4b (*FCCC – Ariazi*, *TGen – Cunliffe*, *GU - Jordan*)
Introduction…… 55
Body (Work Accomplished)…… 55

Task 4c (*TGen – Azorsa/Balagurunathan/Cunliffe*)
Introduction…… 83
Body (Work Accomplished)…… 83

Key Research Accomplishments…… 92

Reportable Outcomes…… 95

Table of Contents continued…..

Conclusions…… 103

References..…… 107

Appendix……… 114

INTRODUCTION

The Center of Excellence Grant is completing four independent, interconnected and synergistic tasks to achieve the goal and answer the overarching question: **to discover the mechanism of estrogen-induced breast cancer cell apoptosis and establish the clinical value of short-term low dose estrogen treatment to cause apoptosis in antihormone resistant breast cancer.** To achieve the goal, we had established an integrated organization (Fig. 1) with a first class advisory board that links clinical trials (**Task 1)** with laboratory models and mechanisms (**Task 2)** proteomics **(Task 3)** and genomics **(Task 4).**

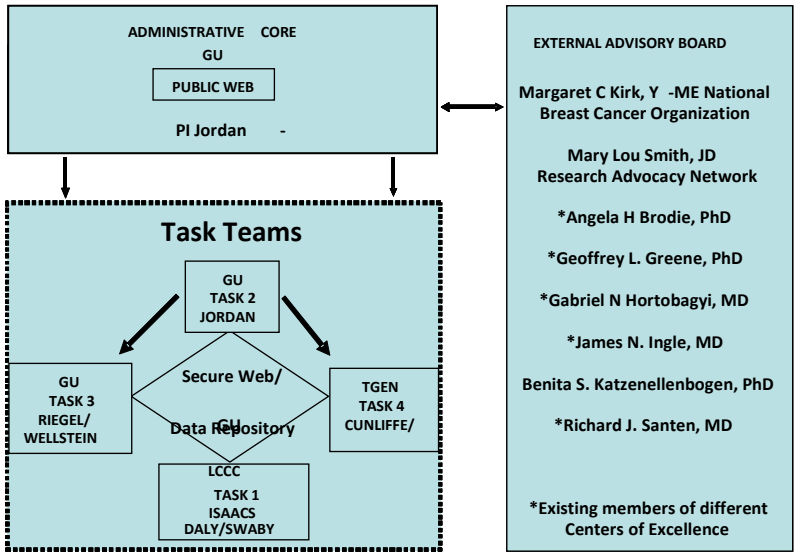


Figure 1 Organization of the COE after May 18, 2011.

Changes in the Organization of the COE

On July 1st, 2009, D r. Jordan assumed the responsibility of Scientific Director and Vice Chairman of the Department of Oncology at the Lombardi Comprehensive Cancer Center (LCCC), Georgetown University, Washington, D.C. With the move at this time to the LCCC, the critical mass of outstanding breast cancer medical scientists who were in position at the LCCC an now interact effectively on a daily basis. The Wellstein and Riegel Laboratory and the Jordan Laboratory continue to use their proteomics database to interrogate the early stages of estrogen-induced apoptosis. Studies with tumors *in vivo* are ongoing to honor the aims and goals of the Center of Excellence (CoE) grant application. Although it has been a challenge to establish the Jordan Laboratory at LCCC, for **Task 2**, this has now been accomplished and financial resources have been marshaled to aid our completion of all the laboratory studies projected in our original application. By necessity, we have had to take steps to move the clinical trial coordinating center (**Task 1**) from the Fox Chase Cancer Center (FCCC), as AstraZeneca has made the unilateral decision to discontinue funding because of their financial situation. Despite this disappointing lack of support by the pharmaceutical industry, these actions are being taken unilaterally by the pharmaceutical industry across the board in all other grant situations. It is our plan with our conserved financial resources from the Department of Defense (DOD), to analyze our collected

clinical material so far, as this is absolutely invaluable to the scientific community. Through this analysis, we will develop preliminary data to apply for future clinical funding to maintain our momentum and leadership in this area.

Dr. Heather Cunliffe, as Principal Investigator of our sub-contract for **Task 4**, will be visiting LCCC to review the enormous developing databases and complete our publications. To aid all of this, the Principal Investigator, Dr. V. Craig Jordan, has carefully and frugally marshaled our valuable financial resources to support continuing interrogation and development of our databases, so that the time lost in having to move from FCCC to LCCC in no way damages our scientific mission and our ability to solve this innovation problem in women's health. Indeed, already our work is having significant impact in the clinical trials community with the recent publication of the Women's Health Initiative study of estrogen replacement therapy alone in hysterectomized women that shows an ***actual*** decrease in the incidence of breast cancer. This exciting new development in women's health finds its scientific foundation in our innovative grant and poised to define the mechanisms necessary to exploit estrogen therapy further in the clinic (see #12 in Appendix). The work that we are refining will form the basis of an invited series of reviews on the molecular mechanism of estrogen-induced apoptosis. Through the award of this Center of Excellence Grant from the DOD, we have demonstrated innovation in solving fundamental problems in women's health at the molecular level.

BODY

Task 1: (LCCC/Isaacs, Swaby/Daly) - To conduct exploratory clinical trials to determine the efficacy and dose response of pro-apoptotic effects of estrogen [Estrace] in patients following the failure of two successful antihormonal therapies.

Task 1a: (Isaacs, Swaby and Daly) - To confirm the efficacy of standard high dose estrogen (Estrace) therapy and then determine a minimal dose to induce tumor regression.

Here we report work completed on Tasks 1a at the FCCC site during year 4 of this COE.

Clinical trial conducted by Ramona Swaby MD, under the direction of Mary Daly MD at FCCC.

DOSE DE-ESCALATION OF ESTROGEN (ESTRACE) TO REVERSE ANTIHORMONE RESISTANCE IN PATIENTS ALREADY EXHAUSTIVELY TREATED WITH ANTIHORMONE THERAPY

WORK ACCOMPLISHED:

During the fourth year of funding, we have continued to actively recruit subjects. The clinical trial was successfully opened at 2 additional sites in addition to Fox Chase Cancer Center: 1) Georgetown University (01-24-2011) 2) Cooper University Hospital (03-11-2011). Additionally, the study was IRB approved (06-28-2010) at the Fox Chase Partner/Pottstown

Memorial Regional Cancer Center and is undergoing IRB review at the Fox Chase Partner/Delaware County Memorial Hospital. In the fourth year of funding, including all sites, 12 subjects were screened and 7 subjects were enrolled. There have been no DLTs (dose limiting toxicities) and/or SAEs (Serious Adverse Events). Of the 11 enrolled subjects, 5 consented to undergo the optional research biopsy for acquisition of tissue samples as proposed in Task 1b. In two of the five cases, no tissue could be visualized or could not feasibly be obtained despite biopsy attempt; an additional subject was unable to be biopsied due to necessary anticoagulant therapy and another subject revoked her consent. Therefore, tissue was able to be obtained from one of the five consented cases.

In total, 11 subjects have been enrolled and 2 subjects remain on study. Preliminary demographic information is available for 9 of the 11 enrolled subjects. The ages of the subjects enrolled range from age 53 – 80 (median age = 64). Eight of the subjects are non-hispanic Caucasian patients and one subject is non-hispanic African American. The population has been heavily pre-treated, as the median number of prior treatments prior to study enrollment including both endocrine and cytotoxic therapies is 8 with a range from 2 to 14 prior treatment regimens. The number of prior endocrine therapies range from 2 to 9 (median = 3). This includes some endocrine agents that were discontinuously used and reinstituted at the time of progression of disease of a separate therapeutic regimen – i.e. anastrazole used following progression of disease on tamoxifen, and then 3 years later used again following progression of disease on capecitabine. The median number of prior cytotoxic therapies prior to enrollment is 1, although the average is 3 with a range from three patients who were chemotherapy naïve to 2 patients who had received 8 and 9 prior cytotoxic treatment regimens prior to enrollment.

Unfortunately, within the past month, AstraZeneca has withdrawn continued funding of the clinical operations. Despite this, we plan to continue the clinical trial and plan to transfer the coordinating center to Georgetown University's Lombardi Comprehensive Cancer Center with Dr. Claudine Isaacs as the Study Chair and Principal Investigator. Institutional funds from the Lombardi Comprehensive Cancer Center will provide support for the continued accrual and conduct of the trial. Accrual at other sites will cease at other institutions but will continue at LCCC. LCCC is planning to advertise for the trial to ensure continued accrual. An amendment to the protocol and consent form outlining these changes is underway and is anticipated to be submitted to the Department of Defense within the next 2 weeks.

TASK 2: (GU/Jordan) - To elucidate the molecular mechanism of E_2 (estrogen) induced survival and apoptosis in breast cancer cells resistant to either selective ER (estrogen receptor) modulators (SERMs) or long-term estrogen deprivation.

Task 2a: (Ariazi and Jordan) - To complete a series of experiments using sets of well defined breast cancer models of E_2-induced survival and apoptosis *in vivo* and *in vitro* [at the FCCC]. FCCC will generate protein samples for proteomic analyses [carried out]

under Task 3 [at GU] and RNA samples for gene expression microarray analyses [carried out] under Task 4 [at Translational Genomics Research Institute (TGen)].

Studies carried out by Eric Ariazi PhD at FCCC in the laboratory of Dr. Jordan.

GENERATION OF CELL LINE SPECIMENS FOR PROTEOMICS AND GENE EXPRESSION MICROARRAY ANALYSES

WORK ACCOMPLISHED:
Task 2a was completed during prior Years 1 – 3 at the FCCC site. The experiments were described in prior Years 1 - 3 Progress Reports. No new samples were generated during Year 4.

TASK 2. GU/Jordan - To elucidate the molecular mechanism of E_2 induced survival and apoptosis in breast cancer cells resistant to either SERMs or long-term estrogen deprivation.

Task 2b-1: Fan and Jordan – To confirm and validate developing pathways of E_2-induced breast cancer cell survival and apoptosis.

Task 2b-1 (Fan and Jordan) - Studies carried out by Dr. Ping Fan in the Jordan laboratory at Georgetown University

ROLE OF C-SRC TYROSINE KINASE ACTIVITY IN REGULATING APOPTOSIS INDUCED BY E_2 IN LONG-TERM ESTROGEN DEPRIVATION-RESISTANT BREAST CANCER CELLS

Here we report work completed on Task 2b-1 at the Lambardi Comprehensive Cancer Center site during year 4 of this COE involving the role of c-Src tyrosine kinase activity in E_2-induced breast cancer cell survival and apoptosis.

Introduction:

Resistance to aromatase inhibitors used for the treatment of ER positive breast cancer is an increasing clinical problem. Previously we showed that physiological concentrations of E_2 could trigger apoptosis of long-term E_2 deprived breast cancer cells (MCF-7:5C) (1). This new targeted strategy provides novel therapeutic approaches to endocrine resistant breast cancer. A recent phase II clinical trial reported that E_2 provided a clinical benefit for aromatase inhibitor-resistant advanced breast cancer patients. However, only 30% of patients receive clinical benefit (2). This prompted us to investigate strategies to increase the therapeutic responsiveness in aromatase inhibitor resistant breast cancer. c-Src is currently of interest, as it mediates survival pathways of breast cancer cells (3). Here, we investigate the mechanisms underlying E_2-induced apoptosis and the therapeutic potential of combination c-Src inhibitor PP2 and E_2 in the long-term estrogen deprived breast cancer cells.

WORK ACCOMPLISHED:

Growth effects of the c-Src tyrosine kinase inhibitor PP2 in different cell lines

The central role of c-Src in mediating survival pathways has validated it as an attractive therapeutic target for the treatment of human breast cancer. To identify inhibitory effects of c-Src tyrosine kinase inhibitor in different human breast cancer cell lines and explore its potential in combination treatment with estrogen to enhance apoptosis in long-term estrogen deprived breast cancer cells, a specific c-Src inhibitor, PP2, was utilized to block c-Src tyrosine kinase. The PP2 acted as an inhibitor to block the phosphorylation of c-Src and inhibited cell growth of breast cancer cell lines including MCF-7, T47D, MDA-MB-231, Sk-Br-3, as well as two long-term estrogen-deprived breast cancer cells MCF-7:5C and MCF-7:2A whereas with different inhibitory rate. The triple negative (ER negative, PR (progesterone receptor) negative, and HER2 (human epidermal growth factor receptor 2) negative) MDA-MB-231 cell was the most sensitive to PP2 among these different cell lines (Fig. 1). The inhibitory efficiency of growth closely correlated with whether the c-Src inhibitor could effectively block survival pathways of different breast cancer cells. Taken together, this study demonstrated variable responses to c-Src inhibitor in different breast cancer cell lines which highlighted the diversity of responses potentially present in the heterogeneous cell populations of clinically observed breast cancer.

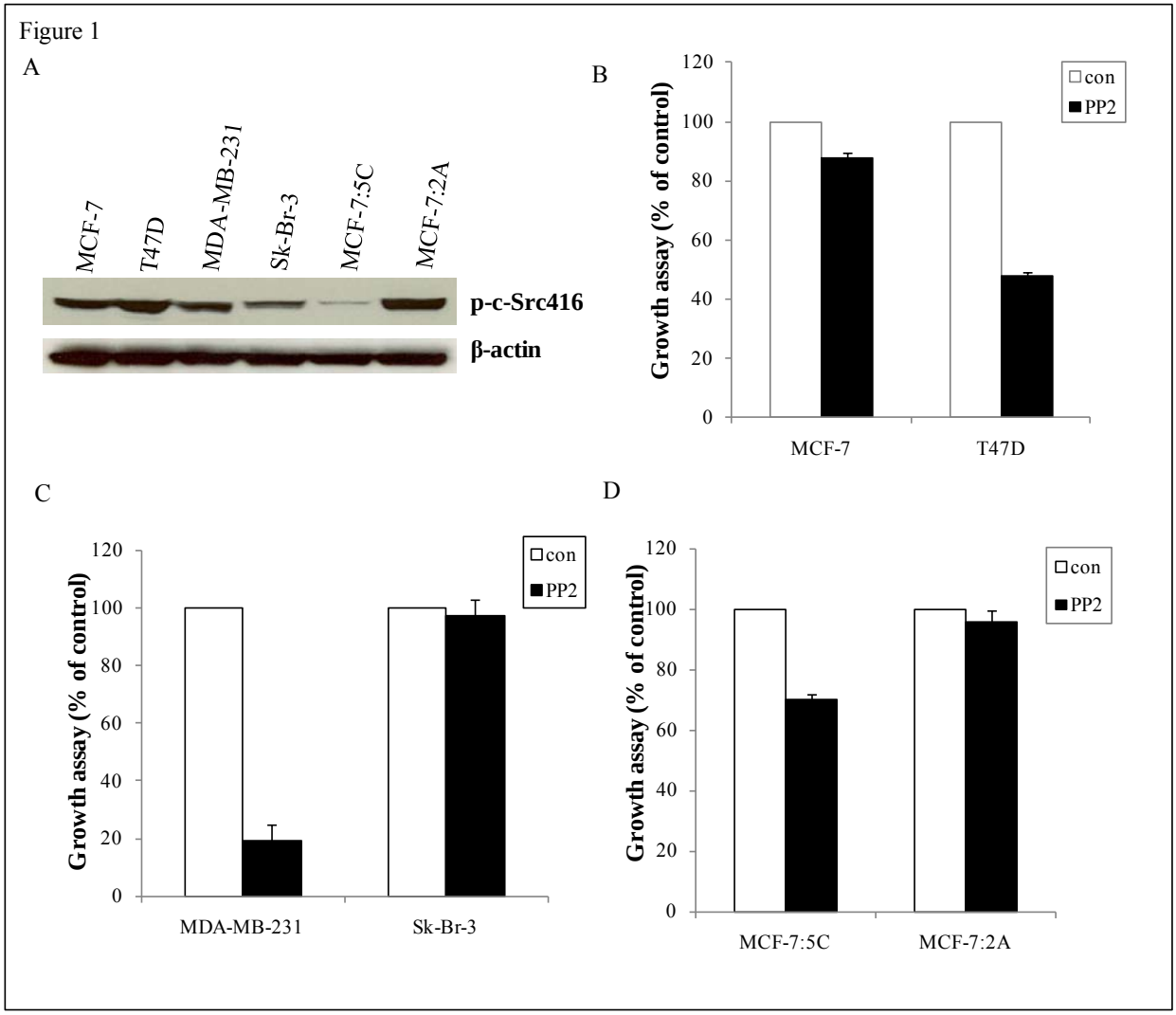


Figure 1. **Different cell lines response to the c-Src inhibitor. A. Levels of c-Src phosphorylation in different cell lines.** Cell lysates were harvested from different cell lines including MCF-7, T47D, MDA-MB-231, Sk-Br-3, MCF-7:5C, and MCF-7:2A cells. The antibody to phospho-c-Src^{Tyr416} was used to examine the phosphorylation level of c-Src. The β-actin was used as loading control. **B. Inhibition effects of the c-Src inhibitor in MCF-7 and T47D cells.** MCF-7 and T47D cells were seeded in the 24-well plates with 10,000 cells/well in triplicate. The next day, cells were treated with PP2 (5 μM) in its culture medium---phenol red RPMI 1640 containing 10% fetal bovine serum. Cells were harvested after 7 days treatment and total DNA was determined using the DNA-binding fluorescent dye Hoechst 33528 and comparison to a standard curve of serially-diluted calf thymus DNA. **C. Inhibition effects of the c-Src inhibitor in MDA-MB-231 and Sk-Br-3 cells.** MDA-MB-231 and Sk-Br-3 cells were seeded in the 24-well plates with 10,000 cells/well in triplicate. The next day, cells were treated with PP2 (5 μM) in its respective culture medium---phenol red DMEM containing 5% whole calf serum and phenol red RPMI 1640 containing 10% fetal bovine serum. Cells were harvested after 7 days treatment and total DNA was determined as in B. **D. Inhibition effects of the c-Src inhibitor in MCF-7:5C and MCF-7:2A cells.** MCF-7:5C and MCF-7:2A cells were seeded in the 24-well plates with 15,000 cells/well in triplicate. The next day, cells were treated with PP2 (5 μM) in its culture medium---phenol red free RPMI 1640 containing 10% charcoal-stripped fetal bovine serum. Cells were harvested after 7 days treatment and total DNA was determined as in B.

c-Src inhibitor could not enhance E_2-induced apoptosis in two long-term estrogen deprived breast cancer cells.

Our previous data have shown that physiological levels of estrogen can induce apoptosis in long-term estrogen deprived breast cancer cells MCF-7:5C and MCF-7:2A cells. Estrogen can quickly induce apoptosis in MCF-7:5C cells but gradually induce apoptosis in MCF-7:2A cells. Although with different levels of c-Src phosphorylation between MCF-7:5C and MCF-7:2A cells (Fig. 1A), c-Src inhibitor could significantly block tyrosine kinase activity of c-Src in both cell lines. The c-Src inhibitor PP2 could block p-MAPK (mitogen-activated protein kinase) and p-Akt in MCF-7:5C cells whereas just reduce p-MAPK but not p-Akt in MCF-7:2A cells, which may result in different inhibitory effects between two cell lines (Fig. 2A and 2B).

Since the c-Src inhibitor could block survival pathways of long-term estrogen deprived breast cancer cells, we investigated whether combination the c-Src inhibitor with estrogen could enhance E_2-induced apoptosis. E_2 alone caused apoptosis as previously reported. Inhibition of c-Src tyrosine kinase by PP2 resulted in moderately growth inhibition of MCF-7:5C and MCF-7:2A cells. However, it was surprising to find that PP2 could block the cell death induced by E_2 in MCF-7:5C and MCF-7:2A cells although PP2 itself acted as an inhibitor in long-term estrogen deprived breast cancer cells (Fig. 2C and 2D). The implication of these results is potentially clinically important that a Src inhibitor should not be combined with E_2 in the treatment of advanced aromatase inhibitor-resistant breast cancer.

Figure 2

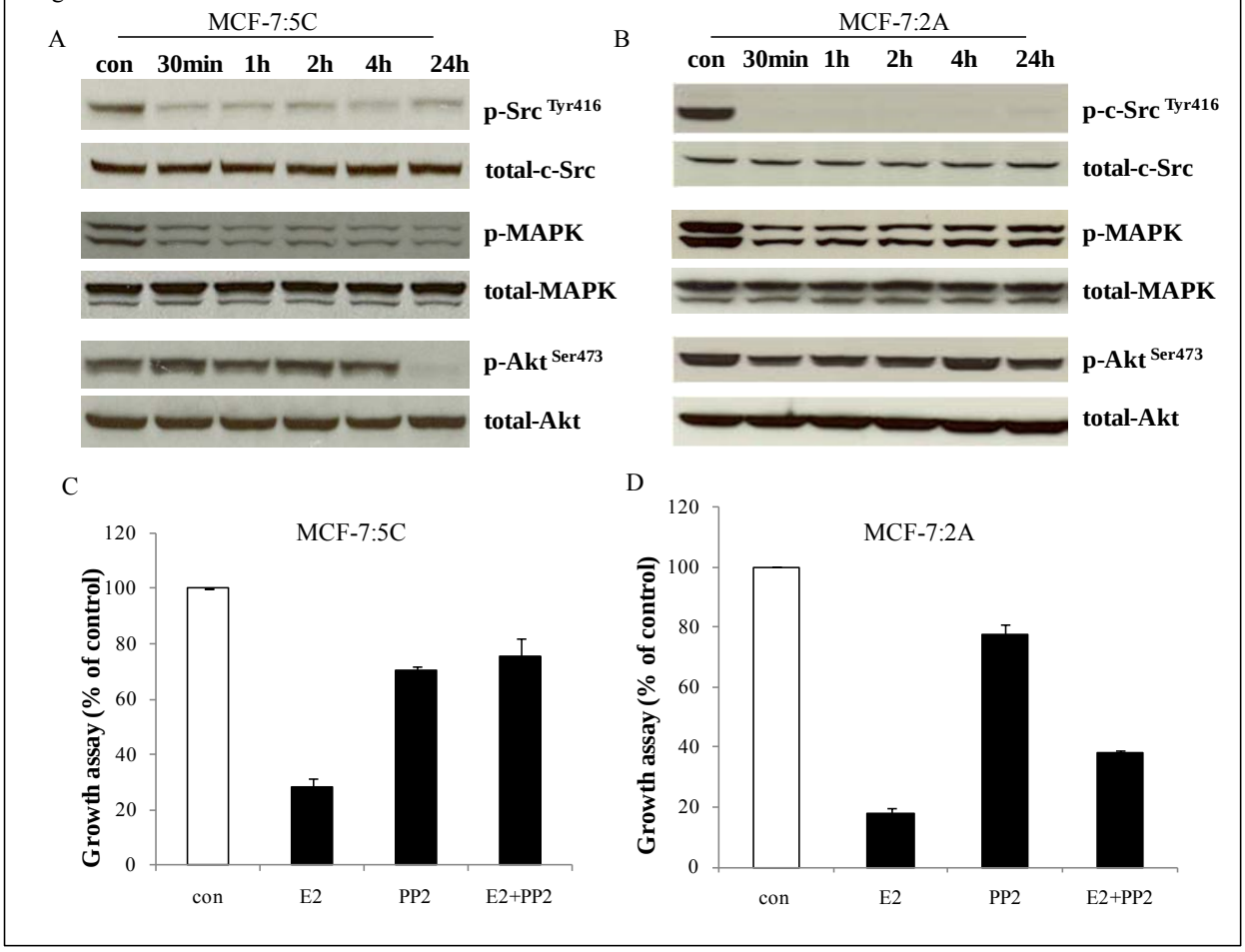


Figure 2. **The c-Src inhibitor prevented E_2-induced cell death in two long-term estrogen deprived breast cancer cells. A. The c-Src inhibitor blocked p-MAPK and p-Akt in MCF-7:5C cells.** MCF-7:5C cells were treated with the c-Src inhibitor PP2 (5 μM). Cell lysates were harvested as indicated time points. The antibodies to phospho-c-Src ^{Tyr416} , phospho-MAPK, and phospho-Akt were used to examine the phosphorylation levels of each signaling. The total c-Src, total MAPK, and total Akt were detected as respective loading controls. **B. The c-Src inhibitor blocked p-MAPK but not p-Akt in MCF-7:2A cells.** MCF-7:2A cells were treated with the c-Src inhibitor PP2 (5 μM). Cell lysates were harvested as indicated time points. The antibodies to phospho-c-Src ^{Tyr416} , phospho-MAPK, and phospho-Akt were used to examine the phosphorylation levels of each signaling. The total c-Src, total MAPK, and total Akt were detected as respective loading controls. C. **The c-Src inhibitor blocked E_2-induced cell death in MCF-7:5C cells.** MCF-7:5C cells were seeded in the 24-well plates with 15,000 cells/well in triplicate. The next day, cells were treated with 0.1% vehicle as control, E_2 (1nM), PP2 (5 μM), and E_2 (1nM) plus PP2 (5 μM) in phenol red free RPMI 1640 containing 10% charcoal-stripped fetal bovine serum. Cells were harvested after 7 days treatment and total DNA was determined by a DNA growth assay kit as in figure 1. **D. The c-Src inhibitor blocked E_2-induced cell death in MCF-7:2A cells.** MCF-7:2A cells were seeded in the 6-well plates with 10,000 cells/well in triplicate. The next day, cells were treated with 0.1% vehicle as control, E_2 (1nM), PP2 (5 μM), and E_2 (1nM) plus PP2 (5 μM) in phenol red free RPMI 1640 containing 10% charcoal-stripped fetal bovine serum. Medium was changed every 2 days with fresh compounds respectively. Cells were harvested after 14 days treatment and total DNA was determined by a DNA growth assay kit as in figure 1.

The c-Src inhibitor PP2 blocked E_2-induced apoptosis.

Our previous data already confirmed that estrogen inhibited MCF-7:5C and MCF-7:2A cell growth through inducing apoptosis. And pure antiestrogen ICI 182,780 could block E_2-induced apoptosis which demonstrated that estrogen utilized estrogen receptor (ER) to trigger apoptosis. The non-receptor tyrosine kinase, c-Src, is an important adapter protein to mediate ER signal pathways (4). However, the c-Src inhibitor could prevent E_2-induced cell death (Fig. 2C and 2D), which clued that the c-Src inhibitor may block E_2-induced apoptosis. We firstly focused on the investigation whether the c-Src inhibitor could block E_2-induced apoptosis in MCF-7:5C cells. MCF-7:5C cells were treated with E_2 plus PP2 and compared with either E_2 alone or PP2 alone treatment. The annexin V binding to externalized phosphatidylserine was a marker of early apoptotic events. Estrogen could significantly increase the percentage of annexin V binding after 72 hours treatment detected through flow cytometry (Fig. 3A). The c-Src inhibitor PP2 could clearly block, and, prevent early stage apoptosis from progressing into late stage apoptosis (Fig. 3A). Another quantitative apoptosis method through determination of cytoplasmic histone-associated-DNA fragments was used to investigate the effect of the c-Src inhibitor on E_2-induced apoptosis. The amount of histone-associated-DNA fragments was normalized by the cell number with different treatment. Significant apoptosis initiated by E_2 could be detected after 96 hours treatment in MCF-7:5C (Fig. 3B). The c-Src inhibitor could clearly block the apoptosis induced by E_2 which further confirmed that the c-Src inhibitor could block the apoptosis induced by E_2. These data also demonstrated that E_2-triggered apoptosis utilized c-Src tyrosine kinase pathway. Two different mechanistic methods to detect apoptosis induced by E_2 in MCF-7:5C cells with different time points which implied that estrogen might firstly act as a knife to cut the cell membrane to trigger apoptosis to increase annexin V binding to the externalized phosphatidylserine in the membrane.

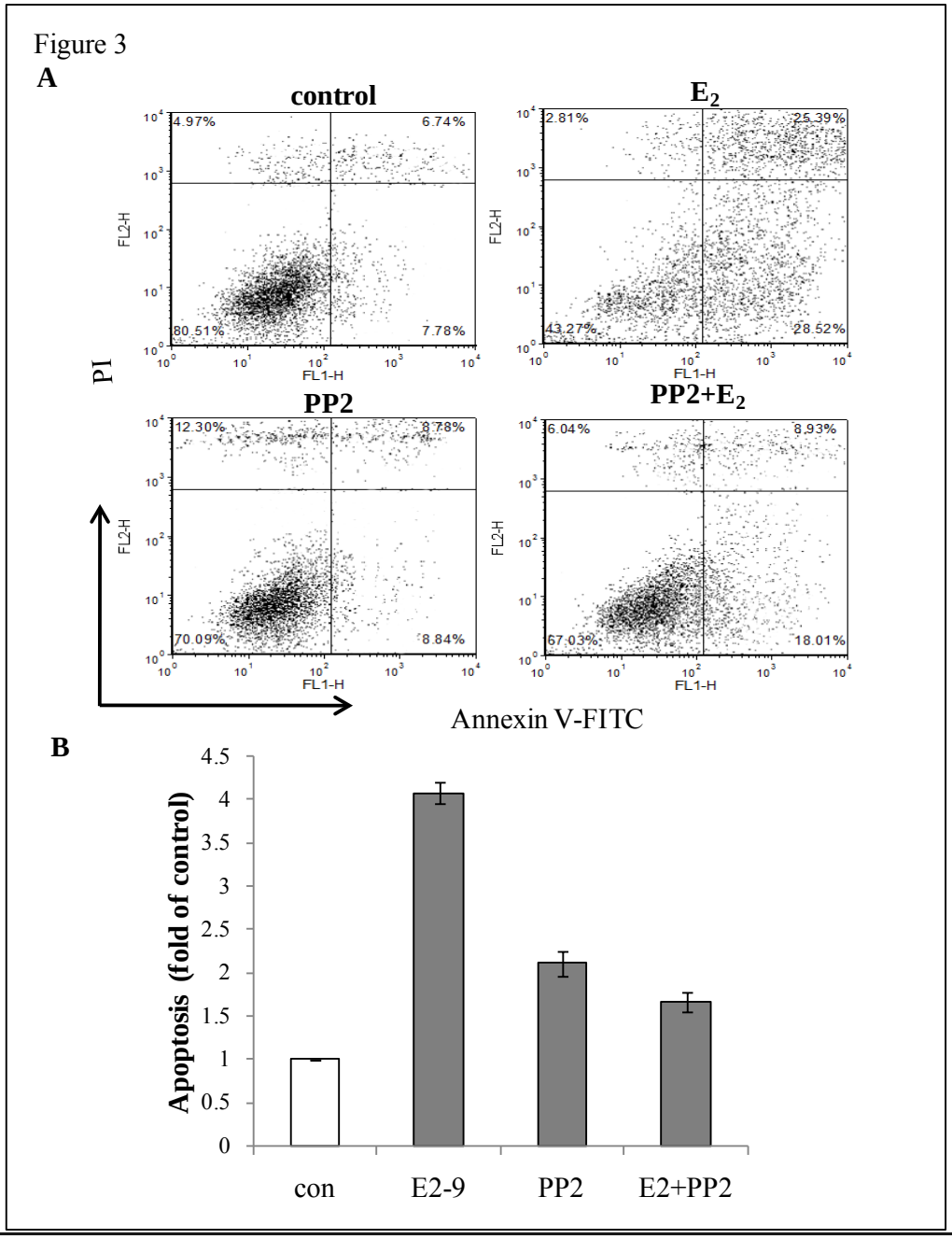


Figure 3. The c-Src inhibitor blocked E_2-induced apoptosis in MCF-7:5C cells. A. The c-Src inhibitor blocked E_2-induced apoptosis through Annexin V-FITC binding assay in MCF-7:5C cells. MCF-7:5C cells were treated with 0.1% vehicle as control, E_2 (1nM), PP2 (5 μM), and E_2 (1nM) plus PP2 (5 μM) in phenol red free RPMI 1640 containing 10% charcoal-stripped fetal bovine serum for 72 hours. Cells were harvested and stained with Annexin V-FITC and PI as manufacturer's protocol. The cells were analyzed trough FACS. **B. The c-Src inhibitor blocked E_2-induced apoptosis through determination of cytoplasmic histone-associated-DNA fragments in MCF-7:5C cells.** MCF-7:5C cells were seeded in the parallel 12-well plates with 50,000 cells/well in triplicate. The next day, cells were treated with 0.1% vehicle as control, E_2 (1nM), PP2 (5 μM), and E_2 (1nM) plus PP2 (5 μM) in phenol red free RPMI 1640 containing 10% charcoal-stripped fetal bovine serum. Medium was changed every 2 days with fresh compounds respectively. After 4 days treatment, cell lysates were harvested as apoptosis ELISA kit's protocol in one plate. The cell numbers were counted in another parallel plate. The apoptosis was normalized by real cell number.

Long-term E_2 plus PP2 treatment completely overcame inhibitory effects of E_2 and PP2 monotherapy on MCF-7:5C cells.

To further investigate the function of c-Src tyrosine kinase in the apoptosis induced by E_2, MCF-7:5C cells were long-term (at least 2 months) treated with E_2 plus PP2 compared with PP2 and E_2 monotherapy respectively. Long-term PP2 treated cells appeared smaller and more contracted, with decreased cell spreading (Fig. 4A). The c-Src inhibitor PP2 inhibited cell growth with clearly G1 arrest (Fig. 4B). Long-term treatment with E_2 initially caused massive apoptosis, but small fraction of surviving cells subsequently re-grew. However, apoptotic impairment could be observed under microscope at this time point (Fig. 4A). Cell cycles analysis demonstrated typical G1 arrest (Fig. 4B). In contrast, a combination of PP2 and E_2 blocked the apoptosis and the resulting cell line (MCF-7:PF) grew vigorously in culture with physiological levels of E_2 (Fig. 4A). This combination treatment completely overcame the G1 arrest exerted by monotherapy and made resulting cell line acquire normal cell cycles compared with MCF-7:5C cells (Fig. 4B).

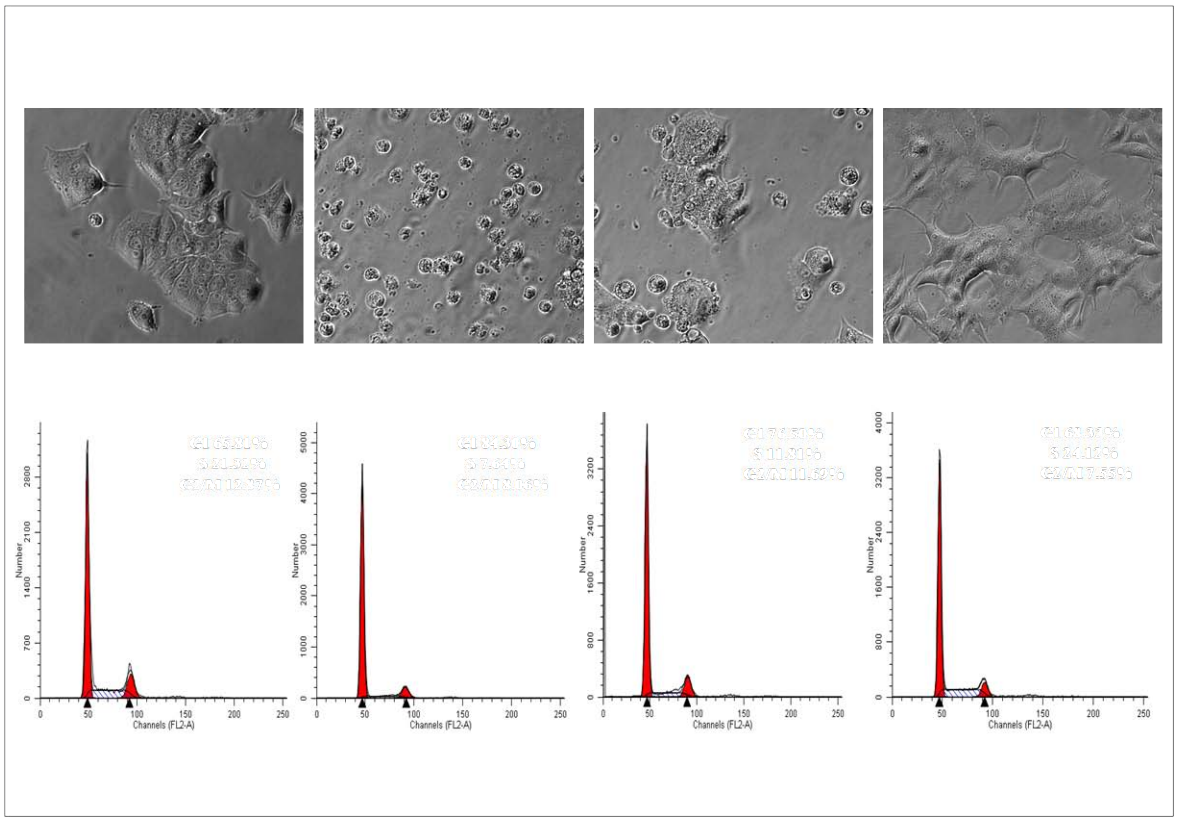


Figure 4. Long-term combination the c-Src inhibitor with E_2 completely blocked E_2-induced apoptosis in MCF-7:5C cells. A. The morphological changes after long-term treatment with E_2 , PP2, and E_2 plus PP2 in MCF-7:5C cells. MCF-7:5C cells were long-term treated with 0.1% vehicle as control, E_2 (1nM), PP2 (5 μM), and E_2 (1nM) plus PP2 (5 μM) in phenol red free RPMI 1640 containing 10% charcoal-stripped fetal bovine serum in T25 flasks. Cells were changed medium every 2 days with fresh compounds in respective flasks. After 2 months treatment, cells were photographed under bright field illumination at (×20) magnification respectively. **B. Analysis of cell cycles after long-term treatment with E_2 , PP2, and E_2 plus PP2 in MCF-7:5C cells.** Differently treated MCF-7:5C cells were harvested separately. After once wash with cold PBS, the cells were gradually fixed with 75% EtOH on ice. Twenty minutes later, they were stained with PI and analyzed through FACS.

The c-Src tyrosine kinase inhibtor converted E_2 from inducing apoptosis to stimulate growth in MCF-7:5C cells.

Since the c-Src inhibitor plus E_2 changed the growth characteristics of MCF-7:5C cells, their response to E_2 alone needed to be re-examined. To our surprise, long-term treatment of MCF-7:5C cells with PP2 plus E_2 not only protected these cells from E_2 -induced apoptosis, instead, allowed E_2 to dramatically stimulate growth of these cells (Fig. 5A). This stimulation by E_2 was blocked by the pure antiestrogen ICI 182,780, confirming that ER mediated proliferation despite its low expression (Fig. 5B). Thus, ERα (ER alpha) must still be expressed in these cells, but at very low levels (Fig. 5C). Intriguingly, physiological levels of E_2 still could induce apoptosis of PP2 alone treated cells if the drug was washed out (Fig. 5A). However, provided including the c-Src inhibitor in the medium which could completely abolish E_2-induced apoptosis in PP2 alone treated cells. These findings further confirmed that E_2-induced apoptosis utilized c-Src tyrosine kinase pathway. In E_2 alone-treated cells, E_2 both induced apoptosis and stimulated growth, but these effects cancelled each other out in terms of total DNA content per well (Fig. 5A). Blocking c-Src tyrosine kinase increased ERα expression after long-term treatment (Fig. 5C). One of the mechanisms whereby blocking c-Src tyrosine kinase could up-regulate ERα may be related to impaired ligand-activated ER alpha ubiquitylation (5,6). As expected, E_2 alone and E_2 plus PP2 treated cells expressed much less ERα due to E_2 down-regulation, which also implied that the c-Src inhibitor could not overcome ERα down-regulation from E_2. The ERα protein expression was consistent with mRNA levels (Fig. 5D).

Figure 5

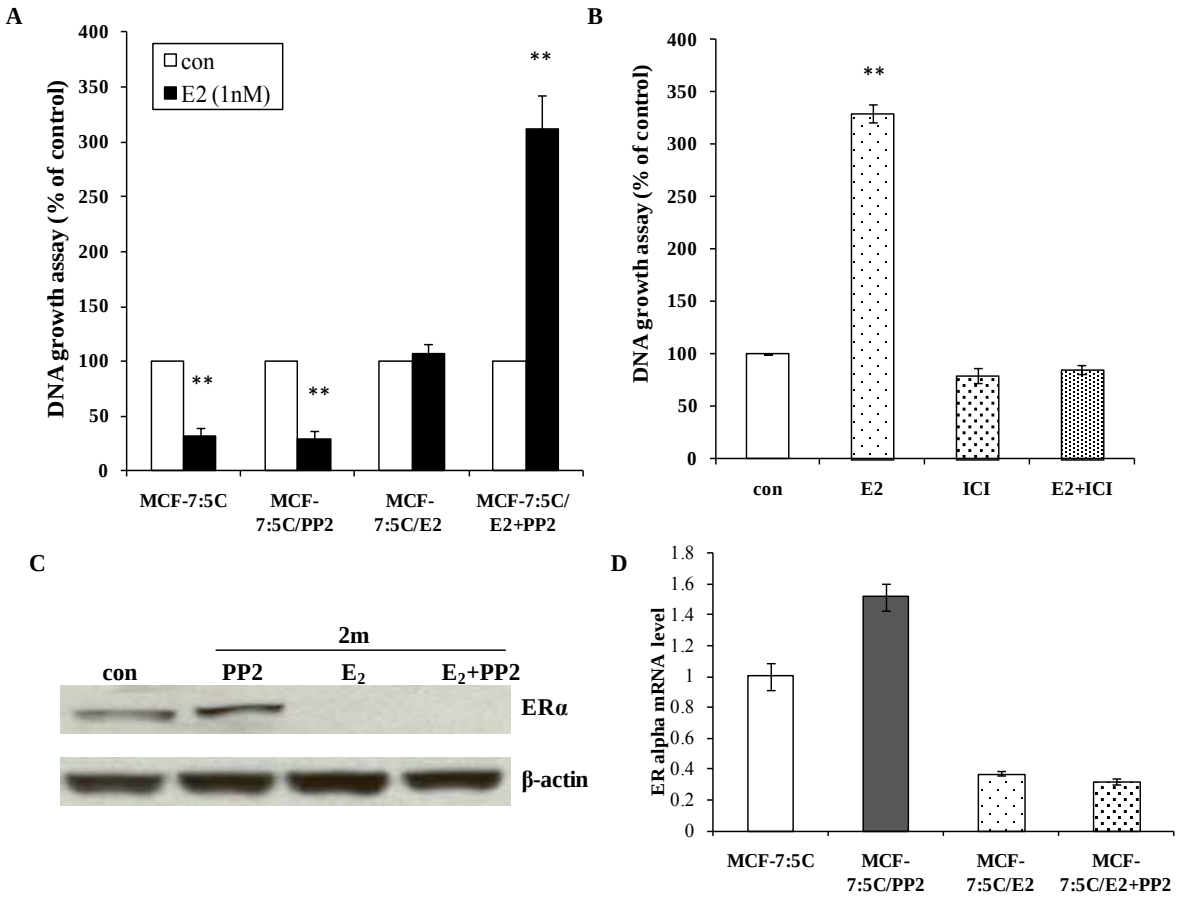


Figure 5. Estrogen stimulated long-term E_2 plus PP2 treated cell growth. A. Differently treated cells response to estrogen. Differently long-term treated cells were seeded in 24-well plates with 15,000 cells/well in triplicate, respectively. After one day, the cells were treated with E_2 (1nM) in estrogen-free medium without any other compounds in the medium. The cells were harvested after 7 days treatment and total DNA was determined using a DNA fluorescence quantitation kit. $P<0.001$, ** compared with MCF-7:5C cells. **B. The proliferation by E_2 could be blocked by ICI 182,780 in long-term E_2 plus PP2 treated cells.** The E_2 plus PP2 treated cells were seeded in 24-well plates with 15,000 cells/well in triplicate without any compound in the medium. After one day, the cells were treated with E_2 (1nM), ICI182,780 (10^{-6} mol/L), and E_2 (1nM) plus ICI182,780 (10^{-6} mol/L) respectively in estrogen-free medium. The cells were harvested after 7 days treatment and total DNA was determined using a DNA fluorescence quantitation kit. $P<0.001$, ** compared with control. **C. Estrogen receptor (ER) expression levels in differently treated cells.** MCF-7:5C cells and differently long-term treated cells were grown in 100mm dishes respectively. Cell lysates were harvested. ER alpha was examined by immunoblotting with primary antibody against it. Immunoblotting for ß-actin was detected for loading control. **D. ER alpha mRNA expression.** MCF-7:5C cells and differently long-term treated cells were grown in six-well plates in triplicates. The RNA was harvested in TRIzol when the cells were 80% confluent for further real-time PCR analysis.

The c-Src inhibitor collaborated with E_2 to elevate endogenous ER target genes after combination treatment.

As shown above, long-term E_2 plus PP2 treated cells were hypersensitive to E_2 despite extremely low ERα expression. The ERE (estrogen response element) ERE activity of E_2 plus PP2 treated cells was similar as other cell lines derived from MCF-7:5C cells which also demonstrated that nuclear ERα functioned well in this resulting cell line (Fig.6A). For the first time, we found that the c-Src inhibitor dramatically elevated E_2 inducible gene pS2 mRNA although the mechanisms were unclear (Fig. 6B). Moreover, the effect of the c-Src inhibitor was additive with E_2 to promote pS2 mRNA in combination treated cells (Fig. 6B). Endogenous PR was undetectable in MCF-7:5C cells compared with wild type MCF-7 cells. However, adding back E_2 in the medium could recover PR expression in E_2 alone treated cells and E_2 plus PP2 treated cells (Fig. 6C). The c-Src inhibitor PP2 alone did not regulate PR expression. Nevertheless, it synergized with E_2 to significantly up-regulate PR mRNA although without consistent highest protein expression, which implied existence of a post-translational modification of PR in E_2 plus PP2 treated cells (Fig. 6D) (7).

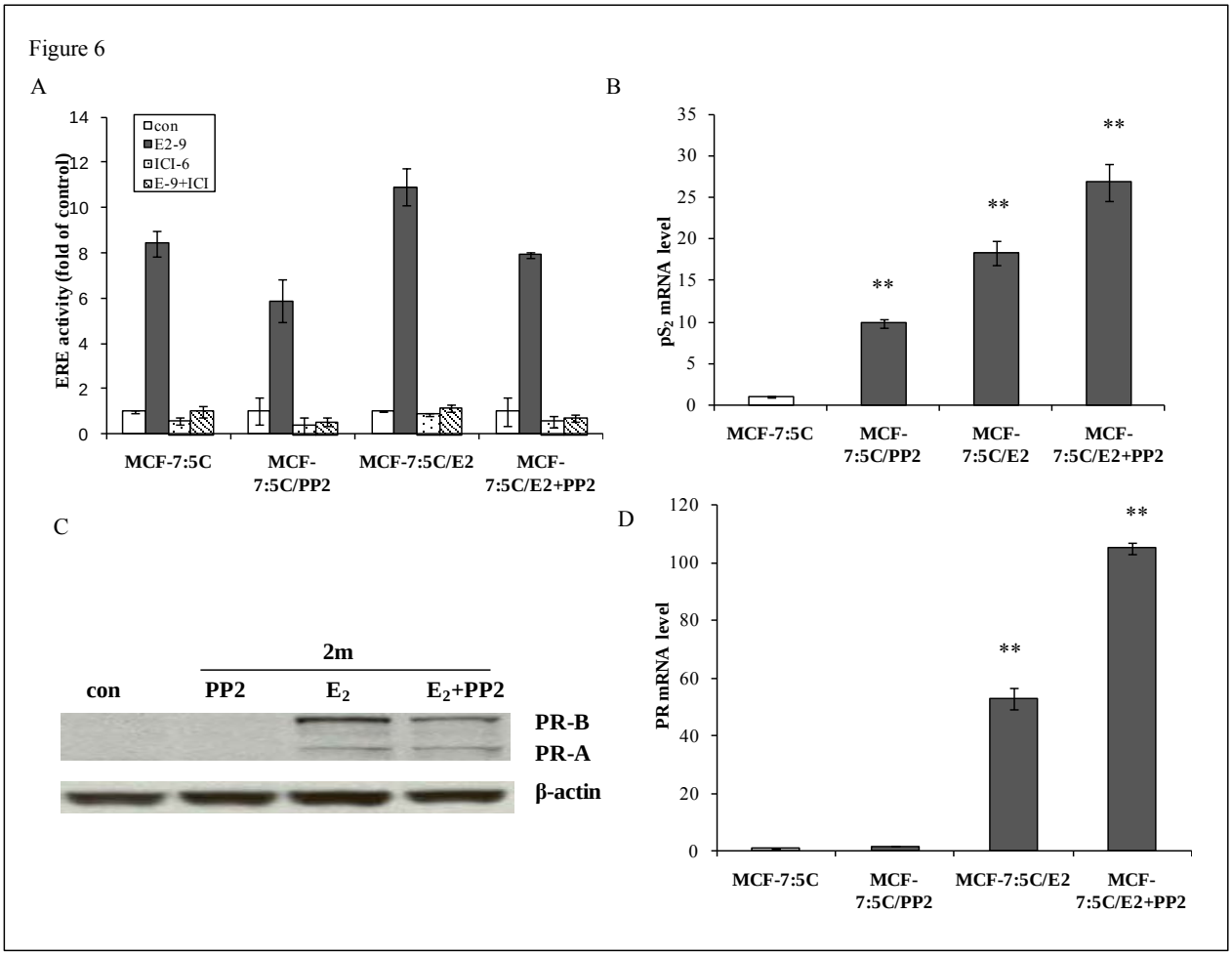


Figure 6. ER target genes were activated after long-term E_2 plus PP2 treated in MCF-7:5C cells. A. ERE activity in different cells. MCF-7:5C and differently long-term treated cells were seeded in 24-well plates in triplicate and transfected with ERE firefly luciferase plasmid plus renilla luciferase plasmid. One day later, they were treated with E_2 (1nM), ICI182,780 (10^{-6} mol/L), and E_2 (1nM) plus ICI182,780 (10^{-6} mol/L) respectively in estrogen-free medium. ERE activity was detected after 24h treatment using luciferase kit. **B. The pS2 mRNA expression.** MCF-7:5C and differently long-term treated cells were grown in 6-well plates in triplicates, respectively. The RNA was harvested in TRIzol when the cells were 80% confluent for further real-time PCR analysis. **C. PR changes after long-term treatment.** MCF-7:5C cells and differently long-term treated cells were grown in 60mm dishes as indicated respectively. PR was examined by immunoblotting with primary antibody against it. Immunoblotting for ß-actin was detected for loading control. D. **PR mRNA expression.** MCF-7:5C cells and differently long-term treated cells were grown in 6-well plates in triplicates, respectively. The RNA was harvested in TRIzol when the cells were 80% confluent for further real-time PCR analysis.

c-Src inhibitor collaborated with E_2 to enhance IGF-1Rβ (type 1 insulin-like growth factor receptor) which is involved in the E_2 stimulation after E_2 plus PP2 treatment.

c-Src mediates the interaction between growth factor receptors and ER in breast cancer . These two growth regulatory pathways are tightly linked in ER positive breast cancer. We found that the c-Src inhibitor could increase IGF-1Rβ expression in MCF-7:5C cells (Fig. 7A). E_2 could also up-regulate IGF-1Rβ (Fig. 7A). Moreover, PP2 and E_2 were additive to elevate IGF-1Rβ in combination treated cells (Fig. 7A and 7B). To investigate the potential role of IGF-1Rβ in combination treated cells, we demonstrated that a specific inhibitor of IGF-1Rβ (AG1024) could inhibit the cell growth and completely abolished E_2 stimulation (Fig. 7C) which provided evidence that IGF-1Rβ played a critical role in E_2-stimulated growth in E_2 plus PP2 treated cells. These data also supported the idea that c-Src was an important adapter protein which mediated the crosstalk between growth factor receptor and estrogen receptor.

Figure 7

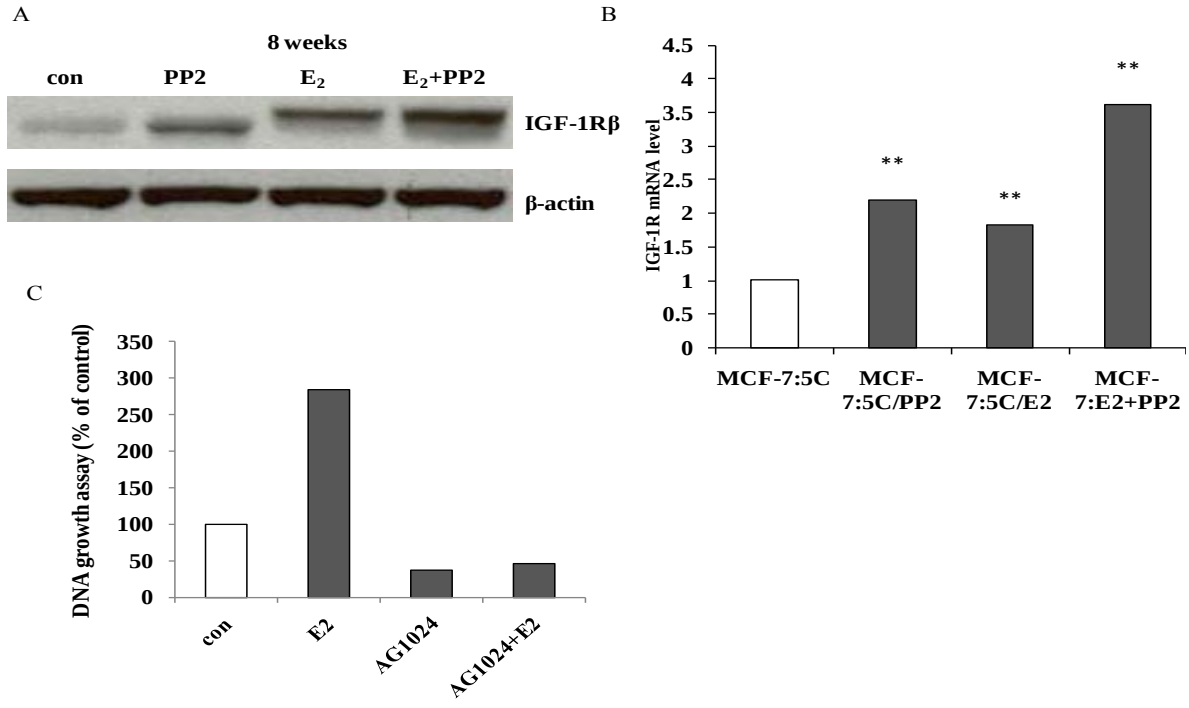


Figure 7. IGF-1Rβ played a critical role in long-term E_2 plus PP2 treated MCF-7:5C cells. A. IGF-1Rβ changes after long-term treatment. MCF-7:5C cells and differently long-term treated cells were grown in 60mm dishes as indicated respectively. PR was examined by immunoblotting with primary antibody against it. Immunoblotting for ß-actin was detected for loading control. **B. The IGF-1Rβ mRNA expression.** MCF-7:5C and differently long-term treated cells were grown in 6-well plates in triplicates, respectively. The RNA was harvested in TRIzol when the cells were 80% confluent for further real-time PCR analysis. **C. IGF-1Rβ inhibitor AG1024 could completely block E2 stimulation in long-term E_2 plus PP2 treated MCF-7:5C cells.** Long-term E_2 plus PP2 treated MCF-7:5C cells were seeded in 24-well plates with 15,000 cells/well in triplicate. After one day, the cells were treated with E_2 (1nM), AG1024 (10 μM), and E_2 (1nM) plus AG1024 (10 μM) in estrogen-free medium. The cells were harvested after 7 days treatment and total DNA was determined using a DNA fluorescence quantitation kit.

Conclusions and Future Directions:

In summary, contrary to our original hypothesis that the c-Src inhibitor PP2 could act with E_2 to additively or synergistically block growth of advanced estrogen deprivation-resistant breast cancer cells growth, long-term treatment with PP2 plus E_2 actually blocked apoptosis and the resulting cell line (MCF-7:PF) was unique, as they grew vigorously in culture with physiological levels of E_2, which could be blocked by the pure antiestrogen ICI 182,780**.** The mechanistic change underlying the action of combination treatment was that the c-Src inhibitor could block apoptosis induced by E_2 and collaborate with E_2 to up-regulate endogenous ERα target genes and IGF-1Rβ. The inhibitor of IGF-1Rβ could completely block stimulation induced by E_2 which also confirmed that IGF-1Rβ played a critical role in this combination treated cell line. These data illustrate that caution must be exercised when considering the evaluation of c-Src inhibitors in clinical trial following the development of acquired resistance to aromatase inhibitors, especially in a combination with physiological levels of E_2.

The c-Src inhibitors have been used in clinical trials. However, if we validate that c-Src inhibitor reverse E_2-induced apoptosis in 3D cell culture and xenograft model experiments, these results may have important clinical implications for appropriately utilizing c-Src inhibitors in Phase II (advanced) antihormone-resistant breast cancers.

We will investigate mechanisms underlying c-Src inhibition in converting responses to E_2 from apoptosis to growth. Our results provide evidence that E_2-induced apoptosis utilize c-Src tyrosine kinase. It is important to find the precise target site by the c-Src inhibitor in the pathways of E_2-induced apoptosis which will further help us to find the mechanisms underlying the E_2-induced apoptosis. Our data indicated that estrogen acted as a normal transcriptional activator in MCF-7:5C cells as in wild-type MCF-7 cells after 24 hour treatment. Various methods demonstrated that E_2-induced apoptosis happened after 72 hours treatment. It is very possible that the c-Src inhibitor blocks the E_2-activated apoptosis related pathways to prevent apoptosis.

As in Task 4, we will use Agilent microarrays and RNAseq to analyze genome-wide changes in gene expression in E_2 plus PP2-treated MCF-7:5C cells compared to vehicle treated, PP2 or E_2 monotherapy MCF-7:5C cells. This will allow identification of a gene signature and biomarkers that could be used to decipher which patient's disease could effectively be treated with c-Src inhibitors. Furthermore, we will functionally validate the involvement of the identified differentially expressed genes in mediating growth responses of the E_2 plus PP2-treated MCF-7:5C cells. Finally, we will find the precise target site of c-Src inhibitor in the process of E_2-induced apoptosis.

TASK 2. GU/Jordan - To elucidate the molecular mechanism of E_2 induced survival and apoptosis in breast cancer cells resistant to either SERMs or long-term estrogen deprivation.

Task 2b-2: Sengupta and Jordan – To confirm and validate developing pathways of E_2-induced breast cancer cell survival and apoptosis.

Task 2b-2 (Sengupta and Jordan) - Studies carried out by Dr. Surojeet Sengupta in the Jordan laboratory at Georgetown University

The Role of Liganded Estrogen Receptor Conformation in Inducing Apoptosis of Estrogen Deprivation-Resistant, MCF7:5C Breast Cancer Cells

Introduction:

High dose estrogen therapy for breast cancer treatment is considered the first chemical therapy to successfully treat any type of cancer (8). Thirty percent patients respond to estrogen therapy (9) and recent clinical trials have confirmed that low dose of estrogen is equally effective in treating the breast cancers as high dose (2). Also, a recent analysis of women treated with estrogen replacement therapy (ERT) in the *Women's Health Initiative* (WHI) double blind, placebo-controlled randomized trial in postmenopausal hysterectomized women revealed a decrease in invasive breast cancer, which was sustained even 5 years after ERT was stopped (10). All these clinical data have established an undisputed clinical benefit of estrogen therapy in breast cancer patients and a possible role in prevention of breast cancers in postmenopausal women (11). However, the precise molecular mechanism(s) by which the paradoxical action of estrogen manifests its therapeutic efficacy are unknown. Previous studies from our laboratory have reported that low concetration of estrogen can induce apoptosis *in vitro* and *in vivo* in MCF7:5C breast cancer cells which are resistant to estrogen deprivation (1, 12). Estrogen receptor α can be activated with various ligands which can be broadly classified as planar (type I) or non-planar (type II) estrogens (13, 14). Here, we have used MCF7:5C cells and planar (type I) and non-planar (type II) estrogens to test the hypothesis that the conformation of the liganded-estrogen receptor alpha is critical in inducing estrogen-induced apoptosis.

WORK ACCOMPLISHED:

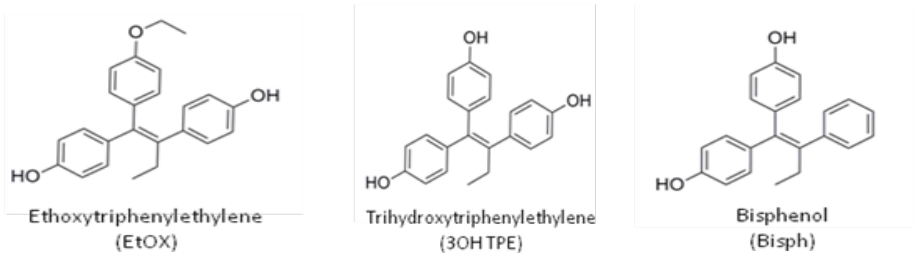
Triphenylethylenes induce proliferation of MCF7:WS8 cells but do not induce effective apoptosis in MCF7:5C cells

To study the biological activity of the triphenylethylenes namely, EtOX (ethoxytriphenylethylene), 3OH TPE (trihydroxytriphenylethylene) and Bisph (bisphenol) (Class II estrogens; Figure 8A) which are the ligands of ER and have been previously reported to act as estrogens (13), we tested their ability to induce cell proliferation in parental MCF7:WS8 cells. As controls we also used active metabolites of tamoxifen, 4OHT (4-hydroxy tamoxifen) and Endox (endoxifen) (Figure 8B) which are known anti-estrogens because of their alkylaminoethoxy side chain. The cells were seeded in 24 well plates and treated with different

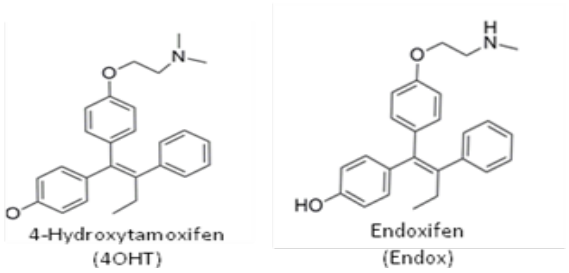
concentration of the compounds over six days and the DNA was measured in each well using a fluoroscent dye. All the triphenylethylenes tested were able to induce cell growth of MCF7:WS8 cells to the maximum level as E_2 (17-beta estradiol), although their agonistic potency was less than E_2 (Figure 9A). EtOX, 3OH TPE and Bisph all induced cell proliferation in a dose dependent manner with maximum stimulation at 1-10 nM as compared to 0.01 nM for E_2. Nonetheless, all of these triphenyethylenes were potent estrogen-agonists in this assay. On the other hand, as expected, the active metabolites of tamoxifen, 4OHT and Endox which are antiestrogens did not induce cell growth of MCF7:WS8 cells.

Figure 8

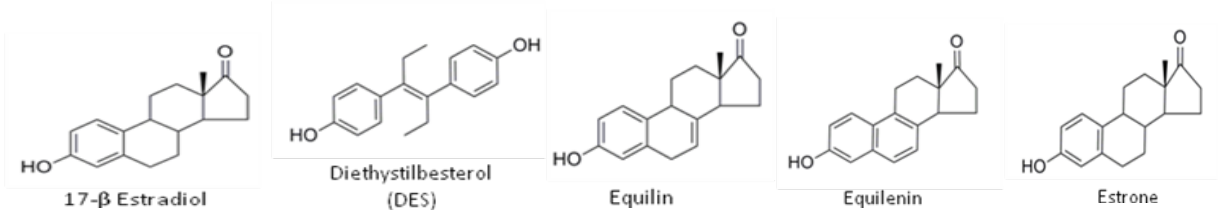
(A)



(B)



(C)



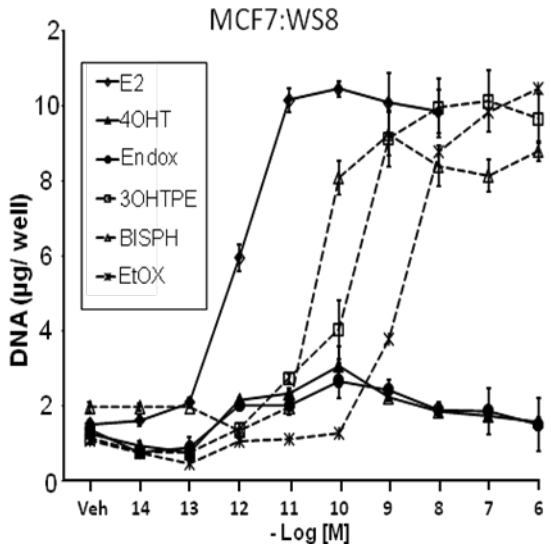
<u>Figure 8.</u> Structure of the compounds used in the experiments. (A) Different Triphenylethylenes. **(B)** Active metabolites of Tamoxifen drug. **(C)** Different Class I estrogens.

Next, we tested if these compounds were able to induce apoptosis in estrogen-deprivation resistant MCF7:5C breast cancer cells as effectively as E_2 induces apoptosis in these cells.

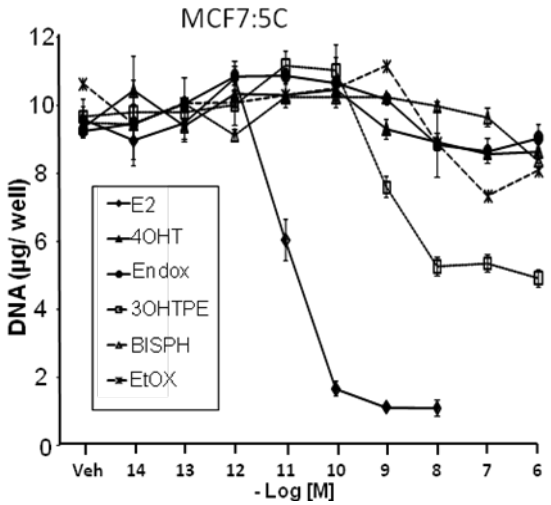
Interestingly, the triphenylethylenes were very ineffective in inducing apoptosis in MCF7:5C cells as compared to E_2 even at higher concentrations (Figure 9B). Compared to E_2, EtOX and Bisph did not show any effective apoptosis even at micro-molar concetration and were comparable to that of 4OHT and Endox which are active metabolites of tamoxifen and known anti-estrogens. However, 3OH TPE was able to induce apoptosis around 50% as comapred to E_2 at higher concentration. E_2, on t he other hand was very effective in inducing apoptosis and achieved maximal apotosis at 0.1 nM concentration. To further investigate the hypothesis that planar and non-planar estrogens may have different abilities to induce apoptosis in MCF7:5C cells we studied the effectiveness of various other planar estrogens namely DES (diethylstibesterol), equilin, equilenin and estrone (Figure 8C) for their ability to induce apoptosis in MCF7:5C cells over a range of concentrations and compared to E_2. All these planar estrogens were able to induce apoptosis as effectively as E_2 (Figure 9C). All the planar estrogens achieved maximal apoptosis in the range of 1-10 nM as compared to E_2 which achieved maximal apoptosis at 0.1 nM. These results strengthened our hypothesis that both planar (Class I) and non-planar (Class II) estrogens function as estrogen agonists in stimulating the cell growth of MCF7:WS8 cells but differ in their action in inducing apoptosis in MCF7:5C cells as all non-planar estrogen tested were ineffective in inducing apoptosis.

Figure 9

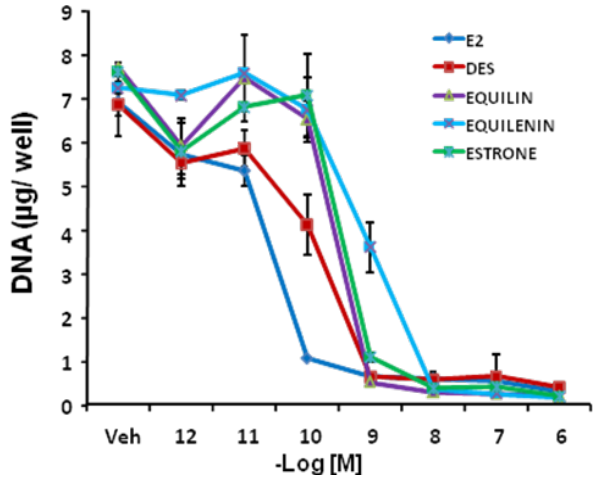
(A)



(B)



(C)



<u>Figure 9.</u> Effect of triphenylethylenes on E_2 induced growth in MCF7:WS8 cells and E_2 induced apoptosis in MCF7:5C cells. **(A)** MCF7:WS8 cells were seeded in 24-well plate and treated with indicated compounds over a range of doses for six days. Cell growth was assessed as DNA content in each well. **(B)** MCF7:5C cells were seeded in 24 well plates and treated with indicated compounds over a range of doses and the extent of apoptosis was determined by measuring the DNA content of the remaining cells in each well. **(C)** MCF7:5C were seeded in 24 well plate and treated with the indicated planar estrogens at various doses and the extent of apoptosis was determined by measuring the DNA content of the remaining cells in each well. Each data point shown is average of 3 replicate +/- SD.

Triphenylethylenes reverses E_2-induced apoptosis in MCF7:5C cells

Since the non-planar triphenylethylenes (3OHTPE, Bisph and EtOX) were not able to induce apoptosis effectively as E_2 and other planar estrogens in MCF7:5C cells we further investigated if the non-planar estrogens were able to block the E_2-induced apoptosis in these cells and function as an estrogen-antagonist in these cells. As evidenced in Figure 3, all the non-planar estrogens were able to reverse the E_2-induced apoptosis in MCF7:5C cells in a dose dependent manner. As expected metabolites of tamoxifen, 4OHT and Endox and the complete estrogen antagonist ICI (ICI 182,780) were also able to completely reverse the E_2-induced apoptosis at 0.1 micro-molar concentration. At 1 micro-molar concentration ICI alone as well as in combination with E_2 was able to block the growth of the cells. Among the triphenylethylenes, Bisph was most potent is reversing the E_2-induced apoptosis in MCF7:5C cells followed by 3OHTPE and EtOX. As noted before the compounds alone did not induce effective apoptosis at 1 micro molar concentration (Figure 10). This data suggests that the triphenylethylenes (non-planar estrogens) function as an estrogen antagonist in MCF7:5C cells apoptosis assay.

Figure 10

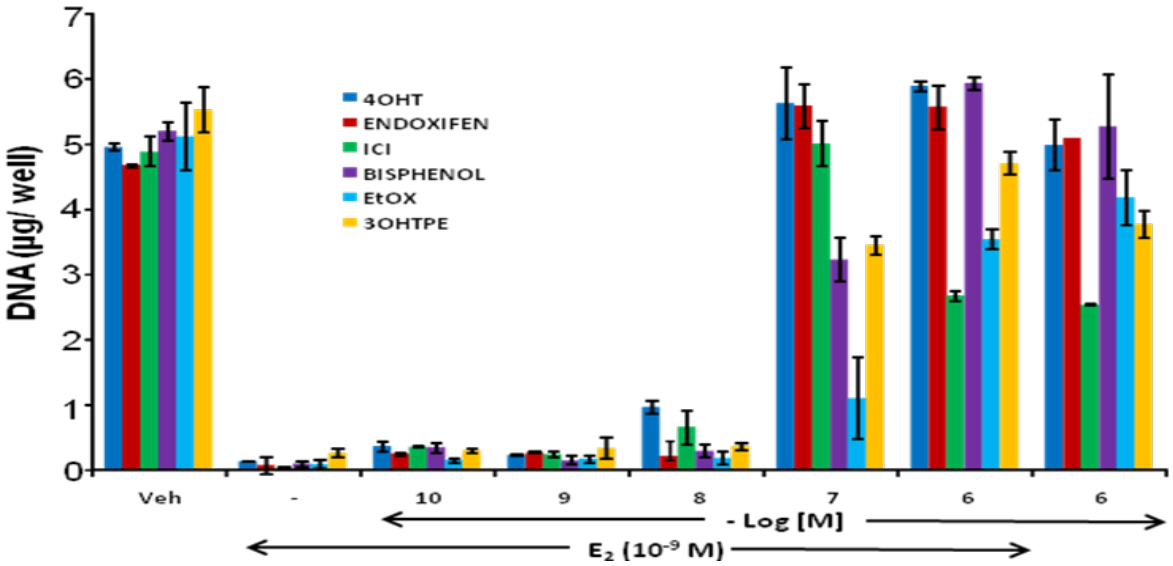


Figure 10. Reversal of E_2-induced apoptosis of MCF7:5C breast cancer cells by triphenylethylenes (non-planar estrogens). MCF7:5C cells were seeded in 24 well plate and treated with 10^{-9}M 17-β estradiol (E2) in presence of increasing concentration of indicated non-planar estrogens, 4-hydroxy tamoxifen (4OHT), endoxifen or ICI 182,780 (ICI). Cells were also treated with either vehicle, E_2 alone or 10^{-6}M concentration of compounds alone as controls.

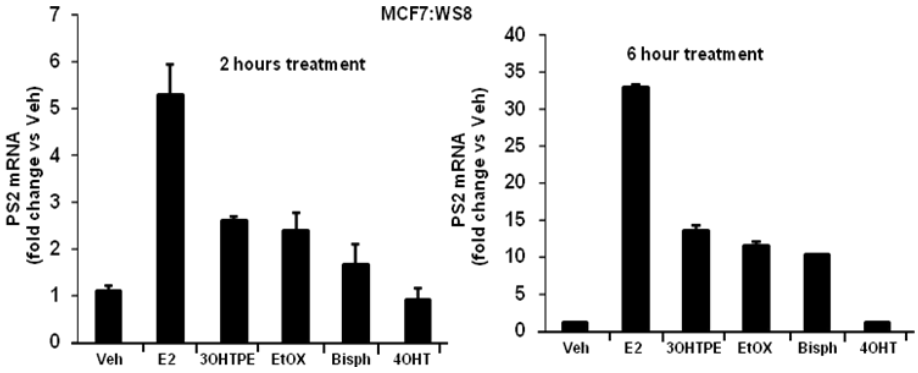
Regulation of estrogen-responsive gene PS2 (TFF1) in MCF7:WS8 and MCF7:5C cells by triphenylethylenes

We further investigated the estrogen response in MCF7:WS8 and MCF7:5C cells at gene level to determine if there were any differences. We chose the gene PS2 (also known as TFF1) which is a very well characterized estrogen-responsive gene (15). PS2 gene is a primary estrogen-responsive gene with a classical estrogen responsive element (ERE) in the proximal

promoter of the gene which is responsible for its estrogen response (16). Therefore, we treated MCF7:WS8 and MCF7:5C cells for 2 or 6 hrs with vehicle (Veh), E_2 (10^{-9}M), 3OHTPE (10^{-6}M), EtOX(10^{-6}M), Bisph (10^{-6}M) or 4OHT (10^{-6}M) and harvested RNA from all the samples. One microgram of total RNA was reverse transcribed to cDNA and q-RTPCR (quantitative real time polymerase chain reaction) was performed using PS2 specific primers. The house keeping gene, 36B4 was used as an internal control and delta-delta Ct method was used to calculate the relative gene expression compared to vehicle treated cells. PS2 gene was stimulated ~ 5 fold by E_2 as expected, in MCF7:WS8 cells after 2 hrs of treatment and more than 30 fold after 6 hrs of treatment (Figure 11A). In contrast 4OHT did not stimulate PS2 gene expression after 2 or 6 hrs of treatment (Figure 11A), whereas all the triphenylethylenes were around 50% as effective as E_2 in MCF7:WS8 cells at both 2 and 6 hrs after treatment (Figure 11A). In case of MCF7:5C cells E_2 was markedly less effective in stimulating PS2 gene after 2 and 6 hrs of treatment (Figure 11B) as only ~4 fold stimulation was observed after 6 hrs. The MCF7:5C cells treated with triphenylethylenes showed did not show any significant increase in PS2 levels after 2 hrs of treatment and about two fold increase after 6 hrs treatment (Figure 11B), whereas 4OHT did not show any increase in PS2 levels at 2 or 6 hrs of treatment.

Figure 11

(A)



(B)

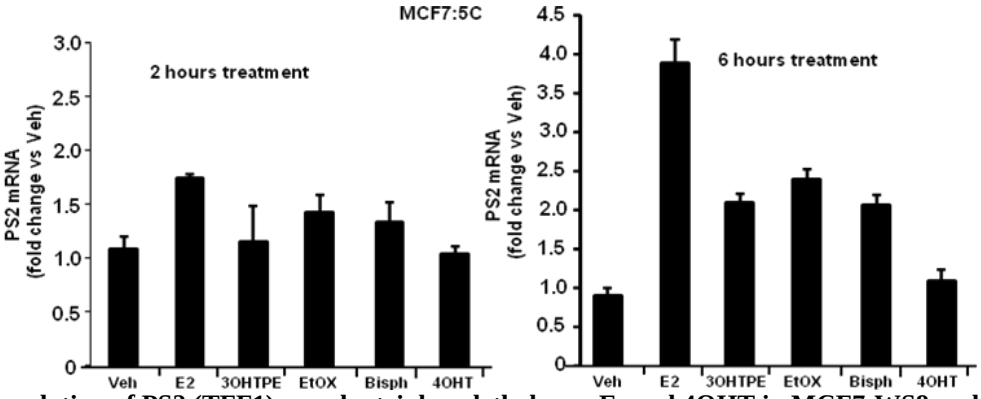


Figure 11. Regulation of PS2 (TFF1) gene by triphenylethylenes, E_2 and 4OHT in MCF7:WS8 and MCF7:5C cells. **(A)** MCF7:WS8 cells were treated with 17-β estradiol (10^{-9}M; E_2), 3-hydroxytriphenylethylene (10^{-6}M; 3OH TPE), ethoxytriphenylethylene (10^{-6}M; EtOX), bisphenol (10^{-6}M; Bisph) and 4-hydroxy tamoxifen (10^{-6}M; 4OHT) for 2 hours or 6 hours. Cells were then harvested and RNA was isolated followed by cDNA synthesis. Expression level of PS2 (TFF1) was assessed using quantitative real time PCR (ABI 7900 HT). Data is represented as fold difference versus vehicle (Veh) treated cells. **(B)** MCF7:5C cells were treated with 17-β estradiol (10^{-9}M; E_2), 3-hydroxytriphenylethylene (10^{-6}M; 3OH TPE), ethoxytriphenylethylene (10^{-6}M; EtOX), bisphenol (10^{-6}M; Bisph) and 4-hydroxy tamoxifen (10^{-6}M; 4OHT) for 2 hours or 6 hours. Expression level of PS2 was assessed identically as mentioned for MCF7:WS8 cells. All data points are average of three replicates +/- S.D.

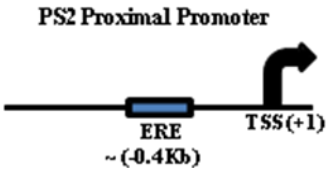
Recruitment of ERα (estrogen receptor α) and SRC3 (steroid co-activator-3) at the proximal promoter of PS2 gene after treatment with triphenylethylenes

To further understand the molecular mechanisms involved in regulation of estrogen-responsive gene PS2 by the triphenylethylenes in MCF7:WS8 and MCF7:5C cells we determined the recruitment of the ERα and SRC-3 protein at the proximal promoter of PS2 gene, which has a classical estrogen responsive element (Figure 12A), using ChIP (chromatin immuno-precipitation) assay after 45 minutes of treatment with triphenylethylenes (10^{-6}M) and compared it with E_2 (10^{-9}M) and 4OHT (10^{-6}M). In MCF7:WS8 cells, E_2 treatment (45 min) was able to recruit very high level of ERα at the PS2 promoter (Figure 12B) as assessed by ChIP assay where more than 8% of input PS2 promoter region was occupied by ERα. On the other hand triphenylethylenes were ~50% as efficient as E_2 treatment in terms of recruiting ERα where as very low level (~20% of E_2) of ERα recruitment was observed after 4OHT treatment. Recruitment of the co-activator SRC3, which is critical in inducing the estrogen responsive gene, was not observed at all after 4OHT treatment at the PS2 promoter (Figure 12B). All the triphenylethylenes tested recruited only about 15-20% of SRC3 as compared to E_2 treatment, which showed around 0.9 % of input PS2 promoter region was occupied by SRC3 protein (Figure 12A). Interestingly, in MCF7:5C cells treated with E_2, around 5% of input PS2 promoter region was occupied by ERα (Figure 12C), which was half as much as observed in MCF7:WS8 cells under identical conditions. SRC3 recruitment was also markedly less (~25%) at the PS2 promoter in MCF7:5C cells (Figure 12C) as compared to MCF7:WS8 cells. In MCF7:5C cells treated with triphenylethylenes for 45 minutes around 50% less ERα occupancy and ~80% less

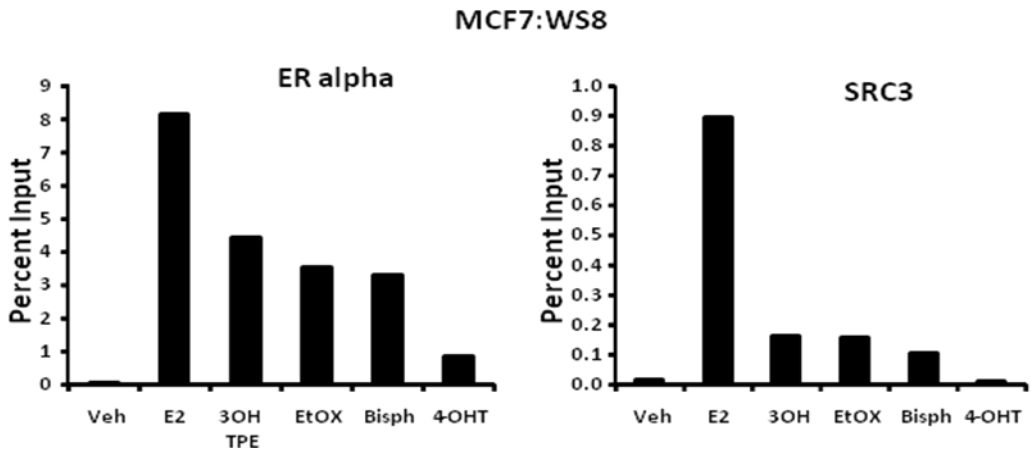
SRC3 occupancy was observed as compared to E_2 treatment in MCF7:5C cells, whereas no SRC3 recruitment was observed after 4OHT treatment. These ChIP data concurs with the PS2 mRNA induction level in MCF7:WS8 and MCF7:5C cells with their respective treatments (Figure 11A and B) and suggests that treatment with triphenylethylenes (non-planar estrogens) in these cells influences the shape of the liganded-ERα complex such that efficiency of ERα binding to ERE region is moderately inhibited whereas binding of SRC3 is severely inhibited as compared to 17β-estradiol treatment which is a planar estrogen. Additionally, of notable importance is that the magnitude of SRC3 recruitment is far less in MCF7:5C cells than MCF7:WS8 cells which may play crucial role in manifesting the functional role of the triphenylethylenes in these cells.

Figure 12

(A)



(B)



(C)

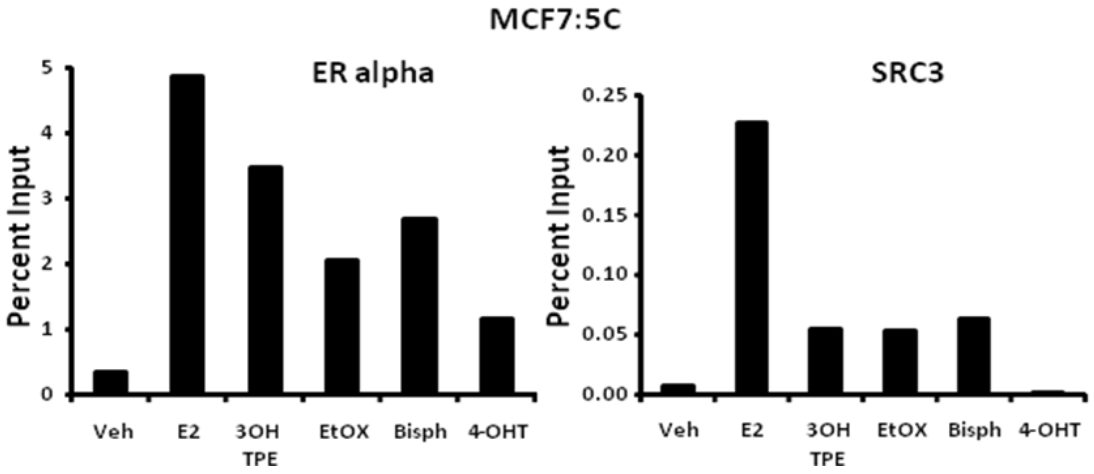


Figure 12. Recruitment of ER alpha and SRC3 (AIB1) at PS2 proximal promoter region containing ERE in MCF7:WS8 and MCF7:5C cells. (A) Depiction of PS2 proximal promoter region and the ERE region relative to TSS (transcription start site). **(B)** MCF7:WS8 cells treated for 45 minutes with 17-β estradiol (10^{-9}M; E_2), 3-hydroxytriphenylethylene (10^{-6}M; 3OH TPE), ethoxytriphenylethylene (10^{-6}M; EtOX), bisphenol (10^{-6}M; Bisph) and 4-hydroxy tamoxifen (10^{-6}M; 4OHT) and ChIP (chromatin immuno-precipitation) assay was performed. Formaldehyde cross-linked and sonicated chromatin was immuno-precipitated using anti ER alpha antibody or SRC-3 (AIB1) antibody. The chromatin was pull down using magnetic beads, reverse cross-linked and DNA was isolated. Isolated DNA was used to amplify the PS2 promoter region by quantitative real time PCR using specific primers to assess enrichment of this region in the pull down. Data is represented as percent input of the starting chromatin used for the ChIP. **(C)** MCF7:5C cells were treated identically as mentioned above and ChIP assay was performed under identical conditions. Data is represented as percent input of the starting chromatin used for the ChIP.

Differential induction of TGFα (transforming growth factor beta) gene by planar and non-planar estrogens (triphenylethylenes) in MDA: MB-231 cells stably transfected with wild type ERα or D351G mutant ERα.

Previous studies from our laboratory has shown that aspartate amino acid at 351 position of ERα plays a critical role in manifestation of estrogenic property of 4-OHT (16, 17). TGFα gene is induced by 4OHT as well as 17β-estradiol (E_2) in MDA:MB-231 cells stably transfected with wild type ERα (MC2 cells) whereas in MDA:MB-231 cells stably transfected with a mutant ERα (JM6 cells), where aspartate at 351 amino acid position is substituted with glycine (D351G), 4OHT fails to induce expression of TGFα gene but E_2 retains its ability to induce the TGFα gene in these cells (16). We therefore used this assay system to interrogate if the triphenylethylenes (3OHTPE, EtOX and Bisph) resembled E_2 or 4OHT in inducing the TGFα gene expression. As expected, all the planar estrogens (E_2, DES, estrone, equilin and equilenin) were able to induce TGFα gene expression (Figure 13A and B) in a concentration dependent manner in both wild type ERα (MC2) and D351G mutant ERα (JM6) cells. On the other hand, the triphenylethylenes (non-planar estrogens), 4OHT and Endox were able to induce TGFα gene expression in MC2 cells (wild type ERα; Figure 13C) in a concentration dependent manner as potently as E_2 but all the triphenylethylenes and the active metabolites of tamoxifen (4OHT and Endox) distinctly failed to induce TGFα gene expression (Figure 13D) in JM6 cells expresses

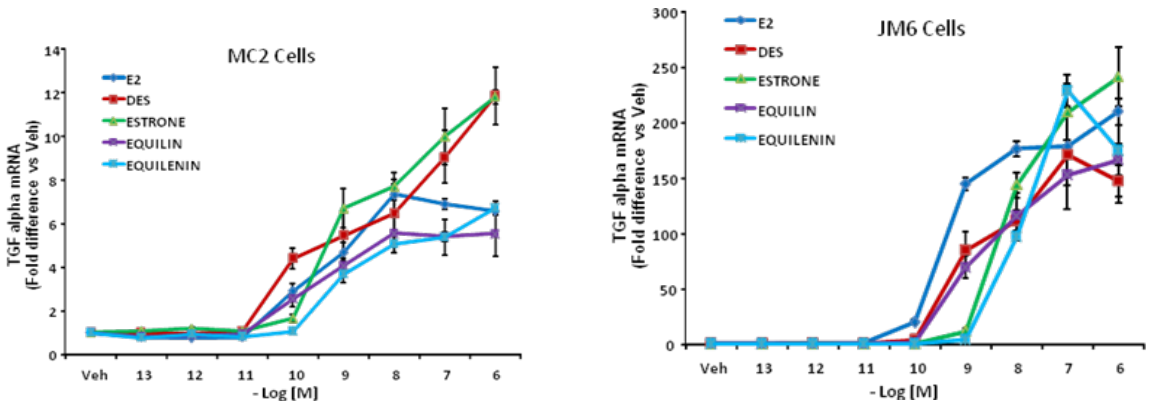
D351G mutant form of the ERα. Notably, in the same experiment E_2 was able to induce TGFα gene expression in JM6 cells. These data clearly indicate that the triphenylethylenes binds with ERα in a manner which is distinctly different from E_2 and other planar estrogens and strikingly resembles the 4OHT and Endox.

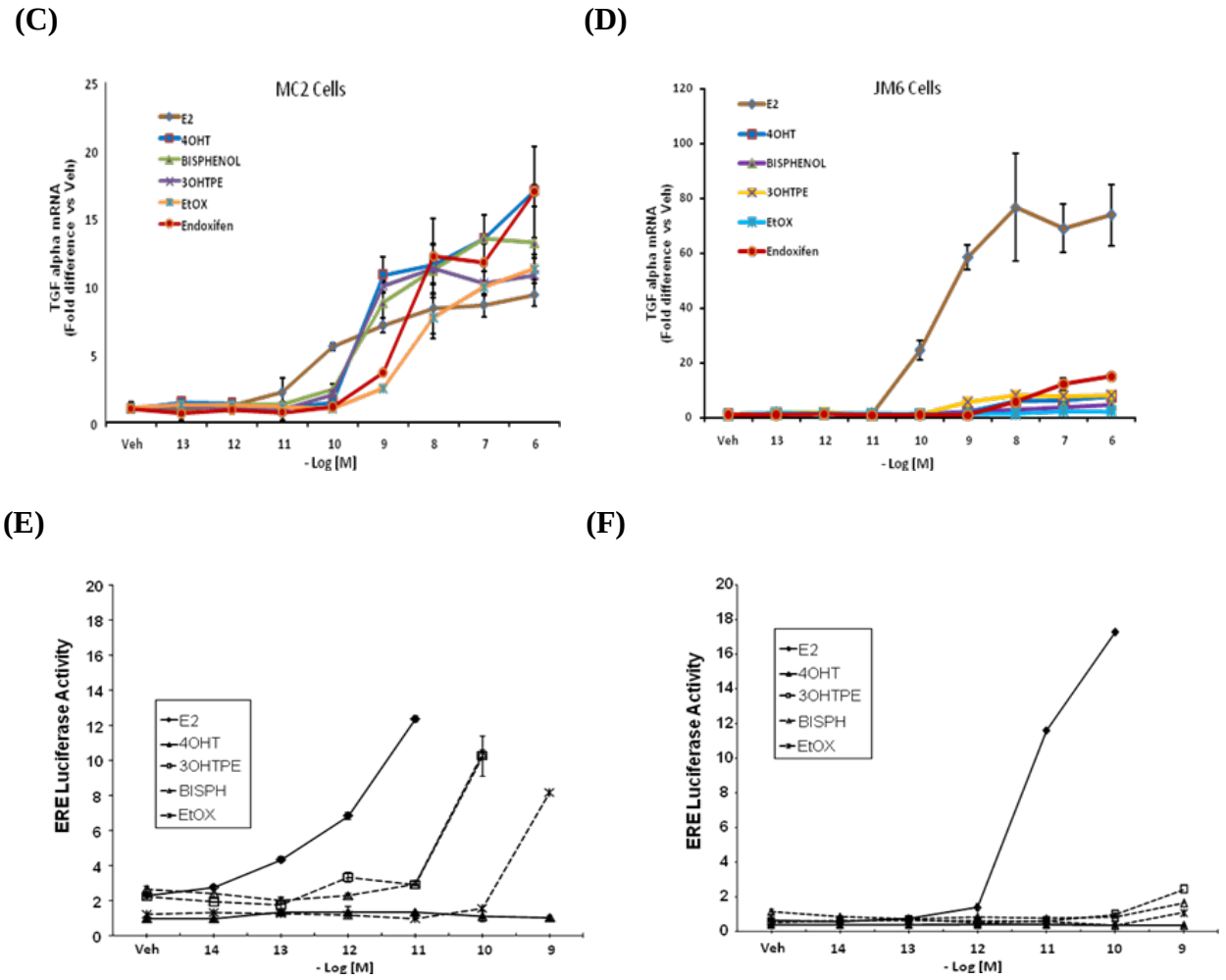
Differential induction of 5X-ERE luciferase by planar and non-planar estrogens (triphenylethylenes) in ERα-negative T47D cells (C42 cells) transiently transfected with wild type or D351G mutant ERα.

We further investigated the ability of planar and non-planar estrogens to induce the expression of luciferase enzyme driven by five repeats of classical estrogen responsive elements (5XERE) by reporter assay. We used an ERα-negative T47D cell line (C42 cells) to transiently transfect with either wild type ERα or D351G mutant ERα plasmid along with 5XERE-luciferase plasmid and renilla luciferase plasmid for normalization of transfection. Subsequently cells were treated with either vehicle or E_2, 4OHT, 3OHTPE, EtOX and Bisph at indicated concentrations for 24 hr s. Using the dual luciferase assay, activity from the 5XERE-firefly-luciferase was assessed and normalized by renilla-luciferase activity. All the compounds with the exception of 4OHT, was able to induce the luciferase activity in the cells transfected with wild type ERα (Figure 13E). However, the potency of the compounds was different. As evident, E_2 was most potent, (as it was able to induce ERE activity at lower concentrations) followed by Bisph and 3OHTPE which was equally potent in inducing ERE activity and the least potent was EtOX. Interestingly, in the C42 cells transfected with mutant (D351G) ERα only E_2 was able to induce ERE activity as all the triphenylethylenes and 4OHT failed to induce luciferase activity from the classical ERE. This further provided evidence that the triphenylethylenes which are non-planar estrogens may have distinctly dissimilar mode of manifesting its estrogenic properties, than the planar estrogens.

Figure 13

(A) **(B)**





<u>Figure 13</u>. Induction of TGFα gene by planar and non-planar estrogens (triphenylethylenes) in MDA:MB 231 cells stably transfected with wild type ERα (MC2) or D351G mutant ERα (JM6) and induction of ERE-luciferase by wild type ERα or D351G mutant ERα in ERα-negative T47D cells (C42). (A) MC2 cells were treated with planar estrogens for 48 hrs at indicated concentrations and expression of TGFα RNA was measured using quantitative real time PCR. **(B)** JM6 cells were treated with planar estrogens for 48 hrs at indicated concentrations and expression of TGFα RNA was measured using quantitative real time PCR. **(C)** MC2 cells were treated with E_2 or non-planar estrogens (triphenyl ethylenes) or active metabolites of tamoxifen (4OHT and Endox) for 48 hrs at indicated concentrations and expression of TGFα RNA was measured using quantitative real time PCR. **(D)** JM6 cells were treated with E_2 or non-planar estrogens (triphenylethylenes) or active metabolites of tamoxifen (4OHT and Endox) for 48 hrs at indicated concentrations and expression of TGFα RNA was measured using quantitative real time PCR. Data **(A-D)** are represented as fold difference versus vehicle treated cells. Each data point is average +/- SD of three replicates. **(E)** C42 cells were transiently transfected with 5XERE-firefly-luciferase, wild type ERα and renilla-luciferase plasmids. Transfected cells were treated with indicated compounds over a range of concentrations for 24 hrs and luciferase activity was measured. **(F)** C42 cells were transiently transfected with 5XERE-firefly-luciferase, D351G ERα and renilla-luciferase plasmids. Transfected cells were treated with indicated compounds over a range of concentrations for 24 hrs and luciferase activity was measured. Data are represented as ratio of enzymatic activity of firefly-luciferase and renilla-luciferase.

Figure 14

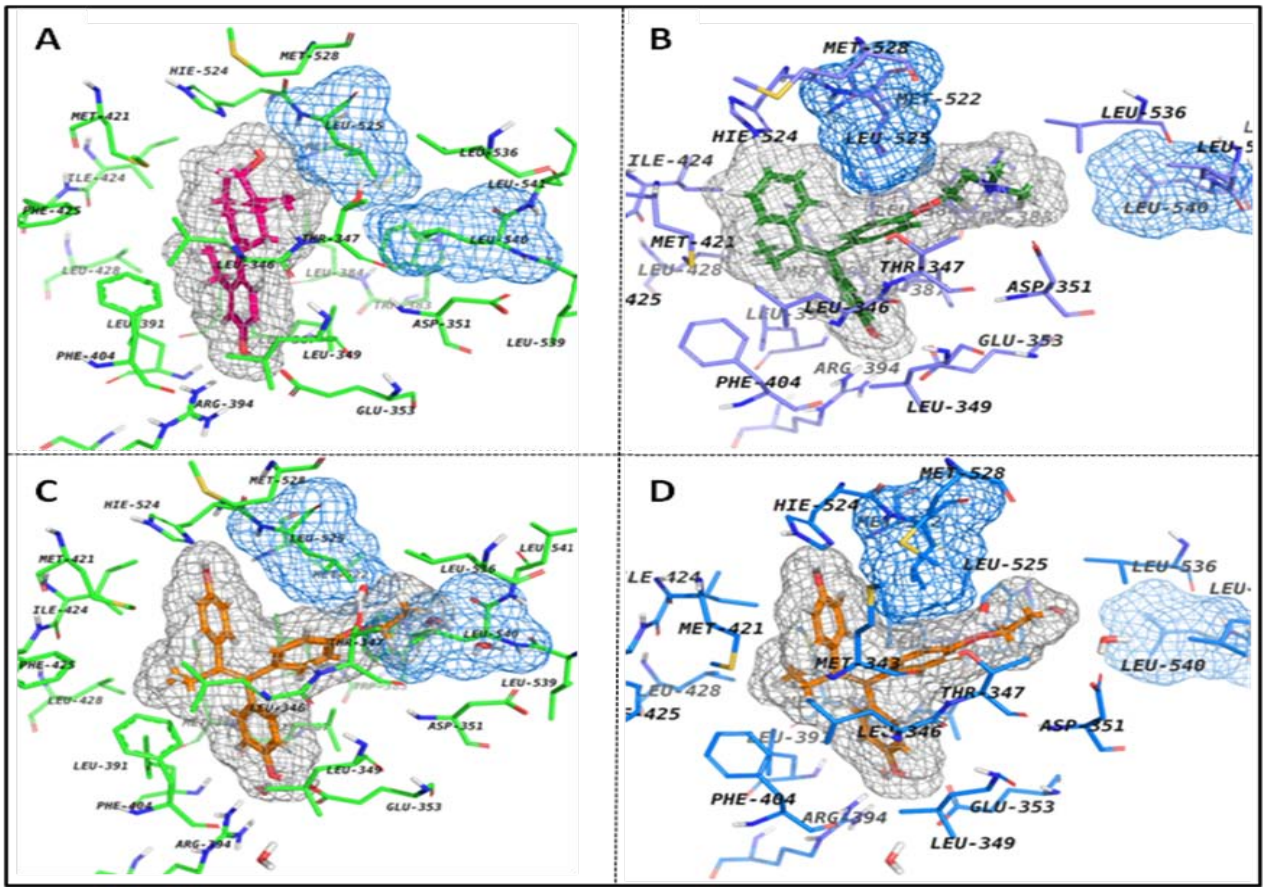


Figure 14. ERalpha binding site presented with E_2, 4OHT or EtOX. All ligands are shown with their corresponding molecular surfaces depicted as gray grids. Also, Leu525 and Leu540 are shown with their molecular surface depicted as blue grids. **A)** The agonist conformation of ERalpha co-crystallized with E_2 (colored in magenta) (PDB code: 1GWR); **B)** 4OHT (depicted in green) co-crystallized with ERalpha - the antagonist conformation of the receptor (PDB code: 3ERT); **C)** EtOX (colored in orange) is superimposed in the agonist conformation of the receptor (PDB code: 1GWR) and **D)** same ligand is docked in the antagonist conformation of ERalpha (3ERT).

Binding of EtOX to the LBD of ER alpha

In an attempt to understand the binding mode of the triphenylethylenes, we studied the binding of EtOX to ERα, the flexible docking of this compound into the LBD (ligand binding domain) of the receptor co-crystallized with 4OHT (Figure 14B) was performed and also, the best ranked ligand-receptor complex was superimposed onto the agonist conformation of ERα (Figure 14A). The results show that when EtOX is fitted in the binding site of the agonist conformation of ERα (1gwr) the ethoxy side chain of the ligand is bumping the side chains of L525 and L540 (Figure 14C) and due to its steric hindrance it is unlikely for the ligand to bind in this conformation of the receptor. In contrast, when EtOX is docked into the binding site of ERα

antagonist conformation (Figure 14D) the top ranked pose is fitted well in the binding cavity and therefore it strongly indicates that it binds to an antagonist-related conformation of the receptor.

TASK 2. GU/Jordan - To elucidate the molecular mechanism of E_2 induced survival and apoptosis in breast cancer cells resistant to either SERMs or long-term estrogen deprivation.

Task 2b-3: Lewis-Wambi and Jordan – Evaluation of a new SERM, bazedoxifene, that is cytotoxic to antihormone resistant breast cancer cells.

Task 2b-3 (Lewis-Wambi and Jordan) - Studies carried out by Dr. Lewis-Wambi at FCCC

WORK ACCOMPLISHED:

Our laboratory is also interested in studying the antitumor effects of the SERM BZA (bazedoxifene). BZA is a third generation SERM that was recently approved for the prevention and treatment of postmenopausal osteoporosis. It has antitumor activity; however, its mechanism of action remains largely unclear. Recently, we characterized the effects of BZA and several other SERMs on the proliferation of hormone-dependent MCF-7 and T47D breast cancer cells and hormone-independent MCF-7:5C and MCF-7:2A cells and examined their mechanism of action in these cells. We found that all of the SERMs inhibited the growth of MCF-7 and T47D cells, however, BZA was the only SERM that inhibited the growth of hormone-independent MCF-7:5C and MCF-7:2A cells (Figure 15) (see #18 in Appendix). Consistent with these growth results, we found that BZA induced G1 blockade in MCF-7:5C and MCF-7:2A cells and it significantly downregulated ERα and cyclin D1 which were constitutively overexpressed in these cells (Figure 16) (see #18 in Appendix). In addition, siRNA knockdown of ERα and/or cyclin D1 significantly reduced the inhibitory effect of BZA in MCF-7:5C cells. Further analysis revealed that BZA downregulated ERα protein by increasing its degradation and it suppressed cyclin D1 protein and promoter activity in MCF-7:5C cells (Figure 16) (see #18 in Appendix). Lastly, molecular modeling studies demonstrated that BZA bound to ERα in an orientation similar to raloxifene and had the tendency to form the same contacts with the aminoacids lining the binding cavity (Figure 17) (see #18 in Appendix).

The manuscript entitled "The Selective Estrogen Receptor Modulator Bazedoxifene Inhibits Hormone-Independent Breast Cancer Cell Growth and Downregulates Estrogen Receptor α and Cyclin D1" is under consideration in *Molecular Pharmacology* and cited as paper #18 in the Reportable Outcomes and Appendix sections.

Figure 15:

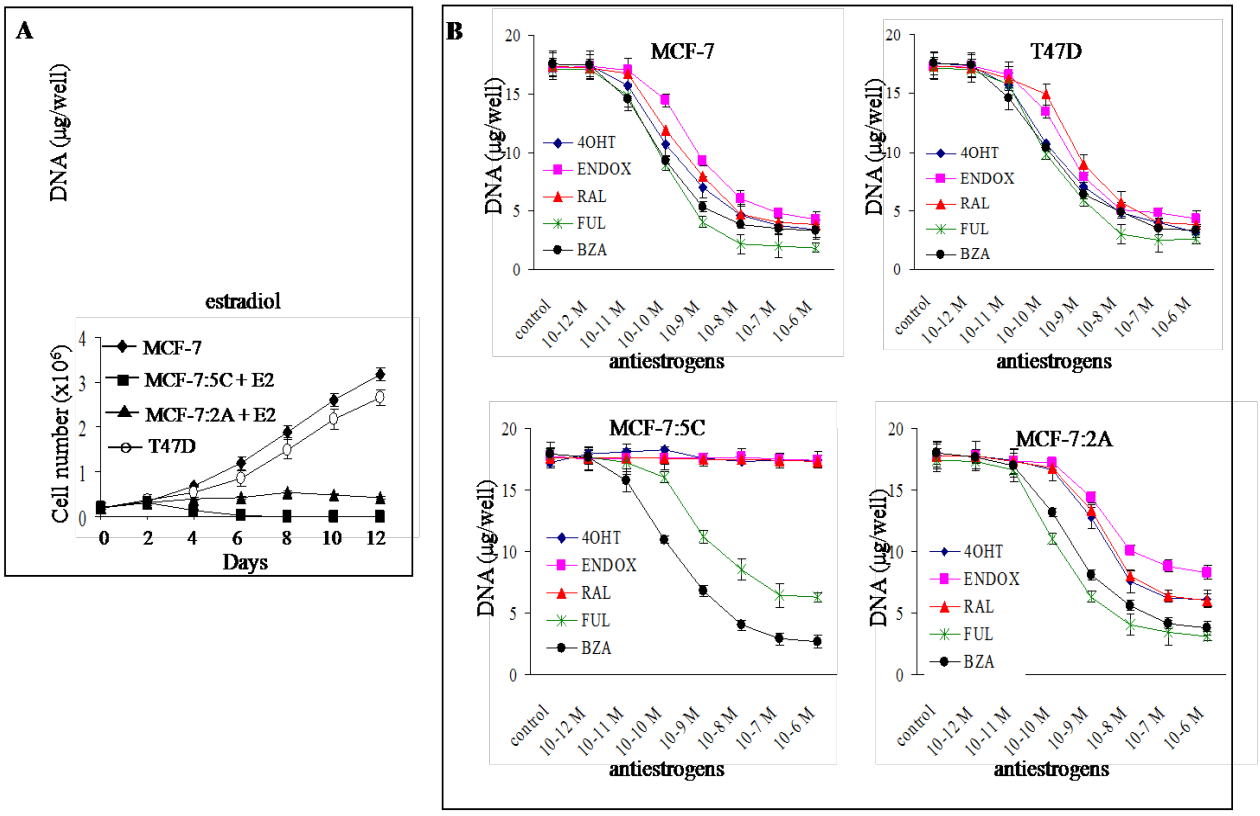


Figure 15: Effects of E_2 and SERMs on the growth of hormone-dependent MCF-7 and T47D cells versus hormone-independent MCF-7:5C and MCF-7:2A cells. **A**, MCF-7 and T47D cells were grown in phenol red-free RPMI medium supplemented with 10% charcoal stripped FBS for 3 days prior to the start of the experiment. On the day of the experiment, all cell lines were seeded in phenol red-free RPMI medium supplemented with 10% charcoal stripped FBS at 30,000 per well in 24-well dishes and after 24 h were treated with 10^{-14} to 10^{-8} M E2 for 7 days, with retreatment every other day. At the conclusion of the experiment, cells were harvested and proliferation was assessed as cellular DNA mass (µg/well) using a DNA quantitation kit. The effect of E_2 on proliferation of the different cell lines over a 12-day period was also determined by cell counting. **B**, the effects of antihormones at inhibiting E_2-stimulated growth in MCF-7 and T47D cells and hormone-independent growth in MCF-7:5C and MCF-7:2A cells. Cells were seeded as described above except MCF-7 and T47D cells were grown in fully estrogenized media and then treated with 10^{-12} M to 10^{-6} M fulvestrant (FUL), bazedoxifene (BZA), raloxifene (RAL), 4-hydroxytamoxifen (4OHT), or endoxifen (ENDOX) for 7 days with retreatment on alternate days. Proliferation was assessed as cellular DNA mass (µg/well) as described in the methods section. **C**, effects of SERMs on reversing E_2-induced growth inhibition of hormone-independent MCF-7:5C cells. Cells were seeded as described above and then treated with 10^{-9} M E_2 alone or E_2 combined with increasing concentrations (10^{-12} M to 10^{-6} M) of BZA, RAL, 4OHT, or ENDOX for 7 days and processed as described above. All data are presented as the mean from three different experiments in triplicate.

Figure 16:

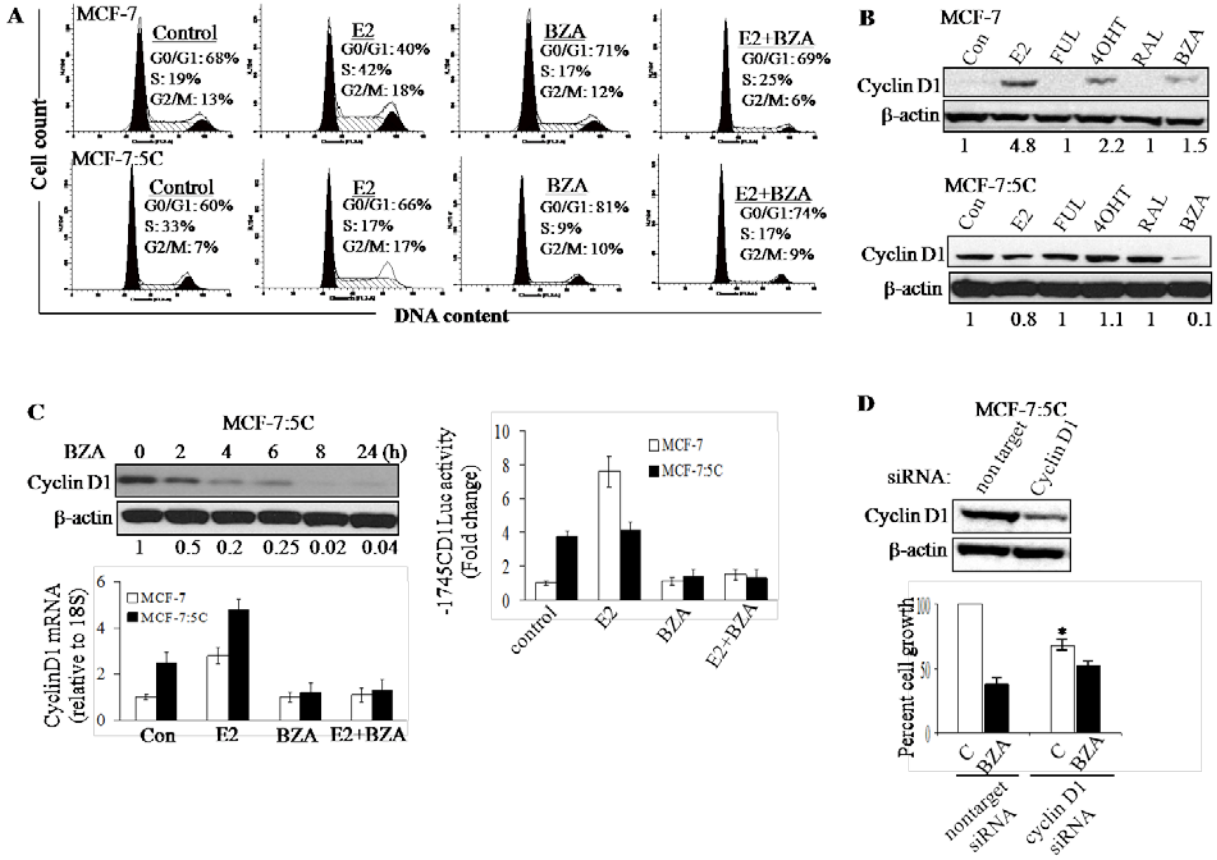


Figure 16: Effects of BZA on cell cycle progression and cyclin D1 regulation in MCF-7 and MCF-7:5C cells. **A**, cell cycle distribution was determined by propidium iodide staining of DNA content and flow cytometry. Cells were treated with 10^{-9} M E_2, 10^{-7} M BZA, or E_2 plus BZA for 24 and 48h. Thirty-thousand cells per sample and three replicates per group were collected. Representative histograms are shown. **B**, Western blot analysis of cyclin D1 expression level in MCF-7 and MCF-7:5C cells following treatment with BZA and other SERMs. Prior to experiment, MCF-7 cells were switched from fully estrogenized media to estrogen-free media for 3 days and then treated with ethanol vehicle (control), 10^{-9} M E_2 alone, or 10^{-9} M E_2 plus FUL (10^{-7} M), RAL (10^{-7} M), 4OHT (10^{-7} M), or BZA (10^{-7} M) for 24 h. MCF-7:5C cells, however, did not require a media switch since they are hormone-independent and are routinely grown in estrogen-free media. MCF-7:5C cells were treated as described above for MCF-7 cells. Quantitated protein levels normalized to β-actin are indicated. **C**, BZA regulation of cyclin D expression and promoter activity in MCF-7:5C cells. Cells were treated with 10^{-7} M BZA for the indicated time points. Cyclin D1 protein and mRNA levels were determined by Western blot and quantitative RT-PCR, respectively with β-actin and 18S rRNA as internal controls. For cyclin D1 promoter activity experiment, MCF-7 and MCF-7:5C cells were cotransfected with a full-length cyclin D1 promoter plasmid (-1745CDLUC) and Renilla luciferase control plasmid overnight and then treated with 10^{-9} M E_2, 10^{-8} M BZA, or E_2 + BZA for 24 h. Luciferase activity was measured as described in materials and methods. **D**, proliferation of MCF-7:5C cells transfected with the nontarget or cyclin D1 siRNA. Cells were transfected and then seeded at 15,000 per well in 24-well dishes. Medium was replenished the day after seeding on day 0 and every other day thereafter. Cells were collected on day 5 and counted using a hemocytometer. All data are presented as the mean from three independent experiments with duplicate (*, $p < 0.01$ versus nontarget transfected cells).

Figure 17:

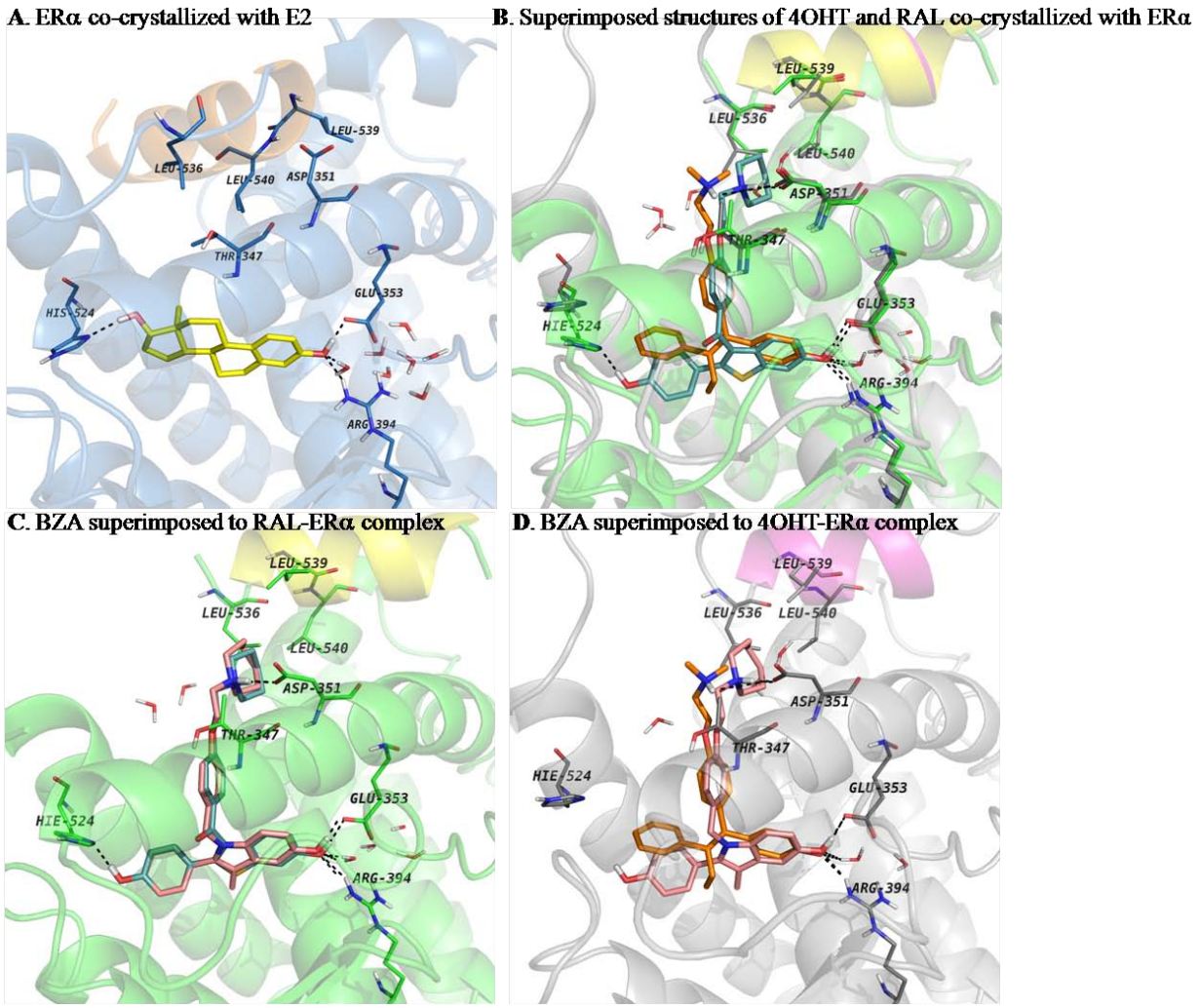


Figure 17: Molecular modelling of ERα binding site with various ligands. A, agonist conformation of ERα co-crystallized with E_2; helix 12 is depicted in orange and lays over the binding site sealing the ligand inside it. The antagonist conformations of the receptor are shown in panels B, C, D, and E. X-ray structures of ERα co-crystallized with 4OHT (B), raloxifene (C), bazedoxifene (D), or fulvestrant (E) docked into the ERα-raloxifene crystal structure. Helix 12 is depicted in magenta for 4OHT bound conformation and yellow for raloxifene and bazedoxifene. Also the key aminoacids lining the binding site are displayed and the network of hydrogen bonds in which they are involved with the ligands is shown in black dashed lines. Carbon atoms are colored in yellow for E_2, orange for 4OHT, cyan for raloxifene and pink for bazedoxifene. These images show the differences between the agonist (A) and antagonist conformation (B, C, E) of ERα and present the alignment of bazedoxifene in the binding site of ERα which is very similar with raloxifene's orientation and the same interactions with the key aminoacids of the binding cavity are encountered

TASK 3: (GU/Riegel and Wellstein) - To decipher cellular signaling pathways using proteomics and to mesh proteomics and mRNA analysis.

Introduction:

Here we report work completed on Task 3 at the GU site during year 4 of this COE. Studies were carried out at GU in the laboratory of Anna Riegel PhD and the laboratory of Anton Wellstein MD PhD, with support from Ben Kagan PhD, Alex Kyriliuck PhD, Zhangzhi Hu PhD and Jordan Li. In years 1-4 of this project we have developed methods of proteomic analysis (18) and undertaken an extensive proteomic comparison of differences in untreated MCF-7 and MCF-7:5C or cells treated with estradiol-17B for short periods of time (Hu et al 2011 *Plos One* in press; see item #16 in the Appendix). In this publication, data was presented that suggests that the nuclear coactivator AIB1 (amplified in breast cancer 1) is a significant driver of E2-controlled growth phenotype in these ER-positive breast cancer cells. Because AIB1 was rate-limiting for the E_2-induced changes in the growth phenotype of MCF-7 and MCF-7:5C cells, we performed AIB1-specific immunoprecipitation of lysates from untreated and E_2-treated (2 hrs) MCF-7 and MCF-7:5C cells to fractionate the respective proteome, which was followed by 1-D PAGE (polyacrylamide gel electrophoresis), and MS (mass spectrophotometry) identification of proteins. Immunoprecipitation of phosphotyrosine-containing protein complexes was also performed to complement the AIB1-specific proteome fractionation .Stringent filtering of the initial proteomic data resulted in a subset of 101 proteins that either interacted with AIB1 or are present in pY-protein complexes with 13 proteins common to both.

In separate experiments with independent mass spectrometry analyses 48% of the proteins reported here were found in two and 16% in three or more experiments. We show the functional categories ascribed to the AIB1-associated (top) and pY-complexed (bottom) proteins. Nearly half of the AIB1-interacting proteins fall into four categories, i.e. cytoskeleton and structural proteins, metabolism, transcription regulation, and signal transduction. The functional categories of pY-complexed proteins of which more than half fall into four major categories: cytoskeleton and structural proteins, transcription regulation, signal transduction, and protein transport and vesicle trafficking. Thirteen proteins were found to be both AIB1-interacting and pY-complexed in MCF-7 and MCF-7:5C cells. Interestingly, 5 proteins were IP'ed (immunoprecipitated) with pY that were unique to the E_2-treated MCF7:5C group, one of which was FAK1 (focal adhesion kinase 1). Independent validation of this interaction with IP Western was demonstrated (Fig 18A). This result is of interest since FAK1 is known to complex with EGFR (epidermal growth factor receptor) and an isoform of AIB1 and contribute to cellular signaling in breast cancer (19). We also identified 18 proteins (CI >95%) that interact with AIB1 in E_2-treated but not in untreated MCF-7:5C cells, 10 of which are also unique to MCF-7:5C cells. These E_2-induced AIB1-interacting proteins in MCF-7:5C cells mainly segregate in the category "transcriptional regulation" (6 of 18), several of which are also known to be involved in the control of apoptosis. For example, PRDM5 (PR domain containing 5), a PR domain and zinc-finger transcriptional regulator is a putative tumor suppressor and has been linked to cancer cell apoptosis (20). TLE3 (transducin-like enhancer protein 3), a transcriptional corepressor that binds to a number of

transcription factors (21), can form a transcriptional repressor complex with RUNX3 (Runt-related transcription factor 3) (22), a known tumor suppressor that has been shown to be involved in apoptosis in gastric and colon cancer (23). TLE3 has also been associated with the development of anti-estrogen resistance (24). The presence of the 83 kDa TLE3 in AIB1 immunoprecipitations (IP) was also validated by IP Western blot analysis (Fig 18B). TLE3, PRDM5 and PRPF6 (pre-mRNA-processing factor 6) were all uniquely identified in E_2-treated MCF-7:5C cells.

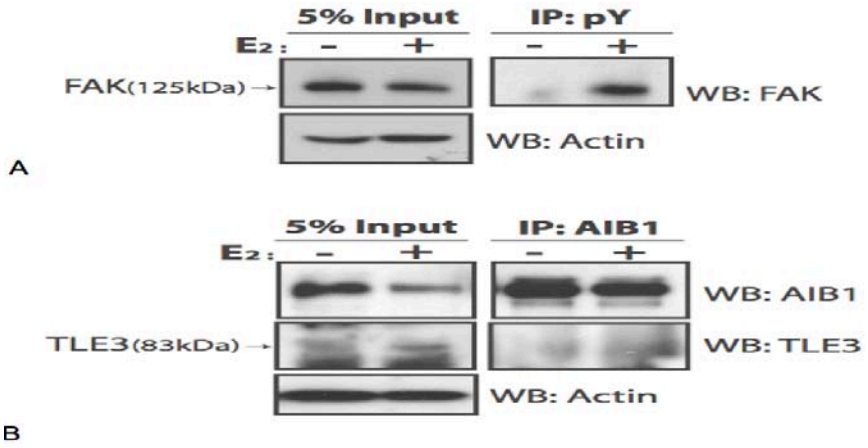


Figure 18: **Western blot analysis confirms that FAK1 and TLE3 are immunoprecipitated from E_2 treated MCF7:5C cells**. MCF-7:5C cells were treated or not with E_2 for 2 hours, and proteins were extracted for IP/Western analysis A) Tyrosine-phosphorylated endogenous proteins were immunoprecipitated with anti-phosphotyrosine monoclonal antibody (4G-10, Millipore) and the immunoprecipitate was resolved on SDS-PAGE (sodium dodecyl sulfate polyacrylamide gel electrophoresis) followed by Western analysis. The input is 5% of the amount of total cell lysates for IP. FAK1 was detected on the blot with FAK antibody (A-17, Santa Cruz). B) AIB1 interacting proteins were immunoprecipitated using anti-AIB1 monoclonal antibody (BD Biosciences). The input is 5% of the amount of total cell lysates for IP. TLE3 was detected on the blot with TLE3 antibody (Abcam).

The canonical pathway mapping analyses of all identified proteins suggest that several pathways are significantly represented both for proteins immunoprecipitated with anti-AIB1 and for those with anti-pY, including GPCRs (G-protein coupled receptors), apoptosis, PI3K (phosphoinositide 3-kinase)/AKT and Wnt/b-catenin and Notch signaling pathways.

Connection of the proteomics pathways identified to transcriptome effects

Comparative mRNA expression profiles of estrogen-deprived MCF-7 and MCF-7:5C cells have been reported and are available for data mining at the NCBI GEO website (GSE10879; ncbi.nlm.nih.gov/). An analysis of mRNA expression regulation after 48 hrs of estradiol treatment of these cells was published recently by the COE group and shows significant differences with respect to mRNA expression of regulators of apoptosis at steady state (25): In MCF-7 cells Bcl-2, a major anti-apoptosis gene, is upregulated by estradiol treatment whereas no

change of Bcl-2 was seen in MCF-7:5C cells. In our analysis Bcl-2 is one of the major hubs in the AIB1 interaction networks. In contrast, the pro-apototic Bcl-2 antagonists Bak, Bax and Bim mRNAs were found upregulated 2- to 7-fold after estradiol treatment of MCF-7:5C cells whereas no expression change was seen in the MCF-7 cells. Our analysis shows that upstream regulators of the canonical intrinsic mitochondrial pathway such as RSKs (ribosomal s6 kinase), were identified in the proteomics approach. The most differentially regulated cell survival and apoptosis modulator was Gadd45beta mRNA that was found upregulated 5-fold in MCF-7:5C and down-regulated 5-fold in MCF-7 cells after E_2 treatment (25). Gadd45beta was described earlier as a factor linked to cell survival in apoptosis resistant cells though it was mostly associated with serum growth factor dependent survival and not with UV or gamma-radiation induced apoptosis (26). In terms of it connectivity, this fits with Gadd45beta being a hub of the MAP kinase pathway signaling cascade that include MAP3K4, MEK6 (methyl ethyl ketone 6), MEK3, MAPK8 interactions and also connected to PCNA and cyclin B1 as well as relA, the NFkappaB p65 subunit (27). Of note is that we also observed components of GPCR signaling in our pathway analysis. This finding corroborates the upregulation of GPR30 (G-protein coupled receptor 30) in MCF7:5C cells after estradiol treatment (28) and it is noteworthy that GPR30 can bind estradiol and mediate rapid, non-genomic effects in breast cancer cells (29). Overall the expression analysis and proteomics data show some interesting convergences especially in apoptotic regulatory pathways which may be functionally relevant as initiators of estradiol–induced apoptosis. In conclusion, the results of the canonical pathway mapping analyses of all identified proteins suggest that several pathways are significantly represented both for proteins immunoprecipitated with anti-AIB1 and for those with anti-pY, including GPCRs, apoptosis, PI3K/AKT, and Wnt/b-catenin and Notch signaling pathways.

PROTEOMIC AND BIOINFORMATIC PATHWAY ANALYSIS OF 17β-ESTRADIOL (E_2)-INDUCED GROWTH VERSUS APOPTOSIS IN ESTROGEN-RESPONSIVE MCF-7 AND ESTROGEN DEPRIVATION-RESISTANT MCF-7:5C CELLS

We concluded from the previously published experiments on the characterization of the MCF7:5C cells that since the ER and AIB1 are not mutated but rather that unique activation of the novel signaling pathways by the ER and coactivator AIB1 must occur in these cells through tyrosine kinase activated signaling pathways that are selectively present in MCF7:5C cells. We now report our 4th year studies investigating these two aspects of estrogen-induced apoptosis and are summarized below.

Under this task we aim to identify signaling events that control estrogen-induced apoptosis in contrast to the induction of cell growth. A crucial model for this is a comparison between MCF-7:5C, a long-term estrogen deprivation-resistant variant line of breast cancer MCF-7 cells that undergo apoptosis in response to E_2, whereas wild-type MCF-7 cells will grow in response to E_2. The major goal during the fourth year of the project at the GU site was to continue our analysis of the proteome in these cell lines and in particular use phospho proteomics data and analysis to further analyze signaling pathways involved in E_2-induced apoptosis versus growth. Specifically during year 4 we based our analysis on examination of kinase activation in E_2-

treated MCF-7 and MCF-7:5C cells and focused much of the analysis on phosphoproteome of the ER and the nuclear coactivator AIB1. From a comparison of these experimental data sets obtained from MCF-7 versus MCF-7:5C cells + E_2 we obtained information on pathways that are involved in the differential response to E_2.

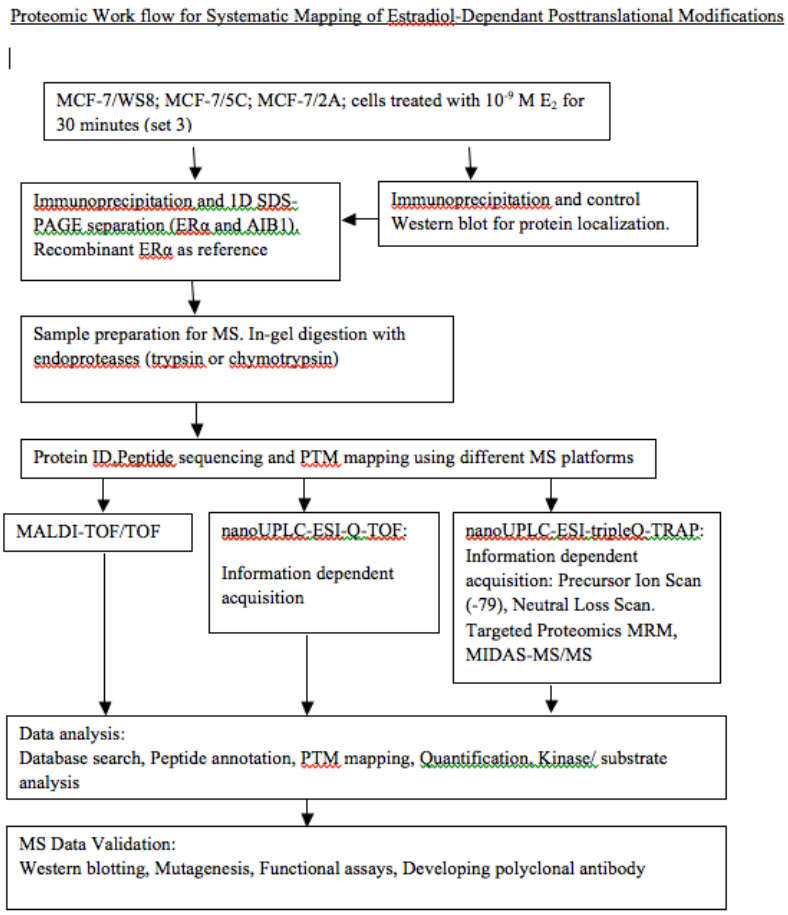
We report here on the new data and new analyses generated during year 4. For some of the experimental details we refer the reader to the reports from year 1-3.

WORK ACCOMPLISHED:

Part 1: Proteomic Analysis of phosphorylation changes in ER and AIB1 related to estrogen induced apoptosis in breast cancer.

We developed proteomic methods for identifying protein posttranslational modifications and analysis of differential regulation of ER and AIB1 proteins isolated from MCF-7 and MCF7:5C +/- E_2. Validation of the novel posttranslational modifications (phosphorylation) of interest detected in AIB1 and ER is ongoing, and involves Western blotting, mutagenesis, functional assays and ultimately developing polyclonal antibodies for detection of phopshorylation changes in specific sites (Figure 19).

Figure 19:



Experiments Completed:

Sets of protein lysates were delivered by Fox Chase Center and GU under Task 1 was used for developing condition suitable for MS analysis of PTM (predictive technology model) profile for ER and AIB1. For optimization of the input for MS analysis a set of immunoprecipitation experiments for ER alpha, were performed from total 15 to 50mg of proteins extract form MCF-7 cells (3 repeats for trypsin digestion of estradiol- treated and untreated cells and 2 repeats - for chymoptypsin digestion of ERα from estradiol-treated cells). The tubes with MCF-7 /5C/2A/WS8 cell lysate had a protein concentration between 20-40ug/ul. Volume per tube was 200-230ul.

For typical experiment: after thawing the lysates were cleared after by centrifugation at 14,000 g for 10 m at 4°C. The required amount of protein for IP was formed by mixing together the lysates from replicated experiments (typically 10-12). A 50 mg aliquot of each lysate was transferred to a pre-chilled 15 ml tube. The lysates were supplemented with 10mM Na_3V0_4, 10ul/ml phosphate inhibitor cocktail 1 (Sigma), 320nM Okadaic acid (50mM Na2MoO4 is optional). Volumes were adjusted with NP-40 (nonyl phenoxypolyethoxylethanol) lysis buffer (composition (50 mM Tris, pH 8.0, 150 mM NaCl, 40 mM b-glycerophosphate, 0.25% sodium deoxycholate, 1% NP-40, 50 mM sodium fluoride, 20 mM sodium pyrophosphate, 1 mM EGTA (ethylene glycol tetraacetic acid), 1 mM sodium orthovanadate) to reach a final concentration of total proteins in the samples as average as 20 ug/ul. The lysates were precleared with 30ul of Protein G-agarose beads for 1h, 4C on a rocker platform. The IP for ER alpha was done overnight with mouse monoclonal antibody (clone F-10, Santa Cruz, sc-8002, or sc-8002CA, conjugated). For each 50mg of lysate we added 150ul of F-10 AB (30mg of antibody). Estrogen receptor- Ab complexes were precipitated with 75 ul of Protein G -agarose beads (bed-volume) for 1h, 4C. Immunocomplexes were washed 5 times with 0.5% NP-40/PBS supplemented with protease and phosphatase inhibitors (Roche). The efficiency of IP was tested by Western blot with F10 AB (dilution 1 to 1000) on lysates before and after IP. Immunopurified ER was resolved on 4–15% gradient NuPAGE gels (Invitrogen) and detected by reversible Coomassie staining (Imperial protein stain, Thermo Scientific). The bands corresponding to ERα protein (Fig 21) were excised and cut into small chunks, using as a reference recombinant ERα and Western blot analysis with anti- ERα antibody.

Gel pieces were washed subsequently with 25 mM ammonium bicarbonate for 15 min, 50% ethanol/ 25 mM ammonium bicarbonate for 20 min and 100% ethanol for 20 min. After that cysteine residues were reduced with 10 mM DTT (Dithiothreitol)/25 mM ammonium bicarbonate for 60 min at 56°C, followed by alkylation with freshly made 55mM iodoacetamide/ 25 mM ammonium bicarbonate for 30 min, in the dark, at room temperature. After 3 times washing with 25 mM ammonium bicarbonate gel pieces were combined with 12.5 ng/ul endoprotease (trypsin or chymotrypsin, sequencing grade) in 25 mM ammonium bicarbonate. In-gel digestion was performed overnight at 37°C. Supernatant was transferred to low binding microcentrifuge tubes (PGC Scientifics). Peptides were extracted with 1% formic acid, 30 min with shaking and combined with liquid from previous step. All samples were evaporated down,

resuspended with LC solvent A and divided into three aliquots and stored at -80°C until used for mass spectrometry.

Peptide mixtures were analyzed with MALDI-TOF/TOF 4800 (AB Sciex, Framingham, MA) or using reversed phase nanoUPLC Acquity (Waters) coupled to ESI-Q-STAR quadrupole/ orthogonal TOF (AB Sciex, Framingham, MA) or on E SI-4000 QTRAP hybrid triple quadrupole/linear ion trap mass spectrometer (AB Sciex, Framingham, MA).

For LC fractionation peptide mixtures were resolved using reversed phase column BEH C18 column (1.7 µm, 75 µm x 150 mm, Waters) on nanoUPLC with buffer A (2% acetonitrile, 0.1% formic acid) and buffer B (98% acetonitrile, 0.1% formic acid). Peptides were eluted over 30 min linear gradient of 0-60% of the solvent B with 300 nl/min flow rate. The nanoUPLC instrument was coupled to ESI-Q-STAR or to 4000QTRAP mass spectrometer equipped with NanoSpray II ionsource (AB Sciex, Framingham, MA). Eluted peptides were ionized in positive mode using a fused silica PicoTip emitter (outer diameter 75 µm inner diameter, 15 µm emitter orifice, New Objective, Woburn, MA) with a spray voltage of 2300 V, a curtain gas of 13 psi, a nebulizer gas of 13 psi, an interface heater temperature of 180°C. 4000QTRAP was set up at unit resolution for Q1 and Q3 in MRM mode, and at low resolution in enhanced product ion scan.

Figure 20:

Coverage of ERα protein as result of MIDAS-MS, 70%

```
  1 MTMTLHTKAS GMALLHQIQG NELEPLNRPQ LKIPLERPLG EVYLDSSKPA
 51 VYNYPEGAAY EFNAAAAANA QVYGQTGLPY GPGSEAAAFG SNGLGGFPPL
101 NSVSPSPLML LHPPPQLSPF LQPHGQQVPY YLENEPSGYT VREAGPPAFY
151 RPNSDNRRQG GRERLASTND KGSMAMESAK ETRYCAVCND YASGYHYGVW
201 SCEGCKAFFK RSIQGHNDYM CPATNQCTID KNRRKSCQAC RLRKCYEVGM
251 MKGGIRKDRR GGRMLKHKRQ RDDGEGRGEV GSAGDMRAAN LWPSPLMIKR
301 SKKNSLALSL TADQMVSALL DAEPPILYSE YDPTRPFSEA SMMGLLTNLA
351 DRELVHMINW AKRVPGFVDL TLHDQVHLLE CAWLEILMIG LVWRSMEHPG
401 KLLFAPNLLL DRNQGKCVEG MVEIFDMLLA TSSRFRMMNL QGEEFVCLKS
451 IILLNSGVYT FLSSTLKSLE EKDHIHRVLD KITDTLIHLM AKAGLTLQQQ
501 HQRLAQLLLI LSHIRHMSNK GMEHLYSMKC KNVVPLYDLL LEMLDAHRLH
551 APTSRGGASV EETDQSHLAT AGSTSSHSLQ KYYITGEAEG FPATV
```

Systematic search for Phosphorylation sites of endogenous ERα and AIB1 employing MRM (Multiple Reaction Monitoring) strategy and MIDAS (MRM-initiated Detection and Sequencing) algorithm.

MRM method is highly sensitive, has very little chemical background and provides confidence in the results even in the absence of a full MS/MS spectrum. MRM/MS relies on simultaneous observation of the peptide precursor ion together with one of its fragment product ions by taking advantage of the characteristic fragmentation pattern of phosphopeptides. It is highly unlikely that isobaric component that may coelute with targeted precursor will also have matching fragment mass. The most important benefit of this technology is a relative PTM

quantitation capability for practically any given peptide. MRM base analysis has significant advantage as it allows simultaneous quantitative monitoring of many novel or previously reported modifications in one experiment. Such analysis provides the quantitative assessment of the stoichiometric level of a modified peptide relative to its unmodified form.

MRM transitions and corresponding collision energy settings for predicted peptides were generated using recommended setting in MRM pilot software (AB Sciex, Framingham, MA). The list of *in-silico* predicted transitions includes the potential variable modification of the oxidated methionine and the fixed modification of the alkylated cysteine.

All peptides containing serine, threonine, or tyrosine residues were interrogated using *in silico* prediction of fragmentation with trypsin or chymotrypsin endoproteases for precursor ions Q1 masses and best collision induced fragment ions for Q3 masses. Short tryptic peptides (3-4 aa long) as well as large peptides were excluded from analysis if they did not contain potentially phosphorylated amino acid residue. Using MRMpilot software, a set of predicted MRMs was generated for each **peptide.** MRMs were tested in initial experiments with commercially availibable ER protein. A final set of optimized MRMs that covered most sequence of ER protein was selected. Optimized MS method combined the analysis of both, unmodified and phosphorylated peptides (Figure 20).

The MS method for 4000QTRAP includes MIDAS algorithm for triggered MS/MS scans. Typically, method for 4000QTRAP mass spectrometer has 3-4 dependent Enhanced Product Ion scans, which are triggered when the MRM signal exceeds a threshold (normally 100 counts/s). Precursor ions were dynamically excluded for one minute after two occurrences.

The list of transition used for quantification and triggering MS/MS is presented. A minimum of two different transitions were used for stoichiometric analysis of each modification in this experiment. As the sample preparation involved an SDS-PAGE method, the sulfoxide forms of each methionine containing peptide are prevailing in the current work. However, peptides with unmodified methionine were analyzed as well. Dwell time of MRMs and total scan time were kept to allow at least seven data points per peak.

Neutral loss scan and Precursor Ion scan (-79)

Peaks were integrated using quantitation software MaltiQuant (AB Sciex, Framingham, MA). An abundance of modified peptides is determined from the shape of their fragment peaks in corresponding MRM using the area under the curve with relation to the signal of related unmodified peptide. Data of estrogen-stimulated signals were normalized to corresponding signals from an unstimulated experiment and presented in Fig 22. as folds on induction.

MIDAS- MS/MS fragment ion data were searched against a human database using Paragon and Mascot algorithm (Matrix Sciences, London, UK) in ProteinPilot 3.0 software (AB Sciex) with mass tolerance for precurcor ions 0.02 Da, fragment ion tolerance 0.8 Da, no miss cleavage, carboxymethylation as fixed modification for cysteine, and several variable modifications such as oxidation for methionine and phosphorylation for serine, threonine and tyrosine.

In addition to MIDAS-MS, we employed a sensitive and specific for phosphorylation scans such as a precursor ion (PI) or neutral loss (NL). In combination with dependant enhanced resolution (ER) and enhanced product ion (EPI) scans. The method is automated by employing Information Dependent Acquisition (IDA). The 4000 Q TRAP system selectively detects characteristic PO3 - fragment ion using precursor ion (PI) scan for negative 79 fragment. For tyrosine phosphorylation sites the 4000 Q TRAP spectrometer was set to detect precursors in PI scan with diagnostic fragment m/z 216 in the a triple quadrupole mode. Phosphorylated serines and threonine were analyzed in Neutral Loss scan (NL) scan of (+) 49.0 for 2+ charge. The first mass analyzer scans all the masses. The second mass analyzer also scans, but at a set offset from the first mass analyzer. This offset corresponds to a neutral loss that is commonly observed for the class of compounds. Neutral loss scans cannot be done with time based MS instruments. In a -neutral-loss scan, both quadrupole are in scan mode simultaneously, but with a mass offset 49.

Data base analysis of triggered NL scan and PI scans were done in similar way as with MIDAS-MS data sets.

The main challenge for ER analysis is very low basal level of protein (see arrowed upper band Fig 21 below) and down regulation/degradation upon estrogen treatment that represent a challenge for mass spectrometry. MALDI-TOF/TOF was unable to identified both ER and AIB1 proteins from pull down. That is why we continued our analysis with LC-MS platforms. ERα and AIB1 proteins were positively identified, validated and pattern of estradiol-induced phosphorylation were collected using MRM methods on 4000QTRAP mass spectrometer. Data, presented in the table reflect position of phosphorylated amino acid residue, Mascot score, and sequence of peptide used for analysis.

Figure 21: CoMassie stain gel of ER alpha immunoprecipitate.

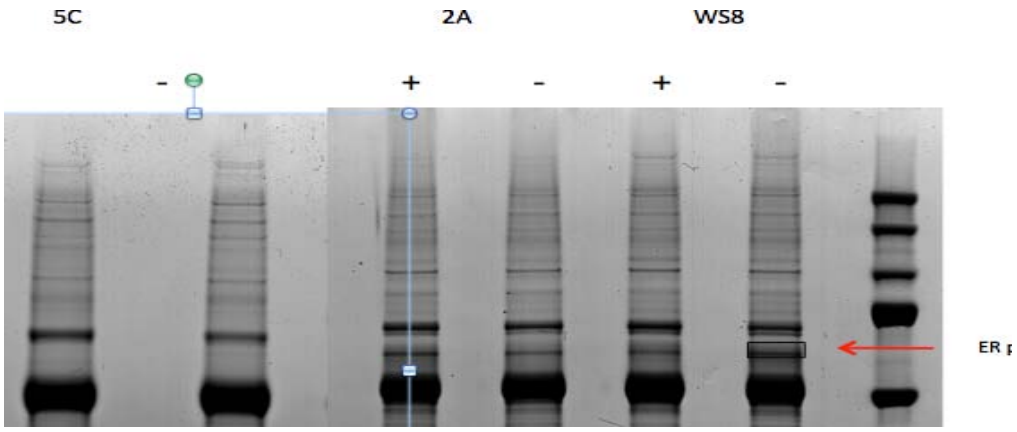


Figure 22:

ERα protein was positively identified, validated and pattern of estradiol-induced phosphorylation were collected using MRM methods on 4000QTRAP mass spectrometer. Data, presented in the table reflect position of phosphorylated amino acid residue, Mascot score, and sequence of peptide used for analysis.

ph-Residue	WS8/E2-	WS8/E2+	2A/E2-	2A/E2+	5C/E2-	5C/E2+
Threonine 7		18 (Ch 6-15)		3(Tr 1-8)		10 (Ch 6-15)
Serine 10		20 (Ch 6-15)		10 (Ch 6-15)		13 (Ch 6-15)
Serine 102		14 (Ch 101-110)		21 (Ch 101-110)		19 (Ch 101-110)
Serine 104				15 (Ch 101-110)		14 (Ch 101-110)
Serine 106		20 (Ch 101-110)		13 (Ch 101-110)		26 (Ch 101-110)
Serines 102/104		20 (Ch 101-110)				9 (Ch 101-110)
Serines 102/106		14 (Ch 101-110)		13 (Ch 101-110)		19 (Ch 101-110)
Serines 104/106		20 (Ch 101-110)		18 (Ch 101-110)		
Serine 118		8 (Ch 111-120)				
Threonine 140		15 (Ch 140-149)		38 (Ch 140-149)		15 (Ch 140-149)
Serine 167				7 (Tr 165-171)		2 (Tr 165-171)
Threonine 168		18 (Tr 165-180)		10 (Tr 165-180)		11 (Tr 165-180)
Serine 173		12 (Tr 172-183)		11 (Tr 165-180)	13 (Tr 172-180)	10 (Tr 172-183)
Serine 178		6 (Tr 172-183)	6 (Tr 172-183)			16 (Tr 172-180)
Serines 173/178		12 (Tr 172-183)		15 (Tr 172-183)		12 (Tr 172-180)
Threonine 182		14 (Tr 172-183)		23 (Tr 172-183)		6 (Tr 172-183)
Serine 173/Threonine 182				7 (Tr 172-183)		11 (Tr 172-183)
Serine 193		6 (Tr 184-206)				
Serine 193/Tyrosine197				23 (Tr 184-206)		
Serine 212				13 (Tr 212-231)		
Tyrosine 219		9 (Tr 212-231)				
Tyrosine 219/Threonines224				7 (Tr 212-231)		
Threonines 224/228			6 (Tr 212-231)			8 (Tr 212-231)
Serine 212/Threonine 228		16 (Tr 212-231)	16 (Tr 212-231)			
Threonine 228						6 (Tr 212-231)
Serine 236		10 (Tr 236-243)				
Tyrosine 246	11 (Tr 245-256)	9 (Tr 245-256)	11 (Tr 245-252)	12 (Tr 245-256)	4 (Tr 245-252)	8 (Tr 245-252)
Serine 282		13 (Tr 278-299)	21 (Tr 278-299)	18 (Tr 278-287)	21 (Tr 278-299)	15 (Tr 278-299)
Serine 294				9 (Tr 278-299)		7 (Tr 278-299)
Serine 282/294		9 (Tr 278-299)				14 (Tr 278-299)
Serine 309		9 (Ch 307-320)				
Serine 311		8 (Ch 307-320)		14 (Ch 307-320)		
Serine 317		23 (Ch 307-320)				
Serine 371				10 (Ch 361-372)		
Serine 433		10 (Ch 430-440)				5 (Tr 417-436)
Serine 432/433						10 (Ch 426-435)
Serine 456		5 (Tr 437-467)		5 (Tr 437-467)		
Serine 450		13 (Tr 437-467)			8 (Tr 450-472)	9 (Tr 437-467)
Serine 463/468		10 (Ch 462-469)		13 (Ch 462-469)		
Serine 463				13 (Ch 462-469)		
Threonine 465			6 (Tr 450-472)	10 (Tr 450-472)		
Serine 464/Threonine 465		7 (Tr 450-465)				
Serine 468						10 (Tr 450-472)
Serine 450/ Serine468						11 (Tr 450-472)
Serine 512		3 (Tr 504-515)		9 (Tr 504-515)		
Serine 518		26 (Tr 516-520)		19 (Tr 516-520)		26 (Tr 516-520)
Tyrosine 526				6(Tr 521-529)		
Serine 527		24(Tr 521-529)	5 (TR 521-529)	14 (Ch 527-539)		18 (Ch 527-539)
Tyrosine 526/Serine 527		9(Tr 521-529)		11(Tr 521-529)		7(Tr 521-529)
Tyrosine 526/537						14 (Ch 526-537)
Tyrosine 537	3 (Tr 532-548)		4 (Tr 532-548)		7 (Tr 532-548)	
Threonine 543	3 (Tr 549-555)					
Threonine 553		13 (Tr 549-555)				11 (Tr 549-555)
Serine 554		18 (Tr 549-555)		11 (Tr 549-555)	3 (Tr 549-555)	20 (Tr 549-555)
Treonine553/Serine 554		12 (Tr 549-555)		2 (Tr 549-555)		5 (Tr 549-555)
Threonine 570		13 (Ch 569-582)				13 (Ch 569-582)
Serine 575		17 (Ch 569-582)		17 (Ch 569-582)		
Threonine 574						12 (Ch 569-579)
Serine 578				17 (Ch 569-579)		
Tyrosine 582		14 (Ch 569-582)		11 (Ch 569-582)		

Figure 22. Data base analysis of triggered MIDAS-MS/MS.

Figure 23:

Domain structure of ERα with reported E_2 -induced phosphorylation sites. Positions of modifications identified in the present work by mass spectrometry are shown below: red- novel sites, blue – phosphosites reported before in literature.

		phos-Residue	Max Mascot score (peptide rresidues)
1			
	A	Threonine 7	18 (6-15)
		Serine 10	20 (6-15)
38		Serine 102	21 (101-110)
		Serine 104	15 (101-110)
		Serine 106	26 (101-110)
		Serine 118	8 (111-120)
		Threonine 140	38 (140-149)
	NTD/AF-1	Serine 167	7 (165-171)
		Threonine 168	18 (165-180)
		Serine 173	13 (172-180)
		Serine 178	16 (172-180)
		Threonine 182	23 (172-183)
		Serine 193	23 (184-206)
		Tyrosine197	23 (184-206)
		Serine 212	16 (212-231)
		Tyrosine 219	9 (212-231)
180		Threonines 224	16 (212-231)
		Threonine 228	16 (212-231)
	DBD	Serine 236	10 (236-243)
		Tyrosine 246	12 (245-256)
		Serine 282	21 (278-299)
263		Serine 294	14 (278-299)
		Serine 309	9 (307-320)
		Serine 311	14 (307-320)
	Hinge	Serine 317	23 (307-320)
		Serine 371	10 (361-372)
		Serine 432	10 (430-440)
302		Serine 433	10 (426-435)
		Serine 456	12 (450-472)
		Serine 450	13 (437-467)
		Threonine460	12 (450-472)
		Serine 463	13 (462-469)
		Threonine 464	10 (450-472)
		Threonine 465	10 (450-472)
	LBD/AF-2	Serine 468	13 (462-469)
		Serine 512	9 (504-515)
		Serine 518	26 (516-520)
		Tyrosine 526	14 (526-537)
		Serine 527	24(521-529)
		Tyrosine 537	14 (526-537)
		Threonine 553	13 (549-555)
		Serine 554	20 (549-555)
553		Threonine 570	13 (569-582)
	F	Serine 575	17 (569-582)
		Threonine 574	12 (569-579)
		Serine 578	17 (569-579)
		Tyrosine 582	14 (569-582)

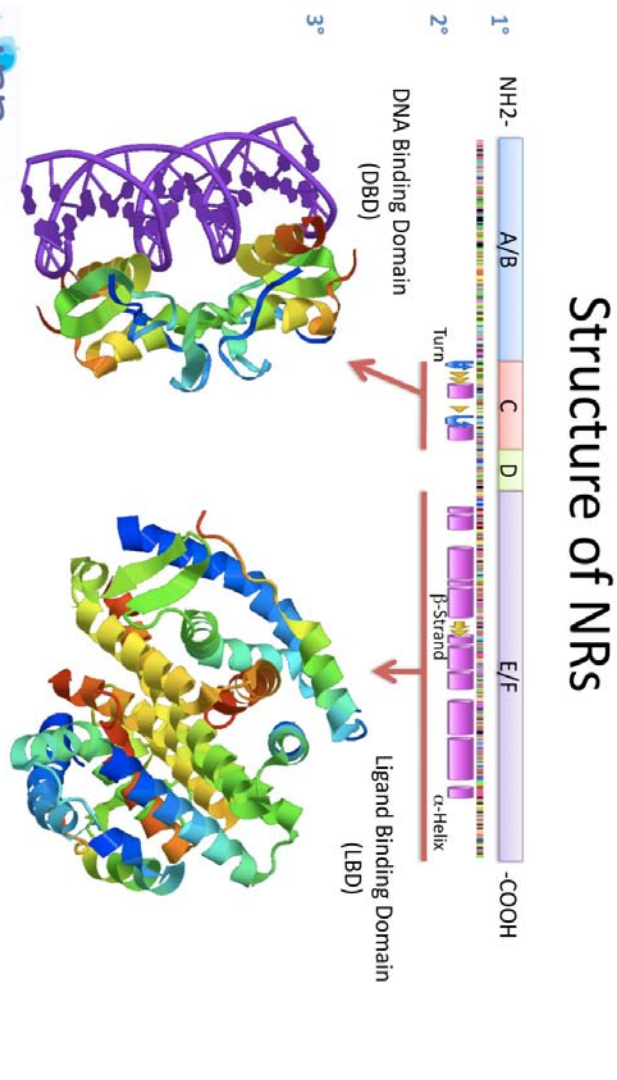


Figure 24:

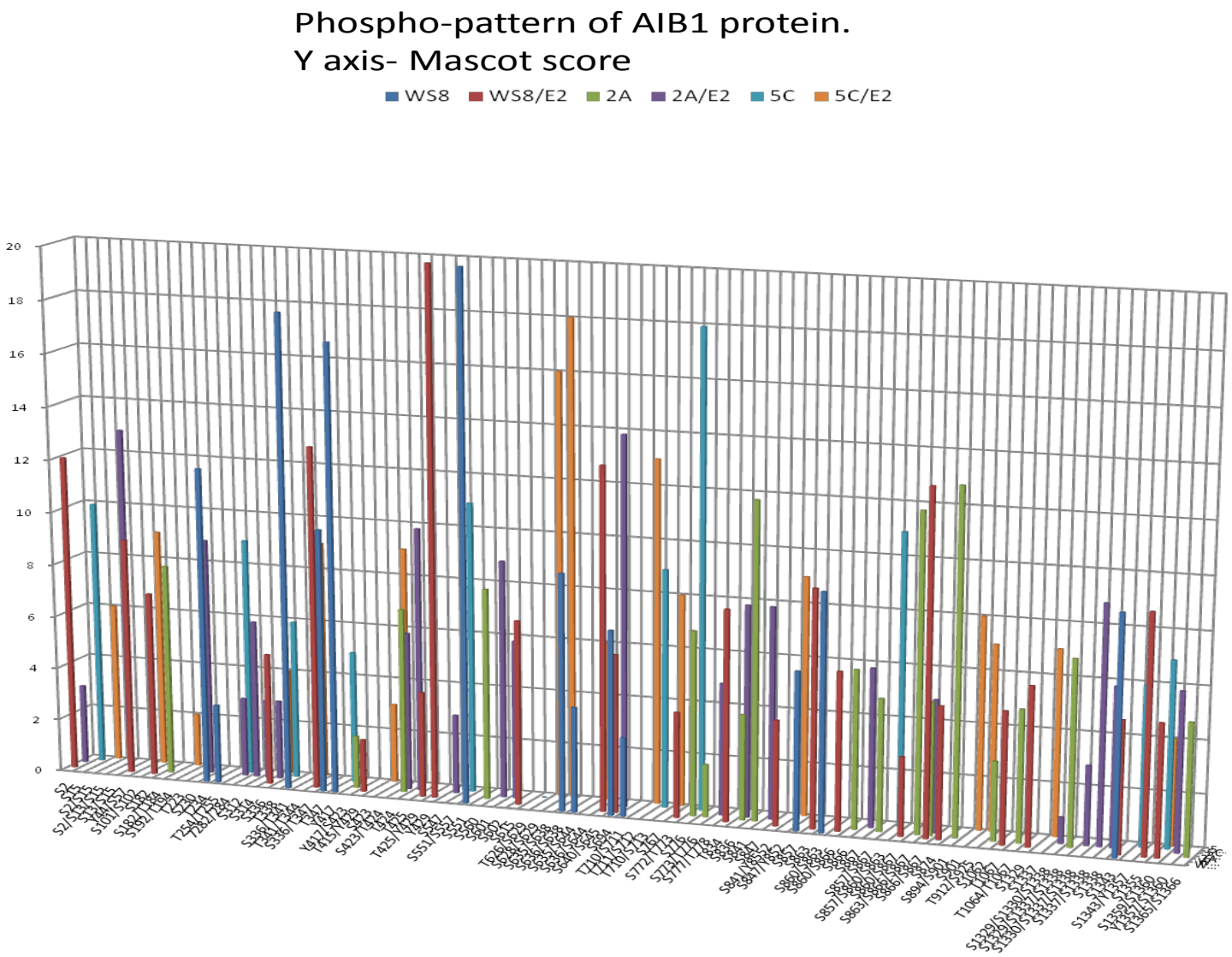


Figure 24A: Overall phosphorylation pattern of AIB1 +/- E_2 in MCF-7 (WS8) or MCF7:5C or MCF7:2A identified by mass spectrometry

Multiple phosphorylations at serine, threonine and some tyrosine residues of AIB1were observed and some of these were regulated by estrogen treatment in the MCF7:5C line but not in the parental MCF-7 cell line. In year 5 we will select several of these sites for further functional analysis for their role in E_2-induced apoptosis.

Figure 24B:

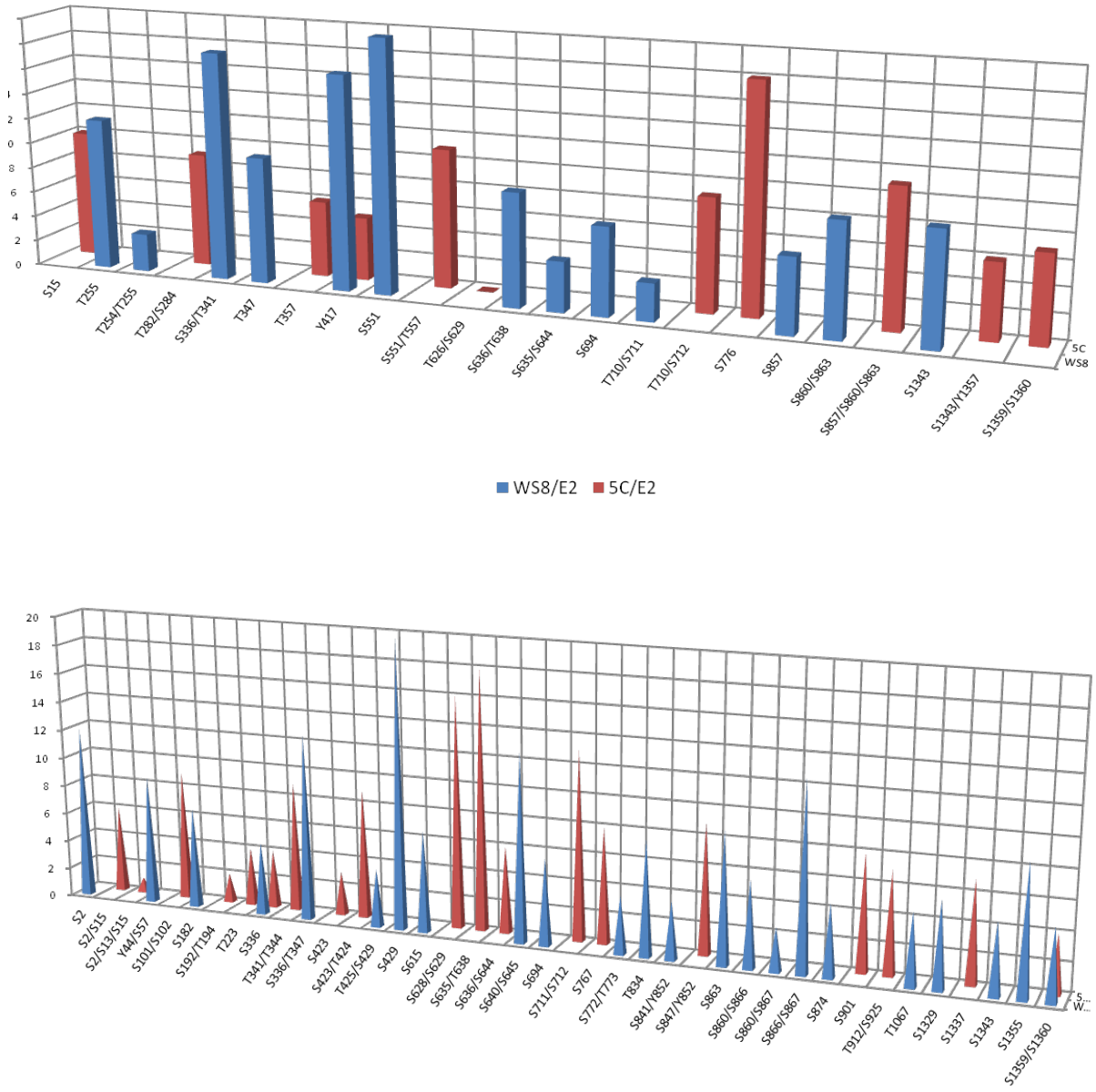


Figure 24B: Overall AIB1 phosphorylation pattern determined by mass spec proteomics in MCF7:5C in the absence (upper) or presence (lower) of estrogen after 2 hrs treatment.

Figure 25:

Estrogen-responsive phosphorylation in AIB1. WS8 cells versus 5C.
Quantitation on the base of MRM analysis. These transitions were verified with MS/MS and Mascot data base search . Position of phosphorylated amino acid residue in the AIB1 protein. MRM transitions including m/z of precursor (Q1 mass) and of fragment ion (Q3 mass), as well as the Mascot score of MS/MS for corresponding phosphopeptides.

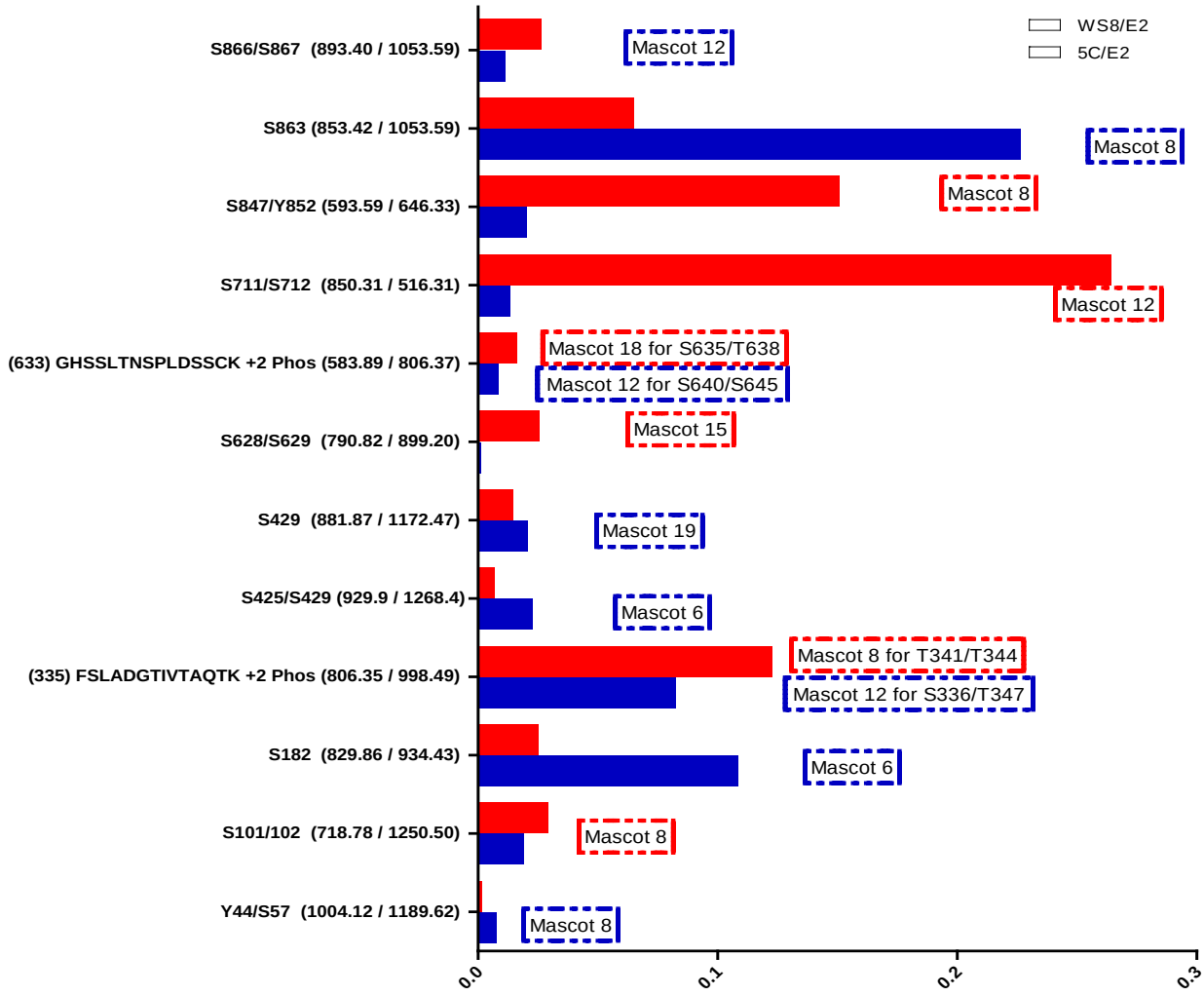


Figure 26:

	$-E_2$	$+E_2$
S15	ND	10
S102	ND	9
S336	ND	9
S423	ND	9
S628	ND	16
S635	ND	18
T711.S712	ND	13
S901	ND	8
S1329	ND	9

Figure 26: Selected sites at which E_2 upregulates AIB1 phosphorylation in MCF7:5C

Part II: regulation of AIB1 phosphorylation in MCF-7 or MCF7:5C by growth factors

A number of recent studies e.g. (30) have indicated that estrogen and HER/EGFR are co-regulated and that there is significant cross talk between these two pathways in the proliferative response in breast cancer epithelial cells and in the development of endocrine resistance. In addition, a pivotal molecule in the responsive to Estrogen and HER2 and EGFR is the nuclear coactivator AIB1 which is involved in estrogen control of HER2 expression and is also involved in control of overall HER2 response in breast epithelium (31, 32). Given the role of AIB1 in HER2 and EGFR signaling in breast cancer we decided to also examine how phosphorylation of AIB1 by these oncogenic growth factors is altered in the MCF-7 vs MCF7:5C pathway. Our first experiments were performed with EGF treatment of AIB1 for short periods in MCF-7 cells followed my IP of AIB1 and resolution by MS proteomics. Although phosphorylation is usually a low % of total protein a predominant phosphorylation peak was detected at Ser 214 after EGF treatment. (Figure 27).

Figure 27:

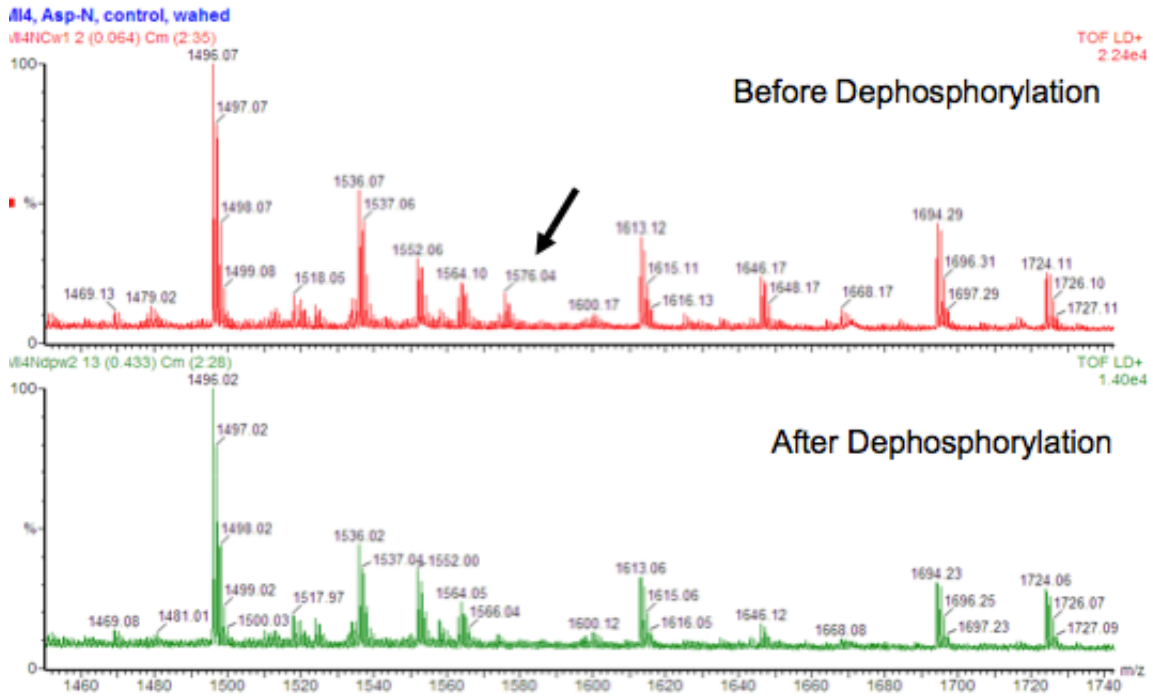
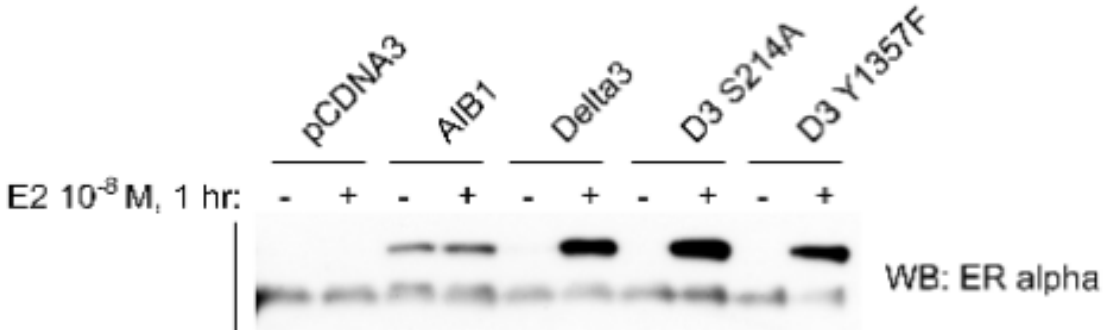


Figure 27: indicates MS species obtained from EGF treated MCF7 cells . AIB1 was IPed and resolved by MS. The peaks were resolved +/- phosphatase and peaks that are removed indicate a phopho-peptide fragment. The phospho peak for phospho Ser 214 is indicated.

To determine whether phosphorylation of Ser 214 altered the interaction of AIB1 with the estrogen receptor we mutated the Ser site and expressed this mutant as a FLAG tagged protein. After IP with a Flag antibody we determined how much of the AIB1 mutant bound to ER vs the wild type AIB1 (Figure 28). Interestingly, mutation of the 214 site appeared to slightly increase the interaction with the ER, which would suggest that EGF phosphorylation would induce less coactivation of ER, and possibly increase interaction with other AIB1 transcription factors such as AP-1.

Figure 28:



Phosphorylation of the Y1357 site has been reported by us previously (33) and in contrast to ser 214, mutation of the Y at 1357 decreases the interaction with the ER (Figure 26).

We decided that the EGF phosphorylation at Ser 214 was of potential interest for non steroidal regulation of the coactivator AIB1 and could play a major role in the switch of AIB1 from interactions with nuclear coactivators to interactions with other transcription factors such as AP-1,SP-1 E2F1 (34) and potentially alter cellular responses to estrogen. We raised a poly clonal antibody to the Ser 214 phospho peptide site and tested the antibody for its interaction with AIB1. The antibody worked for specific IP of AIB1 serine phosphorylated at 214 although it did not work in direct western analysis. Using this antibody we determined that IGF-1 and EGF caused a rapid increase in phosphorylation of Ser 214.

Figure 29:

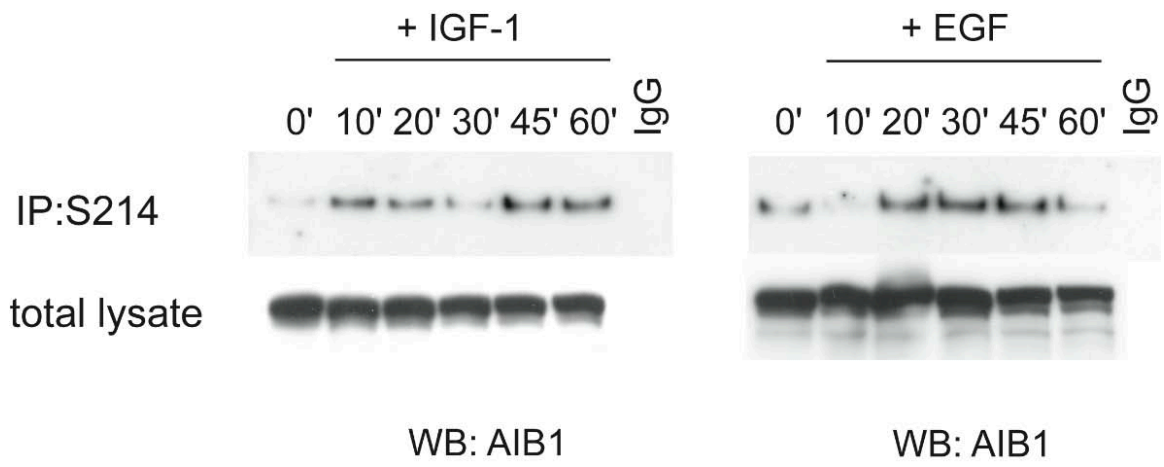


Figure 29: **Growth factors increase phosphorylation of Ser 214 AIB1**. *MCF7 cells were treated with IGF-1 or EGF for the times indicated and cell lysates were prepared. IP with phospho Ser 214 Ab was followed by Western analysis and AIB1 detected with a pan AIB1 antibody*.

Thus, several tyrosine kinase receptors that are activated by growth factors bring about rapid phosphorylation of the Ser 214 site.

The next question was to determine the functional consequence of changes in phosphorylation of this site. It is know that phosphorylation at other sites on AIB1 can lead to changes in protein half life (35) and we determined that was also the case for Ser 214.

Figure 30:

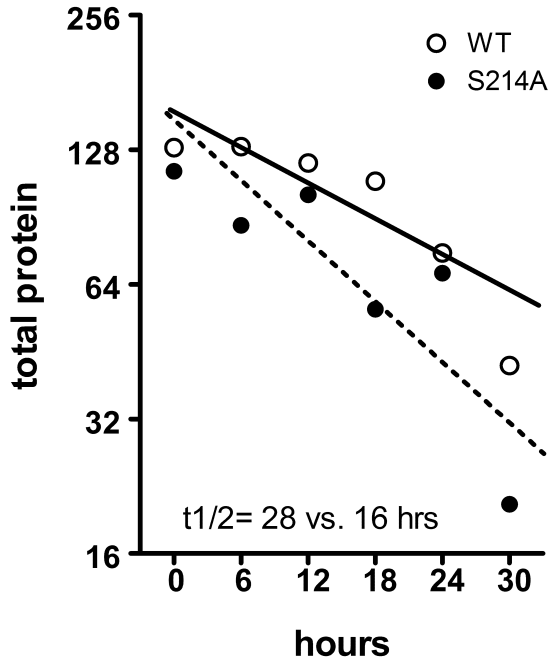
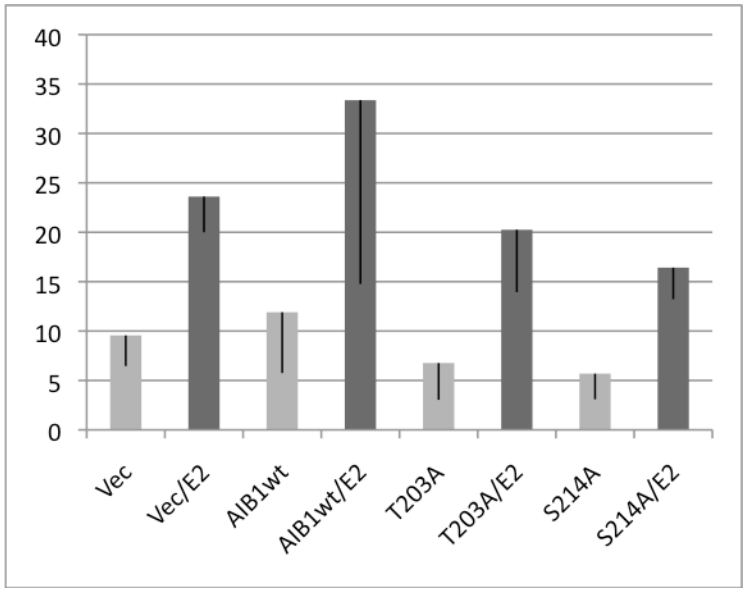


Figure 30: **Phosphorylation of Ser 214 extends the half life of AIB1 from 16hrs to 28 hrs.** Half life of the protein was determined after cycloheximide treatment of MCF-7 cells.

We also determined if mutation of the Ser 214 site affected the transcriptional activity of factors know to bind to AIB1. We tested the Wt vs the Ser 214 A mutation on an estrogen responsive luciferase construct and also an AP-1 responsive promoter (Figure 31). We found that mutation of Ser 214 reduced the basal and estrogen responsive promoter response, however, in contrast the basal and AP-1 responsiveness is increased by mutation of Ser 214. Although the earlier data suggested that mutation of this site increases interaction with ER, it is possible that the shorter half life of the mutant just reduces the amount of available coactivator for the transcription complex. In contrast, despite the reduced half life of the Ser 214 construct. It is still more active than the Wt protein at the Ap-1 site, suggesting that in MCF7 cells EGF induction of phospho Ser 214 would inhibit use of AP-1 sites and would favor cross talk with the estrogen receptor. We are now testing whether this paradigm is altered in the MCF7:5C cells, i.e. does mutation of the phospho sites of AIB1 reveal a regulatory pathway that is activated by HER2/EGF in MCF7:5C that activates an Estrogen -dependent apoptotic gene expression pattern?

Figure 31:

A



B

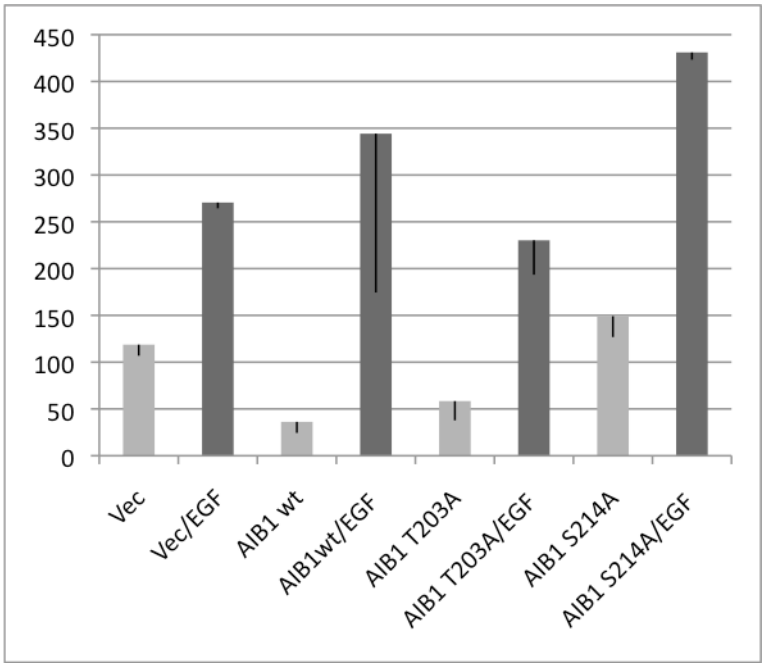


Figure 31: A) Each mutation or WT AIB1 was overexpressed +/- E_2. the reporter readout was an A) ERE-luciferase construct or B) +/- EGF with an AP-1 luciferase reporter

In conclusion: In year 4 of this COE we have performed extensive analysis of the phopshorylation profile of ER and AIB1 induced by Estrogen and growth factors in the MCF7 and MCF7:5C lines. We have found significant regulated differences at specific phosphorylation sites and have now embarked on functional analysis of the role of some of majorly modified site s to determine whether these post transitional modifications play a role in the switch from an estrogen induced proliferative to an estrogen induced apoptotic response.

TASK 4: (FCCC/Ariazi; TGen/Cunliffe; Jordan/LCCC) – To analyze E_2-induced survival and apoptotic pathways using gene arrays and siRNAs.

Task 4a: (Ariazi, Cunliffe, and Jordan) - Catalogue the transcriptional response using array-based expression profiling.

Task 4b: (Ariazi, Cunliffe, and Jordan) - Identify regulatory networks for pathways indicative of differential responses to E_2.

ESTROGEN-INDUCES APOPTOSIS IN ESTROGEN DEPRIVATION-RESISTANT BREAST CANCER VIA STRESS RESPONSES AS IDENTIFIED BY GLOBAL GENE EXPRESSION

Goal of this reporting: This section is critical for the ultimate success of our collaborative CoE grant. Using our unique cell lines, we have generated a time curve over the two weeks of study to precisely quantify each gene in the human genome related to the life and death of breast cancer cells in response to estrogen. This experiment in biology conducted as Task 1 ha s been completed in conjunction with TGen of Task 4. We report here select biological interrogation of our database, as the overall database for this work is too enormous to report here. This reporting will be done in Year 5, with the publication of our work in the *Proceedings of the National Academy of Sciences*. This is still a work in progress and the paper has yet to be submitted. Suffice to say, that our subsequent analysis through gene enrichment pathways will be the basis of all of our future studies to modulate estrogen-induced apoptosis.

Studies/analyses carried out by Eric Ariazi at FCCC in collaboration with Heather Cunliffe at TGen.

Here we report work completed on T asks 4a and 4b dur ing year 4 of this COE. Cell lysate samples were generated at FCCC, RNA was purified from lysates at TGen, microarray hybridizations were conducted at TGen, and analyses and interpretation of the data were conducted at FCCC. Work accomplished for Tasks 4a and 4b are presented in an integrated format.

Introduction/Abstract:

Acquired resistance to long-term antihormonal therapy in breast cancer evolves through two phases over 5 years. Phase I develops within a year, and tumor growth occurs with either E_2 or tamoxifen. Phase II resistance develops after five years of therapy, and tamoxifen still stimulates growth, but E_2 paradoxically induces apoptosis. This is the basis for therapeutic use of estrogen to treat advanced antihormone-resistant breast cancer. We interrogated E_2-induced apoptosis by comparing E_2-regulated gene expression across time (2-96 h) in MCF-7 cell variants which were estrogen-dependent (WS8), or resistant to estrogen deprivation and refractory (2A) or sensitive (5C) to E_2-induced apoptosis. We developed a method termed dAUC (differential area-under-the-curve) analysis that allowed identification of genes differentially regulated by E_2 in 5C compared to both WS8 and 2A cells, and hence, were associated with E_2-induced apoptosis. Estrogen signaling, ERS (endoplasmic reticulum stress) and inflammatory response genes were over-represented among the 5C-specific genes. The identified ERS genes indicated E_2 inhibited protein folding, translation and fatty acid synthesis. Meanwhile, the ERS-associated apoptotic genes BAX, BIM and CASP4 (caspase 4), among others, were induced. Evaluation of a caspase peptide inhibitor panel demonstrated the CASP4 inhibitor z-LEVD-fmk was the most active at blocking E_2-induced apoptosis. F urther, z-LEVD-fmk completely prevented PARP (Poly ADP-ribose polymerase*)* cleavage, E_2-inhibited growth, and apoptotic morphology. The up-regulated pro-inflammatory genes included interleukin, interferon and AA (arachidonic acid)-related genes. Functional testing demonstrated AA and E_2 interacted to super-additively induce apoptosis. Therefore, these data indicate that E_2-induced apoptosis via ERS and inflammatory responses in advanced antihormone-resistant breast cancer.

WORK ACCOMPLISHED: – Task 4a and 4b.

We have developed a series of MCF-7 variants that are either estrogen-dependent for growth [MCF-7:WS8 cells (8)], or resistant to estrogen deprivation (ED) and refractory [MCF-7:2A (37-39)] or sensitive [MCF-7:5C (1, 12, 36)] to E_2-induced apoptosis. To identify genes differentially regulated by E_2 specifically associated with apoptosis, we interrogated these models for changes in E_2-regulated global gene expression as a function of time using Agilent 4x44K oligonucleotide microarrays. We developed a new method termed dAUC (differential area-under-the-curve) analysis to identify genes that exhibited significantly altered regulation by E_2 across time specifically in the apoptosis sensitive 5C cells compared to both the estrogen-dependent WS8 and apoptosis refractory 2A cells. Examination of the identified 5C-specific genes and functional testing indicated that E_2 elicited ERS (endoplasmic reticulum stress) and inflammatory responses, which then led to apoptosis.

Cell Line Characterization. B efore gene expression profiling of WS8, 2A and 5C cells was conducted, we first confirmed the expected growth/apoptotic responses of these cell lines to E_2, biomarker status of ERα, PR, and HER2, and ER-regulated transcriptional activity (Fig. 32). The estrogen-dependent WS8 cells exhibited a 6.8-fold increase in growth after 7 days of 10^{-9} M E_2 treatment compared to control (no E_2) treatment (Fig. 32A). The estrogen deprivation-resistant

2A cells grew robustly in the absence of E_2 over 12 days. E_2 did not affect growth of the 2A cells over the first 6 days, but did inhibit growth beginning at day 7 through day 12 by 62.5% (Fig. 32B). Hence, the 2A cells exhibited an initial phase of E_2-independent growth followed by a second phase of E_2-inhibited growth. The resistant 5C cells continually proliferated in the absence of E_2 over 7 days. The DNA mass per well of the 5C cells also increased in the presence of E_2, but only for the first 4 days. It is important to note that within this period of apparent growth, E_2 caused subtle morphologic changes by day 2 and gross morphologic changes in the 5C cells such as rounding, blebbing and detachment from the plate by day 3 (Fig. 43D). In E_2-treated 5C cells, DNA mass per well steadily decreased from day 4 to day 7 such that by day 7, there was 5% less DNA then at day 1 of the experiment (Fig. 32C). Therefore, the 5C cells displayed a relatively rapid E_2-induced growth inhibitory response compared to the delayed growth inhibitory response in the 2A cells. We previously reported that these growth inhibitory responses to E_2 in 5C cells reflect induction of apoptosis (36).

Protein levels of ERα, PR and HER2 were characterized by semi-quantitative immunoblot analysis in the wild-type WS8 and ED-resistant 2A and 5C cells (Fig. 32D). Both 2A and 5C cells overexpressed ERα, 2A cells by 5.8-fold and 5C cells by 2.3-fold compared to WS8 cells. It is likely that derivation of the 2A and 5C cells under estrogen-free conditions selected for increased ERα expression since this would translate into an increase in unliganded ER activity to promote survival of the cells. Incubation of the cells with 10^{-9} M E_2 for 48h induced PR in WS8 and 2A cells, but not in 5C cells. Thus, WS8 and 2A cells were PR positive (37), whereas 5C cells were PR negative as previously reported (36). HER2 protein levels in control-treated cells were not substantially different in 2A and 5C cells versus WS8 cells, after correction for the loading control β-actin. Therefore HER2 was unlikely to have contributed to the development of ED-resistance in these cells.

ER transcriptional activity was evaluated using an ERE (estrogen responsive element) – regulated dual-luciferase reporter gene assay (40). Cells were transiently co-transfected with an ERE(5x)-TATA box driven firefly luciferase reporter plasmid and a basal TATA box-regulated renilla luciferase reporter plasmid. Cells were then treated with increasing concentrations E_2 for 24 h as indicated in Fig. 37E. Basal (control treatment) ERE-dependent transcriptional activity was 5.8-fold in 2A cells $P < 0.0001$), and 1.7-fold in 5C cells ($P = 0.001$) relative to control-treated WS8 cells (Fig. 37E). Hence, unliganded ER transcriptional activity was higher in the 2A and 5C cells and correlated with increased ERα protein levels (Fig. 37D). E_2 at 10-9 M stimulated ER-dependent transcriptional activity in both ED-resistant cell lines, to a greater extent in resistant 2A cells (22.5-fold) than in wild-type WS8 cells (15.4-fold), and to a lesser extent in resistant 5C cells (7.4-fold), in which E_2-induces apoptosis.

Gene Expression Microarrays and Differential AUC Analysis. To identify genes and pathways/processes associated with E_2-induced apoptosis, differential regulation of global gene expression in response to E_2 was interrogated in ED-resistant/apoptotic-sensitive 5C cells vs. estrogen-dependent WS8 and ED-resistant/apoptotic-refractory 2A cells. Each cell line was treated with 10-9 M E_2 or without E_2 (control) over a 96 h time course consisting of 7 time points

(2, 6, 12, 24, 48, 72, and 96 h). Each RNA sample in all three cell lines were quality controlled for expected induction of TFF1 (trefoil factor 1) and MYC mRNA expression in E_2-treated samples and for no induction in control-treated samples (Fig. 34-36). Gene expression was measured using 2-color Agilent 4x44k human oligonucleotide microarrays. Each individual E_2-treated RNA sample was competitively hybridized to an array against time-point matched and pooled control-treated RNA samples. Gene expression values were extracted from arrays as relative $\log_2$-ratios of E_2/control-treated cells. The AUC of each probe's profile was calculated as a measure of expression across time. The AUCs of each probe were then compared between all pairwise combinations of the 3 cell lines over the entire 2 - 96 time course, and to delineate relatively early and lates genes, over 2 - 24 h and 24 - 96 h time periods. To determine whether a gene's regulation by E_2 was significantly different between cell lines, a method termed differential AUC analysis was developed. In this method, the null hypothesis was there is no real difference in a probe's expression profile between the 2 cell lines being compared. If this is the case, then a probe's actual expression values can be permutated by pooling observed values from both cell lines, shuffling the values, and re-assigning them back to either cell line, all on a time point matched basis. This permutation of expression values was carried out a total of 20,000 times for every probe in each paired cell line comparison, followed by re-calculation of AUCs. This set of 20,000 permuted AUCs provided an estimate of how large and variable the differences in AUCs (or differential AUCs) can be when there is no real difference between the profiles. Then, a probe's profile was considered significantly different between the 2 cell lines being compared if the observed differential AUC was greater than that derived from all 20,000 permutations. This corresponded to a P-value = 0. A second requirement for significance was a probe's differential AUC must have exhibited an average $\log_2$ fold-change of 0.58 (1.5 on a linear scale) across a given time period.

To focus on genes associated specifically with E_2-induced apoptosis, genes were selected which were regulated significantly differently by E_2 in the 5C cells vs. both the WS8 and 2A cells as defined in the methods. A total of 1,142 genes were identified as significantly differentially regulated by E_2 specifically in the 5C cells. These genes were examined for over-representation of those mapping to a particular curated process (or pathway, network etc.) according to GeneGo's Metacore enrichment analysis functions. The top 10 enriched broad category biological processes are shown in Fig. 37A. As expected, estrogen signaling and apoptosis genes were significantly enriched. Within the apoptosis category, ERS was the most enriched subcategory (Fig. 37B). Inflammatory response genes were also enriched, and this was interesting because ERS and inflammatory stress have been linked mechanistically (41). The top scoring process was cell differentiation; yet our purpose was to elucidate how estrogen induces apoptosis. However, we do not discount that genes involved in cell differentiation can also play roles in apoptosis, and if so, those genes should have still been identified. A total of 350 of the 1,142 identified 5C-specific genes mapped to estrogen signaling, apoptosis, and inflammatory response. The relatedness of these 3 processes is illustrated by the Venn diagram in Fig. 37C, in which many of the identified 5C specific genes have overlapping roles.

Estrogen Signaling Genes. Estrogen signaling genes selectively regulated by E_2 in 5C cells relative to both WS8 and 2A cells that are discussed are shown in Fig. 38 (unless otherwise indicated). Examination of these genes reveals alterations at many levels in estrogen signaling during apoptosis such as covalent modification of ERα (SETD7), estrogen metabolism (CYP1B1 and HSD17B11), ERα-related growth factor signaling (AREG, CAV1, ERBB4, IGF1R, PIK3CB, and PIK3R1), ERα-regulated transcription via interactions with other transcription factors, [AR, CEBPB (Fig. 40), FOS, FOXO1, JUN, JUND, NR2F1/COUP-TF1, SMAD3, SP3, THRA/TRα, and XBP1 (Fig. 39)], repression of ERα RNA expression (INHBA, INHBB, RUNX2, SNAI1, ZN217), and ERα-regulated genes [ACOX2 (Fig. 40), BCL9, BMP7, ITGA2, MYBL1, RAB31, RET, RUNX2, VEGFA (vascular endothelial growth factor A) (Fig. 40)]. These genes may modulate estrogen signaling by the following means: SETD7 methylates ER to stabilize the protein, and SETD7 was down-regulated by E_2 selectively in 5C cells which would lead to accelerated E_2-induced ERα protein degradation. In support of this, ERα was expressed at higher levels in 5C cells than WS8, yet E_2 down-regulated the protein to similar levels in both cell lines (Fig. 32D). CYP1B1 and HSD17B11 were up-regulated by E_2 in 5C cells, which is logical since these enzymes metabolically eliminate E_2 to remove the apoptotic signal. The ER co-activator NCOA3 (also AIB1/SRC3) was up-regulated, and facilitates ligand-dependent and independent ER activation. Importantly, we recently found that AIB1 was required for E_2-induced apoptosis in 5C cells (See #16 in Appendix). Multiple transcription factors with which ERα interacts were up-regulated by E_2 in 5C cells including JUN, JUND, FOS, SP3 and SMAD3. Thus, ERα could potentially differentially target a wide array of genes via these factors, and in particular, JUN, JUND and FOS form AP-1 complexes which play roles in apoptosis as discussed later. AR failed to down-regulate in response to E_2 in 5C cells compared to WS8 and 2A cells. Since non-aromatizable androgens can inhibit E_2-stimulated growth of MCF-7 cells (42), AR may have been opposing ERα activity in 5C cells to dampen the apoptotic signal. ERα transcriptional activity can also be suppressed by activin, a TGFβ family member, in MCF-7 cells (43). E_2 induced INHBA (inhibin β A subunit) selectively in 5Cs, while repressing INHA (inhibin α subunit) in all cell lines (not shown) to promote INHBA homodimerization which constitutes Activin A. Several transcription factors were up-regulated that repress ERα RNA expression, i.e. FHL2, SNAI1 (Snail 1), and ZNF217; or compete with ERα for binding extended ERE half-sites, i.e. NR2F1/COUP-TF1 and THRA/TRα. FHL2 (44, 45) and SNAI1 (Snail 1) are also interesting since it promotes epithelial-to-mesenchymal transition, and EMT-related genes were enriched in the 5C-specific gene dataset (Fig. 37B). TGFβ signaling promotes EMT, and E_2 selectively up-regulated in 5C cells the TGFβ pathway-related genes BMP7, RUNX2 and SMAD3. Interestingly, the growth factor BMP7 can stimulate expression of the transcription factor RNX2 (46), which plays a key role in osteoblast differentiation, and RNX2 can interact with SMAD3 (47), forming a potential pathway. PI3K (phosphatidylinositol-3-OH kinase) activates Akt and thereby promotes cell survival, but PI3K's catalytic subunit PIK3CB was down-regulated while its regulatory subunit PIK3R1 was up-regulated by E_2 in 5C cells, suggesting suppression of this survival pathway during E_2-induced

apoptosis. The receptor tyrosine kinase and proto-oncogene RET (rearranged during transfection) was preferentially down-regulated by E_2 in 5Cs. Interestingly mutations in RET are associated with multiple endocrine neoplasia. Hence E_2 suppressed another proliferation/survival pathway. Taken together, E_2-bound ERα was likely antagonized by several incoming pathways to restrain the apoptotic signal, while outgoing pathways from E_2-bound ERα likely suppressed survival and promoted features of EMT (epithelial-mesenchymal transition) in contrast to its normal functions, promoting survival and enforcing epithelial differentiation.

Apoptosis Genes. Apoptosis genes selectively regulated by E_2 in 5C cells relative to both WS8 and 2A cells that are discussed are shown in Fig. 38. Additional enrichment analysis indicated ERS-mediated apoptosis as the top scoring individual pathways comprising the apoptosis category (Fig. 38B). Folding of secreted, membrane bound, and some organelle-target proteins occurs in the endoplasmic reticulum. To promote optimal protein folding, important enzymatic steps and molecular chaperones involved in this process require several factors such as ATP (adenosine triphosphate), calcium (Ca^{2+}) and an oxidizing environment. Protein folding often occurs in an ATP-dependent manner, many chaperones require Ca^{2+} as a bound cofactor, and formation of disulfide bonds requires and an oxidizing environment. When cellular stresses perturb energy levels, the redox state, or the Ca^{2+} concentration, accumulation of unfolded proteins and protein aggregation occurs; this condition is referred to as ERS. To relieve ERS, an UPR (unfolded protein response) is triggered to clear the unfolded proteins and export them to the cytosol for degradation. The UPR is initiated by a key chaperone termed HSPA5/GRP78/BiP (heat shock 70kDa protein 5; glucose-regulated protein, 78kDa; immunoglobulin heavy chain-binding protein). GRP78 not only binds unfolded proteins to facilitate proper folding, but also binds the luminal domains of endoplasmic reticulum transmembrane receptors, preventing their oligomerization. When unfolded proteins accumulate, GRP78 is released from binding the transmembrane receptors, allowing them to oligomerize and autophosphorylate to initiate a UPR signal. Although some unfolded proteins may also directly bind and activate the transmembrane receptors. The critical endoplasmic reticulum transmembrane receptors include EIF2AK3/PERK (eukaryotic translation initiation factor 2-alpha kinase 3; protein kinase-like endoplasmic reticulum kinase), IRE1α/ERN1 (endoribonuclease inositol-requiring enzyme-1α; endoplasmic reticulum to nucleus signaling 1) and ATF6 (activating transcription factor 6). The UPR signals to attenuate protein translation, induce expression of additional chaperones, and export misfolded proteins to the cytosol for ubiquitylation and proteasome-mediated degradation. If the UPR fails to relieve the stress, the function of the UPR switches from promoting cell survival to promoting cell death. Thus, excessive or prolonged ERS typically induces apoptosis (48).

Stimulation of hormonally responsive cells by E_2 leads to global increases in nascent polypeptides which require folding. In WS8, and to a lesser extent in 2A clls, an increased need for protein folding in response to E_2 stimulation was indicated by induction of multiple UPR genes including GRP78 and XBP1 (X-box binding protein 1), a transcription factor which up-regulates many UPR genes including GRP78. However, GRP78 and XBP1 failed to increase in response to E_2 in 5C cells compared to WS8 and 2A cells. The lack of GRP78 and XBP1

induction in 5C cells may indicate a deficiency in mounting a survival UPR, which would lead to pronounced accumulation of unfolded/misfolded proteins. A deficiency in mounting a survival UPR was also indicated by decreased levels in 5C cells of MBTPS1/S1P (membrane-bound transcription factor peptidase, site 1), which cleaves ATF6 to activate its translocation to the nucleus where it induces transcription of UPR genes such as XBP1. Thus decreased S1P in 5C cells compared to WS8 and 5C cells may have contributed to the attenuated induction of XBP1 in 5C vs. WS8 and 2A cells. As a cascade effect of decreased XBP1, its target genes would also show a lack of induction, as observed for HERPUD1/HERP1 (homocysteine-inducible, ERS-inducible, ubiquitin-like domain member 1) and DERL1 (degradation in endoplasmic reticulum protein 1) in 5C cells compared to WS8 and 2A cells. These factors promote degradation of endoplasmic reticulum-resident proteins, and hence decreased expression of HERP1 and DERL1 would lead to reduced clearance of unfolded/misfolded proteins. A deficiency in the UPR in 5C cells was further indicated by a failure to increase protein folding genes localized to the endoplasmic reticulum including ERO1L, FKBP10, PDIA6, and UGGT1. But the deficiency in protein folding was not limited to the endoplasmic reticulum, as cytoplasmic protein folding genes were also down-regulated in 5C cells vs. WS8 and 2A cells including HSP90AB1/HSP90B, PPIAL4A, and PPIF. A global inhibition of protein translation was indicated in E_2-treated 5C cells. In 5C compared to WS8 and 2A cells, E_2 rapidly (within 24 h) up-regulated DNAJC3/p58IPK (protein kinase inhibitor p58). p58IPK binds to and inactivates EIF2AK3/PERK, leading to reduced global translational initiation (41). Several aminoacyl tRNA synthetases and interacting factors also failed to increase in response to E_2 in 5Cs including AIMP1, CARS, LARS (not shown), SARS (not shown), and YARS. Other translational factors which failed in induce in 5C cells include EEF1A1, EEF2K, ETF1, GSPT1/ERF3A, and PABPC4. Taken together, we propose that 5C cells were deficient in folding polypeptides and degrading mal-folded proteins in response to E_2, resulting in pronounced unfolded protein accumulation.

ERS has been implicated in the regulation of lipogenesis involving fatty acid synthesis and cholesterol metabolism. Under physiological levels of ERS, the UPR can increase lipogenesis, but under severe ERS, the UPR can shut down lipogenesis as cells commit to death (41). This was likely the case in E_2-treated 5C cells which showed a lack of induction of critical genes involved in fatty acid synthesis, including ACLY (ATP citrate lyase), SCD/ACOD [stearoyl-CoA desaturase (Δ-9-desaturase); acyl-CoA desaturase], ELOVL1 (elongation of very long chain fatty acids-like 1). ACLY is the primary enzyme responsible for synthesis of acetyl-CoA, the basic building block of fatty acids. SCD introduces a C-C double bound in a spectrum of fatty acyl-CoA substrates including stearoyl-CoA and palmitoyl-CoA; this is key step in producing monounsaturated fatty acids. ELOVL1 condenses both saturated and monounsaturated fatty acids. Interestingly, SCD and ELOVL1 are localized to the endoplasmic reticulum membrane.

In response to ERS, specific BCL2 and BH3-only family members are targeted (48). BCL2 family members possess either pro- or anti-apoptotic activities. Prototypical BCL2 inhibits

cell death by binding and inactivating pro-apoptotic members such as BAX. BH3 (Bcl-2 homology domain 3) -only containing proteins, such as BCL2L11 (BIM, BCL2 interacting mediator of cell death) indirectly activate BAX by binding BCL2 (via the BH3 motif), thereby releasing BAX from the complex. BAX then permeabolizes the mitochondrial outer membrane allowing cytochrome C release to the cytoplasm (49). Under ERS conditions, BAX also interacts with and activates IRE1α. IRE1α then signals to JNK (Jun N-terminal kinase) to simultaneously activate BIM and inhibit BCL2 (50). BIM is implicated in ERS as a variety of inducers of such stress stimulate BIM expression, and BIM is essential in this form of apoptosis in a wide range of cell types (51). This pathway was likely activated by E_2 in 5C cells. E_2 repressed MAPK10 (JNK3) in WS8 and 2A cells, but not in 5C cells indicating higher JNK3 activity in 5C cells. Meanwhile, E_2 selectively up-regulated pro-apoptotic BAX and BIM in 5C cells compared to WS8 and 2A cells. Another BH3-only protein HRK (harakiri) was also upregulated by E_2 in 5C cells, and may have contributed to apoptosis in a similar manner as BIM by promoting BAX activity. Noteworthy, BCL2 remained low in E_2-treated 5C cells compared to its induction in E_2-treated WS8 cells. Yet it was not listed as a 5C-specific gene since BCL2 was lower still in E_2-treated 2A cells compared to 5C cells (Fig. 41). We have previously verified the importance of BAX and BIM by showing that E_2 induced these genes at the protein level in 5C vs. WS8 cells, and that siRNA-mediated knockdown of BAX and BIM dramatically blocked E_2-induced apoptosis by 76% and 85%, respectively, compared to control (1). We further demonstrated that E_2 led to loss of mitochondrial membrane potential (integrity) and caused cytochrome C release into the cytoplasm in 5C cells (1). Therefore, ERS, together with mitochondrial stress, likely led to apoptotic cell death.

Additional pro-apoptotic genes selectively induced by E_2 in 5C cells including CXXC5/CF5, DAPK2/DRP-1, DDIT4/REDD1/RTP801, LGALS1/Galectin 1, and PDCD7/ES18. CF5 induces p53 and apoptosis in response to DNA damage (51). DAPK2/DRP-1 is a Ca^{2+}/calmodulin-regulated Ser/Thr death kinase that mediates membrane blebbing during apoptosis (52). LGALS1 causes flipping of phosphatidylserine to mark cells for phagocytosis (53), and sensitizes MCF-7 cells to apoptosis in conjunction with additional stress stimuli (54). DDIT4/REDD1 is induced by oxidative stress and DNA damage, and its induction involves CEBPB (55), another E_2-up-regulated 5C-specific gene (Fig. 40). PDCD7 is also induced by oxidative stress (56), and its overexpression can provoke apoptosis (57).

Following prolonged ERS, specific caspases are activated to enact cell death. Examination of the 5C-specific differentially regulated genes revealed that, of the caspases, only CASP4 met the stringent significance criteria. CASP1, CASP5 and CASP8 also showed up-regulation in 5C cells, but did not meet the significance requirements (Fig. 41). CASP4 belongs to the inflammatory subgroup of caspases, along with CASP1 and CASP5 in humans (58). These caspases are termed 'inflammatory' because the founding member CASP1 proteolytically activates proIL-1β and proIL-18, cytokines which play critical roles in inflammation (58). CASP4 specifically localizes to the endoplasmic reticulum, undergoes cleavage in response to ERS-inducing agents but not other apoptotic agents, and its depletion by siRNA can prevent

endoplasmic stress-induced apoptosis in multiple model systems (59-63). Therefore CASP4 may be vital for ERS-induced apoptosis. Importantly, CASP4 auto-activates by dimerizing and undergoing interdomain cleavage (64), and thus, simply overexpressing this caspase is sufficient to cause apoptosis (65). CASP4 can also be activated by other proteases, such as calpain under ERS (66), and CAPN12 and CAPN13 were selectively up-regulated in 5C cells.

Inflammatory Response Genes. Inflammatory response genes selectively regulated by E_2 in 5C cells relative to both WS8 and 2A cells that are discussed are shown in Fig. 40. In 5C cells, E_2 elicited up-regulation of many pro-inflammatory cytokine/cytokine receptors including, CSF3/GCSF (colony stimulating factor 3; granulocyte), IL4R (interleukin 4 r eceptor), IL6R, IL6ST/gp130 (IL6 signal transducer), IL17RD/Sef (IL17 receptor D), IL22RA1 (IL22 receptor, alpha 1), IL29/IFNL1 (interleukin 29; interferon lambda 1), and VEGFA. IL4R was induced with early kinetics, indicating it may be a primary response. IL6R was up-regulated shortly after IL4R, while gp130, also an IL4R subunit, was already up-regulated at 2 h. Hence IL6 signaling was likely activated in 5Cs. IL17RD/Sef not only mediates IL17 signaling, its overexpression also leads to JNK activation and apoptosis (67), which links inflammatory responses and ERS. GCSF (granulocyte colony-stimulating factor) and VEGFA are well known as growth and angiogenic factors, respectively, but they can also participate in inflammation. GCSF and VEGFA reciprocally transphosphorylate VEGF-R2 (vascular endothelial growth factor receptor 2) and GCSF receptor, respectively, leading to activation of pro-inflammatory p38 MAPK (68). VEGFA also leads to activation of p38 MAPK and JNK in tamoxifen-resistant MCF-7 cells (69). An interferon response was likely activated since the interferon IL29/IFNL1 and the interferon-responsive genes, IFI6 (interferon, alpha-inducible protein 6), IFI16 (interferon, gamma-inducible protein 16) were up-regulated. CASP4 can also be induced by interferon (70).

A number of inflammatory markers were up-regulated by E_2 specifically in 5C cells including ADM (adrenomedullin), CEBPB (CCAAT/enhancer binding protein (C/EBP), beta), CP (ceruloplasmin, ferroxidase), ITGB2/CD18 (integrin, beta 2; complement component 3 receptor 3 and 4 subunit), LTB/TNF-C (lymphotoxin beta; TNF superfamily, member 3), NTN1 (netrin 1). Some of these markers and other inflammatory genes already mentioned, such as CP, IFI16, IL29/IFNL1, and LTB, showed dramatic increases in expression following 72 h of E_2 exposure indicating these changes may be secondary inflammatory responses. Other inflammatory genes were selectively up-regulated in 5C cells with relatively early kinetic, indicating a more mechanistic role, such as CEBPB, ITGB2, NTN1, and UNC5C. CEBPB plays in important role in induction of IL-6, is activated by ERS (71), is required for nuclear import of CHOP/GADD153 (CAAT-binding homologous protein) in ERS (72), and enhances NFκB signaling (73, 74). ITGB2 is a leukocyte adhesion molecule, but also signals to activate NFκB to induce TNF and other inflammatory cytokines in response to lipopolysaccharide (75). NTN1 is a secreted factor and serves as an inflammatory marker, but protects tissues from inflammatory injury by suppressing cytokine production, repulsing leukocyte infiltration, and acts as an anti-inflammatory and anti-apoptotic ligand of its receptors DCC (deleted in colorectal cancer) and the UNC-5 family members (76). Interestingly, E_2 rapidly down-regulated UNC5C in WS8 and

2A cells within 6 h, but failed to do so resulting in higher UNC5C expression in 5C cells. UNC5C may have a pro-inflammatory role as synovial cells from patients with rheumatoid arthritis and osteoarthritis overexpress UNC5C (769-fold) compared to those of healthy donors (77). The co-ordinated up-regulation of NTN1 and UNC5C indicates an active pathway. In the context of E_2-induced apoptosis, NTN1 may have been up-regulated to limit or resolve the inflammatory response, possibly by neutralizing UNC5C. Since NTN1 is secreted, it has potential to be developed as a circulating marker of E_2 response in the clinic. Further, NTN1 may be selective to E_2-induced apoptosis and therefore targeted blockade of NTN1 activity could potentially increase clinical response rates to E_2 without engaging systemic inflammatory responses.

Arachidonic acid [AA; 20:4n-6)] is a 20-carbon ω-6 PUFA (polyunsaturated fatty acid) with 4 C-C double bonds that plays a key role as an inflammatory mediator. Enzymes involved in AA biosynthesis were up-regulated by E_2 in 5C cells such as FADS1 (fatty acid desaturase 1, Δ-5 desaturase), FADS3 (Δ-6 desaturase), PLA2G10 (phospholipase A2, group X), and PLCD3 (phospholipase C, delta 3). AA is synthesized from the ω-6 PUFA linoleic acid (LA; 18:2n-6). FADS3 and FADS1 catalyze the first and last steps in AA biosynthesis by introducing C-C double-bonds in LA producing gamma-linolenic acid (GLA; 18:3n-6), and in dihomo-γ-linolenic acid (DGLA; 20:3n-6) producing AA, respectively. PLA2s hydrolyze phospholipids releasing AA, while PLCs cleave AA from diacylglycerol (DAG). Other 5C up-regulated enzymes which feed into AA production were MGLL/MAGL (monoglyceride lipase; monoacylglycerol lipase), PPAP2A/LPP1 (phosphatidic acid phosphatase type 2A; lipid phosphate phosphohydrolase 1), and SGMS1/SMS1. MGLL converts manoacylglycerides such as 2-arachidonoylglycerol to free fatty acids including AA. PPAP2A/LPP1 converts phosphatidic acid to DAG, and SGMS1/SMS1 converts ceramide plus phosphatidylcholine into sphingomyelin plus DAG. Thus both of these enzymes produce DAG, providing increased substrate levels for PLCD3 to release AA. ACOX2 (acyl-CoA oxidase 2, branched chain) was rapidly selectively induced within 12 h by E_2 in 5C cells, and ACOX2 can be induced by LA (78). This suggests that the induced ACOX2 expression reflected a possible E_2-induced rise in LA concentrations in 5C cells needed to produce AA. As an inflammatory mediator, AA is utilized as a precursor by COX (cyclooxygenase) and LOX (lipoxygenase) to generate inflammatory prostaglandins and leukotrienes, respectively. The COX pathway was unlikely to have been employed in E_2-induced apoptosis since PTGES (prostaglandin E synthase) was down-regulated in 5C cells compared to WS8 and 2A cells. In hormone-dependent breast cancer cells, E_2 is known to induce PTGES (prostaglandin E synthase) expression via an ERE, which may promote breast cancer proliferation since the increased prostaglandin E_2 may enhance aromatase expression and further promote local productions of estrogens (79). Thus, a failure to induce PTGES may ultimately have served to prevent any potential increases in estrogen concentrations in 5C cells. Considering that ERS likely led to a block of fatty acid synthesis and conversion to monounsaturated fatty acids (i.e. no induction of ACLY and SCD), the selective increases in

AA-related genes indicate the importance of AA in promoting an inflammatory response in E_2-induced apoptosis.

As mentioned previously, ERS and inflammatory pathways intersect. The key ERS genes IRE1α, ATF6, and PERK can all activate NF-κB, which serves as a master regulator of inflammatory response gene transcription (41). NFκB is well known as a pro-survival factor, yet depending on context, it also promotes apoptosis. The NF-κB family consists of 5 members defined by Rel homology domain, NFKB1 (p105/p50), NFKB2 (p100/p52), REL/c-Rel (p65), RELA, and RELB. NFKB1 and NFKB2 are initially synthesized as p105 and p100 precursor proteins, which then undergo maturation to the smaller proteins p50 and p52, respectively. The NF-κB members form homo- and heterodimers in various combinations to regulate distinct subsets of genes. In canonical NF-κB signaling, RELA-containing dimers are retained in the cytoplasm in a latent state by IκBs (inhibitor of NF-κB). Upon an inflammatory stimulus (IL-1, TNF (tumor necrosis factor), others), IKKs (IκB kinase) and predominantly IKKβ, phosphorylate IκBs to signal IκB ubiquitination and degradation, which releases NFκB dimers to translocate to the nucleus. In non-canonical NF-κB signaling, a subset of NFκB-induction stimuli such as by LTB, activate MAP3K14/NIK (NFκB inducing kinase), which in an IKKα-dependent manner, leads to phosphorylation of p100 to promote its processing to p52. The mature p52 then heterodimerizes with RelB, and together translocate to the nucleus to regulate a set of genes distinct from canonical NF-κB complexes (80).

REL was already down-regulated in 5C cells by the first time point at 2 h, and remained so for 48h. Meanwhile, NFKBIZ/IκBζ (NF-kappa-B inhibitor zeta; I-kappa-B-zeta) was selectively up-regulated in 5Cs within 24 h of E_2 exposure. Consistent with kinetics observed here, IκBζ has been shown to be an inflammatory primary response gene that associates with NFκB p50 homodimers in the nucleus to direct transcription of a subset of secondary response genes (41). Additional genes which activate NFκB signaling were also selectively induced by E_2 in 5C cells including BCL10, CXXC5, and LTB. BCL10 is required for both canonical and non-canonical NFκB signaling (81). CXXC5, which as mentioned induces p53 (51), also activates NFκB (82). LTB, as previously mentioned, activates the non-canonical NFκB pathway (80). Also, many of the identified cytokine/cytokine receptors can activate NF-κB pathways. Further, multiple 5C-specific genes have been shown as NFκB responsive including BIM (83, 84), CASP4 (85), CEBPB (86), CP (87), NTN1(88) and VEGFA (89). Moreover, ERα and NFκB can interact to transcriptionally regulate promoters, providing a direct mechanism for E_2 to target a diverse array of inflammatory and apoptotic genes. Therefore, NFκB signaling was very likely involved in E_2-induced apoptosis, and we are pursuing this hypothesis in future studies.

ERS intersects with inflammatory responses not only through NFκB, but also via JNK activated by IRE1α and PERK. JNK then phosphorylates AP-1 transcription factor complexes to switch on expression of inflammatory response genes (41). AP-1 complexes are heterodimers composed of various combinations of JUN, JUND and FOS subunits, and as previously mentioned, all of which were selectively induced by E_2 in 5C cells, with significant FOS

induction within 24 h (Fig. 38). As in the case of NFκB, ERα interacts with AP-1 complexes in promoters and provides a means for ERα to target AP-1-regulated genes.

Functional Involvement of AA and CASP4 in E_2-induced Apoptosis. The involvement of endoplasmic reticulum and inflammatory stresses in E_2-induced apoptosis was functionally examined. First, whether E_2-induced apoptosis could be promoted by the AA was tested. AA was chosen because 1) it is widely recognized as a pro-inflammatory agent; 2) it induces apoptosis (90), likely at least in part by depleting the endoplasmic reticulum of Ca^{2+} thereby inhibiting protein folding and eliciting ERS (91); 3) it can activate NFκB in mammary epithelial cells (92); and 4) several genes which increase AA levels, e.g. FADS1 and PLA2G10, were up-regulated in response to E_2 in 5C vs. WS8 and 2A cells (Fig. 40). 5C cells were exposed to varying concentrations of both AA and E_2 in a factorial design, and then apoptosis was measured by YO-PRO-1 and 7AAD staining and flow cytometry (Fig. 42A). Since E_2-induced apoptosis occurs maximally with 10^{-9} M E_2 after 96 h of exposure, E_2 was used at very low concentrations of 2.5 and 5 × 10-11 M, and apoptosis was assayed at 72 h to allow observation of potential AA effects. The combination of AA plus E_2 at all varied concentrations increased the percentage of apoptotic plus dead cells in a greater than additive manner relative to either agent alone. Fitting the data to a multiple regression model showed the rate of increase (slope) in apoptotic plus dead cells progressively and significantly increased when comparing E_2 alone vs. E_2 + 10 μM AA vs. E_2 + 20 μM AA. Therefore, AA and E_2 showed a statistical interaction indicating functional involvement of AA in E_2-induced apoptosis.

We sought to validate the importance of CASP4 by evaluating a panel of irreversible caspase peptide inhibitors selectively targeting caspases 1 through 9 (except caspase-3 which is not expressed in MCF-7 cells (93). 5C cells were treated with 10^{-9} M E_2 plus each CASP inhibitor as indicated for 96 h to induce apoptosis, which was measured by altered plasma membrane permeability (Fig. 42B). The broad spectrum caspase inhibitor z-VAD-fmk was used as a positive control, since we previously reported this inhibitor completely blocks E_2-induced apoptosis (1), while the inactive inhibitor z-FA-fmk was used as a negative control. In an effort to prevent off-target caspase inhibition, the blockers were used at 10 μM, which was the concentration that reduced apoptosis by approximately one-half rather than complete inhibition by the pan inhibitor z-VAD-fmk. The most active inhibitor was the CASP4 blocker z-LEVD-fmk, which was slightly more effective than the pan CASP inhibitor. The CASP8 inhibitor z-IETD-fmk was the next most active blocker, but was significantly less potent than z-LEVD (P-value = 0.0026). Therefore, in an unbiased comparison of caspases 1 through 9, CASP4 was validated as functionally critical in E_2-induced apoptosis.

The functional activity of CASP4 was further studied. Real-time qPCR and immunoblotting confirmed induction of CASP4 expression at the mRNA and protein levels, respectively, occurred specifically in 5C cells in response to E_2 (Fig. 43A-B). Importantly, in 5C cells z-LEVD at 20 μM completely blocked E_2-induced PARP cleavage (Fig. 43B), reversed E_2-inhibited growth (Fig. 43C), and prevented morphologic alterations associated with apoptosis in 5C cells. Since z-LEVD-fmk was used at 20 μM rather than 10 μM, we do not discount the

possibility that some caspases in addition to CASP4 were also inhibited and that other caspases could still play an important role. Yet these data establish a critical role for CASP4 in E_2-induced apoptosis.

Methods

Cell Lines and Compounds. MCF-7:WS8 human breast cancer cells were clonally selected from MCF-7 cells for sensitivity to E_2-stimulated growth (36-38) and employed here as the wild-type estrogen-dependent reference cell line. Estrogen deprivation (ED)-resistant MCF-7:2A (37-39) and MCF-7:5C (1, 12, 36) human breast cancer cells were also clonally selected from MCF-7 cells for maximal growth under long-term estrogen-free conditions. Wild-type WS8 cells were maintained in fully-estrogenized media [phenol red-containing RPMI-1640 and 10% whole FBS (fetal bovine serum), supplemented with 6 ng/ml insulin, 2 mM glutamine, 100 μM non-essential amino acids, and 100 U of penicillin and streptomycin per ml], while 5C and 2A cells were maintained in estrogen-free medium (phenol red-free RPMI-1640 plus 10% dextran-coated charcoal-stripped FBS and the same supplements as for fully-estrogenized medium) as previously described. Cells were maintained at 37° C in a humidified 5% CO_2 atmosphere. Wild-type WS8 cells were switched to estrogen-free media for 3 days before all experiments. E_2 and DES (diethylstilbestrol) were from Sigma-Aldrich. FUL (Fulvestrant; also termed ICI 182,780, Faslodex) was from Tocris. All cell culture reagents were from Invitrogen. Caspase substrate peptide inhibitors of the generalized sequence z-XXXX-FMK (z, benzyloxycarbonyl; X, any amino acid; FMK, fluoromethyl ketone), were from Biovision. The peptides are derivatized as methyl esters to promote cell permeability and to FMK, which irreversibly inhibits the caspase by alkylating a cysteine residue in the catalytic site. All test agents were added to culture medium at 1:10,000 to 1:1,000 (v/v).

Cellular Proliferation. Cellular proliferation was assessed according to DNA mass per well using Hoechst 33258 (Invitrogen) as previously described (1). WS8 and 5C cells were seeded at 15,000 and 20,000 cells per well, respectively, in 24-well plates and allowed to grow for 7 days. 2A cells were seeded at 30,000 cells per well in 6-well plates and allowed to grow for 12 days. Cells were treated without (control) or with 10^{-9} M E_2 every other day.

Immunoblot Analyses. Whole cell protein lysates were prepared and immunoblotted using 40 μg protein per lane as previously described (40) Membranes were probed using antibodies against ERα (AER6111; Lab Vision), HER2 (EP1045Y; Epitomics), PgR (YR85; Epitomics), CASP4 (CAS4; Sigma-Aldrich), PARP (46D11; Cell Signaling Technology), β-actin (AC-15; Sigma-Aldrich) and GAPDH (14C10; Cell Signaling Technology). Blots were visualized and quantified using the Odyssey Infrared Imaging System (Li-Cor Biosciences). Protein units in figures reflect the relative level of the target protein normalized to the endogenous control protein.

ERE (Estrogen-response Element) Dual-luciferase Assays. ERE dual-luciferase assays were conducted by transfecting cells with an ERE(5x)-regulated (pERE(5x)TA-ffLuc) firefly luciferase expression plasmid, and co-transfected with a basal TATA promoter-regulated (pTA-srLuc) *Renilla* luciferase expression plasmid as previously described (40).

Apoptosis Analysis by Cell Membrane Permeability Assay. The percentage of apoptotic cells was determined based on altered plasma membrane permeability to the nucleic acid stains YO-PRO-1 and 7AAD and analyzed by flow cytometry. Using these dyes, viable cells stain weakly, apoptotic cells stain moderately, and dead (necrotic) cells stain strongly. Adherent cells were harvested by trypsinization and combined with floating cells. Cells were suspended to ~300,000 cells per 300 µl in complete estrogen-free media (containing serum), and incubated with 100 nM YO-PRO-1 (Invitrogen) plus 1 µg/ml 7AAD (7-aminoactinomycin D; Invitrogen) at 37° C for exactly 60 m. Immediately afterwards, cells were kept on ice, and then analyzed using a BD LSR-II flow cytometer (BD Biosciences). Stains were excited using a 488 nm laser, and detected using 530 nm (YO-PRO-1) and 670 nm (7AAD) bandpass filters. Spectral compensation between dyes was accomplished using single-stained cells. Sequential gating of the relevant FSC-A (forward scatter-area) vs. FSC-H (height) and FSC-H vs. SSC-A (side scatter-area) population subsets allowed for the selection of single cells. Data were analyzed using FloJo 7.6.1 for Windows (Tree Star).

RNA Sample Generation for Microarray Analysis. WS8, 2A, and 5C cells were seeded at 2, 4, and 5 million cells per 15 cm plate, respectively, in estrogen-free media. Cells were parsed into 2 groups of 6 replicate plates per treatment per time point, and then treated with either 0.1% ethanol (control) or 10^{-9} M E_2 for 2, 6, 12, 24, 48, 72, and 96 h. At 48h, media of remaining cells was replenished. Cells were harvested for RNA using TRIzol. In full, 252 samples were collected. Total RNA was isolated as previously described (94). RNA samples were controlled for purity and integrity using an Agilent Bioanalyzer by requiring each sample to exhibit an RIN number of 9.8-10.0.

Real-time Quantitative Polymerase Chain Reaction (qPCR) Assays. Real-time qPCR was conducted as previously described (41). Target mRNA levels were normalized to PUM1 [pumilio homolog 1 (Drosophila)] mRNA levels (95). Data were analyzed by comparison to a serial-dilution series of WS8 cell cDNA. PCR primer sequences were as follows: PUM1 forward 5'-AAT GCA GGC GCG AGA AAT-3', PUM1 reverse 5'-TTG TGC AGC TGA GGA ACT AAT GA-3, PUM1 probe 5'-[6FAM]-CCT GTT CGA CTT GTA GCT CCT GCC CC-[BHQ1]-3'; MYC forward 5'-GCC ACG TCT CCA CAC ATC AG-3', MYC reverse 5'-TCT TGG CAG CAG GAT AGT CCT T-3', MYC probe 5'-[6FAM]-ACG CAG CGC CTC CCT CCA CTC-[BHQ1]-3'; TFF1 forward 5'-CAT CGA CGT CCC TCC AGA AGA G-3', TFF1 reverse 5'-CTC TGG GAC TAA TCA CCG TGC TG-3', (no probe for TFF1); CASP4 forward 5'-TTT CCT GGC AAT TGA AAA TGG-3', CASP4 reverse 5'-AAG GTG CTC CTT GAA GTT GAT TAA G-3', CASP4 probe 5'-[6FAM]-AGC CAC AAG CAG CCC AGC CCT-[BHQ1]-3'.

Gene Expression Microarrays. Gene expression profiling was carried out using 2-color Agilent 4x44k Whole Human Genome oligonucleotide microarrays (Palo Alto, CA). RNA labeling, hybridization to the arrays, and quality assessment of hybridizations were performed using protocols recommended by Agilent Technologies as previously described (94). Each individual E_2-treated RNA sample was competitively hybridized against a time point-matched control-treated reference RNA, which consisted of a pool of equal amounts of RNA from 6 replicate control-treated samples (in some cases 5 samples if a sample could not be validated). Individual E_2-treated RNA samples were labeled with Cy3, and control-treated RNA reference pools were labeled using Cy5. All replicate Cy3 samples were competitively hybridized against the same reference pool within each time point. Raw data were extracted, processed and normalized using Agilent's Feature Extraction (FE) software (v10.7) as previously described (94). After applying a set of array hybridization QC criteria (94), 6 arrays were excluded from further analysis – as a result, four of the 21 (cell line/time point) combinations had five replicate array, one had four replicate arrays, and the remaining 16 combinations had six replicate arrays each; in total 120 arrays.

Several steps were taken to minimize variability across this large gene expression microarray series. The cell line treatment series were conducted consecutively (WS8, followed by 5C, followed by 2A). Within each cell line series, the same lot numbers of Qiagen RNeasy kits, Agilent arrays, gasket backings, Cy-dyes labeling kits, hybridization kits and wash buffers were used. All arrays were washed in an ozone-controlled environment (<0.1 ppb). Samples representing replicate (cell line/time point) assays were hybridized to different arrays to minimize any chip to chip variation across replicates.

Differential AUC Analysis. The expression measurements used in all analyses were the *LogRatio* ($\log_2$-ratio) values produced by Agilent's FE software. Prior to analysis, identical probes appearing on multiple spots were replaced by their first occurrence, and probes lacking a valid Entrez identifier (based on Bioconductor annotation) were omitted. Probes which were absent (those with signals indistinguishable from background as defined by FE software) in both channels across all arrays involved in the comparison of interest were removed. Probes which were flagged by FE as "non-uniformity outliers" in any of the replicate arrays were also removed.

For a given cell line (WS8, 2A, 5C) and probe, a measure of the effect of E_2 treatment over all or part of the time-course is given by the area under the $\log_2$-ratio profile over the time period of interest. Let x_{ijk} be the observed $\log_2$-ratio for probe p for cell line i, time t_j ($t_1 = 2,\ldots,$ $t_7 = 96$), and replicate k (where k ranges from 1 to the total number of replicate arrays for cell line i, and time t_j (six, in most cases)), and let x_{ij} be the average $\log_2$-ratio across replicates. Then the area AUC_i under the $\log_2$-ratio profile can be calculated as a sum of trapezoidal areas:

$$AUC_i = \sum_{j=1}^{6} \frac{(t_{j+1} - t_j)(x_{ij\cdot} + x_{i(j+1)\cdot})}{2}$$

This area can be positive or negative, reflecting respectively a net up- or down-regulation with E_2 treatment across the time-course. The difference $\boldsymbol{\Delta}_{obs}^{ij} = AUC_i - AUC_j$ (or differential AUC) provides a measure of differential regulation between two cell lines *i* and *j* across the full time-course. To assess the statistical significance of this difference, we generate a reference distribution for each probe for Δ under the null hypothesis that the true differential AUC is 0: we repeatedly (n = 20,000) permute the cell line labels within each time point and calculate Δ_{perm} for each reordering. The two-sided *P*-value of the test is the proportion of permutations for which the absolute value of the calculated Δ_{perm} exceeds the absolute value of $\boldsymbol{\Delta}_{obs}^{ij}$. Only those probes whose observed $\boldsymbol{\Delta}_{obs}^{ij}$ value (or differential AUC value) exceeded all 20,000 resampled Δ_{perm} values (*i.e*. *P*-value = 0) were considered significant. To select only those probes exhibiting a substantial separation between expression profiles, differential AUCs were also required to exhibit an average $\log_2$ fold difference of at least 0.58 (corresponding to a 1.5-fold change on the linear scale). The average $\log_2$ fold-difference across the time-course is the ratio of $\boldsymbol{\Delta}_{obs}^{ij}$ to the length of the time-course. All three pairwise comparisons between the 3 cell lines were performed. The AUC statistics for the full time course, and the early (t = 2, 6, 12, and 24 h) and late (t = 24, 48, 72, and 96 h) subsets of the time-course were computed. Finally, if multiple distinct probes mapped to the same Entrez gene, only the probe exhibiting the greatest overall expression intensity, measured by the sum of the $\log_2$-intensities in both channels across all arrays in the comparison, was retained. All identified 5C-specific genes are listed in Dataset S1 with full annotation, differential AUC values, and P-values.

In some instances, it was necessary to assess differential expression at a single time point. For these comparisons, we used the *limma* package (96, 97) implemented in the R/Bioconductor platform (98). *Limma* was used to compute empirical Bayes moderated *t*-statistics, analogous to classical *t*-statistics, except that information on all probes is used to produce more stable standard error estimates of log-fold changes. P-values of moderated t-statistics were adjusted for multiple comparisons by using the method of Benjamini and Hochberg (99) to control the FDR (false discovery rate), the expected false positive rate among rejected null hypotheses.

Gene Enrichment and Pathway Analysis. Gene enrichment and pathway analysis (Fig. 37) was conducted using GeneGo's MetaCore version 6.5. This software generates *P*-values based on a hypergeometric test of enrichment, and measures the probability of observing the number of identified genes mapping to a particular curated process by chance, as a function of the total number of identified genes, the number of curated genes in the pathway, and the size of the "full set" of all genes in all curated pathways. Significantly enriched processes/pathways/networks were required to pass a false discovery rate of 0.05.

Statistical Analyses not related to Microarray Data. Excel 2003 for Windows (Microsoft) was used to perform 1-way ANOVA or T tests, as appropriate. Non-linear curve fitting and EC_{50} determinations were performed using Prism 4.03 (GraphPad Software). To assess the interaction between AA and E_2-induced apoptosis, the multiple regression model $Pct = E2 + AA + E2 \times AA$

was fit in which *Pct* was the percentage of apoptotic + dead cells, *E2* was the E_2 concentration, and *AA* was the concentration of arachidonic acid. *AA* was coded as a categorical factor with three levels (0 μM, 10 μM, and 20 μM).

Figure 32

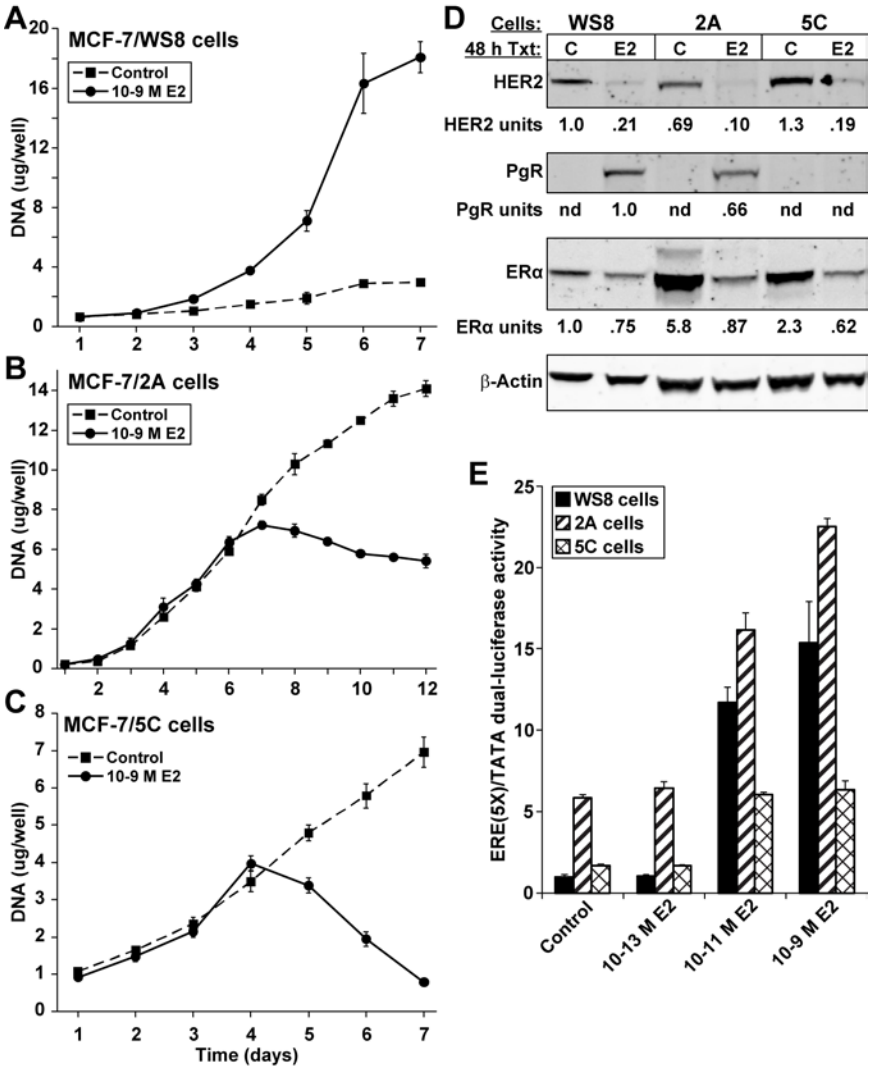


Figure 32: **Characterization of estrogen-dependent MCF-7:WS8 and estrogen deprivation-resistant MCF-7:2A and MCF-7:5C cell lines.** E_2-regulated growth of (*A*) MCF-7:WS8, (*B*) MCF-7:2A and (*C*) MCF-7:5C cell lines. Cells were seeded in 24-well (WS8 and 5C cells) or 6-well plates (2A cells) and allowed to grow in the presence or absence of E_2 over 7 days (WS8 and 5C cells) or 12 days (2A cells). DNA mass per well was measured daily using the DNA-binding fluorescent dye Hoechst 33258 compared to a standard curve. Data shown represent 8 replicate wells and associated SDs per condition and time point.

Figure 33

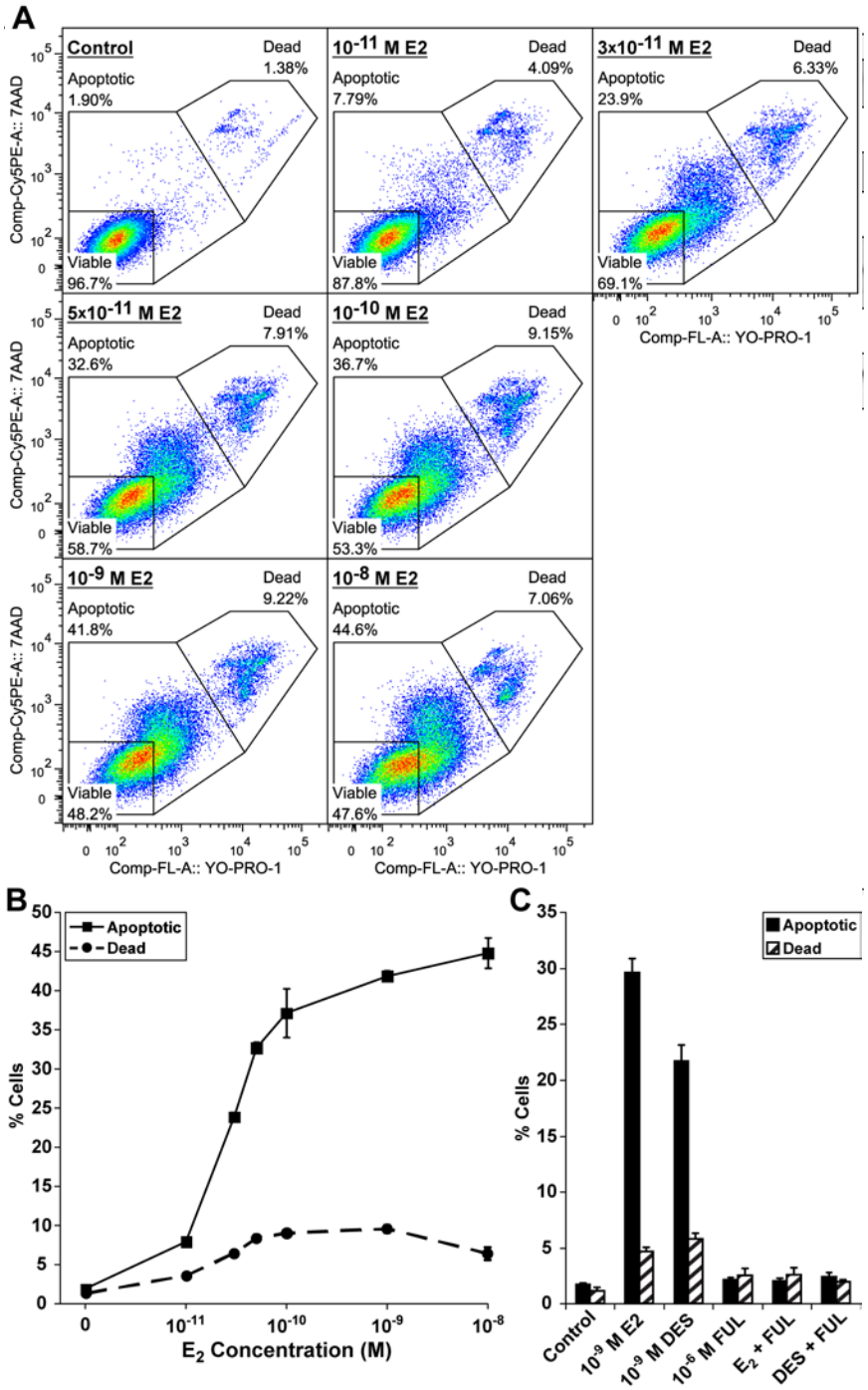


Figure 33: ***E_2* induces apoptosis in 5C cells in a concentration dependent manner via ER.** (*A* and *B*) Concentration response of E_2-induced apoptosis. Apoptosis was determined by flow cytometric analysis of cells stained with the DNA-specific binding dyes YO-PRO-1 and 7AAD. Double-negative staining cells were defined as viable, double-positive staining cells as dead, and intermediately staining cells as apoptotic. Cells were not-treated (Control) or treated with the indicated increasing E_2 concentrations for 96 h. Examples of flow cytometry data are shown in (*A*), and quantitation of apoptotic and dead cells is shown in (*B*). (*C*) ER-dependent apoptosis in 5C cells. ***E_2*** and DES induced apoptosis in 5Cs was completely blocked by FUL. 5C cells were treated with the indicated ER ligands for 96 h, and analysed for apoptotic and dead cells as in (*A*). Data shown in *(B* and *C)* represent triplicates and associated SDs.

Figure 34

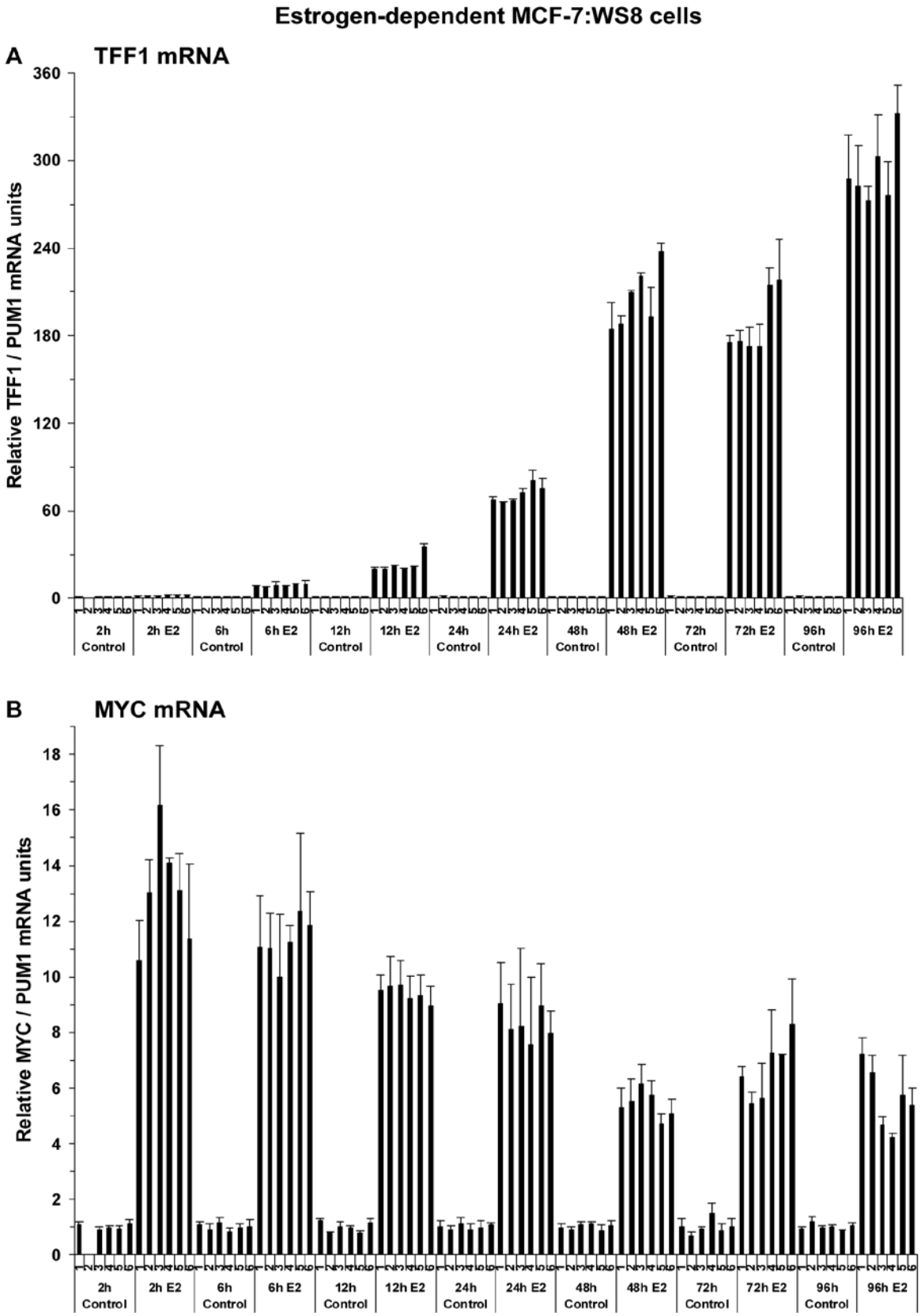


Figure 14: **MCF-7:WS8 RNA sample quality control for estrogenic responses of TFF1 and MYC.** Only samples which passed quality control are shown. TFF1 and MYC were measured by qRT-PCR.

Figure 35

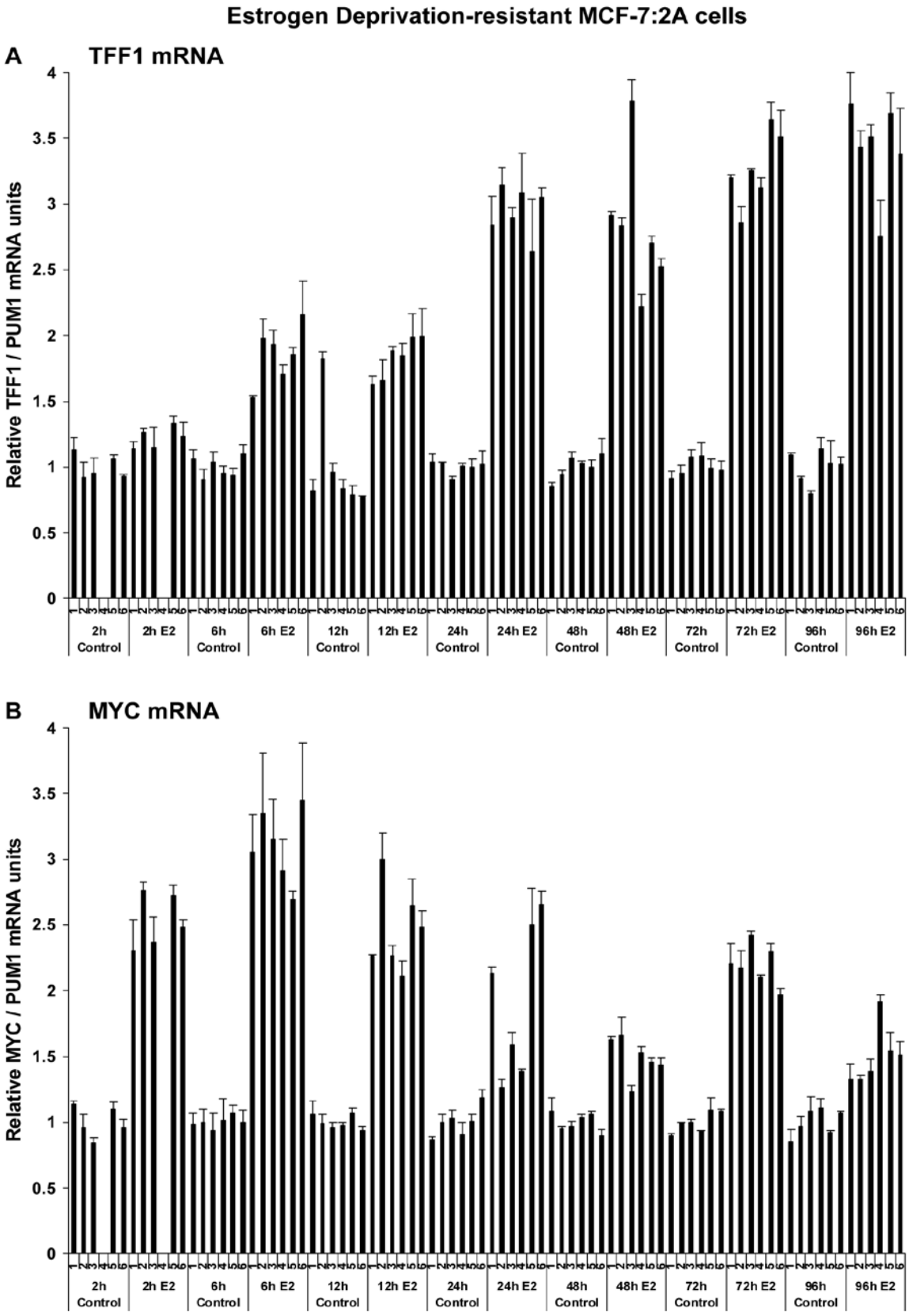


Figure 35: **MCF-7:2A RNA sample quality control for estrogenic responses of TFF1 and MYC.** Only samples which passed quality control are shown. TFF1 and MYC were measured by qRT-PCR.

Figure 36

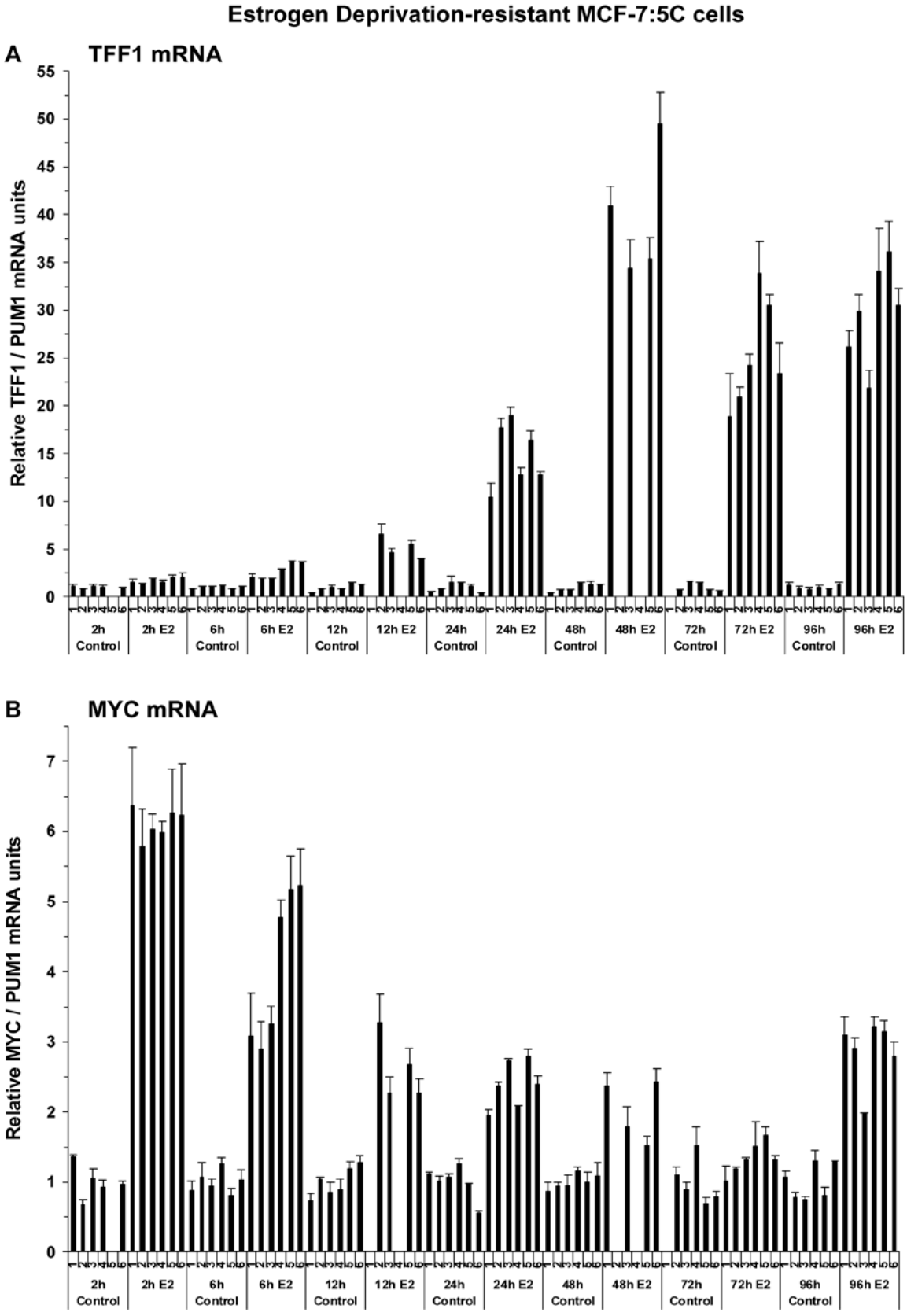


Figure 36: **MCF-7:5C RNA sample quality control for estrogenic responses of TFF1 and MYC.** Only samples which passed quality control are shown. TFF1 and MYC were measured by qRT-PCR.

Figure 37

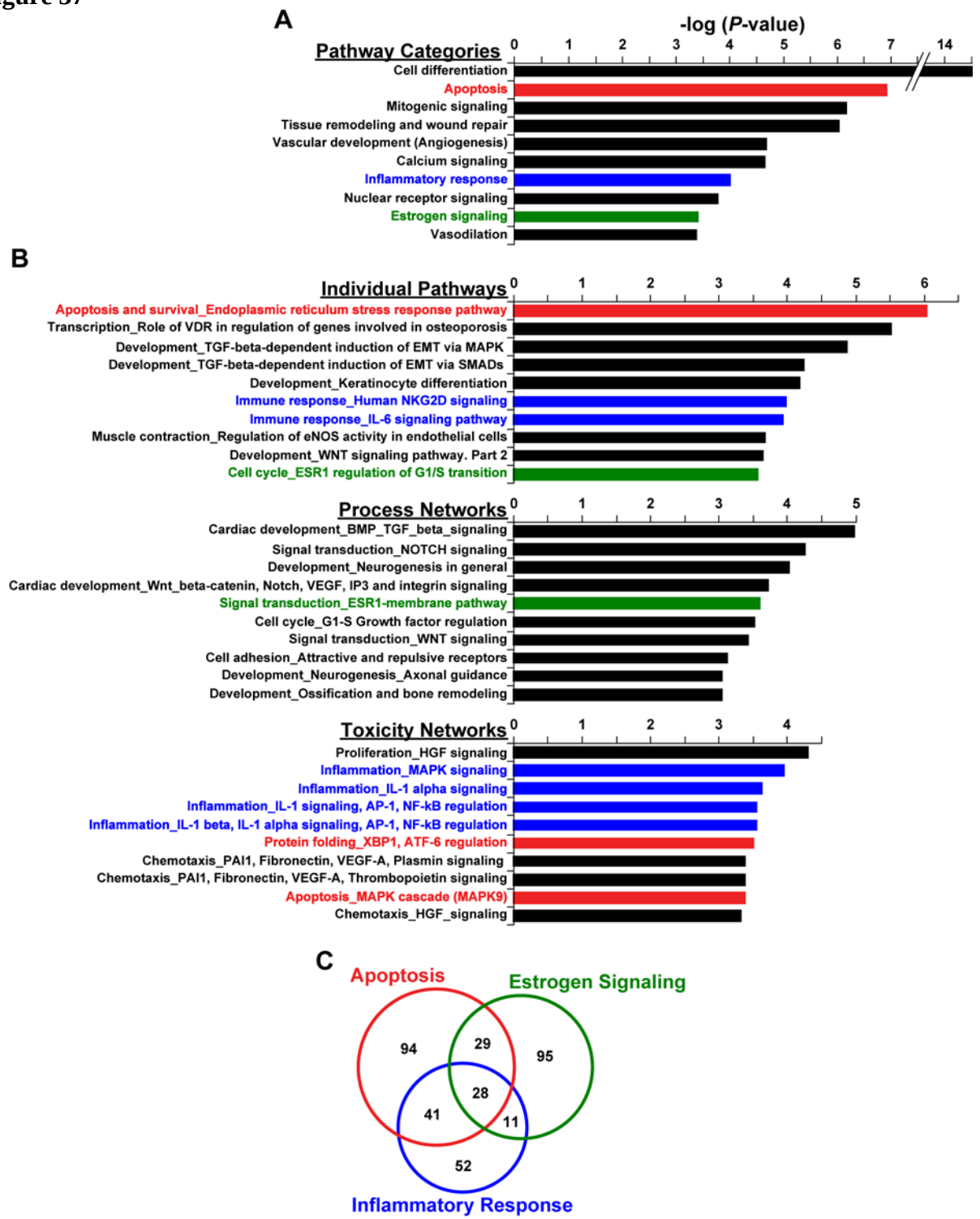


Figure 37: **Gene enrichment analysis of genes differentially regulated by E_2 in 5C cells relative to both WS8 and 5C cells.** (*A*) Broad pathway categories. (*B*) Detailed pathway/network categories. (*C*) Venn diagram showing the total and overlapping number of genes involved in estrogen signaling, inflammatory response, and apoptosis.

Figure 38

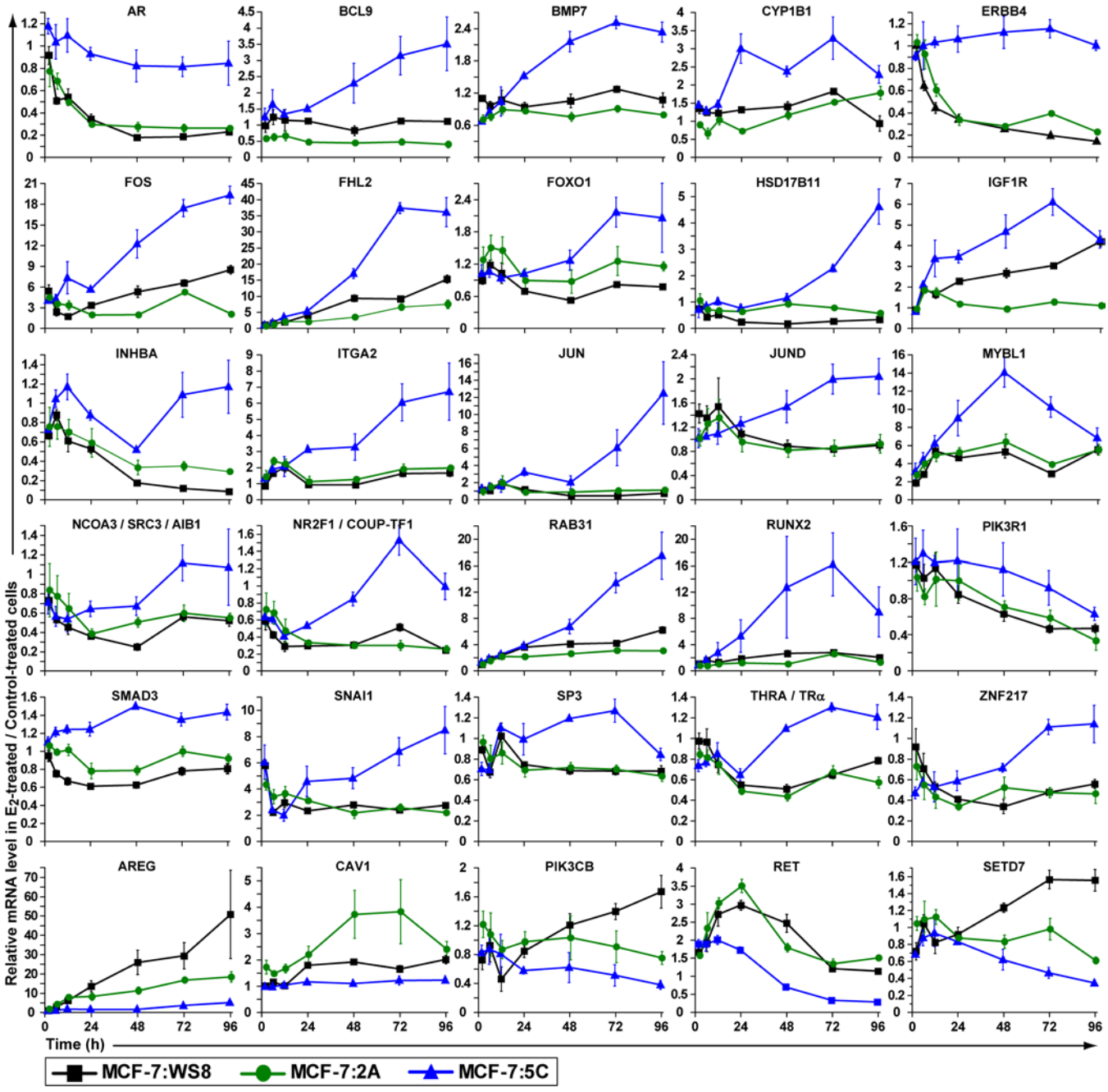


Figure 38: **Examples of estrogen signaling genes.**

Figure 39

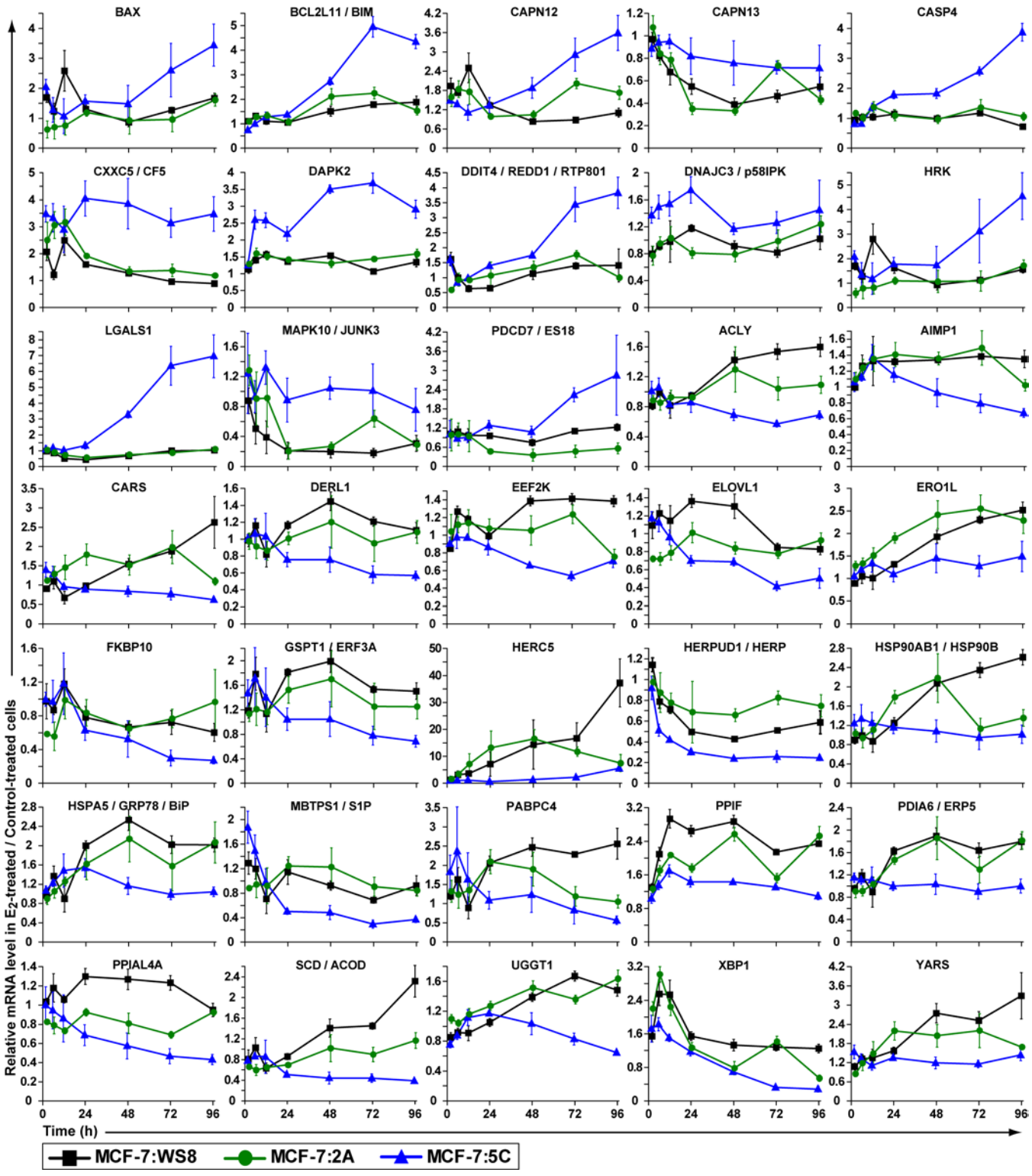


Figure 39: **Examples of apoptosis genes.**

Figure 40

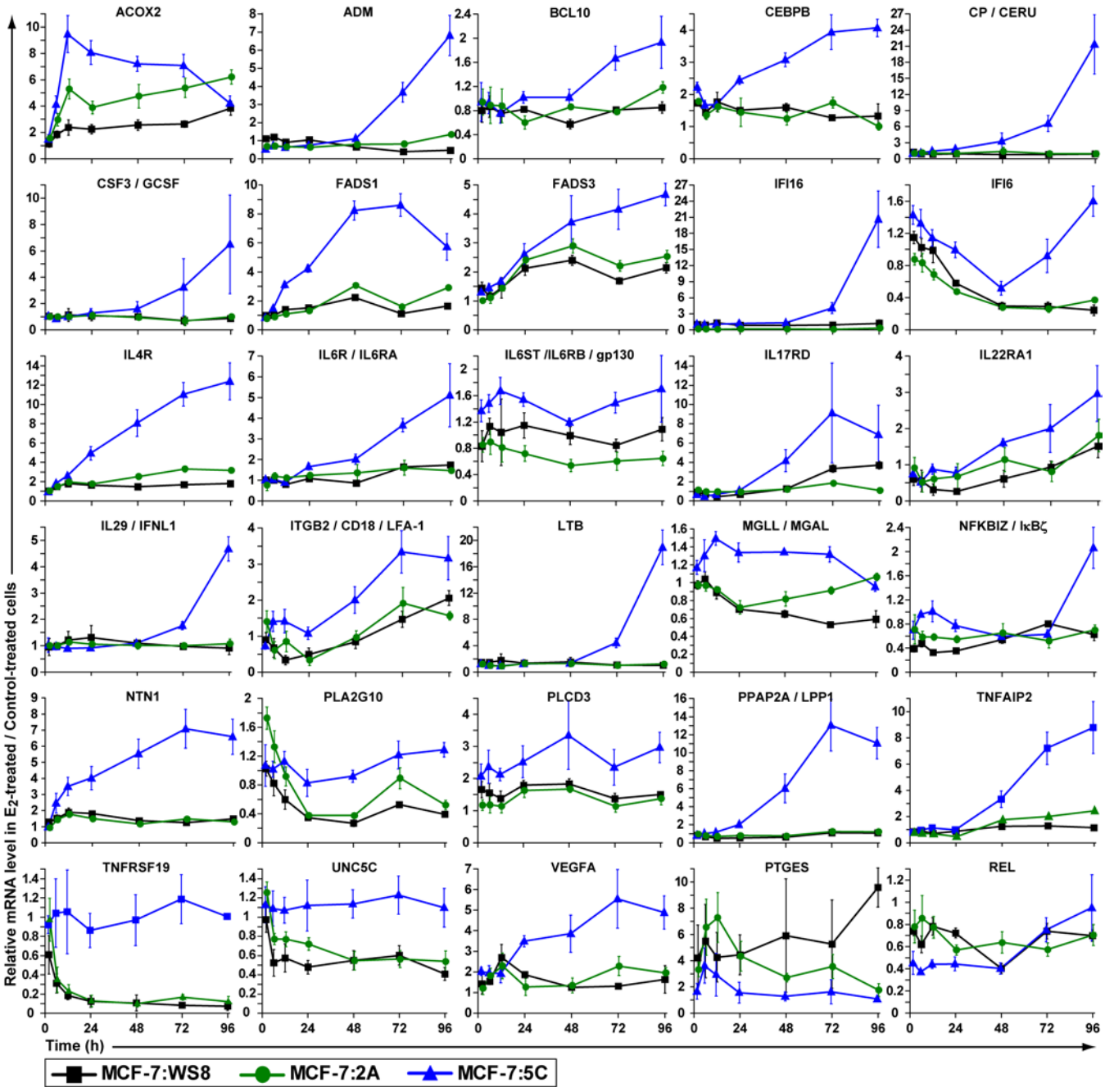


Figure 40: **Examples of inflammatory response genes.**

Figure 41

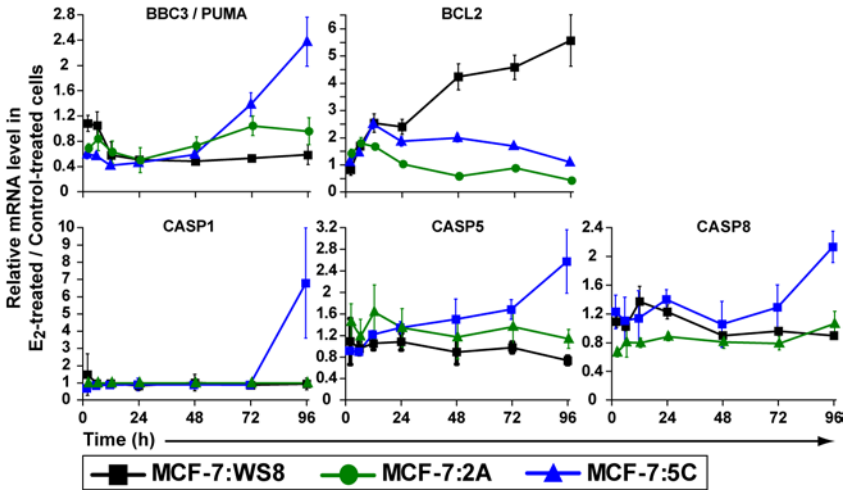


Figure 41: **Apoptotic 5C-specific genes that were below the significance cut-off parameters.**

Figure 42

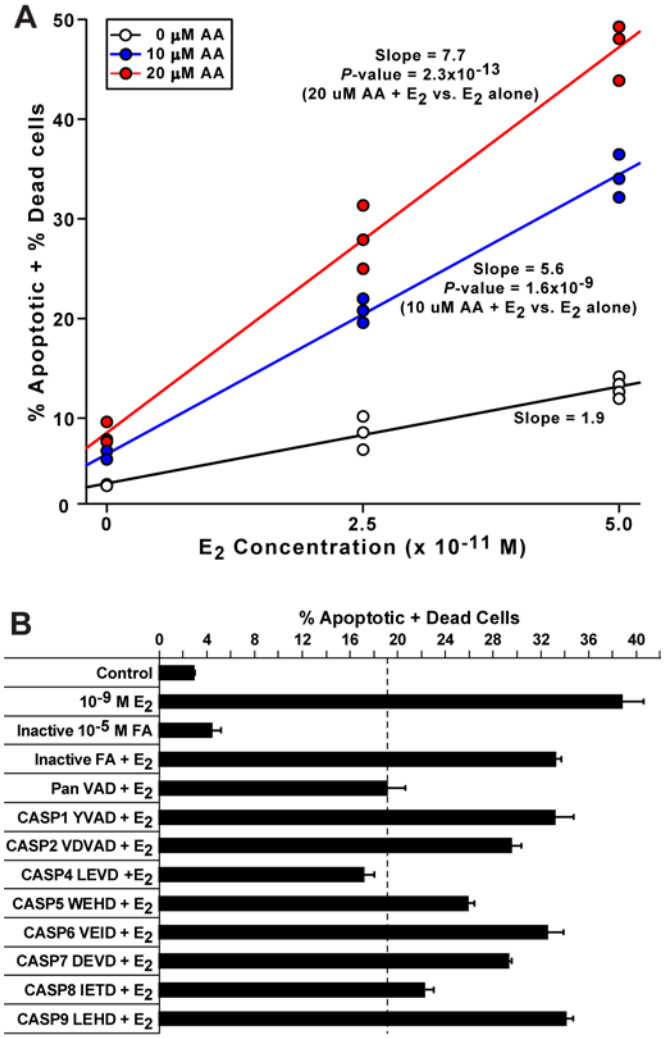


Figure 42: **Functional interrogation of E_2-induced apoptosis.** (*A*) AA a nd ***E_2*** interact to super-additively induce apoptosis. 5C cells were treated with combinations of AA and E_2 as indicated for 72 h. (*B*) Screening of selective CASP inhibitors. The selectivity of the inhibitors for individual caspases is indicated according to the manufacturer. 5C cells were treated with 10-9 M E_2 and 10 µM of each CASP inhibitor as indicated for 96 h. The CASP4 inhibitor Z-LEVD-fmk was the most active of the inhibitors tested. Apoptosis in *(A* and *B)* was quantified by altered plasma membrane permeability as in Fig. 2. Data shown in *(B)* represent triplicates and associated SDs.

Figure 43

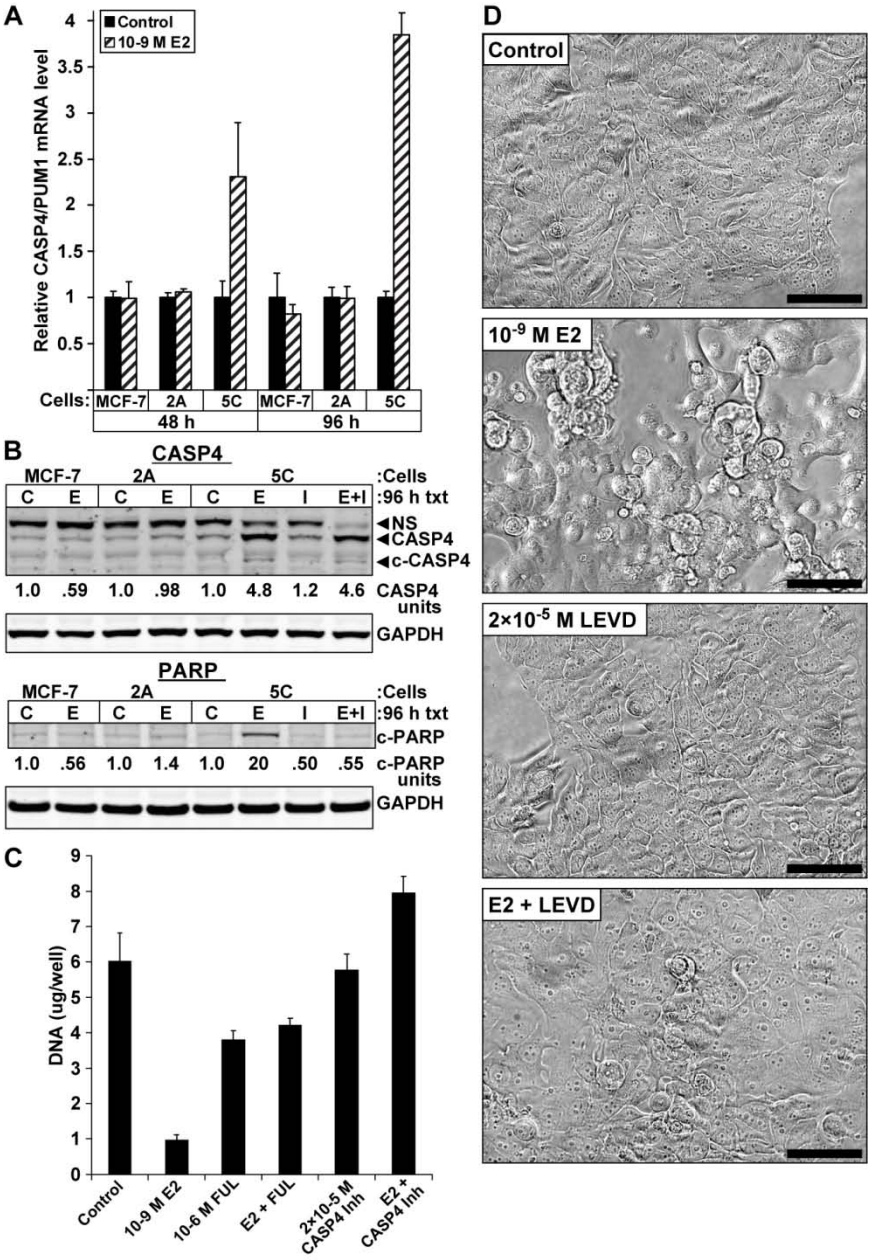


Figure 43: **The inflammatory CASP4 is functionally involved in E_2-induced apoptosis.** (*A*) CASP4 mRNA was induced by E_2 in 5C cells but not in WS8 or 2A cells. (*B*) $\boldsymbol{E_2}$ also induced CASP4 at the protein level specifically in the 5C cells, and led to cleavage of the apoptotic marker PARP, which was blocked by the CASP4 inhibitor z-LEVD-fmk. (*C*) $\boldsymbol{E_2}$-inhibited growth and (*D*) morphologic alterations associated with apoptosis in 5C cells were completely reversed by the CASP4 inhibitor z-LEVD-fmk.

Future Directions:

- We intend to investigate the functional involvement of the NFκB pathway in E_2-induced apoptosis.
- The identified 5C-specific genes may serve as biomarkers to predict response to estrogen therapy. Additionally, since VEGFA and LTB are secreted factors, they could be rapidly developed and assayed from blood samples. These identified 5C-specific genes also provide the basis for potentially improving clinical response rates to estrogen by combining it with agents that promote ERS and/or tumor-specific inflammation. For example neutralizing NTN1 antibodies, AA or its precursor conjugated LA may increase response rates. Further, these findings lead to the conclusion that anti-inflammatory agents prescribed for ancillary clinical problems should not be used during anti-tumor estrogen therapy.

TASK 4: (FCCC/Ariazi; TGen/Cunliffe; Jordan/GU) – To analyze E_2-induced survival and apoptotic pathways using gene arrays and siRNAs.

Task 4c (Azorsa, Balagurunathan, Cunliffe). Interrogate pathways of endocrine resistance using high throughput RNA interference (HT-RNAi)

Introduction:

Here we report work completed on Task 4c at The Translational Genomics Research Institute (TGen) site during year 4. We report completion of the high throughput RNAi screening in three formats: The Kinome, the druggable genome (which includes a significant overlap with the kinome), and validation of candidate hits from these high-density screens in custom-designed "flexiplate" format. Biological duplicate screens were performed for both the druggable genome and kinome screens by Dr. David Azorsa's laboratory at TGen. Candidate genes that were protective against E_2-mediated apoptosis in duplicate screens were selected, and used to custom-design and purchase in flexi-plate format. Flexiplate screens include an additional two siRNA's per candidate gene, and are used specifically to further interrogate the functional significance of candidate genes that are protective of E_2-mediated apoptosis in MCF7:5C cells. In this report, we provide a comprehensive explanation of the high-throughput screening approaches implemented and summarized analysis performed by Dr. Yoganand Balagurunathan at TGen to select candidate hits from the druggable genome screen. Current investigations are focused on 2 key areas: 1) verification and validation of the top hits from the MCF7:5C RNAi screens, 2) Integration of the candidate hits with the E_2-regulated genes significantly deregulated in the temporal expression analysis reported in Task 4a,b.

WORK ACCOMPLISHED - Task 4c, Year 4.

High-throughput siRNA Screen of estrogen deprivation-resistant MCF-7:5C cells (David Azorsa, PhD, Yoganand Balagurunathan, PhD and Heather Cunliffe, PhD)

A detailed assay development summary is provided in Year 3 progress report for high

throughput siRNA screening of MCF-7:5C cells using siRNA libraries. Validation screens were conducted using libraries targeting kinases and apoptosis-associated genes followed by the high throughput, large-scale screen done using a "druggable genome" siRNA library targeting 7000 genes. Details are provided below for each screen.

Kinase siRNA library screen:

An siRNA screen targeting 572 individual kinases was initially conducted. The siRNA library plate set up is shown in Figure 44. MCF-7:5C cells were transfected with two sets of siRNA library plates, with one set treated with vehicle and the other with 3 nM estradiol, which was found to be optimal at inducing E_2-mediated apoptosis in this assay format (Figure 45). The screens were conducted in duplicate. The results of the scatter plot are shown in Figure 46. Assay Run B performed better than A, showing a larger number of genes whose viability in E_2 (y axis) was stronger compared to the same siRNA in the vehicle control plate.

Figure 44

siRNA library plate

	col 01	col 02	col 03	col 04	col 05	col 06	col 07	col 08	col 09	col 10	col 11	col 12	col 13	col 14	col 15	col 16	col 17	col 18	col 19	col 20	col 21	col 22	col 23	col 24
A	REF	REF	lib	lib	lib	lib	lib	lib	lib	lib	lib	lib	lib	lib	lib	lib	lib	lib	lib	lib	lib	lib	Buffer	Buffer
B	REF	REF	lib	lib	lib	lib	lib	lib	lib	lib	lib	lib	lib	lib	lib	lib	lib	lib	lib	lib	lib	lib	Buffer	Buffer
C	REF	REF	lib	lib	lib	lib	lib	lib	lib	lib	lib	lib	lib	lib	lib	lib	lib	lib	lib	lib	lib	lib	Buffer	Buffer
D	REF	REF	lib	lib	lib	lib	lib	lib	lib	lib	lib	lib	lib	lib	lib	lib	lib	lib	lib	lib	lib	lib	Buffer	Buffer
E	REF	REF	lib	lib	lib	lib	lib	lib	lib	lib	lib	lib	lib	lib	lib	lib	lib	lib	lib	lib	lib	lib	Buffer	Buffer
F	REF	REF	lib	lib	lib	lib	lib	lib	lib	lib	lib	lib	lib	lib	lib	lib	lib	lib	lib	lib	lib	lib	NS	NS
G	REF	REF	lib	lib	lib	lib	lib	lib	lib	lib	lib	lib	lib	lib	lib	lib	lib	lib	lib	lib	lib	lib	NS	NS
H	REF	REF	lib	lib	lib	lib	lib	lib	lib	lib	lib	lib	lib	lib	lib	lib	lib	lib	lib	lib	lib	lib	POS	POS
I	REF	REF	lib	lib	lib	lib	lib	lib	lib	lib	lib	lib	lib	lib	lib	lib	lib	lib	lib	lib	lib	lib	POS	POS
J	REF	REF	lib	lib	lib	lib	lib	lib	lib	lib	lib	lib	lib	lib	lib	lib	lib	lib	lib	lib	lib	lib	POS	POS
K	REF	REF	lib	lib	lib	lib	lib	lib	lib	lib	lib	lib	lib	lib	lib	lib	lib	lib	lib	lib	lib	lib	POS	POS
L	REF	REF	lib	lib	lib	lib	lib	lib	lib	lib	lib	lib	lib	lib	lib	lib	lib	lib	lib	lib	lib	lib	POS	POS
M	REF	REF	lib	lib	lib	lib	lib	lib	lib	lib	lib	lib	lib	lib	lib	lib	lib	lib	lib	lib	lib	lib	Scram	Scram
N	REF	REF	lib	lib	lib	lib	lib	lib	lib	lib	lib	lib	lib	lib	lib	lib	lib	lib	lib	lib	lib	lib	Scram	Scram
O	REF	REF	lib	lib	lib	lib	lib	lib	lib	lib	lib	lib	lib	lib	lib	lib	lib	lib	lib	lib	lib	lib	GFP	GFP
P	REF	REF	lib	lib	lib	lib	lib	lib	lib	lib	lib	lib	lib	lib	lib	lib	lib	lib	lib	lib	lib	lib	GFP	GFP

Figure 44: siRNA library plate format Blue reference (REF) wells contain cells, media, transfection reagent, no E_2 or vehicle, and no siRNA. They are used for plate-to-plate normalization. The Qiagen validated kinase library (572 genes, 2 siRNAs per gene) was used. siRNA negative and positive controls are shown on the right two columns.

Figure 45

Treatment of Plates

	col 01	col 02	col 03	col 04	col 05	col 06	col 07	col 08	col 09	col 10	col 11	col 12	col 13	col 14	col 15	col 16	col 17	col 18	col 19	col 20	col 21	col 22	col 23	col 24
A	REF	REF	Veh	Veh	Veh	Veh	Veh	Veh	Veh	Veh	Veh	Veh	Veh	Veh	Veh	Veh	Veh	Veh	Veh	Veh	Veh	Veh	Veh	Veh
B	REF	REF	Veh	Veh	Veh	Veh	Veh	Veh	Veh	Veh	Veh	Veh	Veh	Veh	Veh	Veh	Veh	Veh	Veh	Veh	Veh	Veh	Veh	Veh
C	REF	REF	Veh	Veh	Veh	Veh	Veh	Veh	Veh	Veh	Veh	Veh	Veh	Veh	Veh	Veh	Veh	Veh	Veh	Veh	Veh	Veh	Veh	Veh
D	REF	REF	Veh	Veh	Veh	Veh	Veh	Veh	Veh	Veh	Veh	Veh	Veh	Veh	Veh	Veh	Veh	Veh	Veh	Veh	Veh	Veh	Veh	Veh
E	REF	REF	Veh	Veh	Veh	Veh	Veh	Veh	Veh	Veh	Veh	Veh	Veh	Veh	Veh	Veh	Veh	Veh	Veh	Veh	Veh	Veh	Veh	Veh
F	REF	REF	Veh	Veh	Veh	Veh	Veh	Veh	Veh	Veh	Veh	Veh	Veh	Veh	Veh	Veh	Veh	Veh	Veh	Veh	Veh	Veh	Veh	Veh
G	REF	REF	Veh	Veh	Veh	Veh	Veh	Veh	Veh	Veh	Veh	Veh	Veh	Veh	Veh	Veh	Veh	Veh	Veh	Veh	Veh	Veh	Veh	Veh
H	REF	REF	Veh	Veh	Veh	Veh	Veh	Veh	Veh	Veh	Veh	Veh	Veh	Veh	Veh	Veh	Veh	Veh	Veh	Veh	Veh	Veh	Veh	Veh
I	REF	REF	Veh	Veh	Veh	Veh	Veh	Veh	Veh	Veh	Veh	Veh	Veh	Veh	Veh	Veh	Veh	Veh	Veh	Veh	Veh	Veh	Veh	Veh
J	REF	REF	Veh	Veh	Veh	Veh	Veh	Veh	Veh	Veh	Veh	Veh	Veh	Veh	Veh	Veh	Veh	Veh	Veh	Veh	Veh	Veh	Veh	Veh
K	REF	REF	Veh	Veh	Veh	Veh	Veh	Veh	Veh	Veh	Veh	Veh	Veh	Veh	Veh	Veh	Veh	Veh	Veh	Veh	Veh	Veh	Veh	Veh
L	REF	REF	Veh	Veh	Veh	Veh	Veh	Veh	Veh	Veh	Veh	Veh	Veh	Veh	Veh	Veh	Veh	Veh	Veh	Veh	Veh	Veh	Veh	Veh
M	REF	REF	Veh	Veh	Veh	Veh	Veh	Veh	Veh	Veh	Veh	Veh	Veh	Veh	Veh	Veh	Veh	Veh	Veh	Veh	Veh	Veh	Veh	Veh
N	REF	REF	Veh	Veh	Veh	Veh	Veh	Veh	Veh	Veh	Veh	Veh	Veh	Veh	Veh	Veh	Veh	Veh	Veh	Veh	Veh	Veh	Veh	Veh
O	REF	REF	Veh	Veh	Veh	Veh	Veh	Veh	Veh	Veh	Veh	Veh	Veh	Veh	Veh	Veh	Veh	Veh	Veh	Veh	Veh	Veh	Veh	Veh
P	REF	REF	Veh	Veh	Veh	Veh	Veh	Veh	Veh	Veh	Veh	Veh	Veh	Veh	Veh	Veh	Veh	Veh	Veh	Veh	Veh	Veh	Veh	Veh

	col 01	col 02	col 03	col 04	col 05	col 06	col 07	col 08	col 09	col 10	col 11	col 12	col 13	col 14	col 15	col 16	col 17	col 18	col 19	col 20	col 21	col 22	col 23	col 24
A	REF	REF	E2	E2	E2	E2	E2	E2	E2	E2	E2	E2	E2	E2	E2	E2	E2	E2	E2	E2	E2	E2	E2	E2
B	REF	REF	E2	E2	E2	E2	E2	E2	E2	E2	E2	E2	E2	E2	E2	E2	E2	E2	E2	E2	E2	E2	E2	E2
C	REF	REF	E2	E2	E2	E2	E2	E2	E2	E2	E2	E2	E2	E2	E2	E2	E2	E2	E2	E2	E2	E2	E2	E2
D	REF	REF	E2	E2	E2	E2	E2	E2	E2	E2	E2	E2	E2	E2	E2	E2	E2	E2	E2	E2	E2	E2	E2	E2
E	REF	REF	E2	E2	E2	E2	E2	E2	E2	E2	E2	E2	E2	E2	E2	E2	E2	E2	E2	E2	E2	E2	E2	E2
F	REF	REF	E2	E2	E2	E2	E2	E2	E2	E2	E2	E2	E2	E2	E2	E2	E2	E2	E2	E2	E2	E2	E2	E2
G	REF	REF	E2	E2	E2	E2	E2	E2	E2	E2	E2	E2	E2	E2	E2	E2	E2	E2	E2	E2	E2	E2	E2	E2
H	REF	REF	E2	E2	E2	E2	E2	E2	E2	E2	E2	E2	E2	E2	E2	E2	E2	E2	E2	E2	E2	E2	E2	E2
I	REF	REF	E2	E2	E2	E2	E2	E2	E2	E2	E2	E2	E2	E2	E2	E2	E2	E2	E2	E2	E2	E2	E2	E2
J	REF	REF	E2	E2	E2	E2	E2	E2	E2	E2	E2	E2	E2	E2	E2	E2	E2	E2	E2	E2	E2	E2	E2	E2
K	REF	REF	E2	E2	E2	E2	E2	E2	E2	E2	E2	E2	E2	E2	E2	E2	E2	E2	E2	E2	E2	E2	E2	E2
L	REF	REF	E2	E2	E2	E2	E2	E2	E2	E2	E2	E2	E2	E2	E2	E2	E2	E2	E2	E2	E2	E2	E2	E2
M	REF	REF	E2	E2	E2	E2	E2	E2	E2	E2	E2	E2	E2	E2	E2	E2	E2	E2	E2	E2	E2	E2	E2	E2
N	REF	REF	E2	E2	E2	E2	E2	E2	E2	E2	E2	E2	E2	E2	E2	E2	E2	E2	E2	E2	E2	E2	E2	E2
O	REF	REF	E2	E2	E2	E2	E2	E2	E2	E2	E2	E2	E2	E2	E2	E2	E2	E2	E2	E2	E2	E2	E2	E2
P	REF	REF	E2	E2	E2	E2	E2	E2	E2	E2	E2	E2	E2	E2	E2	E2	E2	E2	E2	E2	E2	E2	E2	E2

Figure 45: Treatment of siRNA plates with E_2 or vehicle control MCF7:5C cells plated in phenol-red free media with charcoal stripped fetal bovine serum, as previously optimized. Cells were transfected at 1000 cells/well by reverse transfection using diluted Dharmafect 3 at an 8:1 lipid to siRNA ratio. At 24 h post transfection, replicate plates were treated with either vehicle control (Veh) or 3nM E_2. At 144 h, cell number was measured using the cell Titer Glo assay.

Figure 46

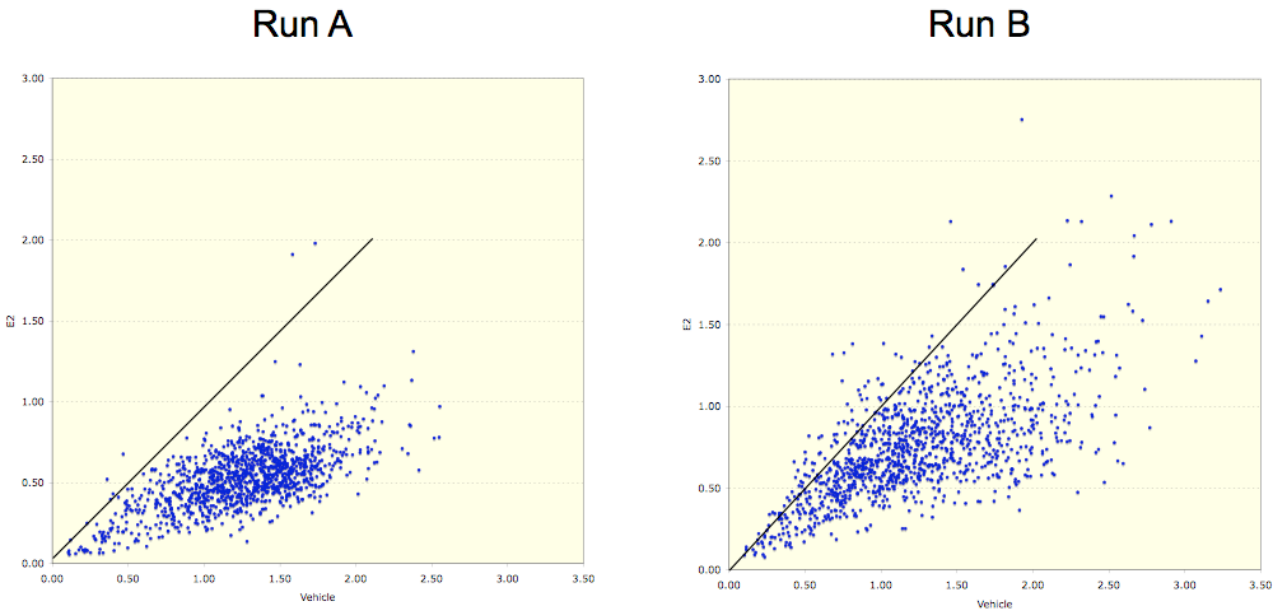


Figure 46: Normalized ratios for each siRNA in replicate kinase screens (Run A and B). The cell titer Glo readout for each siRNA was normalized to the median REF value for each plate. The ratio of E_2-treated (y axis) vs vehicle treated control (x-axis) was then derived. Plotted ratios falling close to the 45 degree line are the candidate hits that are protective against E_2-mediated apoptosis.

Selected gene hits from the kinase screens were further tested in a "flexiplate" format, which included additional functionally validated siRNAs targeting the candidate hits from the screens as well as breast cancer associated genes. Functional evaluation of these kinases on modulating the response of MCF-7:5C cells to E_2 is currently in progress in the laboratories of Drs. Cunlffe and Azorsa. Additionally and importantly, the data sets for the vehicle treated only sets of siRNA will be evaluated separately in order to identify cell specific genes in MCF7:5C that when silenced greatly affect cell growth. These "Achilles' Heel" targets will shed additional light on the molecular mechanisms essential to the survival of MCF7:5C cells in the absence of estrogen.

Druggable Genome siRNA library screen:

For the druggable genome (DG) screen, assay conditions similar to the kinase screen and flexiplate validation assays were used, with the plate setup shown in Figure 47. Similarly, two replicate siRNA screens were performed, both using two sets of druggable genome plates; one treated with vehicle and one treated with 1 nM estradiol.

Figure 47

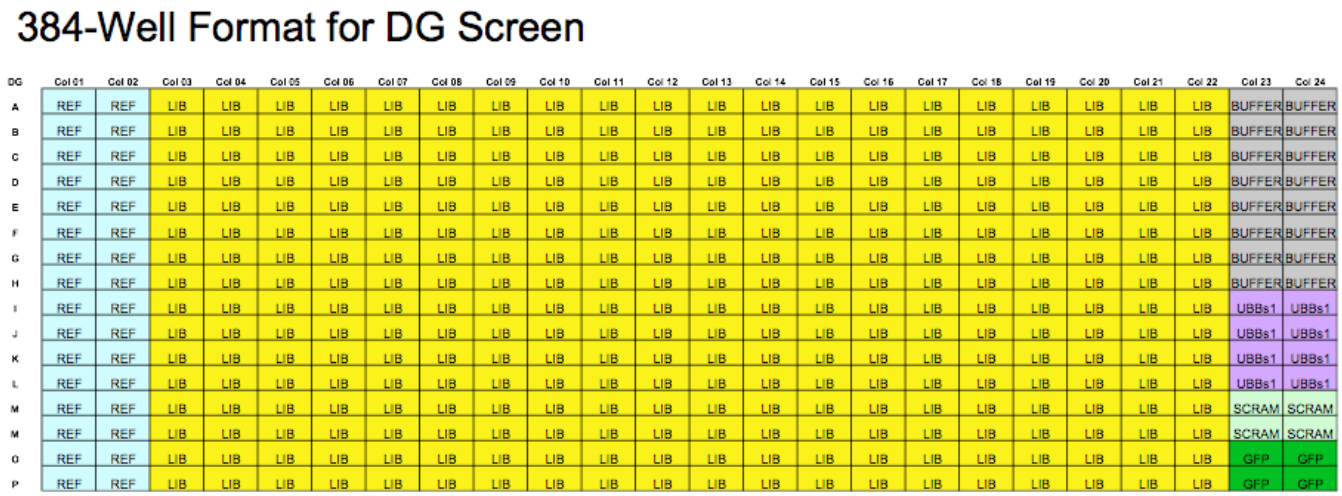


Figure 47: DG siRNA library plate format Blue reference wells as in Figure 4.1. U BBs1 is a lethal siRNA (positive control). SCRAM are scrambled non-targeting siRNAs (negative control). GFP is a positive control for transfection efficiency.

Quality control measurements were conducted for the DG screens to evaluate the robustness of the assay. Measurements included plotting of reference and control wells averages per plate and treatment. An example plot for DG1 is shown in Figure 48. The E_2-treated plates averaged lower values for the control siRNA wells indicating the apoptosis induction by E2. Z-factor measurements were also calculated for each plate and ranged from 0.2-0.8 signifying marginal to excellent assay plate results with the majority of the plates in the good-excellent range. Plotting of the log2 ratios of each well identified the outlier plate sets for the screens. The plotted ratios for DG 1 screen are shown in Figure 49.

Figure 48

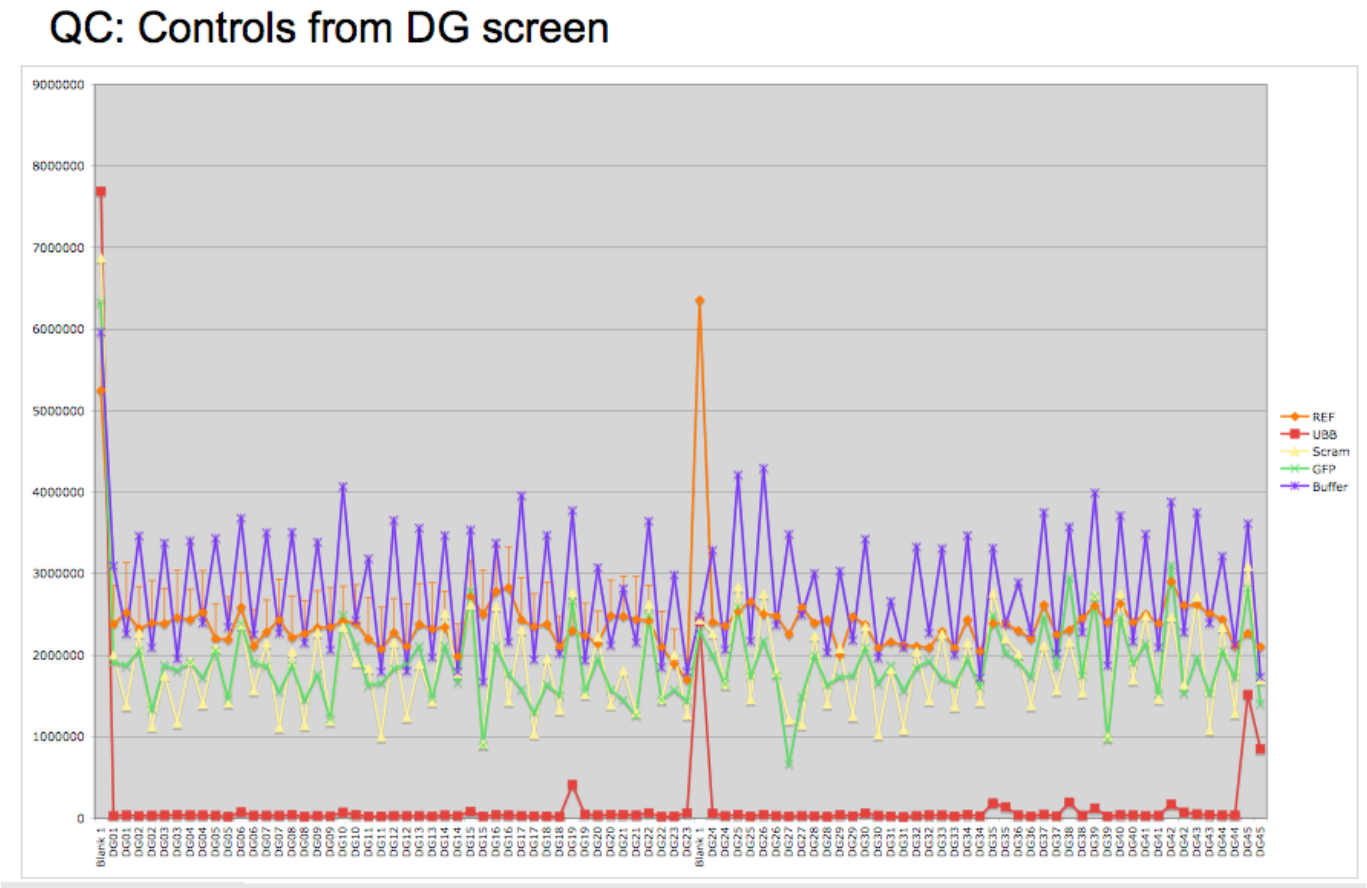


Figure 48. Control siRNA plot for DG screen. siRNA RLU (Relative light units) for each siRNA control are plotted for each plate in the assay. Paired plates without and with E_2 are plotted consecutively (X-axis). The overall RLU for the second plate in each pair shows reduced intensity for the scrambled, GFP and buffer controls as expected, as the E_2 treatment in these plates is causing apoptosis of the MCF7:5C cells (expected drop in RLU is evident in the oscillating pattern). The UBB lethal control siRNA shows complete cell death in each plate, except for the last plate pair, which did not contain any UBB siRNA. The REF controls for each plate display more uniformity across the entire screen (the REF wells contain MCF7:5C cells not treated with either Vehicle or E_2, so they represent the natural variability inherent in the screen, which is ultimately used in the plate local and global normalization during candidate hit selection described later in this report).

Figure 49

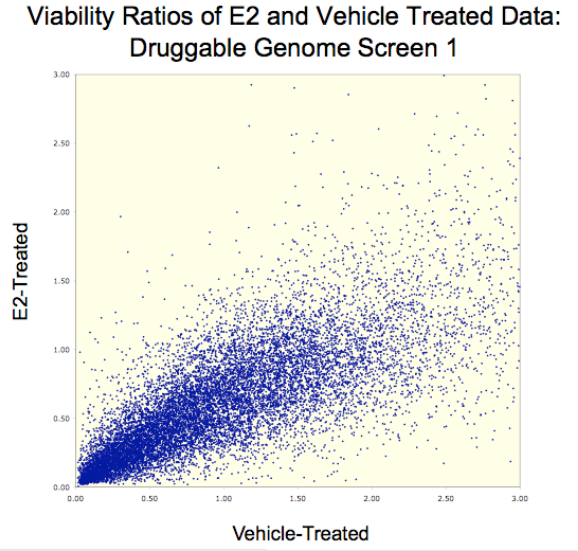


Figure 49. Normalized ratios for siRNA DG screen 1 in MCF7:5C cells. 15,000 siRNA hits representing 7000 genes. Plotted ratios (E_2-treated vs Vehicle control) that meet the 45 degree axis are those protective of E_2-apoptosis in this screen. Genes in the lower right quadrant are not protective of E_2-mediated apoptosis. Several candidate hits were >90 percent effective in blocking E_2-induced apoptosis and are currently being investigated.

Candidate hit identification from RNAi- Druggable genome screens

The experimental setup had observations from 17,280 w ells, spread over 45 plates (384 wells/plate).

Table 1: Control probe count for Run A&B each run contained 45 plates.

Probe/Well type	**Expt. A or B**	**Per Run**
Blank	8 per plate	1224
Reference	32 per plate	1440
Scrambled	8 per plate	178
GFP	8 per plate	178
UBBs	~8 per plate	358

A variety of normalization procedures commonly used in published literature for RNAi screening data. Our data were analyzed in a plate wise format as outlined in our previous study (Y.Balagurunathan, S. Mousses, M.Bittner, siRNA screening: A process model to evaluate hit rate discovery., IEEE Genomics Signal processing and statistics ((GENSiPS) 2008, conference,

pp1-5, June 2008). Methods include: median normalization, median-polish, B score and regression (1st & 2nd order).

After data standardization, the system variability was measured by taking the difference between treated to untreated for the control probes (Reference and Blank Probes). The inherent variability measure of the controls was applied to the rest of the probes after appropriate level shift in significance (1σ, 2σ or 3σ). Any probes that are above the set limits were marked hits (Tables 2a-c). The probes that are on the right side of the distribution are the hits of interest (treated ≥ untreated), as they are associated with protection of E_2-mediated apoptosis in the MCF7:5C cells. The level of acceptance is set by the confidence (user defined). For an example of hits, we present a summary of those selected using our analysis at 2σ, for the 5 different methods of normalization (Table 2a-c). The regression-based normalization methods are global, whereas the rest are local plate based normalization methods. Several of the candidate hits in common to the two DG screens, as outlined in Table 2c are currently under functional investigation in the laboratory. Prioritization to candidates for evaluation are being made with consideration to the data reported in Task 4a,b.

Table 2a. DG screen Run A (Hits at 2σ cutoff)

Normalization Type	**Confidence level**			**Number of Hits**		
	Left	**Right**		**Num-Positive (Right if CI)**	**Num-Neg (Left of CI)**	**Total**
No-Norm	-2.9749	0.6369		263	360	623
Median(local)	-0.0690	0.0716		312	437	749
Median-polish	-1.1487	1.2961		939	972	1911
B-score	-1.4964	1.5514		789	727	1516
Regression(1st order)	-3.6668	1.2812		211	355	566
Regression(2nd order)	-3.6649	1.2707		203	346	549

Table 2b. DG screen Run B (Hits at 2σ cutoff)

Normalization Type	Confidence level			Number of Hits		
	Left	Right		Num-Positive	Num-Neg	Total
No-Norm	-1.9707	0.5823		728	686	1414
Median(local)	-0.0640	0.0553		556	604	1160
Median-polish	-1.1871	1.1561		679	814	1493
B-score	-1.4780	1.5158		656	688	1344
Regression(1st order)	-2.4990	1.0587		627	704	1331
Regression(2nd order)	-2.4877	1.0406		619	713	1332

Table 2c. DG screen Common probes between two experiments A & B **(Hits at 2*σ* cutoff)**

Normalization Type	Hits in Run A & B			
	Run.A	Run.B	Common Hits	Useful (Treated > Untreated & Non Control Probe)
No-Norm	623	1414	133	36
Loc.Median(local)	749	1160	95	15
Median-polish	1911	1493	233	94
B-score	1516	1344	157	65
Regression(1st order)	566	1331	74	13
Regression(2nd order)	549	1332	72	12

Comparison of basal levels of gene expression in MCF7:5C and MCF7:2A compared to wild type MCF7 cells using gene expression microarrays

An important consideration for the interpretation of the RNAi data obtained is knowledge of the basal-levels of gene expression the MCF7:5C and MCF7:2A cell lines relative to wild type MCF7 cells. The gene expression microarray platform used to perform the time course of E_2-induced gene expression in MCF7:5C, MCF7:2A and MCF7:WS8 resulted in identification of valid gene candidates likely to play a role in mediating E_2-induced apoptosis, these dual-color arrays result in gene 'ratio' data which can be compared across experiments. It is thus an electronic challenge to reliably compare the basal level of gene expression between cell lines (without addition of E_2) using this platform, as single channel 'intensity' data cannot be easily normalized across array experiments for comparative analysis. To resolve this important issue, six gene expression microarrays were performed, comparing RNA from exponentially growing cultures of MCF7:5C and MCF7:2A (in the absence of estrogen), and from MCF7 wild type cells growing in replete conditions (with estrogen). RNA from the MFF7:5C and MCF7:2A were hybridized in triplicate against MCF7 wild type cells (therefore 6 hybridizations in total with the same MCF7 reference pool). RNA for the triplicate repeats were isolated from cells seeded on 3 separate occasions for data reproducibility and reliability. Normalized gene expression ratio data was extracted into a filemaker pro database, a weighted average calculated for each array feature. This data is currently being exploited to further prioritize candidate hits from the RNAi screens, and is also available for use by all laboratories integrating data for this study.

Key Research Accomplishments (For All Tasks of the CoE):

Task 1 (LCCC, Isaacs, Swaby/Daly)

- The clinical trial to evaluate dose de-escalation of estrogen (Estrace) to reverse antihormone resistance in patients treated exhaustively with antihormone therapy continues to actively recruit subjects.
- Including all sites, 12 subjects were screened and 7 subjects were enrolled.
- Of the 11 enrolled subjects, 5 consented to undergo the optional research biopsy for acquisition of tissue samples as proposed in Task 1b. In total, 11 subjects have been enrolled and 2 subjects remain on study.
- AstraZeneca has withdrawn continued funding of the clinical operations but we plan to continue the clinical trial and plan to transfer the coordinating center to Georgetown University's Lombardi Comprehensive Cancer Center with Dr. Claudine Isaacs as the Study Chair and Principal Investigator.
- Institutional funds from the Lombardi Comprehensive Cancer Center will provide support for the continued accrual and conduct of the trial. Accrual at other sites will cease at other institutions but will continue at LCCC.
- LCCC is planning to advertise for the trial to ensure continued accrual.

Task 2a (FCCC – Jordan/Ariazi)

- Task 2a was completed during prior Years 1 – 3 at the Fox Chase Cancer Center (FCCC) site. The experiments were described in prior Years 1 - 3 Progress Reports. No new samples were generated during Year 4.

Task 2b-1 (GU – Jordan/Fan)

- The c-Src inhibitor PP2 blocked estrogen-induced apoptosis in long-term estrogen deprived breast cancer cells MCF-7:5C and MCF-7:2A (Fig 2, Fig 3).
- Surprisingly, treatment of MCF-7:5C cells under E_2 plus PP2 conditions produced a cell line in which not only E_2 was unable to induce apoptosis, but E_2 dramatically stimulated growth (Fig. 4, Fig. 5).
- Treatment of MCF-7:5C cells under E_2 plus PP2 conditions also activate endogenous ER target genes and growth factor receptor (Fig. 6, Fig.7).
- The implication of these results is potentially clinically important that a Src inhibitor should not be combined with estrogen to treat advanced aromatase inhibitor resistant breast cancer patients although both are in the clinical trials right now.

Task 2b-2 (GU – Jordan/Sengupta)

- Triphenylethylenes (Non-planar/type II estrogens) act as an anti-estrogen in MCF7:5C cells as they cannot induce effective apoptosis and block E_2-induced apoptosis.
- Triphenylethylene treated MCF7:WS8 or MCF7:5C cells recruit very low levels of co-activator SRC3 as compared to E_2 treatment at the promoter of estrogen-responsive gene PS2 (TFF1).
- The aspartate amino acid at 351 pos ition of estrogen receptor plays a critical role in manifesting the estrogenic properties of the non-planar estrogen (triphenylethylenes).
- Molecular docking studies suggests that ethoxy-triphenylethylene fits into the ligand binding pocket of the estrogen receptor alpha in a antagonistic mode as the non-planar structure prevents it from binding in agonist conformation due to steric hindrance.

Task 2b-3 (FCCC – Jordan/Lewis-Wambi)

- We characterized the effects of BZA and several other SERMs on the proliferation of hormone-dependent MCF-7 and T47D breast cancer cells and hormone-independent MCF-7:5C and MCF-7:2A cells and examined their mechanism of action in these cells.
- We found that all of the SERMs inhibited the growth of MCF-7 and T47D cells, however, BZA was the only SERM that inhibited the growth of hormone-independent MCF-7:5C and MCF-7:2A cells.
- Consistent with these growth results, we found that BZA induced G1 blockade in MCF-7:5C and MCF-7:2A cells and it significantly downregulated ERα and cyclin D1 which were constitutively overexpressed in these cells.

- siRNA knockdown of ERα and/or cyclin D1 significantly reduced the inhibitory effect of BZA in MCF-7:5C cells.
- Further analysis revealed that BZA downregulated ERα protein by increasing its degradation and it suppressed cyclin D1 protein and promoter activity in MCF-7:5C cells. Lastly, molecular modeling studies demonstrated that BZA bound to ERα in an orientation similar to raloxifene and had the tendency to form the same contacts with the aminoacids lining the binding cavity.
- The manuscript entitled "The Selective Estrogen Receptor Modulator Bazedoxifene Inhibits Hormone-Independent Breast Cancer Cell Growth and Downregulates Estrogen Receptor α and Cyclin D1" is under consideration in *Molecular Pharmacology* and cited as paper #18 in the Reportable Outcomes and Appendix sections.

Task 3 (GU – Riegel/Wellstein)

- We have completed validation of a number of proteins that were detected in initial proteomic comparison of AIB1 and pY interacting proteins. This data and proteomic analysis is now in press in PloS one
- We have conducted a phosphor proteomic analysis of the ER alpha in the MCF7, MCF7:5C and MCF7:2A lines in the presence or absence of estrogen
- We have conducted phospho proteomic analysis of AIB1 in alpha in the MCF7, MCF7:5C and MCF7:2A lines in the presence or absence of estrogen
- We have conducted phospho proteomic analysis of AIB1 in alpha in the MCF7, MCF7:5C and MCF7:2A lines in the presence or absence of EGF
- We have determined that Ser 214 is a site that is majorly phosphorylated by EGF in MCF7 cells
- We have determined that phosphorylation at the Ser 214 produces opposite effects on estrogen vs AP-1 responsive gene promoters
- We have determined that mutation of the Ser 214 site significantly alters the half life of the AIB1 protein.

Tasks 4a and 4b (FCCC – Ariazi, TGen – Cunliffe, GU – Jordan)

- We have interrogated E_2-induced apoptosis by identifying differentially-regulated genes across time associated with this process compared to E_2-stimulated and E_2-independent growth using a newly developed method termed differential AUC analysis.
- Over-representation analysis of the identified genes indicated 5C cells respond to E_2 with inflammatory and ERS.
- Inflammatory stress was indicated by up-regulation of cytokines/cytokine receptors (IL4R, IL6R), interferon responsive genes (IFI6, IFI16), AA biosynthetic genes (FADS1, PLA2G10), and other inflammatory markers (NTN1, UNC5C).
- AA interacted with E_2 to super-additively induce apoptosis in 5C cells, indicating AA metabolism was likely involved in E_2-induced apoptosis.

- ERS was indicated by a deficiency in up-regulating genes involved in initiating a UPR (decreased GRP78, XBP1) protein folding (decreased GRP78, PDIA6, UGGT1) and degradation of malfolded proteins (decreased HERP1, DERL1), which would lead to accumulation of unfolded proteins. Meanwhile, expression profiles indicated a widespread inhibition of protein translation (increased p58IPK; decreased AIMP1, aminoacyl tRNA synthetases, EEF2K, ERF3A) which in combination with accumulation of unfolded proteins, would further promote stress and death. ERS was also indicated by induction of BIM and BAX, and the inflammatory caspase CASP4.
- Inhibiting CASP4 activity with z-LEVD-fmk blocked E_2-induced apoptosis. Thus, CASP4 plays an important role in E_2-induced apoptosis.

Task 4c (TGen – Azorsa/Balagurunathan/Cunliffe)

- We have completed replicate kinase RNAi screens, and replicate druggable genome RNAi screens in MCF7:5C cells in the presence and absence of estrogen.
- We have identified several candidate genes that are protective against E_2-mediated apoptosis in MCF7:5C cells.
- We have identified a number of novel "Achilles heel" genes in MCF7:5C cells, without which these cells cannot survive in estrogen-deprived medium. Several of these genes are specific to survival of MCF7:5C cells (siRNA reduction of the same gene in MCF7 cells is non-lethal).
- Gene expression microarray studies have been conducted to identify the basal level of expression of all genes in the MCF7:5C and MCF7:2A cell lines compared to wild type MCF7 cells in the absence of E_2. This work was accomplished to empower integration of multiple analytical approaches, including the RNAi screens, the E_2 time course gene expression microarray data and the comparative proteomic analyses generated from these same cell lines.
- Microarray-based Data integration efforts from all Task 4 components together with the proteomic data are the focus of current efforts, to elucidate the mechanism by which E_2-mediates apoptosis in the MCF7:5C model.

Reportable Outcomes:

Publications

1. Peng J, Jordan VC. Expression of estrogen receptor alpha with a Tet-off adenoviral system induces G0/G1 cell cycle arrest in SKBr3 breast cancer cells. *International Journal of Oncology* 2010: 36(2):451-458.
2. Ariazi EA, Brailoiu E, Yerrum S, Shupp HA, Slifker MJ, Cunliffe HE, Black MA, Donato AL, Arterburn JB, Oprea TI, Prossnitz ER, Dun NJ, Jordan VC. The G Protein-Coupled Receptor GPR30 Inhibits Proliferation of Estrogen Receptor-Positive Breast Cancer Cells. *Cancer Research* 2010: 70:1184-1194. (Selected for Faculty of 1000 Medicine, identified as

an important article published in Medicine for its scientific merit and positive contribution to the medical literature).

3. Patel RR, Sengupta S, Kim HR, Klein-Szanto AJ, Pyle JR, Zhu F, Li T, Ross EA, Oseni S, Fargnoli J, Jordan VC. Experimental treatment of estrogen receptor (ER) positive breast cancer with tamoxifen and brivanib alaninate, a V EGFR-2/FGFR-1 kinase inhibitor: a potential clinical application of angiogenesis inhibitors. *European Journal of Cancer* 2010: 46:1537-1553.
4. Maximov PY, Myers CB, Curpan RF, Lewis-Wambi JS, Jordan VC. Structure-Function Relationships of Estrogenic Triphenylethylenes Related to Endoxifen and 4-Hydroxytamoxifen. *Journal of Medicinal Chemistry* 2010: 53:3273-3283.
5. Sengupta SS, Sharma CGN, Jordan VC. Estrogen Regulation of X-Box Binding Protein-1 and its Role in Estrogen Induced Growth of Breast and Endometrial Cancer Cells. *Hormone Molecular Biology and Clinical Investigation* 2010: 2:235-243.
6. Balaburski G, Dardes RC, Johnson M, Haddad B, Zhu F, Ross EA, Sengupta S, Klein-Szanto A, Liu H, Kim H, Jordan VC. Raloxifene-stimulated experimental breast cancer with the paradoxical actions of estrogen to promote or prevent tumor growth: A unifying concept in anti-hormone resistance. *International Journal of Oncology* 2010: 37:387-398.
7. Vogel VG, Costantino JP, Wickerham DL, Cronin WM, Cecchini RS, Atkins JN, Bevers TB, Fehrenbacher L, Pajon ER, Wade JL, Robidoux A, Margolese RG, James J, Runowicz CD, Ganz PA, Reis SE, McCaskill-StevensW, Ford LG, Jordan VC, Wolmark N. Update of the NSABP Study of Tamoxifen and Raloxifene (STAR) P-2 Trial: Preventing Breast Cancer. *Cancer Prevention Research* 2010: 3:696-706.
8. Maximov P, Sengupta S, Lewis-Wambi JS, Kim HR, Curpan RF, Jordan VC. The conformation of the estrogen receptor directs estrogen-induced apoptosis in breast cancer: a hypothesis. *Hormone Molecular Biology and Clinical Investigation* 2011: 5:27-34.
9. Ko S and Jordan VC. Treatment of osteoporosis and reduction in risk of invasive breast cancer in postmenopausal women with raloxifene. *Expert Opinion on Pharmacotherapy* 2011: 12:657-74.
10. Hu ZZ, Huang H, Wu CH, Jung M, Dritschilo A, Riegel AT, Wellstein A. Omics-based molecular target and biomarker identification. *Methods in Molecular Biology* 2011: 719:547-571.
11. Yang CZ, Yaniger SI, Jordan VC, Klein DJ, Bittner GD. Most Plastic Products Release Estrogenic Chemicals: A Potential Health Problem That Can Be Solved. *Environmental Health Perspectives* 2011 (*Epub ahead of print*).
12. Jordan VC and Ford LS. Paradoxical Clinical Effect of Estrogen on Breast Cancer Risk: A "New" Biology of Estrogen-Induced Apoptosis. *Cancer Prevention Research* 2011: 4:633-637.
13. Sweeney L and Jordan VC. Estrogen Receptor (ER). In: Encyclopedia of Cancer Therapeutic Targets. Springer Science + Business Media, LLC, New York (*in press*).

14. Jordan VC, Obiorah I, Fan P, Kim HR, Ariazi E, Cunlifffe H, Brauch H. Evolution of Long-Term Adjuvant Anti-hormone Therapy: Consequences and Opportunities: The St. Gallen Prize Lecture. *Breast* 2011 (*in press*).
15. Jordan VC. Decades of Discovery: The Selective Estrogen Receptor Modulator (SERM) Story: The St. Gallen Prize. *References en Gynecologie Obstetrique* 2011 (*in press)*.
16. Hu ZZ, Kagan BL, Ariazi E, Rosenthal DS, Zhang L, Li JV, Huang H, Wu C, Jordan VC, Riegel AT, Wellstein A. Proteomic analysis of pathways involved in estrogen-induced growth and apoptosis of breast cancer cells. *PLoS ONE* 2011 (*in press*).
17. Chien CD, Li JV, Kirilyuk AA, Lahusen T, Schmidt MO, Oh As, Wellstein A, Riegel AT. Role of the nuclear receptor co-activator AIB1-4 in the control of gene transcription. *Journal of Biological Chemistry* 2011 (*in press*).
18. Lewis-Wambi JS, Kim H, Curpan R, Grigg R, Sarker MA, Jordan VC. "The Selective Estrogen Receptor Modulator Bazedoxifene Inhibits Hormone-Independent Breast Cancer Cell Growth and Downregulates Estrogen Receptor α and Cyclin D1. *Molecular Pharmacology* 2011 (*in press*).

Abstracts

1. *Abstract was presented at the 27th Annual Miami Breast Cancer Conference, Miami, FL, March 3-6, 2010.*
   Challenges to improve adjuvant endocrine therapy.
   V. Craig Jordan.
2. *Abstract was presented at the 27th Annual Miami Breast Cancer Conference, Miami, FL, March 3-6, 2010.*
   Chemoprevention in the high risk patient.
   V. Craig Jordan.
3. *Abstract was presented at the 27th Annual Miami Breast Cancer Conference, Miami, FL, March 3-6, 2010.*
   Predictor of permanent menopause after chemotherapy.
   V. Craig Jordan.
4. *Abstract #607 was published in the 2010 Proceedings of the 101st Annual Meeting of the American Association for Cancer Research, Washington, DC, April 17-21, 2010.*
   Loss of pigment epithelium derived-factor (PEDF) is associated with breast cancer progression and antihormone drug resistance.
   Joan S. Lewis-Wambi, Helen Kim, V. Craig Jordan.
5. *Abstract #609 was published in the 2010 Proceedings of the 101st Annual Meeting of the American Association for Cancer Research, Washington, DC, April 17-21, 2010.*
   Paradoxical actions of a c-Src inhibitor on estradiol-induced apoptosis in long-term estrogen deprivation breast cancer cells.
   Ping Fan, Helen Kim, V. Craig Jordan.
6. *Abstract #1279 was published in the 2010 Proceedings of the 101st Annual Meeting of the American Association for Cancer Research, Washington, DC, April 17-21, 2010.*

Caspase-4 is critical in estrogen-induced apoptosis in antihormone-resistant breast cancer.

V. Craig Jordan, Eric A. Ariazi, Heather E. Cunliffe, Joan S. Lewis-Wambi, Smitha Yerrum, Helen R. Kim, Catherine G.N. Sharma, Amanda Willis, Pilar Ramos, Coya Tapia, Michael J. Slifker, Suraj Peri, Eric A. Ross.

7. *Abstract was presented at the Cold Spring Harbor Laboratory/Wellcome Trust Scientific Conference, Cambridge UK, August 11-15, 2010.*

   Proteomics and systems analysis of estrogen-induced cell growth or cell death in breast cancer cells.

   Zhang-Zhi Hu, Benjamin L. Kagan, Lihua Zhang, V. Craig Jordan, Anna T. Riegel, Anton Wellstein.

8. *Abstract was presented at the 2010 Taipei International Breast Cancer Symposium, Taiwan, September 4, 2010.*

   Selective Oestrogen Receptor Modulators: Concept to Reality, Drugs and Medicines to Prevent Multiple Diseases in Women.

   V. Craig Jordan.

9. *Abstract was presented at the 2010 Taipei International Breast Cancer Symposium, Taiwan, September 4, 2010.*

   Antihormone Resistance: The New Biology of Low Dose Estrogen Treatment for Breast Cancer.

   V. Craig Jordan.

10. *Abstract was presented at the 1st International Symposium of the Journal: Hormone Molecular Biology and Clinical Investigation, Seefeld, Tyrol, Austria, September 11-14, 2010.*

    Mechanisms of oestrogen-induced apoptosis in breast cancer.

    V. Craig Jordan.

11. *Abstract was presented at the European Molecular Biology Organization Conference Series Chemical Biology 2010: From Functional Genomics to Systems Biology, Heidelberg, Germany, September 22-25, 2010.*

    Proteomics and systems analysis of estrogen-induced cell growth or cell death in breast cancer cells.

    Zhangzhi Hu, Benjamin Kagan, Lihua Zhang, Cathy Wu, Eric Ariazi, V. Craig Jordan, Anna T. Riegel, Anton Wellstein.

12. *Abstract #B61 was published in the 2010 Proceedings of the 3rd Science of Cancer Health Disparities in Racial/Ethnic Minorities and the Medically Underserved Conference of the American Association for Cancer Research, Miami, FL, September 30 – October 3, 2010.*

    Phospholipid scramblase is a critical mediator of estrogen-induced apoptosis in antihormone resistant breast cancer cells.

    Joan S. Lewis-Wambi, Tabitha King, Annalese Smith.

13. *Abstract was presented at the TGen Annual Scientific Retreat, Phoenix Convention Center, September 4, 2009.*
    Investigating mechanisms of PKC signaling deregulation in endocrine-resistant breast cancer: The role of RACK7.
    Pilar Ramos, Amanda L. Willis, JM Chatigny, Megan L. Russell, Joan S. Lewis-Wambi, Eric A. Ariazi, V. Craig Jordan, Heather E. Cunliffe.
14. *Abstract was presented at the Amazon Project 8th Conference, Palermo, Italy, November 15-20, 2010.*
    Estrogen action in the life and death of breast cancer cells.
    V. Craig Jordan.
15. *Abstract was presented at the 12th St. Gallen International Breast Cancer Conference, St. Gallen, Switzerland, March 16-19, 2011.*
    Evolution of long-term adjuvant antihormone therapy: Consequences and opportunities.
    V. Craig Jordan.
16. *Abstract #774 was published in the 2011 Proceedings of the 102nd Annual Meeting of the American Association for Cancer Research, Orlando, FL, April 2-6, 2011.*
    PEDF silencing a novel mechanism of antihormone resistance in breast cancer.
    Joan S. Lewis-Wambi, Min Huang.
17. *Abstract #2291 was published in the 2011 Proceedings of the 102nd Annual Meeting of the American Association for Cancer Research, Orlando, FL, April 2-6, 2011.*
    Inhibition of c-Src restores estrogen-stimulated growth in estrogen-deprivation resistant MCF-7 breast cancer cells.
    Ping Fan, Helen Kim, Russell E. McDaniel, V. Craig Jordan.
18. *Abstract was presented at the Cologne Cancer Club, Cologne, Germany, May 4, 2011.*
    Tamoxifen: a pioneering medicine that gave us SERMs to prevent multiple diseases in women's health.
    V. Craig Jordan.

Presentations

2010:

1. Ramos P. "Investigating mechanisms of PKC signaling deregulation in endocrine-resistant breast cancer: The role of RACK7." Glendale Community College Lecture Series, Glendale, AZ, February 19, 2010.
2. Jordan VC. "Chemoprevention in the High Risk Patient." 27th Annual Miami Breast Cancer Conference, Prevention Strategies, Miami, FL, March 3, 2010.
3. Jordan VC. "Predictor of Permanent Menopause After Chemotherapy." 27th Annual Miami Breast Cancer Conference, Emerging and Controversial Topics in Systemic Adjuvant Therapy, Miami, FL, March 5, 2010.

4. Jordan VC. "Challenges to Improve Adjuvant Endocrine Therapy." 27th Annual Miami Breast Cancer Conference, Future Challenges, Miami, FL, March 6, 2010.
5. Jordan VC. "Overcoming Hormone Therapy Resistance." 5th Annual Georgetown Breast Cancer Update: Emerging Trends in Management of Breast Cancer, Washington, DC, March 13, 2010.
6. Jordan VC. "Amplifying the apoptotic actions of oestrogen to treat metastatic breast cancer." Translational Cancer Medicine, American Association for Cancer Research, Amsterdam, Netherlands, March 22, 2010.
7. Jordan VC. "Targeted Therapy to Steroid Hormone Receptors: Evolution of Ideas Into Lives Saved." AACR 101st Annual Meeting, Walter E. Washington Convention Center, Washington, DC, April 17-21, 2010.
8. Jordan VC. "Estrogen in the life and death of breast cancer cells." NIH/NCI Distinguished Speaker, Distinguished Scientist Lecture Series, National Cancer Institute, Frederick, MD, May 4, 2010.
9. Jordan VC. "The discovery and application of selective estrogen receptor modulators." Department of Pharmacology seminar, Georgetown University Medical Center, Washington DC, May 21, 2010.
10. Obiorah I. "Estrogen regulated growth and apoptosis." Cancer Research Data Meeting, Lombardi Comprehensive Cancer Center, Georgetown University Medical Center, Washington, DC, June 24, 2010.
11. Jordan VC. "The quest for multi-functional medicines: path for progress: the tamoxifen story." Moscow, Russia, July 14-18, 2010.
12. Jordan VC. "The quest for multi-functional medicines: path for progress: the SERM story." Moscow, Russia, July 14-18, 2010.
13. Hu ZZ, Kagan BL, Zhang L, Jordan VC, Riegel AT, Wellstein A. "Proteomics and systems analysis of estrogen-induced cell growth or cell death in breast cancer cells." Systems Biology: Networks Plenary Lecture. Cold Spring Harbor Laboratory/Wellcome Trust Scientific Conference, Cambridge UK, August 11-15, 2010.
14. Jordan VC. "Anti-hormone resistance: the new biology of low dose oestrogen treatment for breast cancer." 2010 T aipei International Breast Cancer Symposium, The Breast Cancer Society of Taiwan, Taipei, Taiwan, September 4, 2010.
15. Jordan VC. "Selective oestrogen receptor modulators: concept to reality. Drugs and medicines to prevent multiple diseases in women." 2010 Taipei International Breast Cancer Symposium, The Breast Cancer Society of Taiwan, Taipei, Taiwan, September 4, 2010.
16. Jordan VC. "Mechanisms of oestrogen-induced apoptosis in breast cancer." 1st International Symposium of the Journal: Hormone Molecular Biology and Clinical Investigation, Seefeld, Tyrol, Austria, September 11-14, 2010.
17. Jordan VC. "Hormone receptor positive disease subgroup update (recent progress)." Stand Up 2 C ancer (SU2C), 2nd AACR Breast Cancer Dream Team (BCDT) Update Meeting, Dallas, TX, September 25-26, 2010.

18. Jordan VC. "Hormone receptor positive disease subgroup follow-on meeting (animal models)." Stand Up 2 C ancer (SU2C), 2nd AACR Breast Cancer Dream Team (BCDT) Update Meeting, Dallas, TX, September 25-26, 2010.
19. Jordan VC. "Estrogen-induced apoptosis in breast cancer." Research Update Seminar Series, Lombardi Comprehensive Cancer Center, Georgetown University Medical Center, Washington, DC, September 29, 2010.
20. Ariazi EA. "Deciphering Global Gene Expression Across Time by Differential Area-Under-the-Curve Analysis to Examine Estrogen-induced Apoptosis in Aromatase Inhibitor-resistant Breast Cancer Cells." Research Update Seminar Series, Lombardi Comprehensive Cancer Center, Georgetown University Medical Center, Washington, DC, October 6, 2010.
21. Jordan VC. "Breast Cancer Chemoprevention: Have We Made Progress?" 12th Annual Lynn Sage Breast Cancer Symposium, Chicago, IL, October 28-31, 2010.
22. Jordan VC. "Oestrogen action in the life and death of breast cancer cells." Amazon Project, 8th Conference, Palermo, Italy, November 15-20, 2010.
23. Fan P. "Modulation of Estrogen-Induced Apoptosis by Inhibiting c-Src in Estrogen-Deprived Resistant MCF-7 Breast Cancer Cells: Potential Clinical Implications." Research Update Seminar Series, Lombardi Comprehensive Cancer Center, Georgetown University Medical Center, Washington, DC, November 17, 2010.
24. Riegel AT. "Co-activators in Malignant Progression." Research Update Seminar Series, Lombardi Comprehensive Cancer Center, Georgetown University Medical Center, Washington, DC, December 8, 2010.
25. Jordan VC. "Evolution of hormone therapy for the prevention and treatment of breast cancer: new opportunities." A New Era In The Diagnosis and Treatment of Breast Cancer, Bangkok, Thailand, December 10-19, 2010.

2011:

1. Jordan VC. "Deciphering the molecular pharmacology of tamoxifen treatment for breast cancer: the critical role of the graduate student." Uniformed Services University, Molecular & Cell Biology Graduate Program, Bethesda, MD, January 13,2011.
2. Jordan VC. "Modulation of Estrogen-Induced Apoptosis in Breast Cancer." Think Tank 21, Breast Cancer Symposium, Montego Bay, Jamaica, January 16-22, 2011.
3. Wellstein A. "Understanding and targeting cancer/stromal interactions." Research Update Seminar Series, Lombardi Comprehensive Cancer Center, Georgetown University Medical Center, Washington, DC, January 26, 2011.
4. Jordan VC. "Evolution of long-term adjuvant anti-hormone therapy: consequences and opportunities." 12th St. Gallen International Breast Cancer Conference, St. Gallen, Switzerland, March 16-19, 2011.
5. Obiorah I. "Modulation of estrogen-induced apoptosis in breast cancer." Cancer Research Data Meeting, Lombardi Comprehensive Cancer Center, Georgetown University Medical Center, Washington, DC, April 14, 2011.

6. Jordan VC. "Tamoxifen: A Pioneering Medicine That Gave Us SERMs to Prevent Multiple Diseases in Women's Health." Cologne Cancer Club, Cologne, Germany, May 4, 2011.

Grants

1. Susan G. Komen For The Cure Award # SAC100009 for the Susan G Komen For The Cure Foundation. "Molecular modification of the estrogen receptor (ER) for estrogen action antagonism and apoptosis." Period: July 1, 2010 – June 30, 2012
2. SU2C (Stand Up 2 Cancer) Grant number SU2C-AACR-DT0409, subcontract under Stand Up 2 Cancer, American Association for Cancer Research (AACR). "An integrated approach to targeting breast cancer molecular subtypes and their "resistance" phenotypes." Period: October 1, 2009 – September 30, 2012

Awards and Honorary Memberships

1. **April 29, 2010**: Dr. V. Craig Jordan appointed to the Susan G. Komen Scientific Advisory Council. Term duration: 2 years, renewable terms. Appointment to the Komen Scientific Advisory Council is reserved for those who have a distinguished record of leadership and commitment to breast cancer research, as well as innovative contributions to breast cancer advancements. Those who are appointed as Council members "will serve as distinguished scholars advising and providing expertise to Susan G. Komen for the Cure in peer review, scientific research, sponsored programs, program development and review, and public policy."
2. **May 24, 2010**: PhD degree awarded to Dr. Philipp Maximov from the Russian State Medical University, Moscow, Russia. Dr. Maximov was formerly Dr. Jordan's PhD Graduate Student (2006-2009) when the Jordan Lab was at the Fox Chase Cancer Center, Philadelphia, PA.
3. **August 2010**: V. Craig Jordan elected as the new President for the Royal Society of Medicine (RSM) Foundation in the United States, 2010-present. In this role, Dr. Jordan is representing the Royal Society of Medicine in the United States and will work closely with the RSM in London to enhance awareness of the opportunities of Fellowship in the Society and to focus on specific educational opportunities in global health to foster exchanges across the Atlantic.
4. **October 8, 2010**: V. Craig Jordan inducted into the Susan G. Komen For The Cure Investigator Hall of Fame as its Inaugural Recipient, at the John F. Kennedy Center, Washington, DC. Awarded for practical contributions to enhancing survivorship in breast cancer.
5. **October 16, 2010**: V. Craig Jordan awarded with the Susan G. Komen For The Cure Scientific and Medical Distinction Award at the John F. Kennedy Center, Washington, DC. Awarded for contributions to developing tamoxifen and SERMs.
6. **February 4, 2011**: V. Craig Jordan selected for inclusion in *Who's Who 2012* in the United Kingdom, the 164th annual edition, the oldest professional biography in the world. Who's Who is the world-renowned biographical reference book, recognized as the source of information on people of distinction, influence and interest in all fields.

7. **March 16, 2011**: V. Craig Jordan awarded the St. Gallen Breast Cancer Award in Clinical Breast Cancer Research to V. Craig Jordan, OBE, PhD, DSc, FMedSci in St. Gallen, Switzerland at the 12th St. Gallen International Breast Cancer Conference. This award recognizes outstanding contributions to the adjuvant therapy of breast cancer and is the most prestigious clinical breast cancer award in the world.
8. **May 11, 2011**: V. Craig Jordan honored at the Embassy of Switzerland, Washington, DC for contributions to breast cancer research and for enhancing the international research cooperation between Switzerland and the United States of America for the past thirty years.

Appointments

1. **Julia J. Tijerina**
   March 17, 2010, Executive Assistant to Dr. V. Craig Jordan
2. **Russell E. McDaniel, BS**
   March 17, 2010, Research Assistant I
3. **Seungsang Ko, MD, PhD**
   July 28, 2010, V isiting Associate Professor from the Cheil General Hospital & Women's Health Care Center, Department of Surgery, KwanDong University College of Medicine, Seoul, South Korea
4. **Philipp Y. Maximov, MD, PhD**
   February 28, 2011, Susan G. Komen Foundation For The Cure Postdoctoral Research Fellow

CONCLUSIONS

The successful transition from FCCC to LCCC has been complex, time-consuming and momentum has been retarded through administrative delays. Despite this challenge and the delays in our projected timetable, we are now completely re-organized, re-invigorated and back to the Tasks in hand to achieve our goal to decipher the molecular mechanisms of estrogen-induced apoptosis in breast cancer. It is, however, important to stress at the outset of this section, that there is growing momentum within the clinical community that our work is an important new dimension in women's health. This is illustrated by three, well-defined facts:

1) Our focus on t he applicability of our laboratory results through the use of low dose estrogen for the treatment of metastatic breast cancer following antihormone drug resistance, is now a general topic of discussion. Our work has been pivotal for the publication of others; the concept we proposed from the laboratory data enhances the treatment of women with breast cancer (2, 100).
2) Our concepts form the basis of a major clinical trial in Europe and around the world, described as the Study of Letrozole Extension (SOLE) (see #11 i n Appendix). The strategy for the study is to examine whether continuous long term antihormone therapy is better or worse for the adjuvant treatment of ER-positive breast cancer than therapy that has three months per year drug holidays, where the women's own estrogen can destroy the antihormone resistant breast cancer cells before drug resistance disease gets a hold.

3) The recent published findings of the Women's Health Initiative (WHI) of estrogen replacement therapy in hysterectomized postmenopausal women showed a reduction in the incidence of breast cancer that in fact continues for five years after estrogen therapy stops (10). We are providing all of the scientific knowledge database to explain this apparently paradoxical finding (estrogen replacement reduces the risk of breast cancer!). We obviously take very seriously, the fact that we are the pioneering group scientifically in this area and through the investment of the DOD CoE grant via their visionary peer-reviewed system, we have been given the responsibility to decipher the mechanisms involved in this new biology of estrogen-induced apoptosis in breast cancer.

It is clear from the aforementioned three broad applications in clinical medicine that we have a responsibility and opportunity to revolutionize women's health through the prudent application of remaining resources to be awarded through our CoE grant. I will systematically create an executive summary conclusion for each of our ongoing Tasks.

The proposed clinical trials (**Task 1**) have suffered from the general withdrawal of the pharmaceutical industry from university, scientific-based programs. Despite this apparent setback, we are moving the coordinating center from FCCC to LCCC, as I have acquired funding to maintain patient accrual through the clinical PI, Dr. Claudine Isaacs. All of the biological materials collected at FCCC are invaluable and will be transferred to LCCC for evaluation, analysis and data mining. It is our intention to maintain patient accrual with our primary objective of sample acquisition, but with the full knowledge that our original concept is already in the clinical domain and available for all clinicians to use in their treatment plans. This demonstrates a clear success story for our commitment to this translational research.

Our major accomplishment on the grant to create a map of the life and death of breast cancer cells in response to physiological estrogen has been achieved (**Task 2a**). This is a new unique dataset that is invaluable, but the complexity of our dataset is currently a challenge to the best brains in bioinformatics in the world, with whom we are currently collaborating. It is important to realize that our visionary approach proposed the equivalence of a movie, of the life and death of breast cancer cells through gene activation and suppression, but every other research group in the world is studying only single photographs of cells and tumors at a single point in time. Nevertheless, it is our accomplishment that has been enhanced by considerable bioinformatics input and the development of new computer modeling systems to analyze gene dosing activation against time for the growth and death of human breast cancer cells in response to estrogen. With my election to the National Academy of Sciences and my induction during this reporting period, we are in the process of submitting our pioneering work as my inaugural paper to the *Proceedings of the National Academy of the Sciences* (*PNAS*) (**Tasks 4a and 4b)**. With our database, we have already identified an initial molecular mechanism for estrogen-induced apoptosis in our endocrine resistant breast cancer cells. Estrogen induces a stress response and activates inflammatory genes. This discovery now allows us to interrogate this mechanism of inflammation-mediated cell death through its modulation with anti-inflammatory agents. Glucocorticoids are used universally in clinical care and are essential in human physiology. Our

preliminary findings are that glucocorticoids inhibit estrogen-induced apoptosis, which potentially will allow us to define and propose clinical strategies to amplify estrogen-induced apoptosis. The other major finding from our database is a definition of the caspase cascade that provokes cell death and destruction following estrogen-induced apoptosis. We have precisely defined and identified caspase 4 as the trigger caspase in the initiation of estrogen-induced apoptosis. However, we now seek to build upon our database and use molecular pharmacology to define and refine the input signal through the estrogen receptor that modulates estrogen-induced apoptosis. We are addressing two issues: 1) What are the basic estrogen-ER related events that trigger estrogen-induced apoptosis (**Tasks 2b-1 and 2b-2**) and 2) Can a SERM be discovered that will kill antihormone resistant breast cancer cells in our laboratory models (**Task 2b-3**).

We have addressed the hypothesis that by blocking cellular survival signaling, we should be able to enhance estrogen-induced apoptosis (**Task 2b-1**). The c-Src oncogene is present in 70% of breast cancers and is clearly a survival pathway of potential importance. We have made the novel discovery that blocking c-Src actually blocks estrogen-induced apoptosis. This counter-intuitive observation that is unique to our laboratory has two important ramifications: 1) Clinically available c-Src inhibitors should not be used or tested in breast cancer patients following drug resistance to antihormones. The c-Src inhibitor has the potential to prevent naturally occurring estrogen-induced apoptosis and this will be of detriment to the patient. 2) Our observation that blockade of c-Src has potential to inhibit estrogen-induced apoptosis has resulted in a collaboration with a new grant (SU2C) to evaluate the molecular mechanism that was previously unknown. It is important to emphasize that this grant at SU2C has now introduced us to a group of the most prominent analytical experts and world leaders in the molecular aspects of breast cancer in the world. This would not have happened but for the investment in our DOD CoE grant.

Another important aspect of the triggering of estrogen-induced apoptosis is the actual shape and conformation of the ER complex in the cell (**Task 2b-2**). Earlier, we described a new classification of synthetic and natural estrogens binding to the estrogen receptor, and this classification really segregated the molecules into planar and non-planar estrogens. As a result of ligand binding, the planar estrogens (Class I) produced a neat protein complex around the planar estrogen. In contrast, non-planar estrogens (Class II) do not allow the estrogen receptor to close neatly around the ligand and at its extreme, an antiestrogen produces an abnormal shape, thereby blocking estrogen action (13). Earlier we discovered that non-steroidal antiestrogens (SERMs) such as 4-hydroxytamoxifen, completely blocked estrogen-induced apoptosis. The shape of the complex clearly was critical to trigger apoptosis. However, we have also extended our investigation using Class II estrogens, although estrogen-like, Class II estrogens stimulate breast cancer cell replication, but do not in fact stimulate estrogen-induced apoptosis. This insight into the modulation of the shape of the ER complex now draws us to the conclusion that co-activators that would normally bind to the ER complex for full estrogen action are clearly critical for estrogen-induced apoptosis. We are currently engaged in a major project studying the structure function relationships of Class II estrogens and their ability to modulate apoptosis and deliver

appropriate co-activators to promoter sites on estrogen target genes. It is important to stress that the goal of this molecular enterprise of the shape of the ER to modulate estrogen-induced apoptosis now perfectly intersects with **Task 3**, the proteomics of estrogen-induced apoptosis (see later).

A central question that we posed was why in some of our antihormone resistant cells is that the antiestrogen and SERM, 4-hydroxytamoxifen, has absolutely no effect on the growth of these cells? Bazedoxifene is a new SERM developed by the pharmaceutical industry that will be used for the treatment of osteoporosis and prevention of breast cancer at the same time. Additionally, bazedoxifene will be administered with estrogen replacement therapy to ameliorate hot flashes in women as they progress through the menopause, but the SERM will protect them from endometrial and breast cancer. Although we have been prohibited from obtaining bazedoxifene from the pharmaceutical industry, one of my colleagues in the Royal Society in England, under contract, has synthesized the drug. We have made a remarkable discovery: bazedoxifene has the ability to kill antihormone resistant breast cancer cells (**Task 2b-3**). Our manuscript, noted in the Appendix, has been accepted by *Molecular Pharmacology* (see Appendix) and we will be continuing this work in our laboratory to refine and define mechanisms.

The role of our proteomic groups (**Task 3**) is to look at the early stages of estrogen receptor mediated estrogen-induced apoptosis to define key components of the ER complex or pathways emanating from an important node. Our proteomics group has integrated a global co-activator signaling network (AIB1) that appears to control the growth and apoptosis of breast cancer cells. The importance of G-protein coupled receptors, PI3 kinase, Wnt and Notch signaling pathways are strongly associated with estrogen-induced proliferation or apoptosis. These findings link in to our prior publication on GPR30 (29; see #2 in Appendix) and our work on the shape of the ER and estrogen-induced apoptosis. In our parallel studies, we concluded that AIB1 is the controlling mechanism to trigger estrogen-induced apoptosis in our antihormone resistant breast cancer cells. In our current studies and for Year 5 of our grant, we are using breast cancer tumors artificially grown in athymic mice to address the same questions we have derived here in cell culture, but *in vivo*.

The genomics program at TGen (**Task 4c**) has accomplished a remarkable analysis of the resting and gene activation states of our antihormone resistant breast cancer cells in culture. These data married with their accomplishment to measure the CGH of each of our cell lines (to determine gene copies) now positions us uniquely to understand what drives antihormone resistant growth. Again, through our collaboration with our new grant (SU2C) and the head of breakthrough breast cancer, Professor Alan Ashworth, FRS, we are collaborating internationally with their group, who has recently published a set sequence of genes that need to be activated to create tamoxifen resistance. Our models are field testing their gene set. In combination with this, TGen has conducted a high-throughput analysis using siRNAs to determine the precise genes activated by estrogen-induced apoptosis. These data are unique and meld perfectly with all of our other tasks.

Overall, our future plans described in our original grant application are moving forward with an integrated approach to deciphering the molecular mechanism (mechanisms) of estrogen-induced apoptosis. Our unique team has built on our strengths and we are now poised to analyze and integrate our data for publication. These data have been used to obtain grants from other sources (SU2C, Susan G. Komen For The Cure) which enhances our capacity for interaction with the best breast cancer research scientists in the world.

REFERENCES

1. Lewis JS, Meeke K, Osipo C, Ross EA, Kidawi N, Li T, Bell E, Chandel NS, Jordan VC. Intrinsic mechanism of estradiol-induced apoptosis in breast cancer cells resistant to estrogen deprivation. *J Natl Cancer Inst* 2005;97(23):1746-59.

2. Ellis MJ, Gao F, Dehdashti F, Jeffe DB, Marcom PK, Carey LA, et al. Lower-dose vs high dose oral estradiol therapy of hormone receptor-positive, aromatase inhibitor-resistant advanced breast cancer: a phase 2 randomized study. *JAMA* 2009;302:774-80.

3. Thomas SN, Brugge JS. Cellular functions regulated by Src family kinases. *Ann Rev Cell Dev Biol* 1997;13:513-609.

4. Fan P, Wang J, Santen RJ, Yue W. Long-term treatment with tamoxifen facilitates translocation of estrogen receptor alpha out of the nucleus and enhances its interaction with EGFR in MCF-7 breast cancer cells. *Cancer Res* 2007; 67(3):1352-60.

5. Chu I, Arnaout A, Loiseau S, et al. Src promotes estrogen-dependent estrogen receptor alpha proteolysis in human breast cancer. *J Clin Invest* 2007;117:2205-15.

6. Kasahara K, Nakayama Y, Kihara A, Matsuda D, Ikeda K, Kuga T, Fukumoto Y, Igarashi Y, Yamaguchi N. Rapid trafficking of c-Src, a non-palmitoylated Src-family kinase, between the plasma membrane and late endosomes/lysosomes. *Exp Cell Res* 2007;313(12):2651-66.

7. Boonyaratanakornkit V, Bi Y, Rudd M, Edwards DP. The role and mechanism of progesterone receptor activation of extra-nuclear signaling pathways in regulating gene transcription and cell cycle progression. *Steroids* 2008;73:922-928.

8. Haddow A, Watkinson JM, Paterson E, Koller PC. Influence of Synthetic Oestrogens on Advanced Malignant Disease. *Br Med J* 1944;2(4368):393-8.

9. Lonning PE, Taylor PD, Anker G, Iddon J, Wie L, Jorgensen LM, et al. High-dose estrogen treatment in postmenopausal breast cancer patients heavily exposed to endocrine therapy. *Breast Cancer Res Treat* 2001;67(2):111-6.

10. LaCroix AZ, Chlebowski RT, Manson JE, Aragaki AK, Johnson KC, Martin L, et al. Health outcomes after stopping conjugated equine estrogens among postmenopausal women with prior hysterectomy: a randomized controlled trial. *JAMA* 2011;305(13):1305-14.

11. Jordan VC, Ford LG. Paradoxical Clinical Effect of Estrogen on Breast Cancer Risk: A "New" Biology of Estrogen-induced Apoptosis. *Cancer Prev Res (Phila)* 2011;4(5):633-7.

12. Lewis JS, Osipo C, Meeke K, Jordan VC. Estrogen-induced apoptosis in a breast cancer model resistant to long-term estrogen withdrawal. *J Steroid Biochem Mol Biol* 2005;94(1-3):131-41.
13. Jordan VC, Schafer JM, Levenson AS, Liu H, Pease KM, Simons LA, et al. Molecular classification of estrogens. *Cancer Res* 2001;61(18):6619-23.
14. Gust R, Keilitz R, Schmidt K. Investigations of new lead structures for the design of selective estrogen receptor modulators. *J Med Chem* 2001;44(12):1963-70.
15. Metivier R, Penot G, Hubner MR, Reid G, Brand H, Kos M, et al. Estrogen receptor-alpha directs ordered, cyclical, and combinatorial recruitment of cofactors on a natural target promoter. *Cell* 2003;115(6):751-63.
16. Levenson AS, Jordan VC. The key to the antiestrogenic mechanism of raloxifene is amino acid 351 (aspartate) in the estrogen receptor. *Cancer Res* 1998;58(9):1872-5.
17. Levenson AS, Tonetti DA, Jordan VC. The oestrogen-like effect of 4-hydroxytamoxifen on induction of transforming growth factor alpha mRNA in MDA-MB-231 breast cancer cells stably expressing the oestrogen receptor. *Br J Cancer* 1998;77(11):1812-9.
18. Hu ZZ, Huang H, Wu CH, Jung M, Dritschilo A, Riegel AT, & Wellstein A. Omics-based molecular target and biomarker identification. *Methods Mol Biol* 2011;719:547-571.
19. Long W, Yi P, Amazit L, Lamarca HL, Ashcroft F, Kumar R, Mancini MA, Tsai, SY, Tsai MJ, & O'malley BW. SRC-3Delta4 mediates the interaction of EGFR with FAK to promote cell migration. *Mol Cell* 2010;37:321-332.
20. Deng Q & Huang S. PRDM5 is silenced in human cancers and has growth suppressive activities. *Oncogene* 2004;23:4903-4910.
21. Brinkmeier ML, Potok MA, Cha KB, Gridley T, Stifani S, Meeldijk J, Clevers H, & Camper SA. TCF and Groucho-related genes influence pituitary growth and development. *Mol Endocrinol* 2003;17:2152-2161.
22. Nagahama Y, Ishimaru M, Osaki M, Inoue T, Maeda A, Nakada C, Moriyama M, Sato K, Oshimura M, & Ito H. Apoptotic pathway induced by transduction of RUNX3 in the human gastric carcinoma cell line MKN-1. *Cancer Sci* 2008;99:23-30.
23. Tong DD, Jiang Y, Li M, Kong D, Meng XN, Zhao YZ, Jin Y, Bai J, Fu SB, & Geng JS. RUNX3 inhibits cell proliferation and induces apoptosis by TGF-beta-dependent and -independent mechanisms in human colon carcinoma cells. *Pathobiology* 2009;76:163-169.
24. van Agthoven T, Sieuwerts AM, Meijer-van Gelder ME, Look MP, Smid M, Veldscholte J, Sleijfer S, Foekens JA, & Dorssers LC. J. Relevance of breast cancer antiestrogen resistance genes in human breast cancer progression and tamoxifen resistance. *J Clin Oncol* 2009;27:542-549.
25. Lewis-Wambi JS & Jordan VC. Estrogen regulation of apoptosis: how can one hormone stimulate and inhibit? *Breast Cancer Res* 2009;11:206.
26. Engelmann A, Speidel D, Bornkamm GW, Deppert W, & Stocking C. Gadd45 beta is a pro-survival factor associated with stress-resistant tumors. *Oncogene* 2008;27:1429-1438.

27. Papa S, Zazzeroni F, Bubici C, Jayawardena S, Alvarez K, Matsuda S, Nguyen DU, Pham CG, Nelsbach AH, Melis T, *et al.* Gadd45 beta mediates the NF-kappa B suppression of JNK signalling by targeting MKK7/JNKK2. *Nat Cell Biol* 2004;6:146-153.
28. Jordan VC, Lewis-Wambi J, Kim H, Cunliffe H, Ariazi E, Sharma CGN, Shupp HA, & Swaby R. Exploiting the apoptotic actions of oestrogen to reverse antihormonal drug resistance in oestrogen receptor positive breast cancer patients. *Breast* 2007;16 Suppl 2:S105-113.
29. Ariazi EA, Brailoiu E, Yerrum S, Shupp HA, Slifker MJ, Cunliffe HE, Black MA, Donato AL, Arterburn JB, Oprea TI, *et al.* The G protein-coupled receptor GPR30 inhibits proliferation of estrogen receptor-positive breast cancer cells. *Cancer Res* 2010;70:1184-1194.
30. Hurtado A, Holmes KA, Geistlinger TR, Hutcheson IR, Nicholson RI, Brown M, Jiang J, Howat WJ, Ali S, & Carroll JS. Regulation of ERBB2 by oestrogen receptor-PAX2 determines response to tamoxifen. *Nature* 2008;456:663-666.
31. Lahusen T, Henke RT, Kagan BL, Wellstein A, & Riegel AT. The role and regulation of the nuclear receptor co-activator AIB1 in breast cancer. *Breast Cancer Res Treat* 2009;116:225-237.
32. Fereshteh MP, Tilli MT, Kim SE, Xu J, O'Malley BW, Wellstein A, Furth PA, & Riegel AT. The nuclear receptor coactivator amplified in breast cancer-1 is required for Neu (ErbB2/HER2) activation, signaling, and mammary tumorigenesis in mice. *Cancer Res* 2008;68:3697-3706.
33. Oh AS, Lahusen JT, Chien CD, Fereshteh MP, Zhang X, Dakshanamurthy S, Xu J, Kagan BL, Wellstein A, & R iegel AT. Tyrosine phosphorylation of the nuclear receptor coactivator AIB1/SRC-3 is enhanced by Abl kinase and is required for its activity in cancer cells. *Mol Cell Biol* 2008;28:6580-6593.
34. York B & O'Malley BW. Steroid receptor coactivator (SRC) family: masters of systems biology. *J Biol Chem* 2010;285:38743-38750.
35. Wu RC, Qin J, Yi P, Wong J, Tsai SY, Tsai MJ, & O'Malley BW. Selective phosphorylations of the SRC-3/AIB1 coactivator integrate genomic responses to multiple cellular signaling pathways. *Mol Cell* 2004;15:937-949.
36. Jiang SY, Wolf DM, Yingling JM, Chang C, & Jordan VC. An estrogen receptor positive MCF-7 clone that is resistant to antiestrogens and estradiol. *Mol Cell Endocrinol* 1992;90(1):77-86.
37. Pink JJ, Jiang SY, Fritsch M, & Jordan VC. An estrogen-independent MCF-7 breast cancer cell line which contains a novel 80-kilodalton estrogen receptor-related protein. *Cancer Res* 1995;55(12):2583-2590.
38. Pink JJ & Jordan VC. Models of estrogen receptor regulation by estrogens and antiestrogens in breast cancer cell lines. *Cancer Res* 1996;56(10):2321-2330.
39. Lewis-Wambi JS, Kim HR, Wambi C, Patel R, Pyle JR, Klein-Szanto AJ, Jordan VC. Buthionine sulfoximine sensitizes antihormone-resistant human breast cancer cells to estrogen-induced apoptosis. *Breast Cancer Res* 2008;10(6):R104.

40. Ariazi EA, Kraus RJ, Farrell ML, Jordan VC, & Mertz JE. Estrogen-related receptor alpha1 transcriptional activities are regulated in part via the ErbB2/HER2 signaling pathway. *Mol Cancer Res* 2007;5(1):71-85.
41. Hotamisligil GS. Endoplasmic reticulum stress and the inflammatory basis of metabolic disease. *Cell* 2010;140(6):900-917.
42. Somboonporn W & Davis SR. Testosterone Effects on the Breast: Implications for Testosterone Therapy for Women. *Endocr Rev* 2004;25(3):374-388.
43. Burdette JE & Woodruff TK. Activin and estrogen crosstalk regulates transcription in human breast cancer cells. *Endocr Relat Cancer* 2007;14(3):679-689.
44. Lee KS, Kim HJ, Li QL, Chi XZ, Komori T, Wozney JM, Kim EG, Choi JY, Ryoo HM, Bae SC. Runx2 is a common target of transforming growth factor beta1 and bone morphogenetic protein 2, and cooperation between Runx2 and Smad5 induces osteoblast-specific gene expression in the pluripotent mesenchymal precursor cell line C2C12. *Mol Cell Biol* 2000;20(23):8783-8792.
45. Tsai AD, Yeh LC, & Lee JC. Effects of osteogenic protein-1 (OP-1, BMP-7) on gene expression in cultured medial collateral ligament cells. *J Cell Biochem* 2003;90(4):777-791.
46. Tou L, Quibria N, & Alexander JM. Transcriptional regulation of the human Runx2/Cbfa1 gene promoter by bone morphogenetic protein-7. *Mol Cell Endocrinol* 2003;205(1-2):121-129.
47. Selvamurugan N, Kwok S, & Partridge NC. Smad3 interacts with JunB and Cbfa1/Runx2 for transforming growth factor-beta1-stimulated collagenase-3 expression in human breast cancer cells. *J Biol Chem* 2004;279(26):27764-27773.
48. Kim I, Xu W, & Reed JC. Cell death and endoplasmic reticulum stress: disease relevance and therapeutic opportunities. *Nat Rev Drug Discov* 2008;7(12):1013-1030.
49. Kim SJ, Zhang Z, Hitomi E, Lee YC, & Mukherjee AB. Endoplasmic reticulum stress-induced caspase-4 activation mediates apoptosis and neurodegeneration in INCL. *Hum Mol Genet* 2006;15(11):1826-1834.
50. Puthalakath H, O'Reilly LA, Gunn P, Lee L, Kelly PN, Huntington ND, Hughes PD, Michalak EM, McKimm-Breschkin J, Motoyama N, Gotoh T, Akira S, Bouillet P, Strasser A. ER stress triggers apoptosis by activating BH3-only protein Bim. *Cell* 2007;129(7):1337-1349.
51. Zhang M, Wang R, Wang Y, Diao F, Lu F, Gao D, Chen D, Zhai Z, Shu H. The CXXC finger 5 protein is required for DNA damage-induced p53 activation. *Sci China C Life Sci* 2009;52(6):528-538.
52. Inbal B, Bialik S, Sabanay I, Shani G, & Kimchi A. DAP kinase and DRP-1 mediate membrane blebbing and the formation of autophagic vesicles during programmed cell death. *J Cell Biol* 2002;157(3):455-468.
53. Stowell SR, Karmakar S, Arthur CM, Ju T, Rodrigues LC, Riul TB, Dias-Baruffi M, Miner J, McEver RP, Cummings RD. Galectin-1 Induces Reversible Phosphatidylserine Exposure at the Plasma Membrane. *Mol Biol Cell* 2009;20(5):1408-1418.

54. Wiest I, Seliger C, Walzel H, Friese K, & Jeschke U. Induction of apoptosis in human breast cancer and trophoblast tumor cells by galectin-1. *Anticancer Res* 2005;25(3A):1575-1580.
55. Lin L, Qian Y, Shi X, & Chen Y. Induction of a cell stress response gene RTP801 by DNA damaging agent methyl methanesulfonate through CCAAT/enhancer binding protein. *Biochemistry* 2005;44(10):3909-3914.
56. Nagaoka-Yasuda R, Matsuo N, Perkins B, Limbaeck-Stokin K, & Mayford M. An RNAi-based genetic screen for oxidative stress resistance reveals retinol saturase as a mediator of stress resistance. *Free Radical Biology and Medicine* 2007;43(5):781-788.
57. Park EJ, Kim JH, Seong RH, Kim CG, Park SD, Hong SH. Characterization of a novel mouse cDNA, ES18, involved in apoptotic cell death of T-cells. *Nucleic Acids Res* 1999;27(6):1524-1530.
58. Martinon F & Tschopp J. Inflammatory caspases and inflammasomes: master switches of inflammation. *Cell Death Differ* 2007;14(1):10-22.
59. Hitomi J, Katayama T, Eguchi Y, Kudo T, Taniguchi M, Koyama Y, Manabe T, Yamagishi S, Bando Y, Imaizumi Km Tsujimoto Y, Tohyama M. Involvement of caspase-4 in endoplasmic reticulum stress-induced apoptosis and A{beta}-induced cell death. *J Cell Biol* 2004;165(3):347-356.
60. Lopez-Anton N, Rudy A, Barth N, Schmitz ML, Pettit GR, Schulze-Osthoff K, Dirsch VM, Vollmar AM. The marine product cephalostatin 1 a ctivates an endoplasmic reticulum stress-specific and apoptosome-independent apoptotic signaling pathway. *J Biol Chem* 2006;281(44):33078-33086.
61. Bian Z-M, Elner SG, & Elner VM. Dual Involvement of Caspase-4 in Inflammatory and ER Stress-Induced Apoptotic Responses in Human Retinal Pigment Epithelial Cells. *Invest Ophthalmol Vis Sci* 2009;50(12):6006-6014.
62. Yamamuro A, Kishino T, Ohshima Y, Yoshioka Y, Kimura T, Kasai A, Maeda S. Caspase-4 Directly Activates Caspase-9 in Endoplasmic Reticulum Stress-Induced Apoptosis in SH-SY5Y Cells. *J Pharmacol Sci* 2011;115(2):239-43
63. Rahmani M, Davis EM, Crabtree TR, Habibi JR, Nguyen TK, Dent P, Grant S. The kinase inhibitor sorafenib induces cell death through a process involving induction of endoplasmic reticulum stress. *Mol Cell Biol* 2007;27(15):5499-5513.
64. Karki P, Dahal GR, & Park IS. Both dimerization and interdomain processing are essential for caspase-4 activation. *Biochem Biophys Res Commun* 2007;356(4):1056-1061.
65. Yukioka F, Matsuzaki S, Kawamoto K, Koyama Y, Hitomi J, Katayama T, Tohyama M. Presenilin-1 mutation activates the signaling pathway of caspase-4 in endoplasmic reticulum stress-induced apoptosis. *Neurochem Int* 2008; 52(4-5):683-687.
66. Matsuzaki S, Hiratsuka T, Kuwahara R, Katayama T, & Tohyama M. Caspase-4 is partially cleaved by calpain via the impairment of Ca2+ homeostasis under the ER stress. *Neurochem Int* 2009;56(2):352-356.

67. Tadagavadi RK, Wang W, & Ramesh G. Netrin-1 regulates Th1/Th2/Th17 cytokine production and inflammation through UNC5B receptor and protects kidney against ischemia-reperfusion injury. *J Immunol* 2010;185(6):3750-3758.
68. Saulle E, Riccioni R, Coppola S, Parolini I, Diverio D, Riti V, Mariani G, Laufer S, Sargiacomo M, Testa U. Colocalization of the VEGF-R2 and the common IL-3/GM-CSF receptor beta chain to lipid rafts leads to enhanced p38 a ctivation. *Br J Haematol* 2009;145(3):399-411.
69. Aesoy R, Sanchez BC, Norum JH, Lewensohn R, Viktorsson K, Linderholm B. An autocrine VEGF/VEGFR2 and p38 s ignaling loop confers resistance to 4-hydroxytamoxifen in MCF-7 breast cancer cells. *Mol Cancer Res* 2008;6(10):1630-1638.
70. Chawla-Sarkar M, Lindner DJ, Liu YF, Williams BR, Sen GC, Silverman RH, Borden EC.Apoptosis and interferons: role of interferon-stimulated genes as mediators of apoptosis. *Apoptosis* 2003;8(3):237-249.
71. Chen C, Dudenhausen EE, Pan YX, Zhong C, & Kilberg MS. Human CCAAT/enhancer-binding protein beta gene expression is activated by endoplasmic reticulum stress through an unfolded protein response element downstream of the protein coding sequence. *J Biol Chem* 2004;279(27):27948-27956.
72. Chiribau CB, Gaccioli F, Huang CC, Yuan CL, & Hatzoglou M. Molecular symbiosis of CHOP and C/EBP beta isoform LIP contributes to endoplasmic reticulum stress-induced apoptosis. *Mol Cell Biol* 2010;30(14):3722-3731.
73. Park SH, Choi HJ, Yang H, Do KH, Kim J, Lee DW, Moon Y. Endoplasmic reticulum stress-activated C/EBP homologous protein enhances nuclear factor-kappaB signals via repression of peroxisome proliferator-activated receptor gamma. *J Biol Chem* 2010;285(46):35330-35339.
74. Cappello C, Zwergal A, Kanclerski S, Haas SC, Kandemir JD, Huber R, Page S, Brand K. C/EBPbeta enhances NF-kappaB-associated signalling by reducing the level of IkappaB-alpha. *Cell Signal* 2009;21(12):1918-1924.
75. Perera PY, Mayadas TN, Takeuchi O, Akira S, Zaks-Zilberman M, Goyert SM, Vogel SN. CD11b/CD18 acts in concert with CD14 and Toll-like receptor (TLR) 4 to elicit full lipopolysaccharide and taxol-inducible gene expression. *J Immunol* 2001;166(1):574-581.
76. Ly NP, Komatsuzaki K, Fraser IP, Tseng AA, Prodhan P, Moore KJ, Kinane TB. Netrin-1 inhibits leukocyte migration in vitro and in vivo. *Proc Natl Acad Sci U S A* 2005;102(41):14729-14734.
77. Schubert T, Denk A, Mägdefrau U, Kaufmann S, Bastone P, Lowin T, Schedel J, Bosserhoff AK. Role of the netrin system of repellent factors on s ynovial fibroblasts in rheumatoid arthritis and osteoarthritis. *Int J Immunopathol Pharmacol* 2009;22(3):715-722.
78. Yeh CS, Wang JY, Cheng TL, Juan CH, Wu CH, Lin SR. Fatty acid metabolism pathway play an important role in carcinogenesis of human colorectal cancers by Microarray-Bioinformatics analysis. *Cancer Lett* 2006;233(2):297-308.

79. Frasor J, Weaver AE, Pradhan M, & Mehta K. Synergistic up-regulation of prostaglandin E synthase expression in breast cancer cells by 17beta-estradiol and proinflammatory cytokines. *Endocrinology* 2008;149(12):6272-6279.
80. Perkins ND. Integrating cell-signalling pathways with NF-[kappa]B and IKK function. *Nat Rev Mol Cell Biol* 2007;8(1):49-62.
81. Bhattacharyya S, Borthakur A, Tyagi S, Gill R, Chen ML, Dudeja PK, Tobacman JK. B-cell CLL/lymphoma 10 (BCL10) is required for NF-kappaB production by both canonical and noncanonical pathways and for NF-kappaB-inducing kinase (NIK) phosphorylation. *J Biol Chem* 2010;285(1):522-530.
82. Matsuda A, Suzuki Y, Honda G, Muramatsu S, Matsuzaki O, Nagano Y, Doi T, Shimotohno K, Harada T, Nishida E, Hayashi H, Sugano S. Large-scale identification and characterization of human genes that activate NF-[kappa]B and MAPK signaling pathways. *Oncogene* 2003;22(21):3307-3318.
83. Sarnico I, Lanzillotta A, Boroni F, Benarese M, Alghisi M, Schwaninger M, Inta I, Battistin L, Spano P, Pizzi M. NF-kappaB p50/RelA and c-Rel-containing dimers: opposite regulators of neuron vulnerability to ischaemia. *J Neurochem* 2009;108(2):475-485.
84. Inta I, Paxian S, Maegele I, Zhang W, Pizzi M, Spano P, Sarnico I, Muhammad S, Hermann O, Inta D, Baumann B, Liou HC, Schmid RM, Schwaninger M. Bim and Noxa are candidates to mediate the deleterious effect of the NF-kappa B subunit RelA in cerebral ischemia. *J Neurosci* 2006;26(50):12896-12903.
85. Lakshmanan U & Porter AG. Caspase-4 Interacts with TNF Receptor-Associated Factor 6 and Mediates Lipopolysaccharide-Induced NF-{kappa}B-Dependent Production of IL-8 and CC Chemokine Ligand 4 (Macrophage-Inflammatory Protein-1). *J Immunol* 2007;179(12):8480-8490.
86. Li X, Massa PE, Hanidu A, Peet GW, Aro P, Savitt A, Mische S, Li J, Marcu KB. IKKalpha, IKKbeta, and NEMO/IKKgamma are each required for the NF-kappa B-mediated inflammatory response program. *J Biol Chem* 2002;277(47):45129-45140.
87. Persichini T, Maio N, di Patti MC, Rizzo G, Colasanti M, Musci G. Interleukin-1beta induces ceruloplasmin and ferroportin-1 gene expression via MAP kinases and C/EBPbeta, AP-1, and NF-kappaB activation. *Neurosci Lett* 2010;484(2):133-138.
88. Paradisi A, Maisse C, Bernet A, Coissieux MM, Maccarrone M, Scoazec JY, Mehlen P. NF-kappaB regulates netrin-1 expression and affects the conditional tumor suppressive activity of the netrin-1 receptors. *Gastroenterology* 2008;135(4):1248-1257.
89. Guadagni F, Ferroni P, Palmirotta R, Portarena I, Formica V, Roselli M. TNF/VEGF cross-talk in chronic inflammation-related cancer initiation and progression: an early target in anticancer therapeutic strategy. *In Vivo* 2007;21(2):147-161.
90. Serini S, Piccioni E, Merendino N, & Calviello G. Dietary polyunsaturated fatty acids as inducers of apoptosis: implications for cancer. *Apoptosis* 2009;14(2):135-152.
91. Rotman EI, Brostrom MA, & Brostrom CO. Inhibition of protein synthesis in intact mammalian cells by arachidonic acid. *Biochem J* 1992;282 (Pt 2):487-494.

92. Martinez-Orozco R, Navarro-Tito N, Soto-Guzman A, Castro-Sanchez L, & Perez Salazar E. Arachidonic acid promotes epithelial-to-mesenchymal-like transition in mammary epithelial cells MCF10A. *Eur J Cell Biol* 2010;89(6):476-488.
93. Kurokawa H, Nishio K, Fukumoto H, Tomonari A, Suzuki T, Saijo N. Alteration of caspase-3 (CPP32/Yama/apopain) in wild-type MCF-7, breast cancer cells. *Oncology reports* 1999;6(1):33-37.
94. Willis AL, Tran NL, Chatigny JM, Charlton N, Vu H, Brown SA, Black MA, McDonough WS, Fortin SP, Niska JR, Winkles JA, Cunliffe HE. The fibroblast growth factor-inducible 14 receptor is highly expressed in HER2-positive breast tumors and regulates breast cancer cell invasive capacity. *Mol Cancer Res* 2008;6(5):725-734.
95. Lyng MB, Laenkholm AV, Pallisgaard N, & Ditzel HJ. Identification of genes for normalization of real-time RT-PCR data in breast carcinomas. *BMC Cancer* 2008;8:20.
96. Smyth GK. Linear models and empirical bayes methods for assessing differential expression in microarray experiments. *Stat Appl Genet Mol Biol* 2004;3:Article3.
97. Cazanave SC, Elmi NA, Akazawa Y, Bronk SF, Mott JL, Gores GJ. CHOP and AP-1 cooperatively mediate PUMA expression during lipoapoptosis. *Am J Physiol Gastrointest Liver Physiol* 2010;299(1):G236-243.
98. Gentleman RC, Carey VJ, Bates DM, Bolstad B, Dettling M, Dudoit S, Ellis B, Gautier L, Ge Y, Gentry J, Hornik K, Hothorn T, Huber W, Iacus S, Irizarry R, Leisch F, Li C, Maechler M, Rossini AJ, Sawitzki G, Smith C, Smyth G, Tierney L, Yang JY, Zhang J. Bioconductor: open software development for computational biology and bioinformatics. *Genome Biol* 2004;5(10):R80.
99. Benjamini Y & Hochberg Y. Controlling the False Discovery Rate: A Practical and Powerful Approach to Multiple Testing. *J R Statist Soc B* 1995;57(1):289-300.
100. Munster PN & Carpenter JT. Estradiol in breast cancer treatment: reviving the past. *JAMA* 2009;302(7):797-8.

APPENDIX

1. Peng J, Jordan VC. Expression of estrogen receptor alpha with a Tet-off adenoviral system induces G0/G1 cell cycle arrest in SKBr3 breast cancer cells. *International Journal of Oncology* 2010: 36(2):451-458.
2. Ariazi EA, Brailoiu E, Yerrum S, Shupp HA, Slifker MJ, Cunliffe HE, Black MA, Donato AL, Arterburn JB, Oprea TI, Prossnitz ER, Dun NJ, Jordan VC. The G Protein-Coupled Receptor GPR30 Inhibits Proliferation of Estrogen Receptor-Positive Breast Cancer Cells. *Cancer Research* 2010: 70:1184-1194. (Selected for Faculty of 1000 Medicine, identified as an important article published in Medicine for its scientific merit and positive contribution to the medical literature).
3. Patel RR, Sengupta S, Kim HR, Klein-Szanto AJ, Pyle JR, Zhu F, Li T, Ross EA, Oseni S, Fargnoli J, Jordan VC. Experimental treatment of estrogen receptor (ER) positive breast

cancer with tamoxifen and brivanib alaninate, a V EGFR-2/FGFR-1 kinase inhibitor: a potential clinical application of angiogenesis inhibitors. *European Journal of Cancer* 2010: 46:1537-1553.

4. Maximov PY, Myers CB, Curpan RF, Lewis-Wambi JS, Jordan VC. Structure-Function Relationships of Estrogenic Triphenylethylenes Related to Endoxifen and 4-Hydroxytamoxifen. *Journal of Medicinal Chemistry* 2010: 53:3273-3283.
5. Sengupta SS, Sharma CGN, Jordan VC. Estrogen Regulation of X-Box Binding Protein-1 and its Role in Estrogen Induced Growth of Breast and Endometrial Cancer Cells. *Hormone Molecular Biology and Clinical Investigation* 2010: 2:235-243.
6. Balaburski G, Dardes RC, Johnson M, Haddad B, Zhu F, Ross EA, Sengupta S, Klein-Szanto A, Liu H, Kim H, Jordan VC. Raloxifene-stimulated experimental breast cancer with the paradoxical actions of estrogen to promote or prevent tumor growth: A unifying concept in anti-hormone resistance. *International Journal of Oncology* 2010: 37:387-398.
7. Vogel VG, Costantino JP, Wickerham DL, Cronin WM, Cecchini RS, Atkins JN, Bevers TB, Fehrenbacher L, Pajon ER, Wade JL, Robidoux A, Margolese RG, James J, Runowicz CD, Ganz PA, Reis SE, McCaskill-StevensW, Ford LG, Jordan VC, Wolmark N. Update of the NSABP Study of Tamoxifen and Raloxifene (STAR) P-2 Trial: Preventing Breast Cancer. *Cancer Prevention Research* 2010: 3:696-706.
8. Maximov P, Sengupta S, Lewis-Wambi JS, Kim HR, Curpan RF, Jordan VC. The conformation of the estrogen receptor directs estrogen-induced apoptosis in breast cancer: a hypothesis. *Hormone Molecular Biology and Clinical Investigation* 2011: 5:27-34.
9. Ko S and Jordan VC. Treatment of osteoporosis and reduction in risk of invasive breast cancer in postmenopausal women with raloxifene. *Expert Opinion on Pharmacotherapy* 2011: 12:657-74.
10. Hu ZZ, Huang H, Wu CH, Jung M, Dritschilo A, Riegel AT, Wellstein A. Omics-based molecular target and biomarker identification. *Methods in Molecular Biology* 2011: 719:547-571.
11. Yang CZ, Yaniger SI, Jordan VC, Klein DJ, Bittner GD. Most Plastic Products Release Estrogenic Chemicals: A Potential Health Problem That Can Be Solved. *Environmental Health Perspectives* 2011 (*Epub ahead of print*).
12. Jordan VC and Ford LS. Paradoxical Clinical Effect of Estrogen on Breast Cancer Risk: A "New" Biology of Estrogen-Induced Apoptosis. *Cancer Prevention Research* 2011: 4:633-637.
13. Sweeney L and Jordan VC. Estrogen Receptor (ER). In: Encyclopedia of Cancer Therapeutic Targets. Springer Science + Business Media, LLC, New York (*in press*).
14. Jordan VC, Obiorah I, Fan P, Kim HR, Ariazi E, Cunlifffe H, Brauch H. Evolution of Long-Term Adjuvant Anti-hormone Therapy: Consequences and Opportunities: The St. Gallen Prize Lecture. *Breast* 2011 (*in press*).
15. Jordan VC. Decades of Discovery: The Selective Estrogen Receptor Modulator (SERM) Story: The St. Gallen Prize. *References en Gynecologie Obstetrique* 2011 (*in press)*.

16. Hu ZZ, Kagan BL, Ariazi E, Rosenthal DS, Zhang L, Li JV, Huang H, Wu C, Jordan VC, Riegel AT, Wellstein A. Proteomic analysis of pathways involved in estrogen-induced growth and apoptosis of breast cancer cells. *PLoS ONE* 2011 (*in press*).
17. Chien CD, Li JV, Kirilyuk AA, Lahusen T, Schmidt MO, Oh As, Wellstein A, Riegel AT. Role of the nuclear receptor co-activator AIB1-4 in the control of gene transcription. *Journal of Biological Chemistry* 2011 (*in press*).
18. Lewis-Wambi JS, Kim H, Curpan R, Grigg R, Sarker MA, Jordan VC. The new selective estrogen receptor modulator, bazedoxifene, inhibits hormone-independent breast cancer cell growth and downregulates estrogen receptor α and cyclin D1. *Molecular Pharmacology* 2011 (*in press*).

Expression of estrogen receptor alpha with a Tet-off adenoviral system induces G0/G1 cell cycle arrest in SKBr3 breast cancer cells

JING PENG and V. CRAIG JORDAN[1]

Fox Chase Cancer Center, 333 Cottman Avenue, Philadelphia, PA 19111, USA

Received August 27, 2009; Accepted October 6, 2009

DOI: 10.3892/ijo_00000519

Abstract. Endocrine therapies targeting estrogen action are pivotal for the prevention and treatment of ER-positive breast cancers. Previous studies sought to recreate hormone responsiveness by the stable expression of ERα in the ER-negative MDA-MB-231 breast cancer cells. Paradoxically, estrogen inhibits breast cancer cell growth when an exogenous ERα is expressed. In this study, we have built on previous studies by developing a Tet-off adenoviral system to express ERα in the ER-negative SKBr3 breast cancer cells that over-express both EGFR and HER2. This system efficiently delivers ERα and the expression level of ERα is controlled by doxycycline in a concentration-dependent manner. The growth of SKBr3 was inhibited by ERα expression and further inhibited in the presence of 1 nM 17ß-estradiol. SKBr3 cells were arrested at G0/G1 cell cycle upon ERα expression, which corresponded to an increase of $p21^{Cip1\ Waf1}$, hypo-phosphorylation of pRb and decrease of E2F1. Estrogen also reduced EGFR and HER2 expression in SKBr3 cells after ERα was expressed. Given that estrogen-induced increase of $p21^{Cip1\ Waf1}$ and decrease of E2F1 was also observed in MDA-MB-231 cells stably transfected with ERα, our results suggest that a common pathway might be shared by different breast cancer cell lines whose growth is suppressed by ectopic ERα and estrogen.

Introduction

Antihormone agents such as tamoxifen and aromatase inhibitors have been widely used to treat estrogen receptor-positive (ER-positive) breast tumors whose growth depends on estrogen (1). However, acquired drug resistance develops as a consequence of long-term antihormone treatment. Interestingly, estrogen exerts apoptotic actions on long-term (>5 years) tamoxifen-resistant breast tumors (2) or long-term (>1 year) estrogen-deprived breast cancer cells (aromatase inhibitor-resistant) (3-5). In addition, the long-term tamoxifen-resistant MCF-7 breast cancer xenografts on ovariectomized athymic mice regrow and become tamoxifen-responsive again after short exposure to physiological estrogen (6). These discoveries suggest a novel strategy to kill antihormone-resistant breast cancer cells with low dose estrogen for short period and re-sensitize the tumors for further antihormone therapy. Phase II clinical trial is now ongoing to treat patients with 12-week course of low-dose estrogen after exhaustive antihormone therapy (7). It seems that estrogen induces apoptosis through different mechanisms in different breast cancer cell models. In one model, estrogen kills LTED breast cancer cells by activating the Fas/FasL signaling pathway (3). However, in another model, estrogen induces apoptosis in MCF-7:5C cells predominantly through a mitochondrial mechanism (5).

Although the development of antihormone therapies is improving cancer care for ER-positive patients, these endocrine therapies are ineffective for the treatment of ER-negative tumors that comprise about 30% of breast cancers. Therefore, it is of value to understand whether the re-introducing of ER expression into ER-negative breast cancer cells that are absolutely antihormone-resistant can modulate responsiveness to endocrine therapies. Multiple approaches are being tested in the laboratory on cultured cell lines and animal models to examine if ER-positive phenotypes can be re-created. Epigenetic methods using DNA methyltransferase (DNMT) inhibitors and/or histone deacetylase (HDAC) inhibitors have been shown to restore ERα expression in ER-negative breast cancer cells, whose growth is then inhibited by antiestrogens (reviewed in ref. 8). Estrogen blocks the growth inhibitory effects of antiestrogen on these cells when ER is restored using the epigenetic methods (9). Additionally, the study of estrogen and antiestrogen action has been described when ectopic ER is expressed in ER-negative cells. One way is to stably transfect ER-negative cells with plasmids encoding ERα. Surprisingly, estrogen treatment leads to growth inhibition rather than stimulation in ER-negative Chinese hamster ovary (CHO) cells and MDA-MB-231 breast cancer cells transfected with a wild-type ERα cDNA (10,11). The estrogen-mediated

Correspondence to: Dr V. Craig Jordan, [1]*Present address:* Department of Oncology, Lombardi Comprehensive Cancer Center, Georgetown University Medical Center, 3970 Reservoir Rd NW, Washington, DC 20057, USA
E-mail: vcj2@georgetown.edu

Key words: ER-negative breast cancer, estrogen receptor, growth factor receptor, Tet-off adenoviral system, SKBr3 cells

growth inhibition of MDA-MB-231 cells stably transfected with ERα seems to require regulation of E2F1 (12). Stable transfection normally takes months for a colony to be selected and expanded, and a more efficient adenoviral system was developed to express ERα (13). The growth of MDA-MB-231 cells that express ERα delivered by the adenoviral system is also suppressed by estradiol (14).

Antihormone-resistance is often linked with excessive growth factor signaling that has elevated ErbB family cell membrane receptor tyrosin kinases such as EGFR (ErbB-1) and HER2/c-neu (ErbB-2) (15). Most studies to express ectopic ERα have used MDA-MB-231 cells that over-express EGFR. It is important to examine how ER-negative breast cancers cells with high HER2 react to estrogen when an exogenous ERα is expressed. Potential new drug targets could be identified in ER-negative cancers if estrogen triggers apoptosis or growth inhibition through a common mechanism shared by different types of ER-negative cancer cells when an exogenous ERα is introduced. In this study, a Tet-off adenoviral system was developed to deliver ERα to ER-negative breast cancer SKBr3 cells that over-express both EGFR and HER2. The Tet-off adenoviral system is highly efficient and the expression level of ERα is controlled by addition of doxycycline in a concentration-dependent manner. Using this system, we examined the function of ERα and estradiol on cell proliferation. The results suggest that estrogen suppresses the proliferation of SKBr3 cells through a similar mechanism as estrogen does in MDA-MB-231 cells when an ectopic ERα is expressed. The mechanism involves upregulation of $p21^{Cip1\ Waf1}$ and down-regulation of E2F1. The effect of estrogen on growth receptor expression was also examined in SKBr3 cells when exogenous ERα was expressed.

Materials and methods

Cells and culture conditions. SKBr3 and MDA-MB-231 cells were obtained from American Type Culture Collection (ATCC, Manassas, VA). MCF-7 cells were from Dr Dean Edwards (University of Texas, San Antonio). MCF-7/F cells were derived from MCF-7 as described (16). SKBr3, MCF-7, and MCF-7/F cells were maintained in full serum RPMI-1640 medium supplemented with 10% fetal bovine serum (FBS), 2 mM L-glutamine, 100 U/ml penicillin, 100 μg/ ml streptomycin, 1X essential amino acid (all from Invitrogen, Carlsbad, CA) and 6 ng/ml bovine insulin (Sigma-Aldrich, St. Louis, MO). MDA-MB-231 cells were maintained in minimal essential medium supplemented with 5% calf serum and other supplements as the RPMI-1640 complete medium. T47D:C42 cells were cloned from T47D (from ATCC) (17,18) and maintained in estrogen-free RPMI medium which is phenol red-free RPMI-1640 supplemented with 10% dextran-coated charcoal-stripped fetal bovine serum (SFS) and other supplements as the full serum RPMI-1640 medium. All cells were grown at 37°C with 5% CO_2.

Adenoviruses and viral infection. Ad-TRE-ERα adenovirus was custom-generated by Vector Biolabs (Philadelphia, PA) using human type 5 adenoviral backbone with E1 and E3 regions deleted. Adeno-X Tet-off adenovirus stock was purchased from Clontech (Mountain View, CA). It was subsequently amplified with Adeno-X Maxi Purification Kit (Clontech) and the titer was measured with Adeno-X Rapid Titer Kit (Clontech), following the instructions from the manufacturer. Ad-CMV-GFP was purchased from Vector Biolabs. For viral infection, SKBr3 cells were cultured in estrogen-free RPMI medium 3 days before the infection and throughout the experiments. Each adenovirus was added to resuspended cells at 30 MOI (multiplicity of infection), then the cells were divided equally and 1 μg/ml doxycycline was added to half of the cells. Subsequently, $3x10^4$ cells/well were seeded in 24-well plates for cell proliferation assay and $1.5x10^5$ cells/well were seeded in 6-well plates for protein or RNA preparation. After 24 h, the medium was replaced with fresh medium with or without 1 μg/ml doxycycline containing ethanol (EtOH), fulvestrant or 17ß-estradiol at concentrations indicated in the figures. The compound-containing medium was replaced every other day until the cells were harvested.

Cell proliferation assay. Cell DNA content was determined as a measure of cell proliferation using the Fluorescent DNA Quantitation Kit (Bio-Rad, Hercules, CA), which includes 10X TEN buffer, Hoechst dye and calf thymus DNA. Briefly, the cells were washed with 1X phosphate-buffered saline (PBS, Invitrogen), incubated in 0.5 ml 0.1X TEN buffer (diluted from the 10X TEN buffer) for 1 h at 4°C then sonicated for 10 sec. Hoechst dye was diluted in 10X TEN buffer to a final concentration of 25 μg/ml, and 20 μl of the diluted dye was incubated with 0.2 ml of the cell lysate for 1 h at room temperature. The fluorescence was measured with a Mithras LB 940 fluorometer (Oak Ridge, TN) and the total DNA amount was calculated based on a standard curve prepared from calf thymus DNA.

Western blot analysis. Cells were washed twice with 1X PBS and lysed in RIPA buffer (Sigma-Aldrich) supplemented with Complete Protease Inhibitor Cocktail Tablets at 1 tablet/10 ml (Roche, Indianapolis, IN). The protein concentration was determined using the BCA Protein Assay Reagent (Thermo, Rockford, IL) following instructions from the manufacturer. Total protein were separated by 4-12% sodium dodecyl sulfate polyacrylamide gel electrophoresis (SDS-PAGE, Invitrogen) and electro-blotted to polyvinylidene fluoride (PVDF) membranes. The membranes were blocked for 1 h at room temperature in TBST buffer (50 mM Tris-HCl, pH 7.5, 150 mM NaCl, 0.1% Tween-20) containing 5% non-fat milk then incubated overnight at 4°C with primary antibodies. After being washed 3 times with TBST, the membranes were incubated with horseradish peroxidase (HRP)-conjugated secondary antibodies for 2 h at room temperature, washed again with TBST and visualized using ECL Western Blotting Detection Reagents (GE Healthcare, Piscataway, NJ). The antibodies against EGFR (Cat# 2232), Rb (Cat# 9309), Rb-P(s807/811) (Cat# 9308) and mTOR (Cat# 2983) were purchased from Cell Signaling (Danvers, MA). Antibodies against HER2 (Ab-20) and ERα (Ab-15) were from Thermo Lab Vision/NeoMarkers (Fremont, CA). Antibody against ß-actin (AC-15) was from Sigma-Aldrich. Antibodies against p21 (Cat# sc-469) and E2F1 (Cat# sc-193) were from Santa Cruz Biotechnology (Santa Cruz, CA). The HRP-conjugated

anti-mouse or anti-rabbit secondary antibodies were from Cell Signaling.

ERE-Luciferase reporter assay. SKBr3 cells were infected and seeded in 24-well plates as described above. Twenty-four hours after infection, 0.3 μg 5X ERE-firefly-luciferase reporter plasmid and 0.1 μg control TA-Renilla-luciferase plasmid (19) were used to transfect each well of cells using 15 μl FuGENE® HD transfection reagent (Roche) following instructions from the manufacturer. After 24 h, the medium was replaced with fresh medium containing different compounds as indicated in the figure. Cells were harvested 48 h after treatment and the activities of firefly and Renilla luciferases were analyzed with Dual-Luciferase® Reporter Assay System (Promega, Madison, WI) following instructions from the manufacturer.

Real-time reverse transcription-polymerase chain reaction (RT-PCR) assay. Total RNA was isolated with RNeasy Mini Kit (Qiagen, Valencia, CA) and quantitated with spectrometer. The cDNA was prepared from 1 μg RNA with the High Capacity cDNA Reverse Transcription Kit (Applied Biosystems, Foster City, CA) in a 20-μl reaction mix assembled according to instructions from the manufacturer. The reaction mix was incubated at 25°C for 10 min and 85°C for 90 min then diluted with 200 μl water. Two microliters of the diluted products were used for subsequent real-time PCR amplification using either Power SYBR® Green PCR Master Mix or Taqman® Universal PCR Master Mix, both from Applied Biosystems. The reactions were performed with 7900 HT Fast Real-Time PCR System (Applied Biosystems) in 384-well plates using the standard settings. The sequences of the primers are as follows: PS2-F, 5'-CATCGACGTCCCT CCAGAAGAG; PS2-R, 5'-CTCTGGGACTAATCACCGTG CTG; PR-F, 5'-CGCGCTCTACCCTGCACTC; PR-R, 5'-TGA ATCCGGCCTCAGGTAGTT; E2F1-F, 5'-CCCAACTCCCT CTACCCTTGA; E2F1-R, 5'-TCTGTCTCCCTCCCTCACT TTC; p21-F, 5'-CTGGAGACTCTCAGGGTCGAA; p21-P, 5'-6ACGGCGGCAGACCAGCATGA[BHQ1]; p21-R, 5'-GGCGTTTGGAGTGGTAGAAATCT; Rb-F, 5'-CTTGCAT GGCTCTCAGATTCAC; Rb-R, 5'-AGAGGACAAGCAGA TTCAAGGTG; 36B4-F, 5'-GTGTTCGACAATGGCAGCAT; 36B4-R, 5'-GACACCCTCCAGGAAGCGA.

Cell cycle analysis. The adenovirus-infected SKBr3 cells were plated at $1x10^6$ per 10-cm culture dish and treated with different compounds for 48 h. All the cells were harvested and fixed in 70% ethanol in 1X PBS overnight at 4°C. The fixed cells were washed twice with 1X PBS and incubated with propidium iodide (PI) staining buffer (1X PBS, 0.1% Triton X-100, 200 μg/ml RNase A, and 50 μg/ml PI) for 30 min at 37°C. The stained cells were analyzed using FACScan flow cytometer (Becton Dickinson, San Jose, CA) and the data were analyzed using FlowJo program (Tree Star Inc., Ashland, OR).

Statistical analysis. Data were expressed as means ± standard deviation (SD) for at least three independent repeated experiments. Statistical significance ($p<0.05$) between two groups was assessed by unpaired, one-tailed t-test.

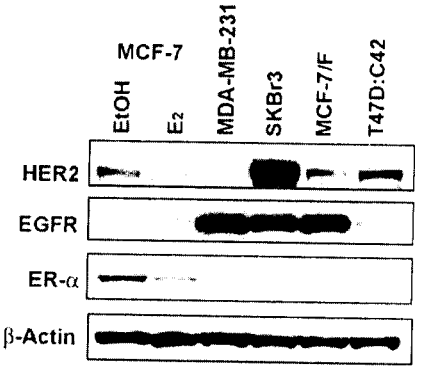


Figure 1. Comparison of HER2, EGFR and ERα expression between SKBr3 and other breast cancer cells. MCF-7 cells were grown in estrogen-free RPMI medium for 4 days then treated with either EtOH control or 1 nM E_2 for 2 more days before harvest. Other cells were grown in medium as described in Materials and methods. Fifty micrograms of total proteins were used for Western blot analysis for HER2, EGFR and ERα. The ß-actin was also examined as a loading control.

Results

Expression of ERα in SKBr3 breast cancer cells with Tet-off adenoviral system. Most studies expressing ectopic ERα in ER-negative breast cancer cells have used MDA-MB-231 cells which have high levels of EGFR, but low levels of HER2. Since about 20% breast cancers are HER2-positive, it is important to examine if hormone-responsiveness could be restored in ER-negative breast cancer cells that over-express HER2. Therefore, we chose SKBr3 cells which over-express both HER2 and EGFR for this study. The expression of HER2, EGFR and ERα were compared between SKBr3 and several other breast cancer cell lines as shown in Fig. 1. The ER-positive MCF-7 cells expressed low levels of EGFR and HER2, and estrogen treatment decreased HER2 expression. MDA-MB-231 cells had high levels of EGFR but little HER2. The ER-negative MCF-7/F cells derived from MCF-7 (16) highly expressed EGFR and moderately expressed HER2. Another ER-negative T47D:C42 cells cloned from ER-positive T47D cells (17,18) had moderate expression of HER2 and little expression of EGFR. Only SKBr3 cell had high levels of both HER2 and EGFR.

A Tet-off adenoviral delivery system was developed to express ERα in SKBr3 cells. The infection efficiency of adenoviruses in SKBr3 cells was analyzed using a green fluorescent protein (GFP) reporter adenovirus (Ad-CMV-GFP). As shown in Fig. 2A, >95% cells were infected and expressing GFP. The adenoviral system is more efficient than plasmid transfection which normally has <50% efficiency, thus a lengthy selection for stable-transfected cell colonies can be avoided using the adenoviral system since almost all the cells were infected and expressed the delivered gene of interest. The expression of ERα can be turned off by doxycycline when cells are co-infected with Adeno-X Tet-Off and Ad-TRE-ERα adenovirus simultaneously. As shown in Fig. 2B, the expression level of ERα decreased as the concentration of doxycycline increased from 0 to 0.8 ng/ml, and ERα expression was almost undetectable as doxycycline concentration was

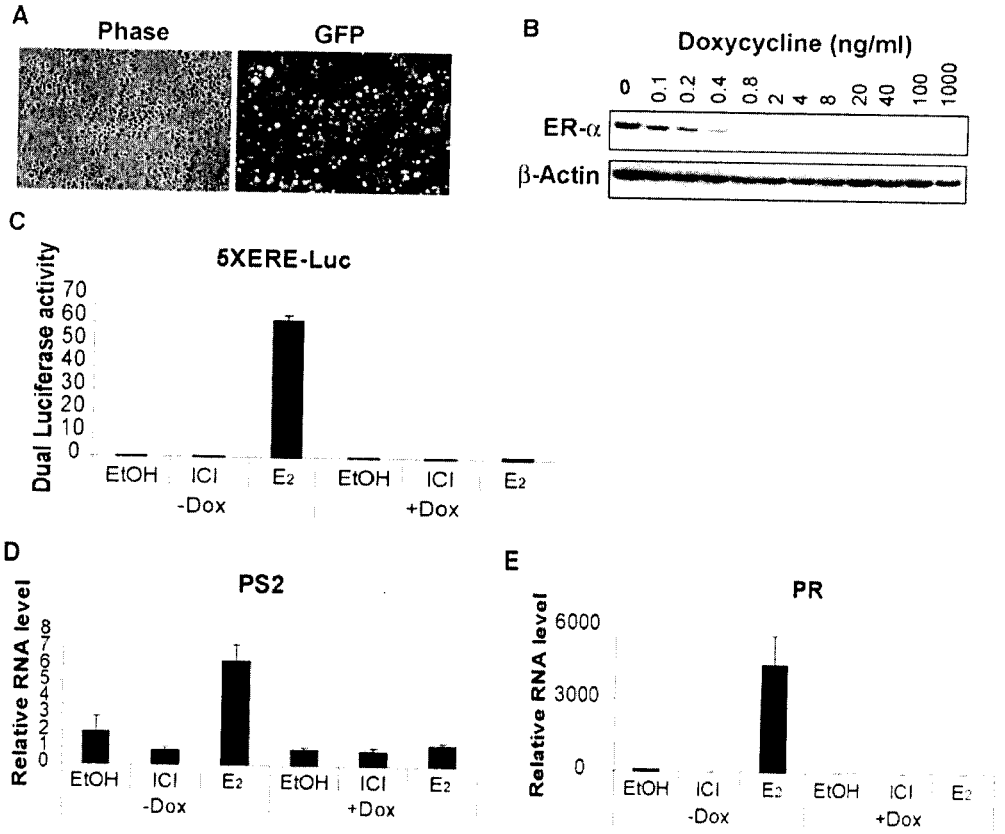


Figure 2. The Tet-off adenoviral system to express ERα in SKBr3 cells. (A) SKBr3 cells were infected with Ad-CMV-GFP and observed 24 h after infection with a TE300 fluorescence microscope (Nikon Instruments, Melville, NY). (B) SKBr3 cells were co-infected by Adeno-X Tet-off and Ad-TRE-ERα in the presence of doxycycline at various concentrations. The cells were harvested 48 h after infection and total protein was extracted for Western blot analysis (C) SKBr3 cells infected by Adeno-X Tet-off and Ad-TRE-ERα in the presence (+Dox) or absence (-Dox) of 1 μg/ml doxycycline were transfected with 5xERE-firefly-luciferase and TA-Renilla-luciferase plasmids. The cells were harvested for dual luciferase activity assay after 48-h treatment with the compounds as indicated. The ratio of firefly luciferase vs Renilla luciferase activities were plotted and the number of the +Dox/EtOH sample was arbitrarily set to be 1 for easy comparison. (D) SKBr3 cells infected by Adeno-X Tet-off and Ad-TRE-ERα in the presence (+Dox) or absence (-Dox) of 1 μg/ml doxycycline were treated with 0.1% EtOH, 1 μM fulvestrant (ICI) or 1 nM 17β-estradiol (E_2) for 48 h. The total RNA was extracted for real-time RT-PCR analysis of PS2 or PR (E) against endogenous control 36B4 using a relative standard curve generated by 10-fold serial dilution of MCF-7 cDNA. The value of the +Dox/EtOH sample was arbitrarily set to be 1 for easy comparison.

above 2 ng/ml. The ERα expressed in SKBr3 cells by the adenovirus is fully functional. It activated luciferase reporter containing 5 estrogen receptor elements (5X ERE) in the presence of 1 nM E_2 while the luciferase reporter was not detected either when ERα was not expressed (+Dox) or when EtOH control or pure antiestrogen fulvestrant (ICI) was added (Fig. 2C). Real-time RT-PCR assay also indicated that the exogenous ERα induced the endogenous estrogen-responsive genes PS2 and progesterone receptor (PR) in response to E_2. The RNA level of PS2 was doubled by expression of ERα itself (compare -Dox/EtOH and +Dox/EtOH), and addition of 1 nM E_2 further increased PS2 RNA to 6-fold (compare -Dox/E_2 and +Dox/EtOH), but addition of fulvestrant did not change PS2 RNA expression (Fig. 2D). The induction of PR RNA was more dramatic, as PR RNA was barely detectable without ERα expression (+Dox) or with ERα but in the presence of EtOH control or antiestrogen fulvestrant. However, E_2 addition increased PR RNA level by thousands of folds when ERα was expressed (compare -Dox/E_2 and +Dox/EtOH, Fig. 2E).

Cell proliferation of SKBr3 cells after ERα expression. We next examined the effects of ERα on SKBr3 cell proliferation by measuring the total cellular DNA content. As shown in Fig. 3A, growth of SKBr3 cells was irresponsive to fulvestrant, 4-hydoxytamoxifen or E_2 if no ERα was expressed. However, expression of ERα itself reduced cell proliferation to about 70% (compare -Dox/EtOH and +Dox/EtOH), although the reduction was not statistically significant, similar inhibition was repeatedly observed in independent experiments. The ERα-mediated growth suppression was abolished by fulvestrant, and addition of 1 nM E_2 or 1 μM 4-hydroxytamoxifen inhibited SKBr3 cell proliferation to about 40 and 50% respectively, which was statistically significant (compare with the +Dox/EtOH control). With the ectopic expression of ERα, E_2 inhibited the growth of SKBr3 cells in a dose-dependent manner, as shown in Fig. 3B. Statistical difference was reached when E_2 concentration was $\geq 10^{-10}$ M (0.1 nM), comparing with the +Dox/EtOH control. Similar results were obtained in the time-dependent growth curve shown in Fig. 3C.

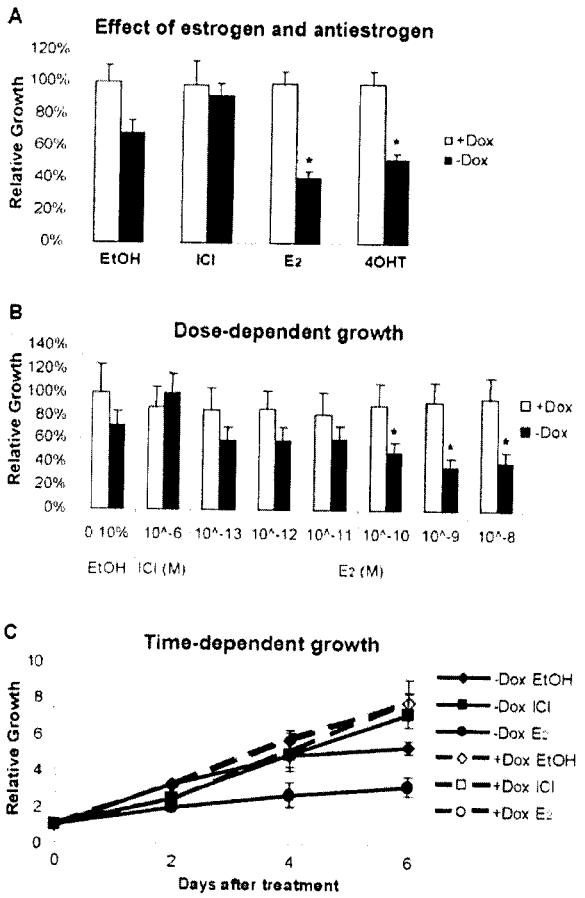


Figure 3. The effects of ERα expression and estrogen/antiestrogen treatment on the proliferation of SKBr3 cells. SKBr3 cells were infected by Adeno-X Tet-off and Ad-TRE-ERα in the presence (+Dox) or absence (-Dox) of 1 μg/ml doxycycline, treated by the 0.1% EtOH (v/v), 1 μM fulvestrant (ICI), 1 μM 4-hydroxytamoxifen (4OHT) or E_2 (at final concentration of 1 nM or as indicated in the graph) and harvested for DNA quantification. (A) Growth with different ER ligands treated for 6 days. (B) Dose-dependent growth with various E_2 concentrations treated for 6 days. (C) Time-dependent growth with cells harvested every 2 days after treatment. *Samples with a statistically significant difference ($p<0.05$ by t-test) from the +Dox/EtOH control.

ERα expression arrests SKBr3 cells at G0/G1 cycle. Next, flow cytometry analysis was performed to examine cell cycle progression of SKBr3 cells when ERα was expressed. As shown in Fig. 4, about 50% cells were at G0/G1 cell cycle without ERα (+Dox) or with ERα but in the presence of fulvestrant (-Dox/ICI). However, the population of cells at G0/G1 cell cycle increased to about 80% when ERα was expressed in the presence of EtOH control or 1 nM E_2. Apoptosis was not observed in SKBr3 cells as there was no significant cell accumulation at sub-G1 phase (cell debris) when ERα was expressed. Annexin V/PI staining, caspase activity assay or PARP-cleavage assay all confirmed that apoptosis did not occur (data not shown).

Modulation of E2F1 cell cycle checkpoint proteins by E_2 and ERα. The transcription factor E2F1 plays an important role in G1 to S cell cycle progression. Before cells enter S phase, hypo-phosphorylated pRb protein binds to E2F1 and prevents it from activating downstream genes essential for DNA replication and cell proliferation. Activation of cyclin-dependent kinases (CDKs) phosphorylates pRb and releases E2F1 for action. CDK inhibitory proteins such as $p21^{Cip1\ Waf1}$, $p27^{Kip1}$ and $p16^{INK4A}$ inhibit CDKs activity thus lead to hypo-phosphorylation of pRb and inactivation of E2F1, which in turn causes cell cycle arrest at G0/G1 phase. Stender *et al* (12) found that E2F1 and p21 were differentially regulated by estrogen in ER-positive MCF-7 cells and ER-stably-transfected MDA-MB-231 cells. Therefore, we also examined modification of $p21^{Cip1\ Waf1}$/pRb/E2F1 pathway proteins by E_2 and ERα in SKBr3 cells. As shown in Fig. 5A, $p21^{Cip1\ Waf1}$ was undetectable without ERα expression (+Dox) or with ERα expression but in the presence of fulvestrant. The $p21^{Cip1\ Waf1}$ protein level was increased by ERα expression and further increased by the addition of E_2, which coordinated with the phosphorylation status of pRb. Opposite regulation of E2F1 was observed by ERα expression and E_2 treatment. The RNA levels of $p21^{Cip1\ Waf1}$ and E2F1 were regulated in a similar patten as the protein levels (Fig. 5B). A moderate down-regulation of pRb at protein level was also observed in ERα-expressing samples but not at the RNA level. This might be resulted from the up-regulation of $p21^{Cip1\ Waf1}$ because $p21^{Cip1\ Waf1}$ mediates pRb protein degradation (20).

The effects of estrogen on HER2 and EGFR expression. Intimate crosstalk between hormone receptor signaling and growth factor receptor signaling is a major contributor to breast cancer progression and endocrine resistance (15). However, an inverse correlation is often found between ER and HER2 (21,22), and estrogen down-regulates HER2 expression in ER-positive MCF-7 cells (23) (Fig. 1). Growth factor signaling is essential for SKBr3 cell proliferation, therefore we examined the effects of estrogen and exogenous ERα on the expression of HER2 and EGFR. As shown in Fig. 6, ERα expression itself had little effect on HER2 and EGFR expression (compare -Dox/EtOH and +Dox/EtOH), however, 2-day treatment with E_2 decreased EGFR protein level and 6-day treatment of E_2 also reduced HER2 protein level. These results suggest that ectopic expression of ERα and E_2 treatment might be a way to switch the more aggressive growth-factor receptor-positive tumors to the prognostically more favorable hormone-sensitive type.

Discussion

Tet-off adenoviral system is a valuable approach to deliver ectopic genes. In this study, we developed a Tet-off adenovirus to express ERα in ER-negative SKBr3 cells. Adenoviruses infect the cells and deliver the gene of interest with over 95% efficiency, thus can be used to study cellular effects of the interested gene in a 'transient expression' experiment. This is not always possible using the traditional plasmid transfection with <50% delivery efficiency because the background is high when most cells are not expressing the gene of interest. Instead, a stably-transfected clone has to be selected and expanded, which is a time-consuming process. In addition, the phenotype of a stably-transfected clone may not be the

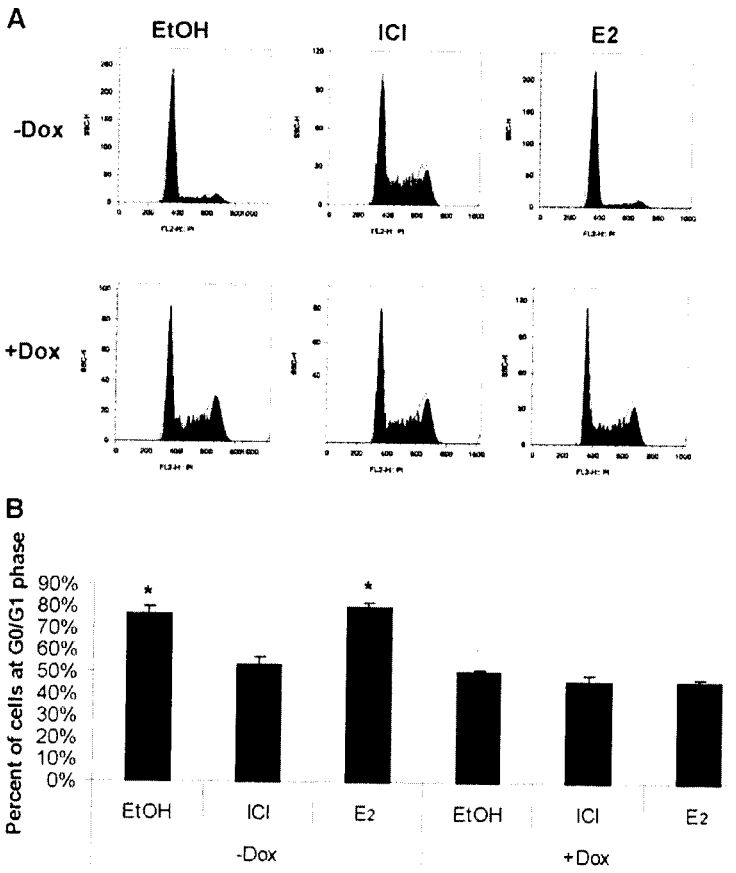


Figure 4. Cell cycle analysis of SKBr3 cells expressing ERα. SKBr3 cells were infected by Adeno-X Tet-off and Ad-TRE-ERα in the presence (+Dox) or absence (-Dox) of 1 μg/ml doxycycline, treated by 0.1% EtOH, 1 μM fulvestrant (ICI) or 1 nM E_2 for 2 days and harvested for cell cycle analysis. (A) Flow cytometry analysis of cell cycle distribution. (B) Percentage of cells at G0/G1 cell cycle from three independent experiments. *Samples with a statistically significant difference ($p<0.05$ by t-test) from the +Dox/EtOH control.

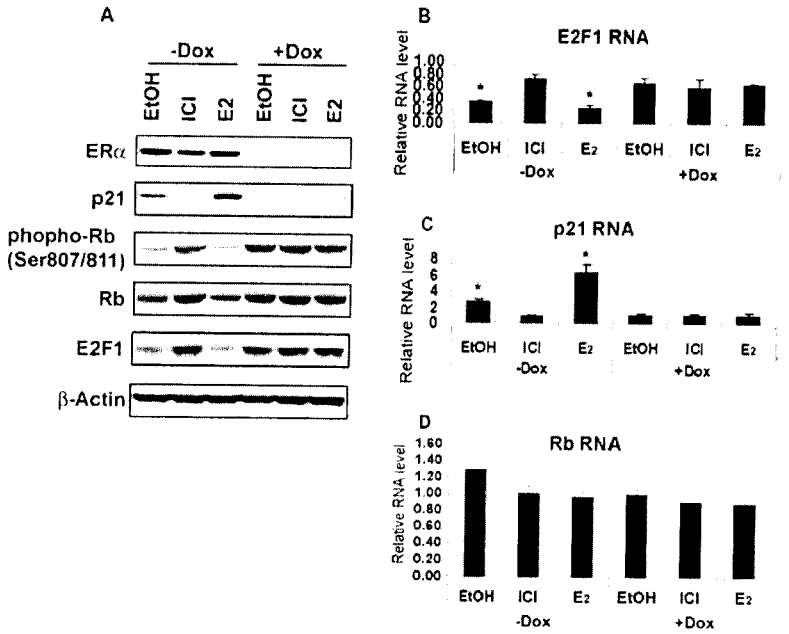


Figure 5. Modification of $p21^{Cip1\ Waf1}$, pRb and E2F1 by ERα/E_2 in SKBr3 cells. SKBr3 cells were infected, treated and harvested as in Fig. 4. Protein was extracted for Western blot analysis (A) and RNA was prepared for real-time RT-PCR analysis to detect E2F1 (B), $p21^{Cip1\ Waf1}$ (C) or pRb (D) as described in Fig. 2. *Samples with a statistically significant difference ($p<0.05$ by t-test) from the +Dox/EtOH control.

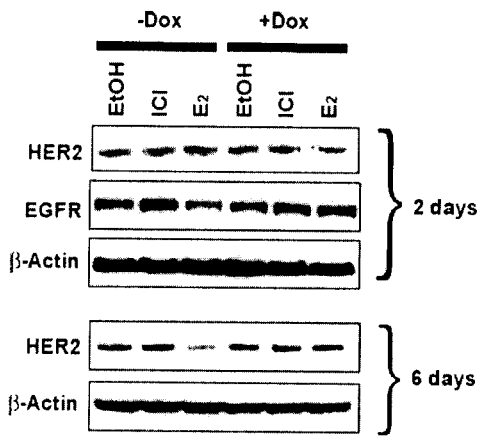


Figure 6. The effects of ERα expression and estrogen treatment on the expression of HER2 and EGFR in SKBr3 cells. SKBr3 cells were infected, treated for 2 days or 6 days then harvested for protein extraction and Western blot analysis.

direct result of the interested gene expression but the result of the random gene insertion at the host genome. The inability of adenoviruses to integrate into the host genome minimizes the complications of destroying or activating other host genes, thus adenoviral vector is a valuable tool to express exogenous genes for gene therapy. Adenovirus-based therapy to express p53 tumor suppressor, Advxin™ (Introgen Therapeutics, Austin, TX), has demonstrated safety profile and clinic efficacy in several tumor types and approval is being sought in Europe and the United States to treat recurrent, refractory head and neck cancer (24). Another similar adenoviral p53 transfer therapy, Gendicine® (Benda Pharmaceutical, China), has been approved to treat head and neck cancer in China (25). Therefore, adenovirus-based vectors could potentially be developed in the future to express ERα in ER-negative breast cancers to restore hormone responsiveness.

The Tet-off system adds another advantage to the expression method by controlling the expression level of interested gene. As shown in Fig. 2B, the amount of ERα expressed is regulated by doxycycline. This provides a valuable approach to study gene function in a dose-dependent manner, which is not achievable using a constitutively-expressing vector. Moreover, expression of the interested gene can be turned on or off by removal or addition of doxycycline at any time, thus studying the gene function in a timely fashion is possible.

Ectopic ERα expression and E_2 treatment arrest SKBr3 cells at G0/G1 cell cycle. In MDA-MB-231 cells, ectopic ERα expression by adenovirus itself had no effect on cell proliferation, but treatment of E_2 suppressed cell proliferation (14). However, in SKBr3 cells, the expression of ERα itself inhibits cell proliferation and E_2 treatment amplifies the growth inhibitory effects, while pure antiestrogen fulvestrant abolished growth inhibitory effects of ERα (Fig. 3). It is possible that ERα has more ligand-independent activity in SKBr3 cells which over-express both HER2 and EGFR than in MDA-MB-231 cells that only over express EGFR. Estrogen exerts similar growth inhibitory effects on MDA-MB-231 and SKBr3 cells when ERα is expressed, but ERα-expressing MDA-MB-231 and SKBr3 cells respond differently to tamoxifen which is ineffective in MDA-MB-231 cells (14) but inhibitory in SKBr3 cells (Fig. 3A). The mechanisms remain to be elucidated and could be that these two cell types have various cellular profile of transcription factors and different levels of nuclear receptor coregulators.

The proliferation inhibition mediated by ERα and E_2 in SKBr3 cells is likely due to cell cycle arrest at G0/G1 phase (Fig. 4), since significant apoptosis was not observed. Similar to MDA-MB-231 cells, E_2 and ERα modify the expression of G1 to S phase checkpoint proteins $p21^{Cip1\ Waf1}$ and E2F1 in SKBr3 cells (Fig. 5), suggesting an important role of E2F1 in hormone-mediated regulation of cell proliferation. E2F1 is critical to control cell cycle progression and apoptosis (26), and its overexpression is often linked to poor prognosis of breast cancer (27-30). Therefore, E2F1 is a potential drug target for breast cancer. In addition, E_2 treatment down-regulates expression of HER2 and EGFR in ERα-expressing SKBr3 cells (Fig. 6), suggesting that growth factor signalling could be diminished by E_2/ERα and that a less aggressive hormone-responsive cancer type can be re-created.

Strategically, it is important to note that the ectopic E_2/ERα complex is able to block cell cycle progression at G0/G1 phase. A similar effect occurs with endogenous E_2/ERα complex in the MCF-7:5C cell line that is resistant to estrogen withdrawal (5). However, in contrast to the MCF-7:5C cells that progress to apoptosis, SKBr3 cells with ectopic ERα do not. It will be important to discover the reason for the failure to trigger apoptosis because the ectopic ERα could be used to define and identify a common pathway for future drug discovery. In other words, a proportion of cancers that never had the ER may have a vestigial pathway that could be activated to provoke apoptosis. The Tet-off adenoviral ERα system may be an approach to discover the veracity of this drug discovery strategy.

Acknowledgements

We appreciate the assistance of Flow Cytometry and Cell Sorting Facility at the Fox Chase Cancer Center for flow cytometry analysis. Dr Jordan is supported by the Department of Defense Breast Program under award number BC050277 Center of Excellence, FCCC Core Grant NIH P30 CA006927, the Genuardi's Fund, the Weg Fund of Fox Chase Cancer Center and the Hollenbach Family Fund. The views and opinions of the author(s) do not reflect those of the US Army or the Department of Defense.

References

1. Jordan VC: A century of deciphering the control mechanisms of sex steroid action in breast and prostate cancer: the origins of targeted therapy and chemoprevention. Cancer Res 69: 1243-1254, 2009.
2. Wolf DM and Jordan VC: A laboratory model to explain the survival advantage observed in patients taking adjuvant tamoxifen therapy. Recent Results Cancer Res 127: 23-33, 1993.
3. Song RX, Mor G, Naftolin F, *et al*: Effect of long-term estrogen deprivation on apoptotic responses of breast cancer cells to 17beta-estradiol. J Natl Cancer Inst 93: 1714-1723, 2001.

4. Lewis JS, Osipo C, Meeke K and Jordan VC: Estrogen-induced apoptosis in a breast cancer model resistant to long-term estrogen withdrawal. J Steroid Biochem Mol Biol 94: 131-141, 2005.
5. Lewis JS, Meeke K, Osipo C, *et al*: Intrinsic mechanism of estradiol-induced apoptosis in breast cancer cells resistant to estrogen deprivation. J Natl Cancer Inst 97: 1746-1759, 2005.
6. Yao K, Lee ES, Bentrem DJ, *et al*: Antitumor action of physiological estradiol on tamoxifen-stimulated breast tumors grown in athymic mice. Clin Cancer Res 6: 2028-2036, 2000.
7. Jordan VC: The 38th David A. Karnofsky lecture: the paradoxical actions of estrogen in breast cancer - urvival or death? J Clin Oncol 26: 3073-3082, 2008.
8. Brinkman JA and El-Ashry D: ER re-expression and re-sensitization to endocrine therapies in ER-negative breast cancers. J Mammary Gland Biol Neoplasia 14: 67-78, 2009.
9. Bayliss J, Hilger A, Vishnu P, Diehl K and El-Ashry D: Reversal of the estrogen receptor negative phenotype in breast cancer and restoration of antiestrogen response. Clin Cancer Res 13: 7029-7036, 2007.
10. Jiang SY and Jordan VC: Growth regulation of estrogen receptor-negative breast cancer cells transfected with complementary DNAs for estrogen receptor. J Natl Cancer Inst 84: 580-591, 1992.
11. Levenson AS and Jordan VC: Transfection of human estrogen receptor (ER) cDNA into ER-negative mammalian cell lines. J Steroid Biochem Mol Biol 51: 229-239, 1994.
12. Stender JD, Frasor J, Komm B, Chang KCN, Kraus WL and Katzenellenbogen BS: Estrogen-regulated gene networks in human breast cancer cells: involvement of E2F1 in the regulation of cell proliferation. Mol Endocrinol 21: 2112-2123, 2007.
13. Lazennec G, Alcorn JL and Katzenellenbogen BS: Adenovirus-mediated delivery of a dominant negative estrogen receptor gene abrogates estrogen-stimulated gene expression and breast cancer cell proliferation. Mol Endocrinol 13: 969-980, 1999.
14. Lazennec G and Katzenellenbogen BS: Expression of human estrogen receptor using an efficient adenoviral gene delivery system is able to restore hormone-dependent features to estrogen receptor-negative breast carcinoma cells. Mol Cell Endocrinol 149: 93-105, 1999.
15. Arpino G, Wiechmann L, Osborne CK and Schiff R: Crosstalk between the estrogen receptor and the HER tyrosine kinase receptor family: molecular mechanism and clinical implications for endocrine therapy resistance. Endocr Rev 29: 217-233, 2008.
16. Liu H, Cheng D, Weichel AK, *et al*: Cooperative effect of gefitinib and fumitremorgin c on cell growth and chemosensitivity in estrogen receptor alpha negative fulvestrant-resistant MCF-7 cells. Int J Oncol 29: 1237-1246, 2006.
17. Murphy CS, Pink JJ and Jordan VC: Characterization of a receptor-negative, hormone-nonresponsive clone derived from a T47D human breast cancer cell line kept under estrogen-free conditions. Cancer Res 50: 7285-7292, 1990.
18. Pink JJ, Bilimoria MM, Assikis J and Jordan VC: Irreversible loss of the oestrogen receptor in T47D breast cancer cells following prolonged oestrogen deprivation. Br J Cancer 74: 1227-1236, 1996.
19. Ariazi EA, Kraus RJ, Farrell ML, Jordan VC and Mertz JE: Estrogen-related receptor alpha1 transcriptional activities are regulated in part via the ErbB2/HER2 signaling pathway. Mol Cancer Res 5: 71-85, 2007.
20. Broude EV, Swift ME, Vivo C, *et al*: p21(Waf1/Cip1/Sdi1) mediates retinoblastoma protein degradation. Oncogene 26: 6954-6958, 2007.
21. Schiff R, Massarweh SA, Shou J, *et al*: Advanced concepts in estrogen receptor biology and breast cancer endocrine resistance: implicated role of growth factor signaling and estrogen receptor coregulators. Cancer Chemother Pharmacol 56 (Suppl. 1): 10-20, 2005.
22. Huang HJ, Neven P, Drijkoningen M, *et al*: Hormone receptors do not predict the HER2/neu status in all age groups of women with an operable breast cancer. Ann Oncol 16: 1755-1761, 2005.
23. Read LD, Keith D Jr, Slamon DJ and Katzenellenbogen BS: Hormonal modulation of HER-2/neu protooncogene messenger ribonucleic acid and p185 protein expression in human breast cancer cell lines. Cancer Res 50: 3947-3951, 1990.
24. Senzer N and Nemunaitis J: A review of contusugene ladenovec (Advexin) p53 therapy. Curr Opin Mol Ther 11: 54-61, 2009.
25. Patil SD, Rhodes DG and Burgess DJ: DNA-based therapeutics and DNA delivery systems: a comprehensive review. AAPS J 7: E61-E77, 2005.
26. De Gregori J and Johnson DG: Distinct and overlapping roles for E2F family members in transcription, proliferation and apoptosis. Curr Mol Med 6: 739-748, 2006.
27. Vuaroqueaux V, Urban P, Labuhn M, *et al*: Low E2F1 transcript levels are a strong determinant of favorable breast cancer outcome. Breast Cancer Res 9: R33, 2007.
28. Baldini E, Camerini A, Sgambato A, *et al*: Cyclin A and E2F1 overexpression correlate with reduced disease-free survival in node-negative breast cancer patients. Anticancer Res 26: 4415-4421, 2006.
29. Han S, Park K, Bae BN, *et al*: E2F1 expression is related with the poor survival of lymph node-positive breast cancer patients treated with fluorouracil, doxorubicin and cyclophosphamide. Breast Cancer Res Treat 82: 11-16, 2003.
30. Zhang SY, Liu SC, Al-Saleem LF, *et al*: E2F-1: a proliferative marker of breast neoplasia. Cancer Epidemiol Biomarkers Prev 9: 395-401, 2000.

Published Online First on January 19, 2010 as 10.1158/0008-5472.CAN-09-3068

Tumor and Stem Cell Biology

Cancer Research

The G Protein–Coupled Receptor GPR30 Inhibits Proliferation of Estrogen Receptor–Positive Breast Cancer Cells

Eric A. Ariazi[1], Eugen Brailoiu[2], Smitha Yerrum[1], Heather A. Shupp[1], Michael J. Slifker[1], Heather E. Cunliffe[3], Michael A. Black[4], Anne L. Donato[1], Jeffrey B. Arterburn[5], Tudor I. Oprea[6], Eric R. Prossnitz[7], Nae J. Dun[2], and V. Craig Jordan[1]

Abstract

The G protein–coupled receptor GPR30 binds 17β-estradiol (E_2) yet differs from classic estrogen receptors (ERα and ERβ). GPR30 can mediate E_2-induced nongenomic signaling, but its role in ERα-positive breast cancer remains unclear. Gene expression microarray data from five cohorts comprising 1,250 breast carcinomas showed an association between increased GPR30 expression and ERα-positive status. We therefore examined GPR30 in estrogenic activities in ER-positive MCF-7 breast cancer cells using G-1 and diethylstilbestrol (DES), ligands that selectively activate GPR30 and ER, respectively, and small interfering RNAs. In expression studies, E_2 and DES, but not G-1, transiently downregulated both ER and GPR30, indicating that this was ER mediated. In Ca^{2+} mobilization studies, GPR30, but not ERα, mediated E_2-induced Ca^{2+} responses because E_2, 4-hydroxytamoxifen (activates GPR30), and G-1, but not DES, elicited cytosolic Ca^{2+} increases not only in MCF-7 cells but also in ER-negative SKBr3 cells. Additionally, in MCF-7 cells, GPR30 depletion blocked E_2-induced and G-1–induced Ca^{2+} mobilization, but ERα depletion did not. Interestingly, GPR30-coupled Ca^{2+} responses were sustained and inositol triphosphate receptor mediated in ER-positive MCF-7 cells but transitory and ryanodine receptor mediated in ER-negative SKBr3 cells. Proliferation studies involving GPR30 depletion indicated that the role of GPR30 was to promote SKBr3 cell growth but reduce MCF-7 cell growth. Supporting this, G-1 profoundly inhibited MCF-7 cell growth, potentially via p53 and p21 induction. Further, flow cytometry showed that G-1 blocked MCF-7 cell cycle progression at the G_1 phase. Thus, GPR30 antagonizes growth of ERα-positive breast cancer and may represent a new target to combat this disease. *Cancer Res; 70(3); 1184–94. ©2010 AACR.*

Introduction

The G protein–coupled receptor GPR30 is a seven-transmembrane domain protein identified as a novel 17β-estradiol (E_2)–binding protein structurally distinct from the classic estrogen receptors α and β (ERα and ERβ). GPR30 can mediate rapid E_2-induced nongenomic signaling events, including stimulation of adenylyl cyclase, and, via transactivation of epidermal growth factor receptors, induces mobilization of intracellular calcium (Ca^{2+}) stores and activation of mitogen-activated protein kinase (MAPK) and phosphoinositide 3-kinase (PI3K) signaling pathways (1, 2). GPR30 also exhibits prognostic utility in endometrial (3), ovarian (4), and breast cancer (5, 6) and can modulate growth of hormonally responsive cancer cells (7–11). Therefore, GPR30 likely plays important roles in modulating estrogen responsiveness and in the development and/or progression of hormonally responsive cancers. Moreover, GPR30 represents a promising new target for drug discovery in hormonally responsive disease.

In addition to E_2, the selective ER modulator (SERM) tamoxifen, one of its active metabolites 4-hydroxytamoxifen (4OHT), and the complete antiestrogen fulvestrant all activate GPR30 (12–14). GPR30 does not significantly bind the nonsteroidal full ER agonist diethylstilbestrol (DES; ref. 12). Drug discovery efforts have yielded two GPR30-selective high-affinity ligands: an agonist termed G-1 (15) and, recently, an antagonist termed G-15 (16). G-1 and G-15 do not bind ERs at concentrations up to 10^{-6} mol/L (15, 16). Moreover, G-1 specificity for GPR30 was illustrated by showing it does not significantly bind 25 other G protein–coupled receptors (17).

GPR30 has been shown to mediate the proliferative effects of E_2 in thyroid (7), endometrial (8, 18), ovarian (9), and

Authors' Affiliations: [1]Fox Chase Cancer Center; [2]Department of Pharmacology, Temple University School of Medicine, Philadelphia, Pennsylvania; [3]Computational Biology Division, The Translational Genomics Research Institute, Phoenix, Arizona; [4]Department of Biochemistry, University of Otago, Dunedin, New Zealand; [5]Department of Chemistry and Biochemistry, New Mexico State University, Las Cruces, New Mexico; and Departments of [6]Biochemistry and Molecular Biology and [7]Cell Biology and Physiology, University of New Mexico School of Medicine, Albuquerque, New Mexico

Note: Supplementary data for this article are available at Cancer Research Online (http://cancerres.aacrjournals.org/).

Current address for V.C. Jordan: Department of Oncology, Lombardi Comprehensive Cancer Center, Georgetown University School of Medicine, Washington, District of Columbia.

Corresponding Author: V. Craig Jordan, Department of Oncology, Lombardi Comprehensive Cancer Center, Georgetown University Medical Center, 3970 Reservoir Road Northwest, Washington, DC 20057. Phone: 202-687-2897; Fax: 202-687-6402; E-mail: vcj2@georgetown.edu.

doi: 10.1158/0008-5472.CAN-09-3068

©2010 American Association for Cancer Research.

ER-negative SKBr3 breast cancer cell lines (9, 10) because GPR30 depletion, using antisense oligonucleotides or RNA interference (RNAi) methodologies, abrogated E_2-stimulated growth in these cells. However, GPR30-mediated growth effects differ in ER-positive MCF-7 breast cancer cells. Ahola and colleagues (11) reported that transient overexpression of GPR30 in MCF-7 cells inhibited bromodeoxyuridine incorporation, an indicator of proliferation.

We investigated GPR30 largely in ER-positive MCF-7 with some comparisons to ER-negative SKBr3 breast cancer cells. First, a statistical association was sought between GPR30 and ERα-positive status in publicly available breast carcinoma microarray data sets. Next, the contribution of ERα and GPR30 in several E_2-responsive activities, including regulation of GPR30 expression, intracellular Ca^{2+} mobilization, cellular growth, and cell cycle progression, was studied using receptor-specific ligands and small interfering RNA (siRNA) methodology.

Materials and Methods

Breast cancer microarray data mining. GPR30 mRNA levels and ER status were extracted from gene expression microarrays comprising 1,250 breast carcinomas across five distinct cohorts. The first cohort or the NKI cohort (n = 295; Netherlands Cancer Institute, Amsterdam, the Netherlands) was derived from van de Vijver and colleagues (19).[8] NKI data were obtained using two-color 60-polymer oligonucleotide arrays. cRNA from one tumor was competitively hybridized against a pooled reference cRNA from all tumors. Expression values corresponded to normalized $\log_2$ ratio intensity units. ER-positive status was supplied with the microarray data (19). Pearson's correlation coefficients were computed between GPR30 and all other genes using the R software package.[9] Cohorts 2 to 5 were obtained from Gene Expression Omnibus (GEO; ref. 20). These cohorts are termed the Uppsala cohort (GSE3494/GSE4922/GSE6532; samples collected in Uppsala County, Sweden), the Stockholm cohort (GSE1456; samples collected at the Karolinska Hospital in Stockholm, Sweden), the EMC cohort (GSE2034/GSE5327; samples collected at the Erasmus Medical Center, Rotterdam, the Netherlands), and the TRANSBIG cohort (GSE7390; samples collected by the translational research network managed by the Breast International Group). The Uppsala and EMC cohorts contained samples processed at the same institution that span multiple GEO accession numbers. These four cohorts used Affymetrix microarray technology. Where available, raw data (in the form of CEL files) were downloaded; otherwise, MAS5.0 normalized data were downloaded (CEL files were available for all studies except GSE2034 and GSE5327). All data preprocessing and MAS5.0 normalization were performed using R software and the justMAS function in the simpleAffy library from Bioconductor (no background correction, target intensity of 600; ref. 21). After normalization, gene expression data were extracted for the GPR30 probe 210640_s_at. ER status was provided via Supplementary Data in GEO.

Compounds and cell lines. E_2, DES, and 2-aminoethyldiphenylborinate (2APB) were from Sigma-Aldrich. G-1 and fulvestrant (ICI 182,780, Faslodex) were from Tocris. Xestospongin C (XeC) and ryanodine (Ry) were from Calbiochem, EMD Biosciences. All agents were added to culture medium at 1:10,000 to 1:1,000 (v/v). Fura-2 AM and all cell culture reagents were from Invitrogen. MCF-7:WS8 human mammary carcinoma cells were used in all experiments indicating MCF-7 cells; they were clonally selected for sensitivity to E_2-stimulated growth (22). SKBr3 cells were purchased from the American Type Culture Collection. Both cell lines were maintained in estrogenized medium [RPMI-1640 plus 10% fetal bovine serum (FBS)]. MCF-7 cells were switched to estrogen-free medium (phenol red–free RPMI-1640 plus 10% charcoal-stripped FBS) for 2 d before all experiments, except where noted.

Real-time quantitative PCR assays. Quantitative PCR (qPCR) was conducted as previously described (23). Target mRNA levels were normalized to PUM1 [pumilio homologue 1 (*Drosophila*)] mRNA levels (24). See Supplementary Materials and Methods for primer sequences. Data were analyzed by comparison with a serial dilution series of MCF-7 cell cDNA. Values in each group were averaged from four biological replicates (unless otherwise indicated), and each biological replicate was averaged from four technical replicates.

siRNA transfection. MCF-7 cells that had been maintained in estrogenized medium were transfected with siRNAs for 6 h in serum-free Opti-MEM (Invitrogen) using Dharmafect 1 (Dharmacon RNAi Technologies) followed by overnight recovery in estrogenized medium. The transfection was carried out a second time, and then the cells were immediately switched to estrogen-free medium and again allowed overnight recovery. siRNAs were transfected at 200 nmol/L final concentration, except in Ca^{2+} experiments in which siRNAs were transfected at 100 nmol/L and cotransfected with siGLO Green, a 6-carboxyfluorescein–labeled inactive double-stranded RNA. See Supplementary Materials and Methods for ERα and GPR30 siRNA sequences (Dharmacon RNAi Technologies).

Ca^{2+} imaging. Cytoplasmic Ca^{2+}concentrations were measured using Fura-2 AM and microscopy as previously described (25). Flat SKBr3 cells were imaged because they were the major morphologic cell type, whereas rounded SKBr3 cells were not imaged. All compounds were administered at 1 min.

Cellular proliferation. Cell growth was assessed using Hoechst 33258 (Invitrogen) and compared with a standard curve of serial-diluted calf thymus DNA as previously described (26, 27).

Cell cycle analyses. Cell cycle distribution was determined by propidium iodide staining and using a fluorescence-activated cell sorter (Becton Dickinson) as previously described (27). Data were analyzed using FlowJo 7.2.5 for Windows (Tree Star).

[8] http://www.rii.com/publications/2002/nejm.html
[9] http://www.R-project.org

Immunoblot analyses. Immunoblotting was carried out using 40 μg protein per lane as previously described (23). Membranes were probed using antibodies against ERα (AER 611; Lab Vision), p53 (DO-1; Calbiochem), p21 (F-5; Santa Cruz Biotechnology), cyclin D1 (DCS-6; Santa Cruz Biotechnology), cyclin B1 (D-11; Santa Cruz Biotechnology), and β-actin (AC-15; Sigma-Aldrich). Membranes were visualized using the Odyssey Infrared Imaging System (LI-COR Biosciences).

Statistical analyses. Mann-Whitney tests were performed using Prism 4.03 for Windows (GraphPad Software). All other statistical analyses were performed using Excel 2003 for Windows (Microsoft). Error is represented by SEMs in Ca^{2+} mobilization experiments and by SDs in all other experiments. Also in the Ca^{2+} experiments, *P* values reflect one-way ANOVA comparing the maximum Ca^{2+} concentration versus the concentration at the treatment start time, unless otherwise stated.

Results

Increased GPR30 mRNA expression associates with ERα-positive status in 1,250 breast carcinomas. Evidence of a relationship between GPR30 and ERα expression was sought by mining publicly available and well-annotated gene expression microarray data sets across five independent cohorts comprising 1,250 breast carcinomas. In the NKI cohort (n = 254), data were collected using two-color oligonucleotide microarrays (Fig. 1A). According to the nonparametric Mann-Whitney rank sum test, GPR30 mRNA levels were significantly higher in ERα-positive versus ERα-negative tumors ($P < 0.0001$). The upper range of GPR30 expression was 7.7-fold higher on a linear scale in the ERα-positive compared with ERα-negative carcinomas. In addition, GPR30 and ERα mRNA levels correlated as continuous variables (Pearson's coefficient $\rho = 0.30$, adjusted $P < 0.0001$). The other four cohorts used one-color Affymetrix oligonucleotide microarrays (Fig. 1B). In each of these four cohorts, GPR30 mRNA levels were significantly higher in the ERα-positive compared with the ERα-negative breast cancers (Uppsala cohort, n = 244, P = 0.040; Stockholm cohort, n = 159, P = 0.0091; EMC cohort, n = 344, P = 0.0050; TRANSBIG cohort, n = 198, P = 0.0024).

E_2 downregulates GPR30 mRNA expression via ER and not GPR30. GPR30 regulation in response to E_2 was investigated. MCF-7 cells were treated with E_2 or without E_2 (control, vehicle only) over a 96-hour time course followed by determination of ERα and GPR30 mRNA levels by qPCR. As expected, E_2 steadily downregulated ERα mRNA levels by 59% over 96 hours (Fig. 2A). E_2 also downregulated GPR30 but with faster kinetics than with ERα (Fig. 2B); GPR30 mRNA levels were decreased by 37% at 2 hours (P = 0.0013) and by 79% at 24 hours ($P < 0.0001$). Afterwards, GPR30 mRNA levels rebounded. Additionally, GPR30 mRNA expression decreased in a concentration-dependent manner from 10^{-12} mol/L E_2 to 10^{-10} mol/L E_2 (Fig. 2C). The GPR30-specific agonist G-1 did not alter GPR30 mRNA expression, but the ER-specific agonist DES did repress GPR30 expression relative to control treatment by 54% P = 0.0009), which was very similar to the effect of E_2 (Fig. 2D). Fulvestrant completely blocked E_2 and DES effects. Therefore, E_2 likely acted via ER and not GPR30 to transiently downregulate GPR30 mRNA expression.

GPR30 and not ERα mediates E_2-induced Ca^{2+} mobilization responses. To begin to delineate whether endogenous ERα and/or GPR30 mediates E_2-induced Ca^{2+} responses in breast cancer cells, changes in intracellular Ca^{2+} concentrations $[Ca^{2+}]_i$ were measured in ER-positive MCF-7 and ER-negative SKBr3 breast cancer cells at the single-cell level using Fura-2 AM (Fig. 3). In ER-positive MCF-7 cells (Fig. 3A), E_2 induced $[Ca^{2+}]_i$ by 112 ± 1.6 nmol/L (n = 47 cells, P = 0.0063), G-1 by 511 ± 3.4 nmol/L (n = 58 cells, P = 0.0007), and 4OHT by 234 ± 3.4 nmol/L (n = 31 cells, P = 0.0017), whereas DES did not significantly increase the $[Ca^{2+}]_i$ (change = 41 ± 0.8 nmol/L, n = 23 cells, P = 0.66). In ER-negative SKBr3 cells (Fig. 3B), the rank order of ligand-induced cytosolic Ca^{2+} increases was the same as in MCF-7 cells, but the magnitude of the increases was much greater and the responses were transitory instead of sustained. In ER-negative SKBr3 cells, E_2 induced oscillating increases in $[Ca^{2+}]_i$ with an average maximum of 294 ± 1.6 nmol/L (n = 36 cells, P = 0.0037). G-1 and 4OHT induced transitory increases in $[Ca^{2+}]_i$ of 1,517 ± 10.3 nmol/L (n = 79 cells, P = 0.0001) and of 558 ± 2.7 nmol/L (n = 37 cells, P = 0.0013), respectively, whereas DES did not ($[Ca^{2+}]_i$ change = 51 ± 1.3 nmol/L, n = 21 cells, P = 0.26). Therefore, because G-1 and two ER ligands that also bind GPR30, E_2 and 4OHT, but not ER-selective DES, elicited Ca^{2+} responses in both ER-positive MCF-7 cells and ER-negative SKBr3 cells, they likely did so via GPR30.

Two of the major Ca^{2+} channels, inositol triphosphate receptors (IP_3R) and Ry receptors (RyR; ref. 28), were tested for whether they mediated G-1–induced Ca^{2+} mobilization. The pharmacologic probes 2APB and XeC, both of which inhibit IP_3Rs, and Ry, which at high concentrations blocks RyRs, were used. Cells were pretreated for 30 min before inducing Ca^{2+} responses with G-1. In MCF-7 cells, both 2APB and XeC blocked G-1–induced $[Ca^{2+}]_i$ increases by 78% (both 2APB + G-1 versus G-1 alone and XeC + G-1 versus G-1 alone, P = 0.0018) but Ry did not. In contrast, in SKBr3 cells, Ry blocked G-1–induced $[Ca^{2+}]_i$ increases by 80% (Ry + G-1 versus G-1 alone, P = 0.0006), whereas XeC did not. In addition, 2APB allowed G-1 to almost fully induce $[Ca^{2+}]_i$ increases, although the response was significantly lower by 17% versus G-1 alone (P = 0.0094), but this was likely due to blockade of store-operated Ca^{2+} entry, another activity of 2APB. Therefore, GPR30 was coupled to IP_3Rs in ER-positive MCF-7 cells but to RyRs in ER-negative SKBr3 cells.

To confirm that GPR30 and not ERα mediates Ca^{2+} mobilization in response to E_2 in MCF-7 cells, cells were transfected with siRNAs targeting these receptors (characterization of siRNAs in Supplementary Materials and Methods) and a nontargeting siRNA pool as a control. First, the GPR30 siRNA was validated by showing that it led to an almost complete blockade of G-1–induced Ca^{2+} responses ($[Ca^{2+}]_i$ increase = 58 ± 1.3 nmol/L, n = 19 cells, P = 0.62; Fig. 4A). Next, E_2-induced Ca^{2+} mobilization responses were investigated

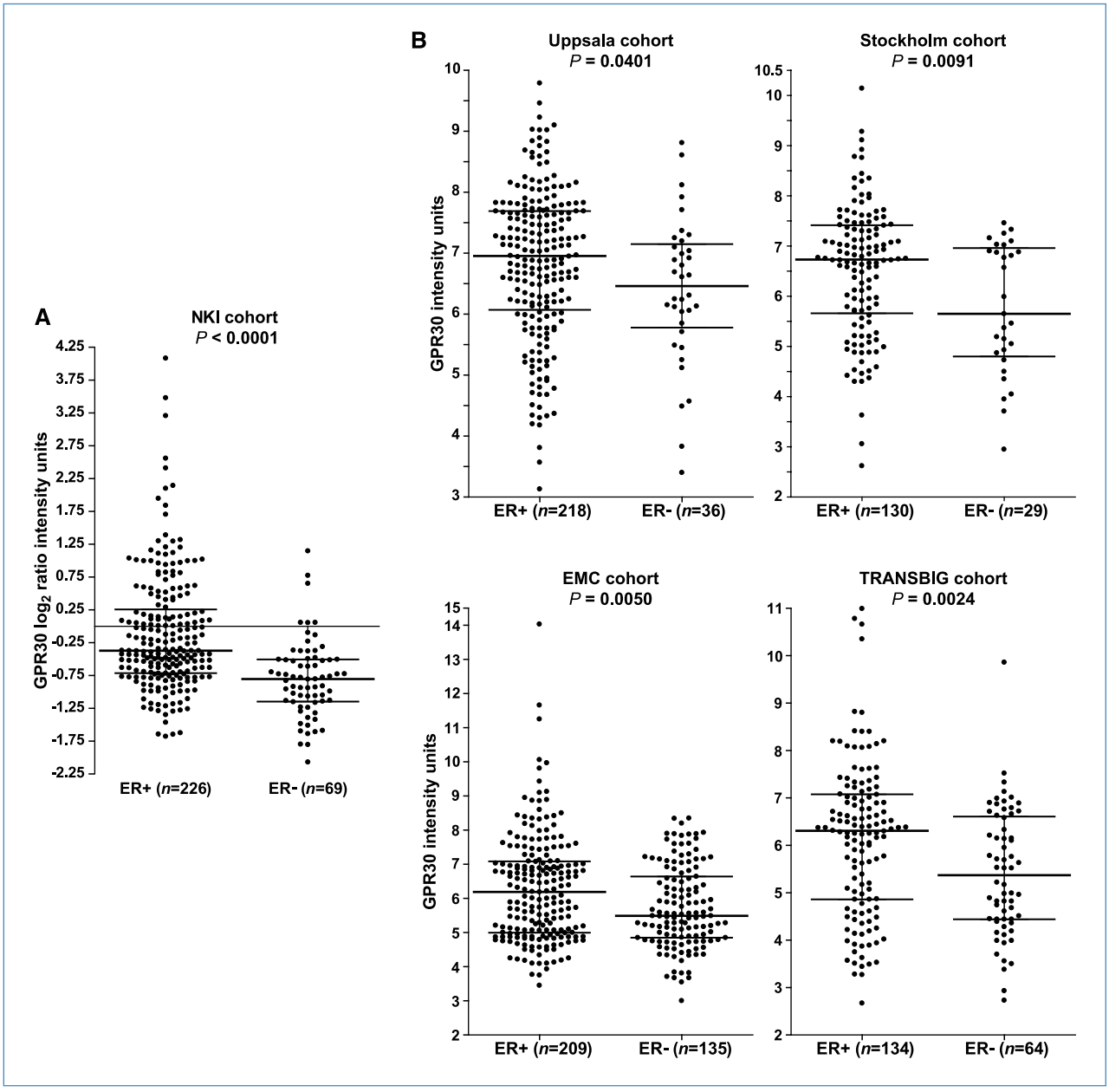


Figure 1. GPR30 mRNA expression shows an association with ERα-positive status in human breast carcinomas. A, GPR30 mRNA levels in the NKI cohort derived from two-color arrays. Expression values are normalized $\log_2$ ratio intensity units corresponding to a single tumor cRNA hybridized against a pooled reference cRNA from all tumors. B, GPR30 mRNA levels in the Uppsala, Stockholm, EMC, and TRANSBIG cohorts all derived from one-color arrays. Expression values are MAS5.0 normalized intensity units. A and B, sample sizes of ERα-positive (*ER+*) and ER-negative (*ER–*) cancers are shown, and bars indicate the 75th, 50th (median), and 25th percentiles. Significance was assessed using the nonparametric Mann-Whitney rank test.

(Fig. 4B). In nontargeting siRNA–transfected cells, E_2 induced an $[Ca^{2+}]_i$ increase of 159 ± 1.6 nmol/L (n = 14 cells, P = 0.0075). However, in ERα siRNA–transfected cells, E_2 caused almost a 2-fold further rise in $[Ca^{2+}]_i$ (314 ± 3.2 nmol/L, n = 17 cells; P = 0.0006). In GPR30 siRNA–transfected cells, the E_2-induced Ca^{2+} response was blocked ($[Ca^{2+}]_i$ increase = 52 ± 0.8 nmol/L, n = 16 cells, P = 0.35). ERα and GPR30 expression were depleted in the appropriate siRNA-transfected cells (Fig. 4C). However, GPR30 mRNA levels were increased by 73% in ERα-depleted cells, a finding consistent with the prior observation that E_2 and DES repressed GPR30 expression (Fig. 2B–D). Hence, the 2-fold potentiation of E_2-induced $[Ca^{2+}]_i$ in ERα-depleted cells likely reflected, at least in part, the increased GPR30 expression.

GPR30 functions to promote growth of ER-negative SKBr3 cells but to inhibit growth of ER-positive MCF-7 cells. The role of GPR30 in cellular proliferation was examined

by transfecting cells with nontargeting and GPR30 siRNAs and then measuring cellular DNA mass after 5 days of growth. First, SKBr3 cells were evaluated (Fig. 5A). The number of cells seeded in each group was similar as indicated by a lack of difference in DNA masses at day 0. After 5 days of growth, DNA mass was 45% lower in GPR30 siRNA compared with nontargeting siRNA–transfected cells ($P < 0.0001$). Thus, the function of GPR30 was to promote growth of SKBr3 cells, in accordance with other reports (9, 10). Next, MCF-7 cells were similarly evaluated (Fig. 5B). Again, equivalent numbers of nontargeting and GPR30 siRNA–transfected cells were seeded as indicated by DNA masses at day 0. After 5 days, GPR30 depletion did not affect basal growth (control treatment). However, GPR30 depletion did potentiate E_2-stimulated growth by 2.1-fold (nontargeting versus GPR30 siRNA–transfected cells, $P < 0.0001$). Analysis of progesterone receptor (PgR) and TFF1 (pS2) mRNA levels by qPCR indicated no significant differences in their induction by E_2 between nontargeting and GPR30 siRNA–transfected cells (data not shown). Therefore, in contrast to SKBr3 cells, the function of GPR30 in MCF-7 cells was to inhibit growth.

The role of GPR30 in MCF-7 cell proliferation was further evaluated by examining effects of G-1 on E_2-stimulated (Fig. 5C) and DES-stimulated (Fig. 5D) growth over 6 days. G-1 blocked the concentration-dependent growth stimulatory response of E_2 (all E_2 treatment groups versus paired E_2 + G-1

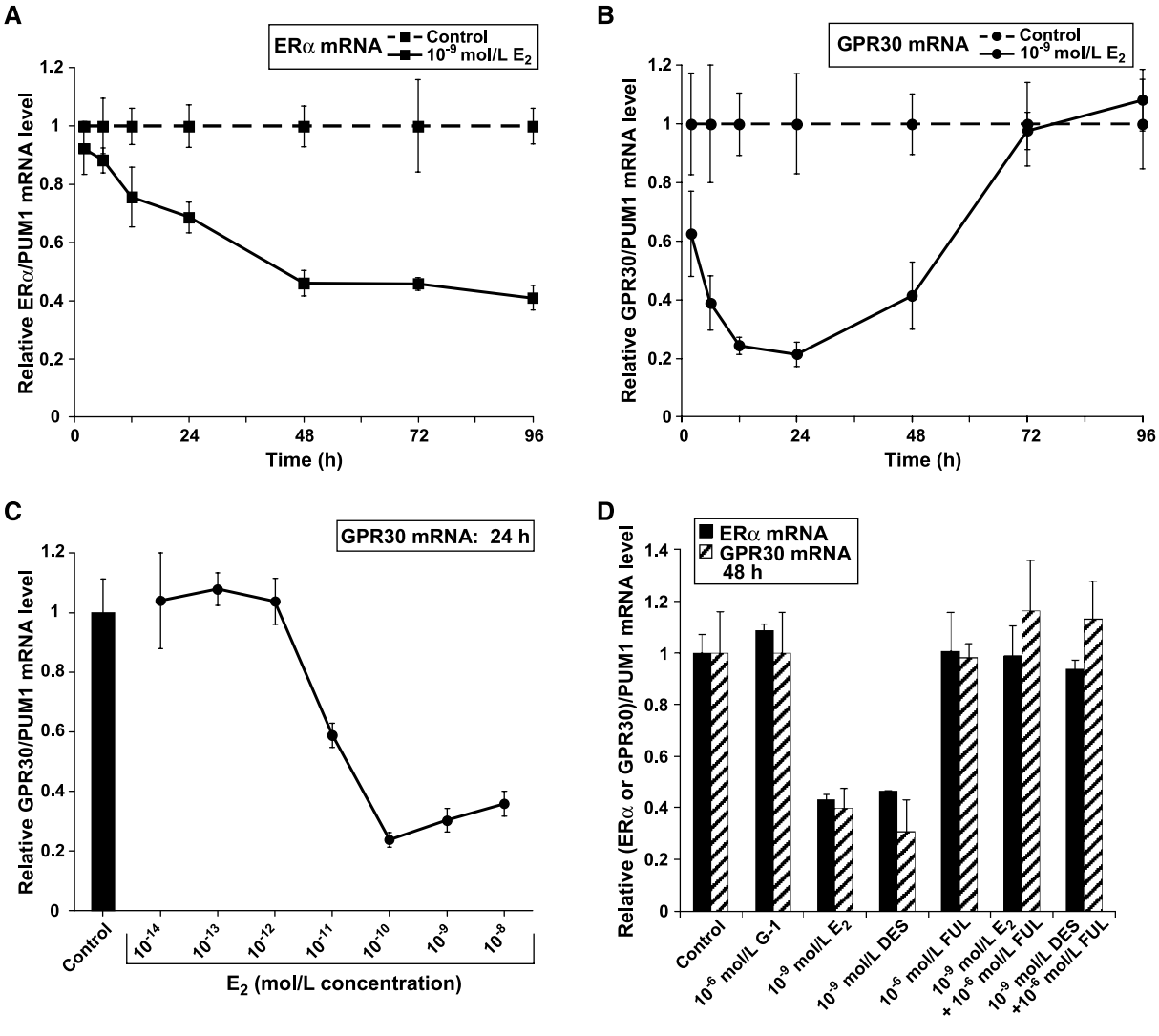


Figure 2. E_2 represses ERα and GPR30 mRNA levels via ER and not GPR30 in MCF-7 cells. E_2 regulation of ERα (A) and GPR30 mRNA (B) levels across a time course. MCF-7 cells were treated with 10^{-9} mol/L E_2 or with the vehicle ethanol alone for 2, 6, 12, 24, 48, 72, and 96 h. C, GPR30 mRNA levels in response to 24-h treatment with a serial dilution series of E_2. D, ERα and GPR30 mRNA levels in response to 48-h treatment with ER and GPR30 ligands as determined by qPCR. Each data point represents the average of six (A and B) or four (C and D) biological replicates. *FUL,* fulvestrant.

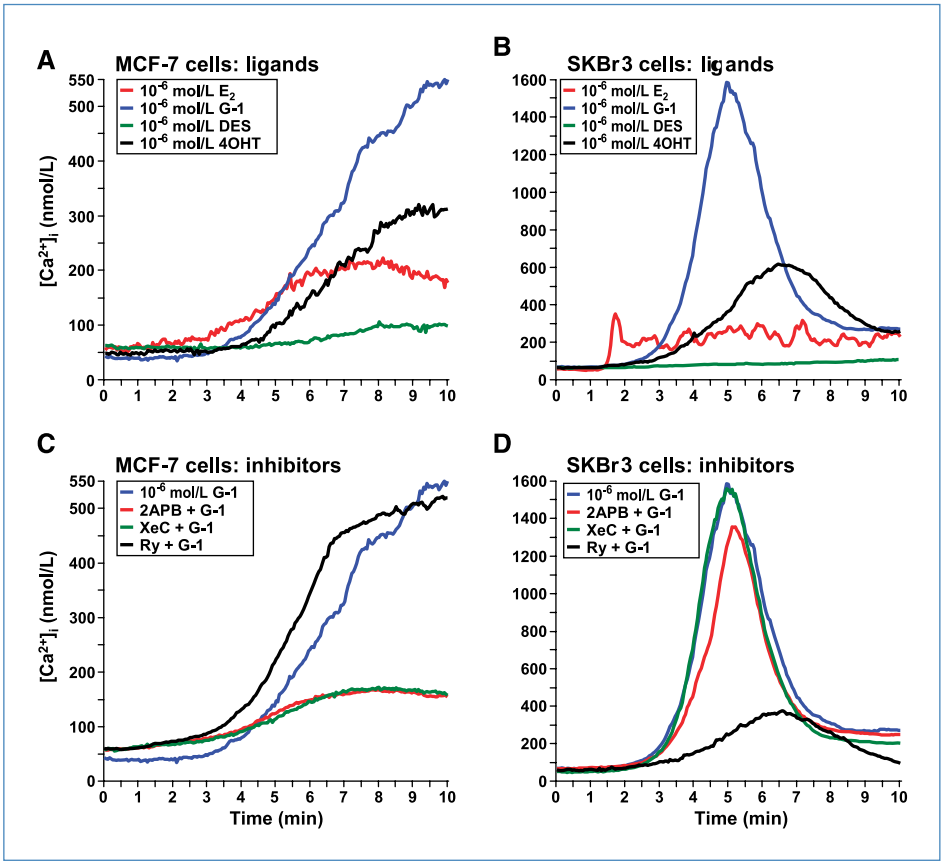


Figure 3. ER ligands that also activate GPR30 induce Ca^{2+} mobilization responses in both ER-positive MCF-7 and ER-negative SKBr3 cells. Ligand-induced Ca^{2+} responses (A and B) and blockade of G-1–induced responses using Ca^{2+} channel inhibitors (C and D) in MCF-7 and SKBr3 cells. Cells were loaded with Fura-2 AM, and intracellular Ca^{2+} concentrations $[Ca^{2+}]_i$ were determined in individual cells versus time using fluorescence microscopy. Cells were perfused with all ligands at 10^{-6} mol/L starting at 1 min. 2APB was used at 10^{-4} mol/L, XeC at 10^{-5} mol/L, and Ry at 10^{-5} mol/L. SKBr3 cells with flat, not rounded, morphology were imaged. G-1–induced Ca^{2+} traces in A and B were redrawn in C and D, respectively.

treatment groups, $P = 0.0001$, one-way ANOVA); in particular, G-1 inhibited 10^{-10} mol/L E_2-stimulated growth by 77% relative to E_2 alone ($P < 0.0001$, t test). G-1 also blocked DES-stimulated growth by 72% (DES versus DES + G-1, $P < 0.0001$). Additionally, in both the E_2 and DES experiments, G-1 inhibited basal (control treatment) growth by 32% ($P < 0.0001$) and 47% ($P < 0.0001$), respectively. Therefore, G-1–activated GPR30 blocked growth of ER-positive breast cancer cells but did so independently of ligand-activated ER.

G-1–activated GPR30 blocks cell cycle progression at G_1 phase. The effect of G-1 on cell cycle progression was investigated. MCF-7 cells were synchronized by estrogen withdrawal and then treated with E_2 and G-1 for 24 hours followed by propidium iodide staining and flow cytometric analysis (Fig. 6A). Treatment with G-1 alone significantly decreased the proportion of S-phase cells from 19.8% (control) to 14.7% (G-1; $P < 0.0001$). Importantly, the addition of G-1 to E_2 led to retention of an additional 11.6% of the cells in G_1 phase (42.7% in E_2-treated cells versus 54.4% in E_2 + G-1–treated cells, $P < 0.0001$) and prevented 13.2% of cells from entering S phase (37.7% in E_2-treated cells versus 24.5% in E_2 + G-1–treated cells, $P < 0.0001$). Therefore, G-1 blocked E_2-stimulated cells from cell cycle progression at the G_1 phase.

The G-1–induced cell cycle block was further investigated by measuring protein expression of the tumor suppressor p53, the cyclin-dependent kinase inhibitor (CDK-I) p21 (Fig. 6B), the G_1-phase–specific cyclin D1, and the G_2/M-phase–specific cyclin B1 (Fig. 6C). MCF-7 cells were treated with E_2 and G-1 and then collected at 24, 48, and 72 hours for immunoblot analysis. Both p53 and p21 proteins were upregulated in G-1 and E_2 + G-1–treated cells across all time points compared with control-treated cells (Fig. 6B). As expected, E_2 upregulated both cyclins D1 and B1 across the time course compared with control treatment, whereas G-1 alone did not (Fig. 6C). However, the addition of G-1 to E_2 potentiated the upregulation of cyclin D1 while nearly completely preventing cyclin B1 accumulation compared with E_2 alone across the time points. Because cyclin D1 is induced during G_1 phase and degraded in S phase (29, 30), whereas cyclin B1 accumulates during G_2-phase and degrades on M-phase entry (31), these data are consistent with G-1 blocking cell cycle progression in G_1 phase before cyclin D1 degradation occurred and before cyclin B1 accumulated.

Discussion

Filardo and colleagues (5) and Kuo and colleagues (6) have previously shown in breast carcinomas a positive association between GPR30 and ERα expression by immunohistochemistry and qPCR, respectively. We confirmed and extended this finding by examining gene expression

microarray data sets of five independent patient cohorts comprising 1,250 breast cancers. In all cohorts, high GPR30 mRNA levels showed an association with ERα positivity (Fig. 1). It is unknown why high GPR30 levels would be selected for in ERα-positive breast carcinomas given GPR30 attenuates growth of ER-positive breast cancer, but some GPR30-dependent functions may be necessary for tumorigenesis and cell survival, such as activation of adenylyl cyclase, PI3K, and MAPK (1, 2). Additional roles of GPR30 may be needed for disease progression, such as in cell migration (15, 32), which may then promote metastasis (5).

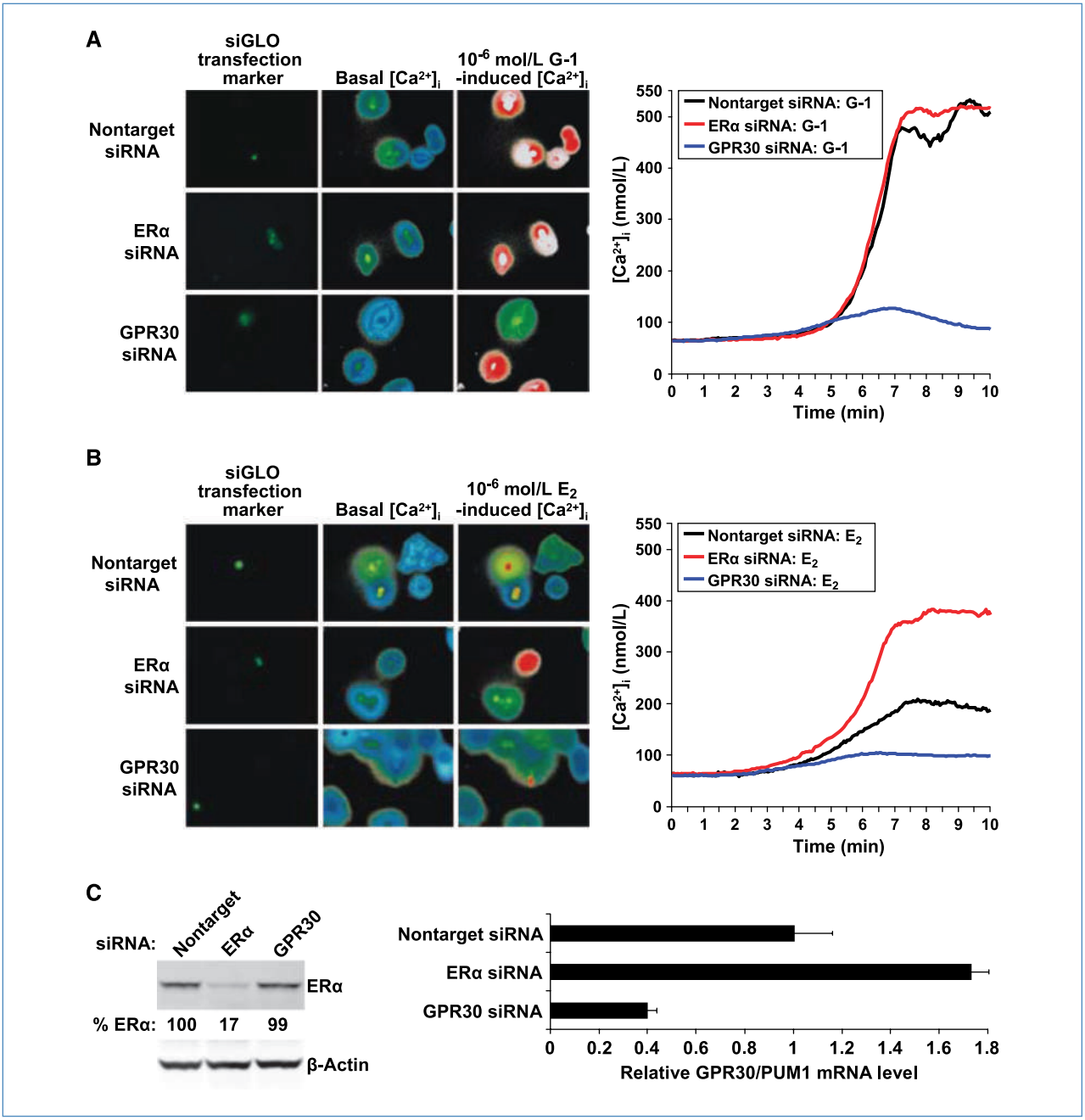


Figure 4. GPR30 and not ERα mediates E_2-induced Ca^{2+} mobilization in MCF-7 cells. G-1–induced (A) and E_2-induced (B) Ca^{2+} responses. Cells were transfected with nontargeting pool, ERα, and GPR30 siRNAs. Transfected cells were labeled using siGLO Green and appear green. Ca^{2+} imaging was performed 48 h following the transfection as in Fig. 3. Low levels of basal $[Ca^{2+}]_i$ are visualized as blue and then green, whereas higher levels of $[Ca^{2+}]_i$ are seen as red and then white. C, ERα protein levels were measured by immunoblotting and GPR30 mRNA levels by qPCR in siRNA-transfected cells 48 h following transfection.

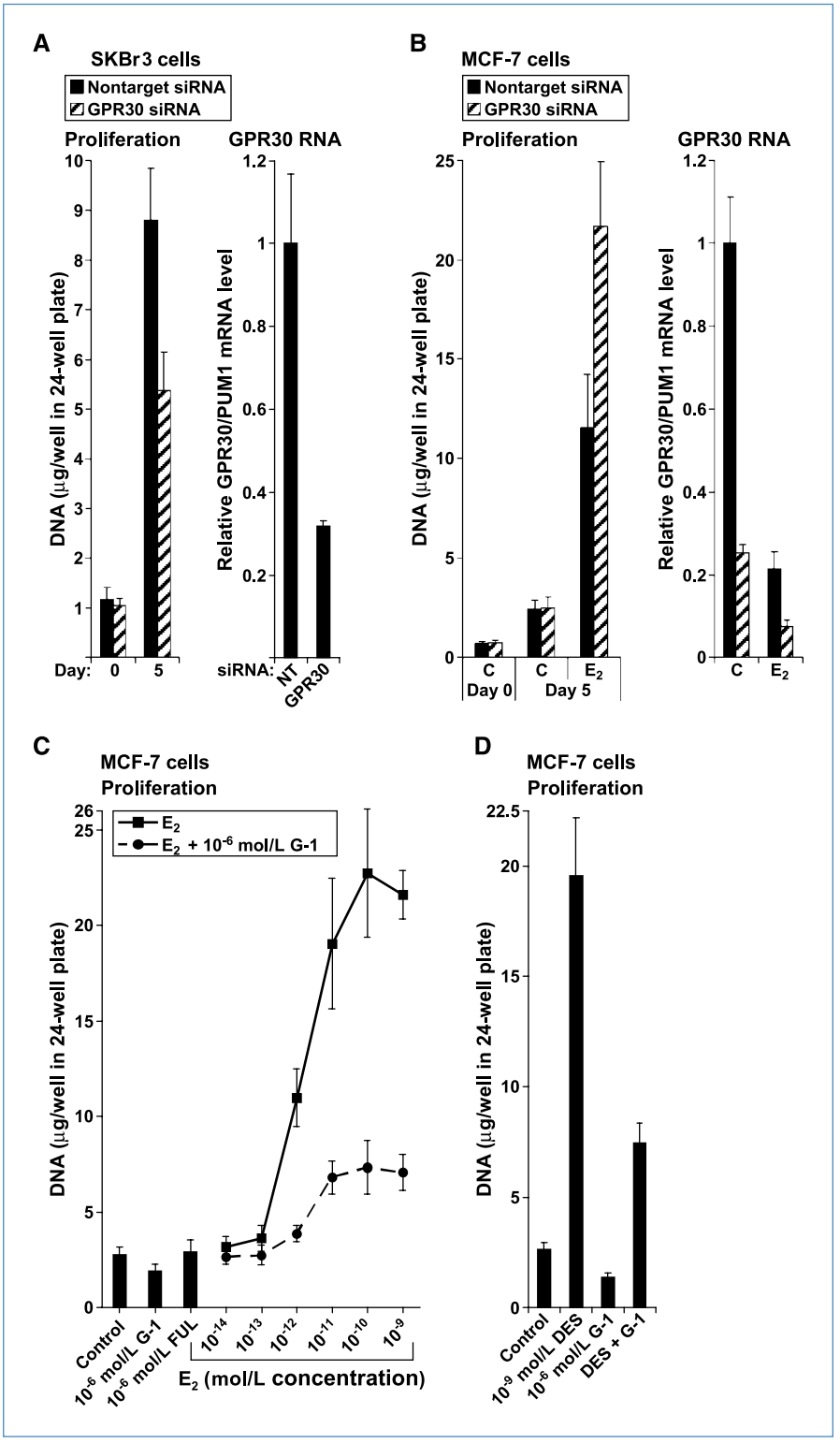


Figure 5. GPR30 promotes growth of ER-negative SKBr3 but inhibits growth of ER-positive MCF-7 cells. Proliferation of SKBr3 (A) and MCF-7 (B) cells transfected with the nontargeting pool and GPR30 siRNAs. Cells were transfected and then seeded at 15,000 per well in 24-well dishes. Medium was replenished the day after seeding on day 0 and every other day thereafter. Cells were collected on days 0 and 5. SKBr3 cells were cultivated in their passage medium, and MCF-7 cells in estrogen-free medium supplemented with 10^{-9} mol/L E_2 or without E_2 [control (*C*)]. Proliferation was assessed as cellular DNA mass (μg/well) using 24 replicate wells. GPR30 mRNA levels were determined by qPCR 48 h following the transfection in both cell lines, and in MCF-7 cells, after 24 h of 10^{-9} mol/L E_2 or control treatment. C and D, proliferation of MCF-7 cells over 6 d treated with a serial dilution series of E_2 (C) or with 10^{-9} mol/L DES (D) in the presence and absence of 10^{-6} mol/L G-1. Twelve replicate wells were used per group.

The interplay between GPR30 and ERα was further investigated using MCF-7 breast cancer cells. E_2 repressed GPR30 expression in a time- and concentration-dependent manner (Fig. 2B and C). In addition, DES but not G-1 downregulated GPR30; therefore, ER mediated this effect (Fig. 2D). The inverse functional relationship between ERα and GPR30 was also shown by depleting ERα, which led to derepression of GPR30 mRNA expression and consequently potentiated

E_2-induced Ca^{2+} mobilization responses (Fig. 4). E_2 is known to downregulate ERα expression in MCF-7 cells as a negative feedback regulatory loop to prevent overresponsiveness (26). Likewise, GPR30 may also be negatively regulated by E_2 via ER to prevent excessive GPR30-dependent activity, such as aberrantly high $[Ca^{2+}]_i$. Interestingly, the maximum increases in $[Ca^{2+}]_i$ were much larger in SKBr3 cells than in MCF-7 cells (Fig. 3B versus Fig. 3A). It is possible that this was due to the lack of ERs in SKBr3 cells, which translated into a lack of negative feedback regulation.

GPR30 depletion decreased growth of SKBr3 cells (Fig. 5A) but potentiated E_2-stimulated growth in MCF-7 cells (Fig. 5B), indicating that GPR30 functions to promote SKBr3 but to inhibit MCF-7 cellular proliferation. Also in MCF-7 cells, G-1 profoundly inhibited E_2-stimulated (Fig. 5C) and DES-stimulated growth (Fig. 5D) as well as decreased the percentage of cells entering S phase (Fig. 6A). However, these G-1 effects occurred in both the presence and the absence of E_2. These findings in MCF-7 cells complement those of Ahola and colleagues (11) who reported that transient

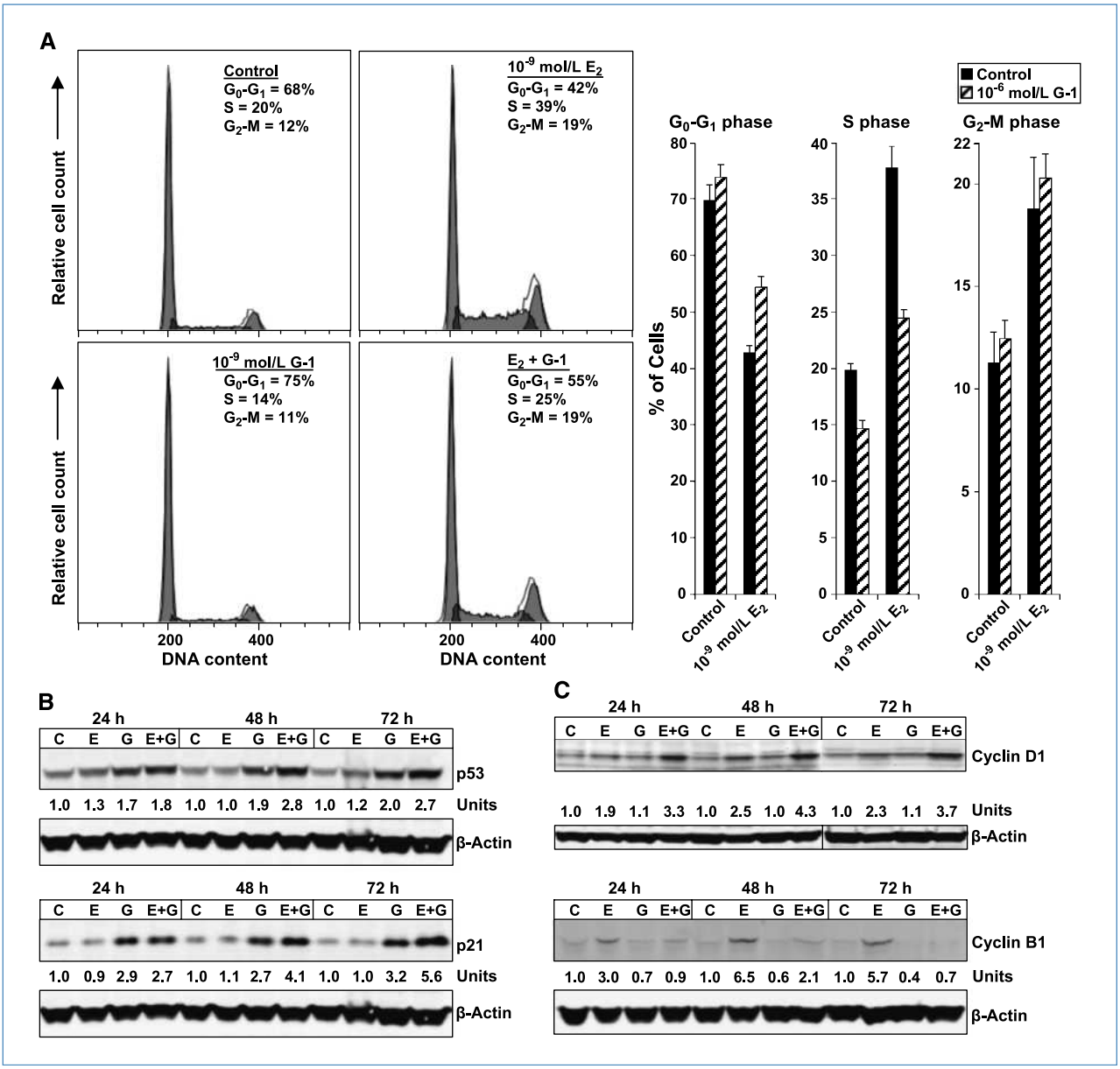


Figure 6. G-1 inhibits cell cycle progression in E_2-stimulated MCF-7 cells by producing a block at G_1 phase. A, cell cycle distribution as determined by propidium iodide staining of DNA content and flow cytometry. Cells were synchronized by 3-d cultivation in estrogen-free medium and then treated as indicated for 24 h. Thirty-thousand cells per sample and three replicates per group were collected. Representative histograms are shown. Immunoblot analyses of p53 and p21 (B) and of cyclin D1 and cyclin B1 (C) protein levels. MCF-7 cells were control (*C*)-, 10^{-9} mol/L E_2 (*E*)-, and 10^{-6} mol/L G-1 (*G*)–treated as indicated. Quantitated protein levels normalized to β-actin are indicated.

GPR30 overexpression decreased the percentage of proliferating MCF-7 cells independent of E_2. Indeed, GPR30 likely does not directly regulate ER transcriptional activity because there were no significant differences in E_2-induced mRNA expression of well-established ER target genes *PgR* and *TFF1* between GPR30 siRNA–transfected and nontargeting siRNA–transfected cells (data not shown).

Rather, we propose that GPR30 antagonizes growth of MCF-7 cells by inducing sustained increases in cytosolic Ca^{2+} concentrations (Figs. 3A and 4), in contrast to transitory increases in SKBr3 cells where GPR30 promotes growth. Aberrant sustained increases in intracellular Ca^{2+} levels can lead to inhibition of proliferation and induce apoptosis (33). For example, the plasma membrane Ca^{2+}-ATPase (PMCA) pumps Ca^{2+} across the plasma membrane out of the cell to lower cytosolic Ca^{2+} levels after Ca^{2+} increases. Partial inhibition of PMCA in MCF-7 cells causes a moderate increase in intracellular Ca^{2+} levels, which leads to inhibition of proliferation by altering cell cycle kinetics (34). Additionally, the mechanism of action of numerous antitumor agents involves increases in $[Ca^{2+}]_i$ (35).

It is possible that differences in GPR30-coupled Ca^{2+} signaling, which mediate sustained versus transitory responses, associate with ER status. In support of this hypothesis, GPR30 was coupled to differing Ca^{2+} channels: to IP_3Rs in ER-positive MCF-7 cells but to RyRs in ER-negative SKBr3 cells. Alternatively, sustained versus transitory Ca^{2+} responses could have been due to potential alterations in factors that participate in lowering cytosolic Ca^{2+}, such as plasma membrane or sarcoplasmic/endoplasmic reticulum Ca^{2+}-ATPase pumps. We intend to explore these possibilities involving differing Ca^{2+} responses in future studies.

As shown by propidium iodide staining and flow cytometry, G-1 induced a cell cycle block at the G_1 phase (Fig. 6A). Consistent with a G_1-phase arrest, G-1 increased accumulation of the tumor suppressor p53, the CDK-I p21, and the G_1-phase–specific cyclin D1 but prevented E_2-induced accumulation of the G_2/M-phase–specific cyclin B1 (Fig. 6B and C). Ca^{2+} signaling has been shown to induce p53 via activation of cyclic AMP–responsive element binding protein (28). In MCF-7 cells, p53 induction by E_2 is Ca^{2+} and calmodulin kinase IV dependent (36). In addition, aberrant Ca^{2+} mobilization in response to anticancer/cytotoxic agents correlates with p53 induction (35). Thus, G-1 could lead to p53 induction via Ca^{2+} mobilization in MCF-7 cells. Then, p53 could induce p21 via a p53 response element to mediate arrest in G_1 phase of the cell cycle (28).

As a SERM, tamoxifen acts as an antiestrogen in ER-positive breast cancer but as an estrogen in the endometrium and bone (37). Similarly, G-1 inhibits growth of ER-positive MCF-7 breast cancer cells but promotes growth of the endometrium (16) and plays an important role in promoting bone growth *in vivo* (38, 39). Thus, the tissue-specific proliferative effects of G-1 may parallel those of tamoxifen. It is interesting to speculate that 4OHT-induced Ca^{2+} mobilization (Fig. 3A and B) may be involved in some of the tissue-specific effects of tamoxifen.

Taken together, GPR30 inhibits growth of ERα-positive breast cancer. Our studies also indicate that pharmacologic activation of GPR30 shows promise in combating ER-positive breast cancer. G-1 would also probably be well tolerated because it, like E_2, exerts beneficial effects against an animal model of multiple sclerosis but without E_2-associated side effects (17, 40). Thus, G-1 may represent the first in a new class of therapeutically relevant agents for use alone or in conjunction with conventional antihormonal therapeutics in breast cancer.

Disclosure of Potential Conflicts of Interest

No potential conflicts of interest were disclosed.

Grant Support

Department of Defense grant BC050277 Center of Excellence (V.C. Jordan; views and opinions of, and endorsements by the author(s) do not reflect those of the US Army or the Department of Defense), and Weg and Genuardis funds (V.C. Jordan) and NIH grants P30CA006927 (Fox Chase Cancer Center), HL090804 and HL090804-01A2S109 (E. Brailoiu), CA127731 (E.R. Prossnitz, T.I. Oprea, and J.B. Arterburn), CA116662 (E.R. Prossnitz), U54MH084690 and CA118100 (University of New Mexico Cancer Center), and NS18710 and HL51314 (N.J. Dun).

The costs of publication of this article were defrayed in part by the payment of page charges. This article must therefore be hereby marked *advertisement* in accordance with 18 U.S.C. Section 1734 solely to indicate this fact.

Received 8/19/09; revised 10/28/09; accepted 11/24/09; published OnlineFirst 1/19/10.

References

1. Prossnitz ER, Arterburn JB, Smith HO, Oprea TI, Sklar LA, Hathaway HJ. Estrogen signaling through the transmembrane G protein–coupled receptor GPR30. Annu Rev Physiol 2008;70:165–90.
2. Prossnitz ER, Barton M. Signaling, physiological functions and clinical relevance of the G protein–coupled estrogen receptor GPER. Prostaglandins Other Lipid Mediat 2009;89:89–97.
3. Smith HO, Leslie KK, Singh M, et al. GPR30: a novel indicator of poor survival for endometrial carcinoma. Am J Obstet Gynecol 2007;196:386.e1–9; discussion 386.e9–11.
4. Smith HO, Arias-Pulido H, Kuo DY, et al. GPR30 predicts poor survival for ovarian cancer. Gynecol Oncol 2009;114:465–71.
5. Filardo EJ, Graeber CT, Quinn JA, et al. Distribution of GPR30, a seven membrane-spanning estrogen receptor, in primary breast cancer and its association with clinicopathologic determinants of tumor progression. Clin Cancer Res 2006;12:6359–66.
6. Kuo WH, Chang LY, Liu DL, et al. The interactions between GPR30 and the major biomarkers in infiltrating ductal carcinoma of the breast in an Asian population. Taiwan J Obstet Gynecol 2007;46:135–45.
7. Vivacqua A, Bonofiglio D, Albanito L, et al. 17β-Estradiol, genistein, and 4-hydroxytamoxifen induce the proliferation of thyroid cancer cells through the G protein–coupled receptor GPR30. Mol Pharmacol 2006;70:1414–23.
8. Vivacqua A, Bonofiglio D, Recchia AG, et al. The G protein–coupled

receptor GPR30 mediates the proliferative effects induced by 17β-estradiol and hydroxytamoxifen in endometrial cancer cells. Mol Endocrinol 2006;20:631–46.
9. Albanito L, Madeo A, Lappano R, et al. G protein–coupled receptor 30 (GPR30) mediates gene expression changes and growth response to 17β-estradiol and selective GPR30 ligand G-1 in ovarian cancer cells. Cancer Res 2007;67:1859–66.
10. Albanito L, Sisci D, Aquila S, et al. Epidermal growth factor induces G protein–coupled receptor 30 expression in estrogen receptor-negative breast cancer cells. Endocrinology 2008;149:3799–808.
11. Ahola TM, Manninen T, Alkio N, Ylikomi T. G protein–coupled receptor 30 is critical for a progestin-induced growth inhibition in MCF-7 breast cancer cells. Endocrinology 2002;143:3376–84.
12. Thomas P, Pang Y, Filardo EJ, Dong J. Identity of an estrogen membrane receptor coupled to a G protein in human breast cancer cells. Endocrinology 2005;146:624–32.
13. Filardo EJ, Quinn JA, Bland KI, Frackelton AR, Jr. Estrogen-induced activation of Erk-1 and Erk-2 requires the G protein–coupled receptor homolog, GPR30, and occurs via trans-activation of the epidermal growth factor receptor through release of HB-EGF. Mol Endocrinol 2000;14:1649–60.
14. Filardo EJ, Quinn JA, Frackelton AR, Jr., Bland KI. Estrogen action via the G protein–coupled receptor, GPR30: stimulation of adenylyl cyclase and cAMP-mediated attenuation of the epidermal growth factor receptor-to-MAPK signaling axis. Mol Endocrinol 2002;16:70–84.
15. Bologa CG, Revankar CM, Young SM, et al. Virtual and biomolecular screening converge on a selective agonist for GPR30. Nat Chem Biol 2006;2:207–12.
16. Dennis MK, Burai R, Ramesh C, et al. *In vivo* effects of a GPR30 antagonist. Nat Chem Biol 2009;5:421–7.
17. Blasko E, Haskell CA, Leung S, et al. Beneficial role of the GPR30 agonist G-1 in an animal model of multiple sclerosis. J Neuroimmunol 2009;214:67–77.
18. Lin BC, Suzawa M, Blind RD, et al. Stimulating the GPR30 estrogen receptor with a novel tamoxifen analogue activates SF-1 and promotes endometrial cell proliferation. Cancer Res 2009;69:5415–23.
19. van de Vijver MJ, He YD, van't Veer LJ, et al. A gene-expression signature as a predictor of survival in breast cancer. N Engl J Med 2002; 347:1999–2009.
20. Barrett T, Suzek TO, Troup DB, et al. NCBI GEO: mining millions of expression profiles-database and tools. Nucleic Acids Res 2005;33: D562–6.
21. Gentleman RC, Carey VJ, Bates DM, et al. Bioconductor: open software development for computational biology and bioinformatics. Genome Biol 2004;5:R80.
22. Jiang SY, Wolf DM, Yingling JM, Chang C, Jordan VC. An estrogen receptor positive MCF-7 clone that is resistant to antiestrogens and estradiol. Mol Cell Endocrinol 1992;90:77–86.
23. Ariazi EA, Kraus RJ, Farrell ML, Jordan VC, Mertz JE. Estrogen-related receptor α1 transcriptional activities are regulated in part via the ErbB2/HER2 signaling pathway. Mol Cancer Res 2007;5:71–85.
24. Lyng MB, Laenkholm AV, Pallisgaard N, Ditzel HJ. Identification of genes for normalization of real-time RT-PCR data in breast carcinomas. BMC Cancer 2008;8:20.
25. Brailoiu E, Churamani D, Cai X, et al. Essential requirement for two-pore channel 1 in NAADP-mediated calcium signaling. J Cell Biol 2009;186:201–9.
26. Pink JJ, Jordan VC. Models of estrogen receptor regulation by estrogens and antiestrogens in breast cancer cell lines. Cancer Res 1996; 56:2321–30.
27. Liu H, Lee E-S, Gajdos C, et al. Apoptotic action of 17β-estradiol in raloxifene-resistant MCF-7 cells *in vitro* and *in vivo*. J Natl Cancer Inst 2003;95:1586–97.
28. Lipskaia L, Lompre AM. Alteration in temporal kinetics of Ca^{2+} signaling and control of growth and proliferation. Biol Cell 2004;96: 55–68.
29. Doisneau-Sixou SF, Sergio CM, Carroll JS, Hui R, Musgrove EA, Sutherland RL. Estrogen and antiestrogen regulation of cell cycle progression in breast cancer cells. Endocr Relat Cancer 2003;10: 179–86.
30. Guo Y, Yang K, Harwalkar J, et al. Phosphorylation of cyclin D1 at Thr 286 during S phase leads to its proteasomal degradation and allows efficient DNA synthesis. Oncogene 2005;24:2599–612.
31. Pines J, Hunter T. Isolation of a human cyclin cDNA: evidence for cyclin mRNA and protein regulation in the cell cycle and for interaction with p34cdc2. Cell 1989;58:833–46.
32. Pandey DP, Lappano R, Albanito L, Madeo A, Maggiolini M, Picard D. Estrogenic GPR30 signaling induces proliferation and migration of breast cancer cells through CTGF. EMBO J 2009;28:523–32.
33. Pinton P, Giorgi C, Siviero R, Zecchini E, Rizzuto R. Calcium and apoptosis: ER-mitochondria Ca^{2+} transfer in the control of apoptosis. Oncogene 2008;27:6407–18.
34. Lee WJ, Robinson JA, Holman NA, McCall MN, Roberts-Thomson SJ, Monteith GR. Antisense-mediated inhibition of the plasma membrane calcium-ATPase suppresses proliferation of MCF-7 cells. J Biol Chem 2005;280:27076–84.
35. Olofsson MH, Havelka AM, Brnjic S, Shoshan MC, Linder S. Charting calcium-regulated apoptosis pathways using chemical biology: role of calmodulin kinase II. BMC Chem Biol 2008;8:2.
36. Qin C, Nguyen T, Stewart J, Samudio I, Burghardt R, Safe S. Estrogen up-regulation of p53 gene expression in MCF-7 breast cancer cells is mediated by calmodulin kinase IV-dependent activation of a nuclear factor κB/CCAAT-binding transcription factor-1 complex. Mol Endocrinol 2002;16:1793–809.
37. Ariazi EA, Jordan VC. Estrogen receptors as therapeutic targets in breast cancer. In: Ottow E, Weinmann H, editors. Nuclear receptors as drug targets. Mörlenbach: Wiley-VCH; 2008, p. 127–99.
38. Martensson UE, Salehi SA, Windahl S, et al. Deletion of the G protein–coupled receptor 30 impairs glucose tolerance, reduces bone growth, increases blood pressure, and eliminates estradiol-stimulated insulin release in female mice. Endocrinology 2009; 150:687–98.
39. Chagin AS, Savendahl L. GPR30 estrogen receptor expression in the growth plate declines as puberty progresses. J Clin Endocrinol Metab 2007;92:4873–7.
40. Wang C, Dehghani B, Li Y, et al. Membrane estrogen receptor regulates experimental autoimmune encephalomyelitis through up-regulation of programmed death 1. J Immunol 2009;182:3294–303.

Supplementary Materials

Characterization of ERα and GPR30 siRNAs

Before examining effects of RNAi-mediated depletion of ERα and GPR30, an ERα siRNA pool, a GPR30 siRNA pool, and the four individual siRNAs in each pool were evaluated (Supplemental Fig. 1). Since ERα regulated expression of GPR30 in MCF-7 cells (Fig. 2B-C), siRNA–mediated depletion of ERα could potentially alter expression of GPR30. Therefore, evaluation of the ERα and GPR30 siRNAs was carried out in a non–breast cancer cell type. ERα–positive ECC-1 endometrial cancer cells were chosen since we had observed that E_2 does not significantly regulate GPR30 mRNA expression in this cell line (data not shown). ECC-1 cells were transfected with the siRNAs as described in the Methods, and 48 h later, ERα protein (Supplemental Fig. 1A) and GPR30 mRNA expression (Supplemental Fig. 1B) were determined by semi-quantitative immunoblot analysis and real-time qPCR, respectively. The ERα pool and individual siRNAs (#11 to #14) all effectively depleted ERα by greater than 90 %. Similarly, the GPR30 pool and individual siRNAs (#6 to #9) depleted GPR30 mRNA expression from 86 % to 71 %. However, the ERα pool siRNA, and ERα siRNAs #11 and #14 decreased GPR30 mRNA expression by 70 %, 44 %, and 62 % respectively, while ERα siRNA #13 did not. Likewise, the GPR30 siRNA pool and siRNAs #6 and #7 significantly decreased ERα protein expression by 92 %, 79 %, and 62 %, respectively, while GPR30 siRNA #8 did not. Since the ERα siRNAs led to varying decreases in GPR30 expression, and similarly since the GPR30 siRNAs led to varying decreases in ERα expression, it was concluded that these effects were off–target. Additionally, while the fourth GPR30 siRNA evaluated, #9, only showed a modest off-target effect of decreasing ERα protein levels by 22 %, it appeared to be toxic (data not shown). Therefore, for

all further siRNA–based experiments presented, the ERα siRNA #13 and GPR30 siRNA #8 were employed as these siRNAs exhibited the least off–target effects.

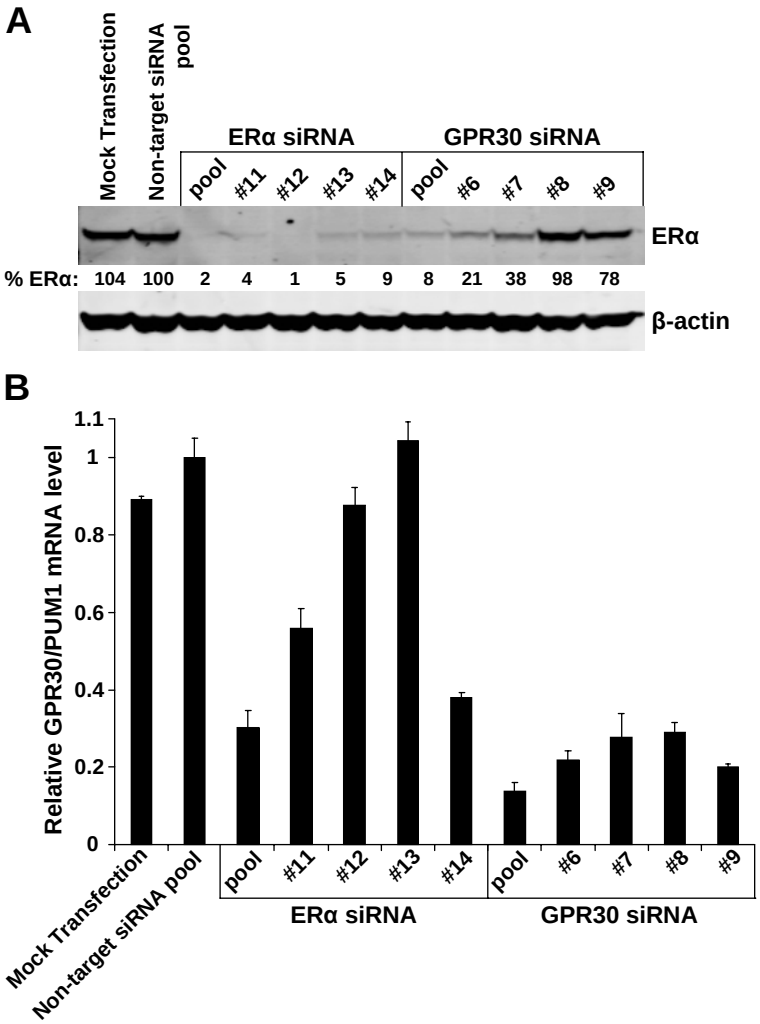
PCR primer sequences

PCR primer sequences used were as follows : ERα forward 5'–GGA GGG CAG GGG TGA A–3', ERα reverse 5'-GGC CAG GCT GTT CTT CTT AGA-3'; GPR30 forward 5'-TGG GGA AGA GGC CAC CA-3', GPR30 reverse 5'-CGT GGA GCT GCT CAC TCT CTG-3'; PUM1 forward 5'-AAT GCA GGC GCG AGA AAT-3', PUM1 reverse 5'-TTG TGC AGC TGA GGA ACT AAT GA-3'.

siRNA sense oligonucleotide sequences

The siRNA sense oligonucleotide sequences were as follows : GPR30 #6 GGG UGA AGC GCC UCA GUU Auu; GPR30 #7 GAC GAG GCC UGC UUC UGU Uuu, GPR30 #8 UAG GAA ACC UCA CGA CUG Guu; GPR30 #9 GGA UGA GCU UCG ACC GCU Auu; ESR1 #11 GAU CAA ACG CUC UAA GAA Guu; ESR1 #12 GAA UGU GCC UGG CUA GAG Auu; ESR1 #13 GAU GAA AGG UGG GAU ACG Auu; ESR1 #14 GCC AGC AGG UGC CCU ACU Auu.

Supplemental Figure 1. Characterization of ERα and GPR30 siRNA pools in ECC-1 endometrial cancer cells. (A) ERα protein levels by immnoblot analysis and **(B)** GPR30 mRNA levels by qPCR in ERα siRNA and GPR30 siRNA-transfected ECC-1 endometrial cancer cells. ECC-1 cells were transfected and assayed under estrogen-free conditions at 48 h following the transfection. The immunoblot was visualized using a Li-Cor Odyssey infrared scanner. Quantitation of ERα protein levels normalized to β-actin is indicated. GPR30 mRNA levels represent the average of 4 biological replicates and error bars their associated SDs. Testing of individual siRNAs indicated that only ERα siRNA #13 and GPR30 siRNA #8 exhibit on-target knockdown without off-target effects.


A
Mock Transfection
Non-target siRNA pool
ERα siRNA
GPR30 siRNA
pool
#11
#12
#13
#14
pool
#6
#7
#8
#9
ERα
% ERα:
104
100
2
4
1
5
9
8
21
38
98
78
β-actin
B
Relative GPR30/PUM1 mRNA level
1.1
1
0.8
0.6
0.4
0.2
0
Mock Transfection
Non-target siRNA pool
pool
#11
#12
#13
#14
pool
#6
#7
#8
#9
ERα siRNA
GPR30 siRNA



available at www.sciencedirect.com

ScienceDirect

journal homepage: www.ejconline.com



Experimental treatment of oestrogen receptor (ER) positive breast cancer with tamoxifen and brivanib alaninate, a VEGFR-2/FGFR-1 kinase inhibitor: A potential clinical application of angiogenesis inhibitors

Roshani R. Patel [a,b], *Surojeet Sengupta* [b,c], *Helen R. Kim* [b,c], *Andres J. Klein-Szanto* [d], *Jennifer R. Pyle* [b], *Fang Zhu* [e], *Tianyu Li* [e], *Eric A. Ross* [e], *Salewa Oseni* [b], *Joseph Fargnoli* [f], *V. Craig Jordan* [b,c,*]

[a] *Dartmouth Hitchcock Medical Center, Dept. of Surgery, Manchester, NH 03104, United States*
[b] *Fox Chase Cancer Center, Philadelphia, PA 19111, United States*
[c] *Lombardi Comprehensive Cancer Center, Washington, DC 20057, United States*
[d] *Fox Chase Cancer Center, Dept. of Pathology, Philadelphia, PA 19111, United States*
[e] *Fox Chase Cancer Center, Dept. of Biostatistics, Philadelphia, PA 19111, United States*
[f] *Bristol Myers Squibb, Princeton, NJ 08543, United States*

ARTICLE INFO

Article history:
Received 12 August 2009
Received in revised form 1 February 2010
Accepted 16 February 2010
Available online 18 March 2010

Keywords:
Breast cancer
Tamoxifen
VEGFR-2
Angiogenesis
Brivanib alaninate
Hormone resistance

ABSTRACT

Purpose: Tamoxifen, a selective oestrogen receptor modulator (SERM), and brivanib alaninate, a vascular endothelial growth factor receptor 2 (VEGFR-2) inhibitor, are two target specific agents that result in a substantial decrease in tumour growth when given alone. Tamoxifen activates SERM stimulated breast and endometrial tumour growth. Tamoxifen and brivanib alaninate have side-effects that can affect therapeutic outcomes. The primary goal of the current study was to evaluate the therapeutic effects of lower doses of both agents when given in combination to mice with SERM sensitive, oestrogen stimulated tumour xenografts (MCF-7 E2 tumours). Experiments were conducted to evaluate the response of SERM stimulated breast (MCF-7 Tam, MCF-7 Ral) and endometrial tumours (EnCa 101) to demonstrate the activity of brivanib alaninate in SERM resistant models.

Experimental design: In the current study, tumour xenografts were minced and bi-transplanted into the mammary fat pads of athymic, ovariectomised mice. Preliminary experiments were conducted to determine an effective oral dose of tamoxifen and brivanib alaninate that had minimal effect on tumour growth. Doses of 125 μg of tamoxifen and 0.05 mg/g of brivanib alaninate were evaluated. An experiment was designed to evaluate the effect of the two agents together when started at the time of tumour implantation. An additional experiment was done in which tumours were already established and then treated, to obtain enough tumour tissue for molecular analysis.

Results: Brivanib alaninate was effective at inhibiting tumour growth in SERM sensitive (MCF-7 E2) and SERM stimulated (EnCa 101, MCF-7 Ral, MCF-7 Tam) models. The effect

* *Corresponding author:* Address: Lombardi Comprehensive Cancer Center, Georgetown University Medical Center, Research Building, Room E501, 3970 Reservoir Road, NW, Washington, DC 20057-1468, United States.
E-mail address: vcj2@georgetown.edu (V.C. Jordan).
0959-8049/$ - see front matter © 2010 Elsevier Ltd. All rights reserved.
doi:10.1016/j.ejca.2010.02.018

of the low dose drug combination as an anti-tumour strategy for SERM sensitive (MCF-7 E2) in early treatment was as effective as higher doses of either drug used alone. In established tumours, the combination is successful at decreasing tumour growth, while neither agent alone is effective. Molecular analysis revealed a decreased phosphorylation of VEGFR-2 in tumours that were treated with brivanib alaninate and an increase in VEGFA transcription to compensate for the blockade of VEGFR-2 by increasing the transcription of VEGFA. Tamoxifen increases the phosphorylation of VEGFR-2 and this effect is abrogated by brivanib alaninate. There was also increased necrosis in tumours treated with brivanib alaninate.

Conclusion: Historically, tamoxifen has a role in blocking angiogenesis as well as the blockade of the ER. Tamoxifen and a low dose of an angiogenesis inhibitor, brivanib alaninate, can potentially be combined not only to maximise therapeutic efficacy but also to retard SERM resistant tumour growth.

© 2010 Elsevier Ltd. All rights reserved.

1. Introduction

Angiogenesis is a major requirement for tumours to grow successfully and spread. Early work[1–3] characterised many of the factors involved in the regulation of angiogenesis and how these factors can become disregulated in tumour pathogenesis.[4–6] One of the most important factors in the positive modulation of angiogenesis is the vascular endothelial growth factor (VEGF) family of growth factors and their corresponding receptors. Angiogenesis in tumours is different from physiological angiogenesis seen with normal development and wound healing. In wound healing, angiogenesis is a carefully orchestrated process and occurs in a short time. By contrast, the blood vessels that form in the tumour bed are thin, disorganised and leaky. The growth of such vessels persists over years as long as viable tumour tissue is present.[3]

In oestrogen receptor (ER) positive breast cancer, it is clear that adjuvant anti-oestrogenical therapy must be extended to 5 years and beyond to prevent recurrence and improve survival.[7–9] However, toxicities, the development of resistance to anti-hormonal therapy, and side-effects from therapy such as clots and endometrial cancer with tamoxifen[10,11] and fractures and joint pain with aromatase inhibitors[11,12] often limit long-term treatment. Clearly new treatment strategies need to be developed to enhance the activity of anti-hormonal therapy by improving efficacy. Oestrogen enhances the angiogenic cascade critical for tumour growth, primarily through the release of VEGF.[13–16] Tamoxifen has a historical role in the prevention of tumour angiogenesis as it was one of the three drugs in the 'Navy Regimen' developed by Folkman.[17] Tamoxifen is also reported[18] to reduce angiogenesis for ER negative tumours. An anti-oestrogen for the treatment of ER positive breast cancer can potentially regulate VEGF production. However, with the development of acquired resistance[10] in breast and endometrial tumours it is axiomatic that selective oestrogen receptor modulator (SERM) (tamoxifen and raloxifene) stimulated tumours must induce angiogenesis to grow. We hypothesise that limiting angiogenesis with angiogenic drugs during anti-hormonal therapy could potentially improve adjuvant therapeutic regimens. However, there are significant toxicities with current antiangiogenic drugs that limit their usefulness for long-term therapy.

Several antiangiogenic agents are either used in clinical practice or are in clinical trials. Most notably, bevacizumab, a monoclonal antibody that binds to VEGFA and as a result, prevents phosphorylation and activation of its target receptors, vascular endothelial growth factor receptors 1 and 2 (VEGFR-1 and VEGFR-2), has shown promise in combination with chemotherapy for breast cancer.[19–21] In a phase 3 trial of 722 patients, the disease-free survival time in patients with metastatic breast cancer has been shown to double (5.9 versus 11.8 months) when treated with paclitaxel in conjunction with bevacizumab.[21] Unfortunately, the overall survival does not change when bevacizumab is included as a part of therapy. Toxicities such as infection (9.3% versus 2.9%), proteinuria (3.6% versus 0.0%), hypertension (14.8% versus 0.0%) and cerebrovascular ischaemia (1.9% versus 0.0%) also limit long-term therapy.[21] Part of the problem with the therapeutic use of monoclonal antibodies is that VEGFA is not the only ligand that can bind to these receptors. Other members of the VEGF family such as VEGFC and VEGFD can bind to VEGFR-2, while VEGFB has been shown to bind and activate VEGFR-1.[19,22] With this in mind, other agents, which target the tyrosine kinase domain of the receptor, have been developed and several pre-clinical and clinical trials are investigating the use of such agents.[2,23] Many of the newer agents that are being developed also target other growth factor receptor tyrosine kinases such as PDGF, FGFR, and c-Kit with the idea that blocking several receptors will prevent resistance to therapy that results from the activation of alternate pathways by co-regulatory proteins.[2]

One dual-targeting drug is brivanib alaninate (BMS 582664, Bristol Myers Squibb, Princeton, NJ), a VEGFR-2/FGFR-1 inhibitor. Pre-clinical studies *in vivo* have shown that brivanib alaninate is effective in reducing the growth of a lung tumour xenograft, L2987, a panel of human derived hepatocellular carcinomas,[24] and an ER negative breast tumour H3396.[25] Pharmacological studies in a phase I clinical trials have shown that doses of brivanib alaninate below 800 mg/d are tolerable, but have associated toxicities such as hypertension (>150/100), elevated transaminases, fatigue and dizziness as the dosage increases from a baseline of 180 mg/d. Several phase 1 clinical trials are underway in patients with a variety of solid tumours.[26,27]

We have addressed the hypothesis that combining tamoxifen, a SERM with a sub-therapeutic dose of brivanib alaninate would be a beneficial strategy for long-term therapy in the treatment of breast cancer. We report the first studies testing the efficacy of brivanib alaninate to control tumour growth of ER regulated SERM sensitive (MCF-7 E2) and SERM stimulated (MCF-7 Ral, MCF-7 Tam), and endometrial (EnCa 101) tumours. We find that the combination of tamoxifen and brivanib alaninate in a laboratory model provided a therapeutic advantage for the control of breast tumour growth over tamoxifen or brivanib alaninate alone.

2. Materials and methods

2.1. Tumour xenografts

SERM sensitive tumours were previously developed by injecting the mammary fat pads of ovariectomised, BALB/c athymic mice (Harlan Sprague Dawley, Madison, WI) with 1×10^7 WS8 human breast cancer cells.[28] Tumour growth was sustained with 0.3 cm silastic capsules containing estradiol (Sigma, St. Louis, MO) delivering 83.8 ± 34.6 pg/mL oestrogen over an eight-week period.[29] Over time, the tumours were serially passaged by bi-transplanting the established tumours into the mammary fat pads of estradiol treated mice. The development and characterisation of the SERM stimulated EnCa 101 endometrial cancer model,[30] MCF-7 Ral model,[31] and MCF-7 Tam model[32] have been reported previously.

For the experiments in the current study, athymic ovariectomised CrTac: NCr-Foxn1nu mice were obtained from Taconic (Hudson, NY). Mice were placed under anaesthesia, using a mixture of isoflurane and 100% oxygen delivered via inhalation. Healthy tumour tissue was sectioned into 1 mm^3 pieces and implanted bilaterally into the mammary fat pads. Estradiol capsules (0.3 cm silastic capsule) were placed subcutaneously on the dorsal surface of the mice to maintain tumour growth.

Tumours were measured with calipers once a week. Cross-sectional areas (CSAs) were calculated by measuring the length and width of the tumours and then using an Excel (Microsoft) spreadsheet to calculate the CSA (length (cm) × width (cm) × $\pi/4$). Growth curves were derived from the determining the average CSA per treatment group per week. In the case of EnCa 101 endometrial tumours, growth characteristics were atypical with a prolonged latent period of tumour spreading subcutaneously with an eventual rapid haemorrhagical growth phase reminiscent of the 'angiogenic trigger'. Tumour volumes were measured for EnCa 101 using the formula $4/3\pi r^3$.

Six sets of experiments were completed. The first experiment was specifically conducted to evaluate where VEGFR-2 and VEGFA are expressed and how expression changes in response to hormonal and anti-hormonal manipulation. Experiments 2–5 were conducted to determine dosing of brivanib alaninate to prevent the growth in MCF-7 E2, a SERM sensitive tumour, and MCF-7 Ral, MCF-7 Tam, and EnCa 101 SERM stimulated tumours. The fourth experiment determined the dosing of tamoxifen to block estradiol stimulated tumour growth in MCF-7 E2 tumours. The fifth and sixth experiments determined the effects of combined therapy when started 24 h after initial tumour implantation versus giving the drug to animals with the established tumours for a two-week time period.

2.2. Drug preparation

Bristol Myers Squibb (Princeton, NJ) provided brivanib alaninate in powder form. The drug was suspended in a citric acid buffer solution and the pH was gradually titrated to a pH of 3.5 after the drug dissolved. The final concentration was 10 mg/mL.

Tamoxifen (Sigma Chemical Co., St. Louis, MO) was weighed and suspended in 10% Tween 80/polyethylene glycol (PEG) 400 (99.5% PEG 400/0.5% Tween 80) and 90% carboxymethylcellulose (CMC, 1% CMC dissolved in double distilled water). The final concentration of the tamoxifen solution was 2.5 mg/mL and administered by gavage at the doses indicated. Administration of tamoxifen to animals bearing EnCa 101 tumours was at a dose of 500 μg/mouse by gavage.

Raloxifene (Evista, Eli Lilly, IN) was prepared by placing five raloxifene tablets in a conical tube and dissolving them via centrifugation in 27 mL double distilled water. Once the tablets were dissolved, 3 mL of 90% CMC and 10% PEG 400/Tween 80 was added to the raloxifene solution. The final concentration was 10 mg/mL. Raloxifene was administered at a daily dose of 1.5 mg/mouse by gavage.

Estradiol capsules were prepared by plugging one end 0.3 cm length of medical grade silastic tubing and filling it with 17β-estradiol (Sigma Chemical Company, St. Louis, MO) mixed 1:3 with elastomer. Capsules sealed by placing elastomer at the open ends and then sterilised with radiation (20,000 rad).[33]

Fulvestrant (Faslodex, AstraZeneca, Wilmington, DE) was purchased from the pharmacy at Fox Chase Cancer Center as a solution of fulvestrant suspended in EtOH and castor oil (50 mg/ml).

2.3. Drug administration

Brivanib alaninate was dosed orally 7 d a week, according to the weight of each mouse. Mice were weighed once weekly. For the high dose, a 20 g mouse was given 200 μL (2 mg) and for the low dose a 20 g mouse was given 100 μL (1 mg). Tamoxifen was also administered 7 d a week. Dosing of tamoxifen was as follows: 125 μg (50 μL), for 250 μg (100 μL), or 500 μg (200 μL). Fulvestrant was administered as 2 mg (40 μL) injections 5 d per week.

2.4. Experiment 1: the effect of hormonal manipulation on VEGFA and VEGFR-2 expression

Tumours were grown in the presence of estradiol (0.3 cm silastic capsule) until the tumours reached 0.4 cm^2. The mice were then treated with different drug regimens for 2 weeks. The treatments after tumours reached 0.4 cm^2 were as follows:

(1) continue estradiol (0.3 cm silastic capsule),
(2) withdraw estradiol,

(3) estradiol + 125 μg tamoxifen daily,
(4) withdraw estradiol (0.3 cm silastic capsule) and 2 mg/40 μL fulvestrant injections given subcutaneously daily.

2.5. Experiment 2: effects of different doses of brivanib alaninate on SERM sensitive MCF-7 E2 tumours

We evaluated the effects of a high dose and low dose of brivanib alaninate. The brivanib alaninate treatment was started 24 h after tumour implantation. Treatment groups (five animals) were as follows:

(1) estradiol (0.3 cm silastic capsule) + placebo given orally (citric acid buffer: pH 3.5),
(2) estradiol (0.3 cm silastic capsule) + low dose brivanib alaninate given orally (.05 mg/g),
(3) estradiol (0.3 cm silastic capsule) + high dose brivanib alaninate given orally (0.1 mg/g).

2.6. Experiment 3: the effects of brivanib alaninate on SERM stimulated tumours

2.6.1. Experiment 3A: the effects of different doses of brivanib alaninate on SERM resistant MCF-7 Ral tumours

We evaluated the effects of a high dose and low dose of brivanib alaninate. The brivanib alaninate treatment was started 24 h after tumour implantation. Treatment groups (five animals) were as follows:

placebo (citric acid buffer),
1.5 mg raloxifene,
2 mg fulvestrant – pure anti-oestrogen (subcutaneous),
1.5 mg raloxifene + high dose VEGFR antagonist (0.1 mg/g).

2.6.2. Experiment 3B: the effect of brivanib alaninate on established SERM resistant MCF-7 Ral tumour models

Tumours were grown up to an average 0.5 cm^2 CSA. The mice were randomised to receive 2 weeks of therapy with the high dose brivanib alaninate.

Groups:
10 mice each after randomisation:

1.5 mg raloxifene,
1.5 mg raloxifene + high dose brivanib alaninate (0.1 mg/g).

2.6.3. Experiment 3C: the effect of brivanib alaninate on SERM resistant MCF-7 Tam tumours

We examined the effects of the high dose brivanib alaninate on another SERM resistant model. There were two components to this experiment. The first was to determine whether brivanib alaninate inhibited tumour growth and the second was to determine whether brivanib alaninate was effective in established tumours

(1) 1.5 mg tamoxifen first 48 d of the experiment (8 mice, 16 tumours),
  – this group was used for the second part of the experiment,
(2) placebo: citric acid buffer (0.15 mL) (5 mice, 10 tumours),
(3) 1.5 mg tamoxifen + 0.1 mg/g brivanib alaninate (4 mice, 6 tumours).

Once the tumours in group one reached a CSA of 0.5 cm^2, 48 d after tumour implantation, group 1 was subdivided:

(1) continue 1.5 mg tamoxifen for two more weeks (4 mice, 8 tumours),
(2) 1.5 mg tamoxifen + high dose brivanib alaninate (0.1 mg/g) for 2 weeks (4 mice, 8 tumours).

2.6.4. Experiment 3D: the effect of brivanib alaninate on EnCa Tam endometrial tumours

This experiment determined whether brivanib alaninate inhibited the growth of endometrial tumours that normally grow with 500 μg of tamoxifen daily. Tumours initially are not evident until after one month after which they grow rapidly. Twenty mice were treated with tamoxifen for 40 d and then randomised into two groups. After randomisation, treatments were given for 3 weeks.

Control group: 500 μg tamoxifen daily(10 mice).
Experimental group: 500 μg tamoxifen daily + 0.1 mg/g brivanib alaninate (started on day 40) (10 mice).

2.7. Experiment 4: determination of tamoxifen dosing in SERM sensitive MCF-7 E2 tumours

We determined a dose response curve of various oral doses of tamoxifen to determine the lowest dose that was effective in decreasing the rate of tumour growth

(1) no estradiol,
(2) estradiol (0.3 cm silastic capsule),
(3) estradiol (0.3 cm silastic capsule) + 500 μg tamoxifen given orally,
(4) estradiol (0.3 cm silastic capsule) + 250 μg tamoxifen given orally,
(5) estradiol (0.3 cm silastic capsule) + 125 μg tamoxifen given orally.

2.8. Experiment 5: the combined effect of a lower dose of tamoxifen and brivanib alaninate in SERM sensitive MCF-7 E2 tumours

This experiment determined the combined effects of a sub-maximal dose of tamoxifen and a sub-maximal dose of brivanib alaninate on oestrogen stimulated tumour growth. Drug dosing was commenced 24 h after tumour implantation

(1) control with estradiol (0.3 cm silastic capsule),
(2) experimental group with estradiol (0.3 cm silastic capsule) + 125 μg tamoxifen given orally,
(3) experimental group with estradiol (0.3 cm silastic capsule) + low dose brivanib alaninate (.05 mg/g dose) given orally,

(4) experimental group with estradiol (0.3 cm silastic capsule) + 125 μg tamoxifen given orally + low dose brivanib alaninate (0.05 mg/g dose) given orally.

2.9. *Experiment 6: the combined effect of a lower dose of tamoxifen and brivanib alaninate in established SERM sensitive MCF-7 E2 tumours*

Experiment 8 was similar to Experiment 7 with one exception. The tumours were grown to an average CSA of 0.43 mm^3 and drug therapy was given for 2 weeks.

2.10. *Western immunoblotting*

Tumours were harvested and placed in foils and frozen immediately in liquid nitrogen. Tumours were kept at –80 °C until they were processed. For processing, tumours were placed in liquid nitrogen and homogenised using a mortar and pestle. The extract was suspended in RIPA buffer (Sigma, St. Louis, MO) with protease (Roche, Nutley, NJ) and phosphatase (Calbiochem, San Diego, CA) inhibitors. The mixture was briefly sonicated and centrifuged for 10 min at 5000*g*. The supernatant was removed and protein concentration was determined using the Bradford assay (BCA assay, Pierce, Rockford, IL) with a Spectramax machine (Molecular Devices, Sunnyvale, CA). Equal amounts (25 μg) and concentrations of protein were loaded into 4–12% Nupage Bis-tris (Invitrogen, Carlsabad, CA) gels, and transferred to nitrocellulose membranes. Immunoblotting was carried out with the following antibodies: total VEGFR-2 (1:1000, rabbit polyclonal, Cell Signaling Technologies, Beverly, MA), phospho-VEGFR-2 Tyr ^{951}(1:200, rabbit polyclonal, Santa Cruz, Biotechnology, Santa Cruz, CA), total FGFR-1 and total VEGFR-3 (1:200, rabbit polyclonal, Santa Cruz Biotechnology, Santa Cruz, CA), total VEGFR-1 (rabbit polyclonal, 1:200, Labvision, Fremont, CA), total ER alpha (ERα) (rabbit polyclonal, 1:200, G20, Santa Cruz, Santa Cruz, CA), phospho-ERα (rabbit monoclonal, 1:2000, Ser 118, clone NL 44, Upstate, Billerica, MA), β-actin (mouse monoclonal, 1:30,000, Sigma–Aldrich, St. Louis, MO).

2.11. *Real time polymerase chain reaction (RT-PCR)*

Total RNA was extracted from frozen tumour tissues using RNA mini easy kit (Qiagen, Venlo, The Netherlands) as per the manufacturer's instructions. Two micrograms of total RNA were reverse transcribed using a cDNA high capacity reverse transcription kit (Applied Biosystem, Carlsbad, CA) in 20 μL of total volume, as per manufacturer's instruction. The resulting cDNA was diluted to a total volume of 200 μL using sterile water. The real time PCR was carried out on an ABI 7900 HT Fast Real Time PCR system using 1X SYBR green PCR master mix (Applied Biosystem, Carlsbad, CA) and 100 nM of forward and reverse primers. All the forward and reverse primers (Table 1) were designed using Primer Express 3 software (Applied Biosystem, Carlsbad, CA) except ERα[34] and mouse and human 36B4.[35,36] The fold change in the expression of each gene was calculated by the ΔΔCt[37] method using 36B4, a ribosomal phospho-protein as an internal control.

Table 1 – Primers used for RTPCR.

VEGFA	Fwd: 5′ GGGCAGAATCATCACGAAGTG 3′
	Rev: 5′ TCAGGGTACTCCTGGAAGATGTC 3′
VEGFB	Fwd: 5′ AGCCAGTGTGAATGCAGACCTA 3′
	Rev: 5′ AGTCCCAGCCCGGAACAG 3′
VEGFC	Fwd: 5′ CCTCAGCAAGACGTTATTTGAAATT 3′
	Rev: 5′ TGGCAAAACTGATTGTTACTGGTT 3′
VEGFD	Fwd: 5′ CGTACATTTCCAAACAGCTCTTTG 3′
	Rev: 5′ GGCAAGCACTTACAACCTGTATGA 3′
VEGFR-1	Fwd: 5′ TTCTCACAGGATCTAGTTCAGGTTCA 3′
	Rev: 5′ CTGCTTCCCCCCTGCAT 3′
VEGFR-2	Fwd: 5′ CAGAGTGGCAGTGAGCAAAGG 3′
	Rev: 5′ TTGTAGGCTCCAGTGTCATTTCC 3′
Mouse VEGFR-1	Fwd: 5′ TCCTATCGGCTGTCCATGAAA 3′
	Rev: 5′ CCAAATAGCGAGCAGACTTCAA 3′
Mouse VEGFR-2	Fwd: 5′ ACCAGCATGGCATCGTGTAC 3′
	Rev: 5′ CCTAGCGCAAAGAGACACATTG 3′
Mouse VEGFR-3	Fwd: 5′ GTATGAAATTGACCCGTACGAAAA 3′
	Rev: 5′ AGGAAATGAGGCTTGAGAGAAGATC 3′
VEGFA	Fwd: 5′ GGGCAGAATCATCACGAAGTG 3′
	Rev: 5′ TCAGGGTACTCCTGGAAGATGTC 3′
VEGFB	Fwd: 5′ AGCCAGTGTGAATGCAGACCTA 3′
	Rev: 5′ AGTCCCAGCCCGGAACAG 3′
VEGFC	Fwd: 5′ CCTCAGCAAGACGTTATTTGAAATT 3′
	Rev: 5′ TGGCAAAACTGATTGTTACTGGTT 3′
VEGFD	Fwd: 5′ CGTACATTTCCAAACAGCTCTTTG 3′
	Rev: 5′ GGCAAGCACTTACAACCTGTATGA 3′
VEGFR-1	Fwd: 5′ TTCTCACAGGATCTAGTTCAGGTTCA 3′
	Rev: 5′ CTGCTTCCCCCCTGCAT 3′
VEGFR-2	Fwd: 5′ CAGAGTGGCAGTGAGCAAAGG 3′
	Rev: 5′ TTGTAGGCTCCAGTGTCATTTCC 3′
Mouse VEGFR-1	Fwd: 5′ TCCTATCGGCTGTCCATGAAA 3′
	Rev: 5′ CCAAATAGCGAGCAGACTTCAA 3′
Mouse VEGFR-2	Fwd: 5′ ACCAGCATGGCATCGTGTAC 3′
	Rev: 5′ CCTAGCGCAAAGAGACACATTG 3′
Mouse VEGFR-3	Fwd: 5′ GTATGAAATTGACCCGTACGAAAA 3′
	Rev: 5′ AGGAAATGAGGCTTGAGAGAAGATC 3′

2.12. *Immunohistochemistry (IHC)/histology*

Staining (IHC) was done to determine VEGFR-2 and VEGFA expressions on tumour tissue from Experiments 2 and 6. Tumours were placed in formalin for 48 h and subsequently embedded in paraffin. Fixation was done with phosphate buffered formaldehyde 10% (F79-4, Fisher Scientific, Pittsburgh, PA). Xenografts were placed in the fixative for 48 h and subsequently embedded in paraffin. Paraffin sections were dewaxed using xylenes and hydrated using a series of ethanol. Antigen retrieval was performed with citrate buffer pH 6 for 10 min in a microwave oven (1500 W, 2 min at high and 8 min at the lowest power). Endogenous peroxidases were quenched with 0.3% hydrogen peroxide in methanol for 30 min. Sections were incubated overnight with the primary antibody raised against VEGFR-2 and VEGFA. Total VEGFR-2 (55B11) rabbit monoclonal antibody from Cell Signaling Technology (Beverly, MA) and anti-VEGF (A-20) purified rabbit polyclonal antibody from Santa Cruz (Santa Cruz, CA) were

diluted 1/100 (2 μg/mL) in phosphate buffered saline (PBS), washed the next day with PBS, incubated with biotinylated secondary antibodies (Vector Labs), incubated with Vecta Elite ABC kit (Vector Labs), developed with a DAB kit (Vector Labs) and lightly counterstained with Gill's haematoxylin. Negative controls were stained without primary antibody or with the corresponding concentration of rabbit IgG isotype. Specimens were documented photographically using a Nikon Optiphot microscope, equipped with an Optronics CCD camera. The stained sections were scored on the basis of staining intensity. The vast majority of tissues stained diffusely and all or more than 70% of the tumour tissue was stained in the positive specimens. The score was defined as weak (1+), positive (2+) or strong (3+).

For CD31 staining, in Experiment 3C, the sections were washed in PBS and then treated with 3% H_2O_2 for 10 min to block endogenous peroxidase activity and were blocked with normal rabbit serum. Then, the sections were incubated with rat anti-mouse CD31 (PECAM-1) monoclonal antibody (BD Pharmingen, San Diego, CA) at a 1:300 dilution overnight at 4 °C. Negative controls were incubated with the rat serum IgG at the same protein concentration. All sections were washed in PBS containing 0.05% Tween-20, and were then incubated with a second antibody, mouse anti-rat IgG (Vector laboratories, Burlingame, CA) at a 1:200 dilution for 30 min at room temperature again followed by washing with PBS containing 0.05% Tween-20. The sections were incubated in a 1:400 dilution of Extravadin Peroxidase (Sigma, St. Louis, MO) for 30 min. After washing in PBS containing 0.05% Tween-20, the sections were incubated in peroxidase substrate (Vector laboratories, Burlingame, CA) for 5 min. After washing we used a Biotinyl-Tyramide enhancement kit (TSA/Biotin Tyramide Reagent Pack, Perkin Elmer, Waltham, MA) according to the manufacturer's instructions. The sections were washed in PBS containing 0.05% Tween-20 and were counterstained with Gill's haematoxylin.

For general morphological evaluations, sections from each tumour were stained with haematoxylin and eosin (H and E).

2.13. Statistical analysis

Tumour growth data were analysed using random effects growth curve models, where tumour CSA was fit assuming a quadratic function of time. Let A_{ijt} be the CSA of tumour i on mouse j, in treatment group k, measured t days after treatment (or control) initiation. The growth curve model was of the following form:

$$A_{ijkt} = \beta_{0j} + t\beta_{1ij} + t^2\beta_{2ij} + \sum_{z=1,\ldots,K} \gamma_{0z} I(k = z) + \sum_{z=1,\ldots,K} t\gamma_{1z} I(k = z) + \sum_{z=1,\ldots,K} t^2\gamma_{2z} I(k = z) + \varepsilon_{ijkt}$$

where the βs were assumed random terms with mean zero, the γs were fixed effects and K is the number of treatment groups. Random effects were included to allow deviation of individual tumours from the mean growth of the group and to account for within-animal clustering. The estimated curves were plotted and the fit examined. Linear contrasts were used to estimate mean tumour size differences (and associated standard error) at a specified time t between any two pre-specified experimental groups. Wald tests were used to test the null hypothesis of equal tumour size between two experimental groups at time t. For experiments with randomisation and treatment initiated after day 0, only observations taken after randomisation were analysed. For example, in Experiment 8, only observations after initiation of brivanib alaninate or tamoxifen treatment ($\geqslant$35 d) were analysed. Bonferroni corrections were used to adjust for multiple testing within each experiment for these analyses. The experiment-wise type I error was 5%. The RNA expression data measured by RTPCR with high/low dose of VEGFR-2 inhibitor and combination treatment were analysed using Wilcoxon rank-sum tests. The RTPCR analyses were confirmatory and, therefore no adjustment of the type I error for multiple testing was used. All tests were two-sided. Statistical analyses were performed using STATA version 10.1.

For the CD31 counts that were done for the MCF-7 Tam model, the statistical analysis was done using a two tailed Student's t-test and a p-value that was less than 0.05 was considered significant.

3. Results

3.1. Immunohistochemistry

Immunohistochemistry was performed on representative MCF-7 E2 tumours to determine whether the VEGFR-2 receptor was expressed in response to estradiol and 2 weeks of tamoxifen. We also determined VEGFR-2 receptor expression in response to estradiol, estradiol withdrawal and the treatment with the pure anti-oestrogen, fulvestrant. This analysis demonstrated the presence of VEGFR-2 on both tumour cells and endothelial cells (Fig. 1A). In addition, VEGFR-2 and VEGFA expressions were increased on tumour cells in the presence of estradiol. It is interesting to note that the combination of estradiol and 2 weeks of 125 μg tamoxifen did not apparently change VEGFR-2 or VEGFA expression in comparison to estradiol treatment alone. However, as noted in Fig. 6A, tamoxifen was not effective at controlling established estradiol stimulated tumour growth during the two-week treatment period. With estradiol withdrawal alone, and the subsequent destruction of the ER with fulvestrant, there was very little expression of VEGFR-2 or VEGFA on the tumour cells (Fig. 1A and B).

3.2. Effects of different doses of brivanib alaninate in SERM sensitive MCF-7 E2 tumours

We evaluated the effects of a low dose (0.05 mg/g) and high dose (0.1 mg/g) of brivanib alaninate on estradiol stimulated tumour growth. The high dose was based on data demonstrating the highest effective dose with minimal toxicity and the low dose that was chosen was half of the high dose and the minimally effective dose as determined by Bristol Myers Squibb (Princeton, NJ).[38] Statistical comparisons were done to determine whether there was a difference in the average CSA of tumours treated with estradiol versus those that received the high dose (0.1 mg/g) or low dose (0.05 mg/g) of brivanib alaninate in the presence of estradiol. Estradiol caused tumour growth, while the high dose of brivanib alaninate pro-

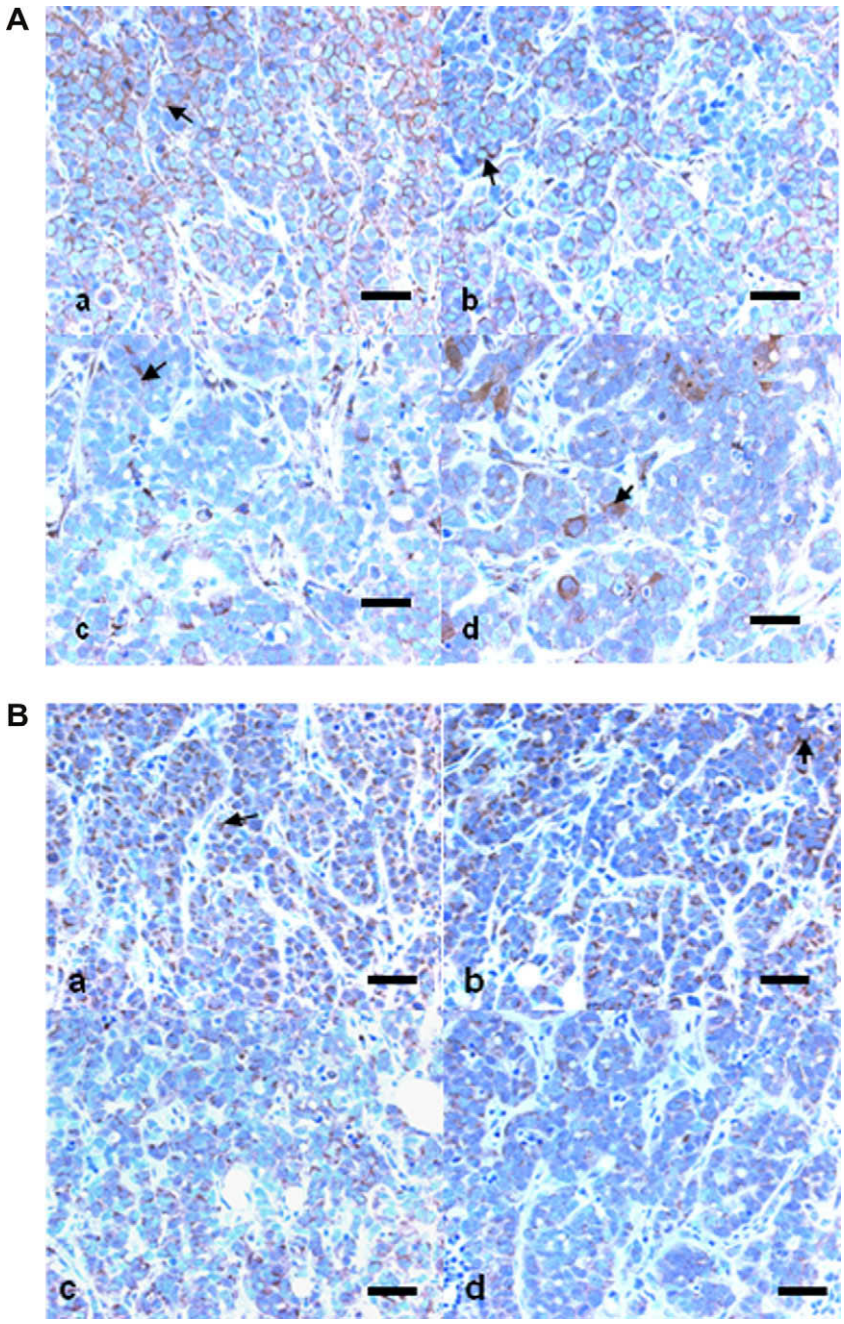


Fig. 1 – The distribution of the VEGFR-2 receptor (A) and VEGFA (B) in the MCF-7 E2 tumour model. Tumour bearing animals were treated with estradiol (a), estradiol and 2 weeks of 125 μg tamoxifen (b), estradiol and then 2 weeks of estradiol withdrawal (c), and estradiol followed by 2 weeks of estradiol withdrawal and fulvestrant (d). VEGFA and VEGFR-2 expressions decreased with estradiol withdrawal. The bars represent 50 μm.

duced a dramatic decrease in estradiol-stimulated growth (Fig. 2A). The average difference in tumour CSA at 6 weeks in the mice that received the high dose of the brivanib alaninate and estradiol versus estradiol was –0.37 cm^2 ($p = 0.001$, $\alpha = 0.025$). There was no significant difference (0.13 cm^2) in the average CSA of tumours treated with estradiol only and those treated with estradiol and the low dose of brivanib alaninate ($p = 0.202$, $\alpha = 0.025$).

The tumour tissue was further evaluated with H and E staining (Fig. 2B). The purpose of this analysis was to detect differences in the amount of necrotic tissue. In tumours in which angiogenesis and thus, oxygen and nutrient delivery is blocked, there would be a decrease in tumour cell viability and hence an increase in necrosis. In tumours that received brivanib alaninate, there was an increase in tissue necrosis as exemplified by the areas that stain pink only. The necrosis was most prominent in the tumours treated with the high dose of the brivanib alaninate. There was mild necrosis in the tumours that were treated with the low dose of the brivanib alaninate.

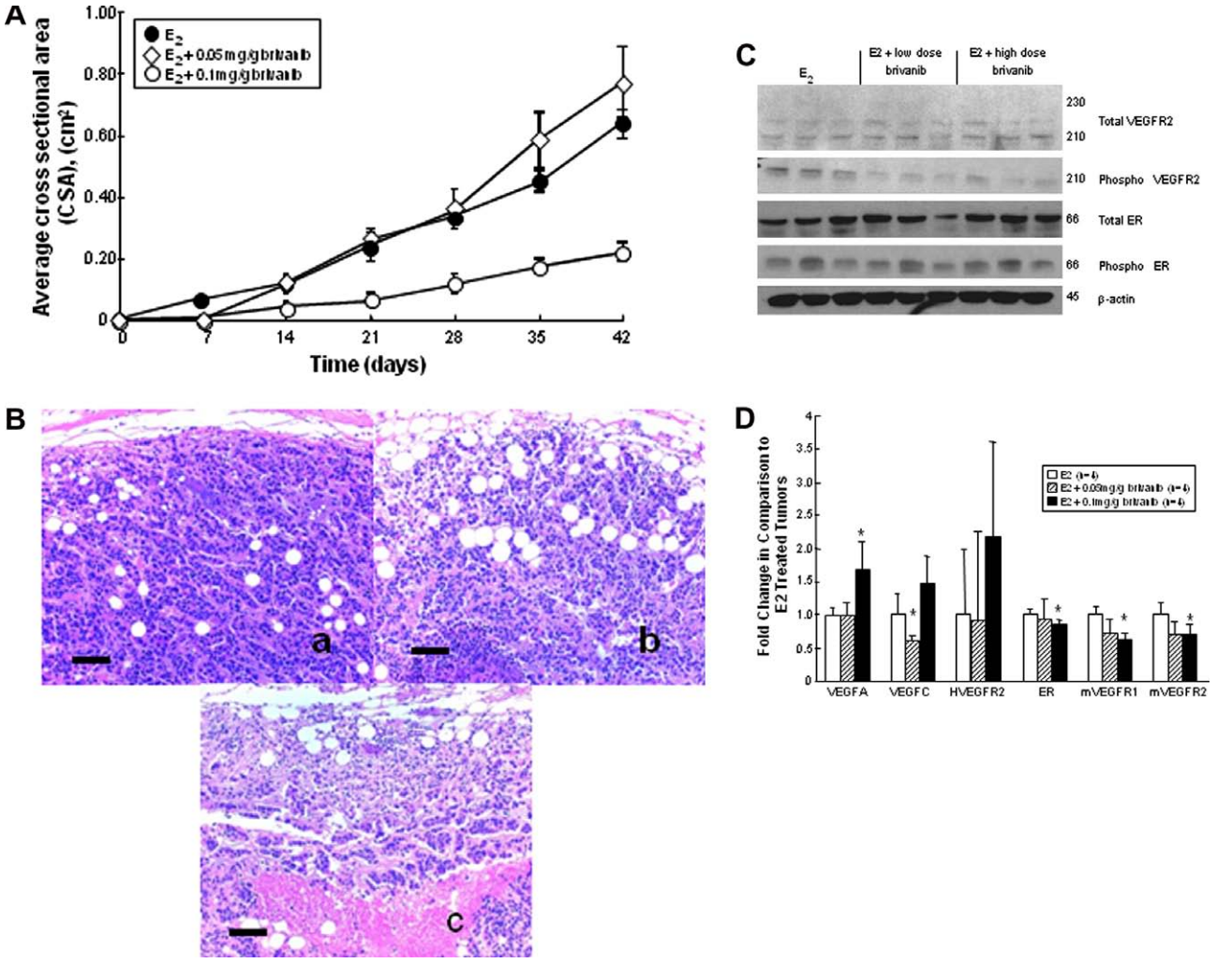


Fig. 2 – The growth characteristics of MCF-7 E2 tumours treated with estradiol alone or with estradiol and the lower (0.05 mg/g) and higher doses (0.1 mg/g) of brivanib alaninate. There were five ovariectomised, athymic mice and 10 tumours per group. The drug treatment resulted in a decreased average CSA of the tumours at the higher dose (0.1 mg/g) ($p = .001$, $\alpha = 0.025$), but there was no difference between the group treated with the low dose (0.05 mg/g) of brivanib alaninate and the oestrogen only group ($p = 0.2$, $\alpha = 0.025$). There were no significant differences in animal body weights between groups. H and E staining is shown in panel B and reveals that with increases in the dosing of the drug, there was an increase in the amount of necrotic tissue (*). The bar represents 100 μm. Panel C demonstrates that there was no significant change in the total amount of VEGFR-2 expressed by the tumours, but there was a decrease in the phosphorylation pattern of the tumours treated with brivanib alaninate, regardless of the dose given. The presence of ER and its phosphorylated form was indicative of active tumour tissue in all the samples. Panel D demonstrates analysis by RTPCR. There was a significant increase in VEGFA in the high dose group in comparison with tumours treated with oestrogen only ($p = 0.02$). There was a small, but significant decrease in ER mRNA in the high dose (0.1 mg/g) group ($p = 0.04$). VEGFC transcription decreased significantly in tumours treated with the low dose (0.05 mg/g) of brivanib alaninate. Mouse VEGFR-1 and mouse VEGFR-2 mRNA, which represented the endothelial component of the tumour, significantly decreased in the high dose (0.1 mg/g) group ($p = 0.02$, $p = .04$).

Western immunoblotting of tumour extracts did not reveal a difference in total VEGFR-2, but there was less phosphorylation at the tyrosine 951 residue of VEGFR-2 in brivanib alaninate treated animals (Fig. 2C). The presence of ER and phospho-ER demonstrated active tumour tissue and an activated ER. There was very little VEGFR-1, VEGFR-3 or FGFR-1 (data not shown) detected by immunoblotting. The use of RTPCR analysis confirmed a significant increase in VEGFA ($p = 0.02$) and a non-significant increase in human VEGFR-2 in tumours that were treated with the high dose of brivanib alaninate (Fig. 2D). There was a significant decrease in mouse VEGFR-1 and mouse VEGFR-2 in tumours that were treated with the higher ($p = 0.02$, $p = 0.04$) dose of brivanib alaninate. ER mRNA decreased slightly, but significantly (Fig. 2C) in those tumours that were treated with the higher dose of brivanib alaninate ($p = 0.04$), but there was no increase in ER protein by Western blotting analysis (Fig. 2C). There was a significant decrease in transcription of VEGFC mRNA ($p = 0.04$) in tumours treated with the lower dose of brivanib alaninate (Fig. 2D). There was very little or no VEGFB, VEGFD, mouse

VEGFR-3 or human VEGFR-1 present in the tumours as evidenced by high CT values (>35) detected by RTPCR analysis (data not shown).

3.3. *Effect of brivanib alaninate on SERM stimulated tumour growth*

To establish that an inhibitor of VEGFR-2 would block the growth of SERM stimulated tumours and as a consequence, would have the potential to retard the development of acquired SERM resistance in ER positive cancers, a series of models and designs was explored. The MCF-7 Ral tumour model[39] grows without raloxifene, and to a greater extent in the presence of raloxifene. Fulvestrant retards tumour growth.[39] This is illustrated in Fig. 3A. Statistical comparisons were done to determine whether there was a difference in the average CSA of tumours treated with raloxifene versus those treated with placebo, fulvestrant or high dose brivanib alaninate (0.1 mg/g). Raloxifene stimulated tumour growth was significantly decreased in the presence of high dose brivanib alaninate (0.1 mg/g) administered with raloxifene and the difference in average CSA was 0.391 cm^2 after 8 weeks ($p < 0.001$, $\alpha = 0.016$). A similar difference in average CSA (0.366 cm^2) was also observed with tumours treated with raloxifene versus tumours treated with fulvestrant ($p < 0.001$, $\alpha = 0.016$). There was no significant difference between the average CSAs of tumours (0.212 cm^2) in the presence or absence of raloxifene ($p = 0.024$, $\alpha = 0.016$). The addition of high dose brivanib alaninate (0.1 mg/g) to a daily regimen of 1.5 mg of raloxifene (0.1 mg/g) caused a rapid decrease in tumour growth (decrease in average CSA = –0.294 cm^2) ($p < 0.001$, $\alpha = 0.025$) in established raloxifene stimulated tumours (Fig. 3B) over a two-week period. At the time of randomisation, the group that was treated with raloxifene (1.5 mg) and brivanib alaninate (0.1 mg/g) demonstrated no difference in average CSA (–.0146 cm^2) than those that received raloxifene (1.5 mg) only ($p = 0.73$, $\alpha = 0.025$).

Our MCF-7 Tam SERM stimulated model showed similar effects with brivanib alaninate. Statistical comparisons were done to determine whether there was a difference in the average CSA of tumours treated with 1.5 mg tamoxifen daily versus vehicle or 1.5 mg tamoxifen + 0.1 mg/g brivanib alaninate. The difference in CSA between those tumours that received 1.5 mg tamoxifen daily versus 1.5 mg tamoxifen and the high dose brivanib alaninate (0.1 mg/g) daily ($p < 0.001$, $\alpha = 0.025$) was 0.395 cm^2. A similar difference in CSA (0.484 cm^2) was observed between tumours treated with tamoxifen alone versus control treated with vehicle only ($p < 0.001$, $\alpha = 0.025$). The tamoxifen (1.5 mg/daily) treated group was then randomised to continue 1.5 mg/d tamoxifen or 1.5 mg/d tamoxifen + high dose brivanib alaninate for 2 weeks. At the time of randomisation, the group that was treated with tamoxifen (1.5 mg) and brivanib alaninate (0.1 mg/g) demonstrated no difference in average CSA than those that received tamoxifen (1.5 mg/g) only ($p = 0.76$, $\alpha = 0.25$). The addition of brivanib alaninate (0.1 mg/g) caused a rapid tumour regression (difference in average CSA = –0.261 cm^2) of established tumours after 2 weeks of treatment ($p < 0.001$, $\alpha = 0.025$) (Fig. 3C). There was a significant decrease in blood vessel density (CD31 counts) in the group that received 0.1 mg/g brivanib alaninate and 1.5 mg tamoxifen for 2 weeks (average MVD/sq. mm = 76) in comparison with the group that continued receiving 1.5 mg tamoxifen (average MVD sq./mm = 156) ($p = 0.003$).

Finally, the tamoxifen-stimulated EnCa 101 endometrial tumour model[30] was also used to evaluate the efficacy of brivanib alaninate (0.1 mg/g). Animals with bi-transplanted tumours were treated with 500 μg of tamoxifen daily by oral gavage for 40 d and then randomised. One group received 500 μg of tamoxifen and 0.1 mg/g brivanib alaninate daily. The other group continued to receive 500 μg of tamoxifen. At the time of randomisation, the group that was treated with tamoxifen (500 μg) and brivanib alaninate (0.1 mg/g) had a larger average volume (difference = 40 mm^3) than those that received tamoxifen (500 μg) only ($p = 0.002$, $\alpha = 0.025$). Despite this initial difference, over a three-week period, animals treated with tamoxifen alone subsequently had an average tumour volume (difference = 0.168 mm^3) that was much greater than those animals treated with brivanib alaninate in combination with tamoxifen ($p < 0.001$, $\alpha = 0.025$) (Fig. 3D). All models demonstrated that a VEGFR-2 inhibitor, brivanib alaninate would prevent the growth of SERM stimulated tumours.

3.4. *Determination of tamoxifen dosing in SERM sensitive MCF-7 E2 tumours*

We determined an anti-oestrogenical dose of tamoxifen that would be approximately 50% effective in blocking estradiol stimulated tumour growth. Previously, 1.5 mg/d of tamoxifen has been used to almost completely block oestrogen stimulated tumour growth.[40] The differences in the CSAs of tumours treated with estradiol and 125 μg tamoxifen (–0.368 cm^2, $p = 0.01$, $\alpha = 0.016$), estradiol and 250 μg tamoxifen (–0.479 cm^2, $p = 0.001$, $\alpha = 0.016$) or estradiol and 500 μg tamoxifen (–0.479 cm^2, $p < 0.001$, $\alpha = 0.016$) versus estradiol alone were significant (Fig. 4). A dose of 125 μg was chosen for further testing in combination with brivanib alaninate to determine whether there would be an improvement in therapeutic efficacy.

3.5. *The combined effect of a lower dose of tamoxifen and brivanib alaninate in SERM sensitive MCF-7 E2 tumours*

We hypothesise that a sub-therapeutic dose of brivanib alaninate may enhance a sub-optimal effective daily dose of tamoxifen (125 μg) and thus improve tumour growth control. The strategy of limiting angiogenesis would optimise long-term anti-oestrogen therapy. Statistical comparisons were done to determine whether there was a difference in the average CSA of tumours treated with 125 μg tamoxifen + 0.05 mg/g brivanib alaninate versus 125 μg tamoxifen or 0.05 mg/g brivanib alaninate. The results illustrated in Fig. 5 demonstrated that the combination of 125 μg of tamoxifen and 0.05 mg/g of brivanib alaninate significantly improved the anti-tumour action tamoxifen or brivanib alaninate alone after 6 weeks. The difference in average CSAs of tumours treated with 125 μg tamoxifen and 0.05 mg/g brivanib alaninate versus those treated 125 μg tamoxifen (–0.128 cm^2, $p = 0.01$, $\alpha = 0.025$) was significant. Similarly, there was a significant difference in the CSA of those tumours treated with the combination therapy and those treated with brivanib alaninate (–0.449 cm^2, $p < 0.001$, $\alpha = 0.025$).

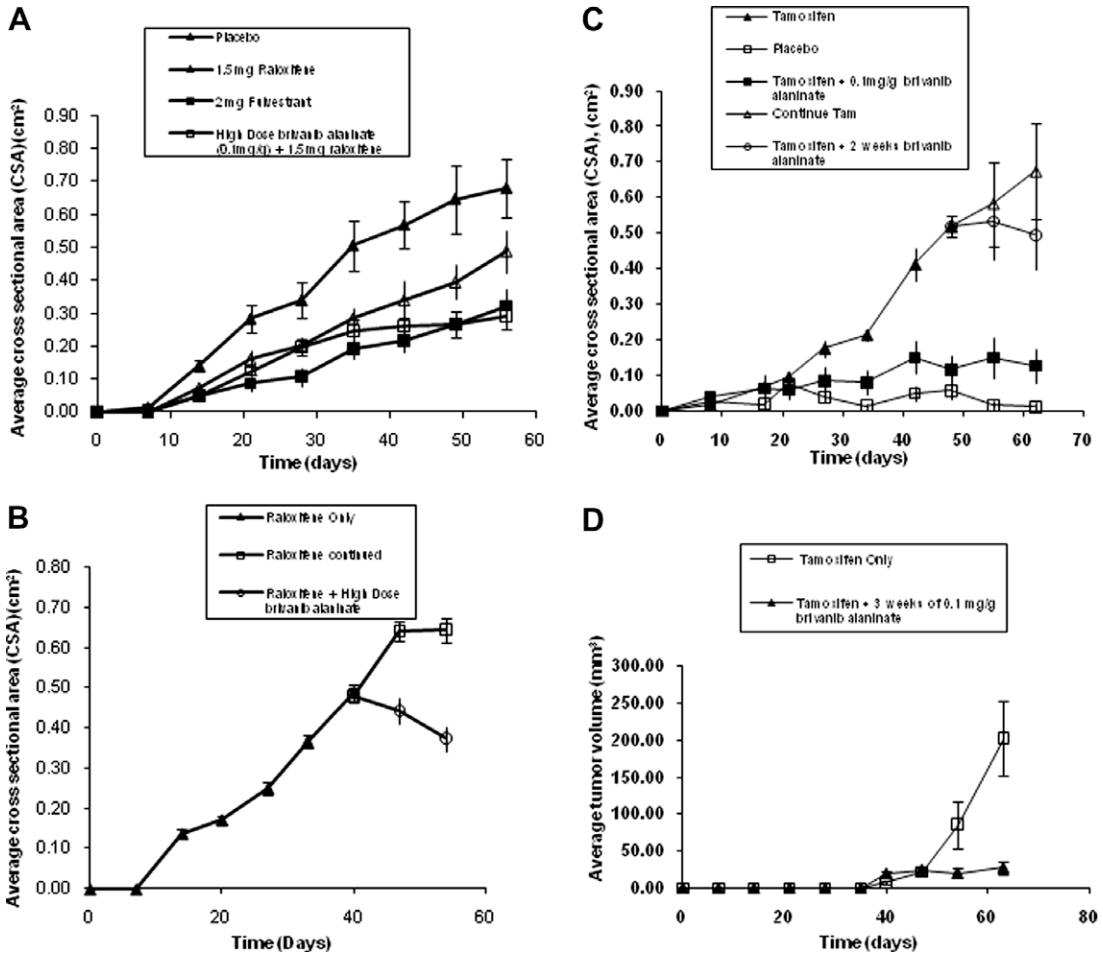


Fig. 3 – The anti-tumour effects of high dose (0.1 mg/g) brivanib alaninate on the growth of human tumours with acquired resistance to the SERMs raloxifene or tamoxifen. There were no significant differences in animal body weights between groups. Unless stated otherwise, all groups had 5 ovariectomised athymic mice with 10 tumours. (A) Raloxifene stimulated MCF-7 Ral. Groups were treated with raloxifene (1.5 mg daily by gavage), vehicle, fulvestrant (2 mg SQ 5 d per week), or raloxifene plus brivanib alaninate (0.1 mg/g by gavage). Brivanib alaninate (0.1 mg/g) significantly prevented the growth of raloxifene treated tumours ($p < 0.001$, $\alpha = 0.016$). (B) Raloxifene (1.5 mg daily by gavage) stimulated MCF-7 RAL. Twenty ovariectomised athymic mice were randomised into two groups of 10 mice each with continued raloxifene treatment (total of 17 tumours in the group) or raloxifene plus high dose brivanib alaninate (0.1 mg/g by gavage) (total of 19 tumours in the group). There was a significant decrease in tumour size with brivanib alaninate ($p < 0.001$, $\alpha = 0.025$). (C) Tamoxifen (1.5 mg daily by gavage) stimulated MCF-7 TAM tumours. Athymic, ovariectomised mice were initially placed into three groups to receive 1.5 mg tamoxifen (8 mice, 16 tumours), 1.5 mg tamoxifen plus 0.1 mg/g brivanib alaninate (4 mice, 6 tumours) or control vehicle (5 mice, 10 tumours). The group that received tamoxifen was randomised to continue tamoxifen (4 mice, 8 tumours) or receive tamoxifen with 0.1 mg/g brivanib alaninate (4 mice, 8 tumours) once the tumours reached an average CSA of 0.5 cm^2. The VEGFR inhibitor produced significant decreases in tamoxifen-stimulated growth rate in early implanted ($p < 0.001$, $\alpha = 0.025$) or established ($p < 0.001$, $\alpha = 0.025$) tumours. (D) Treatment of tamoxifen-stimulated (500 μg tamoxifen by gavage daily) EnCa 101 endometrial tumours was continued in two groups of 10 ovariectomised, athymic mice (20 tumours per group for 40 d). One group then received concomitant high dose brivanib alaninate (0.1 mg/g by gavage) for 3 weeks. Tumour volume was significantly decreased in animals treated with brivanib alaninate and tamoxifen compared to tamoxifen alone ($p < 0.001$, $\alpha = 0.025$).

3.6. *The combined effect of a lower dose of tamoxifen and brivanib alaninate in established SERM sensitive MCF-7 E2 tumours*

The goal of this experiment was to obtain sufficient tumour tissue for molecular analysis to evaluate the actions of tamoxifen and brivanib alaninate. The results are summarised in Figs. 6 and 7. The short-term combination of brivanib alaninate and tamoxifen decreased tumour size during the two-week period, whereas neither tamoxifen alone nor the brivanib alaninate alone prevented an increase in established tumour size (Fig. 6A). Statistical comparisons were done to determine whether there was a difference in the average CSA of tumours treated with 125 μg tamoxifen + 0.05 mg/g

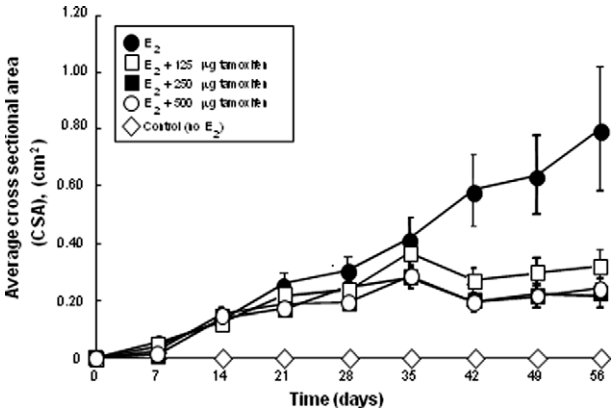


Fig. 4 – The effect of daily oral tamoxifen dosing on the estradiol-stimulated growth of MCF-7 E2 tumours delivered by an implanted 0.3 cm sustained release silastic capsule. There were five ovariectomised, athymic mice and 10 tumours per group. There was a dose-dependent decrease in estradiol stimulated tumour growth. The tumours did not grow without estradiol. The lowest dose of tamoxifen, 125 µg, suppressed tumour growth by 63%, whereas the higher doses (250 µg and 500 µg) suppressed tumour growth by 75%. There were no significant differences in animal body weights between groups.

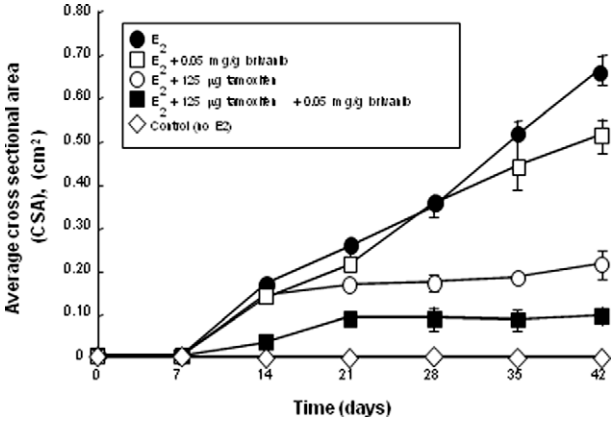


Fig. 5 – The effect of a combination of tamoxifen (125 µg daily oral dose) and 0.05 mg/g brivanib alaninate on the growth of established estradiol stimulated MCF-7 E2 tumours. There were five ovariectomised, athymic mice and 10 tumours per group. The combination of 125 µg tamoxifen with 0.05 mg/g brivanib alaninate improved the effects of 125 µg tamoxifen ($p < 0.01$, $\alpha = 0.025$) or 0.05 mg/g brivanib alaninate ($p < 0.001$, $\alpha = 0.025$). There were no significant differences in animal body weights between groups.

brivanib alaninate versus 125 µg tamoxifen or 0.05 mg/g brivanib alaninate. There was no difference in size at the time of randomisation (tamoxifen versus combination therapy ($p = 0.87$) and brivanib versus combination therapy ($p = 0.29$)). The average CSA was significantly different between tumours treated with 125 µg tamoxifen versus those treated with 125 µg tamoxifen and .05 mg/g brivanib alaninate (–0.292 cm^2, $p = 0.01$, $\alpha = 0.025$). The same observation was noted for those tumours treated with 0.05 mg/g brivanib alaninate versus those treated with 0.05 mg/g brivanib alaninate and 125 µg tamoxifen (–0.341 cm^2, $p = 0.007$, $\alpha = 0.025$).

Consistent with our findings, illustrated in Fig. 2B, representative histological analysis in this experiment confirmed (Fig. 6B) increased necrosis in tumours that received only brivanib alaninate or brivanib alaninate plus tamoxifen.

Western immunoblotting (Fig. 6C) demonstrated a decrease in phosphorylation of the VEGFR-2, but not total VEGFR-2 in the two groups that received brivanib alaninate. Total ER expression was reduced in the group receiving tamoxifen and the brivanib alaninate compared to tamoxifen alone.

RTPCR analysis (Fig. 6D) demonstrated an increase in mRNA for mouse VEGFR-1 and mouse VEGFR-2 in tumours that receive brivanib alaninate with ($p = 0.002$, $p = 0.002$) or without ($p = 0.001$, $p = 0.001$) tamoxifen. VEGFA mRNA is increased with tamoxifen ($p = 0.01$), brivanib alaninate ($p = 0.001$) or both drugs ($p = 0.002$) in combination. VEGFC increased with the tamoxifen treated group ($p = 0.001$), but decreased in the groups treated with the brivanib alaninate ($p = 0.004$). ER mRNA levels increased ($p = 0.04$) with the tamoxifen treated group, but decreased with the group that received both the VEGFR inhibitor and tamoxifen ($p = 0.04$).

We further validated our molecular studies with immunohistochemistry. There was little change in total VEGFR-2 (Fig. 7A), which was consistent with the findings in Western immunoblotting. VEGFA staining intensity increased in the tumours treated with tamoxifen and brivanib alaninate, which is consistent with the increased VEGFA mRNA seen in RTPCR analysis (Fig. 7B). The nuclear staining of the VEGF in the presence of brivanib (Fig. 7C) could be consistent with the report by Rosenbaum-Dekel et al.[41] with the nuclear localisation of L-VEGF, but no specific antibody was available to test the hypothesis.

4. Discussion

We report the first study to explore the potential of combining tamoxifen with low dose brivanib alaninate to block the growth of ER positive breast cancer. Previous studies have demonstrated the efficacy of brivanib in mouse models of human hepatocellular carcinoma[24] and to inhibit growth in ER negative H3396 xenografts in athymic mice.[25] Our strategy is to employ an anti-oestrogen (tamoxifen) to block oestrogen stimulated VEGF production and to use a combination with blockers of VEGFR-2 to reduce angiogenic survival mechanisms in both the tumour and endothelial cells to enhance tumour cell death. Our results demonstrate that the strategy is feasible. We have advanced the idea with the demonstration that a VEGFR-2 inhibitor, brivanib alaninate can not only inhibit the growth of small SERM stimulated implants derived from MCF-7 cells with acquired resistance to tamoxifen and raloxifene, but also can inhibit SERM stimulated growth of established tumours in athymic mice (Fig. 3A–C). Additionally, brivanib alaninate inhibits tamoxifen-stimulated endometrial cancer (EnCa 101) growth (Fig. 3D). Thus, the ability of a VEGFR-2 inhibitor to block the growth of tumours with acquired SERM resistance supports the idea that this strategy might improve adjuvant therapies.

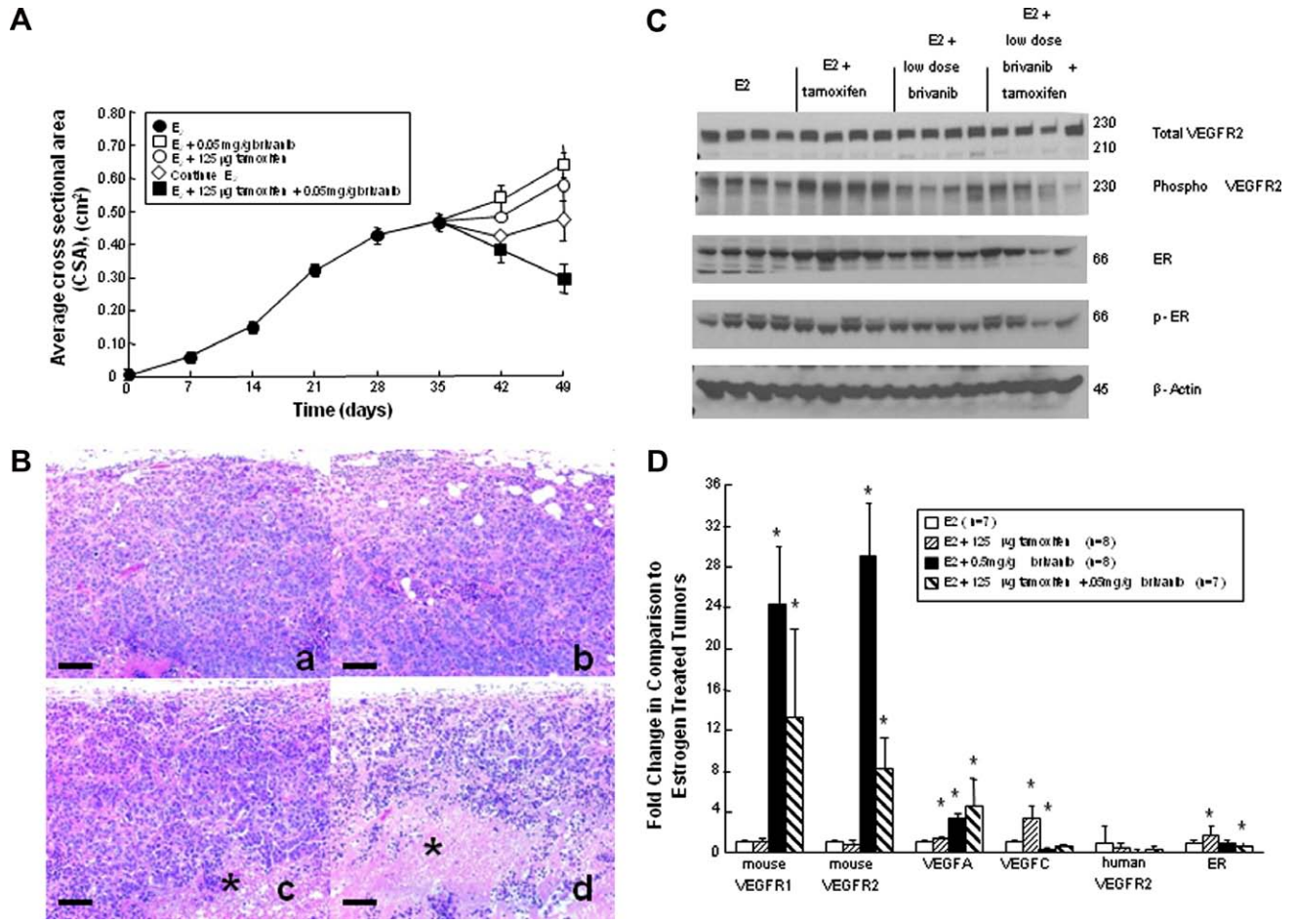


Fig. 6 – *Panel A:* the efficacy of a combination of 125 μg tamoxifen and 0.05 mg/g brivanib alaninate on the growth of established estradiol stimulated MCF-7 E2 tumours. There were five ovariectomised, athymic mice and 10 tumours per group. Tumours were grown to approximately 0.46 cm^2 and treated with the treatment regimens as indicated. There were no significant differences in animal body weights between groups. However, the decrease in average CSA was significant when comparing the combination treatment to tamoxifen (125 μg) treated tumours ($p = 0.01$, $\alpha = 0.025$) or those treated with 0.05 mg/g brivanib alaninate ($p = 0.007$, $\alpha = 0.025$). *Panel B:* H and E staining demonstrated an increase in necrotic tissue when brivanib alaninate was given alone or with tamoxifen. Once again, the bar represented a 100 μm distance. *Panel C:* Western blot analysis of tumour tissue did not illustrate a decrease in total VEGFR-2, regardless of the treatment group. The addition of brivanib alaninate, decreased the phosphorylation of VEGFR-2. Expression of ER and phosphorylated ER in all tumours, demonstrated the presence of active tumour tissue. *Panel D:* relative fold change in the mRNA levels of angiogenic factors in tumours relative to estradiol treatment alone. Mouse VEGFR-1 and mouse VEGFR-2 mRNA increased dramatically in tumours that received the inhibitor ($p = 0.001$, $p = 0.001$) or the inhibitor plus tamoxifen ($p = 0.002$, $p = 0.002$). VEGFA mRNA increased in tumours in response to tamoxifen treatment ($p = 0.01$) brivanib alaninate treatment ($p = 0.001$) and the combination of brivanib alaninate plus tamoxifen ($p = 0.002$). VEGFC increased in tamoxifen treated tumours ($p = 0.001$) and decreased in tumours treated with brivanib alaninate ($p < 0.004$). There was a significant, but small decrease in ER mRNA ($p = 0.04$) in tumours treated with the combination of tamoxifen plus brivanib alaninate and an increase in ER mRNA in tamoxifen treated tumours ($p = 0.04$).

Angiogenesis is important for tumour growth and metastasis. Stable transfection of MCF-7 cells with the VEGF gene results in hormone independent growth *in vivo* and tamoxifen resistance.[42] This is supported by the recent work by Aesoy and coworkers[43] using an anti-oestrogen resistant cell line (LCC2) *in vitro* that has constitutive VEGF secretion relative to wildtype MCF-7 cells. MCF-7 cells respond to 4-hydroxytamoxifen with a reduction in VEGF, but the anti-oestrogen resistant variant LCC2 does not. Oestrogen has been shown to increase the synthesis of VEGFA[13] and anti-oestrogens inhibit the process.[13,43] This observation was validated in our tumour models as the expression of VEGFA and VEGFR-2 is increased in the presence of oestrogen and decreased with oestrogen withdrawal (Fig. 1A and B). As there is strong evidence for the oestrogen mediated regulation of angiogenesis, combining an anti-oestrogen with an antiangiogenic inhibitor to diminish tumour growth is a reasonable therapeutic approach.

There are fewer side-effects such as malignant hypertension with angiogenesis inhibitors when used lower doses.[44]

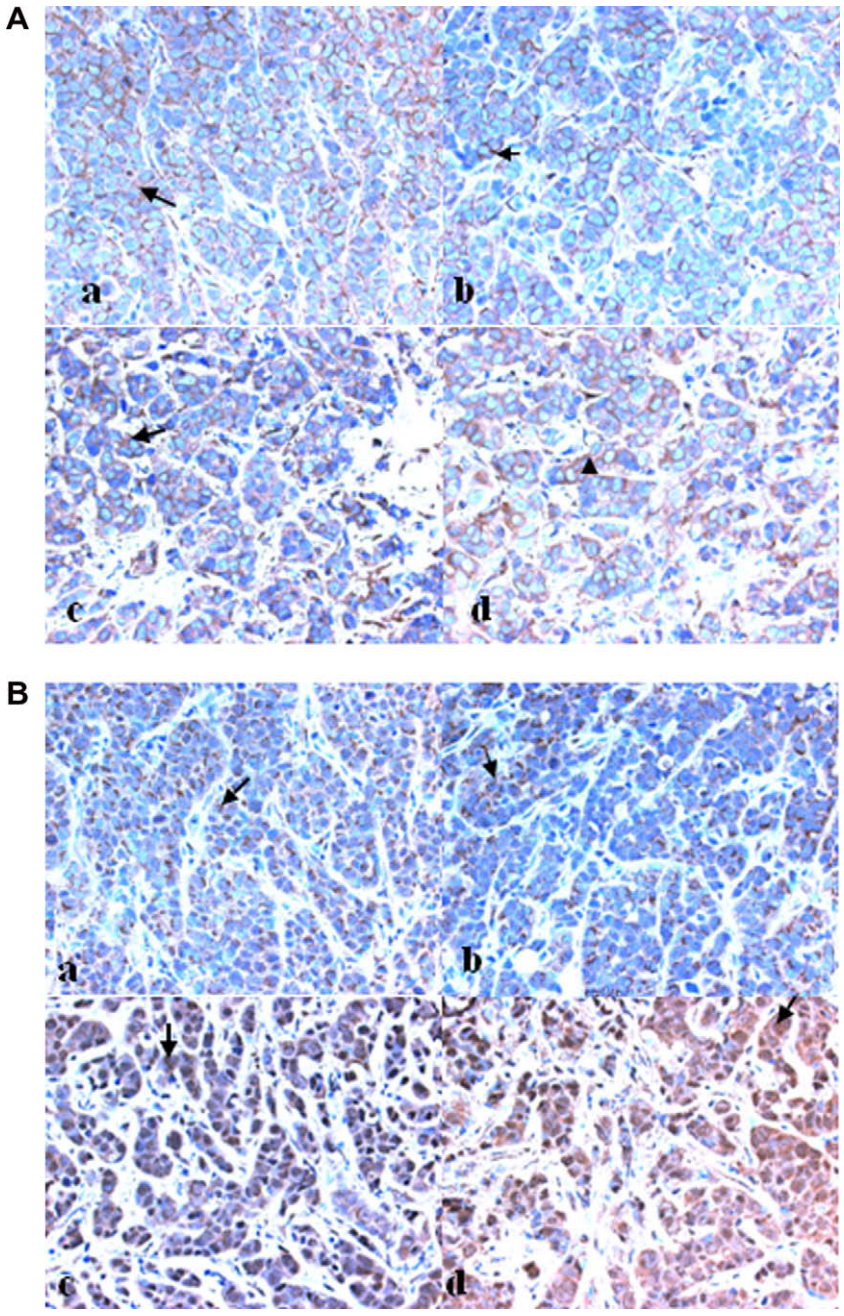


Fig. 7 – *Panel A*: there is no change in total VEGFR-2 expression by IHC in MCF-7 E2 tumours treated with estradiol (a), estradiol and 2 weeks of 125 μg tamoxifen (b), estradiol and 2 weeks of 0.05 mg/g brivanib alaninate (c), or estradiol and 2 weeks of the combination of 125 μg tamoxifen and 0.05 mg/g brivanib alaninate (d). *Panel B*: by IHC, the VEGFA staining intensity is greatest with 2 weeks of the combination of 125 μg tamoxifen and 0.05 mg/g brivanib alaninate (d). Staining intensity is the same with estradiol (a), estradiol and 2 weeks of 125 μg tamoxifen (b), estradiol, and 2 weeks of 0.05 mg/g brivanib alaninate (c). The bars represent 50 μm.

At higher doses, therapeutic efficacy may be diminished when drug dosing is reduced or abbreviated. Therefore, we advanced the concept of dual inhibition of angiogenesis further and tested a combination of sub-effective tamoxifen (125 μg) daily and the sub-therapeutic VEGFR-2 inhibitor brivanib alaninate (0.05 mg/g daily). The combination significantly decreased tumour growth compared with estradiol and either drug alone. This was true for the prevention of early tumour development following initial implantation (Fig. 5) or during the short-term treatment of established tumours (Figs. 6 and 7). Thus, we have shown that using a combination of lower, more tolerable doses of two drugs that are as efficacious as higher, less tolerable doses of either drug used alone, is a viable alternative for adjuvant therapy.

Drug treatments were evaluated in established tumours to provide tissue to investigate molecular mechanisms. Total

VEGFR-2 levels did not change in the tumours with treatment (Figs. 6C and 7A), but the phosphorylation patterns were different (Fig. 6C). Brivanib alaninate inhibits phosphorylation of the VEGFR-2 receptor. This confirmed the reported mechanism of action[24] of brivanib alaninate as an inhibitor of the VEGFR-2 tyrosine kinase. Treatment of established tumours with tamoxifen alone increased phosphorylation of VEGFR-2 and this increase in phosphorylation was inhibited when brivanib alaninate was combined with tamoxifen. Thus, it is possible to explain why a significant decrease in tumour size resulted from the use of a two-drug combination rather than a single drug that was individually ineffective in established tumours.

Similarly, transcription of VEGFC mRNA increased during tamoxifen treatment, but this was abrogated with brivanib alaninate. This is an important finding because VEGFC also activates VEGFR-2.[22] There was a compensatory rise in VEGFA with tamoxifen, brivanib alaninate, or the combination of the two drugs. However, with the combination of tamoxifen and brivanib alaninate, the compensatory mechanisms of the tumour to overcome blockade of the ER and VEGFR-2 failed as evidenced by increased tumour necrosis. The compensatory rise in VEGFA was validated by IHC in tumours treated with the combination of tamoxifen and brivanib alaninate. Overall, our findings confirm and extend the recent findings of Aesoy and co-workers[43] who demonstrate a breast cancer cell survival of VEGF/VEGFR-2/p38 feedback loop in cells resistant to anti-oestrogens.

Classically, the VEGF pathway in tumours has been thought to result from VEGF secretion from tumour cell activation of VEGF receptors on endothelial cells. However, accumulating evidence suggest that VEGFR-2 is most likely found on both cancer cells and endothelial cells.[43,45–47] By using IHC to localise VEGFR-2 in the MCF-7 tumour model, there is demonstrable expression of VEGFR-2 on the breast cancer cells (Fig. 1A). Moreover, there is evidence of oestrogen mediated regulation of VEGFR-2 expression on tumour cells as VEGFR-2 expression decreases with the withdrawal of 17β-estradiol. Ryden[48] also demonstrated that VEGFR-2 is expressed on tumour material from patients. These findings strengthen the argument to target VEGFR-2 in breast cancer.

By using RTPCR to differentiate between mouse and human VEGFR-2, we were able to evaluate the response to therapy in the endothelial (mouse) and the tumour cell (human) components. Interestingly, when the brivanib alaninate is started at the time of implantation there is a significant decrease in mouse VEGFR-1 and VEGFR-2. There was a trend towards an increase in human VEGFR-2 in mice treated with the higher dose of brivanib alaninate, with a significant decrease in mouse VEGFR-2 mRNA. When the angiogenesis inhibitor was given to mice with established tumours, there was a trend towards a decrease in human VEGFR-2 mRNA with a significant increase in mouse VEGFR-1 and VEGFR-2 mRNA. Thus, when the human VEGFR-2 is blocked, this then affects the endothelial component and the cells attempt to manufacture more receptor.

The ER is central to oestrogen-regulated events. As reported in previous studies, tamoxifen blocks the E2-mediated down-regulation of ER mRNA (Fig. 6D) and there is an increase in total ER expression[49] (Fig. 6C). Interestingly, the co-administration of brivanib alaninate prevented the tamoxifen induced increase in ER mRNA (Fig. 6C) and there was a decrease in total ER expression (Fig. 6D). It appears that the administration of an inhibitor of VEGFR-2 can modulate the ER during the anti-tumour process and this is an area worthy of further investigation. Conversely, the expression of VEGFR-2 on the cancer cells in response to oestrogen is clearly important to maintain control of tumour growth. These observations further validate the use of a combination of an anti-oestrogen and an angiogenesis inhibitor.

In addition to inhibiting VEGFR-2, the inhibitor has also shown activity against FGFR-1 in other tumour models, and is thus useful as a dual inhibitor for angiogenesis.[24] In the present study, however, we were unable to detect FGFR-1 in our specific model.

Despite the encouraging results obtained in the present study, several recent reports[50–52] of either the development of resistance to antiangiogenic drugs[50] or enhanced metastatic spread with low dose antiangiogenic drugs[51,52] deserve consideration. Clinical trials have shown that the majority of human tumour types do not respond to inhibitors of integrin as an antiangiogenic strategy. Laboratory models now show[52] that low concentrations of $\alpha_v\beta_3$ and $\alpha_v\beta_5$ inhibitors increase tumour growth via VEGFR-2 trafficking. This promotes endothelial cell migration to VEGF. In related studies, inhibitors of VEGFR can either enhance tumour cell seeding in 'metastatic assays'[51] or cause adaptive–evasive responses by tumours with greater malignancy and increased invasiveness.[50] Clearly, the complexity of the angiogenic survival signalling pathways present a challenge to seek the clinical relevance of pre-clinical pharmacology. Nevertheless, in a recent review, Ebos and co-workers[53] contend that it remains unclear whether antiangiogenic therapy will lead to increased invasion or metastases after long- or short-term treatments. There are more than 40+ adjuvant clinical trials in progress, so the question of the premature tumour resistance caused by low dose antiangiogenesis inhibitors will probably be answered first in the clinical setting.[53]

With this concern in mind, we are currently considering an initial short-term testing platform in ER positive metastatic breast cancer that has failed exhaustive endocrine therapy.[54,55] It is known that apoptosis and tumour regression can be induced by both high or low dose oestrogen clinically,[56,57] but we propose to use low dose oestrogen to reduce thromboembolic events. The therapeutic application of low dose oestrogen treatment is a direct translation of laboratory studies over the past 15 years.[58,59] By combining a dose escalation schedule of brivanib alaninate, we will be able to monitor tumour response precisely for the 12-week treatment schedule. These preliminary clinical data will guide our future adjuvant applications.

In summary, antiangiogenic agents have been utilised clinically in patients who have breast cancer that is refractory to other agents.[44] In these instances, to see a partial clinical benefit, higher doses that are potentially toxic have to be used. The observations that elevations of VEGFA and VEGFR-2 are associated with poor prognosis and response to tamoxifen therapy[48,60] suggests that a strategy to combine

anti-hormone treatment with an antiangiogenic strategy may have merit to test in clinical trials. Based on an increasing laboratory database that implicates an elevation in angiogenic factors in endocrine resistant breast cancer in the presence of tamoxifen,[43] we have provided evidence that a combination of tamoxifen plus a low dose dual inhibitor of VEGFR-2 and FGFR-1, brivanib alaninate, effectively controlled tumour growth. The strategy of combining a tyrosine kinase inhibitor of VEGFR-2 has the advantage of reducing toxicity, permitting long-term therapy and therefore compliance to enhance efficacy for adjuvant tamoxifen therapy. Indeed, the strategy of inhibiting angiogenesis, might in fact, improve responsiveness of those ER positive tumours that are refractory to tamoxifen alone. We believe this issue should be addressed in clinical trial.

Role of the funding source

Roshani Patel's salary is supported by 5T32CA10365-03. Surojeet Sengupta, Helen Kim, and Jennifer Pyle's salaries, as well as laboratory supplies supported by the following: the Department of Defense Breast Program under award number BC050277 Center of Excellence, SPORE in Breast Cancer CA 89018 (VCJ), Genuardis Fund (VCJ), FCCC Core Grant NIH P30 CA006927, the Avon Foundation and the Weg Fund of Fox Chase Cancer Center (VCJ). Bristol Myers Squibb provided funding for this research, as well as the drug, brivanib alaninate.

Conflict of interest statement

A research grant was provided as partial funding of this project by Bristol Myers Squibb. Brivanib alaninate was also provided by Bristol Myers Squibb.

Acknowledgements

This work was supported by the following grants: Department of Defense Breast Program under award number BC050277 Center of Excellence (Views and opinions of, and endorsements by the author(s) do not reflect those of the US Army or the Department of Defense) (VCJ), SPORE in Breast Cancer CA 89018 (VCJ), Genuardis Fund (VCJ), FCCC Core Grant NIH P30 CA006927, the Avon Foundation and the Weg Fund of Fox Chase Cancer Center (VCJ), Bristol Myers Squibb (VCJ), 5T32CA10365-03 (R.R.P.).

Special thanks to the animal histopathology laboratory at Fox Chase Cancer Center: Catherine Renner, Fangping Chen and Huafen Li. Technical Assistance: Korey Griffin at Santa Cruz Biotechnology, and Sheree Beane at Cell Signaling.

REFERENCES

1. Folkman J. Angiogenesis. *Annu Rev Med* 2006;**57**:1–18.
2. Folkman J. Angiogenesis: an organizing principle for drug discovery? *Nat Rev Drug Discov* 2007;**6**:273–86.
3. Naumov GN, Akslen LA, Folkman J. Role of angiogenesis in human tumor dormancy: animal models of the angiogenic switch. *Cell Cycle* 2006;**5**:1779–87.
4. Jain RK. Normalization of tumor vasculature: an emerging concept in antiangiogenic therapy. *Science* 2005;**307**:58–62.
5. Jain RK, Carmeliet PF. Vessels of death or life. *Sci Am* 2001;**285**:38–45.
6. Carmeliet P, Jain RK. Angiogenesis in cancer and other diseases. *Nature* 2000;**407**:249–57.
7. Goss PE, Ingle JN, Pater JL, et al. Late extended adjuvant treatment with letrozole improves outcome in women with early-stage breast cancer who complete 5 years of tamoxifen. *J Clin Oncol* 2008;**26**:1948–55.
8. Muss HB, Tu D, Ingle JN, et al. Efficacy, toxicity, and quality of life in older women with early-stage breast cancer treated with letrozole or placebo after 5 years of tamoxifen: NCIC CTG intergroup trial MA.17. *J Clin Oncol* 2008;**26**:1956–64.
9. Mamounas EP, Jeong JH, Wickerham DL, et al. Benefit from exemestane as extended adjuvant therapy after 5 years of adjuvant tamoxifen: intention-to-treat analysis of the national surgical adjuvant breast and bowel project B-33 trial. *J Clin Oncol* 2008;**26**:1965–71.
10. Jordan VC. Selective estrogen receptor modulation: concept and consequences in cancer. *Cancer Cell* 2004;**5**:207–13.
11. Buzdar A, Howell A, Cuzick J, et al. Comprehensive side-effect profile of anastrozole and tamoxifen as adjuvant treatment for early-stage breast cancer: long-term safety analysis of the ATAC trial. *Lancet Oncol* 2006;**7**:633–43.
12. Crivellari D, Sun Z, Coates AS, et al. Letrozole compared with tamoxifen for elderly patients with endocrine-responsive early breast cancer: the BIG 1-98 trial. *J Clin Oncol* 2008;**26**:1972–9.
13. Takei H, Lee ES, Jordan VC. In vitro regulation of vascular endothelial growth factor by estrogens and antiestrogens in estrogen-receptor positive breast cancer. *Breast Cancer* 2002;**9**:39–42.
14. Hyder SM, Nawaz Z, Chiappetta C, et al. Identification of functional estrogen response elements in the gene coding for the potent angiogenic factor vascular endothelial growth factor. *Cancer Res* 2000;**60**:3183–90.
15. Hyder SM. Sex-steroid regulation of vascular endothelial growth factor in breast cancer. *Endocr Relat Cancer* 2006;**13**:667–87.
16. Hyder SM, Stancel GM, Chiappetta C, et al. Uterine expression of vascular endothelial growth factor is increased by estradiol and tamoxifen. *Cancer Res* 1996;**56**:3954–60.
17. Kirk E. Dog's tale of survival opens door in cancer research. USA Today 2002. Available from: http://www.usatoday.com/news/health/2002-07-24-cover-cancer_x.htm.
18. Blackwell KL, Haroon ZA, Shan S, et al. Tamoxifen inhibits angiogenesis in estrogen receptor-negative animal models. *Clin Cancer Res* 2000;**6**:4359–64.
19. Ferrara N, Hillan KJ, Gerber HP, et al. Discovery and development of bevacizumab, an anti-VEGF antibody for treating cancer. *Nat Rev Drug Discov* 2004;**3**:391–400.
20. Wedam SB, Low JA, Yang SX, et al. Antiangiogenic and antitumor effects of bevacizumab in patients with inflammatory and locally advanced breast cancer. *J Clin Oncol* 2006;**24**:769–77.
21. Miller K, Wang M, Gralow J, et al. Paclitaxel plus bevacizumab versus paclitaxel alone for metastatic breast cancer. *N Engl J Med* 2007;**357**:2666–76.
22. Ferrara N. Vascular endothelial growth factor: basic science and clinical progress. *Endocr Rev* 2004;**25**:581–611.
23. Eskens FA, Verweij J. The clinical toxicity profile of vascular endothelial growth factor (VEGF) and vascular endothelial

growth factor receptor (VEGFR) targeting angiogenesis inhibitors; a review. *Eur J Cancer* 2006;**42**:3127–39.
24. Huynh H, Ngo VC, Fargnoli J, et al. Brivanib alaninate, a dual inhibitor of vascular endothelial growth factor receptor and fibroblast growth factor receptor tyrosine kinases, induces growth inhibition in mouse models of human hepatocellular carcinoma. *Clin Cancer Res* 2008;**14**:6146–53.
25. Bhide RS, Cai ZW, Zhang YZ, et al. Discovery and preclinical studies of (R)-1-(4-(4-fluoro-2-methyl-1H-indol-5-yloxy)-5-methylpyrrolo[2,1-f][1,2,4]triazin-6-yloxy)propan-2-ol (BMS-540215), an in vivo active potent VEGFR-2 inhibitor. *J Med Chem* 2006;**49**:2143–6.
26. Rosen LS, Wilding G, Sweeney C, et al. Phase I dose escalation study to determine the safety, pharmacokinetics and pharmacodynamics of BMS-582664, a VEGFR/FGFR inhibitor in patients with advanced/metastatic solid tumors. *J Clin Oncol* 2006;**24**:3051.
27. Jonker DJ, Rosen LS, Sawyer M, et al. A phase I study of BMS-582664 (brivanib alaninate), an oral dual inhibitor of VEGFR and FGFR tyrosine kinases, in patients (pts) with advanced/metastatic solid tumors: safety, pharmacokinetic (PK), and pharmacodynamic (PD) findings. *J Clin Oncol* 2007;**25**:3559.
28. Gottardis MM, Robinson SP, Jordan VC. Estradiol-stimulated growth of MCF-7 tumors implanted in athymic mice: a model to study the tumoristatic action of tamoxifen. *J Steroid Biochem* 1988;**30**:311–4.
29. O'Regan RM, Cisneros A, England GM, et al. Effects of the antiestrogens tamoxifen, toremifene, and ICI 182, 780 on endometrial cancer growth. *J Natl Cancer Inst* 1998;**90**:1552–8.
30. Gottardis MM, Robinson SP, Satyaswaroop PG, et al. Contrasting actions of tamoxifen on endometrial and breast tumor growth in the athymic mouse. *Cancer Res* 1988;**48**:812–5.
31. O'Regan RM, Gajdos C, Dardes RC, et al. Effects of raloxifene after tamoxifen on breast and endometrial tumor growth in athymic mice. *J Natl Cancer Inst* 2002;**94**:274–83.
32. Gottardis MM, Jordan VC. Development of tamoxifen-stimulated growth of MCF-7 tumors in athymic mice after long-term antiestrogen administration. *Cancer Res* 1988;**48**:5183–8187.
33. Robinson SP, Jordan VC. Antiestrogenic action of toremifene on hormone-dependent, -independent, and heterogeneous breast tumor growth in the athymic mouse. *Cancer Res* 1989;**49**:1758–62.
34. Stossi F, Barnett DH, Frasor J, et al. Transcriptional profiling of estrogen-regulated gene expression via estrogen receptor (ER)α or ERβ in human osteosarcoma cells: distinct and common target genes for these receptors. *Endocrinology* 2004;**145**:3473–86.
35. Gowri PM, Sengupta S, Bertera S, et al. Lipin1 regulation by estrogen in uterus and liver: implications for diabetes and fertility. *Endocrinology* 2007;**148**:3685–93.
36. Frasor J, Danes JM, Komm B, et al. Profiling of estrogen up- and down-regulated gene expression in human breast cancer cells: insights into gene networks and pathways underlying estrogenic control of proliferation and cell phenotype. *Endocrinology* 2003;**144**:4562–74.
37. Livak KJ, Schmittgen TD. Analysis of relative gene expression data using real-time quantitative PCR and the 2(–$\Delta\Delta$C(T)) method. *Methods* 2001;**25**:402–8.
38. Cai ZW, Zhang Y, Borzilleri RM, et al. Discovery of brivanib alaninate ((S)-((R)-1-(4-(4-fluoro-2-methyl-1H-indol-5-yloxy)-5-methylpyrrolo[2,1-f][1,2,4]triazin-6-yloxy)propan-2-yl)2-aminopropanoate), a novel prodrug of dual vascular endothelial growth factor receptor-2 and fibroblast growth factor receptor-1 kinase inhibitor (BMS-540215). *J Med Chem* 2008;**51**:1976–80.
39. O'Regan RM, Osipo C, Ariazi E, et al. Development and therapeutic options for the treatment of raloxifene-stimulated breast cancer in athymic mice. *Clin Cancer Res* 2006;**12**:2255–63.
40. Dardes RC, O'Regan RM, Gajdos C, et al. Effects of a new clinically relevant antiestrogen (GW5638) related to tamoxifen on breast and endometrial cancer growth in vivo. *Clin Cancer Res* 2002;**8**:1995–2001.
41. Rosenbaum-Dekel Y, Fuchs A, Yakirevich E, et al. Nuclear localization of long-VEGF is associated with hypoxia and tumor angiogenesis. *Biochem Biophys Res Commun* 2005;**332**:271–8.
42. Qu Z, Van Ginkel S, Roy AM, et al. Vascular endothelial growth factor reduces tamoxifen efficacy and promotes metastatic colonization and desmoplasia in breast tumors. *Cancer Res* 2008;**68**:6232–40.
43. Aesoy R, Sanchez BC, Norum JH, et al. An autocrine VEGF/VEGFR2 and p38 signaling loop confers resistance to 4-hydroxytamoxifen in MCF-7 breast cancer cells. *Mol Cancer Res* 2008;**6**:1630–8.
44. Burstein HJ, Elias AD, Rugo HS, et al. Phase II study of sunitinib malate, an oral multitargeted tyrosine kinase inhibitor, in patients with metastatic breast cancer previously treated with an anthracycline and a taxane. *J Clin Oncol* 2008;**26**:1810–6.
45. Kranz A, Mattfeldt T, Waltenberger J. Molecular mediators of tumor angiogenesis: enhanced expression and activation of vascular endothelial growth factor receptor KDR in primary breast cancer. *Int J Cancer* 1999;**84**:293–8.
46. Scherbakov AM, Lobanova YS, Shatskaya VA, et al. Activation of mitogenic pathways and sensitization to estrogen-induced apoptosis: two independent characteristics of tamoxifen-resistant breast cancer cells? *Breast Cancer Res Treat* 2006;**100**:1–11.
47. Weigand M, Hantel P, Kreienberg R, et al. Autocrine vascular endothelial growth factor signalling in breast cancer. Evidence from cell lines and primary breast cancer cultures in vitro. *Angiogenesis* 2005;**8**:197–204.
48. Ryden L, Linderholm B, Nielsen NH, et al. Tumor specific VEGF-A and VEGFR2/KDR protein are co-expressed in breast cancer. *Breast Cancer Res Treat* 2003;**82**:147–54.
49. Pink JJ, Jordan VC. Models of estrogen receptor regulation by estrogens and antiestrogens in breast cancer cell lines. *Cancer Res* 1996;**56**:2321–30.
50. Paez-Ribes M, Allen E, Hudock J, et al. Antiangiogenic therapy elicits malignant progression of tumors to increased local invasion and distant metastasis. *Cancer Cell* 2009;**15**:220–31.
51. Ebos JM, Lee CR, Cruz-Munoz W, et al. Accelerated metastasis after short-term treatment with a potent inhibitor of tumor angiogenesis. *Cancer Cell* 2009;**15**:232–9.
52. Reynolds AR, Hart IR, Watson AR, et al. Stimulation of tumor growth and angiogenesis by low concentrations of RGD-mimetic integrin inhibitors. *Nat Med* 2009;**1**:392–400.
53. Ebos JM, Lee CR, Kerbel RS. Tumor and host-mediated pathways of resistance and disease progression in response to antiangiogenic therapy. *Clin Cancer Res* 2009;**15**:5020–5.
54. Jordan VC, Lewis-Wambi J, Kim H, et al. Exploiting the apoptotic actions of oestrogen to reverse antihormonal drug resistance in oestrogen receptor positive breast cancer patients. *Breast* 2007;**16**:S105–13.
55. Jordan VC, Lewis-Wambi JS, Patel RR, et al. New hypotheses and opportunities in endocrine therapy: amplification of oestrogen-induced apoptosis. *Breast* 2009;**18**:S10–7.
56. Lonning PE, Taylor PD, Anker G, et al. High-dose estrogen treatment in postmenopausal breast cancer patients heavily exposed to endocrine therapy. *Breast Cancer Res Treat* 2001;**67**:111–6.

57. Ellis MJ, Gao F, Dehdashti F, et al. Lower-dose vs high-dose oral estradiol therapy of hormone receptor-positive, aromatase inhibitor-resistant advanced breast cancer: a phase 2 randomized study. *JAMA* 2009;**302**:774–80.
58. Wolf DM, Jordan VC. *A laboratory model to explain the survival advantage observed in patients taking adjuvant tamoxifen therapy. Recent results in cancer research*. Heidelberg: Springer-Verlag; 1993. p. 23–33.
59. Yao K, Lee ES, Bentrem DJ, et al. Antitumor action of physiological estradiol on tamoxifen-stimulated breast tumors grown in athymic mice. *Clin Cancer Res* 2000;**6**:2028–36.
60. Ryden L, Stendahl M, Jonsson H, et al. Tumor-specific VEGF-A and VEGFR2 in postmenopausal breast cancer patients with long-term follow-up. Implication of a link between VEGF pathway and tamoxifen response. *Breast Cancer Res Treat* 2005;**89**:135–43.

Journal of Medicinal Chemistry Article

J. Med. Chem. **2010,** *53,* 3273–3283 **3273**
DOI: 10.1021/jm901907u

Structure−Function Relationships of Estrogenic Triphenylethylenes Related to Endoxifen and 4-Hydroxytamoxifen

Philipp Y. Maximov,[†,‡] Cynthia B. Myers,[†] Ramona F. Curpan,[§] Joan S. Lewis-Wambi,[†] and V. Craig Jordan*[,∥]

[†]*Fox Chase Cancer Center, Philadelphia, Pennsylvania,* [‡]*Russian State Medical University, Moscow, Russia,* [§]*Institute of Chemistry, Romanian Academy, Timisoara, Romania, and* [∥]*Lombardi Comprehensive Cancer Center, Georgetown University, 3970 Reservoir Road, NW, Research Building, E501, Washington, DC 20057-1468*

Received December 23, 2009

Estrogens can potentially be classified into planar (class I) or nonplanar (class II) categories, which might have biological consequences. 1,1,2-Triphenylethylene (TPE) derivatives were synthesized and evaluated against 17β-estradiol (E2) for their estrogenic activity in MCF-7 human breast cancer cells. All TPEs were estrogenic and, unlike 4-hydroxytamoxifen (4OHTAM) and Endoxifen, induced cell growth to a level comparable to that of E2. All the TPEs increased ERE activity in MCF-7:WS8 cells with the order of potency as followed: E2 > 1,1-bis(4,4′-hydroxyphenyl)-2-phenylbut-1-ene (**15**) > 1,1,2-tris(4-hydroxyphenyl)but-1-ene (**3**) > *Z* 4-(1-(4-hydroxyphenyl)-1-phenylbut-1-en-2-yl)phenol (**7**) > *E* 4-(1-(4-hydroxyphenyl)-1-phenylbut-1-en-2-yl)phenol (**6**) > *Z*(4-(1-(4-ethoxyphenyl)-1-(4-hydroxyphenyl)but-1-en-2-yl)phenol (**12**) > 4-OHTAM. Transient transfection of the ER-negative breast cancer cell line T47D:C4:2 with wild-type ER or D351G ER mutant revealed that all of the TPEs increased ERE activity in the cells expressing the wild-type ER but not the mutant, thus confirming the importance of Asp351 for ER activation by the TPEs. The findings confirm E2 as a class I estrogen and the TPEs as class II estrogens. Using available conformations of the ER liganded with 4OHTAM or diethylstilbestrol, the TPEs optimally occupy the 4OHTAM ER conformation that expresses Asp351.

Introduction

Breast cancer is one of the most frequently diagnosed cancers among women in the United States, with an estimated 192370 new cases of invasive disease and 40170 deaths in 2009.[1] Although the exact etiology of breast cancer is not known, there is strong evidence that estrogen plays a role in its development and progression.[2] The effects of estrogen are mediated via the estrogen receptors (ERs[a]), ER-alpha (ERα) and ER-beta (ERβ), which are present in more than 80% of breast tumors. With regard to the therapy of breast cancer, ERα remains the most important target and its presence in breast tumors is routinely used to predict response to selective ER modulators (SERMs), such as tamoxifen (TAM).[3,4] TAM (Figure 1) is also the first chemotherapeutic drug to target ER-positive breast cancer cells[5] and prevent tumorigenesis in high-risk women.[6] TAM is available worldwide to treat patients with ER-positive breast cancers.

TAM is a substituted derivative[7,8] of the long-acting estrogen triphenylethylene.[9] TAM efficacy depends on the formation of clinically active metabolites 4-hydroxytamoxifen (4OHTAM)[10] and Endoxifen[11] (Figure 1), which have a greater affinity to ERα and a much higher antiestrogenic potency in breast cancer cells compared to the parent drug.

We are unaware of the subtle molecular changes that occur when estrogen binds to the ER to produce the ER complex because the whole complex has not been crystallized. As a consequence of this gap in our knowledge, the modulation of ERα can only be deduced by exploring structure−function relationships. However, the ligand binding domain (LBD) of ERα has been crystallized[12,13] with the estrogens 17β-estradiol (E2), diethylstilbestrol (DES), and the SERMs, 4OHTAM and raloxifene (Figure 1). The resolution of the structure of the estrogen: LBD complex by X-ray crystallography demonstrates that the planar estrogens E2 and DES are sealed within the LBD by helix 12.[12,13] This activates activating function (AF)-2 at the upper surface of helix 12 by the interaction with coactivators to facilitate full estrogen action. In contrast, the bulky side chain of 4OHTAM and raloxifene prevents helix-12 from sealing the LBD and this produces antiestrogenic action.[12,13] However, although AF-2 is deactivated, the 4OHTAM:ERα complex has estrogen-like activity,[14] whereas raloxifene does not.[15] This is believed to be because the side chain of raloxifene shields and neutralizes asp351 to block estrogen action.[16] In contrast, the side chain of tamoxifen is too short. It appears that when helix 12 is not positioned correctly the exposed asp351 can interact with AF-1 to produce estrogen action. This estrogen-like activity can be

*To whom correspondence should be addressed. Phone: (202) 687-2795. Fax: (202) 687-6402. E-mail: vcj2@georgetown.edu.

[a] Abbreviations: ER, estrogen receptor; SERM, selective estrogen receptor modulators; TAM, tamoxifen; 4OHTAM, 4-hydroxytamoxifen; LBD, ligand binding domain; E2, 17β-estradiol; DES, diethylstilbestrol; AF, activating function; TPE, triphenylethylene; EC_{50}, effective concentration 50%; ERE, estrogen response element; rmsd, root-mean-square deviation; THF, tetrahydrofuran; RPMI, Roswell Park Memorial Institute; FBS, fetal bovine serum; SFS, stripped fetal bovine serum; PBS, phosphate buffered saline; OPTI-MEM, Optimum Eagle's Minimum Essential Media; RCSB, Research Collaboratory for Structural Bioinformatics; PDB, Protein Data Bank; OPLS, optimized potential for liquid simulations; IFD, induced fit.

© 2010 American Chemical Society

Published on Web 03/24/2010

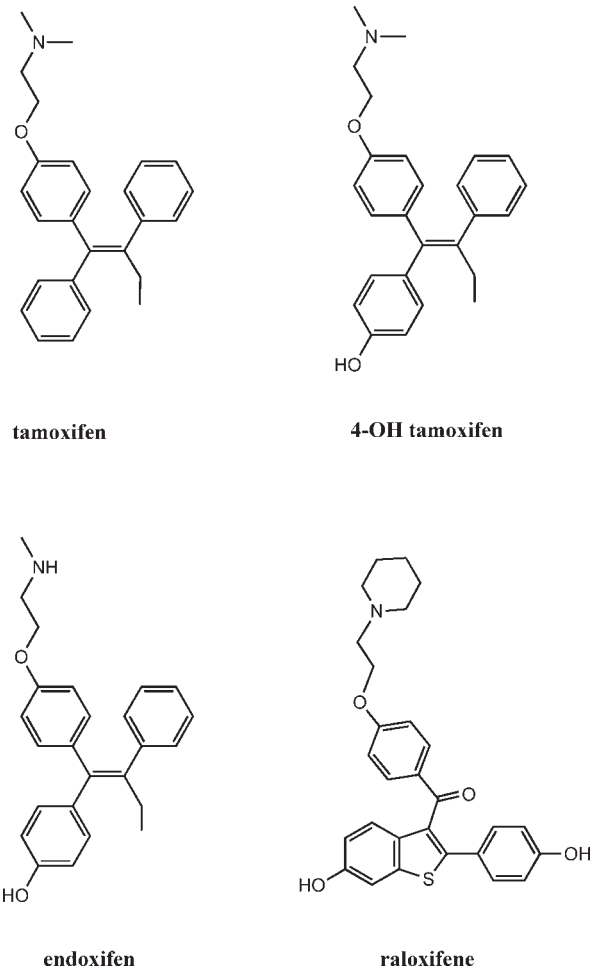


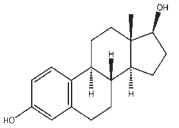
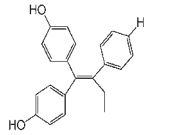
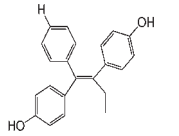
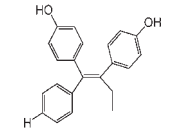
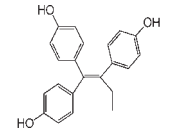
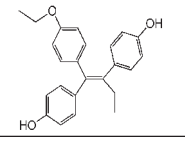
Figure 1. The formula of tamoxifen and its hydroxylated metabolites Endoxifen, and 4OHTAM. The related SERM raloxifene is shown for comparison.

inhibited by substituting asp351 for glycine an uncharged amino acid.[17]

Planar or nonplanar compounds are both classified as estrogens based on their actions to cause growth of the immature rodent uterus or provoke vaginal cornification in castrate animals. However, knowledge of the structure of the 4OHTAM:ER LBD complex[13] led to the idea that all estrogens may not be the same in their interactions with ER.[18] Previous studies suggest that nonplanar triphenylethylenes (TPEs) with a bulky phenyl substituent prevents helix-12 from completely sealing the LBD pocket.[18] This physical event creates a putative "antiestrogen like" configuration within the complex. However, the complex is not antiestrogenic because Asp351 is exposed to communicate with AF-1, thereby causing estrogen-like action. Thus, there are putative class I (planar) and class II (nonplanar) estrogens.[18] A similar classification and conclusion has been proposed,[19] but the biological consequences of this classification are unknown.

In this report, we further addressed the hypothesis that the shape of the ER complex can be controlled by the shape of an estrogen. We have synthesized a range of hydroxylated TPEs to establish new tools to investigate the relationship of shape with estrogenic activity through the exposure of Asp351. For convenience, the structure of nonsteroidal antiestrogens described in the text are illustrated in Figure 1 and the test compounds in Table 1.

Table 1. The EC_{50} Values for E2 and the Tested Triphenylethylenes in MCF-7:WS8 Cells Proliferation Assays

Compound	Structure	EC_{50}
E2		$1x10^{-3}$ nM
15		$5x10^{-2}$ nM
6		$1x10^{-1}$ nM
7		$1x10^{-1}$ nM
3		$1.5x10^{-1}$ nM
12		4.0 nM

Results

Chemistry. The general synthetic routes used to prepare substituted 1,1,2-tribenzyl-but-1-ene compounds are outlined in Scheme 1. Desoxyanisoin was treated with potassium *t*-butoxide followed by reflux with ethyl iodide to give **1** in 74% yield. Intermediate **1** was refluxed with the formed Grignard reagent of 4-bromoanisole and then treated with phosphoric acid to yield **2**. Removal of the methoxide groups was accomplished with boron tribromide to give **3**. Isomers **6**−**7** were synthesized from **1** by treatment with the formed Grignard reagent of bromobenzene followed by reflux in phosphoric acid to yield isomers **4**−**5**. Removal of the two methoxides was accomplished with boron tribromide resulting in isomers **6**−**7**. Compounds **11**−**12** were obtained by reaction of desoxyanisoin with glacial acetic acid and hydroiodic acid to give **8** in 90% yield. Dihydroxy **8** was protected using 3,4-dihydro-2*H*-pyran and *p*-toluene sulfonic acid to form **9**. Compound **9** was treated with potassium *t*-butoxide followed by reflux with ethyl iodide to yield **10** in 87%. Compound **10** was refluxed with the formed Grignard reagent of 4-bromophenetole, followed by acid hydrolysis using phosphoric acid to yield isomers **11**−**12**. Synthesis of 15 proceeded from reaction of anisole with 2-phenylbutyryl chloride to form monomethoxide **13** in 94% yield. Compound **13** was coupled with 4-methoxyphenyl magnesium bromide, followed by phosphoric acid to produce **14**. The methoxides of **14** were treated with boron tribromide to give dihydroxy **15**.

Pharmacology. We compared and contrasted the estrogen-like properties of the hydroxylated TPEs to promote proliferation in the ERα-positive human breast cancer cell

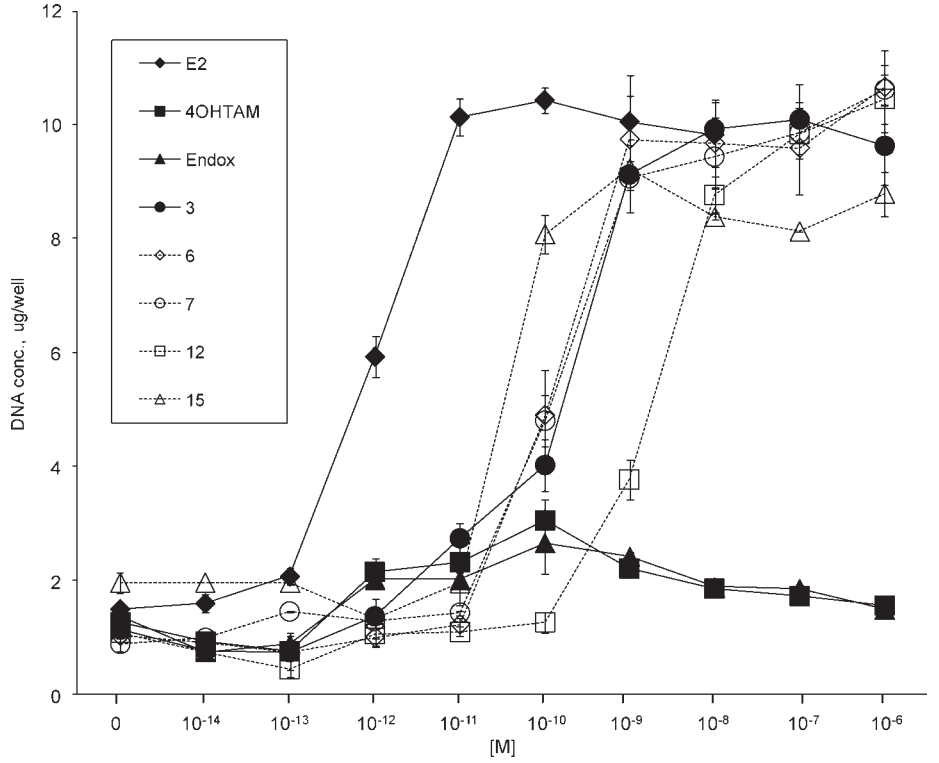
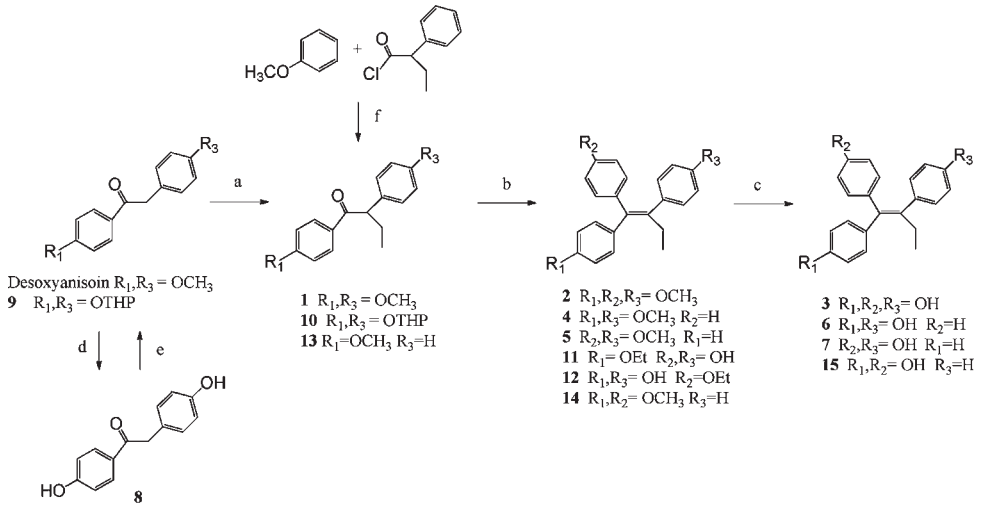


Figure 2. Effects of E2, test TPEs **3**, **6**, **7**, **12**, and **15** and antiestrogens 4OHTAM and Endoxifen on the proliferation of MCF-7:WS8 breast cancer cells. Cells were treated with the indicated compounds for 7 days.

Scheme 1. Synthesis of Substituted 1,1,2-Tribenzyl-but-1-ene Compounds[a]



[a] Reaction conditions: (a) KOtBu, ether, 1 h, then, EtI, reflux 12 h; (b) 4-$BrMgC_6H_4R_2$, THF, refluxed 12 h, then, H_3PO_4, refluxed 2 h; (c) BBr_3, CH_2Cl_2, 4 days; (d) HI, AcOH, 130−140 °C, 4 h; (e) C_5H_8O, *p*-$CH_3C_6H_4SO_3H$-H_2O, 0 °C 4.5 h; (f) $AlCl_3$, CS_2, 20 °C, 22 h.

line MCF-7:WS8. Compounds were compared with the tamoxifen metabolites 4-OHTAM and Endoxifen, which have a high affinity for the ER (because of the appropriately positioned phenolic hydroxyl) but are antiestrogenic because of the alkylaminoethoxy-side chain. To compare the biological activities of the tested TPEs, we employed DNA proliferation assays which are described in the Materials and Methods.

Figure 2 shows that our MCF-7:WS8 human breast cancer cells were exquisitely sensitive to E2, which produced a concentration-dependent increase in growth with maximal stimulation at 1×10^{-11} M. All of the TPE's were potent agonists with the ability to stimulate MCF-7:WS8 breast cancer cell growth, however, their agonist potency was less compared to E2, which had an effective concentration 50% (EC_{50}) of 1×10^{-12} M. The most potent of the phenolic TPEs was bisphenol (**15**), with an EC_{50} of approximately 5×10^{-11} M. The second potent were the *E* and *Z*-isomers of the diphenolic TPEs, compounds **6** and **7**, which both had an EC_{50} of approximately 1×10^{-10} M. The triphenolic TPE (**3**) was slightly less active, with an EC_{50} of approximately 1.5×10^{-10} M, whereas the ethoxy TPE (**12**) was the least potent, with an EC_{50} of approximately 4×10^{-9} M. The EC_{50} values for all the tested compounds are outlined

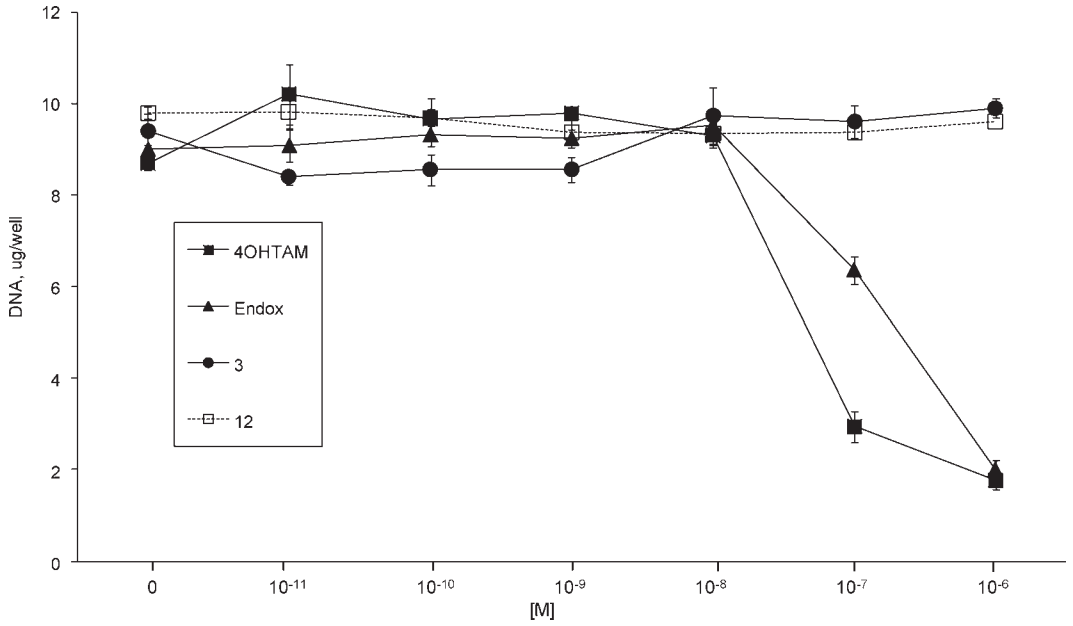


Figure 3. The ability of the tested TPEs **3** and **12** and 4OHTAM and Endoxifen to inhibit estradiol-stimulated MCF-7:WS8 breast cancer cell growth. Cells were treated with indicated compounds for 7 days.

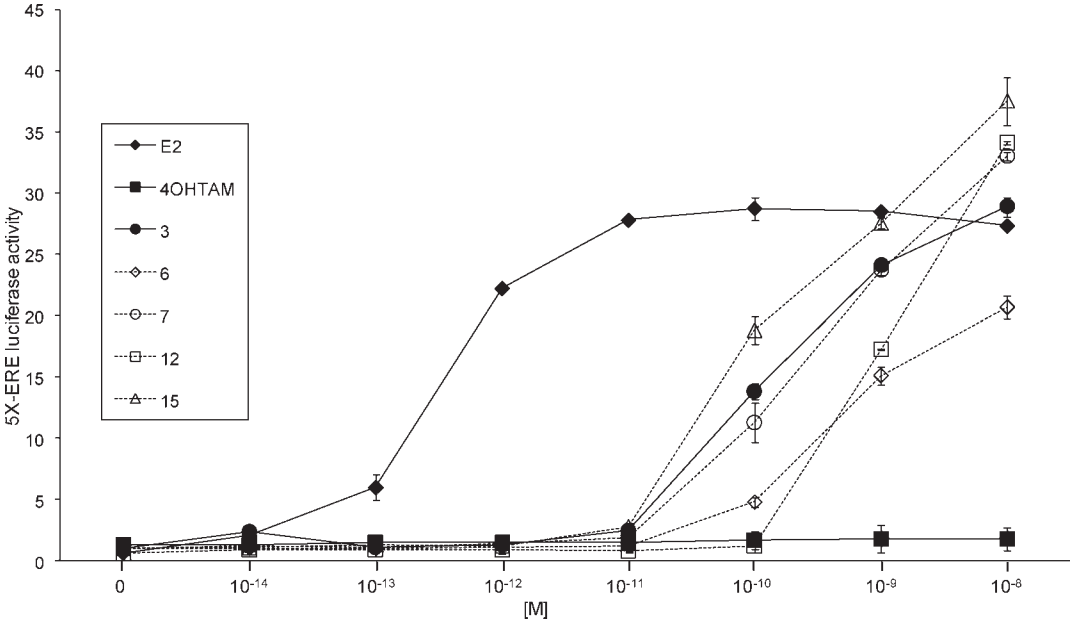


Figure 4. ERE luciferase assay in MCF-7:WS8 cells transiently transfected with an ERE luciferase construct and treated with E2, test TPEs **3**, **6**, **7**, **12**, and **15** and 4OHTAM.

in Table 1. The compound **12** was prepared to replicate a molecule without the alkyl nitrogen group of 4-OHTAM or Endoxifen, and this derivative had reduced estrogenic potency comparison to the other TPEs, however, the molecule remained a full estrogen agonist in our proliferation assays. The metabolites, 4-OHTAM and Endoxifen, had no significant agonist effect in MCF-7:WS8 cells, however, these compounds at 1 μM were able to completely inhibit estradiol-stimulated MCF-7:WS8 breast cancer cell growth (Figure 3), thus confirming their role as antagonists/antiestrogens. Similar experiments performed with compounds **3** and **12** showed an inability to block estradiol-stimulated growth in MCF-7:WS8 cells at concentrations up to 1 μM (Figure 3). On the basis of these findings, compounds **3** and **12** were classified as estrogens with a pharmacology, in this assay, indistinguishable from the natural planar estrogen E2.

It is interesting to note that compounds **6** and **7**, which are the *E*- and *Z*-isomers of the diphenolic TPEs, were equivalent in their agonistic potency, thus suggesting that isomerization occurs in vitro given an equilibrium mixture. This phenomenon has been noted previously with the *E*-isomer of 4-OHTAM,[20] but the true pharmacology of the separate isomers was eventually resolved by the synthesis of fixed ring analogues.[20,21] Both the *E*- and *Z*-isomers of 4-OHTAM are antiestrogenic because they block the proliferation of estradiol-stimulated growth in MCF-7 breast cancer cells and they inhibit estradiol-stimulated prolactin gene activation.

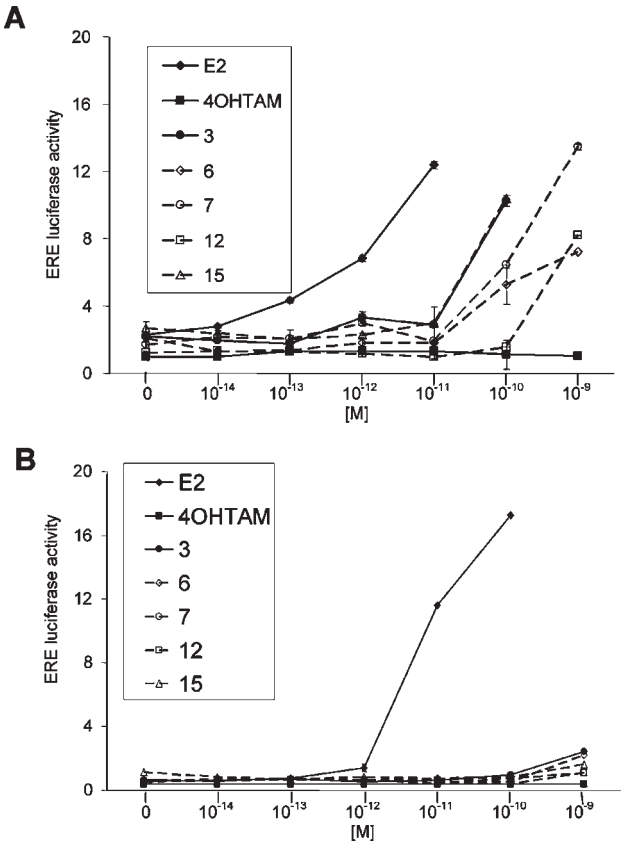


Figure 5. Luciferase assay in ER-negative T47D:C4:2 cells, transiently transfected with ERE luciferase and wild type (A) and D351G (B) mutant ER constructs, respectively, and treated with E2, tested TPEs **3**, **6**, **7**, **12**, and **15** and 4OHTAM. Results demonstrate that substitution of Asp351 to Gly in ER abrogates the agonistic activity on all tested TPEs (class II estrogens), except planar E2 (class I estrogen).

The *E*-isomer is however approximately 1/100 the potency of the *Z*-isomer.

To determine the ability of the test TPEs to activate the ER, MCF-7:WS8 cells were transiently transfected with an estrogen response element (ERE)-luciferase reporter gene encoding the firefly reporter gene with five consecutive EREs under the control of a TATA promoter. The binding of ligand-activated ER complex at the EREs in the promoter of the luciferase gene activates transcription. The measurement of the luciferase expression levels permits a determination of agonist activity of the TPE:ER complex. Figure 4 shows that all the phenolic TPEs were estrogenic, but E2 was 100 times more potent than the most potent TPE bisphenol (**15**). The order of potency was as follows: E2 > **15** > **3** > **7** > **6** > **12** > 4-OHTAM. None of the tested TPEs were antiestrogenic in this assay.

Our goal was to confirm and advance the hypothesis that the shape of the estrogen ER complex was different for planar and nonplanar (TPE -like) estrogens. This hypothesis has been advanced independently by ourselves[18,22] and Gust's group.[19] Through a series of studies using mutant ER expression in an ER negative breast cancer cell line, we found that the mutant D351G ER completely suppressed estrogen-like properties of 4-OHTAM at an endogenous TGFα target gene.[17] Use of this assay led us to classify planar estrogens (DES or E2) as class I and nonplanar estrogens (TPE-type) as class II. A broad group of compound structures were used in this study to establish whether a class II compound could become nonestrogenic with the D351G ER mutant.

Our series of phenolic TPEs were evaluated in the ER-negative breast cancer cell line T47D:C42,[23] which was transiently transfected with an ERE luciferase plasmid and either the wild-type ER or the D351G mutant ER. Figure 5A shows that in the presence of the wild-type ER all of the tested TPE compounds were potent agonists with the ability to significantly enhance ERE luciferase activity. In contrast, when the D351G mutant ER gene was transfected with the ERE luciferase reporter, only the planar E2 was estrogenic, whereas the TPEs did not activate the ERE reporter gene (Figure 5B). Overall, these results confirm the importance of Asp351 in ER activation by TPE ligands to trigger estrogen action.

Analysis of the Induced Fit Models for Tested TPEs. Data analysis was performed on top ranked poses for each of the tested TPEs and for comparison reasons on 4OHTAM (Figure 6A). The top ranked structure from induced fit for 4OHTAM has a ligand root-mean-square deviation (rmsd) of 0.55 Å compared with the experimental structure. In addition to the low ligand rmsd, there is a good similarity between the 3ert crystal structure and the top-ranked structures from docking (Figure 6B), the conformations of D351, E353, R394, T347, H524, and the rest of amino acids which line the binding site are nearly superimposable in both structures. Also, the well-known network of H-bonds is formed between 4OHTAM and E353, R394, and water molecules. The most significant difference is that in the top docked pose of 4OHTAM, the antiestrogenic chain is moved closer to D351 to form the interaction between the amino group of 4OHTAM and carboxylate of D351. Induced fit docking of the TPE derivatives: **3**, **6**, **7**, **12**, **15**, and Endoxifen in the ligand binding domain of ERα (3ert) has yielded ligand poses which display a binding mode (Figure 6B) very similar with that of 4OHTAM in the ER binding site (Figure 6A). Thus, the superimposition of the top ranked poses of each ligand onto the 4OHTAM cocrystallized with ERα (binding cavity filled with water) shows the ligands binding to the receptor in a similar mode with 4OHTAM, having the propensity to form the same hydrophobic contacts with the amino acids lining the binding cavity. Furthermore, the complex H-bond network is formed with E353, R394, H524, and a highly ordered water molecule positioned between E353 and R394 (Figure 6B). Interestingly, a H-bond has been noticed between the hydroxyl group of **15**, **3**, **7**, and the side chain of T347 is stabilized by an additional interaction with a water molecule from close proximity and precludes the interaction of the ligands with D351. The situation is different when water is removed from the binding site. In this case, the OH is shifted so that the H interacts with the carboxylate group of D351 and the HO group of T347 is shifted to form a H-bond with the oxygen. (data not shown). The molecular docking results have shown that most of the compounds form the H-bond network encountered in the case of agonists (E353, R394, H524, water) and display hydrophobic interactions with the amino acids lining the binding site. An interesting interaction is the hydrogen bond with T347 which seems to be stabilized by a water molecule and it was observed in different docking simulations (flexible and rigid). However, analysis of other ER crystal structures has not revealed additional data to confirm this interaction. Additional work has to be done to verify the hypothesis

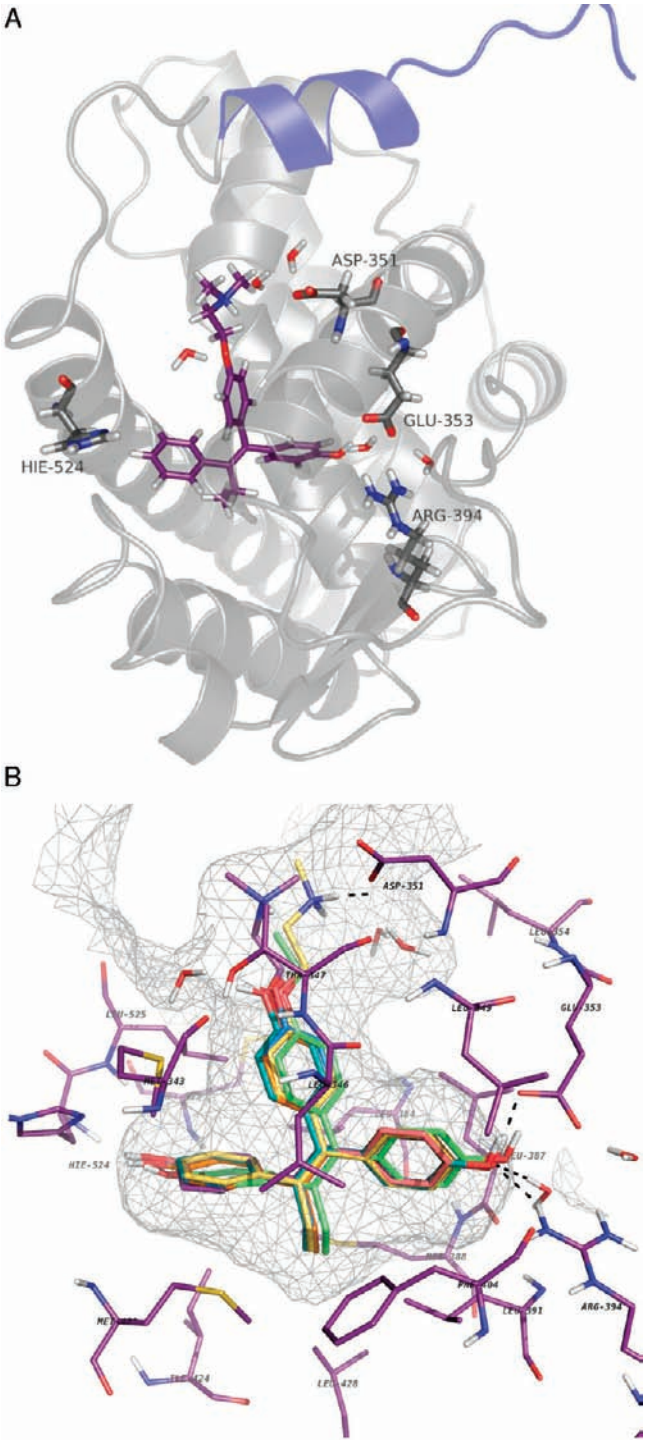


Figure 6. (A) Cartoon representation of the human ERα ligand binding domain complexed with 4-hydroxy tamoxifen, the antagonist conformation of the receptor. Helix 12 is depicted in blue, the amino acids involved in the H-bond network with the ligand are displayed as sticks. and the ligand is colored in purple. (B) Molecular docking of TPE derivatives into the binding site of ERα. For comparison reasons, the top ranked ligand−protein complex is superimposed on the crystal structure of the receptor cocrystallized with 4-OHT; the amino acids lining the biding sites of both complexes are shown and the complex H-bond network between ligand and the binding site is displayed. The induced fit docking poses of the ligands are colored as follow: **15** in cyan, **3** in blue, **6** in orange, **7** in pink, **12** in green, Endoxifen in yellow, while the crystal structure is depicted in purple.

(docking, binding energy calculations through semiempircal and/or ab initio methods, etc.). The interaction with D351 is weak (3.8−4 Å), and it was mostly noticed when the simulations were run with the receptor without water in the binding site. This would mean that D351 is exposed and not shielded so it could communicate intrinsic estrogenic properties of the complex to AF-1.

The best poses of the tested TPEs **3**, **6**, **7**, **12**, **15**, and Endoxifen, obtained from docking simulations ran against the antagonist conformation of the ER, were superimposed on the experimental agonist conformation of the ER (ER cocrystallized with estradiol, PDB code 1GWR) (Figure 7A). This has shown that these ligands are unlikely to be accommodated in the agonist conformation of the ER due to the sterical clashes between "Leu crown", mostly Leu525 and Leu540, helix 12, and ligands as depicted in Figure 7B, indicating, that these ligands most likely bind to ER's conformation more closely related with the antagonist form.

Discussion

The aim of this structure function relationship study was to evaluate the pharmacological properties of synthetic TPEs as estrogens in MCF-7 human breast cancer cells using the DNA proliferation assay and ERE luciferase assays. Our results show that all of the synthesized TPEs possess potent estrogen-like properties in our MCF-7 human breast cancer cells. These TPEs markedly increased cell growth and enhanced ERE luciferase activity. In contrast, the tamoxifen metabolites 4OHTAM and Endoxifen, which possess an alkylaminoethoxy side chain in their structure, failed to induce growth or increase ERE luciferase activity, thus confirming their role as antiestrogens.

X-ray crystallography of ER-4OHTAM and ER-Raloxifene complexes demonstrate that the presence of the alkyaminoethoxy side chain of 4OHTAM is crucial for the ER to gain an antagonistic conformation by displacing the H12 of the receptor by 4OHTAM's bulky side chain, thus preventing the binding of the coactivators.[13] On the basis of the results of our proliferation assays and the luciferase assays, it is clear that repositioning of the hydroxyl groups changed the biological potencies of the tested TPE compounds, which lowered their estrogenic potency compared to that of E2. However, the fact that these TPEs were able to significantly induce growth and ERE activation in MCF-7:WS8 cells demonstrated that they are still full agonists. The absence of the alkyaminoethoxy side chain on the tested TPEs does not allow these compounds to act as antiestrogens, like 4-OHTAM or Endoxifen, which possesses the alkyaminoethoxy side chain.[13] However, despite the changes in biological potencies of the tested TPEs, due to repositioning of the hydroxyl groups and addition of the ethoxy group, these compounds also maintained their ability to activate the ERE as was demonstrated in our ERE luciferase assays.

Another interesting aspect in our study is the importance of Asp351 in activation of the ER thereby acting as a molecular test for the presumed structure of the TPE:ER complex. On the basis of the X-ray crystallography of the ER in complex with 4OHTAM[13] and Raloxifene,[12] it was determined that the basic side chains of these antiestrogens are in proximity of Asp351 in the ER. It was hypothesized that this interaction with Raloxifene actually neutralizes and shields Asp351, preventing it from interacting with ligand-independent activating function 1 (AF-1). In contrast, 4OHTAM possesses some estrogenic activity because the side chain is too short.[13] Substitution of Asp351 with glycine leads to loss of estrogenic

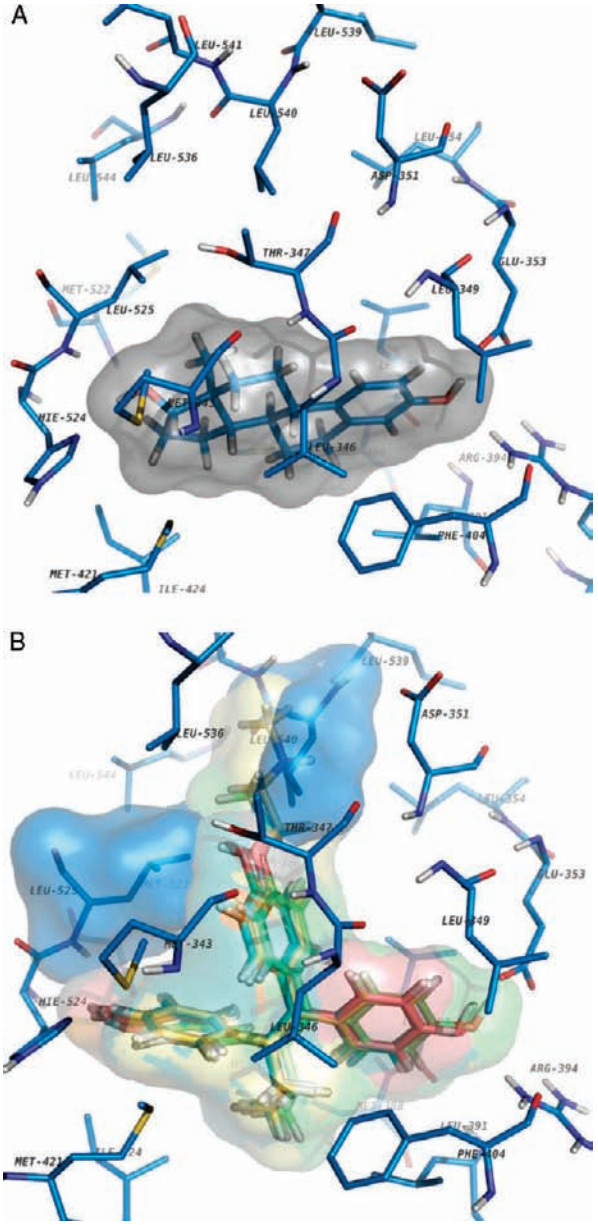


Figure 7. (A) View of ERα binding cavity. The X-ray crystal structure of ERα complexed with estradiol (PDB code 1GWR), the agonist conformation of the receptor. The amino acids lining the binding site are depicted as sticks colored by element. The color code is blue for carbon, red for oxygen, gray for nitrogen, and yellow for sulfur. The ligand is represented as sticks having the same colored code like the receptor and the ligand's surface is colored in gray. (B) View of ERα binding cavity. The best poses of BisPhen, TriOHTPE, EDiOHTPE, ZDiOHTPE, Z4EthoxDiOHTPE, Endox obtained from docking simulations ran against the antagonist conformation of the receptor are superimposed on the agonist conformation of the receptor, ERα cocrystallized with estradiol (PDB code 1GWR). The amino acids involved in steric clashes with the ligands, Leu525 and Leu540, are depicted as molecular surfaces colored in blue while the rest of amino acids lining the binding site are depicted as sticks colored by element, the color code is blue for carbon, red for oxygen, gray for nitrogen, and yellow for sulfur. The ligands are represented in sticks with the associated molecular surfaces. They respect the same coloring code with the exception of carbons which are colored as follow: BisPhen in cyan, TriOHTPE in blue, EDiOHTPE in orange, ZDiOHTPE in pink, ZEthoxDiOHTPE in green, Endoxifen in yellow. For clarity, waters and hydrogen atoms were omitted from the binding site.

activity of the ER bound with 4OHTAM.[17,24] Results from ERE luciferase assays in T47:C4:2 cells transiently transfected with wild type and D351G mutant ER expression plasmids demonstrated that wild type ER was activated by all of the tested TPEs, however substitution of Asp351 by Gly prevented the increase of ERE luciferase activity by all TPEs and only planar E2, which does not interact with Asp351 at all, or exposes it on the surface of the complex, was able to activate ERE in D351G ER transfected cells. This confirms and expands the classification of estrogens, where planar estrogens such as E2 are classified as class I and all TPE-related estrogens are classified as class II estrogens based on the mechanism of activation of the ER.[18]

It is important to note that all of the tested TPEs were agonists in our wild type ER assay systems, however, extensive studies of the structure−function relationship of phenolic TPEs by Gust and co-workers,[25,26] demonstrated that some of these compounds were potent antagonists in their MCF-7:2A cells stably transfected with an ERE luciferase plasmid. Specifically, these investigators found that compounds 1,1,2-tris(4-hydroxyphenyl)but-1-ene and 1,1-bis(4,4′-hydroxyphenyl)-2-phenylbut-1-ene, which correspond to compounds **3** and **15** in this study, were able to completely inhibit estradiol-stimulated ERE luciferase activity at 100 nM. The antagonistic potency of these compounds, however, did not correlate with results from the cytotoxicity assays performed in their wild-type MCF-7 cells.[25,26] Both compounds 1,1,2-tris(4-hydroxyphenyl)but-1-ene (designated as **3** in this study) and 1,1-bis(4,4′-hydroxyphenyl)-2-phenylbut-1-ene (designated as **15** in this study) produced weak cytotoxic effects only at concentrations above 5 uM, which were well beyond the concentration range used in our study. Thus it is possible that the variation in findings between our laboratory and that of Gust and co-workers[25,26] might be due to differences in our in vitro model systems and our experimental design.

Conclusions

We have confirmed and advanced the hypothesis[18,19,22] that estrogens can be classified into planar class I compounds (E2) and nonplanar class II compounds (TPEs). Armed with these new tools, we are now poised to examine the biological consequences of estrogen classification based on the shape of the resulting ER complex.

Materials and Methods

Chemistry. 1,1,2-Tris(4-hydroxyphenyl)but-1-ene (3). 1,1,2-Tris(4-hydroxyphenyl)but-1-ene (**3**) was synthesized according to the method of Lubczyk, Bachmann, and Gust.[26]

1,2-Bis(4-methoxyphenyl)butanone (1). Potassium *tert*-butoxide (1.35 g, 12 mmol) was added to a solution of desoxyanisoin (2.55 g, 10 mmol) in anhydrous ether under a nitrogen atmosphere, and the mixture was stirred for 1 h. At which time, iodoethane (0.8 mL, 10 mmol) was added dropwise and the mixture was refluxed for 12 h. Water (40 mL) was added, and the product was extracted with ether. The ether extracts were combined, dried over sodium sulfate, and evaporated under reduced pressure. The crude product was dissolved in carbon tetrachloride (10 mL), and petroleum ether was added to crystallize unreacted desoxyanisoin. Dexosyanisoin was filtered off, and the filtrate was evaporated in vacuo to yield **1** as colorless oil (2.11 g, 74%). ^{1}H NMR ($CDCl_3$): δ = 0.88 (t, 3H, J = 7.5 Hz), 1.81 (m, 1H), 2.15 (m, 1H), 3.75 (s, 3H, OCH_3), 3.82 (s, 3H, CH_3), 4.34 (t, 1H, J = 7.5 Hz), 6.84 (d, 2H, J = 8.7 Hz), 6.88

(d, 2H, J = 9.0 Hz), 7.26 (d, 2H, J = 9.0 Hz), 7.97 (d, 2H, J = 9.0 Hz).

***E*/*Z*-4,4′-(1-Phenylbut-1-ene-1,2-diyl)bis(methoxybenzene) (4) and (5).** Bromobenzene (1.12 mL, 1.664 g, 10.6 mmol) was added dropwise over 30 min to a stirred solution of magnesium turnings (0.26 g, 10.6 mmol) in dry tetrahydrofuran (THF) (10 mL) under a nitrogen atmosphere. Once the Grignard reagent formed and went into solution, **1** (2.03 g, 7.0 mmol) in THF (10 mL) was added dropwise over 60 min. The reaction was refluxed for 12 h then quenched with water (10 mL) and the THF removed under reduced pressure. The aqueous layer was extracted with ether (3 × 50 mL). The ether extracts were washed with saturated sodium bicarbonate and water and dried over sodium sulfate. The crude carbinol was refluxed with 85% phosphoric acid (10 mL) in dry THF (20 mL) for 2 h. The reaction mixture was diluted with water (30 mL) and extracted with of dichloromethane (3 × 50 mL). The dichloromethane layers were washed with sodium bicarbonate and water and dried over sodium sulfate. It was filtered and the solvent removed under reduced pressure, yielding a brown oil. Purification by flash chromatography over silica (3.0 × 30 cm) and elution with 200 mL of petroleum ether, 300 mL of 5% ether 95% pet ether, and 500 mL of 10% ether 90% petroleum ether yielded two isomers. Isomer *E* **4** (0.322 g; 15% yield) was collected in fractions 17 to 19 while *Z*-isomer **5** was collected in fractions 20 to 28 (0.746 g, 31% yield). ^{1}H NMR *E*-isomer ($CDCl_3$): δ = 0.96 (t, 3H, J = 7.5 Hz), 2.49 (q, 2H, J = 7.5 Hz), 3.76 (s, 3H), 3.84 (s, 3H), 6.71 (d, 2H, 8.7 Hz), 6.89 (dd, 4H, J = 8.7 and 2.1 Hz), 6.88−7.05 (m, 5H), 7.15 (d, 2H, J = 8.7). ^{1}H NMR *Z*-isomer ($CDCl_3$): δ = 0.93 (t, 3H, J = 7.5 Hz), 2.44 (q, 2H, J = 7.5 Hz), 3.71 (s, 3H), 3.78 (s, 3H), 6.57 (d, 2H, 8.7 Hz), 6.72 (d, 2H, J = 8.7 Hz), 6.89 (d, 2H, J = 8.7 Hz), 7.05 (d, 2H, J = 8.7), 7.22−7.37 (m, 5H).

***E*/*Z*-4-(1-(4-Hydroxyphenyl)-1-phenylbut-1-en-2-yl)phenol (6) and (7).** Boron tribromide (1.23 mL; 3.25 g; 0.0129 mols) in dichloromethane (5 mL) was added dropwise over 60 min to 4,4′-(1-phenylbut-1-ene-1,2-diyl)bis(methoxybenzene) **4** or **5** (0.746, 2.17 mmol) in dry dichloromethane (20 mL) cooled in a dry ice/ethanol bath while stirring under a nitrogen atmosphere. The solution turned dark immediately and was allowed to warm to room temperature after the addition was complete. The reaction mixture was stirred for a total of 4 days at room temperature. Excess boron tribromide was removed using a nitrogen stream then anhydrous methanol (3 × 25 mL) was added and it was evaporated in vacuo three times. It was recrystallized from benzene and purified further by preparative HPLC using 70% methanol 30% water. Fractions were collected as follows: *E*-isomer **6** (28−39 min, 1.814 abs; 40 mg); *Z*-isomer **7** (41−58 min, 2.007 Abs; 78 mg). ^{1}H NMR *E*-isomer **6** (MeOD): δ = 0.90 (t, 3H, J = 7.5 Hz), 2.47 (q, 2H, J = 7.5 Hz), 6.39 (d, 2H, J = 8.4 Hz), 6.65 (d, 2H, J = 8.7), 6.76 (d, 2H, J = 8.4 Hz), 7.02 (d, 2H, J = 8.7), 7.07−7.12 (m, 5H). ^{1}H NMR *Z*-isomer **7** (MeOD): δ = 0.90 (t, 3H, J = 7.5 Hz), 2.38 (q, 2H, J = 7.5 Hz), 6.43 (d, 2H, 8.4 Hz), 6.59 (d, 2H, J = 8.4 Hz), 6.66 (d, 2H, J = 8.4 Hz), 6.93 (d, 2H, J = 8.4 Hz), 7.16−7.32 (m, 5H). MS m/z calcd for $C_{22}H_{20}O_2$ 315.14 $(M - H)^-$; found 315 for both samples.

1,2-Bis(4-hydroxyphenyl)ethanone (8). Desoxyanisoin (1.0 g; 3.90 mmol) was dissolved in glacial acetic acid (1 mL) with stirring. Next, hydroiodic acid (5 mL, 36.5 mmol) was added and the solution was heated to 130−140 °C for 4 h. The reaction mixture was poured into water (50 mL) and the blue−gray colored solid was filtered and washed with water. It was dried in vacuo to yield **9** (0.80 g; 90%). Melting point 205−208 °C. ^{1}H NMR (MeOD): δ = 4.13 (s, 2H), 6.71 (d, 2H, J = 8.7 Hz), 6.83 (d, 2H, J = 8.7 Hz), 7.06 (d, 2H, J = 8.7 Hz), 7.93 (d, 2H, J = 8.7 Hz).

1,2-Bis(4-(tetrahydro-2*H*-pyran-2-yloxy)phenyl)ethanone (9). 1,2-Bis(4-hydroxyphenyl)ethanone (**8**) (700 mg, 3.07 mmol) was suspended in benzene (35 mL) with stirring under nitrogen atmosphere. Then, 3,4-dihydro-2*H*-pyran (6 mL, 65.6 mmol) was added, followed by *p*-toluenesulfonic acid monohydrate (53 mg, 0.28 mmol), and the solution was stirred at 0 °C for 4.5 h. The solution changed from purple to pink to clear. It was poured into saturated sodium bicarbonate solution and extracted with ethyl acetate. The combined ethyl acetate layers were washed with water, dried over magnesium sulfate, and evaporated in vacuo to a yellow solid. The residue was triturated with carbon tetrachloride to remove unreacted pyran. The white solid (548 mg) was collected by filtration, and the filtrate was purified by column chromatography over silica (2.7 × 4 on 2.7 × 22). The product was eluted with 100 mL of pet ether, 200 mL of 10% ether 90% pet ether, 200 mL of 20% ether 80% pet ether, 200 mL of 30% ether 70% pet ether, and 200 mL of 40% ether 60% pet ether. Fractions 33−40 were combined and evaporated in vacuo to give 243 mg of additional product (791 mg, 65% yield). ^{1}H NMR ($CDCl_3$): δ = 1.59−2.00 (m, 12H), 3.60 (m, 2H), 3.86 (m, 2H), 4.16 (s, 2H), 5.38 (t, 1H, J = 3.0 Hz), 5.50 (t, 1H, J = 3.0 Hz), 7.00 (d, 2H, J = 8.7 Hz), 7.07 (d, 2H, J = 8.7 Hz), 7.17 (d, 2H, J = 8.7 Hz), 7.97 (d, 2H, J = 9.0 Hz).

1,2-Bis(4-(tetrahydro-2*H*-pyran-2-yloxy)phenyl)butan-1-one (10). Potassium *tert*-butoxide **9** (229 mg, 2.04 mmol) was added to 1,2-bis(4-(tetrahydro-2*H*-pyran-2-yloxy)phenyl)ethanone (**9**) (672 mg, 1.69 mmol) dissolved in anhydrous THF (25 mL) under a nitrogen atmosphere with stirring. The mixture was stirred at room temperature for 1 h. Next, iodoethane (0.136 mL 1.70 mmol) was added dropwise, and the reaction mixture was refluxed for 6 h. After cooling, the THF was removed under reduced pressure. Water (30 mL) was added, and the product was extracted with ether. The ether extracts were combined, dried over sodium sulfate, and evaporated under reduced pressure to **10** (623 mg, 87% yield). ^{1}H NMR ($CDCl_3$): δ = 0.88 (t, 3H, J = 7.2 Hz), 1.60−1.97 (m, 12H), 2.13 (m, 2H, J = 7.2 Hz), 3.58 (m, 2H), 3.864 (m, 2H), 4.34 (t, 1H, J = 7.2 Hz), 5.34 (t, 1H, J = 3.0 Hz), 5.46 (t, 1H, J = 3.0 Hz), 6.95 (d, 2H, J = 8.4 Hz), 7.01 (d, 2H, J = 8.4 Hz), 7.20 (d, 2H, J = 8.7 Hz), 7.93 (d, 2H, J = 8.7 Hz).

***E*/*Z*(4-(1-(4-ethoxyphenyl)-1-(4-hydroxyphenyl)but-1-en-2-yl)-phenol (11) and (12).** 4-Bromophenetole (0.160 mL, 1.11 mmol) in dry THF (10 mL) was added dropwise over 30 min to magnesium turnings (27 mg, 1.11 mmol) with stirring under a nitrogen atmosphere. An iodine crystal was added to initiate the reaction, and it was refluxed until the magnesium turnings dissolved. Next, 1,2-bis(4-(tetrahydro-2*H*-pyran-2-yloxy)phenyl)-butan-1-one (**10**) (0.311 g; 0.735 mmol) was added and the reaction was refluxed for 12 h. After cooling, the reaction mixture was evaporated in vacuo to an orange residue. Water (20 mL), dichloromethane (20 mL), and acetic acid (1 drop) were added to the orange residue, and the aqueous layer was extracted with dichloromethane (3 × 25 mL). The organic extracts were washed with saturated sodium bicarbonate and water and dried over sodium sulfate. Filtration and evaporation provide the crude carbinol, which was hydrolyzed by refluxing for 2 h with 85% phosphoric acid (1 mL) in dry THF (10 mL). The reaction mixture was diluted with water (30 mL) and extracted with dichloromethane (3 × 50 mL). The dichloromethane was washed with sodium bicarbonate and water and dried over sodium sulfate. It was filtered, and the solvent was removed under reduced pressure to a yellow oil. It was purified by prep HPLC over C-18 Delta Pak column eluting with 40% H_2O and 60% MeOH. Flow rate was 100 mL/min. The elution was monitored by UV set to 254. Two fractions were collected: *E*-isomer **11** (54−64 m, 14 mg) and *Z*-isomer **12** (92−100 m, 16 mg). ^{1}H NMR **11** ($CDCl_3$): δ = 0.92 (t, 3H, J = 7.5 Hz), 1.34 (t, 3H, J = 6.9 Hz), 2.44 (q, 2H, J = 7.5 Hz), 3.90 (q, 2H, J = 6.9 Hz), 6.55 (d, 2H, J = 8.7 Hz), 6.63 (d, 2H, J = 8.4 Hz), 6.76 (d, 2H, J = 8.7 Hz), 6.80 (d, 2H, J = 8.7 Hz), 6.97 (d, 2H, J = 8.7 Hz), 7.12 (d, 2H, J = 8.4 Hz). ^{1}H NMR **12** ($CDCl_3$): δ = 0.92 (t, 3H, J = 7.5 Hz), 1.40 (t, 3H, J = 6.9 Hz), 2.45 (q, 2H, J = 7.5 Hz), 4.02 (q, 2H, J = 6.9 Hz), 6.49 (d, 2H, J = 8.7 Hz), 6.63

(d, 2H, J = 8.4 Hz), 6.73 (d, 2H, J = 7.8 Hz), 6.86 (d, 2H, J = 8.4 Hz), 6.97 (d, 2H, J = 8.4 Hz), 7.12 (d, 2H, J = 8.7 Hz). MS m/z calcd for $C_{24}H_{24}O_3$ 360; $(M - H)^-$ found 359; $(M + H)^+$ found 361.

1-(4-Methoxyphenyl)-2-phenylbutan-1-one (13). Anisole (5.861 g, 54.2 mmol) and 2-phenylbutyryl chloride (9.90 g, 54.2 mmol) were dissolved in 20 mL of carbon disulfide with stirring under a nitrogen atmosphere. The reaction mixture was cooled in an ice bath while $AlCl_3$ (7.6 g, 57.0 mmol) was added, keeping the temperature between 10 and 20 °C. It was stirred at room temperature for 20 h. The dark-red reaction mixture was poured into ice, and the aqueous layer was extracted with ether (3 × 75 mL). The combined ether layers were washed with 10% KOH, 10% HCl, and saturated sodium bicarbonate solutions. The ether layer was then dried over $MgSO_4$ and evaporated under reduced pressure to a yellow solid **18** (13.01 g; 94% yield); mp 41−42.5 °C. TLC: ($CHCl_3$) R_f = 0.57. NMR ($CDCl_3$): δ = 0.90 (t, 3H, J = 7.2 Hz), 1.84 (m, 1H, J = 7.2 Hz), 2.19 (m, 1H, J = 7.2 Hz), 3.82 (s, 3H), 4.40 (t, 1H, J = 7.2 Hz), 6.86 (d, 2H, J = 9 Hz), 7.16−7.41 (m, 5H), 7.96 (d, 2H, J = 9 Hz).

1,1-Bis(4,4′-methoxyphenyl)-2-phenylbut-1-ene (14). Compound **18** (1.0 g, 3.93 mmol) in 10 mL of THF was added dropwise over 15 min to a 1 M THF solution of 4-methoxyphenyl magnesium bromide (5.8 mL, 5.8 mmol) cooled in an ice bath under a nitrogen atmosphere with stirring. The solution was refluxed for 17.5 h. The reaction mixture was poured into 20 mL of water and 8 mL of 6N acetic acid. The aqueous layer was extracted with ether (3 × 50 mL). The ether extracts were washed with saturated sodium bicarbonate and brine, dried over sodium sulfate, and evaporated under reduced pressure to an oil. The crude carbinol was refluxed with 85% phosphoric acid (10 mL) in dry THF (20 mL) for 2 h. The reaction mixture was diluted with water (60 mL) and extracted with dichloromethane (3 × 50 mL). The dichloromethane layers were washed with sodium bicarbonate and water then dried over sodium sulfate. The solvent was removed under reduced pressure, yielding a cream solid. Purification by flash chromatography over silica (2.7 × 37 cm) and elution with 500 mL of hexanes gave pure **19** in fractions 7−18, which were combined and evaporated in vacuo; yield 1.30 g (96%); mp 116−118 °C. TLC: ($CHCl_3$) R_f = 0.68. NMR ($CDCl_3$): δ = 0.93 (t, 3H, J = 7.5 Hz), 2.48 (q, 2H, J = 7.5 Hz), 3.68 (s, 3H), 3.83 (s, 3H), 6.54 (d, 2H, J = 9 Hz), 6.77 (d, 2H, J = 9 Hz), 6.88 (d, 2H, J = 9 Hz), 7.07−7.19 (m, 7H).

1,1-Bis(4,4′-hydroxyphenyl)-2-phenylbut-1-ene (15). Compound **19** (1.9 g, 3.79 mmol) in 18 mL dry dichloromethane was cooled to −55 °C under a nitrogen atmosphere with stirring. Then, BBr_3 (2.17 mL, 22.95 mmol) in 10 mL of dichloromethane was added over 30 min while the temperature was kept at −55 °°C. The reaction mixture was stirred at room temperature for 90 h. The reaction was quenched by addition of methanol. The methanol was evaporated, and this was performed three more times, which resulted in a green residue. The crude product was purified by flash chromatography on a silica column (4 cm × 26 cm) equilibrated with hexane. It was eluted with chloroform:methanol (85:15), and 20 mL fractions were collected. Fractions 18−27 were combined and evaporated under reduced pressure. The resulting solid was recrystallized from chloroform but contained a small impurity by HPLC. It was purified by prep HPLC over C-18 Delta Pak column eluting with 20% H_2O and 80% MeOH. Flow rate was 30 mL/min. The UV detector was set to 254λ. The product was collect from 20 to 24 min, and the solvent was evaporated in vacuo to give **20** (75 mg, 5% yield); mp 206−206.5 °C. TLC: ($CHCl_3$ 9: methanol 1) R_f = 0.50. NMR ($CDCl_3$): δ = 0.92 (t, 3H, J = 7.5 Hz), 2.47 (q, 2H, J = 7.5 Hz), 4.48 (s, 1H), 4.71 (s. 1H), 6.46 (d, 2H, J = 8.4 Hz),; 6.73 (d, 2H, J = 8.4 Hz),; 6.81 (d, 2H, J = 8.4 Hz), 7.10−7.16 (m, 7H).

Cell Culture. The ER-positive human breast cancer cell line MCF-7:WS8 and the ER-negative breast cancer cell line T47D:C4:2 were used in our study. MCF-7:WS8 cells were cloned from wild type MCF-7 cells that were originally obtained from Dr. Dean Edwards (University of Texas, San Antonio, TX) and were maintained in phenol-red RPMI 1640 medium containing 10% fetal bovine serum (FBS), 2 mM glutamine, penicillin at 100 units/mL, streptomycin at 100 μg/mL, 1× nonessential amino acids (all from Invitrogen, Carlsbad, CA), and bovine insulin at 6 ng/mL (Sigma-Aldrich, St. Louis, MO). The hormone-independent T47D:C4:2 cells were subcloned from T47D:C4 clones of T47D cells that were originally obtained from the ATCC (Rockville, MD). The T47D:C4:2 cells are ER-negative hormone-independent cells and they do not re-express ERα following growth in estrogen-containing media.[23] T47D:C4:2 cells were maintained in estrogen-free RPMI 1640 medium, containing 10% dextran charcoal-stripped fetal bovine serum (SFS). All cells were cultured in T185 culture flasks (Nalge Nunc International, Rochester, NY) and passaged twice a week in 1:4 ratio. All cultures were grown in 5%CO_2, 37 °C.

Cell Proliferation Assays. MCF-7:WS8 cells were cultured in estrogen-free medium (phenol red-free RPMI 1640 media supplemented with 10% charcoal-stripped FBS) for 4 days before beginning the proliferation assay. On day 0 of the experiment, MCF-7:WS8 cells were seeded in estrogen-free RPMI media containing 10% SFS at a density of 20000 cells per well respectively in NunclonΔ Surface 24-well plates (Nalge Nunc International, Rochester, NY). After 24 h, cells were treated with various concentrations of the tested compounds, prepared via serial dilutions. All concentration points were performed in triplicate. The compound-containing medium was changed on days 3 and 5, and the experiment was stopped on day 7. Cells were washed with cold PBS (Invitrogen, Carlsbad, CA) at least twice and analyzed with Fluorescent DNA quantification kit (Bio-Rad, Hercules, CA) according to manufacturers instructions, and samples were read on Mithras LB540 fluorometer/luminometer (Berthold Technologies, Oak Ridge, TN) in black wall 96-well plates (Nalge Nunc International, Rochester, NY) .

DNA Plasmids. Estrogen Response Element activity was determined via Luciferase assays with pERE(5X)TA-ffLuc and pTA-srLuc reporter plasmids. These plasmids contained the TATA-box basal promoter firefly and the *Renilla* luciferase reporter genes, respectively, and were constructed by insertion via *Hin*dIII linkers of the nucleotides −31 and +31 region of the herpes simplex virus thymidine kinase promoter into pGL3-Basic and phRG-B (Promega, Madison, WI).[27] For transient expression of wild-type ERα and 351 aspartate-to-glycine-substituted mutant ERα, pSG5HEGO and pSG5D351-GER plasmids were used, respectively. pSG5HEGO was originally provided by Professor Pierre Chambon, University of Strasbourg, France, and pSG5D351GER was generated using QuichChange Site-Directed Mutagenesis Kit (Stratagene, La Jolla, CA) and pSG5HEGO as a template.[17] All plasmids for this study were purified using HiSpeed Plasmid Maxi Kit (Qiagen, Valencia, CA) and were grown via OneShot TOP10 Chemically Competent *Escherichia coli* cells (Invitrogen, Carlsbad, CA).

Transient Transfections and Luciferase Activity Assays. MCF-7:WS8 cells were cultured in estrogen-free RPMI media for 24 h prior to transfection. On the day of the experiment, cells were seeded in estrogen-free media at a density of 100000 cells per well in 24-well plates. After 24 h, MCF-7:WS8 cells were transfected with 28.8 μg of pERE(5X)TA-ffLuc and 9.6 μg of pTA-srLuc reporter plasmids, using 3 μL of TransIT-LT1 transfection reagent (Mirus Biolabs, Madison, WI) per 1 μg of plasmid DNA in 52.5 mL of OPTI-MEM serum-free media (Invitrogen, Carlsbad, CA). Transfection mix containing transfection complexes of the transfection reagent and plasmid DNA in OPTI-MEM media was added to cell in growth media to a final concentration of 0.3 μg pERE(5X)TA-ffLuc and 0.1 μg of pTA-srLuc reporter plasmids per well. After 18 h, transfection reagents were removed and fresh media was added. Cells were then treated with the various test compounds for 24 h. At the indicated time point, cells were washed once with cold PBS (Invitrogen, Carlsbad, CA), lysed, and ERE luciferase activity

was determined using the Dual-Luciferase Reporter Assay System (Promega, Madison, WI) according to manufacturers recommendations. Samples were then read on a Mithras MB540 fluorometer/luminometer (Berthold Technologies, Oak Ridge, TN).

T47D:C4:2 cells were seeded in estrogen-free RPMI 1640 media at a density of 200000 cells per well in 24-well plates. T47D:C4:2 cells are ER-negative cells, therefore these cells were transiently transfected with wild-type ERα (pSG5HEGO) or D351G mutant ERα (pSG5D351GER), along with pERE-(5X)TA-ffLuc and pTA-srLuc reporter plasmids. Transfection mix contained 7.2 μg of pSG5HEGO or 7.2 μg of pSG5D351GER, 7.2 μg of pERE(5X)TA-ffLuc, and 2.4 μg of pTA-srLuc reporter plasmids, and 3 μL of FuGene HD transfection reagent (Roche Diagnostics, Indianapolis, IN) per 1 μg of plasmid DNA, and 13 mL of OPTI-MEM serum-free media (Invitrogen, Carlsbad, CA) for 1 × 24-well plate. Transfection complexes of the reagent and plasmid DNA were added to cells in growth media to a final concentration of 0.3 μg of pSG5HEGO or 0.3 μg of pSG5D-351GER, 0.3 μg of pERE(5X)TA-ffLuc, and 0.1 μg of pTA-srLuc per well. After 18 h, transfection reagents were removed and fresh media was added. Cell were then treated with the various test compounds for 24 h, and ERE luciferase activity was determined as described above.

Reagents and Supplies. Estradiol (E2), 4-hydroxy-tamoxifen (4OHTAM), and bovine insulin, was obtained from Sigma, St. Louis, MO. Endoxifen (*Z*-isomer) was a kind gift from Dr. James Ingle (Mayo Clinic). Fetal bovine serum (FBS), 2 mM glutamine, penicillin at 100 units/mL, streptomycin at 100 μg/mL, 1× nonessential amino acids, RPMI 1640 with phenol-red media, PBS buffer, RPMI 1640 phenol-red-free media, and OPTI-MEM serum-free media were all obtained from Invitrogen, Carlsbad, CA. Fluorescent DNA quantification kit obtained from Bio-Rad, Hercules, CA. HiSpeed Plasmid Maxi Kit was obtained from Qiagen, Valencia, CA. TransIT-LT1 transfection reagent was obtained from Mirus Biolabs, Madison, WI. FuGene HD transfection reagent was obtained from Roche Diagnostics, Indianapolis, IN. Dual-Luciferase Reporter Assay System was obtained from Promega, Madison, WI. Anhydrous ether was purchased from Fisher. Potassium *tert*-butoxide, desoxyanisoin, magnesium turnings, bromobenzene, boron tribromide, anhydrous methylene chloride, 3,4-dihydro-2*H*-pyran, oxalyl chloride, *N*,*O*-dimethylhydroxylamine, aluminum chloride, and cyclohexene were purchased from Acros. Ethyl iodide, hydroiodic acid (55% ACS unstabilized), *p*-toluene sulfonic acid monohydrate, 2-fluoro-3-trifluoromethylbenzoic acid, 2,4-dimethoxymagnesium bromide (0.5 M solution in THF), anisole, 2-phenylbutyryl chloride, phenyl magnesium bromide (1 M solution in THF), sodium hydride (60% in mineral oil), and allylbromide was purchased from Aldrich. Carbon disulfide was purchased from Baker. THF was distilled and stored over calcium hydride. Benzene was distilled from calcium hydride and stored over molecular sieves. Flash chromatography was run using Whatman 230−400 mesh silica gel 60. Preparative chromatography was run on a Waters Delta Prep 3000 HPLC system using a prep pak C-18 delta-pak column (47 nn × 300 mm). UV detection was set at 254λ. Flow rate was 50 mL per min. ^{1}H NMR was performed on a Bruker WB Advance 300 MHz instrument. MS analysis performed by HT Laboratories (San Diego, CA) using electrospray ionization. LC-MS was performed using a Waters 2545 binary gradient module and a 2487 dual wavelength detector set to 254 and 365, a 2424 ELS detector, and a 3100 MS detector. The gradient was linear 5% MeOH 95% H_2O to 95% MeOH 5% H_2O over 20 min. The column was a Waters Delta Pak C-18 15μ 100A 3.9 mm × 300 mm (catalogue number 11797) run at a flow rate of 0.8 mL per min. The purity of all compounds was determined by LC-MS to be 95% or greater.

Molecular Modeling. The coordinates for the antagonist conformation of human ER ligand binding domain cocrystallized with 4OHTAM were extracted from the RCSB Protein Data Bank (PDB),[28] entry 3ert, was selected for further modeling with ER in antagonist conformation and 1GWR was selected for modeling of the ER in the agonist conformation. The protein was prepared for the docking experiments using the Protein Preparation Workflow (Protein Preparation Wizard, Schrödinger, LLC, Portland, OR) implemented in Schrödinger suite and accessible from within the Maestro program (Maestro 8.5, Schrödinger, LLC, Portland, OR). Briefly, the hydrogen atoms were added, water molecules beyond 5 Å from the ligand were deleted, and the orientation of hydroxyl groups, Asn, Gln, and the protonation state of His were optimized to maximize hydrogen bonding. All Asp, Glu, Arg, and Lys residues were left in their charged state. Finally, the ligand−protein complex was refined with a restrained minimization performed by Impref utility, which is based on the Impact molecular mechanics engine (Impact 4.5, Schrödinger, LLC, Portland, OR) and the OPLS2001 force field, setting a max rmsd of 0.30.

Ligands preparation for docking was performed with LigPrep (LigPrep 2.1, Schrödinger, LLC, Portland, OR) application which consists of a series of steps that perform conversions, apply corrections to the structure, generate ionization states and tautomers, and optimize the geometries.

Molecular docking was performed using Glide 4.5 (Glide 4.5, Schrödinger, LLC, Portland, OR) followed by the Induced Fit protocol (Induced Fit protocol, Schrödinger, LLC, Portland, OR), which is intended to circumvent the inflexible binding site and accounts for the side chain or backbone movements, or both, upon ligand binding.[29] In the first stage of the IFD protocol, softened-potential docking step, 20 poses per ligand were retained. In the second step, for each docking pose, a full cycle of protein refinement was performed, with Prime 1.6 (Prime 1.6, Schrödinger, LLC, Portland, OR) on all residues having at least one atom within 8 Å of an atom in any of the 20 ligand poses. The Prime refinement starts with a conformational search and minimization of the side chains of the selected residues and after convergence to a low-energy solution, an additional minimization of all selected residues (side chain and backbone) is performed with the truncated-Newton algorithm using the OPLS parameter set and a surface Generalized Born implicit solvent model. The obtained complexes are ranked according to Prime calculated energy (molecular mechanics and solvation), and those within 30 kcal/mol of the minimum energy structure are used in the last step of the process, redocking with Glide 4.5 (extended precision), and scoring. In the final round, the ligands used in the first docking step is redocked into each of the receptor structures retained from the refinement step. The final ranking of the complexes is done by a composite score which accounts for the receptor−ligand interaction energy (GlideScore) and receptor strain and solvation energies (Prime energy).[29]

Acknowledgment. We thank Dr. Richard Schneider from the Organic Synthesis Core Facility at Fox Chase Cancer Center for his help in synthesis of the tested compounds. We particularly thank Helen Kim, Laboratory Manager at the Lombardi Comprehensive Cancer Center for her dedicated work assembling this manuscript for publication. This work was supported by the Department of Defense Breast Program under award no. BC050277 (V.C.J.), Fox Chase Cancer Center Core Grant no. NIH P30 CA006927-47, NIH Career Development Grant K01CA120051-01A2 (J.S.L.W.), American Cancer Society Grant IRG-92-027-14 (J.S.L.W.), and the Hollenbach Family Fund (J.S.L.W.).

References

(1) *Cancer Facts and Figures*; www.cancer.org **2009**.
(2) Russo, I. H.; Russo, J. Role of hormones in mammary cancer initiation and progression. *J. Mammary Gland Biol. Neoplasia* **1998**, *3*, 49–61.

(3) EBCTCG. Tamoxifen for early breast cancer: an overview of the randomised trials. Early Breast Cancer Trialists' Collaborative Group. *Lancet* **1998**, *351*, 1451−1467.
(4) EBCTCG. Effects of chemotherapy and hormonal therapy for early breast cancer on recurrence and 15-year survival: an overview of the randomised trials. *Lancet* **2005**, *365*, 1687−1717.
(5) Jordan, V. C Tamoxifen: catalyst for the change to targeted therapy. *Eur. J. Cancer* **2008**, *44*, 30–38.
(6) Fisher, B.; Costantino, J. P.; Wickerham, D. L.; Redmond, C. K.; Kavanah, M.; Cronin, W. M.; Vogel, V.; Robidoux, A.; Dimitrov, N.; Atkins, J.; Daly, M.; Wieand, S.; Tan-Chiu, E.; Ford, L.; Wolmark, N. Tamoxifen for prevention of breast cancer: report of the National Surgical Adjuvant Breast and Bowel Project P-1 Study. *J. Natl. Cancer Inst.* **1998**, *90*, 1371–1388.
(7) Harper, M. J.; Walpole, A. L. Contrasting endocrine activities of cis and trans isomers in a series of substituted triphenylethylenes. *Nature* **1966**, *212*, 87.
(8) Harper, M. J.; Walpole, A. L. A new derivative of triphenylethylene: effect on implantation and mode of action in rats. *J. Reprod. Fertil.* **1967**, *13*, 101–119.
(9) Robson, J. M.; Schonberg, A. Estrous reactions, including mating, produced by triphenyl ethylene. *Nature* **1937**, *140*, 196.
(10) Jordan, V. C.; Collins, M. M.; Rowsby, L.; Prestwich, G. A monohydroxylated metabolite of tamoxifen with potent antioestrogenic activity. *J. Endocrinol.* **1977**, *75*, 305–316.
(11) Johnson, M. D.; Zuo, H.; Lee, K. H.; Trebley, J. P.; Rae, J. M.; Weatherman, R. V.; Desta, Z.; Flockhart, D. A.; Skaar, T. C. Pharmacological characterization of 4-hydroxy-*N*-desmethyl tamoxifen, a novel active metabolite of tamoxifen. *Breast Cancer Res. Treat.* **2004**, *85*, 151–159.
(12) Brzozowski, A. M.; Pike, A. C.; Dauter, Z.; Hubbard, R. E.; Bonn, T.; Engstrom, O.; Ohman, L.; Greene, G. L.; Gustafsson, J. A.; Carlquist, M. Molecular basis of agonism and antagonism in the oestrogen receptor. *Nature* **1997**, *389*, 753–758.
(13) Shiau, A. K.; Barstad, D.; Loria, P. M.; Cheng, L.; Kushner, P. J.; Agard, D. A.; Greene, G. L. The structural basis of estrogen receptor/coactivator recognition and the antagonism of this interaction by tamoxifen. *Cell* **1998**, *95*, 927–937.
(14) Levenson, A. S.; Tonetti, D. A.; Jordan, V. C. The oestrogen-like effect of 4-hydroxytamoxifen on induction of transforming growth factor alpha mRNA in MDA-MB-231 breast cancer cells stably expressing the oestrogen receptor. *Br. J. Cancer* **1998**, *77*, 1812–1819.
(15) Levenson, A. S.; Catherino, W. H.; Jordan, V. C. Estrogenic activity is increased for an antiestrogen by a natural mutation of the estrogen receptor. *J. Steroid Biochem. Mol. Biol.* **1997**, *60*, 261–268.
(16) Levenson, A. S.; Jordan, V. C. The key to the antiestrogenic mechanism of raloxifene is amino acid 351 (aspartate) in the estrogen receptor. *Cancer Res.* **1998**, *58*, 1872–1875.
(17) MacGregor Schafer, J.; Liu, H.; Bentrem, D. J.; Zapf, J. W.; Jordan, V. C. Allosteric silencing of activating function 1 in the 4-hydroxytamoxifen estrogen receptor complex is induced by substituting glycine for aspartate at amino acid 351. *Cancer Res.* **2000**, *60*, 5097–5105.
(18) Jordan, V. C.; Schafer, J. M.; Levenson, A. S.; Liu, H.; Pease, K. M.; Simons, L. A.; Zapf, J. W. Molecular classification of estrogens. *Cancer Res.* **2001**, *61*, 6619–6623.
(19) Gust, R.; Keilitz, R.; Schmidt, K. Investigations of new lead structures for the design of selective estrogen receptor modulators. *J. Med. Chem.* **2001**, *44*, 1963–1970.
(20) Jordan, V. C.; Koch, R.; Langan, S.; McCague, R. Ligand interaction at the estrogen receptor to program antiestrogen action: a study with nonsteroidal compounds in vitro. *Endocrinology* **1988**, *122*, 1449–1454.
(21) Murphy, C. S.; Langan-Fahey, S. M.; McCague, R.; Jordan, V. C. Structure−function relationships of hydroxylated metabolites of tamoxifen that control the proliferation of estrogen-responsive T47D breast cancer cells in vitro. *Mol. Pharmacol.* **1990**, *38*, 737–743.
(22) Bentrem, D.; Fox, J. E.; Pearce, S. T.; Liu, H.; Pappas, S.; Kupfer, D.; Zapf, J. W.; Jordan, V. C. Distinct molecular conformations of the estrogen receptor alpha complex exploited by environmental estrogens. *Cancer Res.* **2003**, *63*, 7490–7496.
(23) Pink, J. J.; Bilimoria, M. M.; Assikis, J.; Jordan, V. C. Irreversible loss of the oestrogen receptor in T47D breast cancer cells following prolonged oestrogen deprivation. *Br. J. Cancer* **1996**, *74*, 1227–1236.
(24) Levenson, A. S.; MacGregor Schafer, J. I.; Bentrem, D. J.; Pease, K. M.; Jordan, V. C. Control of the estrogen-like actions of the tamoxifen−estrogen receptor complex by the surface amino acid at position 351. *J. Steroid Biochem. Mol. Biol.* **2001**, *76*, 61–70.
(25) Lubczyk, V.; Bachmann, H.; Gust, R. Investigations on estrogen receptor binding. The estrogenic, antiestrogenic, and cytotoxic properties of C2-alkyl-substituted 1,1-bis(4-hydroxyphenyl)-2-phenylethenes. *J. Med. Chem.* **2002**, *45*, 5358–5364.
(26) Lubczyk, V.; Bachmann, H.; Gust, R. Antiestrogenically active 1,1,2-tris(4-hydroxyphenyl)alkenes without basic side chain: synthesis and biological activity. *J. Med. Chem.* **2003**, *46*, 1484–1491.
(27) Ariazi, E. A.; Kraus, R. J.; Farrell, M. L.; Jordan, V. C.; Mertz, J. E. Estrogen-related receptor alpha1 transcriptional activities are regulated in part via the ErbB2/HER2 signaling pathway. *Mol. Cancer Res.* **2007**, *5*, 71–85.
(28) Berman, H. M.; Westbrook, J.; Feng, Z.; Gilliland, G.; Bhat, T. N.; Weissig, H.; Shindyalov, I. N.; Bourne, P. E. The Protein Data Bank. *Nucleic Acids Res.* **2000**, *28*, 235–242.
(29) Sherman, W.; Day, T.; Jacobson, M. P.; Friesner, R. A.; Farid, R. Novel procedure for modeling ligand/receptor induced fit effects. *J. Med. Chem.* **2006**, *49*, 534–553.

Horm Mol Biol Clin Invest 2010;2(2):235–243 © 2010 by Walter de Gruyter • Berlin • New York. DOI 10.1515/HMBCI.2010.025

Estrogen regulation of X-box binding protein-1 and its role in estrogen induced growth of breast and endometrial cancer cells

Surojeet Sengupta[1], Catherine G.N. Sharma[2] and V. Craig Jordan[1,*]

[1]Department of Oncology, Lombardi Cancer Center, Georgetown University Medical Center, Washington, DC, USA
[2]Fox Chase Cancer Center, Philadelphia, PA, USA

Abstract

Background: X-box binding protein 1 (XBP1), a transcription factor involved in unfolded protein response, is also an estrogen-regulated gene and strongly correlates with estrogen receptor alpha (ERα) expression in breast cancers. We investigated the functional role of XBP1 in estrogen responsive breast and endometrial cancer cells as its functions are not fully understood.
Materials and methods: ERα positive breast (MCF7) and endometrial (ECC1) cancer cells were used to study XBP1 gene regulation by 17-β-estradiol (E2) and to investigate the role of XBP1 in E2-mediated growth using short interfering RNA. Quantitative real-time PCR and Western blot were used to assess RNA and protein levels. Recruitment of ERα and other cofactors at the promoter and enhancer region of the XBP1 gene was investigated by chromatin immunoprecipitation. Estrogen responsive element (ERE)-mediated transcriptional activity was evaluated by a luciferase reporter assay.
Results: E2 induced the transcription of XBP1 in both MCF7 and ECC1 cells. E2-dependent recruitment of ERα, steroid receptor coactivator (SRC)-1 and SRC-3, and RNA polymerase II were observed at the promoter and/or enhancer region of the XBP1 gene. Depletion of XBP1 markedly inhibited the E2-induced growth in MCF7 and ECC1 cells. However, ERE-mediated transcription was not altered in XBP1-overexpressing or XBP1-depleted MCF7 cells.
Conclusion: Our results confirm E2-induced transcription of XBP1 and demonstrate the crucial role of XBP1 in E2-induced growth of ERα positive breast and endometrial cancer cells without modulating the classical ERE-mediated transcription by ER. This knowledge creates new opportunities for therapeutic interventions.

*Corresponding author: V. Craig Jordan, OBE, PhD, DSc, FMedSci, Scientific Director, Lombardi Comprehensive Cancer Center, Vice Chair of Department of Oncology, Professor of Oncology and Pharmacology, Georgetown University Medical Center, 3970 Reservoir Rd NW, Washington, DC 20057, USA
Phone: +1-202-687-2897, Fax: +1-202-687-6402,
E-mail: vcj2@georgetown.edu
Received September 16, 2009; accepted March 23, 2010; previously published online June 11, 2010

Keywords: breast cancer; estrogen; estrogen receptor; X-box binding protein 1 (XBP1).

Introduction

Estrogen is the principal growth mediator of the estrogen receptor (ER) positive breast and endometrial cancers (1). Estrogen acts by binding to ERα or β and the resulting complex can activate transcription of estrogen responsive genes. Examples of estrogen responsive genes include the transcription factors which crucially regulate estrogen-dependent growth. X-box binding protein 1 (XBP1) is a transcription factor, identified as basic region leucine zipper belonging to the ATF/CREB family, strongly coexpressed in ERα positive luminal epithelial breast cancers (2, 3). Several DNA microarray studies have also found XBP1 as an estrogen-regulated gene in ER positive breast cancer cell lines as well as in breast cancers (4–9). In addition, recruitment of ERα on the XBP1 promoter as well as enhancer regions has been confirmed using chromatin immunoprecipitation (ChIP) followed by tiled microarray on human chromosomes 21 and 22 (10).

XBP1 is an important component of unfolded protein response (UPR) where it activates a distinct set of genes and regulates endoplasmic reticulum stress-mediated apoptosis (11). Studies have found that XBP1 is essential for survival of mouse embryonic fibroblasts and is also required for tumor growth of human fibrosarcoma cells under hypoxic conditions, as XBP1-deficient cells show impaired survival (12). Consistent with these findings, XBP1 knockout mice are found to be embryonic lethal as embryonic livers at 13.5 day from $XBP^{-/-}$ mouse exhibited increased apoptosis compared with wild type embryos (13). Further studies show that embryonic lethality of the $XBP^{-/-}$ can be rescued by selectively expressing XBP1 in the hepatocytes. However, these animals died in early postnatal period with pancreatic insufficiency (14). Likewise, XBP1 is essential for UPR and differentiation of plasma cells (15). In multiple myeloma, a plasma cell malignancy, XBP1 deficiency can induce apoptosis in response to endoplasmic reticulum stress (16). A recent study observed apoptosis in XBP1-depleted intestinal epithelial cells from mouse and a concurrent increase in their susceptibility to developing inflammatory bowel disease (17).

Interestingly, XBP1 is reported (18) to interact with ERα in a ligand-independent manner and can also induce transcription from estrogen responsive element (ERE) containing luciferase reporter gene even in the absence of estrogen. Fur-

ther studies found large-scale chromatin unfolding associated with XBP1-mediated increase in ERα transcriptional activity (19). Although these findings strongly suggest an interaction of XBP1 with ERα and its involvement in the ERα-mediated transcriptional process, the precise underlying mechanisms are unknown in ER positive breast and endometrial cancers.

Overexpression of XBP1 in ER positive breast cancer cells not only induces estrogen-independent growth of ER positive breast cancer cells but also confers resistance to the anti-estrogen tamoxifen (20). However, no data are available to explain the relevance of endogenous level of XBP1 and also how estrogen mediated upregulation of XBP1 could have a functional role in estrogen-induced growth of ERα positive breast and endometrial cancer cells.

We report the estrogen regulation of endogenous XBP1 and show that coactivators steroid receptor coactivator (SRC)-1 and SRC-3 along with ERα are recruited at the promoter and/or enhancer elements of the XBP1 gene. By depleting XBP1 levels using siRNA, we also show that XBP1 is required to mediate the estrogen-induced growth of MCF7 breast and ECC1 endometrial cancer cells.

Materials and methods

Cell culture and reagents

Cell culture media were purchased from Invitrogen Inc. (Grand Island, NY, USA) and fetal calf serum (FCS) was obtained from HyClone Laboratories (Logan, UT, USA). The ER positive breast cancer cells MCF7:WS8 used in this study were derived from MCF7 cells obtained from the American Type Culture Collection as reported previously (21). The ER positive endometrial cancer cells ECC1 cells were originally from Dr. Myles Brown's lab. MCF7 cells were routinely maintained in RPMI media and ECC1 cells were maintained in Dulbecco's Modified Eagle Medium media supplemented with 10% FCS, 6 ng/mL bovine insulin and penicillin and streptomycin. Three to four days prior to harvesting, cells were switched to phenol red-free media containing 10% charcoal dextran treated FCS. Media was changed every other day. The cells were treated with indicated reagents for the specified time and were subsequently harvested for total RNA isolation or protein lysate. Cycloheximide (CHX) and 5,6-dichloro-1-β-D-ribofuranosylbenzimidazole (DRB) were purchased from Sigma chemicals (St. Louis, MO, USA) and fulvestrant (FUL) was from Tocris Pharmaceuticals (Ellisville, MI, USA). Cells were pretreated for 30 min with CHX, DRB or FUL before treating with 17β-estradiol (E2) or vehicle for specified times as mentioned in Figure legends. All experiments were repeated at least three times, in triplicate to confirm the results.

Total RNA isolation and real-time polymerase chain reaction (PCR)

Total RNA was isolated using TRIzol reagent (Invitrogen, Carlsbad, CA, USA) and an RNeasy kit (Qiagen Inc.) according to the manufacturer's instructions. Real-time PCR was performed by reverse transcribing 1 μg of total RNA in a total volume of 20 μL using a high-capacity cDNA reverse transcription kit (Applied Biosystems, Foster City, CA, USA) as per manufacturer's instructions and subsequently diluted to 200 μL with sterile water. The real-time PCR was performed in a 20 μL reaction which included 1× SYBR green PCR master mix (Applied Biosystems), 100 nM each of forward and reverse primers and 2 μL of diluted cDNA using an ABI Prism 7900 HT Sequence Detection System (Applied Biosystems) for 40 cycles (95°C for 15 s, 60°C for 1 min) following an initial 10 min incubation at 95°C. The fold change in expression of transcripts was calculated using the ΔΔCt method, with the ribosomal protein 36B4 mRNA as the internal control (22). The primer sequences used were the same as previously reported for XBP1 (10) and 36B4 (23).

Growth assay

Cells were grown in 10 cm plates in charcoal-stripped media for 4 days before plating for the growth assay. In total, 12,000 cells were plated in each well of 24-well plates and allowed to attach for at least 16 h before treating them with vehicle or 1 nM E2. One untreated plate was collected at the start day of treatment and this served as the baseline for the comparison of the growth of cells. Cells were then collected on the second, fourth and sixth days of treatment and frozen in –30°C. The growth was assessed by measuring the DNA content in each well using a fluorescent DNA quantitation kit (Bio-Rad, Hercules, CA, USA) according to the manufacturer's instructions. Calf thymus DNA was used to plot the standard curve for the DNA assay with each set of quantitation. The experiments were repeated three times in quadruplicates to confirm the data.

Chromatin immunoprecipitation (ChIP) assay

ChIP was performed as described by Shang et al. (24) with minor modifications. Cells were grown in 15 cm plates in phenol red-free RPMI media containing 10% charcoal stripped fetal bovine serum for 3 days before treating with vehicle or 1 nM estradiol for 45 min. Cells were then washed with phosphate buffered saline (PBS) followed by crosslinking with 1% formaldehyde at room temperature for 15 min and then stopped it using 125 mM glycine. Cells were then rinsed with PBS and collected in PBS containing protease inhibitors (Roche Diagnostics, Indianapolis, IN, USA) and 10 mM dithiothreitol (DTT), followed by centrifuging at 2000×*g* for 5 min at 4°C. Subsequently, cells were resuspended in nuclei isolation buffer (50 mM Tris Cl, 60 mM KCl, 0.5% NP40, protease inhibitors and 10 mM DTT) followed by centrifugation to isolate the nuclei. Isolated nuclei were resuspended in sodium dodecyl sulfate (SDS) lysis buffer (50 mM Tris Cl, 1% SDS, 10 mM EDTA, pH 8.1 with protease inhibitors) and sonicated (Microson ultrasonic dismembrator) three times at setting '10' followed by centrifugation at 14,000×*g* for 20 min at 4°C. Fixed chromatin supernatant was diluted using ChIP dilution buffer (0.01% SDS, 1.1% Triton X-100, 1.2 mM EDTA, 16.7 mM Tris-HCl, pH 8.1, 167 mM NaCl with 1× protease inhibitors) followed by immunoclearing using normal rabbit serum and 60 μL of protein A agarose (Upstate Cell Signaling Solutions, Temecula, CA, USA). Immunoprecipitation was performed overnight with antibodies against ERα, SRC-1, SRC-3 and phospho-2-serine-RNA polymerase II (p-RNA polII). The immunocomplexes were precipitated using 60 μL of protein A agarose and incubated for an additional 2 h followed by centrifugation at 700×*g* for 5 min. The beads bound to immunocomplexes were sequentially washed 10 min each using buffer I (20 mM Tris Cl, 2 mM EDTA, 0.1% SDS, 1% Triton X-100 and 150 mM NaCl), buffer II (20 mM Tris Cl, 2 mM EDTA, 0.1% SDS, 1% Triton X-100 and 250 mM NaCl), buffer III (0.25 M LiCl, 1% NP-40, 1% deoxycholate, 1 mM EDTA, 10 mM Tris-HCl, pH 8.1). Precipitates were then washed twice with TE buffer and extracted twice with freshly made 1% SDS and 0.1 M $NaHCO_3$. Pooled elutes were decrosslinked using 200 μM of NaCl and heated at 65°C overnight.

The DNA fragments were purified using a Qiaquick PCR purification kit (Qiagen Inc.). Then, 1–2 μL of eluted DNA was used for real-time PCR analysis. The primer sequences used are as follows: XBP1 promoter: 5′TCTGGAAAGCTCTCGGTTTG3′ (forward); 5′AATCCCTGGCCAAAGGTACT3′ (reverse); XBP1 enhancer: 5′ATACTTGGCAGCCTGTGACC3′ (forward); 5′GTGCCACAAAGCAGGAAAAA3′ (reverse). The data are expressed as percent input of 1/20th part of starting chromatin material and are representative of three separate experiments with similar results.

Western immunoblotting

MCF7 and ECC1 cells were grown in phenol red-free media containing charcoal stripped serum. After treatments with the compounds for the indicated time periods, cells were rinsed with cold PBS and then lysed by RIPA buffer (Sigma Chemicals, St. Louis, MO, USA) supplemented with protease inhibitors (Roche Diagnostics, Indianapolis, IN, USA) and phosphatase inhibitor cocktails I and II (Calbiochem, La Jolla, CA, USA). Cell lysates were collected, sonicated (3× for 10 s, on ice) and centrifuged at 14,000 rpm for 20 min at 4°C. Cell supernatants were aliquoted and stored at −80°C. Protein concentration was determined using a BCA Protein Assay Kit (Pierce, Rockford, IL, USA). Proteins (20–40 μg) were separated by electrophoresis using 10% polyacrylamide gels containing sodium dodecyl sulfate (SDS-PAGE) and transferred onto PVDF transfer membranes (GE Healthcare Bio-Sciences Corp., Piscataway, NJ, USA). Primary antibodies used for Western blotting were raised against XBP1 (Santa Cruz, CA, USA) and β-actin (Sigma-Aldrich Corp., St. Louis, MO, USA). The bands were visualized using an ECL Western blotting detection system (GE Healthcare Bio-Sciences Corp) as per manufacturer's instructions. The experiments were repeated at least three times with similar results.

Short interfering RNA (siRNA) experiments

For siRNA experiments, MCF7 or ECC1 cells were grown in 10 cm plates, in antibiotic-free media. Cells were transfected with 100 nM XBP1 siRNA (on target plus, cat #009552; Dharmacon, Inc.) or control siRNA (on target plus, non-targeting pool, cat #D-001810; Dharmacon, Inc.) using 20 μL of Dharmafect transfection reagent as per manufacturer's instruction, for 48 h. Cells were allowed to recover in complete medium (without antibiotics) for 16 h, followed by reseeding in 24-well plates for growth assay or in 6-well plates for RNA and protein isolation. Cells were then treated with vehicle or E2 for indicated times. RNA and protein was extracted by methods as mentioned earlier. The experiments were repeated at least three times, in triplicate to confirm the results.

Luciferase reporter assays

Plasmid pERE(5X)TA-ffLuc (25) containing five tandem copies of the consensus palindromic ERE and firefly luciferase was transfected to assess the ERE-mediated transcriptional activity in the MCF7 cells. Plasmid pTA-srluc (25) expressing *renilla* luciferase reporter gene was cotransfected as an internal control. Then, 300 ng of pERE(5X)TA-ffLuc and 50 ng of pTA-srluc was cotransfected in each well containing 10^5 cells treated with control or XBP1 siRNA. Cells were further treated with vehicle or E2 for 48 h before harvesting for the assay.

In another set of experiments, cells were cotransfected with either 20 ng or 500 ng of XBP1 expressing plasmid along with 300 ng of pERE(5X)TA-ffLuc and 50 ng of pTA-srluc. The entire assay was performed using dual luciferase assay kits (Promega). All data are represented in terms of ratio of firefly/renilla RLU values. The experiments were repeated three times, in quadruplicates to confirm the results.

Statistics

Statistical significance of our data were assessed using the Student t-test. A p-value <0.05 was considered as statistically significant.

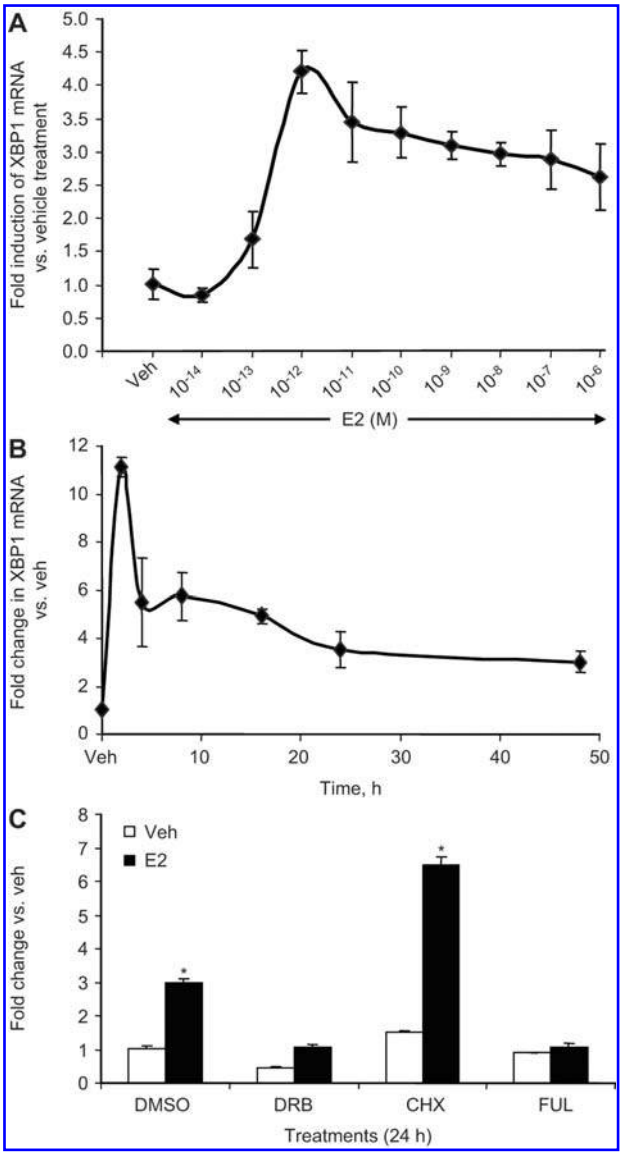


Figure 1 E2-mediated upregulation of XBP1 in MCF7 cells. MCF7 cells were treated with different concentrations of E2 for 8 h and expression of XBP1 was measured using quantitative real-time PCR and compared with vehicle-treated cells (A). MCF7 cells treated with E2 (1 nM) for 2, 4, 8, 16, 24 or 48 h and expression of XBP1 was measured using quantitative real-time PCR and compared with vehicle-treated cells (B). MCF7 cells were treated with CHX (10 μg/mL), DRB (75 μM) or FUL (1 μM) in absence or presence of E2 (1 nM) for 24 h and expression of XBP1 was assessed using real-time PCR (C). *$p<0.05$ compared with respective vehicle-treated group.

Results

Estrogen upregulates XBP1 in MCF7 and ECC1 cells and is a primary responsive gene

We first studied the dose-response of E2 on XBP1 mRNA regulation in MCF7 breast cancer cells after 8 h of E2 treatment using quantitative real-time PCR. Our data show that XBP1 mRNA was induced by E2 in a dose-dependent manner (Figure 1A). Low dose of E2 (10^{-14} M) was not able to induce any upregulation of XBP1 levels, whereas 10^{-12} M of E2 achieved the peak induction. Higher doses of E2 treatment induced XBP1 levels similar to 10^{-12} M of E2. We then studied the regulation of the XBP1 at various time points after 1 nM (10^{-9} M) E2 treatment and found that it was upregulated as early as 2 h after estrogen treatment and maintained an elevated level even after 48 h of estrogen treatment in breast cancer (MCF7) as well as in endometrial cancer (ECC1) cells (Figures 1B and 2A). This upregulation was completely abrogated in the presence of FUL, a complete anti-estrogen, indicating an ERα-mediated mechanism (Figures 1C and 2B). Pretreatment with CHX, an inhibitor of protein synthesis, in the presence of E2 did not alter the E2-mediated upregulation suggesting that de novo protein synthesis is not required for the estrogen-mediated upregulation of XBP1 (Figures 1C and 2B). Conversely, pretreatment with DRB, a transcriptional inhibitor, completely blocked the upregulation of XBP1 demonstrating involvement of transcriptional machinery in upregulation of XBP1 by estrogen (Figures 1C and 2B).

We also studied the regulation of XBP1 in ER negative breast cancer cells SKBR3 and MDA MB 231 cells. As expected, XBP1 was not regulated by E2 in these cells (Figure 2C). Furthermore, we investigated the levels of XBP1 in long-term estrogen-deprived MCF7 cells, known as MCF7:5C cells (26) which are estrogen-deprived resistant cells. Paradoxically, low levels of E2 induce apoptosis in these cells (27). Basal levels of XBP1 mRNA were found to be around 23-fold higher in MCF7:5C cells compared with MCF7 cells (Figure 2D). Interestingly, E2 treatment for 48 h

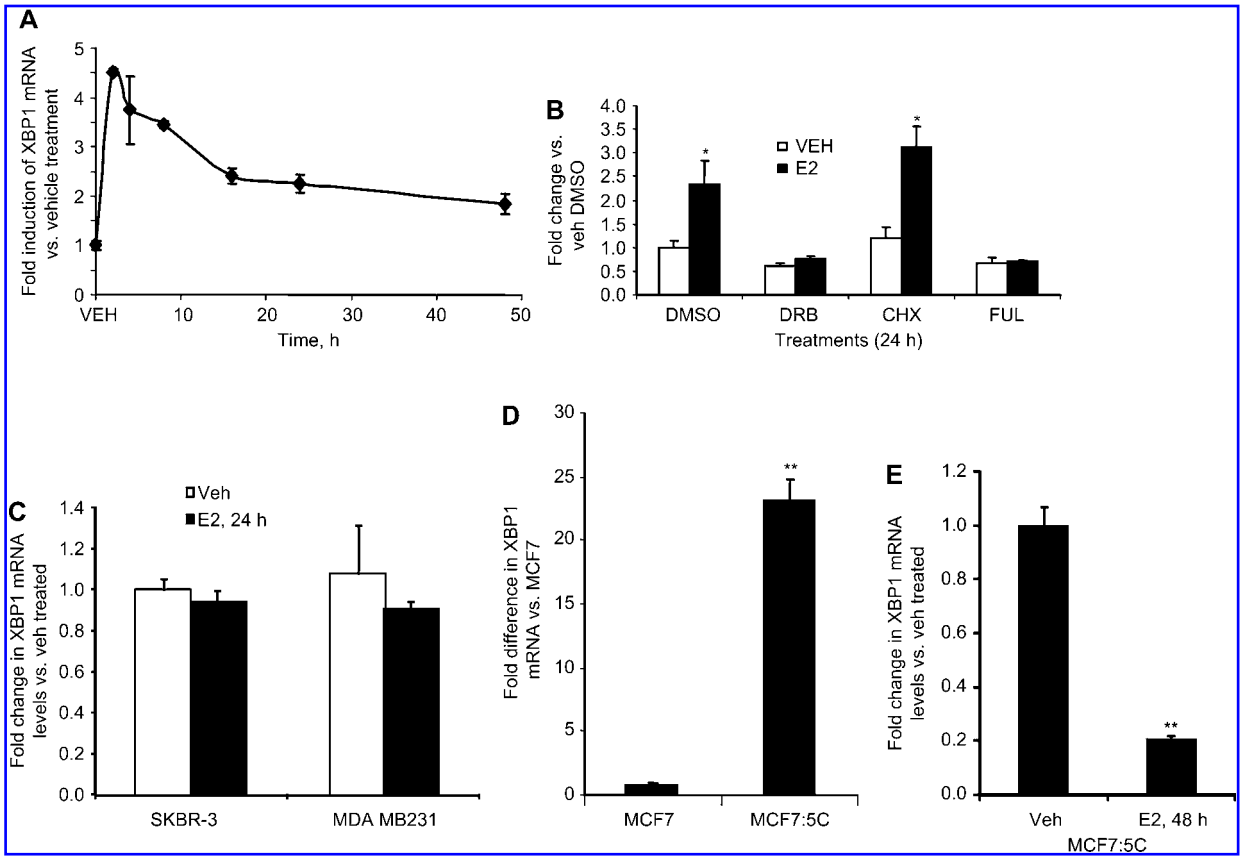


Figure 2 E2-mediated upregulation of XBP1 in ECC1 cells. ECC1 cells treated with E2 (1 nM) for 2, 4, 8, 16, 24 or 48 h and expression of XBP1 was measured using quantitative real-time PCR and compared with vehicle-treated cells (A). ECC1 cells were treated with CHX (10 μg/mL), DRB (75 μM) or FUL (1 μM) in absence or presence of E2 (1 nM) for 24 h and expression of XBP1 was assessed using real-time PCR (B). SKBR-3 and MDA-MB-231 cells were treated with E2 (1 nM) or vehicle (0.1% ethanol) for 24 h and expression of XBP1 was measured using quantitative real-time PCR and compared with vehicle-treated cells (C). Total RNA from MCF7 and MCF:5C was isolated and expression of XBP1 was measured using quantitative real-time PCR relative to MCF7 cells (D). MCF7:5C cells were treated with vehicle (0.1% ethanol) or E2 (1 nM) for 48 h and expression of XBP1 was measured using quantitative real-time PCR and compared with vehicle-treated cells (E). *$p<0.05$ compared with vehicle-treated group (B). **$p<0.05$ compared with MCF7 cells (D) or vehicle-treated group (E).

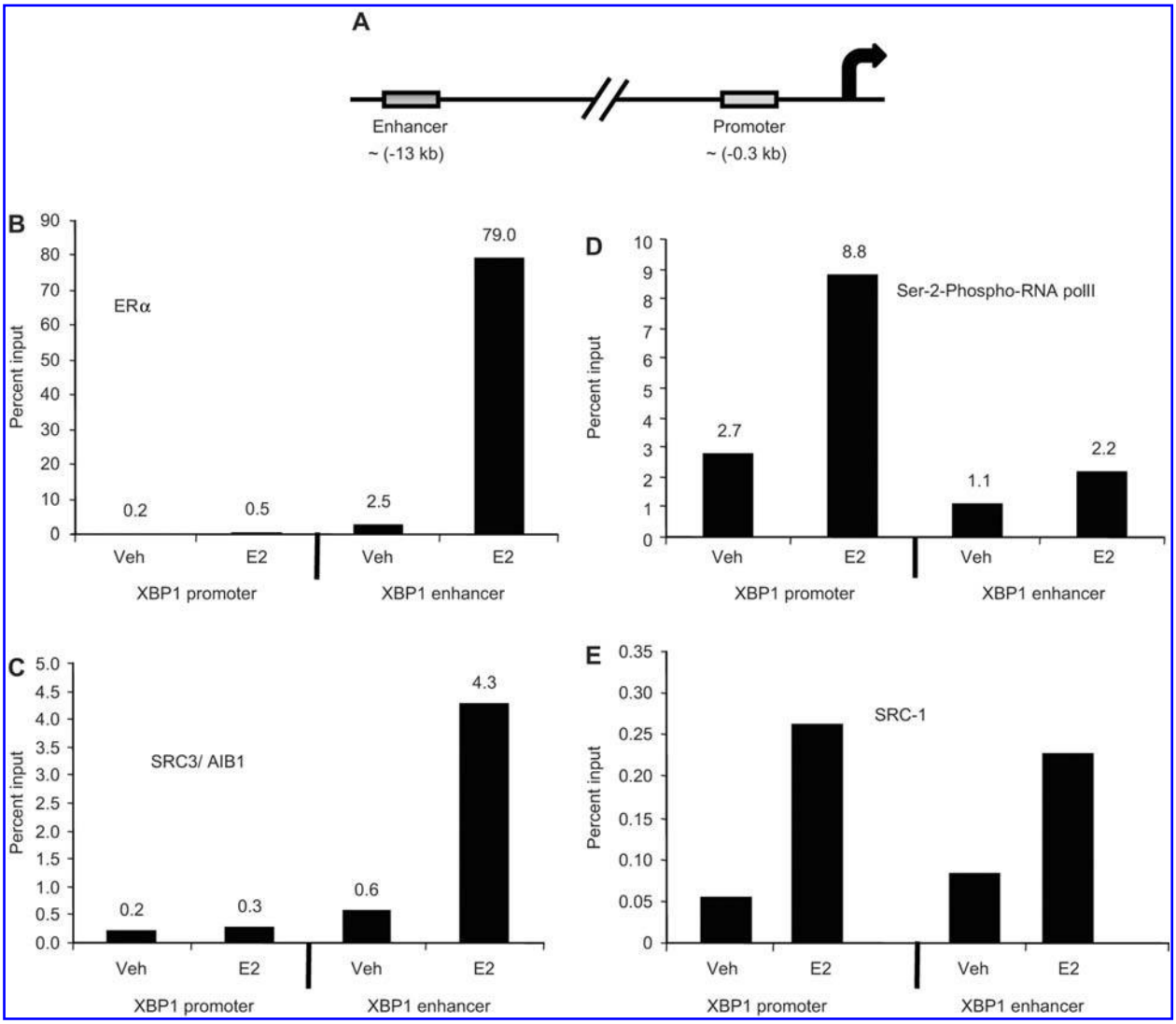


Figure 3 Recruitment of ERα, phospho-serine-2-RNA polII, SRC-1 and SRC-3, at the proximal promoter and distal enhancer region of the XBP1 gene assessed by chromatin immunoprecipitation (ChIP) assay. MCF7 cells were treated with vehicle or E2 (1 nM) for 45 min and ChIP assay was performed as mentioned in the materials and methods section. Schematic representation of the promoter and enhancer regions of the XBP1 gene (A). The extent of recruitment of the factors indicated is shown for promoter and enhancer region of the XBP1 gene. The data are expressed as percent input of 1/20th part of starting chromatin material in each case after subtracting non-specific binding. The data shown are representative of three separate experiments with similar results.

drastically downregulated the XBP1 levels in MCF7:5C cells (Figure 2E), which coincides with estrogen-induced apoptosis in these cells.

Recruitment of ERα and other factors at the promoter and enhancer regions of the XBP1 gene

To further confirm the direct involvement of ERα in transcriptional induction of the XBP1 gene, we performed ChIP assay to assess the recruitment of ERα, SRC-1, SRC-3 and serine-2-phosphorylated RNA polymerase II at ~0.3 kb (promoter) and ~13 kb (enhancer) upstream of the transcription start site of the XBP1 gene (Figure 3A) in the MCF7 cells treated with vehicle or 1 nM E2 for 45 min. We found higher occupancy of ERα and SRC-3 at the enhancer region but not at the promoter region. The occupancy of these factors at the enhancer region was further stimulated after 45 min of E2 treatment compared with vehicle treatment (Figure 3B and C). In contrast, serine-2-phosphorylated RNA polymerase II was found to be recruited 4-fold more at the promoter region than at the enhancer region after 45 min of E2 treatment (Figure 3D). Occupancy of SRC-1 was stimulated after E2 treatment in both the promoter and enhancer regions of the XBP1 gene (Figure 3E). These results indicate that the enhancer region of XBP1 is involved in the regulation of estrogen-induced transcriptional stimulation of the XBP1 gene.

XBP1 depletion inhibits estrogen-mediated growth

To investigate the functional importance of XBP1, we evaluated the effect through loss-of-function using a pool of

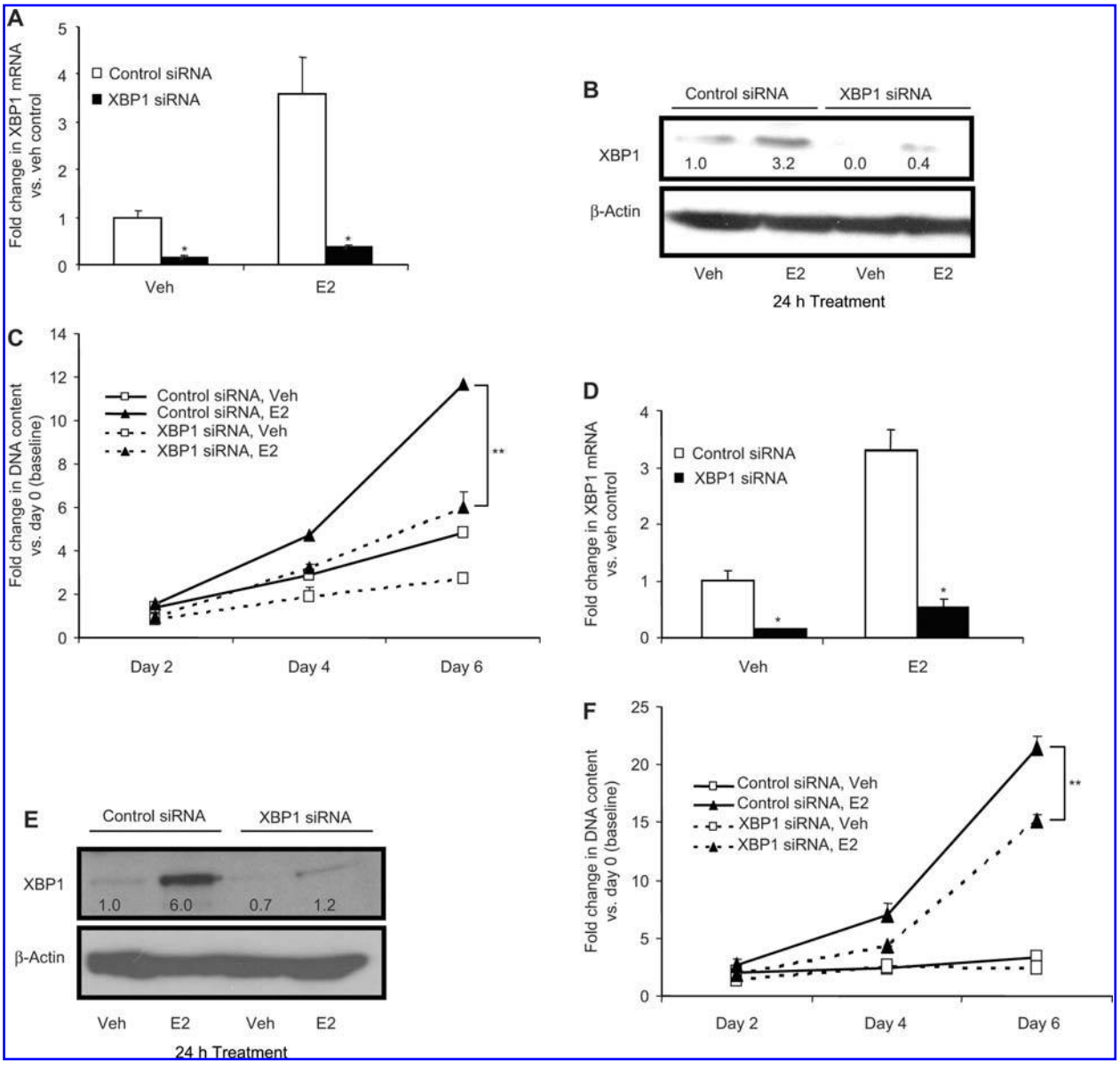


Figure 4 Short interfering RNA (siRNA)-mediated knockdown of XBP1 inhibits growth of MCF7 and ECC1 cells and its effect on estrogen-mediated growth. MCF7 and ECC1 cells, transfected with XBP1 siRNA or control siRNA, were treated with E2 (1 nM) or vehicle for 24 h and the extent of knockdown was assessed using quantitative real-time PCR compared with control siRNA, vehicle-treated cells (A and D) and Western blotting (B and E). Subsequently, cells were reseeded and the growth of the cells was monitored over a 6-day period. Total DNA content was measured as a marker of growth and the fold change in DNA content was calculated compared with the number of cells at the time of the start of the treatment (baseline) (C and F). *$p < 0.05$ compared with control siRNA group and **$p < 0.005$, using the unpaired Student t-test. The Western blots were scanned and quantified. Levels of XBP1 normalized for β-actin, relative to control siRNA-vehicle treated cells, are indicated below each band.

siRNA against XBP1 in MCF7 and ECC1 cells. The extent of XBP1 knockdown was confirmed by real-time PCR and Western blotting (Figure 4A and B; Figure 4D and E, respectively). A growth assay was performed after XBP1 knockdown by siRNA and total DNA content was used as a measure to determine the cell growth over a 6-day period. A parallel identical growth assay was performed using pool of non-targeting control siRNA for comparison. XBP1 knockdown attenuated the E2-induced growth of MCF7 and ECC1 cells by 49% and 30%, respectively, compared with cells treated with control siRNA (Figure 4C and F). These data indicated that the level of XBP1 expression is critical for inducing estradiol-mediated growth of breast and endometrial cancer cells.

We further investigated if the levels of ERα were altered in the XBP1-depleted MCF7 cells compared with control siRNA-treated MCF7 cells. No differences were detected in levels of ERα in XBP1-depleted cells compared with control siRNA-treated cells in presence of vehicle or E2 for 24 h (Figure 5). This rules out the possibility that growth

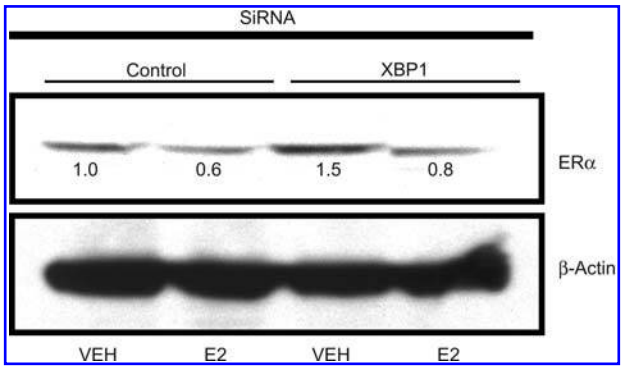


Figure 5 ERα levels in MCF7 cells treated with control or XBP1 siRNA. MCF7 cells were transfected with control or XBP1 siRNA and subsequently treated with vehicle or E2 for 24 h. ERα levels were assessed by Western blotting. Levels of β-actin are shown as loading control. The Western blots were scanned and quantified. Levels of ERα protein normalized for β-actin, relative to control siRNA-vehicle treated cells, are indicated below each band.

inhibition of XBP1-depleted cells was due to altered ERα levels.

XBP1 overexpression or XBP1 depletion does not affect ERE-mediated transcriptional activity

To understand the underlying mechanism by which XBP1 can influence estrogen-mediated growth, we examined the effect of XBP1 overexpression or depletion on the transcriptional activity of ER from a classical ERE. We performed an ERE-luciferase reporter assay in the MCF7 cells transiently transfected with XBP1 expression plasmid or XBP1 siRNA. No differences were observed (Figure 6A and B) in transcriptional activity (as measured by luciferase activity) of the ERE-luciferase reporter in the cells either overexpressing XBP1 or the cells depleted of XBP1 compared with their respective controls. This result suggests that levels of XBP1 in the cell might not affect the classical transcriptional activity of ERα mediated through the direct binding of ERE.

Discussion

Estrogen is the prime growth regulator of ER positive breast and endometrial cancer cells. To better understand the induction of estrogen-mediated growth in breast cancer, some studies (6, 28) have explored the estrogen-induced transcriptional network using DNA microarrays to identify downstream pathways. In these studies, many of the estrogen-regulated genes are identified as transcription factors which could be collectively responsible for the phenotypic manifestations of estrogen-induced growth of ER positive cancer cells. However, in the majority of cases, the precise role of the downstream events in growth is not understood. One solution which can be used to dissect the complexities of clinical tissues is to interrogate estrogen responsive cell lines. One such recent study (29) has noted that the genes are similarly regulated by estrogen in breast

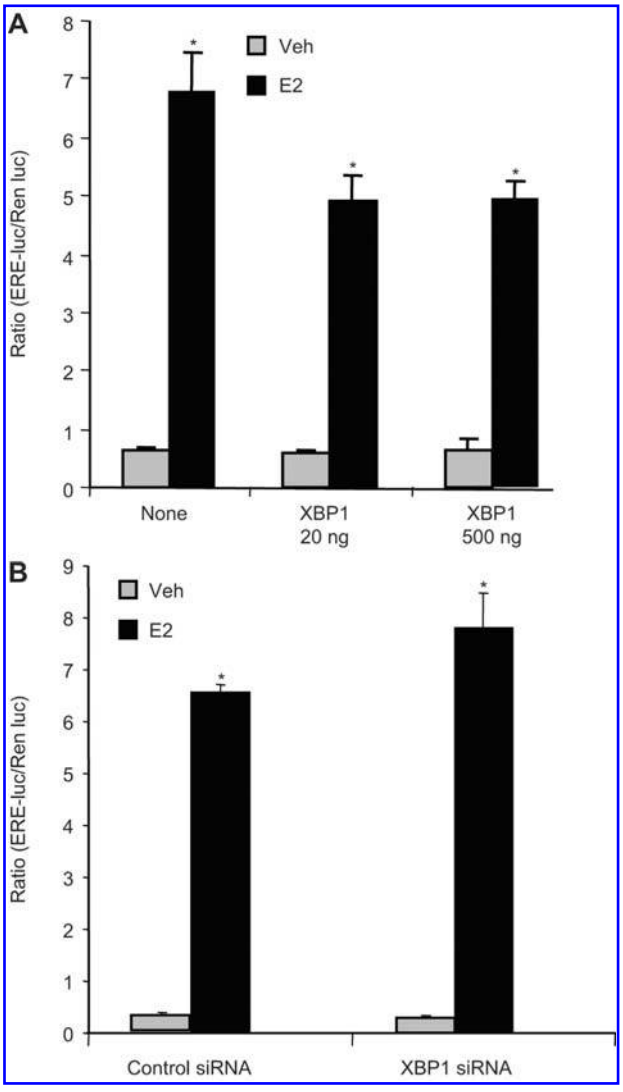


Figure 6 ERE-mediated luciferase activity in XBP1 overexpressing or XBP1 depleted cells. MCF7 cells were transfected with empty vector (none), 20 ng or 500 ng of XBP1-expressing plasmid and ERE-mediated luciferase activity was assessed in absence or presence of 1 nM E2 (A). MCF7 cells transfected with control or XBP1 siRNA were used to assess ERE-mediated luciferase activity in presence or absence of 1 nM E2 (B). Renilla luciferase activity was used as internal control and all values are represented as a ratio of ERE-luciferase and renilla luciferase activity. The values are average of at least four replicates ±SD. *$p < 0.05$ compared with respective vehicle-treated group.

cancer cells in vitro and human breast tumors. This provides a unique opportunity to study the underlying mechanism by manipulating specific genes in the cells, which can influence the progression of ER positive cancers and also provide potential targets for therapeutic intervention. In this context, some recent reports have identified the important roles played by the estrogen-regulated genes such as FOXA1 (10, 30, 31), GREB1 (32) and GATA-3 (30, 33) in regulating estrogen-induced growth in breast cancers.

In the present study, we evaluated the phenotypic effects of the E2-regulated gene XBP1, which has been consistently

shown to be highly coexpressed with ERα in breast cancer patients and is also known to be upregulated by estrogen in the ER positive breast cancer cells in vitro (4–9, 29). Although it is well established that XBP1 plays a key role in UPR and endoplasmic reticulum stress by acting as a transcription factor for the genes involved in UPR, its role in E2-dependent ER positive cancers is not fully understood.

Our results confirm that XBP1 is an E2-regulated gene which is in agreement with previous studies (6, 10). The E2-induction of XBP1 is mediated by ERα and does not need de novo protein synthesis for the upregulation, as CHX did not alter the regulation. Treatment with DRB, an inhibitor of transcription, completely blocked the upregulation of XBP1 by estrogen, indicating transcriptional regulation. The ChIP data further confirmed direct binding of ERα, SRC-1, SRC-3 and serine-2-phosphorylated RNA polymerase II at the promoter and/or enhancer region of the XBP1 gene. Interestingly, recruitment of ERα and SRC-3 (AIB1) was higher at the enhancer region of the XBP1 gene and very minimal at the promoter region. ERα recruitment was induced dramatically at the enhancer region after 45 min of E2 treatment. Recruitment of ERα was also accompanied by SRC-1 and SRC-3 at the enhancer region. However, as expected, recruitment of serine-2-phosphorylated RNA polymerase II was higher at the promoter region than the enhancer region. These data strongly suggest that the enhancer region of the XBP1 gene, which is approximately 13 kb upstream of the transcription start site, is involved in the transcriptional regulation of XBP1 by ER. Indeed, recent studies (34–36) have indicated that distal enhancers of E2-induced genes GREB1 and carbonic anhydrase 12 are involved in the transcriptional regulation by ER. It has been shown that the distal enhancer can interact with the proximal promoter region of these estrogen-regulated genes by intrachromosomal looping.

This study reports for the first time that the XBP1 level is critical for E2-induced growth of ER positive breast and endometrial cancer cells, as evidenced by marked inhibition of E2-induced growth of XBP1-deficient MCF7 and ECC1 cells. This specifically demonstrates that the endogenous level of XBP1 and its upregulation by estrogen is intimately involved in the growth regulation of estrogen responsive breast and endometrial cancer cells. A recent study demonstrated that overexpression of XBP1 in ER positive breast cancer cells can lead to anti-estrogen resistance, by regulating genes associated with apoptosis and cell cycle progression (20).

To further understand the mechanism by which XBP1 can influence E2-induced growth, we hypothesized that levels of XBP1 could affect the ERE-mediated transcriptional activity of ER. To test this we depleted or overexpressed XBP1 and performed an ERE-luciferase reporter assay. Our data show that the level of XBP1 in the MCF7 cells does not affect the transcriptional activity of ER mediated through classical ERE binding. This indicates that XBP1 can influence the growth of the cells by either regulating a subset of genes directly under the control of XBP1 or can also modulate the E2 regulation of the genes which are not exclusively regulated by classical ERE-mediated transcription. These data are, however, in contrast to a previous study (19) where XBP1 overexpression activated ER transcriptional activity in a ligand-independent manner. The differences in the results could be attributed to the exogenous overexpression of ERα in the previous study, whereas in the present study we relied on the intrinsic activity of ER in the MCF7 cells. Further investigations are required to address the associated mechanism of action.

In summary, our results demonstrate that XBP1 expression is estrogen regulated at the transcriptional level and the enhancer region of the XBP1 gene can play a critical role in regulating E2-mediated transcriptional activation. Our findings show that expression level of XBP1 is critical in achieving optimal E2-induced growth in breast and endometrial cancer cells without influencing the classical ERE-mediated transcriptional activity. Our findings also provide an explanation for the strong correlation observed between ERα and XBP1 expression in breast cancer patients. Taken together, we suggest that this novel mechanism for the regulation of cancer cell growth via XBP1 can be exploited as a novel drug target in future studies of anti-hormonal resistance in ER positive cancer cells.

Acknowledgements

This research was supported by the Department of Defense Breast Program under award number BC050277 Center of Excellence; Fox Chase Cancer Center Core Grant NIH P30 CA006927; the Weg Fund of Fox Chase Cancer Center; the Genuardi fund and the Hollenbach Family Fund. The views and opinions of the author(s) do not reflect those of the US Army or the Department of Defense.

References

1. Jensen EV, Jordan VC. The estrogen receptor: a model for molecular medicine. Clin Cancer Res 2003;9:1980–9.
2. van't Veer LJ, Dai H, van de Vijver MJ, He YD, Hart AA, Mao M, Peterse HL, van der Kooy K, Marton MJ, Witteveen AT, Schreiber GJ, Kerkhoven RM, Roberts C, Linsley PS, Bernards R, Friend SH. Gene expression profiling predicts clinical outcome of breast cancer. Nature 2002;415:530–6.
3. Finlin BS, Gau CL, Murphy GA, Shao H, Kimel T, Seitz RS, Chiu YF, Botstein D, Brown PO, Der CJ, Tamanoi F, Andres DA, Perou CM. RERG is a novel ras-related, estrogen-regulated and growth-inhibitory gene in breast cancer. J Biol Chem 2001; 276:42259–67.
4. Wang DY, Fulthorpe R, Liss SN, Edwards EA. Identification of estrogen-responsive genes by complementary deoxyribonucleic acid microarray and characterization of a novel early estrogen-induced gene: EEIG1. Mol Endocrinol 2004;18:402–11.
5. Tozlu S, Girault I, Vacher S, Vendrell J, Andrieu C, Spyratos F, Cohen P, Lidereau R, Bieche I. Identification of novel genes that co-cluster with estrogen receptor alpha in breast tumor biopsy specimens, using a large-scale real-time reverse transcription-PCR approach. Endocr Relat Cancer 2006;13:1109–20.
6. Cunliffe HE, Ringner M, Bilke S, Walker RL, Cheung JM, Chen Y, Meltzer PS. The gene expression response of breast cancer to growth regulators: patterns and correlation with tumor expression profiles. Cancer Res 2003;63:7158–66.

7. Bertucci F, Nasser V, Granjeaud S, Eisinger F, Adelaide J, Tagett R, Loriod B, Giaconia A, Benziane A, Devilard E, Jacquemier J, Viens P, Nguyen C, Birnbaum D, Houlgatte R. Gene expression profiles of poor-prognosis primary breast cancer correlate with survival. Hum Mol Genet 2002;11:863–72.
8. Bertucci F, Houlgatte R, Benziane A, Granjeaud S, Adelaide J, Tagett R, Loriod B, Jacquemier J, Viens P, Jordan B, Birnbaum D, Nguyen C. Gene expression profiling of primary breast carcinomas using arrays of candidate genes. Hum Mol Genet 2000;9:2981–91.
9. Fujimoto T, Onda M, Nagai H, Nagahata T, Ogawa K, Emi M. Upregulation and overexpression of human X-box binding protein 1 (hXBP-1) gene in primary breast cancers. Breast Cancer 2003;10:301–6.
10. Carroll JS, Liu XS, Brodsky AS, Li W, Meyer CA, Szary AJ, Eeckhoute J, Shao W, Hestermann EV, Geistlinger TR, Fox EA, Silver PA, Brown M. Chromosome-wide mapping of estrogen receptor binding reveals long-range regulation requiring the forkhead protein FoxA1. Cell 2005;122:33–43.
11. Koong AC, Chauhan V, Romero-Ramirez L. Targeting XBP-1 as a novel anti-cancer strategy. Cancer Biol Ther 2006;5: 756–9.
12. Romero-Ramirez L, Cao H, Nelson D, Hammond E, Lee AH, Yoshida H, Mori K, Glimcher LH, Denko NC, Giaccia AJ, Le QT, Koong AC. XBP1 is essential for survival under hypoxic conditions and is required for tumor growth. Cancer Res 2004;64:5943–7.
13. Reimold AM, Etkin A, Clauss I, Perkins A, Friend DS, Zhang J, Horton HF, Scott A, Orkin SH, Byrne MC, Grusby MJ, Glimcher LH. An essential role in liver development for transcription factor XBP-1. Genes Dev 2000;14:152–7.
14. Lee AH, Chu GC, Iwakoshi NN, Glimcher LH. XBP-1 is required for biogenesis of cellular secretory machinery of exocrine glands. EMBO J 2005;24:4368–80.
15. Iwakoshi NN, Lee AH, Glimcher LH. The X-box binding protein-1 transcription factor is required for plasma cell differentiation and the unfolded protein response. Immunol Rev 2003;194:29–38.
16. Lee AH, Iwakoshi NN, Anderson KC, Glimcher LH. Proteasome inhibitors disrupt the unfolded protein response in myeloma cells. Proc Natl Acad Sci USA 2003;100:9946–51.
17. Kaser A, Lee AH, Franke A, Glickman JN, Zeissig S, Tilg H, Nieuwenhuis EE, Higgins DE, Schreiber S, Glimcher LH, Blumberg RS. XBP1 links ER stress to intestinal inflammation and confers genetic risk for human inflammatory bowel disease. Cell 2008;134:743–56.
18. Ding L, Yan J, Zhu J, Zhong H, Lu Q, Wang Z, Huang C, Ye Q. Ligand-independent activation of estrogen receptor alpha by XBP-1. Nucleic Acids Res 2003;31:5266–74.
19. Fang Y, Yan J, Ding L, Liu Y, Zhu J, Huang C, Zhao H, Lu Q, Zhang X, Yang X, Ye Q. XBP-1 increases ERα transcriptional activity through regulation of large-scale chromatin unfolding. Biochem Biophys Res Commun 2004;323:269–74.
20. Gomez BP, Riggins RB, Shajahan AN, Klimach U, Wang A, Crawford AC, Zhu Y, Zwart A, Wang M, Clarke R. Human X-box binding protein-1 confers both estrogen independence and antiestrogen resistance in breast cancer cell lines. FASEB J 2007;21:4013–27.
21. Pink JJ, Jordan VC. Models of estrogen receptor regulation by estrogens and antiestrogens in breast cancer cell lines. Cancer Res 1996;56:2321–30.
22. Livak KJ, Schmittgen TD. Analysis of relative gene expression data using real-time quantitative PCR and the 2(-Delta Delta C(T)) Method. Methods 2001;25:402–8.
23. Frasor J, Danes JM, Komm B, Chang KC, Lyttle CR, Katzenellenbogen BS. Profiling of estrogen up- and down-regulated gene expression in human breast cancer cells: insights into gene networks and pathways underlying estrogenic control of proliferation and cell phenotype. Endocrinology 2003;144:4562–74.
24. Shang Y, Hu X, DiRenzo J, Lazar MA, Brown M. Cofactor dynamics and sufficiency in estrogen receptor-regulated transcription. Cell 2000;103:843–52.
25. Ariazi EA, Kraus RJ, Farrell ML, Jordan VC, Mertz JE. Estrogen-related receptor α1 transcriptional activities are regulated in part via the ErbB2/HER2 signaling pathway. Mol Cancer Res 2007;5:71–85.
26. Lewis JS, Osipo C, Meeke K, Jordan VC. Estrogen-induced apoptosis in a breast cancer model resistant to long-term estrogen withdrawal. J Steroid Biochem Mol Biol 2005;94:131–41.
27. Lewis JS, Meeke K, Osipo C, Ross EA, Kidawi N, Li T, Bell E, Chandel NS, Jordan VC. Intrinsic mechanism of estradiol-induced apoptosis in breast cancer cells resistant to estrogen deprivation. J Natl Cancer Inst 2005;97:1746–59.
28. DeNardo DG, Kim HT, Hilsenbeck S, Cuba V, Tsimelzon A, Brown PH. Global gene expression analysis of estrogen receptor transcription factor cross talk in breast cancer: identification of estrogen-induced/activator protein-1-dependent genes. Mol Endocrinol 2005;19:362–78.
29. Creighton CJ, Cordero KE, Larios JM, Miller RS, Johnson MD, Chinnaiyan AM, Lippman ME, Rae JM. Genes regulated by estrogen in breast tumor cells in vitro are similarly regulated in vivo in tumor xenografts and human breast tumors. Genome Biol 2006;7:R28.
30. Lacroix M, Leclercq G. About GATA3, HNF3A, and XBP1, three genes co-expressed with the oestrogen receptor-alpha gene (ESR1) in breast cancer. Mol Cell Endocrinol 2004;219:1–7.
31. Laganiere J, Deblois G, Lefebvre C, Bataille AR, Robert F, Giguere V. From the cover: location analysis of estrogen receptor alpha target promoters reveals that FOXA1 defines a domain of the estrogen response. Proc Natl Acad Sci USA 2005; 102:11651–6.
32. Rae JM, Johnson MD, Scheys JO, Cordero KE, Larios JM, Lippman ME. GREB 1 is a critical regulator of hormone dependent breast cancer growth. Breast Cancer Res Treat 2005;92:141–9.
33. Eeckhoute J, Keeton EK, Lupien M, Krum SA, Carroll JS, Brown M. Positive cross-regulatory loop ties GATA-3 to estrogen receptor alpha expression in breast cancer. Cancer Res 2007;67:6477–83.
34. Barnett DH, Sheng S, Charn TH, Waheed A, Sly WS, Lin CY, Liu ET, Katzenellenbogen BS. Estrogen receptor regulation of carbonic anhydrase XII through a distal enhancer in breast cancer. Cancer Res 2008;68:3505–15.
35. Deschenes J, Bourdeau V, White JH, Mader S. Regulation of GREB1 transcription by estrogen receptor alpha through a multipartite enhancer spread over 20 kb of upstream flanking sequences. J Biol Chem 2007;282:17335–9.
36. Sun J, Nawaz Z, Slingerland JM. Long-range activation of GREB1 by estrogen receptor via three distal consensus estrogen-responsive elements in breast cancer cells. Mol Endocrinol 2007;21:2651–62.

Raloxifene-stimulated experimental breast cancer with the paradoxical actions of estrogen to promote or prevent tumor growth: A unifying concept in anti-hormone resistance

GREGOR M. BALABURSKI[1], RITA C. DARDES[2], MICHAEL JOHNSON[3], BASSEM HADDAD[3], FANG ZHU[1], ERIC A. ROSS[1], SUROJEET SENGUPTA[3], ANDRES KLEIN-SZANTO[1], HONG LIU[4], EUN SOOK LEE[4], HELEN KIM[3] and V. CRAIG JORDAN[3]

[1]Fox Chase Cancer Center, 333 Cottman Avenue, Philadelphia, PA 19111, USA; [2]Department of Gynecology, Federal University of São Paulo (UNIFESP), Rua João Cachoeria 488cj 602, CEP 04535-001 São Paulo, Brasil; [3]Georgetown University Medical Center, Lombardi Comprehensive Cancer Center, 3970 Reservoir Road NW, Washington, D.C. 20057; [4]Robert H. Lurie Comprehensive Cancer Center, Feinberg School of Medicine, Northwestern University, Chicago, IL 60611, USA

Received March 29, 2010; Accepted May 2, 2010

DOI: 10.3892/ijo_00000687

Abstract. We have previously demonstrated that prolonged treatments with raloxifene (RAL) *in vitro* will result in phase II RAL resistance and RAL-induced tumor growth. Clinical interest prompted us to re-examine RAL resistance *in vivo*, particularly the effects of long-term treatments (a decade or more) on the evolution of RAL resistance. In this study, we have addressed the question of this being a reproducible phenomenon in wild-type estrogen receptor (ER)-positive human breast cell line MCF-7. MCF-7 cells cultured under estrogen-deprived conditions in the presence of 1 μM RAL for more than a year develop RAL resistance resulting in an independent cell line, MCF7-RAL. The MCF7-RAL cells grow in response to both estradiol E_2 and RAL. Fulvestrant (FUL) blocks RAL and E_2-mediated growth. Transplantation of MCF7-RAL cells into athymic ovariectomized mice and treatment with physiologic doses of E_2 causes early E_2-stimulated tumor growth. In contrast, continuous treatment of implanted animals with daily oral RAL (1.5 mg daily) causes growth of small tumors within 15 weeks. Continuous re-transplantation of the tumors growing in RAL-treated mice indicated that RAL stimulated tumor growth. Tumors in the untreated mice did not grow. Bi-transplantation of MCF7-E_2 and MCF7-RAL tumors into the opposing mammary fat pads of the same ovariectomized animal demonstrated that MCF7-E_2 grew with E_2 stimulation and not with RAL. Conversely, MCF7-RAL tumors grew with RAL and not E_2, a characteristic of phase II resistance. Established phase II resistance of MCF7-RAL tumors was confirmed following up to 7 years of serial transplantation in RAL-treated athymic mice. The ERα was retained in these tumors. The cyclical nature of RAL resistance was confirmed and extended during a 2-year evolution of the resistant phases of the MCF7-RAL tumors. The MCF7-RAL tumors that initially were inhibited by E_2 grew in the presence of E_2 and subsequently grew with either RAL or E_2. RAL remained the major grow stimulus and RAL enhanced E_2-stimulated growth. Subsequent transplantation of E_2 stimulated tumors and evaluations of the actions of RAL, demonstrated robust E_2-stimulated growth that was blocked by RAL. These are the characteristics of the anti-estrogenic actions of RAL on E_2-stimulated breast cancer growth with a minor component of phase I RAL resistance. Continuous transplantation of the phase I RAL-stimulated tumors for >8 months causes reversion to phase II resistance. These data and literature reports of the cyclical nature of anti-androgen/androgen responsiveness of prostate cancer growth, illustrate the generality of the evolution of anti-hormonal resistance in sex steroid-sensitive target tissues.

Correspondence to: Dr V. Craig Jordan, Georgetown University Medical Center, Lombardi Comprehensive Cancer Center, 3970 Reservoir Road NW, Washington, D.C. 20057, USA
E-mail: vcj2@georgetown.edu

Key words: raloxifene, tamoxifen, osteoporosis, breast cancer

Introduction

Selective estrogen receptor (ER) modulators (SERMs) are compounds that bind to the ER and based on tissue specificity, act as agonists or antagonists (1). Tamoxifen (TAM), the first SERM, is a proven agent for treatment of breast cancer (2) and breast cancer chemoprevention (3,4). Laboratory studies during the 1980s demonstrated that long-term tamoxifen treatment stimulated the growth of ER-positive MCF-7 breast tumors *in vivo* (5,6). This unique form of acquired resistance to a cancer therapy raised clinical concerns

about extending adjuvant tamoxifen therapy. However, the risk of developing endometrial cancer during the use of tamoxifen for chemoprevention of breast cancer (4) prompted the examination of other compounds that would capitalize on the gains in breast cancer prevention made with tamoxifen but with a superior safety profile.

Raloxifene (also known as keoxifene or LY156,758) (7), a second generation SERM, inhibits the growth of 7,12-dimethylbenzanthracene (DMBA)-induced tumors in rats (8), prevents the development and growth of estrogen-dependent N-nitrosomethylurea (NMU)-induced mammary carcinoma in rats (9) and maintains bone density in ovariectomized rats (10). The recognition that non-steroidal anti-estrogens like tamoxifen and raloxifene selectively exhibited estrogen-like effects in bone and anti-estrogenic effects in breast and mammary tissue (9,10) suggested a new strategy to prevent breast cancer by treating post-menopausal women to prevent and treat osteoporosis and prevent breast cancer at the same time (11).

The clinical finding that patients treated with raloxifene to improve bone density (12) exhibited significant decrease in the rates of breast cancer (13), provided a clinical proof of the laboratory principle and demonstrated raloxifene's potential as a breast cancer chemopreventive agent. Data from the study of tamoxifen and raloxifene (STAR) trial (14), which directly compared raloxifene to tamoxifen for breast cancer chemoprevention, indicated that raloxifene has similar chemopreventive properties as tamoxifen but with a significantly better safety profile. A subsequent clinical trial (15) examining the effects of raloxifene on coronary heart disease (CHD) did not achieve its goals but confirmed the role of raloxifene as a breast cancer chemoprevention agent with no increase in endometrial cancer. The evaluation by Martino and coworkers (16) that long-term raloxifene treatment for the prevention of osteoporosis does not increase endometrial cancer but maintains an inhibiting effect on breast cancer incidence suggests that the clinical community may use raloxifene for indefinite periods. However, the discovery that acquired tamoxifen resistance evolves (17,18) raises new questions about acquired resistance to raloxifene treatments.

Acquired tamoxifen resistance is sub-divided into 3 phases: i) phase I, in which estrogen and the SERM stimulate tumor growth, ii) phase II, in which the SERM stimulates tumor growth and estrogen induces tumor regression; iii) phase III resistance or autonomous growth (1). Laboratory studies indicate that long-term SERM treatments result in hypersensitivity to low, physiological doses of estrogen resulting in breast tumor regression and possibly estrogen-induced apoptosis. It is important to note that these observations were initially made with an estrogen-supersensitive clone of MCF-7 breast cancer cells (WS8) using only tamoxifen treatment for 5-10 years *in vivo* (17,18) and raloxifene-resistant model (19,20) *in vitro* and few weeks (20) or a year or two (19,20) *in vivo*. These data are not confined to SERM-resistant models as similar observations were made in long-term estrogen-deprived breast cancer cells (21-24). The findings that physiological estrogen causes dramatic tumor repression in anti-hormone-resistant breast cancer (17,18) are reminiscent of the early clinical trials utilizing high doses of diethylstilbestrol (DES) (25,26) to treat breast cancer in post-menopausal patients many years after their menopause. Moreover, recent clinical trial (27,28) evaluating the role of estrogen treatments in women with advanced breast cancer following acquired resistance to anti-hormone therapy noted a 31% objective response and indicated a substantial role for high dose estrogen treatments in hormone-dependent breast cancer resistant to conventional endocrine therapies.

The current 10-year laboratory study has paralleled the translation of the new biology of apoptotic action (17,18,21,23) to clinical trials (27,28). Most importantly, the increasing clinical use of raloxifene for the prevention of osteoporosis in post-menopausal women implies that breast cancer that develops during a decade or more of raloxifene treatment will have developed raloxifene resistance. It is important to address this emerging clinical problem.

Our goal was to revisit this question by utilizing wild-type MCF-7 cells to recreate a raloxifene-resistant variant of MCF7 cells *in vitro*. The failure of wild-type MCF-7 cells to create acquired resistance *in vivo* would expose an inadequacy of laboratory models or imply that acquired raloxifene resistance would not occur in the clinic. This was not the case as the answer is yes to the first question and the answer to the second question requires clinical investigation. We subsequently used the new model *in vivo* to evaluate the actions of physiological estrogen and raloxifene on the growth responses of raloxifene-stimulated tumors passaged over a decade in ovariectomized athymic mice. This laboratory strategy mimics the clinical duration of raloxifene exposure.

Materials and methods

Cell lines and tissue culture. The MCF7 breast cells were a generous gift of Dr Myles Brown (Harvard) in 1995. The MCF7 cells were maintained in a DMEM red medium (Invitrogen, Carlsbad, CA) supplemented with 10% fetal bovine serum (FBS), 2 mM glutamine, 100 U/ml penicillin, 100 μg/ml streptomycin and 10 mM non-essential amino acids (NEAA). Raloxifene-resistant MCF7 cells (MCF7-RAL) were derived by continuously culturing the MCF7 cells for up to 10 years in estrogen-free media: DMEM yellow media with 10% charcoal-stripped FBS, 2 mM glutamine, 100 U/ml penicillin, 100 μg/ml streptomycin and 10 mM NEAA, supplemented with 1 μM raloxifene-HCl. All cell lines were cultured at 37°C, 5% CO_2 and 95% humidity.

Verification of cell line identity by DNA fingerprinting. The identity of the cell lines was verified by DNA fingerprinting using the commercially available kit, PowerPlex® 1.2 System (Promega). This system allows the co-amplification and two-color detection of nine loci (eight STR loci and the Y-specific Amelogenin) and provides a powerful level of discrimination in excess of 1 in 10^8 (29). The following STR markers were tested: CSF1PO, TPOX, TH01, vWA, D16S539, D7S820, D13S317 and D5S818. The cells were harvested by trypsinization and DNA was isolated from the resultant cell pellets using standard methods (30). The PCR amplification was performed according to the manufacturer's recommended protocol. Fragment analysis of the PCR product was achieved using an ABI 3100 capillary sequencer (Applied Biosystems,

Foster City, CA). The GeneMapper® software (Applied Biosystems) was used to score the fragment sizes and generate an alphanumeric score for each locus. The data generated were then compared to allelic alphanumeric scores for MCF-7 and ECC-1 reported in the ATCC STR database generated using the same assay (ATCC, VA).

DNA growth assay. MCF7 and MCF7-RAL cells were seeded in estrogen-free media 4 days prior to start of the experiment. After 3 days of ligand starvation the appropriate numbers of cells were seeded in a 24-well plate. Twenty-four hours later, which was denoted as day 0, the cells were appropriately treated. The media containing treatments were changed every other day. All drugs were solubilized in ethanol and were added as 1:1000 dilutions. Following 15 days of treatment the DNA content of the cells was measured as previously described (31) with VersaFluor fluorometer (Bio-Rad Laboratories, Hercules, CA).

Animal procedures

MCF7 tumor models. The MCF7-E_2 breast tumor model was developed by bilaterally injecting $1x10^7$ MCF7 cells into the mammary fat pads of ovariectomized athymic CrTac: NCR-Foxn1<nu> mice (Taconic, Hudson, NY) (32), 4-6 weeks of age, implanted with silastic 17ß-estradiol capsules. The raloxifene-resistant MCF7-RAL model was similarly developed by injecting $1x10^7$ raloxifene-resistant MCF7-RAL cells into the mammary fat pads of ovariectomized female mice. RAL treatments were started 24 h post-implantation by administering 1.5 mg RAL or .005 mg TAM via oral gavage. The MCF7-RAL tumor xenograft model was maintained by excising the established MCF7-RAL tumors, removing all extraneous tissues and dissecting them into approximately 1-2 mm^3 pieces that were then implanted by trochar into the mammary fat pads of naïve mice subsequently treated with RAL. The RAL-resistant MCF7-RAL model was continuously passaged into RAL-treated athymic mice over a 10-year period. Established tumors were measured every week or as needed with Vernier calipers and cross sectional area of the tumor was calculated utilizing the formula: Length (l) x width (w) x $\pi/4$.

Drug administration. The raloxifene solution for oral gavage was prepared by grinding 10 commercially available Evista® tablets and dissolving them into 10% PEG 400/Tween-80 (Sigma, St. Louis, MO) solution to a final concentration of 15 mg/ml. Silastic 17ß-estradiol capsules were manufactured as previously described (33) and were subcutaneously implanted in the mice dorsal region. The 0.3-cm capsule delivered the equivalent of menopausal levels of estrogen while the 1.0-cm capsule delivered the equivalent of pre-menopausal levels of estrogen (34). Fulvestrant (Fasoldex/ICI 182,780, AstraZeneca) is commercially available and was purchased from the hospital pharmacy. Total fulvestrant (FUL) (10 mg) was injected bi-weekly, subcutaneously (35). All animal studies were approved by the Fox Chase institutional animal care and use committee.

RNA extractions, reverse transcriptase reactions and real-time qPCR. Total RNA was extracted with TRIzol reagent (Invitrogen) and further purified using RNeasy Mini and Midi kits (Qiagen, Valencia, CA). Total RNA (1 μg) was reversely transcribed with the High Capacity cDNA reverse transcriptase kit (Applied Biosystems) following manufacturer's instructions. The sequences of the primers utilized for real-time qPCR are as follows: *tff1* forward primer, 5'-CATC GACGTCCCTCCAGAAGAG-3'; *tff1* reverse primer, 5'-CTC TGGGACTAATCACCGTGCTG-3'; *36B4* forward primer, 5'-GTGTTCGACAATGGCAGGCAT-3'; *36B4* reverse primer, 5'-GACACCCTCCAGGAAGCGA-3'; c-myc forward primer, 5'-GCCACGTCTCCACACATCAG-3'; c-myc reverse primer, 5'-TCTTGGCAGCAGGAATAGTCCTT-3'; ebag9 forward primer, 5'-CTGGCAGAGGACGGAAATTA-3'; ebag9 reverse primer, 5'-TCATCCCAGGAAGTCCACTC-3'; the primer sets for *egfr* and *her2* were previously described (36,37). Real-time qPCR was performed using the 7900HT real-time PCR system (Applied Biosystems), the amplicons were detected with SYBR-Green and analysis was performed utilizing the $2^{-\Delta\Delta t}$ method (38).

Transient transfections and luciferase assays. MCF7 and MCF7-RAL cells were maintained in estrogen-free medium for 3 days and seeded at confluency of 150,000 cells per 6-well plate. The cells were co-transfected with 5ERE(5X)-TA ffluc and pTA-srluc utilizing TransIT LT1 transfection agent (Mirus, Madison, WI) (39). Luciferase activity was measured utilizing the Dual-luciferase reporter assay system (Promega) with Mithras LB 940 (Berhold Technologies, Bad Wildbad, Germany) microplate reader.

Protein isolation and Western blot. The MCF7 and MCF7-RAL cells were cultured in estrogen-free media for 3 days and seeded at 50-60% confluency. Twenty-four hours post-seeding the cells were treated with the appropriate drug or drug combination. Following 24-h treatment, the cells were washed with PBS and scraped off the plates. After brief centrifugation at 4°C the PBS was aspirated and the cells were resuspended in RIPA buffer (Sigma) supplemented with complete mini protease inhibitor cocktail tablets (Roche Diagnostics, Indianapolis, IN), phosphatase inhibitor cocktail set (EMD Biosciences, La Jolla, CA) and benzonase (Call Biochem, La Jolla, CA). The cells were then incubated for additional 30 min at 4°C with rotation. The debris was removed with centrifugation at 12000 rpm for 30 min at 4°C.

Tumor protein lysates were generated by pulverizing flash-frozen tumors to a fine powder with a Bio-pulverizer (BioSpec Products Inc., Bartlesville, OK) and resuspending them in 400 μl of RIPA buffer supplemented with complete mini protease inhibitor cocktail tablets and phosphatase inhibitors cocktail set. The suspension was than sonicated 3 times at maximum power and centrifuged at 12000 rpm for 20 min at 4°C. Supernatants were collected and stored at -80°C.

Protein quantitation was performed with the Bicinchoninic acid (BCA) Protein Assay (Pierce, Rockford, IL) as per the manufacturer's protocol. Readings were obtained with a microplate reader (SpectraMax Plus, Molecular Devices, Sunnyvale, CA). Protein (50 μg) was resolved by SDS-PAGE and Western blotting was performed as previously described (40). Antibodies used were as follows: ERα G-20 (Santa Cruz Biotechnology, Inc., Santa Cruz, CA), phospho

A.

cell line:	D5S818 allele 1	D5S818 allele 2	D13S317 allele 1	D13S317 allele 2	D7S820 allele 1	D7S820 allele 2	D16S539 allele 1	D16S539 allele 2	vWA allele 1	vWA allele 2	TH01 allele 1	TH01 allele 2	Amelogenin allele 1	Amelogenin allele 2	TPOX allele 1	TPOX allele 2	CSF1PO allele 1	CSF1PO allele 2
MCF-7 ATCC	11	12	11	11	8	8	11	12	14	15	6	6	X	X	8	12	10	10
MCF7-WS8 p24		12	11	11	8	8	11	12		15	6	6	X	X	8	12	10	10
MCF7/5C p217		12	11	11	8	8	11	12	14	15	6	6	X	X	8	12	10	
MCF7/2A p549		12	11	11	8	8	11	12	14	15	6	6	X	X	8	12	10	10
MCF7/ICI p42		12	11	11	8	8	11	12		15	6	6	X	X	8	12	10	10
MCF7/RAL p83	12		11	11	8	8	11	12	14	15	6	6	X	X	8	12	10	10

B.

cell line	D5S818 allele 1	D5S818 allele 2	D13S317 allele 1	D13S317 allele 2	D7S820 allele 1	D7S820 allele 2	D16S539 allele 1	D16S539 allele 2	vWA allele 1	vWA allele 2	TH01 allele 1	TH01 allele 2	Amelogenin allele 1	Amelogenin allele 2	TPOX allele 1	TPOX allele 2	CSF1PO allele 1	CSF1PO allele 2
MCF-7 ATCC	11	12	11	11	8	8	11	12	14	15	6	6	X	X	8	12	10	10
MCF7 (GMB) p184	11	12	11	11	8	8	11	12	14	15	6	6	X	X	8	12	10	10
MCF7-RAL (GMB) p74	11	12	11	11	8	8	11	12	14	15	6	6	X	X	8	12	10	10
ECC1 ATCC		11			8				14	15			X	X				

Figure 1. Verification of cell line identity by DNA fingerprinting. See Materials and methods.

p42/44 MAPK (Thr202/Tyr204) (E10) antibody (Cell Signalling), p42/44 MAP kinase antibody (Cell Signalling). ß-actin antibody AC-15 (Sigma) was used as a loading control. Appropriate horseradish peroxidase-conjugated secondary antibody was used to visualize bands using an Amersham Western Blotting Detection kit (GE Healthcare).

Histology and immunohistochemistry. Tissues were fixed in 10% phosphate-buffered formaldehyde for 48 h, subsequently embedded in paraffin, sectioned and stained. Hematoxylin and eosin (H&E) staining was used to evaluate tumor tissue morphology and extent of necrosis. Immunohistochemistry for Ki-67 (dilution 1:6000) was performed using rabbit polyclonal antibodies from Vector Labs (Burlingame, CA) and Cell Signalling, respectively. Immunostaining was preceded by antigen retrieval in citrate buffer pH6 using a 750 W microwave oven, boiling the slides at maximum setting for 3 min and at low setting for another 7 min. A rabbit Vectastain kit (Vector) was used to develop the immunohistochemical reaction using diaminobenzidine as chromogen. Microphotographs were taken using a Nikon Optiphot research microscope with a x10 and x20 Plan/Apo objectives and a x10 ocular lens connected to a digital photographic camera (Optronics, Magnafire camera, Optronics, Goleta, CA).

Statistical analysis. The growth rates in Fig. 2A and B were estimated for each individual test by fitting the weight of DNA/well to the linear time term. The rates were compared using Wilcoxon rank-sum tests. The tumor growth data were analyzed using growth curve models, where tumor cross sectional area (CSA) was fit assuming a linear function of time. The intercepts and the slopes were used as random effects at the individual tumor level to allow deviation of individual tumor growth from the mean growth of the group. Random mouse effects were included to account for within-animal clustering. The estimated curves were plotted and the fit examined. The differences in rates were estimated by the interaction term between time and the treatment. The comparisons of either the DNA weight/well or CSA at each time point were also conducted by using Wilcoxon rank-sum tests. All tests were 2-sided with 0.05 type I error.

Results

Verification of cell line identity. DNA profiling of the cell lines was conducted using the PowerPlex 1.2 System resulting in the generation of allelic scores for 8 polymorphic STR loci and the amelogenin locus which are presented in Fig. 1A along with the scores for MCF-7 and ECC-1 cells reported in the ATCC STR database. Data from the amelogenin gene amplification were consistent with all samples being of female origin as expected. Allelic score data from the 8 polymorphic STR loci reveal a pattern almost identical among the 5 MCF7 lines that is very closely related to the scores reported for MCF-7 by the ATCC, and consistent with their presumptive identity. Scores for 5 of the 8 loci (D13S317, D7S820, D16S539, TH01 and TPOX) were identical among the study and ATCC MCF-7 cells (Fig. 1A, areas of identity

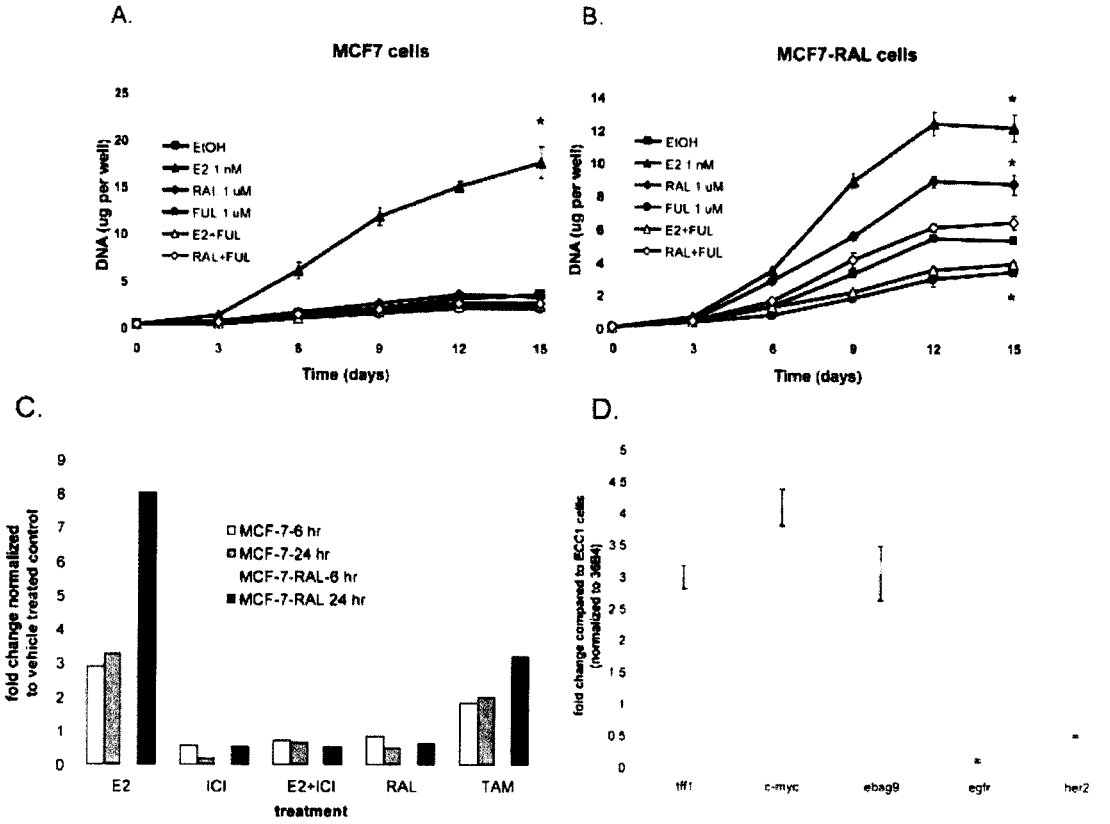


Figure 2. The MCF7-RAL cells are spontaneously growing cells that are stimulated by raloxifene (RAL) and 17β-estradiol (E_2). (A) Three days before seeding the MCF7 cells were cultured in E_2-free conditions, RPMI-yellow media with charcoal stripped FBS. The MCF-7 cells were than seeded in a 24-well plate and 24-h post seeding the cells were treated with vehicle, 1 nM E_2, 1 μM RAL, 1 μM fulvestrant (FUL) and combination of drugs as described in Materials and methods. (B) MCF7-RAL cells were seeded and treated in an identical manner as in (A). (C) MCF-7 and MCF7-RAL cells were either E_2 or RAL starved for 3 days before transfection with the appropriate reporters. Twenty-four h post transfection the cells were treated with vehicle control (EtOH), 1 nM E_2, 1 μM RAL, 1 μM TAM, 1 μM FUL and combination of 1 nM E_2 and1 μM FUL. Luciferase activity was measured 6 and 24 h after post treatment. (D) Expression of ERα-regulated genes in MCF7-RAL cells in steady state. Error bars = standard error of the mean (SEM); *p<0.05, statistically significant finding as compared to EtOH-treated cells.

highlighted in pink), but there was some evidence of genetic drift in some of the study lines. ATCC MCF-7 cells have D5S818 allelic scores of 11 and 12, whereas 4 of the study lines (WS8, 5C, 2A and ICI) only have one allele (12) (allelic loss highlighted in green), whereas the MCF7-RAL cells have two alleles at this locus: 12 and 13 (variant allele highlighted in blue). Similarly, for the vMA locus, the ATCC cells have alleles 14 and 15, as do the 5C, 2A and RAL cells, whereas the WS8 and ICI cells only have one allele; 15. Scores for the CSF1PO locus were identical among the lines showing a single allele (10), with the exception of the 5C cells that have an additional allele at this locus (11). The minor variations in the DNA profile exhibited by the MCF-7 cells are similar to the sort of genetic drift that has been seen previously among sub-lines of cells cultured independently (41), and overall these fingerprinting data confirm the presumptive identity of the lines as being of MCF-7 origin. Furthermore, the profiles from the study cell lines derived from MCF-7 (WS8) show that they are more closely related to each other than to the ATCC MCF-7 cells, again consistent with their having been derived from a common ancestor subline.

Development of a novel raloxifene-resistant tumor cell line, MCF7-RAL. To examine the effects of long-term raloxifene treatments on breast cancer cell growth we derived a novel breast raloxifene-resistant cell line, MCF7-RAL (GMB). The MCF7-RAL (GMB) cells were developed by continuously passaging cells in estrogen-free media supplemented with 1 μM raloxifene for at least 1 year. The fingerprinting data from the independently obtained MCF7 cells p184 and MCF7-RAL p74 (GMB) cells reveal a pattern of allelic scores that is identical to the scores reported for the ATCC MCF-7 cells, and highly divergent from the pattern reported for non-related cells such as the ATCC ECC-1 cells (Fig. 1B). These data suggest that the cell lines used in this study are in fact of ATCCMCF-7 origin and not a variant of the MCF-7WS8 clone. For clarity the MCF-7RAL (GMB) are referred to as MCF-7RAL throughout this paper.

Currently, the MCF7-RAL cells have been propagated in RAL containing medium for approximately 10 years. The growth characteristics *in vitro* were compared and contrasted with wild-type MCF-7. Within 3 days of treatment the MCF7 cells are significantly (p=0.02) stimulated by 1 nM E_2, 2.2-fold increase as compared to vehicle-treated controls (Fig. 2A).

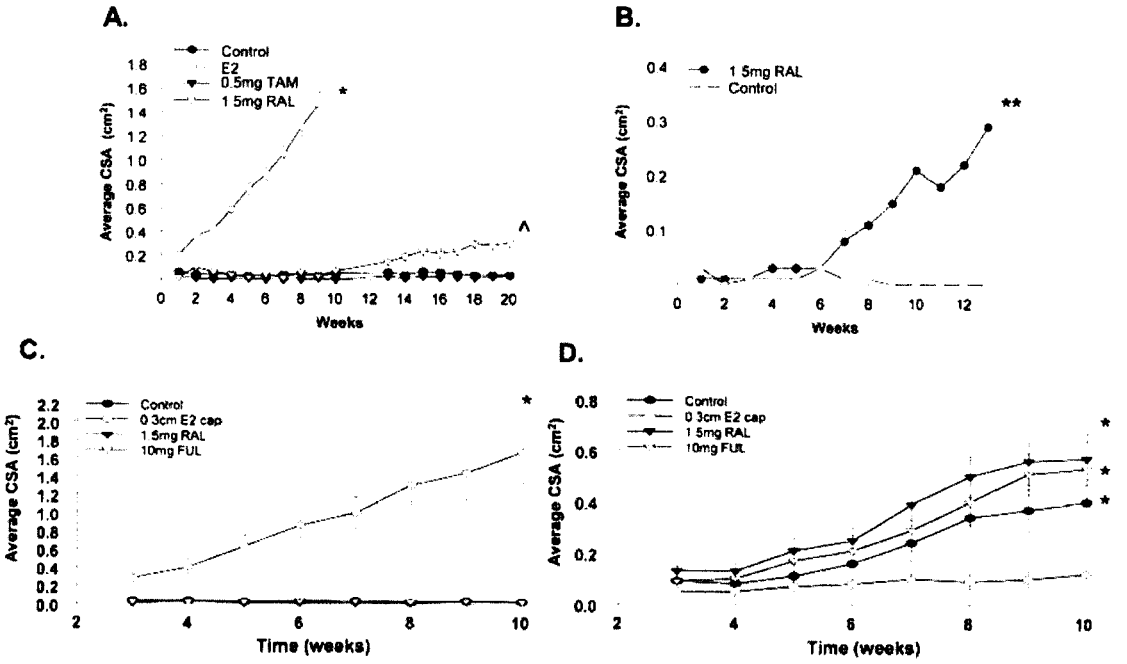


Figure 3. Establishment of MCF7-RAL tumor xenograft model. (A) MCF7-RAL-resistant cells ($1x10^7$) were injected into the axillary mammary fat pads of ovariectomized athymic mice. The mice were then divided into 4 groups and treated as follows: placebo, implanted with silastic 0.3-cm E_2 capsule, orally gavaged with RAL (1.5 mg daily) and TAM (1.5 mg daily). (B) A single tumor from the RAL-treated group was transplanted (passage 1) into 20 naïve ovariectomized athymic mice and divided into 2 groups: placebo and RAL treated. Error bars = SEM; *p<0.0001, E_2 vs. all other treatment groups; ^p=0.048 RAL vs. control. **p=0.05, RAL vs. control (C) MCF7-E_2 and MCF7-RAL tumor xenogratfs were bi-transplanted into each ovariectomized athymic mouse (total of 40). The MCF7-E_2 tumor was implanted in the left and the MCF7-RAL tumor was implanted in the right axillary mammary fat pad. The mice were randomized into groups of 10 and implanted with 0.3-cm E_2 capsule or treated with RAL (1.5 mg daily), FUL (5 mg s.c., twice a week) or no treatment (control). (C) MCF7-E_2 tumors; (D) MCF7-RAL tumors; error bars = SEM; *p<0.05, E_2 vs. all other treatment groups.

Maximum induction, 4.8-fold increase as compared to control was observed at day 15. The E_2-induced growth of the MCF7 cells was blocked by 1 μM FUL treatments. In contrast to E_2, 1 μM RAL did not stimulate the growth of the MCF7 cells. Similarly to the MCF7 cells, within 3 days of treatments, E_2 significantly (p=0.02) induced the growth of the MCF7-RAL cells (Fig. 2B). Maximum E_2 induction was observed at day 9, 2.67-fold increase as compared to control. At day 3 of treatment RAL also significantly (p=0.02) induced the growth of the MCF7-RAL cells. Maximum RAL induction was observed at day 6, 2.1-fold increase as compared to the controls. The E_2 and RAL-induced growth of the MCF7-RAL cells was significantly inhibited by 1 μM FUL treatments within 3 (p=0.04) and 6 days (p=0.02) of treatment, respectively. In addition, the MCF7-RAL cells were spontaneously growing.

To further characterize the RAL-resistant phenotype of the MCF7-RAL cells we determined the protein expression levels of ERα. To determine the protein levels of ERα in MCF7 and MCF7-RAL cells we treated the cells with EtOH, 1 μM RAL, 1 nM E_2 and 1 μM FUL for 48 h. The ERα protein levels in the MCF7-RAL cells are regulated in an identical manner as in the parental MCF7 cells (data not shown). Treatments with 1 nM E_2 and 1 μM FUL decreased the protein levels of ERα, while treatments with 1 μM RAL maintained the protein expression of ERα. The levels of total MAPK and total AKT in the MCF7-RAL cells appeared to remain unchanged, regardless of treatment, when compared to the parental, MCF7 cells. However, the levels of phosphorylated MAPK, increased in the EtOH-treated MCF7-RAL cells (data not shown). Luciferase reporter assays indicated that 1 nM E_2 treatments significantly induced transcriptional activation of the reporter in MCF7 and MCF7-RAL cells (Fig. 2C) consistent indicating similar activity of ERα in the parental and resistant cell line. Fulvestrant (FUL) and RAL treatments did not induce activation of the reporter. Furthermore, FUL treatments abolished the E_2-dependent reporter activity. TAM treatments significantly induced reporter activity in both MCF7 and MCF7-RAL cells at the 24-h time point.

The MCF7-RAL cells grew spontaneously and were inhibited by FUL treatment (Fig. 2B). To further characterize the RAL-resistant phenotype of the MCF7-RAL cells at steady state, we determined by quantitative real-time PCR, the basal mRNA expression of ERα-regulated genes in MCF7 and MCF7-RAL cells (Fig. 2D). In the basal state, the MCF7-RAL cells exhibited 3-fold up-regulation of *tff-1*, 4.1-fold up-regulation of the *c-myc* and 3.1-fold up-regulation of *ebag9*. In contrast, the levels of *egfr* and *her2* were down-regulated by 7.7- and 1.99-fold, respectively.

Development of an MCF7-RAL xenograft tumor model. To develop MCF7-RAL xenograft tumor model *in vivo*, $1x10^7$ MCF7-RAL cells were injected into the mammary fat pads of nude athymic mice as described in Materials and methods. The mice were treated with vehicle, implanted with 0.3-cm

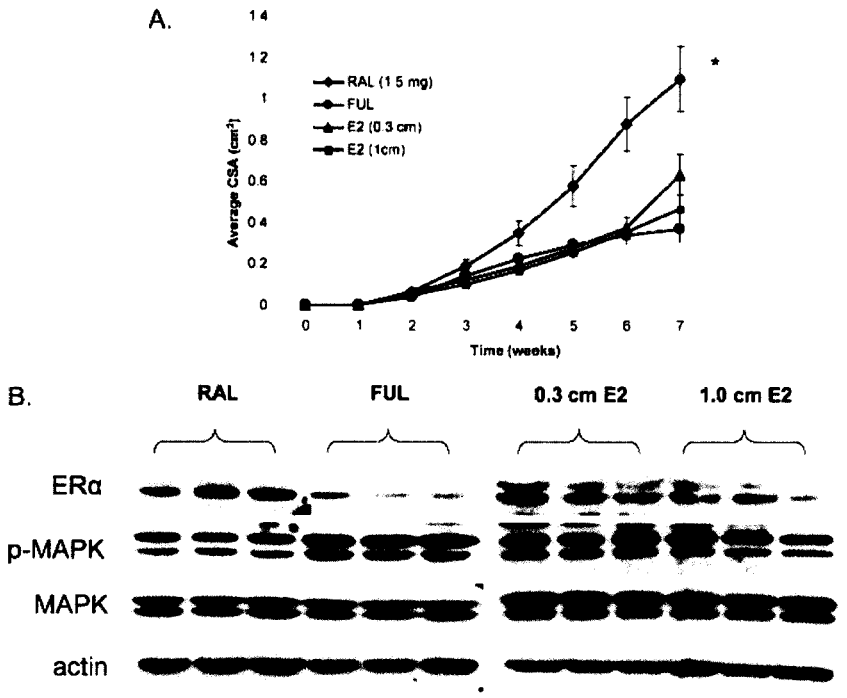


Figure 4. Pre- and post-menopausal concentrations of E_2 significantly impair the growth of long-term RAL-treated MCF7-RAL xenografts. (A) MCF7-RAL tumor xenografts serially transplanted for at least 8 years were implanted into 45 ovariectomized athymic mice. The animals were treated with RAL (1.5 mg daily), FUL (5 mg s.c twice weekly) or implanted with either 0.3-cm or 1.0-cm silastic E_2 capsules. (B) Western blot analysis of protein extracts collected from (A). *p=0.001 RAL vs. all other treatment groups.

silastic E_2 capsule or orally gavaged with 1.5 mg daily RAL or 0.5 mg daily TAM. At week 9, average cross sectional area (CSA) of the estradiol-treated group was 1.47 cm^2, significantly greater ($p<0.0001$) than the control and the other treatment groups (Fig. 3A). The E_2-treated mice grew large tumors and were sacrificed at week 10 because of ethical considerations. By week 15, palpable tumors were observed in the RAL-treated group (average CSA = 0.24 cm^2) which were significantly larger than the control group ($p=0.048$) (Fig. 3A). At week 20, a single tumor from the raloxifene-treated group was excised, resected and transplanted into 20 ovariectomized athymic mice (Fig. 3B). The mice were divided into control (no treatment) and a RAL- (1.5 mg daily) treated group. Starting at week 7, RAL promoted tumor growth which by the conclusion of the experiment at week 13 was statistically significant as compared to the control group ($p<0.05$) (Fig. 3B).

To further characterize the MCF7-RAL tumor xenograft model and to determine the effects of E_2 and RAL on estrogen and raloxifene-dependent breast tumor growth, we bi-transplanted MCF7-E_2 and MCF7-RAL tumors on opposite sides in the axillary mammary fat pads of the same animal. MCF7-E_2 xenografts were implanted into the left and the MCF7-RAL xenografts were implanted into the right mammary fat pad of 40 ovariectomized athymic mice. As anticipated the E_2-treated MCF7-E_2 tumors displayed robust tumor growth and at week 10 the mean tumor size was 1.67 cm^2 (Fig. 3C). No tumor growth was observed in the control, RAL- and FUL-treated groups (Fig. 3C). In contrast, at week 10, RAL and FUL stimulated MCF7-RAL tumor growth while the E_2-treated tumors exhibited minimal growth (Fig. 3D). At week 10, the mean size of the RAL- and FUL-treated tumors was 0.57 and 0.53 cm^2, respectively. Interestingly, spontaneous tumor growth was observed in the control MCF7-RAL (at this point considered passage 3) (mean tumor size = 0.4 cm^2, $p<0.05$ as compared to the E_2 group) (Fig. 3D).

Long-term RAL treatments of the MCF7-RAL tumor xenografts. To determine the effects of E_2 on long-term RAL-treated MCF7-RAL xenografts, we evaluated the effects of pre- and post-menopausal levels of E_2 (34) on the growth of MCF7-RAL tumors that were serially transplanted and continuously treated with RAL for at least 8 years. The MCF7-RAL tumor xenografts were transplanted into 45 ovariectomized athymic mice that were treated with RAL, FUL and 0.3- or 1.0-cm silastic E_2 capsules (Fig. 4A). At week 7, the RAL-treated xenografts exhibited a statistically significant ($p<0.001$) RAL-stimulated growth (mean CSA = 1.1 cm^2) as compared to the FUL, 0.3 and 1.0 cm E_2-treated tumors (mean CSA = 0.37, 0.63, 0.46 cm^2, respectively). There were no statistical differences between the FUL, 0.3 and 1.0 cm E_2-treated tumors. To further characterize the effects of E_2 on the long-term RAL-treated MCF7-RAL tumor xenografts we analyzed the ERα expression of the xenografts (Fig. 4B). The long-term RAL-treated MCF7-RAL xenografts continue to express ERα and RAL treatments increased the expression of ERα while FUL treatments down-regulated the expression of ERα. No differences in ERα protein expression was observed between the two different concentrations of E_2-treated tumors.

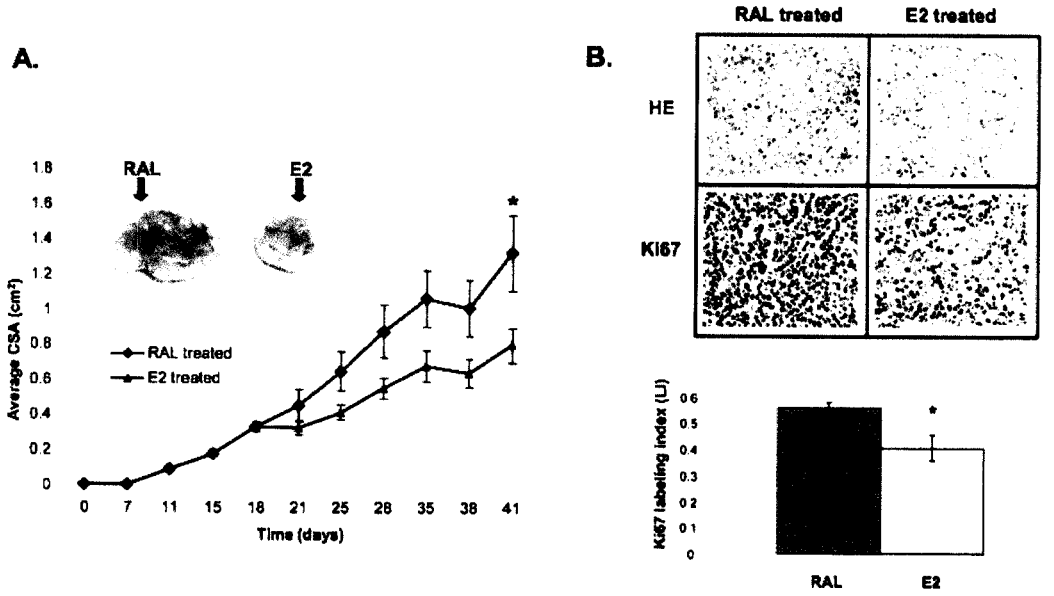


Figure 5. 17ß-estradiol treatments impair the growth of established MCF7-RAL xenografts. (A) Long-term RAL-treated MCF7-RAL xenografts were implanted into 30 ovariectomized athymic mice and the animals were treated with RAL until the cross sectional area (CSA) of the tumors reached 0.3 cm^2. The animals were than randomized into 2 groups: continued RAL treatments or implanted with 0.3-cm E_2 capsules. Estradiol treatments significantly impaired the growth of the MCF7-RAL xenografts by day 38 (20 days post-introduction of E_2). Insert: representative images of E_2- and RAL-treated tumors. (B) Histological analysis of tumors from (A). *p=0.02 RAL vs. E_2.

Estrogen treatments inhibit the growth of established MCF7-RAL tumors. To determine the effects of E_2 on established MCF7-RAL tumors, MCF7-RAL tumor xenografts were implanted into ovariectomized athymic nude mice and the animals were treated with RAL until the average CSA of the tumors reached 0.3 cm^2. At this point the animals were randomized into 2 groups: 1) continued RAL treatments and 2) implanted with 0.3-cm E_2 capsules (Fig. 5A). Within 3 days post-E_2 implantation, there were visible morphological and size differences between the RAL- and E_2-treated tumors (Fig. 5A insert). At day 7, the mean CSA was 0.64 cm^2 for the RAL-treated and 0.41 cm^2 for the E_2-treated tumors. At day 17 the CSA of the RAL-treated tumors was 1.00 cm^2 and the CSA of the E_2-treated tumors was 0.64 cm^2 (p=0.03). At the end-point of the experiment statistically significant differences (p=0.02) were observed between the RAL-treated tumors (average CSA = 1.32 cm^2) and the E_2-treated tumors (average CSA = 0.79 cm^2) (Fig. 5A).

Histological analysis of the RAL- and E_2-treated tumors at the conclusion of the experiment (Fig. 5B) by hematoxylin and eosin staining indicated that there are no significant morphological changes between the two treatment groups. However, significant differences in the expression of Ki-67, a known marker of proliferation, were observed between the two groups. There were significant statistical differences (p=0.02) between the average labeling index (LI) of the RAL-treated group and the E_2-treated group which were 0.56±0.04 and 0.40±0.09, respectively.

Effects of long-term estrogen treatments on the growth of MCF7-RAL tumors. To determine the effects of long-term E_2 treatments on the growth of MCF7-RAL tumor xenografts we transplanted long-term RAL-treated MCF7-RAL tumors into 45 ovariectomized athymic mice. The mice were divided into 3 groups: no treatment, RAL and 0.3 cm E_2 (Fig. 6A). Three weeks post-implantation the average CSA of the tumors were 0.17, 0.08 and 0.09 cm^2 for the RAL, placebo and the 0.3-cm E_2-treated tumors. At week 5, differences could be observed between the treatment groups; the average CSA of the RAL-treated tumors was 0.41 cm^2 and the average CSA of the 0.3-cm E_2-treated tumors was 0.11 cm^2. The average CSA of the untreated tumors was 0.2 cm^2 indicating spontaneously growing tumors. The 0.3-cm E_2 treatment was continued for additional 5 weeks and at week 10 the average CSA was 0.32 cm^2. At that point the E_2-treated tumors were excised, resected and bitransplanted into 25 ovariectomized athymic mice. The animals were divided into 5 groups: RAL, placebo, 0.3 cm E_2, FUL and combination of E_2- and RAL-treated (Fig. 6B). Treatment with RAL continued to induce the growth of the MCF7-RAL tumor and at week 8, the average CSA was 1.3 cm^2. At week 8, the average CSA of the placebo and the FUL-treated tumors was 0.36 and 0.29 cm^2. Unexpectedly, E_2 treatments either individually or in combination with RAL induced the growth of the MCF7-RAL xenografts. At week 8 the average CSA of the E_2-treated tumors was 0.64 cm^2 and combination of E_2 and RAL treatments resulted in tumor growth (average CSA = 1.15 cm^2). The placebo, E_2 and FUL treatments were continued and at week 10 the average CSA of the tumors was: 0.49, 1.16 and 0.52 cm^2. The growth rates of the RAL-treated tumors were significantly different compared to the placebo (p=0.003) and FUL-treated, tumors (p=0.005). However, the growth rate of the E_2- and E_2 + RAL-treated tumors was indistinguishable from the RAL-treated tumors. At week 10 the E_2-treated tumors were

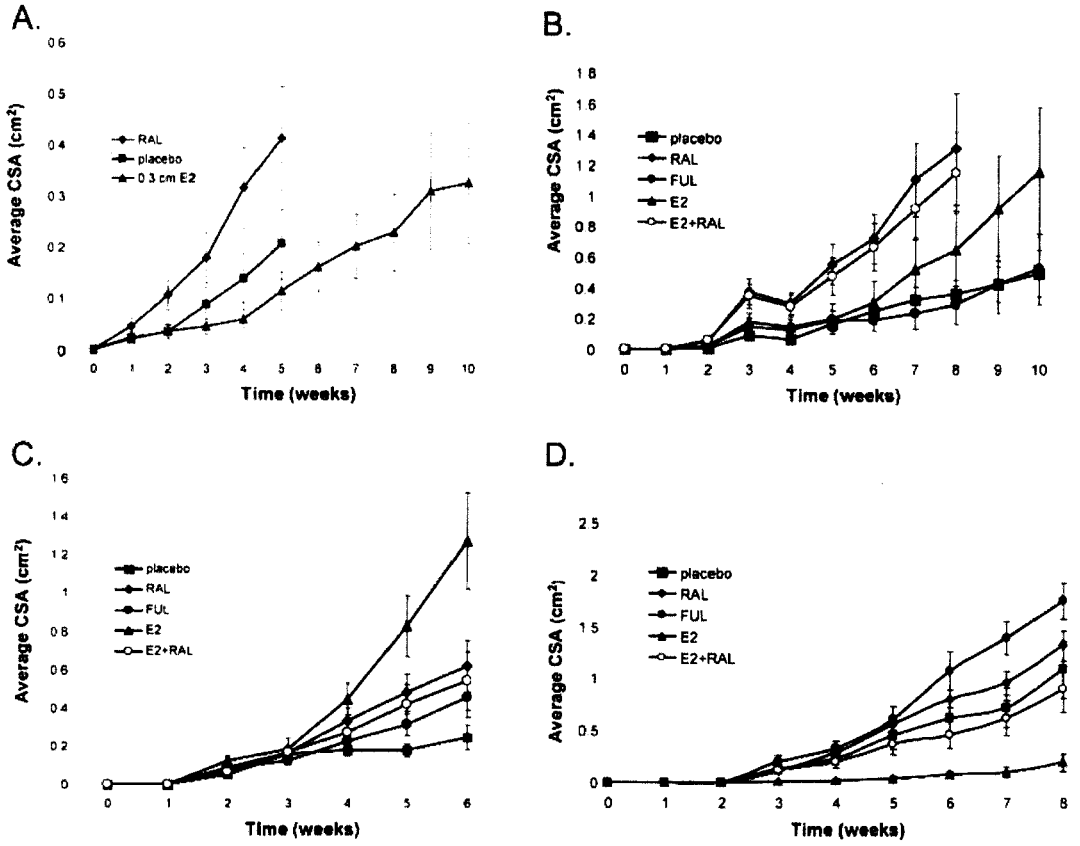


Figure 6. Long-term estrogen and raloxifene treatments result in changes in the phases of SERM resistance. (A) MCF7-RAL tumor xenografts were implanted into 45 ovariectomized athymic mice, the mice were divided into 3 groups and were either left untreated, treated with RAL (1.5 mg/daily) or implanted with 0.3-cm E_2 capsules. (B) E_2-treated tumors from (A) were resected and re-transplanted into 25 ovariectomized athymic mice that were either left untreated or treated with RAL (1.5 mg/daily), FUL (5 mg subcutaneously, twice weekly), implanted with 0.3-cm E_2 capsules and combination of RAL and E_2. (C) E_2-treated tumors from (B) were serially retransplanted into 25 ovariectomized athymic mice that were either left untreated or treated with RAL, FUL, implanted with 0.3-cm E_2 capsules and combination of RAL and E_2. (D) RAL-treated tumors from (C) were implanted into naïve animals and continuously treated with RAL for 28 weeks before being implanted into 25 naïve animals that were either left untreated or treated with raloxifene, FUL, implanted with 0.3-cm E_2 capsules and combination of RAL and E_2. See Results for a precise description of the evolution of raloxifene resistance and statistical significance of the findings in the individual experiments.

excised, resected and implanted into 25 naïve animals. The treatments were identical to the previous experiment and consisted of placebo, RAL, FUL, E_2 and combination of E_2 and RAL (Fig. 6C). At week 3 post-implantation there were no significant differences in the average CSA between the various treatments, and the average CSA was 0.05, 0.08, 0.08, 0.12 and 0.06 cm^2 for the placebo, RAL-, FUL-, E_2- and the E_2 + RAL-treated tumors. However, dramatic changes were observed at week 4 as E_2 treatments started to induce significant tumor growth (average CSA = 0.44 cm^2). In contrast RAL inhibited the estrogen-induced tumor growth as the combination of E_2 + RAL treatments average CSA was 0.27 cm^2. The average CSA of the RAL-treated tumors was 0.33 cm^2 and the placebo- and FUL-treated tumors were 0.18 and 0.22 cm^2, respectively. At conclusion of the experiment at week 6, the E_2-treated tumors reached average CSA of 1.27 cm^2. The average CSA of the RAL-treated tumors was 0.62 cm^2 and the E_2 + RAL group was 0.54 cm^2. The growth rate of the E_2-treated group was significantly different ($p<0.01$) from all other groups with the exception of the RAL-treated tumors, but approached significance ($p=0.06$). Upon conclusion of the experiment at week 6 the RAL-treated tumors were excised, resected and implanted into ovariectomized athymic animals that were continuously treated with RAL. Following 28 weeks of continuous RAL treatments the long-term treated MCF7-RAL tumor xenografts were implanted into 25 animals that were divided into 5 groups and treated as follows: placebo, RAL, E_2, FUL and E_2 + RAL (Fig. 6D). Within 3 weeks of treatments highly statistically significant differences ($p<0.01$) emerged between the E_2-treated tumors and all other treatment groups. At week 3 tumor growth was observed in the placebo, FUL, RAL and E_2 + RAL while negligible tumor growth was observed in the E_2-treated group (average CSA = 0.008 cm^2). These differences persisted throughout the duration of the experiment and at its conclusion at week 7, the average CSA of the E_2-treated tumors was 0.1 cm^2. In contrast, significant tumor growth was observed in all other treatment groups. Paradoxically, maximum tumor growth was observed in the FUL treatment groups (average CSA = 1.4 cm^2). Significant tumor growth was also observed in the RAL group (CSA = 0.96 cm^2) and in the placebo group (CSA

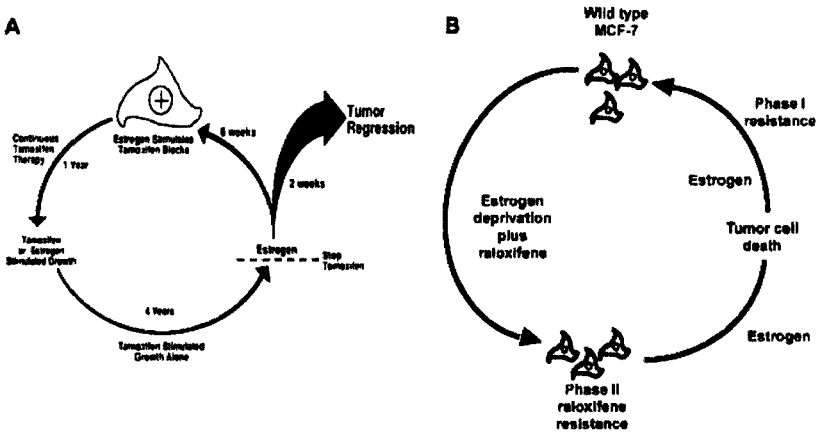


Figure 7. Proposed model of the evolution of acquired raloxifene resistance in ERα-positive MCF-7 breast cancer. On the left (Fig. 7A) is our original proposal from cyclical evolution of acquired resistance to tamoxifen in a clonal derivative (MCF-7 WS8) of wild-type MCF-7 cells originally acquired from Dr Dean Edwards (University of Texas, San Antonio, TX) in 1985. All steps in the cycle (17,18) were documented with experimental data in the peer reviewed literature. On the right (Fig. 7B) is a summary of our current results that illustrate the cyclical evolution of acquired resistance to raloxifene in wild-type MCF-7 cells (MCF-7 GMB) acquired from Dr Myles Brown (Dana Farber Cancer Center, Harvard University, Boston, MA) in 1995. The technique of employing an estrogen-deprived environment with raloxifene accelerates the evolution to phase II-acquired resistance where estradiol causes tumor regression. This process can be reversed through phase I-acquired resistance in a continuous estrogenic environment so tumor growth is again controlled by raloxifene treatment. Continuous raloxifene does again cause phase II-acquired resistance and exposes estrogen-induced tumor regression.

= 0.72 cm^2). The average CSA of the E_2 + RAL group was 0.62 cm^2, indicating that E_2 treatments significantly inhibited the RAL-stimulated tumor growth (p=0.03).

Discussion

In a previous study, we used a select clone of MCF7 cells (MCF7-WS8) (42) that is extremely sensitive to estrogen stimulation, to create an MCF7 raloxifene-resistant cell line *in vitro* (MCF7-RAL) (20). In a short-term growth experiment *in vivo* MCF7-RAL cells grew into tumors in response to raloxifene and tamoxifen but estradiol inhibited tumor growth (20). This biological response to SERMs and estradiol is classified as phase II SERM resistance (1). We have now addressed the question of the predictable creation and evolution of SERM resistance with raloxifene *in vivo* using a wild-type MCF7 cell line from a source that is external to our laboratory. The origins of the line (MCF7 GMB) were confirmed by genotyping (Fig. 1) and unlike the MCF7-WS8 cells were similar to the wild-type MCF7 from ATCC and the original MCF7 cells derived by Soule (43). We created a new MCF7-RAL cell line that is able not only to grow in response to raloxifene *in vitro* but eventually grow in response to raloxifene *in vivo* with phase II resistance, i.e. estradiol-inhibited tumor growth (Fig. 3). However, in this 10-year re-transplantation study *in vivo* we demonstrate the reversal of the biological characteristics of phase II anti-hormone-resistant tumor growth with long-term estradiol therapy to phase I resistance; i.e., estradiol- or raloxifene-stimulated growth, and then predominately estradiol-stimulated growth. Raloxifene now acts as an anti-estrogen, inhibiting estradiol-stimulated growth (Fig. 6C). Thus raloxifene has the potential to cause the classic evolution of SERM resistance in the clinical setting and reverse the process during long-term physiologic estrogen therapy. Nevertheless clinical studies need to be considered to evaluate the efficacy of estrogen on patients whose breast tumors develop during long-term raloxifene treatment to prevent osteoporosis (16). Current anti-hormonal therapies used for the treatment of breast cancer (tamoxifen or aromatase inhibitors) can develop acquired resistance in the clinical cells. The best clinical responses to estrogen are observed with high-dose (15 mg) DES therapy following exhaustive anti-hormonal therapy (27). Indeed, one patient had a complete response during the 5-year to DES therapy administered continuously and a further 5-year disease-free response following the cessation of therapy (44). In contrast, no complete responses were observed in the study of Ellis *et al* (28) probably because the patient population was not selected based on exhaustive anti-hormonal therapy but only failure of therapy following aromatase inhibitors. Experience in the laboratory demonstrates that long-term (>5 years) tamoxifen treatment is necessary to cause the evolution of tamoxifen resistance *in vivo* to expose the apoptotic actions of physiologic estrogen (18). Consistent with these observations, a profound antitumor effect was noted with physiologic estrogen after 10 years of alternating treatments with raloxifene and physiologic estrogen (Fig. 6D).

With regard to treatment strategies for SERM-resistant disease, it is important to note that the response to the injectable steroidal pure anti-estrogen fulvestrant is unpredictable (Fig. 6). At some stages of acquired resistance, fulvestrant acts as an antitumor agent but at other stimulates tumor growth (Fig. 6). This may in part explain the low reported efficacy of fulvestrant in clinical trials treating patients who already have acquired resistance to tamoxifen or aromatase inhibitors. However, it also appears that the recommended monthly doses of fulvestrant used clinically may be sub-optimal and in fact actually enhance tumor growth in tumors with phase II resistance with physiologic estrogen present (45). A recent clinical study on metastatic breast cancer demonstrates that doubling the monthly dose of fulvestrant enhances antitumor activity (46). In a laboratory study, an antitumor dose of fulvestrant in athymic animals implanted

with phase II-resistant tumors reversed the apoptotic actions of estrogen (45). In the present study, despite using repeated subcutaneous injections of fulvestrant weekly, tumor growth was enhanced in some tumor passages with long-term acquired resistance to raloxifene (Fig. 6D). It appears that the efficacy of fulvestrant may depend both upon bioavailability, pharmacokinetics and, as yet, unresolved pharmacodynamic factors of the steroidal antiestrogens at unknown targets within the tumor with acquired raloxifene resistance.

Two further conclusions emerged from the present study. The variant of MCF7 cells that is closely related to wild-type MCF-7 from ATCC could develop acquired resistance to raloxifene *in vitro* and the resulting cell line MCF7-RAL grew in response to either estradiol or raloxifene (Fig. 2). MCF7-RAL cells exhibited gene activation consistent with autonomous growth (Fig. 2C). The cells responded to estradiol both *in vitro* and *in vivo* as a growth stimulus but only developed raloxifene-stimulated tumors *in vivo* after 5 months of continuous treatment. This was confirmed by re-transplantation into raloxifene-treated ovariectomized athymic mice (Fig. 3B). In contrast to MCF7-RAL cells *in vitro*, estradiol is no longer a growth stimulus *in vivo* and completely inhibits tumor development (Fig. 3D). This new biology of estrogen action classifies the MCF7-RAL cells as phase II-resistant *in vivo*. Secondly, the observation that treatment with tamoxifen *in vivo* (Fig. 3A) did not result in tumor growth and that this MCF7 variant could not be used to develop acquired tamoxifen resistance *in vitro* (H. Liu, unpublished), was unusual and unanticipated based on previous studies over two decades. All cells died during incubation with 4-hydroxy-tamoxifen. This observation is currently under investigation as it may provide insight into the cytocidal actions of tamoxifen.

Based on this long-term study, and studies using prostate cancer cells, a general principle is emerging in cancer endocrinology. An androgen-independent cell line, LNCaP 104 R2 was derived from the androgen-dependent cell line, LNCaP 104 S (47). The LNCaP 104 R2 cells are androgen-independent, continue to express the androgen receptor (AR) and low concentrations of androgen in the media inhibited their growth. Implantation of the LNCap104-R2 cells in male athymic-castrated nude mice resulted in tumor growth, that was inhibited by implantation of testosterone capsules (48). In a subsequent study utilizing the LNCaP 104-R2 tumor model, Chuu *et al* (49) significantly impaired established tumor growth with androgen treatments; approximately 2 months post-cell injections. However, within 40 days of initiation of androgen treatments tumor growth resumed, which was a clear indication that the tumors adapted to the presence of the androgen and utilized it for growth. Subsequent androgen withdrawal inhibited tumor growth. These data are consistent with the assumption that androgen-dependent and androgen-independent tumor cells coexist in prostate cancer patients resulting in positive selection of androgen-independent tumor cells during androgen ablation therapies, resulting in androgen-independent growth. Therefore, intermittent androgen replacement therapy has been tested in recent years (50).

Nearly 20 years ago, we first described the antitumor potential of physiologic estrogen to destroy what is now known as phase II-acquired tamoxifen resistance (17) We noted that the interplay of apoptotic estrogen and tamoxifen would create a cyclical method for controlling the growth of ER-postitive breast cancer by purging with estrogen at the appropriate time and then continuing anti-hormone therapy (17). The cycles could be repeated. This original work is summarized in Fig. 7. Our current 10-year *in vitro* and *in vivo* study of the evolution of acquired raloxifene resistance was initiated to explore the potential of raloxifene to exhibit acquired resistance in breast cancer during the long-term treatment and prevention of osteoprosis (16). We conclude that the predictable evolution of acquired resistance to the SERM tamoxifen and estrogen deprivation (aromatase inhibitors) also occurs with raloxifene. The current conclusions are summarized in Fig. 7, following the creation of MCF7-RAL cells *in vitro* is a raloxifene/estrogen-free environment which was then transplanted into athymic mice. The development of phase II-acquired resistance i.e.: estrogen-induced apoptosis or estrogen-inhibited tumor growth (51) occurs with raloxifene and the principle is also true for the evolution of acquired androgen withdrawal in prostate cancer in the laboratory (47-49). Preliminary studies to translate these laboratory findings to aid patients have shown merit (27, 28,44). Further understanding of the mechanism of sex steroid-induced apoptosis (52) and the definition of vulnerable tumors following exhaustive anti-hormonal therapy have the potential to identify appropriate patient populations to amplify the effectiveness of a sex steroid apoptotic trigger in metastatic breast cancer and possibly prostate cancer (53).

Acknowledgements

These studies were supported by the following grants: the Department of Defense Breast Program under award number BC050277 Center of Excellence, SPORE in Breast Cancer CA89018 (VCJ), Genuardi's Fund (VCJ), FCCC Core Grant NIH P30 CA006927, the Lynn Sage Breast Cancer Research Foundation (VCJ), the Weg Fund of Fox Chase Cancer Center (VCJ), and the Cancer Center Support Grant (CCSG) Core Grant NIH P30 CA051008. The views and opinions of the author(s) do not reflect those of the US Army or the Department of Defense.

References

1. Jordan VC: Selective estrogen receptor modulation: Concept and consequences in cancer. Cancer Cell 5: 207-213, 2004.
2. Tamoxifen for early breast cancer: An overview of the randomised trials. Early breast cancer trialists' collaborative group. Lancet 351: 1451-1467, 1998.
3. Jordan VC: Chemoprevention of breast cancer with selective oestrogen-receptor modulators. Nat Rev Cancer 7: 46-53, 2007.
4. Fisher B, Costantino JP, Wickerham DL, *et al*: Tamoxifen for prevention of breast cancer: Report of the National Surgical Adjuvant Breast and Bowel project P-1 study. J Natl Cancer Inst 90: 1371-1388, 1998.
5. Gottardis MM and Jordan VC: Development of tamoxifen-stimulated growth of MCF-7 tumors in athymic mice after long-term antiestrogen administration. Cancer Res 48: 5183-5187, 1988.
6. Gottardis MM, Wagner RJ, Borden EC and Jordan VC: Differential ability of antiestrogens to stimulate breast cancer cell (MCF-7) growth in vivo and in vitro. Cancer Res 49: 4765-4769, 1989.
7. Black LJ, Jones CD and Falcone JF: Antagonism of estrogen action with a new benzothiophene derived antiestrogen. Life Sci 32: 1031-1036, 1983.

8. Clemens JA, Bennett DR, Black LJ and Jones CD: Effects of a new antiestrogen, keoxifene (ly156758), on growth of carcinogen-induced mammary tumors and on lH and prolactin levels. Life Sci 32: 2869-2875, 1983.
9. Gottardis MM and Jordan VC: Antitumor actions of keoxifene and tamoxifen in the N-nitrosomethylurea induced rat mammary carcinoma model. Cancer Res 47: 4020-4024, 1987.
10. Jordan VC, Phelps E and Lindgren JU: Effects of anti-estrogens on bone in castrated and intact female rats. Breast Cancer Res Treat 10: 31-35, 1987.
11. Jordan VC: Chemosuppression of breast cancer with tamoxifen: Laboratory evidence and future clinical investigations. Cancer Invest 6: 589-595, 1988.
12. Ettinger B, Black DM, Mitlak BH, *et al*: Reduction of vertebral fracture risk in postmenopausal women with osteoporosis treated with raloxifene: Results from a 3-year randomized clinical trial. Multiple outcomes of raloxifene evaluation (more) investigators. JAMA 282: 637-645, 1999.
13. Cummings SR, Eckert S, Krueger KA, *et al*: The effect of raloxifene on risk of breast cancer in postmenopausal women: Results from the more randomized trial. Multiple outcomes of raloxifene evaluation. JAMA 281: 2189-2197, 1999.
14. Vogel VG, Costantino JP, Wickerham DL, *et al*: Effects of tamoxifen vs raloxifene on the risk of developing invasive breast cancer and other disease outcomes: The NSABP study of tamoxifen and raloxifene (STAR) P-2 trial. JAMA 295: 2727-2741, 2006.
15. Barrett-Connor E, Mosca L, Collins P, *et al*: Effects of raloxifene on cardiovascular events and breast cancer in postmenopausal women. N Engl J Med 355: 125-137, 2006.
16. Martino S, Cauley JA, Barrett-Connor E, *et al*: Continuing outcomes relevant to evista: Breast cancer incidence in postmenopausal osteoporotic women in a randomized trial of raloxifene. J Natl Cancer Inst 96: 1751-1761, 2004.
17. Wolf DM and Jordan VC: A laboratory model to explain the survival advantage observed in patients taking adjuvant tamoxifen therapy. Recent Results Cancer Res 127: 23-33, 1993.
18. Yao K, Lee ES, Bentrem DJ, *et al*: Antitumor action of physiological estradiol on tamoxifen-stimulated breast tumors grown in athymic mice. Clin Cancer Res 6: 2028-2036, 2000.
19. O'Regan RM, Osipo C, Ariazi E, *et al*: Development and therapeutic options for the treatment of raloxifene-stimulated breast cancer in athymic mice. Clin Cancer Res 12: 2255-2263, 2006.
20. Liu H, Lee ES, Gajdos C, *et al*: Apoptotic action of 17beta-estradiol in raloxifene-resistant MCF-7 cells in vitro and in vivo. J Natl Cancer Inst 95: 1586-1597, 2003.
21. Song RX, Mor G, Naftolin F, *et al*: Effect of long-term estrogen deprivation on apoptotic responses of breast cancer cells to 17beta-estradiol. J Natl Cancer Inst 93: 1714-1723, 2001.
22. Song RX, Zhang Z, Mor G and Santen RJ: Down-regulation of BCL-2 enhances estrogen apoptotic action in long-term estradiol-depleted ER(+) breast cancer cells. Apoptosis 10: 667-678, 2005.
23. Lewis JS, Meeke K, Osipo C, *et al*: Intrinsic mechanism of estradiol-induced apoptosis in breast cancer cells resistant to estrogen deprivation. J Natl Cancer Inst 97: 1746-1759, 2005.
24. Lewis JS, Osipo C, Meeke K and Jordan VC: Estrogen-induced apoptosis in a breast cancer model resistant to long-term estrogen withdrawal. J Steroid Biochem Mol Biol 94: 131-141, 2005.
25. Kennedy BJ: Diethylstilbestrol versus testosterone propionate therapy in advanced breast cancer. Surg Gynecol Obstet 120: 1246-1250, 1965.
26. Haddow A, Watkinson JM, Paterson E and Koller PC: Influence of synthetic oestrogens on advanced malignant disease. Br Med J 2: 393-398, 1944.
27. Lonning PE, Taylor PD, Anker G, *et al*: High-dose estrogen treatment in postmenopausal breast cancer patients heavily exposed to endocrine therapy. Breast Cancer Res Treat 67: 111-116, 2001.
28. Ellis MJ, Gao F, Dehdashti F, *et al*: Lower-dose vs high-dose oral estradiol therapy of hormone receptor-positive, aromatase inhibitor-resistant advanced breast cancer: A phase 2 randomized study. JAMA 302: 774-780, 2009.
29. Lins AM, Micka KA, Sprecher CJ, *et al*: Development and population study of an eight-locus short tandem repeat (STR) multiplex system. J Forensic Sci 43: 1168-1180, 1998.
30. Jamerson MH, Johnson MD, Korsmeyer SJ, Furth PA and Dickson RB: Bax regulates c-myc-induced mammary tumour apoptosis but not proliferation in MMTV-c-myc transgenic mice. Br J Cancer 91: 1372-1379, 2004.
31. Labarca C and Paigen K: A simple, rapid, and sensitive DNA assay procedure. Anal Biochem 102: 344-352, 1980.
32. Dardes RC, Schafer JM, Pearce ST, Osipo C, Chen B and Jordan VC: Regulation of estrogen target genes and growth by selective estrogen-receptor modulators in endometrial cancer cells. Gynecol Oncol 85: 498-506, 2002.
33. Robinson SP and Jordan VC: Antiestrogenic action of toremifene on hormone-dependent, -independent, and heterogeneous breast tumor growth in the athymic mouse. Cancer Res 49: 1758-1762, 1989.
34. O'Regan RM, Cisneros A, England GM, *et al*: Effects of the antiestrogens tamoxifen, toremifene, and ICI 182,780 on endometrial cancer growth. J Natl Cancer Inst 90: 1552-1558, 1998.
35. Ariazi EA, Lewis-Wambi JS, Gill SD, *et al*: Emerging principles for the development of resistance to antihormonal therapy: Implications for the clinical utility of fulvestrant. J Steroid Biochem Mol Biol 102: 128-138, 2006.
36. Ariazi EA, Kraus RJ, Farrell ML, Jordan VC and Mertz JE: Estrogen-related receptor alpha1 transcriptional activities are regulated in part via the erbb2/her2 signaling pathway. Mol Cancer Res 5: 71-85, 2007.
37. Rae JM, Johnson MD, Scheys JO, Cordero KE, Larios JM and Lippman ME: Greb 1 is a critical regulator of hormone dependent breast cancer growth. Breast Cancer Res Treat 92: 141-149, 2005.
38. Livak KJ and Schmittgen TD: Analysis of relative gene expression data using real-time quantitative PCR and the 2-(delta)(delta)ct method. Methods 25: 402-408, 2001.
39. Ariazi EA, Clark GM and Mertz JE: Estrogen-related receptor alpha and estrogen-related receptor gamma associate with unfavorable and favorable biomarkers, respectively, in human breast cancer. Cancer Res 62: 6510-6518, 2002.
40. Pink JJ and Jordan VC: Models of estrogen receptor regulation by estrogens and antiestrogens in breast cancer cell lines. Cancer Res 56: 2321-2330, 1996.
41. Rae JM, Creighton CJ, Meck JM, Haddad BR and Johnson MD: MDA-MB-435 cells are derived from M14 melanoma cells - loss for breast cancer, but a boon for melanoma research. Breast Cancer Res Treat 104: 13-19, 2007.
42. Jiang SY, Langan-Fahey SM, Stella AL, McCague R and Jordan VC: Point mutation of estrogen receptor (ER) in the ligand-binding domain changes the pharmacology of anti-estrogens in ER-negative breast cancer cells stably expressing complementary DNAs for ER. Mol Endocrinol 6: 2167-2174, 1992.
43. Brooks SC, Locke ER and Soule HD: Estrogen receptor in a human cell line (MCF-7) from breast carcinoma. J Biol Chem 248: 6251-6253, 1973.
44. Lonning PE: Additive endocrine therapy for advanced breast cancer - back to the future. Acta Oncol 48: 1092-1101, 2009.
45. Osipo C, Gajdos C, Liu H, Chen B and Jordan VC: Paradoxical action of fulvestrant in estradiol-induced regression of tamoxifen-stimulated breast cancer. J Natl Cancer Inst 95: 1597-1608, 2003.
46. Robertson JF, Llombart-Cussac A, Rolski J, *et al*: Activity of fulvestrant 500 mg versus anastrozole 1 mg as first-line treatment for advanced breast cancer: Results from the first study. J Clin Oncol 27: 4530-4535, 2009.
47. Kokontis J, Takakura K, Hay N and Liao S: Increased androgen receptor activity and altered c-myc expression in prostate cancer cells after long-term androgen deprivation. Cancer Res 54: 1566-1573, 1994.
48. Umekita Y, Hiipakka RA, Kokontis JM and Liao S: Human prostate tumor growth in athymic mice: Inhibition by androgens and stimulation by finasteride. Proc Natl Acad Sci USA 93: 11802-11807, 1996.
49. Chuu CP, Hiipakka RA, Fukuchi J, Kokontis JM and Liao S: Androgen causes growth suppression and reversion of androgen-independent prostate cancer xenografts to an androgen-stimulated phenotype in athymic mice. Cancer Res 65: 2082-2084, 2005.
50. Abrahamsson PA: Potential benefits of intermittent androgen suppression therapy in the treatment of prostate cancer: A systematic review of the literature. Eur Urol (In press).
51. Jordan VC: The 38th David A. Karnofsky lecture: The paradoxical actions of estrogen in breast cancer - survival or death? J Clin Oncol 26: 3073-3082, 2008.
52. Maximov PY, Lewis-Wambi JS and Jordan VC: The paradox of oestradiol-induced breast cancer cell growth and apoptosis. Curr Signal Transduct Ther 4: 88-102, 2009.
53. Jordan VC: A century of deciphering the control mechanisms of sex steroid action in breast and prostate cancer: The origins of targeted therapy and chemoprevention. Cancer Res 69: 1243-1254, 2009.

Research Article
See perspectives pp. 681, 686, and 689

Cancer Prevention Research

Update of the National Surgical Adjuvant Breast and Bowel Project Study of Tamoxifen and Raloxifene (STAR) P-2 Trial: Preventing Breast Cancer

Victor G. Vogel[1,2,7], Joseph P. Costantino[3,4], D. Lawrence Wickerham[1,5], Walter M. Cronin[3], Reena S. Cecchini[3], James N. Atkins[1,8], Therese B. Bevers[1,9], Louis Fehrenbacher[1,10], Eduardo R. Pajon[1,11], James L. Wade III[1,12], André Robidoux[1,13], Richard G. Margolese[1,14], Joan James[15], Carolyn D. Runowicz[1,16], Patricia A. Ganz[1,17], Steven E. Reis[1,6], Worta McCaskill-Stevens[18], Leslie G. Ford[18], V. Craig Jordan[1,15], and Norman Wolmark[1,5]; for the National Surgical Adjuvant Breast and Bowel Project[19]

Abstract

The selective estrogen-receptor modulator (SERM) tamoxifen became the first U.S. Food and Drug Administration (FDA)–approved agent for reducing breast cancer risk but did not gain wide acceptance for prevention, largely because it increased endometrial cancer and thromboembolic events. The FDA approved the SERM raloxifene for breast cancer risk reduction following its demonstrated effectiveness in preventing invasive breast cancer in the Study of Tamoxifen and Raloxifene (STAR). Raloxifene caused less toxicity (versus tamoxifen), including reduced thromboembolic events and endometrial cancer. In this report, we present an updated analysis with an 81-month median follow-up. STAR women were randomly assigned to receive either tamoxifen (20 mg/d) or raloxifene (60 mg/d) for 5 years. The risk ratio (RR; raloxifene:tamoxifen) for invasive breast cancer was 1.24 (95% confidence interval [CI], 1.05–1.47) and for noninvasive disease, 1.22 (95% CI, 0.95–1.59). Compared with initial results, the RRs widened for invasive and narrowed for noninvasive breast cancer. Toxicity RRs (raloxifene:tamoxifen) were 0.55 (95% CI, 0.36–0.83; $P = 0.003$) for endometrial cancer (this difference was not significant in the initial results), 0.19 (95% CI, 0.12–0.29) for uterine hyperplasia, and 0.75 (95% CI, 0.60–0.93) for thromboembolic events. There were no significant mortality differences. Long-term raloxifene retained 76% of the effectiveness of tamoxifen in preventing invasive disease and grew closer over time to tamoxifen in preventing noninvasive disease, with far less toxicity (e.g., highly significantly less endometrial cancer). These results have important public health implications and clarify that both raloxifene and tamoxifen are good preventive choices for postmenopausal women with elevated risk for breast cancer. *Cancer Prev Res; 3(6); 696–706. ©2010 AACR.*

Introduction

Despite improvements in the detection and treatment of breast cancer, this disease still accounted for 192,000 new cases and 40,000 deaths in the United States in 2009 (1). Therefore, the concept of preventing the development of invasive breast cancer remains an attractive one. The selective estrogen-receptor modulator (SERM) tamoxifen has well-known benefits in the treatment of receptor-positive invasive breast cancer (2) and has been shown to be an effective chemoprevention therapy (3–6). However, in spite of its impressive efficacy in the prevention of breast cancer, tamoxifen has not been widely used for prevention because, in large part, of the increased risk of endometrial

Authors' Affiliations: [1]National Surgical Adjuvant Breast and Bowel Project (NSABP); [2]University of Pittsburgh Cancer Institute; [3]NSABP Biostatistical Center; [4]University of Pittsburgh Graduate School of Public Health, Department of Biostatistics; [5]Allegheny General Hospital; [6]University of Pittsburgh Cardiovascular Institute, Pittsburgh, Pennsylvania; [7]American Cancer Society, Atlanta, Georgia; [8]Southeast Cancer Control Consortium - CCOP, Winston-Salem, North Carolina; [9]MD Anderson Cancer Center, Houston, Texas; [10]Kaiser Permanente Northern California, Vallejo, California; [11]Colorado Cancer Research Program, Denver, Colorado; [12]Central Illinois CCOP, Decatur, Illinois; [13]CHUM-Hôtel-Dieu; [14]Jewish General Hospital, McGill University, Montreal, Quebec, Canada; [15]Fox Chase Cancer Center, Philadelphia, Pennsylvania; [16]University of Connecticut Health Center, Farmington, Connecticut; [17]Division of Cancer Prevention and Control Research, Jonsson Comprehensive Cancer Center, University of California, Los Angeles, California; [18]National Cancer Institute - Division of Cancer Prevention, Bethesda, Maryland; [19]For more information about this study and the NSABP, please see http://clinicaltrials.gov/ct2/show/study/NCT00003906 and http://www.nsabp.pitt.edu/

Note: Clinical Trial Registration for NSABP P-2: NCT00003906. The work described in this manuscript is original research and has not been previously published. The following recent related work has been published: ref. 9 and Land SR et al., JAMA 2006;295:2742–51. For earlier related publications, please see the references.

Corresponding Author: D. Lawrence Wickerham, NSABP, Four Allegheny Center, 5th floor, Pittsburgh, PA 15212. Phone: 412-330-4600; Fax: 412-330-4661; E-mail: larry.wickerham@nsabp.org.

doi: 10.1158/1940-6207.CAPR-10-0076

©2010 American Association for Cancer Research.

cancer and thromboembolic events associated with its use. Another SERM, raloxifene, has been shown to reduce the incidence of breast cancer in a series of clinical trials designed primarily to evaluate it for treatment and prevention of osteoporosis in postmenopausal women (7, 8).

The National Surgical Adjuvant Breast and Bowel Project (NSABP) protocol P-2, the Study of Tamoxifen and Raloxifene (STAR), directly compared tamoxifen with raloxifene in 19,747 healthy postmenopausal women at an increased risk for development of breast cancer. With 47 months of follow-up, the initial STAR results demonstrated no significant difference between the two trial arms in the incidence of invasive breast cancer, both with an estimated decreased incidence of approximately 50% (vs untreated women; ref. 9). Raloxifene did not appear to be as effective as tamoxifen in reducing the incidence of noninvasive breast cancer (ductal carcinoma *in situ* [DCIS] and lobular carcinoma *in situ* [LCIS] combined). The toxicity and side-effect evaluations favored the raloxifene group, in which women had significantly fewer deep-vein thromboses and pulmonary emboli, cataracts, and hysterectomies for benign disease. The raloxifene group also had a nonsignificant reduction in endometrial cancer. This report provides updated STAR results.

Materials and Methods

STAR was a two-arm, randomized, double-blinded trial of tamoxifen versus raloxifene for the reduction of breast cancer incidence; participants and their physicians were unaware of the treatment that was being administered until the trial was unblinded in April 2006. All participants provided written informed consent that was reviewed and approved by the National Cancer Institute and the institutional review boards of all participating institutions. The details of the trial methodology, including the definition of endpoints and the methods used for randomization, schedule of patient follow-up, patient testing, and trial monitoring, are described in the initial report of 2006, for which the data were cut off as of December 31, 2005 (9). The update in the present report is based on a cut-off date of March 31, 2009, providing a median follow-up of 81 months. We focus here on updating findings for the primary endpoint (incidence of invasive breast cancer) and for all key secondary endpoints, including noninvasive breast cancer, endometrial and other cancers, and vascular-related events. In the original STAR report, no difference between treatment groups was noted for the secondary endpoints ischemic heart disease, stroke, and osteoporotic fractures. Because our new analyses confirmed that this lack of differences continued in the longer term, these endpoints are not included in this report.

Participant characteristics

Only women who were postmenopausal, at least 35 years of age, and who had a 5-year predicted breast cancer risk of at least 1.66% were eligible for STAR. The risk determination was based on the Gail model, as modified and applied in the Breast Cancer Prevention Trial (BCPT P-1; ref. 10). Participants were also required to meet the following criteria: not taking either tamoxifen or raloxifene, hormone therapy, oral contraceptives, or androgens for at least 3 months before randomization; not currently taking warfarin or cholestyramine; no history of stroke, transient ischemic attack, pulmonary embolism, or deep-vein thrombosis; no atrial fibrillation, uncontrolled diabetes, or uncontrolled hypertension; no psychiatric condition that would interfere with adherence; a performance status that would not restrict normal activity; and no history of previous malignancy except basal cell or squamous cell carcinoma of the skin, carcinoma *in situ* of the cervix, or LCIS of the breast. Eligible women were randomly assigned to receive either 20 mg/d of tamoxifen plus placebo, or 60 mg/d of raloxifene plus placebo for 5 years; the placebo tablets were necessary to maintain the double blinding of treatment assignment because the formulations of tamoxifen and raloxifene tablets were dissimilar.

A total 19,747 women were randomly assigned to one of the two groups between July 1, 1999, and November 4, 2004, and 19,471 of these women (9,726 tamoxifen; 9,745 raloxifene) were included in the analysis of the original report. Two hundred seventy-four women were not included because of a lack of follow-up information (146 tamoxifen; 128 raloxifene). Two other women (in the raloxifene group) were excluded because they had received a prophylactic bilateral mastectomy before randomization and were not at risk for the development of invasive breast cancer. Since the time of the initial report, follow-up information was collected on 20 of the women (10 tamoxifen; 10 raloxifene) who lacked follow-up information at the time of the original report. One woman (in the raloxifene group) in the original report has been excluded from the follow-up analyses because she was discovered to have been diagnosed with invasive breast cancer before randomization. Therefore, this update report includes the findings for 19,490 women—9,736 in the tamoxifen group and 9,754 in the raloxifene group.

The characteristics of the participants included in the current analysis are shown in Table 1. The mean age at entry to the trial was 58.5 years (SD, 7.4). Nine percent of the women were younger than 50 years, 49.8% were between ages 50 and 59, 32.4% were between ages 60 and 69, and 8.8% were aged 70 years or older. The percentages of racial/ethnic groups were as follows: White = 93.5%, African American = 2.4%, Hispanic = 2.0%, and "other" = 2.1%. More than half (51.5%) of the participants had undergone a hysterectomy before entry to the study; over 70% had a first-degree female relative with a history of breast cancer; and 23% had a history of atypical hyperplasia of the breast. The mean 5-year predicted breast cancer risk at entry was 4.03% (SD, 2.2), subdivided as follows: 30.2% with risks between 2.01% and 3.00%, 31.4% between 3.01% and 5.00%, and 27.3% greater than 5.00%. The mean lifetime risk was 14.73% (SD, 7.4).

Table 1. Characteristics at entry to the NSABP STAR Trial (P-2) for women included in the STAR-update analyses

Participant characteristics	Tamoxifen		Raloxifene	
	No.	%	No.	%
Age (years)				
≤49	884	9.1	878	9.0
50–59	4,856	49.9	4,855	49.8
60–69	3,137	32.2	3,174	32.5
≥70	859	8.8	847	8.7
Race/ethnicity				
White	9,105	93.5	9,115	93.4
African-American	233	2.4	243	2.5
Hispanic	192	2.0	193	2.0
Other	206	2.1	203	2.1
No. 1° relatives with breast cancer				
0	2,838	29.1	2,791	28.6
1	5,046	51.8	5,135	52.6
2	1,532	15.7	1,561	16.0
≥3	320	3.3	267	2.7
History of hysterectomy				
No	4,739	48.7	4,717	48.4
Yes	4,997	51.3	5,037	51.6
History of lobular carcinoma *in situ*				
No	8,844	90.8	8,865	90.9
Yes	892	9.2	889	9.1
History of breast atypical hyperplasia				
No	7,545	77.5	7,513	77.0
Yes	2,191	22.5	2,241	23.0
5-year predicted breast cancer risk (%)*				
≤2.00	1,055	10.8	1,102	11.3
2.01-3.00	2,993	30.7	2,893	29.7
3.01-5.00	3,042	31.2	3,086	31.6
≥5.01	2,646	27.2	2,673	27.4
Total	9,736	100.0	9,754	100.0

Abbreviation: NSABP STAR, National Surgical Adjuvant Breast and Bowel Project Study of Tamoxifen and Raloxifene.
*Determined by the Gail model.

The mean duration of treatment was 43.5 months (SD, 20.7) for the tamoxifen group and 46.8 months (SD, 20.0) for the raloxifene group. Participant adherence to 5 years of therapy was within the limits anticipated when the trial was designed. Also, since the original report and unblinding of treatment assignment, any woman who had not completed her 5-year course of tamoxifen was offered the option to switch to raloxifene for the remaining portion of her treatment course. A total of 879 women chose this option.

Statistical analyses

Analyses included all randomly assigned at-risk women for whom follow-up information was available. All analyses were based on the intention-to-treat principle and used the treatment assignment determined at randomization, regardless of the treatment status at the time of analysis. Rates per 1,000 person-years for each of the study endpoints were determined for each treatment group by dividing the number of events within each treatment group by the total number of event-specific person-years of follow-up within the group. Comparisons of rates between treatment groups were based on the risk ratio (RR) and the 95% confidence interval (CI) for the RR. The RR was determined as the rate in the raloxifene group divided by the rate in the tamoxifen group. The 95% CI for each RR was determined assuming a Poisson distribution, conditioning on the total number of events and the person-years at risk. RRs for which the 95% CI did not include 1.00 were considered to be statistically significant. Plots of the cumulative incidence over time of follow-up were also developed. The cumulative incidence accounted for the competing risk of death (11). *P*-values to assess statistically significant differences between treatment group–specific cumulative incidence curves were determined by the log-rank test. All *P*-values are 2-sided using $P < 0.05$ to determine statistical significance. Analyses were performed using SAS version 9.1 software (SAS Institute, Inc.).

Results

Breast cancer

The updated findings for invasive breast cancer are shown in the left panel of Fig. 1. In contrast with the results documented in the original report, there is now a significant difference between the treatment groups, with 310 cases of invasive breast cancer in the raloxifene group and 247 in the tamoxifen group. The invasive breast cancer RR (raloxifene:tamoxifen) is 1.24 (95% CI, 1.05–1.47), indicating that the rate in the raloxifene group is about 24% higher than the rate in the tamoxifen group. As demonstrated in the BCPT, compared with placebo, tamoxifen reduces the risk of invasive breast cancer by about 50% (3). Therefore, if there were no breast cancer RR effect from raloxifene, the expected rate of breast cancer in the raloxifene group would be about twice the rate in the tamoxifen group, yielding an RR of 2.00. Based on this information and the actual 1.24 RR observed in this study, one can extrapolate that raloxifene is about 76% as effective as tamoxifen in reducing breast cancer risk [{(2.00–1.24)/(2.00–1.00)} × 100 = 76%]. Then, compared with placebo, raloxifene would reduce the risk of invasive breast cancer by about 38% (50% × 76% = 38%), versus the 50% reduction seen with tamoxifen.

The rate of invasive breast cancer by participant demographic characteristics is provided in Table 2. The number of events and the point estimates of the rate are higher in the raloxifene arm than in the tamoxifen arm for all categories of participant characteristics, and there is no indication of a quantitative interaction between treatment and any of the participant characteristics.

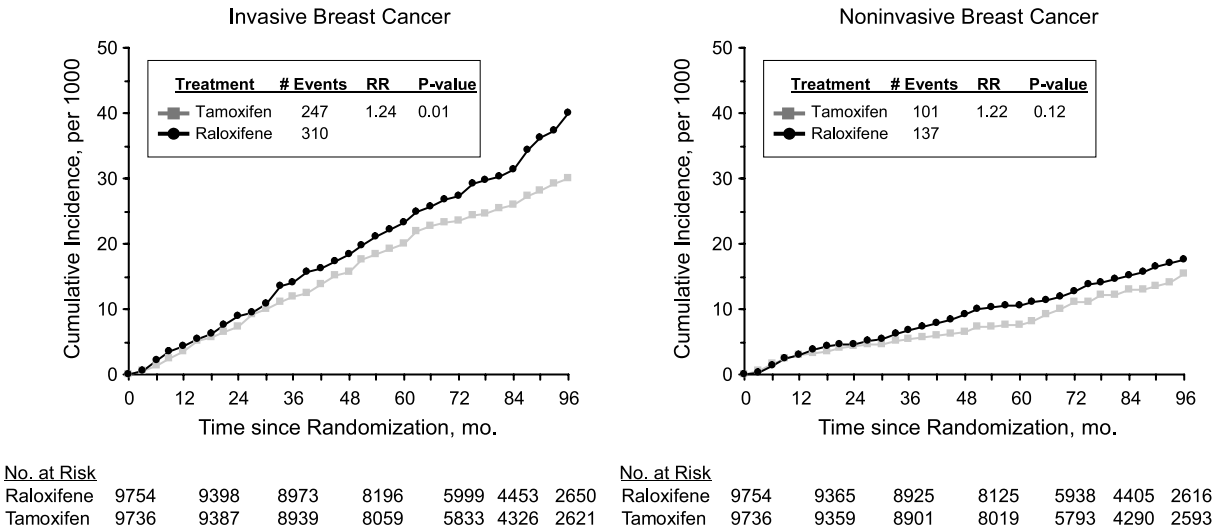


Fig. 1. Cumulative incidences of invasive and noninvasive breast cancer.

In our original report, the difference between treatment groups for the rate of noninvasive breast cancer was borderline for statistical significance (RR = 1.40; 95% CI, 0.98–2.00; P = 0.052). Currently, the difference between treatment groups for this event is less than originally seen (right panel of Fig. 1). There are 137 cases in the raloxifene group compared with 111 in the tamoxifen group, for an RR of 1.22 (95% CI, 0.95–1.59). The difference between

Table 2. Annual rates of invasive breast cancer—NSABP STAR Trial (P-2)

Participant characteristic at baseline	Number of events		Rate per 1000			RR*	RR (95% CI)
	Tamoxifen	Raloxifene	Tamoxifen	Raloxifene	Difference†		
Age at entry (years)							
≤49	10	15	1.84	2.80	−0.96	1.53	0.64–3.80
50-59	125	155	4.09	5.03	−0.94	1.23	0.97–1.57
≥60	112	140	4.47	5.48	−1.01	1.22	0.95–1.58
History of lobular carcinoma *in situ*							
No	197	253	3.54	4.50	−0.96	1.27	1.05–1.54
Yes	50	57	9.14	10.34	−1.20	1.13	0.76–1.69
History of atypical hyperplasia							
No	187	218	3.90	4.52	−0.62	1.16	0.95–1.42
Yes	60	92	4.58	6.79	−2.21	1.48	1.06–2.09
5-year predicted breast cancer risk (%)							
≤3.00	61	81	2.39	3.21	−0.82	1.34	0.95–1.90
3.01-5.00	84	91	4.43	4.63	−0.20	1.05	0.77–1.42
≥5.01	102	138	6.13	8.17	−2.04	1.33	1.02–1.74
No. 1^0 relatives with breast cancer							
0	82	105	4.77	6.17	−1.40	1.29	0.96–1.75
1	112	135	3.51	4.10	−0.59	1.17	0.90–1.51
≥2	53	70	4.44	5.96	−1.52	1.34	0.93–1.96
Total	247	310	4.04	5.02	−0.98	1.24	1.05–1.47

Abbreviations: CI, confidence interval; NSABP STAR, National Surgical Adjuvant Breast and Bowel Project Study of Tamoxifen and Raloxifene; RR, risk ratio.

*Risk ratio for women in the raloxifene group compared to women in the tamoxifen group.

†Rate in the tamoxifen group minus rate in the raloxifene group.

Table 3. Annual rates of noninvasive breast cancer and uterine disease/hysterectomy—NSABP STAR Trial (P-2)

Disease/uterine event type	Events, *n*		Rate per 1,000			RR*	RR (95% CI)
	Tamoxifen	Raloxifene	Tamoxifen	Raloxifene	Difference†		
Noninvasive breast cancer							
DCIS	70	86	1.15	1.40	−0.25	1.22	0.88–1.69
LCIS	33	34	0.54	0.55	−0.01	1.02	0.61–1.70
Mixed	8	17	0.13	0.28	−0.15	2.11	0.86–5.64
Total	111	137	1.83	2.23	−0.40	1.22	0.95–1.59
Uterine disease and hysterectomy‡							
Invasive Cancer	65	37	2.25	1.23	1.02	0.55	0.36–0.83
Hyperplasia§	126	25	4.40	0.84	3.56	0.19	0.12–0.29
Without atypia§	104	21	3.63	0.70	2.93	0.19	0.11–0.31
With atypia§	22	4	0.77	0.13	0.64	0.17	0.04–0.51
Hysterectomy during follow-up	349	162	12.08	5.41	6.67	0.45	0.37–0.54

Abbreviations: CI, confidence interval; DCIS, ductal carcinoma *in situ*; LCIS, lobular carcinoma *in situ*; NSABP STAR, National Surgical Adjuvant Breast and Bowel Project Study of Tamoxifen and Raloxifene; RR, risk ratio.

*Risk ratio for women in the raloxifene group compared with women in the tamoxifen group.

†Rate in the tamoxifen group minus rate in the raloxifene group.

‡Women at risk were those with an intact uterus at entry (see Table 1).

§Among women not diagnosed with uterine cancer.

treatment groups in noninvasive breast cancer appears to be limited to cases of pure DCIS or cases of mixed DCIS and LCIS (top portion of Table 3). There was no difference between the groups for pure LCIS cases; the numbers of women diagnosed with this condition were 33 (tamoxifen) and 34 (raloxifene; RR = 1.02; 95% CI, 0.61–1.70). In parallel with the analysis presented above for invasive breast cancer, tamoxifen was shown in the BCPT to reduce the risk of noninvasive breast cancer by about 50%. Therefore, if there were no noninvasive breast cancer risk reduction effect of raloxifene, the expected rate of noninvasive breast cancer in the raloxifene group would be about twice the rate in the tamoxifen group, yielding an RR (raloxifene:tamoxifen) of 2.00. Based on this information and the actual 1.22 RR observed in this study, one can extrapolate that raloxifene is about 78% as effective as tamoxifen in reducing noninvasive breast cancer risk [{(2.00-1.22)/(2.00-1.00)} × 100 = 78%]. Then, compared with placebo, raloxifene reduces the risk of noninvasive breast cancer by about 39% (50% × 78% = 39%).

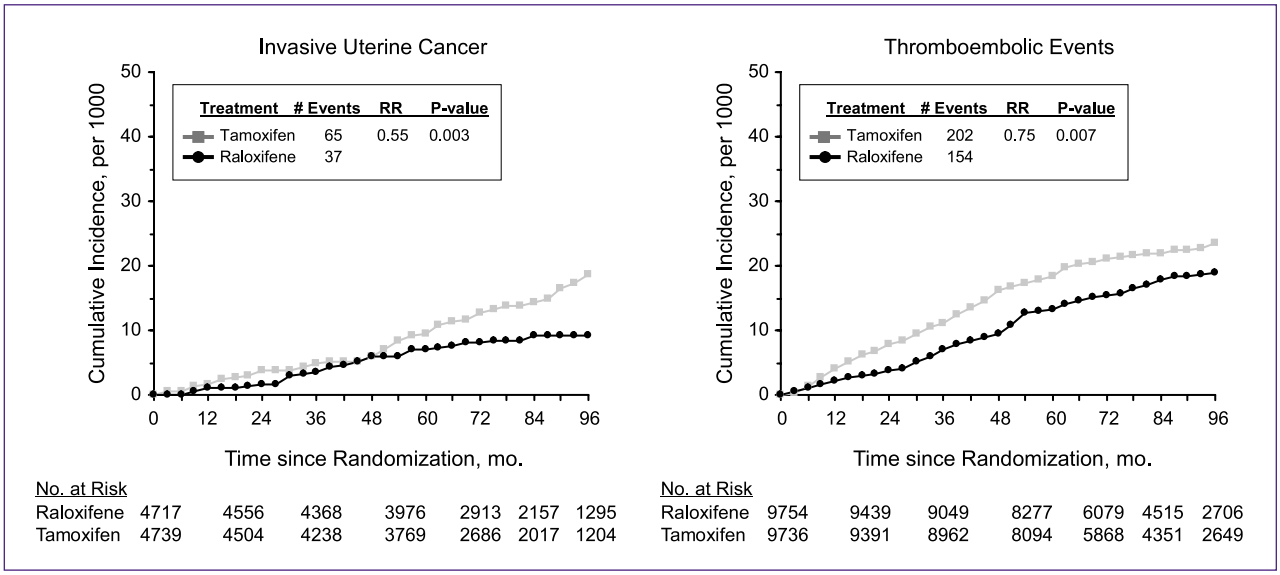


Fig. 2. Cumulative incidences of invasive uterine cancer and thromboembolic events.

Uterine disease

Invasive uterine cancer and uterine hyperplasia are well-established toxicities associated with tamoxifen treatment. When compared with tamoxifen, raloxifene does not have such a profile (bottom portion of Table 3). The incidence of invasive uterine cancer is significantly lower in the raloxifene group (P = 0.003; left panel of Fig. 2). The annual average rate per 1,000 was 2.25 in the tamoxifen group compared with 1.23 in the raloxifene group (RR = 0.55; 95% CI, 0.36–0.83). In our original report, the difference between treatment groups for the rate of invasive uterine cancer was not statistically significant. The average annual incidence rate of uterine hyperplasia, the majority of which was hyperplasia without atypia, was 5 times higher in the tamoxifen group (4.40 per 1,000) than in the raloxifene group (0.84 per 1,000; RR = 0.19; 95% CI, 0.12–0.29). The number of hysterectomies performed in the tamoxifen group (349), including those done for benign disease, was more than double that performed in the raloxifene group (162; RR = 0.45; 95% CI, 0.37–0.54).

Other cancers

Comparisons between treatment groups for the average annual rates of invasive cancer at sites other than the breast or uterus are presented in Table 4. These data are consistent with those in the original report, which also showed no significant differences for cancers other than in breast or uterus cancer.

Thromboembolic events

Pulmonary embolism and deep-vein thrombosis are other toxicities with a well-recognized association with tamoxifen treatment. The incidence of such events was

Table 4. Annual rates of site-specific invasive cancer cases other than breast and uterine cancer—NSABP STAR Trial (P-2)

Site of cancer	Events, *n*		Rate per 1000			RR*	RR (95% CI)
	Tamoxifen	Raloxifene	Tamoxifen	Raloxifene	Difference†		
Adrenal gland	0	1	0	0.02	–0.02	—	—
Bone/cartilage/connective tissue	3	4	0.05	0.06	–0.01	1.32	0.22–8.98
Buccal cavity and pharynx	4	6	0.06	0.10	–0.04	1.48	0.35–7.13
Cervix	3	0	0.05	0	0.05	—	—
Colorectal	48	45	0.78	0.72	0.06	0.93	0.60 to 1.42
Esophagus	2	0	0.03	0	0.03	—	—
Eye	1	1	0.02	0.02	0	0.99	0.01–77.48
Gallbladder	5	2	0.08	0.03	0.05	0.39	0.04–2.41
Kidney	14	21	0.23	0.34	–0.11	1.48	0.72–3.15
Larynx	0	1	0	0.02	–0.02	—	—
Leukemia/other lymph/hemato	60	53	0.97	0.85	0.12	0.87	0.59–1.28
Liver	7	2	0.11	0.03	0.08	0.28	0.03–1.48
Lung, trachea, bronchus	57	64	0.92	1.02	–0.10	1.11	0.76–1.61
Nasal/middle ear/sinuses	1	1	0.02	0.02	0	0.99	0.01–77.48
Nervous system	9	10	0.15	0.16	–0.01	1.10	0.40–3.05
Other gyn	2	2	0.03	0.03	0	0.99	0.07–13.62
Ovary	21	34	0.50	0.79	–0.29	1.58	0.89–2.86
Pancreas	12	11	0.19	0.18	0.01	0.90	0.36–2.24
Retroperitoneum	7	4	0.11	0.06	0.05	0.56	0.12–2.22
Skin	25	24	0.40	0.38	0.02	0.95	0.52–1.73
Small intestine	0	2	0	0.03	–0.03	—	—
Spleen	0	2	0	0.03	–0.03	—	—
Stomach	5	1	0.08	0.02	0.06	0.20	0.004–1.76
Thyroid gland	18	32	0.29	0.51	–0.22	1.76	0.96–3.32
Urinary bladder	15	12	0.24	0.19	0.05	0.79	0.34–1.81
Site unspecified/unspecified nature	15	19	0.24	0.30	–0.06	1.25	0.60–2.64
Secondary/uncertain	4	5	0.06	0.08	–0.02	1.23	0.27–6.22

Abbreviations: CI, confidence interval; gyn, gynecologic; hemato, hematopoietic; lymph, lymphatic; NSABP STAR, National Surgical Adjuvant Breast and Bowel Project Study of Tamoxifen and Raloxifene; RR, risk ratio.

*Risk ratio for women in the raloxifene group compared with women in the tamoxifen group.

†Rate in the tamoxifen group minus rate in the raloxifene group.

Table 5. Rates of thromboembolic events, cataracts, and cataracts surgery—NSABP STAR Trial (P-2)

Type of event	Events, *n*		Rate per 1,000			RR*	RR (95% CI)
	Tamoxifen	Raloxifene	Tamoxifen	Raloxifene	Difference†		
Thromboembolic events	202	154	3.30	2.47	0.83	0.75	0.60–0.93
Pulmonary embolism	84	68	1.36	1.09	0.27	0.80	0.57–1.11
Deep-vein thrombosis	118	86	1.93	1.38	0.55	0.72	0.54–0.95
Cataracts and Cataract Surgery							
Developed cataracts during follow-up‡	739	603	14.58	11.69	2.89	0.80	0.72–0.89
Developed cataracts and had cataract surgery‡	575	462	11.18	8.85	2.33	0.79	0.70–0.90

Abbreviations: CI, confidence interval; NSABP STAR, National Surgical Adjuvant Breast and Bowel Project Study of Tamoxifen and Raloxifene; RR, risk ratio.

*Risk ratio for women in the raloxifene group compared to women in the tamoxifen group.

†Rate in the tamoxifen group minus rate in the raloxifene group.

‡Women at risk were those with no prior history of cataracts at entry (8,341 and 8,336 tamoxifen and raloxifene participants, respectively).

significantly elevated in the tamoxifen group compared with the raloxifene group ($P = 0.007$; right panel of Fig. 2 and top of Table 5). The average annual rates of thromboembolic events were 3.30 per 1,000 (tamoxifen) and 2.47 per 1,000 (raloxifene; RR = 0.75; 95% CI, 0.60–0.93).

Cataracts

When compared with the results in the placebo group in the BCPT, tamoxifen increased the incidence of cataract development and cataract surgery (3). Raloxifene does not have this effect. In the original report of STAR, cataract events were significantly elevated in the tamoxifen group compared with the raloxifene group, and these differences persisted in the current analysis (bottom of Table 5). The rate of cataract development (RR = 0.80; 95% CI, 0.72–0.89) and the rate of cataract surgery (RR = 0.79; 95% CI, 0.70–0.90) are about 20% less in the raloxifene group than in the tamoxifen group.

Mortality

The number of deaths observed during follow-up is shown in Table 6. There is no statistically significant mortality difference between the treatment groups. Overall, 236 deaths occurred in the tamoxifen group and 202 deaths in the raloxifene group, for an RR of 0.84, which was not statistically significant (95% CI, 0.70–1.02). When the differences between treatment groups are compared by specific causes of death, the data are consistent with variation due to chance.

Discussion

Tamoxifen has been shown to reduce the risk of contralateral breast cancer in women with invasive breast cancer and DCIS (12, 13). The benefit appears to be very durable. After 2 to 5 years of adjuvant tamoxifen, the contralateral breast cancer reduction continued through at least 15 years of follow-up (2, 14). In primary prevention trials of tamoxifen in women at risk for the future development of breast cancer, 5 to 8 years of tamoxifen significantly reduced the incidence of invasive breast cancer, and this benefit persisted for at least 7 to 12 years (6, 15, 16).

Raloxifene has also been shown to reduce the incidence of primary invasive breast cancer (compared with placebo). The Multiple Outcomes of Raloxifene Evaluation (MORE) trial randomized 7,704 postmenopausal women with osteoporosis; with a median follow-up of 45 months, raloxifene (given for 4 years) reduced the incidence of breast cancer by 76% (RR = 0.24; 95% CI, 0.13–0.44; ref. 7). In the Raloxifene Use for the Heart (RUTH) trial, 10,101 postmenopausal women with coronary heart disease or multiple risk factors for this disease were assigned to either raloxifene (60 mg/d) or placebo. With 5.6 years median follow-up, raloxifene reduced the incidence of invasive breast cancer by a significant 44% (hazard ratio [HR] = 0.56; 95% CI, 0.38–0.83; ref. 17). As detailed in the initial report of STAR, after a median follow-up of 47 months, raloxifene was as effective as tamoxifen in reducing the risk of invasive breast cancer. The updated results reported here demonstrate that after a median follow-up of 81 months, which represents 60 months of treatment plus an additional 21 months of follow-up, raloxifene no longer appears to be as effective as tamoxifen in preventing primary invasive breast cancer. Raloxifene does appear, however, to retain approximately 76% of tamoxifen's effectiveness, which represents as much as a 38% reduction in invasive breast cancer (compared with an untreated group). The initial STAR report also suggested that raloxifene may not be as effective as tamoxifen in preventing the development of noninvasive breast cancers (LCIS and DCIS combined). The updated results show that the difference between the treatment groups has narrowed, and much like its effect against invasive breast cancer, raloxifene is about 78% as effective as tamoxifen in reducing the risk of noninvasive breast cancer. Patients with a history of LCIS or atypical hyperplasia of the breast

have a 4-fold to 10-fold increased risk of subsequent invasive disease, and tamoxifen and raloxifene were equally effective in reducing this risk in the initially reported STAR results. The current analyses indicate that this equality is no longer the case for STAR women with a history of atypical hyperplasia (RR = 1.48; 95% CI = 1.06-2.09), although results for the LCIS group remain similar to those reported originally (RR = 1.13; 95% CI, 0.76–1.69).

Only a slight difference was evident between treatment groups in the cumulative incidence of both invasive and noninvasive breast cancer (Fig. 1) through the first 20 months of the study. After 30 months, a clear separation of the treatment curves was observed, with a higher cumulative incidence of both invasive and noninvasive breast cancer in the raloxifene group. Why are we seeing this apparent diminution of raloxifene's benefits with longer follow-up? When the initial STAR results were published, all participants were notified of the results, and women who were still receiving tamoxifen were offered the option of crossing over to raloxifene therapy for the remainder of their 5 years of treatment. Only 879 women (9%) chose this option. The cross-over is unlikely to fully explain our updated findings.

Is nonadherence with the medication an issue? Only about 2% of orally administered raloxifene becomes bioavailable, and the biological half-life of raloxifene is much shorter than that of tamoxifen. Missing a day or 2 of raloxifene may result in a greater reduction of effectiveness than would similarly skipped doses of tamoxifen. However, overall adherence to protocol medication, as measured by pill counts, was similar in the two groups, and the protocol medication drop-off rates were higher in the tamoxifen group (38.9% versus 27.4%), indicating that nonadherence or drop-offs in the raloxifene group do not provide the answer. Raloxifene may simply be less potent than is tamoxifen. It was originally developed as a drug to treat breast cancer but was less effective than was tamoxifen in that setting as well (18).

The superiority of tamoxifen over raloxifene in reducing breast cancer risk comes with a cost: significantly more endometrial cancers, hysterectomies for benign disease, thromboembolic events, and cataracts. These toxicities may be acceptable for the treatment of breast cancer but have proved to be a barrier to the use of tamoxifen for preventing primary breast cancers. It is important to point out that, unlike raloxifene, tamoxifen is approved for use in premenopausal women, and the BCPT (NSABP P-1) showed no excessive risk of endometrial cancers or thromboembolic events in the tamoxifen-treated premenopausal group compared with the placebo group. For premenopausal women at increased risk, particularly those with biopsy-proven risk factors such as LCIS or atypical hyperplasia, tamoxifen has a positive risk/benefit ratio and should be presented as a treatment option. A similar risk/benefit ratio may exist in younger postmenopausal women with elevated Gail scores and a prior hysterectomy.

Our results demonstrate that raloxifene (compared with tamoxifen) retains substantial benefit in reducing the risk of invasive breast cancer and has fewer life-threatening side effects, including significantly fewer endometrial cancers, and these results are in keeping with those in the placebo-controlled raloxifene trials. We saw no significant increases in other primary cancers, although there were numerically more ovarian cancers and thyroid cancers. Neither of these tumors was noted to be of concern in the other raloxifene trials, but we plan to continue to follow STAR patients with particular attention to all potential long-term side effects.

The 5-year duration of therapy in STAR was a carryover from the P-1 trial of tamoxifen versus placebo, in which 5 years of tamoxifen was chosen based on the duration of treatment in adjuvant trials. In the combined results of MORE and the Continuing Outcomes Relevant to Evista (CORE) trial, which involved as much as 8 years of raloxifene therapy, a 66% reduction in the incidence of invasive breast cancer was seen in the raloxifene-treated group compared with the placebo group (HR = 0.34; 95% CI, 0.22–0.50). The women in the MORE/CORE studies were not selected based on breast cancer risk, and the majority had Gail scores below 1.66%, although some high-risk women were included.

Laboratory studies demonstrate that the antitumor actions of raloxifene and related hydroxylated SERMs depend on the duration of administration (19–21). In other words, longer administration periods are necessary to control tumorigenesis with short-acting SERMs with poor bioavailability (20). It may be that the long-term benefit of tamoxifen in controlling tumorigenesis occurs because of the development and evolution of a sophisticated SERM-resistant disease that becomes vulnerable to the apoptotic actions of physiologic estrogen (22) once tamoxifen is stopped. In contrast, the evolution of acquired SERM resistance may not advance as quickly with raloxifene as with tamoxifen, and raloxifene only remains therapeutically effective as long as it is given (8). It is unlikely that the optimal duration of raloxifene for chemoprevention will be evaluated in a breast cancer prevention setting; however, the use of raloxifene in treating and preventing osteoporosis is approved for an indefinite period of time. Therefore, continuing raloxifene therapy beyond 5 years might be an approach that would preserve its full chemopreventive activity.

Large randomized cancer-prevention trials with long-term clinical follow-up of a carefully characterized population of individuals provide a valuable resource beyond the primary aims of the study. In the NSABP STAR (P-2) and BCPT (P-1), baseline blood samples have been collected and stored from more than 30,000 women at an increased risk for breast cancer, as have tumor specimens from breast cancer events. Various studies have already been conducted using these resources, and others are underway, including a genome-wide-association study by NSABP in collaboration with the National Institutes of Health Pharmacogenetics Research Network (PGRN) and the RIKEN Yokohama Institute Center for Genomic Medicine; this study includes

Table 6. Distribution of Deaths - NSABP STAR Trial (P-2)

Cause of death	Deaths, *n*	
	Tamoxifen	Raloxifene
Cancer	101	86
Bladder	1	3
Bone, articular cartilage and connective tissue	1	1
Brain	6	4
Breast	11	4
Colon	4	3
Endocrine gland	0	1
Gallbladder	2	1
Kidney	1	1
Liver	7	1
Lung	25	28
Lymphatic/hematopoietic	12	11
Oral	2	1
Ovary	8	7
Pancreas	7	5
Peritoneum	2	0
Skin	2	0
Spleen	0	1
Stomach	2	1
Thyroid	1	0
Uterus	2	2
Other, uncertain, and unspecified sites	5	11
Circulatory/vascular disease	42	42
Aortic	1	2
Atherosclerosis	0	1
Cerebrovascular disease, unspecified	1	0
Hypertensive disease	1	4
Ischemic heart disease	13	8
Other heart disease	9	14
Peripheral vascular disease, unspecified	0	1
Polyarteritis nodosa	0	1
Pulmonary embolism	3	2
Primary pulmonary hypertension	1	0
Stroke	13	9
Other	93	74
Accident, auto	3	4
Accident, fire	1	0
Alcohol dependence syndrome	1	1
Asphyxiation and strangulation	1	0
Complications of surgery	0	1
Dementia	0	1
Diabetes	1	3
Disorders of metabolism	1	0
Emphysema	1	0
Injury, intracranial	2	2

(*Continued on the following page*)

Table 6. Distribution of Deaths - NSABP STAR Trial (P-2) (Cont'd)

Cause of death	Deaths, *n*	
	Tamoxifen	Raloxifene
Injury, other	1	0
Interferon toxicity	0	1
Intestinal infectious disease	0	1
Other conditions of the blood	0	2
Other conditions of the brain/neurological system	7	3
Other diseases of the digestive system	7	6
Other Diseases of the urinary system	2	1
Other respiratory disease	13	7
Pneumonia	2	4
Poisoning	2	0
Septicemia	4	3
Skin infections	0	1
Symptoms, signs, and ill-defined conditions	2	3
Unknown	42	30
Total deaths (rate per 1,000)	236 (3.81)	202 (3.22)
Risk ratio (95% CI)	0.70–1.02)	

Abbreviations: CI, confidence interval; NSABP STAR, National Surgical Adjuvant Breast and Bowel Project Study of Tamoxifen and Raloxifene.

a detailed evaluation of cytochrome P450 2D6 (CYP2D6) status (refs. 23–27; access to these data and specimens is not restricted to NSABP members; the pathology section of the NSABP web site, ref. 28, describes the process by which one can submit applications for such projects).

In conclusion, with a median follow-up of 81 months, our long-term, updated results show that raloxifene retained 76% of the effectiveness of tamoxifen in preventing invasive disease, that its level of effectiveness grew closer over time to that of tamoxifen (78% as effective) in preventing noninvasive disease, and that raloxifene remained far less toxic (e.g., now with highly statistically significantly fewer endometrial cancers). These relative effects of the drugs in the longer term—including greater potency of tamoxifen in preventing invasive and noninvasive disease and significantly less endometrial toxicity with raloxifene—are more consistent with the profiles that were expected on the basis of findings from other published studies. With deep public-health implications, these results help to clarify that both raloxifene and tamoxifen are good preventive choices for higher-risk postmenopausal women, depending largely on a woman's personal risk factors for breast cancer. For postmenopausal women with elevated risk, these results should encourage widespread acceptance of raloxifene for breast cancer risk reduction, especially in women with an intact uterus who also face a risk of osteoporosis and fracture. The results should also promote greater acceptance of tamoxifen (given its greater efficacy) by premenopausal women who are at a very high risk for breast cancer. Such increased acceptances of both SERMs for breast cancer risk reduction ultimately would reduce the public health burden of the disease.

Disclosure of Potential Conflicts of Interest

V.G. Vogel: commercial research grant, Astra-Zeneca; honoraria from speakers bureau, Eli Lilly and Astra-Zeneca; consultant/advisory board, Eli Lilly and Astra-Zeneca. D.L. Wickerham: honoraria from speakers bureau, Astra-Zeneca; consultant/advisory board, Eli Lilly. The other authors disclosed no potential conflicts of interest.

Acknowledgments

The authors wish to thank Barbara G. Good, Ph.D., and Wendy L. Rea for editorial assistance.

Grant Support

Public Health Service grants U10-CA-12027, U10-CA-69651, U10-CA-37377, and U10-CA-69974 from the National Cancer Institute, Department of Health and Human Services.

Received 03/08/2010; revised 04/01/2010; accepted 04/04/2010; published OnlineFirst 04/19/2010.

References

1. Jemal A, Siegel R, Ward E, Hao Y, Xu J, Thun MJ. Cancer statistics 2009. CA Cancer J Clin 2009;59:225–49.
2. Early Breast Cancer Trialists' Collaborative Group. Effects of chemotherapy and hormonal therapy for early breast cancer on recurrence and 15-year survival: an overview of the randomised trials. Lancet 2005;365:1687–717.
3. Fisher B, Costantino JP, Wickerham DL, et al. Tamoxifen for prevention of breast cancer: report of the National Surgical Adjuvant

Breast and Bowel Project P-1 Study. J Natl Cancer Inst 1998;90: 1371–88.
4. Cuzick J, Forbes J, Edwards R, et al. First results from the International Breast Cancer Intervention Study (IBIS-1): a randomised prevention trial. Lancet 2002;360:817–24.
5. Cuzick J, Powles T, Veronesi U, et al. Overview of the main outcomes in breast cancer prevention trials. Lancet 2003;361:296–300.
6. Powles TJ, Ashley S, Tidy A, Smith IE, Dowsett M. Twenty-year follow-up of the Royal Marsden randomized, double-blinded tamoxifen breast cancer prevention trial. J Natl Cancer Inst 2007;99:283–90.
7. Cummings SR, Eckert S, Krueger KA, et al. The effect of raloxifene on risk of breast cancer in postmenopausal women: results from the MORE randomized trial. Multiple Outcomes of Raloxifene Evaluation. JAMA 1999;281:2189–97.
8. Martino S, Cauley JA, Barrett-Conner E, et al. Continuing Outcomes Relevant to Evista: breast cancer incidence in postmenopausal osteoporotic women in a randomized trial of raloxifene. J Natl Cancer Inst 2004;96:1751–61.
9. Vogel VG, Costantino JP, Wickerham DL, et al. Effects of tamoxifen vs raloxifene on the risk of developing invasive breast cancer and other disease outcomes: The NSABP Study of Tamoxifen and Raloxifene (STAR) P-2 trial. JAMA 2006;295:2727–41.
10. Costantino JP, Gail MH, Pee D, et al. Validation studies for models to project the risk of invasive and total breast cancer incidence. J Natl Cancer Inst 1999;91:1541–8.
11. Korn EL, Dorey FJ. Applications of crude incidence curves. Stat Med 1992;11:813–29.
12. Early Breast Cancer Trialists' Collaborative Group. Tamoxifen for early breast cancer: An overview of the randomised trials. Lancet 1998;351:1451–67.
13. Fisher B, Dignam J, Wolmark N, et al. Tamoxifen in treatment of intraductal breast cancer: National Surgical Adjuvant Breast and Bowel Project B-24 randomised controlled trial. Lancet 1999;353: 1993–2000.
14. Fisher B, Jeong JH, Bryant J, et al. Treatment of lymph-node-negative, oestrogen-receptor-positive breast cancer: long-term findings from National Surgical Adjuvant Breast and Bowel Project randomised clinical trials. Lancet 2004;364:858–68.
15. Fisher B, Costantino J, Wickerham DL, et al. Tamoxifen for the prevention of breast cancer: Current status of the National Surgical Adjuvant Breast and Bowel Project P-1 study. J Natl Cancer Inst 2005;97:1652–62.
16. Cuzick J, Forbes JF, Sestak I, et al. Long-term results of tamoxifen prophylaxis for breast cancer – 96-month follow-up of the randomized IBIS-1 trial. J Natl Cancer Inst 2007;99:272–82.
17. Barrett-Conner E, Mosca L, Collins P, et al. Effects of raloxifene on cardiovascular events and breast cancer in postmenopausal women. N Engl J Med 2006;355:125–37.
18. Buzdar AU, Marcus C, Holmes F, Hug V, Hortobagyi G. Phase II evaluation of Ly156758 in metastatic breast cancer. Oncology 1998;45:344–5.
19. Gottardis MM, Jordan VC. The antitumor actions of keoxifene (raloxifene) and tamoxifen in the N-nitrosomethylurea-induced rat mammary carcinoma model. Cancer Res 1987;47:4020–4.
20. Jordan VC, Allen KE. Evaluation of the antitumor activity of the nonsteroidal antioestrogen monohydroxytamoxifen in the DMBA-induced rat mammary carcinoma model. Eur J Cancer 1980;16: 239–51.
21. Jordan VC, Gosden B. Inhibition of the uterotrophic activity of estrogens and antiestrogens by the short acting antiestrogen LY117018. Endocrinology 1983;113:463–8.
22. Jordan VC. The 38th David A. Karnofsky lecture: The paradoxical actions of estrogen in breast cancer—survival or death? J Clin Oncol 2008;26:3073–82.
23. Abramson N, Costantino JP, Garber JE, Berliner N, Wickerham DL, Wolmark N. Effect of Factor V Leiden and prothrombin G20210→A mutations on thromboembolic risk in the National Surgical Adjuvant Breast and Bowel Project cancer prevention trial. J Natl Cancer Inst 2006;98:904–10.
24. Cushman M, Costantino JP, Tracy RP, et al. Tamoxifen and cardiac risk factors in healthy women: Suggestion of an anti-inflammatory effect. Arterioscler Thromb Vasc Biol 2001;21:255–61.
25. King MC, Wieand S, Hale K, et al. Tamoxifen and breast cancer incidence among women with inherited mutations in BRCA1 and BRCA2: National Surgical Adjuvant Breast and Bowel Project (NSABP-P-1) Breast Cancer Prevention Trial. JAMA 2001;286: 2251–6.
26. Cushman M, Costantino JP, Bovill EG, et al. Effect of tamoxifen on venous thrombosis risk factors in women without cancer: The breast cancer prevention trial. Br J Haematol 2003;120: 109–16.
27. Beattie MS, Costantino JP, Cummings SR, et al. Endogenous sex hormones, breast cancer risk, and tamoxifen response: an ancillary study in the NSABP breast cancer prevention trial (P-1). J Natl Cancer Inst 2006;98:110–5.
28. Available from: http://www.nsabp.pitt.edu.

Horm Mol Biol Clin Invest 2011;5(1):27–34 © 2011 by Walter de Gruyter • Berlin • New York. DOI 10.1515/HMBCI.2010.047

The conformation of the estrogen receptor directs estrogen-induced apoptosis in breast cancer: a hypothesis

Philipp Maximov[1,a], Surojeet Sengupta[2,a], Joan S. Lewis-Wambi[1], Helen R. Kim[2], Ramona F. Curpan[3] and V. Craig Jordan[2,*]

[1]Fox Chase Cancer Center, Philadelphia, PA, USA
[2]Department of Oncology, Lombardi Cancer Center, Georgetown University Medical Center, Washington, DC, USA
[3]Institute of Chemistry, Romanian Academy, Timisoara, Romania

Abstract

Background: Estrogens are classified as type I (planar) and type II (angular) based on their structures. In this study, we used triphenylethylenes (TPEs) compounds related to 4-hydroxytamoxifen 4OHT to address the hypothesis that the conformation of the liganded estrogen receptor (ERα) can dictate the E2-induced apoptosis of the ER+ breast cancer cells.

Materials and methods: ERα positive MCF7:5C cells were used to study apoptosis induced by E2, 4OHT and TPEs. Growth and apoptosis assays were used to evaluate apoptosis and the ability to reverse E2-induced apoptosis. ERα protein was measured by Western blotting to investigate the destruction of ERα by TPEs in MCF7 cells. Chromatin immunoprecipitation (ChIP) assays were performed to study the in vivo recruitment of ERα and SRC3 at classical E2-responsive promoter TFF1 (PS2) by TPEs. Molecular modeling was used to predict the binding mode of the TPE to the ERα.

Results: TPEs were not only unable to induce efficient apoptosis in MCF7:5C cells but also reversed the E2-induced apoptosis similar to 4OHT. Furthermore, the TPEs and 4OHT did not reduce the ERα protein levels unlike E2. ChIP assay confirmed very weak recruitment of SRC3 despite modest recruitment of ERα in the presence of TPEs. Molecular modeling suggests that TPE would bind in antagonistic mode with ERα.

Conclusion: Our results advances the hypothesis that the TPE liganded ERα complex structurally resembles the 4OHT bound ERα and cannot efficiently recruit co-activator SRC3. As a result, the TPE complex cannot induce apoptosis of ER+ breast cancer cells, although it can cause growth of the breast cancer cells. The conformation of the estrogen-ER complex differentially controls growth and apoptosis.

Keywords: breast cancer; estrogen; estrogen receptor; tamoxifen; triphenylethylenes.

Introduction

High dose estrogen therapy for the treatment of breast cancer is a pioneering application of translational research, as this was the first chemical therapy to be successful for the treatment of any type of cancer (1). High dose estrogen therapy for the treatment of breast cancer in postmenopausal women became an accepted standard of care for the treatment of breast cancer prior to the introduction of tamoxifen in the 1970s. Response rates to high dose estrogen therapy were dependent upon the duration of time from the menopause; patients treated in their seventies would have a response rate of 30%, whereas patients treated in their fifties had very few tumor responses. Although it was not realized at the time, the antitumor actions of estrogen were based upon estrogen deprivation. Sir Alexander Haddow FRS pioneered the development of high dose estrogen therapy, but in 1970, when he was selected as the inaugural Karnofsky lecturer at the American Society for Clinical Oncology, he remarked that little progress was being made in targeted therapeutics, and with regard to his own contribution of high dose estrogen treatment, he stated, ''…the extraordinary extent of tumor regression observed in perhaps 1% of post-menopausal cases (with estrogen) has always been regarded as of major theoretical importance, and it is a matter for some disappointment that so much of the underlying mechanisms continues to elude us…'' (2).

Now, some 40 years later, based upon decades of research on the impact of long-term adjuvant antihormone therapy on the evolution of drug resistance, a vulnerability of breast cancers has emerged, that was unanticipated. Selective estrogen receptor modulators (SERMs), e.g., tamoxifen and raloxifene, initially cause drug resistance in breast cancer cells that is identified by SERM stimulated growth and the tumor cells are also stimulated to grow with physiological estrogen (3, 4). However, this form of drug resistance occurs within approximately a year with SERM treatment; but, because successful 5 years of adjuvant tamoxifen therapy is given routinely to enhance survivorship (5), one would imagine other mechanisms of drug resistance occurring for micrometastatic disease during 5 years of adjuvant therapy. This would be a reasonable explanation for the lack of recurrences and increasing survivorship after tamoxifen is stopped (5). Studies in the laboratory demonstrate that drug resistance to

[a] These authors contributed equally.

*Corresponding author: V. Craig Jordan, OBE, PhD, DSc, FMedSci, Scientific Director, Lombardi Comprehensive Cancer Center, Vice Chair of Department of Oncology, Professor of Oncology and Pharmacology, Georgetown University Medical Center, 3970 Reservoir Rd NW, Washington, DC 20057, USA
Phone: +1-202-687-2897, Fax: +1-202-687-6402,
E-mail: vcj2@georgetown.edu

Received September 9, 2010; accepted September 24, 2010; previously published online March 4, 2011

SERMs evolves over approximately 5 years into a phase that is SERM-stimulated for growth, but physiological estrogen causes apoptosis and tumor regression (4, 6). The hypothesis has been offered that in fact long-term adjuvant tamoxifen therapy can reconfigure antihormone resistant breast cancer cells so that they are particularly sensitive to the apoptotic actions of physiological estrogen (from the patient's body) once 5 years of adjuvant tamoxifen has been stopped (7). Aromatase inhibitors are also administered to postmenopausal ER positive breast cancer patients for 5 years of adjuvant therapy (8, 9). Laboratory studies show that estrogen deprivation for prolonged periods sensitizes the resulting cells that are estrogen independent for growth to the apoptotic actions of estrogen (10, 11).

Using laboratory models for SERM and aromatase inhibitor resistant disease, mechanisms are emerging to define intrinsic and extrinsic pathways of estrogen-induced apoptosis (12). However, the question arises of how the estrogen receptor (ER) complex in one context can stimulate estrogen-stimulated growth, but the same complex will induce apoptosis in antihormone resistant cells. To address this paradox, we have drawn upon our previous contribution on the molecular classification of estrogens (13, 14) to interrogate the ER complex with structural derivatives of the antiestrogen, 4-hydroxytamoxifen (4OHT) and endoxifen (15). The molecular classification of estrogens is based upon the published X-ray crystallographic data for the planar estrogen diethylstilbestrol (DES) (incidentally, the synthetic estrogen earlier selected for high dose estrogen therapy for breast cancer) and 4OHT (the potent antiestrogenic metabolite of tamoxifen) (16). Simply stated, DES binds to the ligand binding domain (LBD) and is sealed within the cavity with helix 12 being the cap. In contrast, 4OHT, with its ''bulky side chain'' in the triphenylethylene (TPE) structure, pushes helix 12 back because of steric hindrance. The DES ER structure sealed with helix 12 allows the ER complex to be activated through activating function-2 (AF-2) that collaborates and cooperates with AF-1 at the opposing end of the ER. In this manner, the co-activators recruited to the complex initiate estrogen-stimulated growth and gene transcription. In contrast, the 4OHT ER complex cannot activate AF-2, but AF-1 is able to be activated through the exposed Asp351 that is inadequately neutralized and shielded by the dimethyl aminoethoxy side chain of 4OHT. This is classified as an antiestrogen complex, but it mechanistically explains the promiscuous estrogen-like activity of 4OHT (17, 18). Indeed, substitution of Asp351 for the non-ionic amino acid glycine completely abrogates the estrogen-like actions of the 4OHT ER complex (17).

In this paper, we offer the hypothesis that the shape of the ER complex with either planar estrogens (Class I) or angular estrogens (Class II) can modulate the apoptotic actions of estrogen through the shape of the resulting complex. We have previously synthesized a range of estrogenic TPEs, and all of these compounds will stimulate estrogen-stimulated growth of MCF-7 cells (15). Here, we investigate the actions of 4OHT and our model TPEs on estradiol-induced apoptosis in MCF-7:5C cells (19). We have discovered that the angular TPE estrogens do not cause rapid estrogen-induced apoptosis, even though they are potent stimulators of breast cancer cell growth. They do, in fact, block estradiol-induced apoptosis as effectively as 4OHT, a known antiestrogen. We propose the hypothesis that the shape of the ER complex and its ability to bind co-activators and transport them to the correct part of the cell is fundamentally important for the initiation of estrogen-induced apoptosis.

Materials and methods

Cell culture and reagents

Media for cell culture were purchased from Invitrogen Inc. (Grand Island, NY, USA) and fetal calf serum (FCS) was obtained from HyClone Laboratories (Logan, UT, USA). Compounds E2 and 4OHT were obtained from Sigma, St. Louis, MO, USA. The compounds trihydroxytriphenylethylene (3OHTPE) and ethoxytriphenylethylene (EtOX) were synthesized and the details of the synthesis have been reported previously (15). The ER positive breast cancer cells MCF-7:WS8 (hereafter mentioned as MCF7) and estrogen-deprived MCF7:5C were derived from MCF7 cells obtained from the Dr. Dean Edwards, San Antonio, TX, USA as reported previously (20). MCF7 cells were maintained in RPMI media supplemented with 10% FCS, 6 ng/mL bovine insulin and penicillin and streptomycin. MCF7:5C cells were maintained in phenol-red free RPMI media containing 10% charcoal dextran treated FCS, 6 ng/mL bovine insulin and penicillin and streptomycin. Three to four days prior to harvesting, the MCF7 cells were cultivated in phenol red-free media containing 10% charcoal dextran treated FCS. The cells were treated with indicated compounds (with media changes every 48 h) for the specified time and were subsequently harvested for protein lysate or growth assay. All the experiments were repeated at least three times, in triplicate to confirm the results.

Growth assay

For growth assay, 12,000 MCF7:5C cells were plated in each well of 24-well plates and the treatment of the cells with specific concentration of indicated compounds were started 24 h later (day 0). The media containing the compounds were changed on day 2 and day 4. On day 6, the cells were harvested for assessing the total DNA content in each well using a fluorescent DNA quantitation kit (Bio-Rad, Hercules, CA, USA) according to the manufacturer's instructions. Calf thymus DNA was used to plot the standard curve for the DNA assay with each set of quantitation. The experiments were repeated three times in triplicate to confirm the data.

Western immunoblotting

The MCF7 cells were seeded on 10-cm Petri dishes at a density of 3 million cells per plate and were incubated overnight in phenol red-free RPMI 1640 media containing 10% charcoal dextran treated FCS, 6 ng/mL bovine insulin and penicillin and streptomycin. The cells were treated for 24 h with the indicated compounds and the cells were subsequently washed with cold phosphate buffered saline (PBS; Invitrogen, Carlsbad, CA, USA) twice and were lysed using 1× Lysis buffer (Cell Signaling Technology Inc., Denvers, MA, USA) that contained a 1× Complete Mini Protease Inhibitor Cocktail (Roche Diagnostics, Indianapolis, IN, USA) and 1× phosphatase inhibitors (Calbiochem, Gibbstown, NJ, USA). The cells were lysed for 30 min on ice and subsequently centrifuged at 12,000 rpm

(15,000×*g*) for 20 min. Supernatants were transferred in fresh tubes and stored on ice, the concentration of proteins in the lysates were measured via a fluorescent Quant-iT Protein Assay Kit (Invitrogen, Carlsbad, IN, USA). Then, 20 μg of each protein sample diluted in a NuPAGE LDS loading dye was loaded and separated on NuPAGE 4%–12% Bis-Tris Gel (Invitrogen, Carlsbad, CA, USA). After electrophoresis, the samples were transferred onto Hybond-ECL Nitrocellulose Membranes (Amersham Biosciences, Piscataway, NJ, USA), which were subsequently blocked with blocking solution TBS-T (50 nM Tris-HCl pH 7.5, 150 nM NaCl, 0.1% Tween-20), containing 5% skim milk for 1 h at room temperature. The membranes were subsequently probed with primary antibodies anti-ERα (Santa Cruz, Biotechnology, Santa Cruz, CA, USA) and with anti-β-actin (Sigma-Aldrich, St. Louis, MO, USA) diluted in blocking buffer at ratios recommended by the supplier at 4°C. The membranes were washed three times (10 min each) with the TBS-T buffer and subsequently incubated with the appropriate HRP-linked secondary antibodies (anti-mouse or anti-rabbit from Santa Cruz, Biotechnology, Santa Cruz, CA, USA) diluted in blocking buffer for 1 h at room temperature. The membranes were washed again as described above with TBS-T buffer and the signal was visualized using ECL Western Blotting Detection Reagents (GE Healthcare UK, Birminghamshire, UK).

Apoptosis assay

In total, 20,000 MCF7:5C cells were seeded in each well of a 96-well plate. Then, 24 h later cells were treated with indicated compounds in triplicate. Media containing the appropriate compounds were changed every 48 h. At the end of day 5, the cells were harvested using a colorimetric dye based apoptosis kit, APOPercentage™ (Biocolor Ltd., Carrickfergus, Antrim, UK) according to the manufacturer's instructions. Briefly, 30 min prior to the harvesting of the cells 5 μL of APOPercentage dye (which is selectively imported by the cells undergoing apoptosis) was added to each well and incubated for 30 min at 37°C, 5% CO_2 incubator. Subsequently, the cells were very carefully washed twice with PBS to wash off the unimported dye. The dye was thereafter released from the cells using a dye releasing reagent and the amount of dye imported was measured spectrophotometrically at 550 nm. The O.D. at 550 nm was directly proportional to the apoptosis of the cells.

Chromatin immunoprecipitation (ChIP) assay

ChIP was performed as described previously (21) with minor modifications. Briefly, cells were grown in phenol red-free RPMI media containing 10% charcoal stripped fetal bovine serum for 3 days before treating with vehicle, 1 nM E2, 4OHT (10^{-6} M) 3OHTPE (10^{-6} M) or EtOX (10^{-6} M) for 45 min. Cells were then washed with PBS and crosslinked with 1.25% formaldehyde. After stopping the crosslinking, cells were collected in PBS [containing protease inhibitors (Roche Diagnostics, Indianapolis, IN, USA) and 10 mM dithiothreitol (DTT)], centrifuged and resuspended in nuclei isolation buffer (50 mM Tris-Cl, 60 mM KCl, 0.5% NP40, protease inhibitors and 10 mM DTT). Nuclei were isolated by centrifugation and resuspended in SDS lysis buffer (50 mM Tris-Cl, 1% SDS, 10 mM EDTA, pH 8.1 with protease inhibitors) followed by sonication and centrifugation at 14,000×*g* for 20 min at 4°C. The supernatant (fixed chromatin) were diluted using ChIP dilution buffer followed by immunoclearing using normal rabbit serum and 20 μL of Magna ChIP protein A agarose magnetic beads (Upstate Cell Signaling Solutions, Temecula, CA, USA). Immunoprecipitation was performed overnight with antibodies against ERα (1:1 mixture of cat # sc-543 and sc-7207; Santa Cruz Biotechnology, Inc.) and SRC-3 (cat # 13066; Santa Cruz Biotechnology, Inc.). The immune complexes were precipitated using 20 μL of Magna ChIP protein A agarose magnetic beads (Upstate Cell Signaling Solutions) and incubating for an additional 2 h followed by precipitating using a magnet. The beads bound to immunocomplexes were sequentially washed using buffer I (20 mM Tris-Cl, 2 mM EDTA, 0.1% SDS, 1% Triton X-100, and 150 mM NaCl), buffer II (20 mM Tris-Cl, 2 mM EDTA, 0.1% SDS, 1% Triton X-100, and 250 mM NaCl), buffer III (0.25 M LiCl, 1% NP-40, 1% deoxycholate, 1 mM EDTA, 10 mM Tris-HCl, pH 8.1). Precipitates were then washed twice with TE buffer and extracted twice with freshly made 1% SDS and 0.1 M $NaHCO_3$. Pooled elutes were decrosslinked using 200 μM NaCl and heating at 65°C overnight. The DNA fragments were purified using the Qiaquick PCR purification kit (Qiagen, Valencia, CA, USA). Then, 2 μL of eluted DNA was used for real time PCR analysis. The primer sequences used are as follows: PS2 promoter: 5′-TGGGCTTCATGAGCTCCTTC-3′ (forward); 5′-TTCATAGTGAGAGATGGCCGG-3′ (reverse); the data are expressed as percent input of starting chromatin material after subtracting the percent input pulldown of the negative control (normal rabbit IgG).

Molecular modeling

The molecular modeling study was performed using the available X-ray crystallographic structures of ERα in the agonist and antagonist conformations. The 3D coordinates of ERα co-crystallized with E2 (1gwr) and 4OHT (3ert) were extracted from RCSB Protein Data Bank (PDB) (22) and these structures were prepared for docking using the Protein Preparation Workflow (Schrödinger, LLC, New York, NY, USA, 2008), accessible from within the Maestro 9.1 program (Schrödinger, LLC).

The ligand was prepared for docking with LigPrep 2.1 application (Schrödinger, LLC) and molecular docking was carried out with Glide 4.5 (Schrödinger, LLC) followed by the Induced Fit protocol (Schrödinger, LLC) using default parameters and 10 poses per ligand were retained for analysis.

Results

Reversal of E2-induced apoptosis in MCF7:5C cells by 4OHT, 3OHTPE and EtOX

17-β Estradiol induces apoptosis in ER+ MCF7:5C cells (19) which are long-term E2-deprived MCF7 breast cancer cells. Our aim was to evaluate the 4OHT and the TPEs, 3OHTPE and EtOX (Figure 1), for their ability to reverse the apoptosis induced by E2 in MCF7:5C cells in a concentration-dependent manner. Interestingly, the triphenylethylenes 3OHTPE and EtOX had previously been reported to be completely estrogenic as they can induce proliferation of MCF7 cells, unlike 4OHT (15). We found that 3OHTPE and EtOX were able to block the E2-induced apoptosis of MCF7:5C cells similar to the 4OHT in a concentration-dependent manner (Figure 2) as evident by DNA growth assay. The compounds alone at 10^{-6} M concentration were not able to induce significant apoptosis of MCF7:5C cells (Figure 2), whereas, as expected, drastic apoptosis was induced by E2 (1 nM) alone.

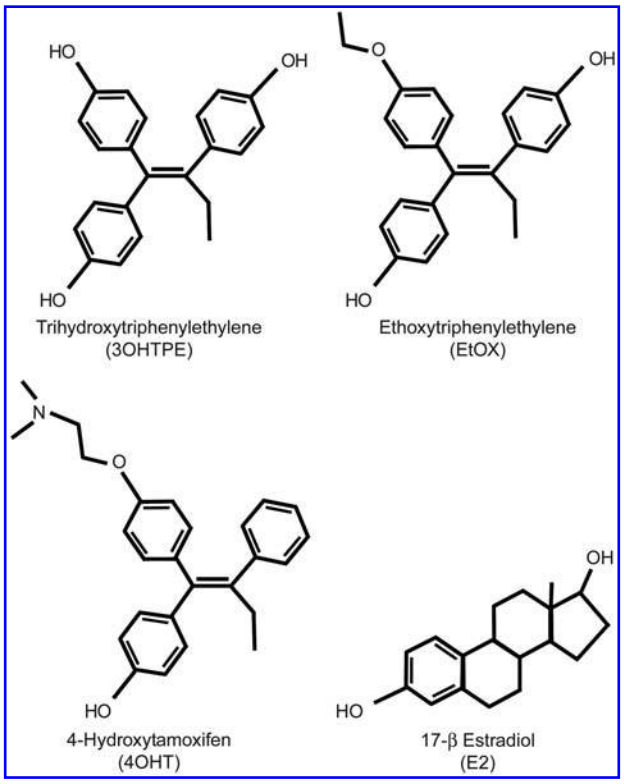


Figure 1 Structure of the compounds used in the study. Trihydoxytriphenylethylene (3OHTPE), ethoxytriphenylethylene (EtOX), 4-hydroxytamoxifen (4OHT) and 17-β estradiol (E2).

Estrogen receptor α levels are not decreased by 4OHT, 3OHTPE and EtOX

Treatment with estrogen in MCF7 cells causes a rapid destruction of ERα protein levels, whereas 4OHT impedes the destruction of ERα levels (23). Interestingly, despite acting as an estrogen agonist in MCF7 cells (15), the triphenylethylenes, 3OHTPE and EtOX, did not reduce the protein levels of ERα after 24 h of treatment at 10^{-6} M concentration, as evident by Western blot analysis of ERα protein levels which is similar to 4OHT treatment (Figure 3). As expected, ERα protein levels were drastically reduced after treatment with E2 (1 nM) for 24 h in MCF7 cells (Figure 3).

Induction of apoptosis by E2, 4OHT, 3OHTPE and EtOX

We further evaluated the apoptotic induction by 4OHT, 3OHTPE and EtOX and compared it with E2 in MCF7:5C cells using a dye-based kit which can measure the cells undergoing apoptosis as detailed in the Materials and methods section. We found that E2 (1 nM) produced a drastic increase in apoptotic cells after 5 days of treatment, whereas 4OHT (10^{-6} M) was completely ineffective (Figure 4). 3OHTPE (10^{-6} M) induced a modest level of apoptosis and a very slight apoptotic induction was observed after EtOX (10^{-6} M) treatment for 5 days (Figure 4).

Recruitment of ERα and SRC3/AIB1 at the promoter of PS2 (TFF1) gene by E2, 4OHT, 3OHTPE and EtOX

PS2 (TFF1) transcription is induced by E2 through a classical estrogen responsive element (ERE) at the promoter of the gene and its mechanism has been extensively studied (24, 25). We therefore evaluated the binding of the ERα and SRC3/AIB1 to the PS2 promoter after 45 min of treatment with 4OHT (10^{-6} M), 3OHTPE (10^{-6} M) or EtOX (10^{-6} M) in comparison with E2 (1 nM) in the MCF7:5C cells. Around a 17-fold increase in ERα recruitment was recorded with E2 treatment compared with vehicle treatment at the PS2 promoter (Figure 5A). In comparison, approximately 15-fold and approximately 11-fold increases in ERα recruitment was

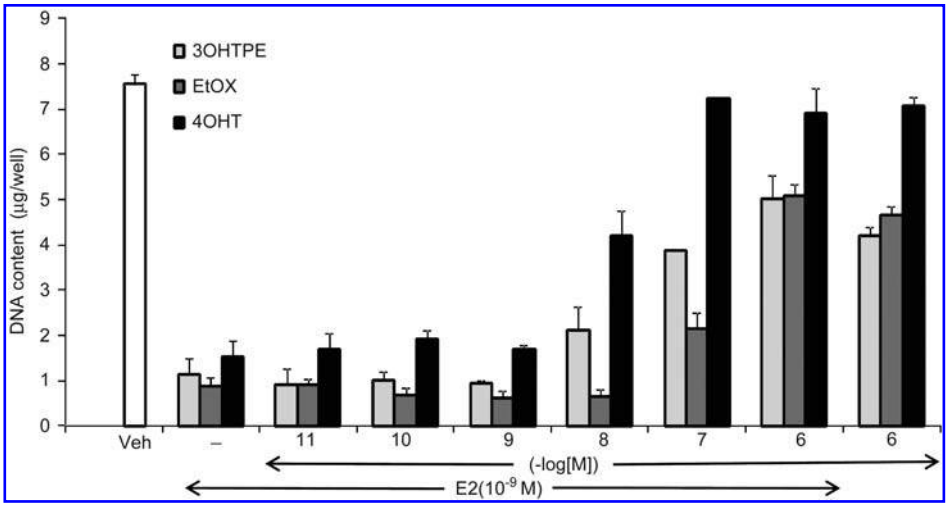


Figure 2 Reversal of E2-induced apoptosis of MCF7:5C cells by 4OHT, 3OHTPE and EtOX. MCF7:5C cells were treated with either vehicle (Veh), E2 (10^{-9} M) alone or E2 in combination with increasing concentration of the indicated compounds. Cells were also treated with compounds alone at 10^{-6} M concentration. After 7 days of treatment, the total DNA in the wells were estimated as a measure of cell survival.

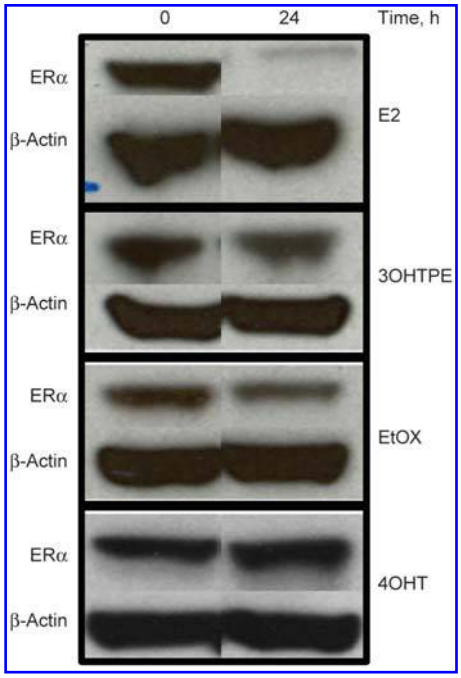


Figure 3 Levels of ERα protein after treatment with E2, 3OHTPE, EtOX or 4OHT. MCF7 cells were treated with E2 (10^{-9} M), 3OHTPE (10^{-6} M), EtOX (10^{-6} M) or 4OHT (10^{-6} M) for 24 h and total protein was isolated to estimate the ERα levels by Western blotting. Levels of β-actin were measured to ensure equal loading.

observed after treatment with 3OHTPE and EtOX, respectively, whereas only an approximately 5-fold increase in ERα recruitment was observed with 4OHT treatment (Figure 5A). Interestingly, in the case of SRC3/AIB1, very low levels of recruitment were observed after treatment with 3OHTPE and EtOX compared with E2 treatment (Figure 5B), whereas

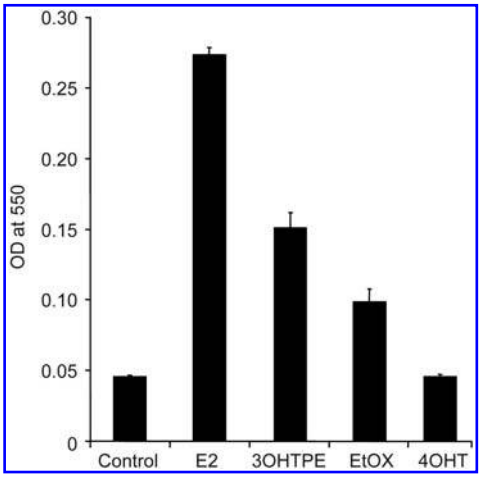


Figure 4 Induction of apoptosis by E2, 3OHTPE, EtOX or 4OHT. MCF7:5C cells were treated with E2 (10^{-9} M), 3OHTPE (10^{-6} M), EtOX (10^{-6} M) or 4OHT (10^{-6} M) and the induction of apoptosis was measured using a dye-based kit as detailed in Materials and methods section.

SRC3/AIB1 was not recruited at all after treatment with 4OHT (Figure 5B).

Binding of EtOX to the LBD of ERα

In an attempt to clarify the binding mode of EtOX to ERα, the flexible docking of this compound into the LBD of the receptor co-crystallized with 4OHT (Figure 6B) was performed, and also the best ranked ligand-receptor complex was superimposed onto the agonist conformation of ERα (Figure 6B). The results show that when EtOX is fitted in the binding site of the agonist conformation of ERα (1gwr), the ethoxy side chain of the ligand is bumping the side chains of L525 and L540 (Figure 6C) and it is unlikely for the ligand to bind in this conformation of the receptor. In contrast, when EtOX is docked into the binding site of ERα antagonist conformation (Figure 6D), the top ranked pose is fitted well in the binding cavity and it probably binds to an antagonist-related conformation of the receptor.

Discussion

Estrogen-induced apoptosis can be reversed in a concentration-related manner by the non-steroidal antiestrogen 4OHT. It is important to point out that in the ER+ MCF-7:5C cells

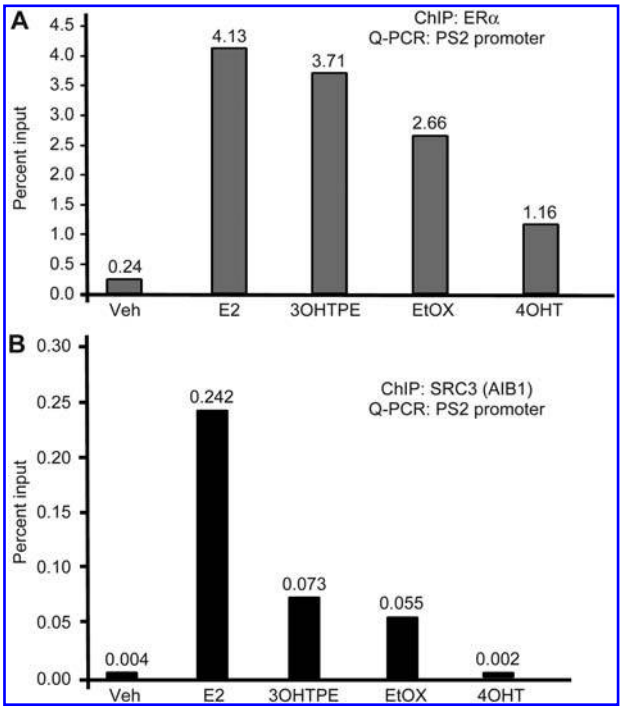


Figure 5 Recruitment of ERα (A) or SRC3 (AIB1) (B) at the promoter of PS2 (TFF1) gene. MCF7:5C cells were treated with E2 (10^{-9} M), 3OHTPE (10^{-6} M), EtOX (10^{-6} M) or 4OHT (10^{-6} M) for 45 min and cells were fixed with 1.25% formaldehyde before isolating the chromatin. ChIP was performed using ERα or SRC3 antibody and the immunoprecipitated DNA was quantified using specific primers for PS2 promoter by quantitative real time PCR. The values at the top of each bar represent the percent input after subtracting the negative control (rabbit IgG).

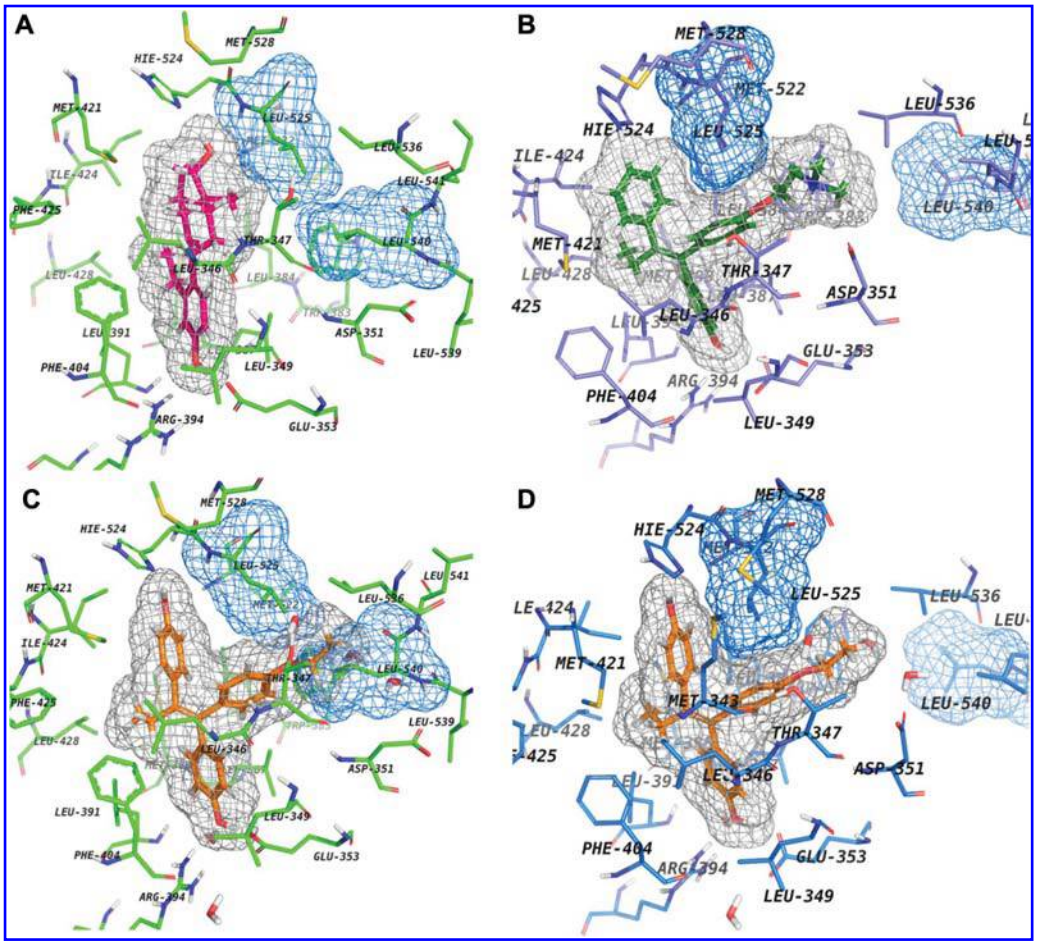


Figure 6 ERα binding site presented with different ligands. All ligands are shown with their corresponding molecular surfaces depicted as gray grids. Also, Leu525 and Leu540 are shown with their molecular surface depicted as blue grids. (A) The agonist conformation of ERα co-crystallized with E2 (colored in magenta) (PDB code: 1GWR); (B) 4OHT (depicted in green) co-crystallized with ERα – the antagonist conformation of the receptor (PDB code: 3ERT); (C) EtOX (colored in orange) is superimposed in the agonist conformation of the receptor (PDB code: 1GWR) and (D) same ligand is docked in the antagonist conformation of ERα (3ERT).

used in this study, 4OHT, although it binds to the ER, blocking apoptosis, does not produce any effect on cell growth when administered alone. These cells are completely resistant to the actions of nonsteroidal antiestrogens. The major finding in this study is that the test TPEs that are all fully estrogenic on cell replication in MCF-7 cells (15) also inhibit estrogen-induced apoptosis. Based on our previous study on the molecular classifications of estrogens (13), this leads to the suggestion that the angular TPEs are creating a shaped ER complex that is analogous to that observed in X-ray crystallography with 4OHT (26). Indeed, molecular modeling (Figure 6) demonstrates that the angular TPE would be unlikely to fit in the estradiol ER complex because steric hindrance would prevent helix 12 from sealing the LBD.

It seems that the TPEs can affect the ER complex in ways similar to 4OHT. 4OHT is known to impede the destruction of the 4OHT ER complex (23, 27). Similarly, the TPEs do not facilitate the rapid destruction of the TPE ER complex (Figure 3). Thus, Western blot analysis shows that the TPE ER levels are analogous to 4OHT ER levels rather than estradiol ER-like, i.e., rapidly destroyed. Indeed, the LeClercq group (28) have recently confirmed and extended our molecular classifications of estrogens, with a larger series of compounds and have also shown that an angular TPE does not cause the destruction of the ER complex in a manner analogous to estradiol when MCF-7 cells are examined by immunohistochemistry for the ER.

In a preliminary study, we have examined, using the ChIP assay, the binding of the ERα in the promoter region of the TFF1 (PS2) gene. The E2-ER complex has robust binding in the promoter region (Figure 5A) and SRC-3 is detected presumably bound to the ER complex (Figure 5B). In contrast, 4OHT ER complexes only have modest binding of ERα and virtually no SRC-3 in the promoter region. The TPEs permit some binding of the TPE ER complex in the promoter region but there are lower levels of SRC-3 and a reduced ability to stimulate PS2 synthesis (data not shown). A major conclusion of LeClerq's paper (28) is that the putative Class II estrogens (angular estrogens) that do not permit the appropriate sealing of the LBD with helix 12 do not efficiently bind co-activators. Our respective studies are therefore in agreement.

In summary, the proposed hypothesis is that the TPE-ER complex significantly changes the shape of the ER to adopt a conformation that mimics that adopted by 4OHT when it binds to the ER. A co-activator now has difficulty in binding to the TPE-ER complex appropriately, but whereas this does affect cell replication, it dramatically impairs the events that must be triggered to cause apoptosis. Future studies will confirm or refute our hypothesis based on the known intrinsic activity of mutant ERs and their capacity to investigate estrogen-target genes. Naturally, the absolute proof of our hypothesis would be the solution of the X-ray crystallography of a TPE-ER complex.

Acknowledgements

This research was supported by the Department of Defense Breast Program under award number BC050277 Center of Excellence; the SU2C [American Association for Cancer Research (AACR)] grant; the Susan G. Komen fund and the Cancer Center Support Grant (CCSG) Core Grant NIH P30 CA051008. Part of this research was supported (R.F.C.) by Consiliul National al Cercetarii Stiintifice din Invatamantul Superior-Unitatea Executiva pentru Finantarea Invatamantului Superior si a Cercetarii Stiintifice Universitare (CNCSIS-UEFISCU) (Romania), project code PN-II-PCE-ID no. 1268 agreement 248/2007. The views and opinions of the author(s) do not reflect those of the US Army or the Department of Defense.

References

1. Haddow A, Watkinson JM, Paterson E. Influence of synthetic oestrogens upon advanced malignant disease. Br Med J 1944; 2:393–8.
2. Haddow A. David A. Karnofsky memorial lecture. Thoughts on chemical therapy. Cancer 1970;26:737–54.
3. Gottardis MM, Jordan VC. Development of tamoxifen-stimulated growth of MCF-7 tumors in athymic mice after long-term antiestrogen administration. Cancer Res 1988;48:5183–7.
4. Balaburski GM, Dardes RC, Johnson M, Haddad B, Zhu F, Ross EA, Sengupta S, Klein-Szanto A, Liu H, Lee ES, Kim H, Jordan VC. Raloxifene-stimulated experimental breast cancer with the paradoxical actions of estrogen to promote or prevent tumor growth: a unifying concept in anti-hormone resistance. Int J Oncol 2010;37:387–98.
5. Early Breast Cancer Trialists' Collaborative Group (EBCTCG). Effects of chemotherapy and hormonal therapy for early breast cancer on recurrence and 15-year survival: an overview of the randomised trials. Lancet 2005;365:1687–717.
6. Yao K, Lee ES, Bentrem DJ, England G, Schafer JI, O'Regan RM, Jordan VC. Antitumor action of physiological estradiol on tamoxifen-stimulated breast tumors grown in athymic mice. Clin Cancer Res 2000;6:2028–36.
7. Wolf DM, Jordan VC. A laboratory model to explain the survival advantage observed in patients taking adjuvant tamoxifen therapy. Recent Results Cancer Res 1993;127:23–33.
8. Howell A, Cuzick J, Baum M, Buzdar A, Dowsett M, Forbes JF, Hoctin-Boes G, Houghton J, Locker GY, Tobias JS. Results of the ATAC (Arimidex, Tamoxifen, Alone or in Combination) trial after completion of 5 years' adjuvant treatment for breast cancer. Lancet 2005;365:60–2.
9. Thurlimann B, Keshaviah A, Coates AS, Mouridsen H, Mauriac L, Forbes JF, Paridaens R, Castiglione-Gertsch M, Gelber RD, Rabaglio M, Smith I, Wardley A, Price KN, Goldhirsch A. A comparison of letrozole and tamoxifen in postmenopausal women with early breast cancer. N Engl J Med 2005;353: 2747–57.
10. Song RX, Mor G, Naftolin F, McPherson RA, Song J, Zhang Z, Yue W, Wang J, Santen RJ. Effect of long-term estrogen deprivation on apoptotic responses of breast cancer cells to 17beta-estradiol. J Natl Cancer Inst 2001;93:1714–23.
11. Lewis JS, Meeke K, Osipo C, Ross EA, Kidawi N, Li T, Bell E, Chandel NS, Jordan VC. Intrinsic mechanism of estradiol-induced apoptosis in breast cancer cells resistant to estrogen deprivation. J Natl Cancer Inst 2005;97:1746–59.
12. Maximov PY, Lewis-Wambi JS, Jordan VC. The paradox of oestradiol-induced breast cancer cell growth and apoptosis. Curr Signal Transduct Ther 2009;4:88–102.
13. Jordan VC, MacGregor Schafer JI, Levenson AS, Liu H, Pease KM, Simons LA, Zapf JW. Molecular classification of estrogens. Cancer Res 2001;61:6619–23.
14. Bentrem D, Fox JE, Pearce ST, Liu H, Pappas S, Kupfer D, Zapf JW, Jordan VC. Distinct molecular conformations of the estrogen receptor alpha complex exploited by environmental estrogens. Cancer Res 2003;63:7490–6.
15. Maximov PY, Myers CB, Curpan RF, Lewis-Wambi JS, Jordan VC. Structure-function relationships of estrogenic triphenylethylenes related to endoxifen and 4-hydroxytamoxifen. J Med Chem 2010;53:3273–83.
16. Jordan VC, Collins MM, Rowsby L, Prestwich G. A monohydroxylated metabolite of tamoxifen with potent antioestrogenic activity. J Endocrinol 1977;75:305–16.
17. MacGregor Schafer J, Liu H, Bentrem DJ, Zapf JW, Jordan VC. Allosteric silencing of activating function 1 in the 4-hydroxytamoxifen estrogen receptor complex is induced by substituting glycine for aspartate at amino acid 351. Cancer Res 2000;60: 5097–105.
18. Liu H, Lee ES, De Los Reyes A, Zapf JW, Jordan VC. Silencing and reactivation of the selective estrogen receptor modulator-estrogen receptor alpha complex. Cancer Res 2001;61: 3632–9.
19. Lewis JS, Osipo C, Meeke K, Jordan VC. Estrogen-induced apoptosis in a breast cancer model resistant to long-term estrogen withdrawal. J Steroid Biochem Mol Biol 2005;94:131–41.
20. Jiang SY, Wolf DM, Yingling JM, Chang C, Jordan VC. An estrogen receptor positive MCF-7 clone that is resistant to antiestrogens and estradiol. Mol Cell Endocrinol 1992;90:77–86.
21. Sengupta S, Sharma CGN, Jordan VC. Estrogen regulation of X-box binding protein-1 and its role in estrogen induced growth of breast and endometrial cancer cells. Horm Mol Biol Clin Invest 2010;2:235–43.
22. Berman HM, Westbrook J, Feng Z, Gilliland G, Bhat TN, Weissig H, Shindyalov IN, Bourne PE. The protein data bank. Nucleic Acids Res 2000;28:235–42.
23. Wijayaratne AL, McDonnell DP. The human estrogen receptor-alpha is a ubiquitinated protein whose stability is affected differentially by agonists, antagonists, and selective estrogen receptor modulators. J Biol Chem 2001;276:35684–92.
24. Metivier R, Penot G, Hubner MR, Reid G, Brand H, Kos M, Gannon F. Estrogen receptor-alpha directs ordered, cyclical, and combinatorial recruitment of cofactors on a natural target promoter. Cell 2003;115:751–63.
25. Carroll JS, Liu XS, Brodsky AS, Li W, Meyer CA, Szary AJ, Eeckhoute J, Shao W, Hestermann EV, Geistlinger TR, Fox EA, Silver PA, Brown M. Chromosome-wide mapping of estrogen receptor binding reveals long-range regulation requiring the forkhead protein FoxA1. Cell 2005;122:33–43.

26. Shiau AK, Barstad D, Loria PM, Cheng L, Kushner PJ, Agard DA, Greene GL. The structural basis of estrogen receptor/coactivator recognition and the antagonism of this interaction by tamoxifen. Cell 1998;95:927–37.
27. Pink JJ, Jordan VC. Models of estrogen receptor regulation by estrogens and antiestrogens in breast cancer cell lines. Cancer Res 1996;56:2321–30.
28. Bourgoin-Voillard S, Gallo D, Laios I, Cleeren A, Bali LE, Jacquot Y, Nonclercq D, Laurent G, Tabet JC, Leclercq G. Capacity of type I and II ligands to confer to estrogen receptor alpha an appropriate conformation for the recruitment of coactivators containing a LxxLL motif – relationship with the regulation of receptor level and ERE-dependent transcription in MCF-7 cells. Biochem Pharmacol 2010;79:746–57.

Expert Opinion

1. Introduction
2. Raloxifene
3. Conclusion
4. Expert opinion

Treatment of osteoporosis and reduction in risk of invasive breast cancer in postmenopausal women with raloxifene

Seung Sang Ko & V Craig Jordan†
Lombardi Comprehensive Cancer Center, Georgetown University Medical Center, Washington, DC, USA

Introduction: Raloxifene, a non-steroidal selective estrogen receptor modulator (SERM), offers a new dimension for the treatment and prevention of osteoporosis and risk reduction of invasive breast cancer in postmenopausal populations at high risk. Both osteoporosis and breast cancer are important public health issues for postmenopausal women. It is well known that estrogen and estrogen receptors play an important role in the pathogenesis of both diseases. Initially, hormone replacement therapy (HRT) was used for the purpose of preventing and treating postmenopausal osteoporosis. However, HRT significantly contributed to an increase in breast cancer risk. The SERM, raloxifene, is used for the prevention and for the treatment of postmenopausal osteoporosis and reducing the risk of invasive breast cancer in postmenopausal women.

Areas covered: This article reviews the emerging evidence of the efficacy of raloxifene in postmenopausal women, summarizes the results and places in perspective their therapeutic uses for women having either a high risk of osteoporosis or breast cancer. Emerging clinical evidence suggests bisphosphonates, currently used as drugs for the treatment of osteoporosis, may also reduce breast cancer risk. The status of other SERMs and bisphosphonates are included for completeness. A Medline search of raloxifene, osteoporosis, breast cancer and SERMs was used to derive a database of 355 references.

Expert opinion: Readers will understand the value of raloxifene to prevent osteoporosis and breast cancer in postmenopausal women. Although most women do not require pharmacotherapy for menopausal symptoms, many are severely affected by osteoporosis or breast cancer at and beyond menopause and, for such women, pharmacologic intervention is important if they are to retain an acceptable quality of life. It is reasonable to use raloxifene or bisphosphonate as an appropriate drug that targets symptom-free postmenopausal women for treatment and prevention of osteoporosis but raloxifene is proven to reduce the incidence of invasive breast cancer.

Keywords: bisphosphonate, breast cancer, lasofoxifene, osteoporosis, raloxifene, selective estrogen receptor modulator

Expert Opin. Pharmacother. (2011) 12(4):657-674

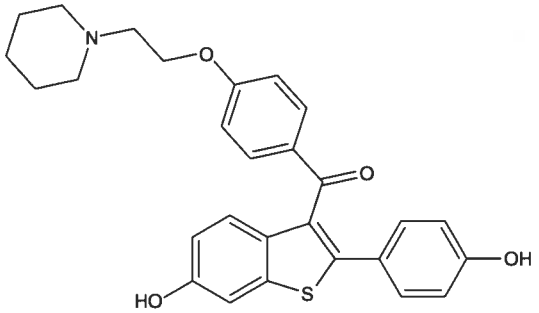
1. Introduction

Menopause is a biological process that occurs as part of aging in women, and the key factor of the menopause is estrogen deficiency. Estrogen and its receptors mediate the modulation of bone density. Estrogen deficiency is the main cause of postmenopausal osteoporosis [1] and its occurrence after menopause leads to an

informa
healthcare

10.1517/14656566.2011.557360 © 2011 Informa UK, Ltd. ISSN 1465-6566
All rights reserved: reproduction in whole or in part not permitted

Box 1. Drug summary.

Drug name	Raloxifene hydrochloride
Phase	Approved by the FDA
Indication	Treating and preventing osteoporosis in postmenopausal women Reducing the risk of invasive breast cancer in postmenopausal women at increased risk of breast cancer
Pharmacology description	Selective estrogen receptor modulator
Route of administration	Parenteral
Chemical structure	
Pivotal trial(s)	MORE: Multiple Outcomes of Raloxifene Evaluation [18-20] CORE: Continuing Outcomes Relevant to Evista [21,22] RUTH: Raloxifene Use for the Heart [23] STAR: Study of Tamoxifen and Raloxifene [9,24,25]

Pharmaprojects – Copyright to Citeline Drug Intelligence (an Informa business). Readers are referred to Informa-Pipeline (http://informa-pipeline.citeline.com) and Citeline (http://informa.citeline.com).

increase in bone remodeling, resulting in an imbalance between bone resorption and formation. This is reflected in a decrease in bone mineral density (BMD) and an increase in fracture risk. Osteoporotic fractures lead to morbidity and mortality. The incidence of osteoporosis and the associated economic burden will rise as the population ages. In the US, an estimated 52.4 million people aged 50 and over have low bone mass or osteoporosis [2]. Accordingly, the number of women of this age group with osteoporosis is estimated at 9.1 million; those with low bone mass at 26 million. By 2020, these numbers are predicted to increase to 10.5 and 30.4 million, respectively [2]. As there is a close relationship between estrogen deficiency and osteoporosis, the use of hormonal replacement therapy (HRT) with estrogen alone (estrogen replacement therapy; ERT) or a combination with a progestin after menopause has been well accepted for decades. However, the prolonged use of HRT is associated with a significant increased risk of breast cancer [3,4]. The weight of evidence indicates that exposure to estrogen is an important determinant of the risk of breast cancer [5]. Therefore, HRT may not be a good choice in the management of postmenopausal women with osteoporosis. If agents could function like estrogen in terms of bone, but without estrogen's stimulation of the breast, they might be a better choice.

Recently, selective estrogen receptor modulators (SERMs) have represented a major therapeutic advance for clinical practice [6]. Unlike estrogens, which are uniformly agonists, and anti-estrogens, which are uniformly antagonists, the SERMs exert selective agonist or antagonist effects on various estrogen target tissues [6]. The unique properties of SERMs lie in their bulky side chain. This blocking effect in turn prevents key co-regulator proteins (co-activators) from interacting with the receptor, and thus prevents activation [7,8]. The mechanisms of the tissue-selective, mixed agonist–antagonist action of SERMs, although still only partly understood, are gradually becoming clearer [8]. Most of the unique pharmacology of SERMs can be explained by three interactive mechanisms: differential ER subtype (ERα and ERβ) expression in a given target tissue, differential ER conformation on ligand binding, and differential expression and binding to the ER of co-regulator proteins [8].

2. Raloxifene

2.1 Overview of the market of raloxifene

Raloxifene (**Box 1**) is a non-steroidal SERM which has been marketed for use in prevention and treatment of postmenopausal osteoporosis for a decade in the US, the EU and elsewhere. One of the consequences of the evaluation of ERT and HRT through the Women's Health Initiative (WHI) has been increased interest in the SERMs because of the potential to retain most of the beneficial effects of estrogen while avoiding some of the adverse effects [7]. Raloxifene binds to estrogen receptors (ERs), with estrogen agonistic effects in some tissues and estrogen antagonistic effects in others. In the last few years, pivotal clinical studies have been published on

the effects of raloxifene on osteoporosis, the risk of invasive breast cancer and cardiovascular diseases. There are a number of other SERMS currently under investigation but raloxifene is the only SERM currently on the market for the treatment and prevention osteoporotic fractures and reduction in risk of invasive breast cancer (raloxifene is approved for breast cancer risk reduction in the US but not the EU) [9,10]. A review of the effects of raloxifene in some target tissues, results of clinical trials, along with a discussion of the usefulness of raloxifene in the prevention of osteoporosis and reduction of breast cancer risk in postmenopausal women are given below.

2.2 Introduction of compound

SERMs are compounds that were first believed to be predominantly estrogen antagonists but are now known to possess tissue-selective estrogen agonist or antagonist properties depending on their interaction with the ER and post-translational effects [11]. A number of SERMs are available for clinical use for infertility management (clomiphene), risk reduction in breast cancer (tamoxifen), breast cancer treatment (tamoxifen, toremifene) and the prevention and treatment of osteoporosis (raloxifene). Preclinical trials with raloxifene (originally named keoxifene), a non-steroidal benzothiophene, revealed many of the desirable properties of a SERM such as inhibition of bone loss and lowering cholesterol without stimulating breast or uterine tissue development. Raloxifene is currently approved for the prevention and treatment of postmenopausal osteoporosis and the reduction in risk of invasive breast cancer in postmenopausal women with osteoporosis and postmenopausal women at high risk for invasive breast cancer.

2.3 Chemistry of raloxifene

Raloxifene hydrochloride (**Box 1**) belongs to the benzothiophenes. It is designated methanone-[6-hydroxy-2-(4-hydroxyphenyl)benzo[b]thien-3-yl]-[4-[2-(1-piperidinyl)ethoxy]phenyl]-hydrochloride. The molecular mass is 510.05 kDa and molecular formula is $C_{28}H_{27}NO_4S{\cdot}HCl$.

Inactive ingredients in raloxifene tablets include anhydrous lactose, carnauba wax, crospovidone, FD & C Blue No. 2, aluminium lake, hydroxypropyl methylcellulose, lactose monohydrate, magnesium stearate, modified pharmaceutical glaze, polyethylene glycol, polysorbate 80, povidone, propylene glycol and titanium dioxide. The tablet (60 mg) is marketed as Evista® (Lilly, Indianapolis, IN, USA).

2.4 Pharmacodynamics of raloxifene

The ER was discovered in the 1960s and at that time it was felt that a single pathway was responsible for the mediation of the biological effects of estrogen [12]. The classical pathway of steroid hormone action was thought to involve high-affinity binding of the estrogen ligand to its receptor, movement of the ligand–receptor complex to the nucleus and subsequent transcriptional activation of nuclear genomic elements. Although the precise mechanism of action of estrogen and SERMs is still unknown, the pathways of estrogen action are clearly much more complex [13]. There appear to be multiple potential interactions for estrogen and its receptors (membrane-bound and nuclear) in the activation of genomic and non-genomic pathways, the subtype of the ER involved in nuclear transcription and multiple co-regulatory factors involved in nuclear responses.

There is evidence that some of the rapid actions of estrogen (e.g., vasodilatation) may be mediated by way of a cell membrane-bound ER and involve non-genomic interactions, such as activation of MAPK signal transduction pathways [14].

The nuclear action of estrogen is mediated through at least two different ERs, ERα and ERβ, which have different relative distributions in different target tissues but with considerable overlap [15]. For example, both subtypes are found in the bone, uterus, breast, prostate and brain. Both ERs have a ligand binding and a DNA-binding domain. After ligand–receptor binding, this ER complex dissociates from its heat-shock proteins and dimerizes with co-activator or corepressor molecules before initiating transcription at DNA promoter sites containing the estrogen response element.

Estrogen binding to its receptor causes a helical region (helix 12) of the receptor to move across the binding site. When raloxifene binds to the ER, helix 12 shifts rightward to block the activation factor-2 site [16]. The anti-estrogenic side chain of raloxifene also interacts with a critical surface amino acid (D351) of the ER to neutralize or shield its charge [11].

It is interesting to note that raloxifene stimulates the production of osteoprotegerin (OPG) from osteoblasts, carrying out their anti-resorption activity, at least in part, as a means of the OPG/receptor activator of NF-κB ligand system. In a prospective, randomized, placebo-controlled study, serum OPG levels in the raloxifene treatment group are statistically significant increased ($p < 0.001$) versus baseline ($p = 0.007$) versus placebo [17].

There is still incomplete knowledge of SERM interaction with ER binding and SERM interaction with all of the potential co-activators or corepressors that are involved in modulating estrogen and SERM gene transcription.

2.5 Pharmacokinetics and metabolism of raloxifene

The approved dose of raloxifene for osteoporosis prevention and treatment is 60 mg/day, without regard to meals. Approximately 60% is rapidly absorbed after oral administration but absolute bioavailability is only 2%. Raloxifene is mostly excreted in the feces and primarily metabolized through hepatic glucuronidation and the half-life is ~ 28 h. The absence of non-glucuronidated metabolites suggests that the CYP pathways do not metabolize raloxifene.

2.6 Clinical efficacy of raloxifene

Many different types of SERMs have undergone large clinical trials. Among them, raloxifene may be the most attractive agent because at least three large trials (**Tables 1 – 3**), including the Multiple Outcomes of Raloxifene Evaluation (MORE) [18-20],

Table 1. Summary of basic characteristics of raloxifene related studies (based on ASCO guideline) [10].

	MORE	CORE	RUTH	STAR
No. of patients randomized	5129 (RAL) 2576 (PLA)	2725 (RAL) 1286 (PLA)	5044 (RAL) 5057 (PLA)	9872 (TAM) 9875 (RAL)
Age, years	≤ 80	≤ 80	≥ 35	≥ 35
Entry dates	1994 - 1999	1999 - 2000	1998 - 2000	1999 - 2004
Follow-up, years	4 (median, 3.4)	4 + time in MORE trial (median, 7.9)	7 (median, 5.6)	6 (median, 4.6)
Primary outcome	Vertebral fractures (incidence of BC secondary)	Incidence of invasive BC	Incidence of invasive BC and coronary events	Incidence of invasive BC
Risk assessment	≤ 80 years	≤ 80 years	≥ 55 years	≥ 35 years with increased risk of BC (≥ 1.66 modified Gail model)
	Postmenopausal Osteoporosis	Postmenopausal Osteoporosis	Postmenopausal CHD or increased risk of CHD	Postmenopausal LCIS
LCIS	Not specified	Not specified	Not specified	Included
Atypical hyperplasia	Not specified	Not specified	Not specified	Included
HT	Excluded (no concurrent HT or if on HT for more than one cycle within 6 months before trial, with the exception of occasional use of oral or topical estrogen for menopausal symptoms)		Excluded (no concurrent HT or use of oral or transdermal estrogen within 6 months before randomization)	Excluded (no concurrent HT or use of oral contraceptives or androgens within before randomization)
Deep vein thrombosis or pulmonary embolism	Excluded	Excluded	Excluded	Excluded
Previous cancer	Excluded (if estrogen-dependent malignancy or any type of cancer within 5 years before randomization, except if superficial skin cancer)		Excluded	Excluded (except if > 5 years, or if basal or squamous cell skin cancer, or *CIS* of cervix)

According to the National Cancer Institute Breast Cancer Risk Assessment Tool.

ASCO: American Society of Clinical Oncology; BC: Breast cancer; CHD: Chronic heart disease; CIS: Carcinoma *in situ*; CORE: Continuing Outcomes Relevant to Evista; HT: Hormonal therapy; LCIS: Lobular carcinoma *in situ*; MORE: Multiple Outcomes of Raloxifene Evaluation; PLA: Placebo; RAL: Raloxifene; RR: Relative risk; RUTH: Raloxifene Use for the Heart; STAR: National Surgical Adjuvant Breast and Bowel Project Study of Tamoxifen and Raloxifene P2; TAM: Tamoxifen.

Continuing Outcomes Relevant to Evista (CORE) [21,22] and Raloxifene Use for the Heart (RUTH) [23], have shown practical and promising results when using raloxifene for the prevention and management of postmenopausal women with osteoporosis or osteopenia. (The RUTH trial included women with cardiovascular disease or at high risk for cardiovascular disease.) In these trials, raloxifene not only decreased the incidence of osteoporosis-associated complications, such as vertebral fractures and possible non-vertebral fractures, but also offered benefits for reduction in risk of breast cancer, with a dramatic decrease in the incidence of ER-positive invasive breast cancers. In addition, two other trials have demonstrated raloxifene to be a potential candidate and choice for postmenopausal women: the Study of Tamoxifen and Raloxifene (STAR, **Tables 1** and 4) [9,24,25] and Evista Versus Alendronate (EVA) [26]. The STAR trial further confirmed the efficacy of raloxifene in reduction in risk of invasive breast cancer and showed it has similar efficacy to the well-known anti-breast cancer drug tamoxifen. The EVA trial was in fact stopped early due to insufficient recruitment within the planned timeline, resulting in insufficient power to show non-inferiority between therapies. Thus, only a safety profile was addressed by the study. Nevertheless, these clinical studies do highlight the opportunities for innovation in the selective modulation of estrogen target tissues, especially with raloxifene for the prevention and treatment of estrogen deficiency related osteoporosis and reducing the incidence of estrogen stimulated ER-positive invasive breast cancers.

Because raloxifene has shown the above benefits, the aims of this article will be to offer data to support the rationale for using raloxifene in postmenopausal women, especially in a given population. We review the emerging evidence of the efficacy of raloxifene in relation to both major health problems – osteoporosis and breast cancer – in postmenopausal women, summarize the results, and place in perspective their therapeutic uses for women having either a high risk of osteoporosis or a high risk of breast cancer.

Three large prospective clinical trials have studied the value, benefits and risks of raloxifene in the management of postmenopausal women (**Tables 1 - 3**).

Table 2. Summary of adverse events or side effects of raloxifene use in raloxifene/placebo trials (based on ASCO guideline) [10].

	CORE (subset of MORE)				MORE				RUTH			
Result	**Statistic**	**95% CI**	**AR/1000***	**NNH***	**Statistic**	**95% CI**	**AR/1000***	**NNH***	**Statistic**	**95% CI**	**AR/1000***	**NNH***
Trial details												
Sample size included in analyses												
Raloxifene	2725				5129				5044			
Placebo	1286				2576				5057			
Median follow-up period, months												
Initial	48 (treatment) [21]				–				–			
Entire period	96 (MORE and CORE) [21]				40 [19,77]				67.2 [23]			
Adverse event/side effect												
Death (any cause)												
Initial	p = 0.027	NR										
Entire period	NR				HR = 0.61	0.36 – 1.03			HR = 0.92	0.82 – 1.03		
Thromboembolic events (overall)												
Initial	RR = 2.17	0.83 – 5.70										
Entire period	p = 0.094	NR			NR				HR = 1.44	1.06 – 1.95	7	150
Deep vein thrombosis												
Initial	p = 0.49	NR										
Entire period	p = 0.32	NR			p = 0.002	NR	NR	NR	HR = 1.37	0.94 – 1.99		
Pulmonary embolism												
Initial	p = 0.07	NR										
Entire period	p = 0.05	NR	NR	NR	HR = 3.97‡	0.91 – 17.3			HR = 1.49	0.89 – 2.49		
Cerebrovascular (overall)												
Initial	NR											
Entire period	NR				HR = 0.93‡	0.64 – 1.36			NR			
Stroke												
Initial	NR											
Entire period	NR				HR = 0.68‡	0.43 – 1.07			HR = 1.10	0.92 – 1.32		

*Computed by guideline authors using incidence data from published results. AR/1000 and NNH are shown only for statistically significant events.

‡Published data pooled doses of raloxifene (60 and 120 mg/day) for analyses.

§Vaginal bleeding; includes only women with intact uterus at baseline of MORE trial.

¶Includes benign gynecologic growths, hyperplasia, bleeding and 'other conditions'.

#Vertebral fractures; assessed at 36 months.

**Vertebral fractures; non-vertebral fractures HR = 0.96; 95% CI, 0.84 – 1.10.

AR/1000: Absolute risk difference/1000 women for specified median follow-up period (using published cumulative or annual incidence rates); ASCO: American Society of Clinical Oncology; CORE: Continuing Outcomes Relevant to Evista; HR: Hazard ratio; MORE: Multiple Outcomes of Raloxifene Evaluation; NNH: Number needed to harm (the number needed to treat to observe adverse event or side effect for specified median follow-up period); NR: Not reported in published literature; RR: Relative risk; RUTH: Raloxifene Use for the Heart.

Table 2. Summary of adverse events or side effects of raloxifene use in raloxifene/placebo trials (based on ASCO guideline) [10] (continued).

	CORE (subset of MORE)				MORE				RUTH			
Result	**Statistic**	**95% CI**	**AR/1000***	**NNH***	**Statistic**	**95% CI**	**AR/1000***	**NNH***	**Statistic**	**95% CI**	**AR/1000***	**NNH***
Transient ischemic attack												
Initial	NR											
Entire period	NR				NR				NR			
Headaches												
Initial	NR											
Entire period	NR				NR				NR			
Endometrial cancer												
Initial	p = 0.69	NR										
Entire period	p = 0.75	NR			HR = 0.69‡	0.22 – 2.18			p = 0.53	NR		
Gynecologic symptoms												
Initial	p > 0.99§	NR										
Entire period	p = 0.87§	NR			p = 0.99§	NR			p = 0.74¶	NR		
Vasomotor symptoms												
Initial	p = 0.61	NR										
Entire period	p < 0.001	NR	NR	NR	P < 0.001	NR			p < 0.001	NR	NR	NR
Breast complaints												
Initial	NR											
Entire period	NR				p = 0.94	NR						
Developing cataracts												
Initial	NR											
Entire period	NR				NR				p = 0.56	NR		
Fractures												
Initial	NR											
Entire period	p < 0.05#[18]	NR			RR = 0.66	0.55 – 0.81	NR	NR	HR = 0.65**	0.47 – 0.89	7	138

*Computed by guideline authors using incidence data from published results. AR/1000 and NNH are shown only for statistically significant events.

‡Published data pooled doses of raloxifene (60 and 120 mg/day) for analyses.

§Vaginal bleeding; includes only women with intact uterus at baseline of MORE trial.

¶Includes benign gynecologic growths, hyperplasia, bleeding and 'other conditions'.

#Vertebral fractures; assessed at 36 months.

**Vertebral fractures; non-vertebral fractures HR = 0.96; 95% CI, 0.84 – 1.10.

AR/1000: Absolute risk difference/1000 women for specified median follow-up period (using published cumulative or annual incidence rates); ASCO: American Society of Clinical Oncology; CORE: Continuing Outcomes Relevant to Evista; HR: Hazard ratio; MORE: Multiple Outcomes of Raloxifene Evaluation; NNH: Number needed to harm (the number needed to treat to observe adverse event or side effect for specified median follow-up period); NR: Not reported in published literature; RR: Relative risk; RUTH: Raloxifene Use for the Heart.

Table 3. Summary of breast cancer incidence in raloxifene vs placebo prevention trials (based on ASCO guideline) [10].

	CORE (Subset of MORE)				MORE*				RUTH			
Result	**Statistic**	**95% CI**	**AR/1000‡**	**NNH‡**	**Statistic**	**95% CI**	**AR/1000‡**	**NNH‡**	**Statistic**	**95% CI**	**AR/1000‡**	**NNH‡**
Trial details												
Sample size included in analyses												
Raloxifene												
Initial	3510				5129				–			
Entire period	5129				5111				5044			
Placebo												
Initial	1703				2576				–			
Entire period	2576				2571				5057			
Median follow-up period (months)												
Initial	48 (CORE trial only) [21]				40 [19]				–			
Entire period	96 (MORE and CORE combined) [21]				48 (includes only women with known hormonal treatment status)				67.2 [23]			
Breast cancer incidence												
Breast cancer (overall)												
Initial	HR = 0.50	0.30 – 0.82	11	89	RR = 0.35	0.21 – 0.58	9	107				
Entire period	HR = 0.42	0.29 – 0.60	NR	NR	RR = 0.38	0.24 – 0.58	NR	NR	HR = 0.67	0.47 – 0.96	5	200
Invasive breast cancer												
Initial	HR = 0.41	0.24 – 0.71	12	81	RR = 0.24	0.13 – 0.44	9	111				
Entire period	HR = 0.34	0.22 – 0.50	22	45	RR = 0.28	0.17 – 0.46	NR	NR	HR = 0.56	0.38 – 0.83	7	150
ER-positive												
Initial	HR§ = 0.34	0.18 – 0.66	10	96	RR = 0.10	0.04 – 0.24	NR	NR				
Entire period	HR = 0.24	0.15 – 0.40	19	52	RR = 0.16	0.09 – 0.30	NR	NR	HR = 0.45	0.28 – 0.72	7	150
ER-negative												
Initial	HR = 1.13	0.29 – 4.35			RR = 0.88	0.26 – 3						
Entire period	HR = 1.06	0.43 – 2.59			NR				HR = 1.44	0.61 – 3.36		
Non-invasive BC												
Initial	HR = 1.78	0.37 – 8.61			NR							
Entire period	HR = 1.12	0.46 – 2.73			NR				HR = 2.17	0.75 – 6.24		

*Published data pooled doses of raloxifene (60 and 120 mg/day) for analyses.

‡Computed by guideline authors using incidence data from published results. AR/1000 and NNT are shown only for statistically significant events.

§Among CORE enrollees, ER status was only determined on 73% of the breast cancers.

AR/1000: Absolute risk difference/1000 women for specified median follow-up period (using published cumulative or annual incidence rates); ASCO: American Society of Clinical Oncology; BC: Breast cancer; CORE: Continuing Outcomes Relevant to Evista; ER: Estrogen receptor; HR: Hazard ratio; MORE: Multiple Outcomes of Raloxifene Evaluation; NNT: Number needed to treat to prevent one additional outcome for specified median follow-up period; NR: Not reported in published literature; RR: Relative risk; RUTH: Raloxifene Use for the Heart.

Table 4. Summary of the updated STAR trial [9].

Outcome	Raloxifene		Tamoxifen		Relative risk	95% CI
	No.	Rate/1000*	No.	Rate/1000*		
Breast cancer incidence						
Invasive	310	5.02	247	4.04	1.24	1.05 – 1.47
Non-invasive	137	2.23	111	1.83	1.22	0.95 – 1.59
DCIS	86	1.40	70	1.51	1.22	0.88 – 1.69
LCIS	34	0.55	33	0.54	1.02	0.61 – 1.70
Adverse event/side effect						
Death (all causes)	202	3.22	236	3.81	0.84	0.70 – 1.02
Endometrial cancer	37	1.23	65	2.25	0.55	0.36 – 0.83
Thromboembolic event (all)	154	2.47	202	3.30	0.75	0.60 – 0.93
Deep vein thrombosis	86	1.38	118	1.93	0.72	0.54 – 0.95
Pulmonary embolism	68	1.09	84	1.36	0.80	0.57 – 1.11
Developing cataracts	603	11.69	739	13.58	0.80	0.72 – 0.89

Median follow-up period is 81 months; sample size is 9754 for raloxifene and 9736 for tamoxifen.
*Average annual rate/1000 women.
DCIS: Ductal carcinoma *in situ*; LCIS: Lobular carcinoma *in situ*; STAR: National Surgical Adjuvant Breast and Bowel Project Study of Tamoxifen and Raloxifene P2.

MORE. The MORE trial is a multi-center, randomized, double-blind trial in which women taking raloxifene at 60 or 120 mg/day (5129 women) or a placebo (2576 women) were evaluated [18-20]. A total of 7705 postmenopausal women (mainly in the US and Europe), younger than 81 years (mean age, 66.5) and with osteoporosis as defined by the presence of vertebral fractures or a femoral neck or spine T-score of at least 2.5 s.d. below the mean for young healthy women were studied. The MORE trial was initiated in 1994 to examine the effect of raloxifene on the skeleton (the risk of vertebral and non-vertebral fractures) [18] to determine whether treatment with raloxifene reduces the risk of breast cancer and assess the safety of treatment with raloxifene [19]. The initial results from the 3-year MORE trial showed very promising findings, including a 30% reduction of relative risk in any new vertebral fractures [18], and a 76% reduction of invasive breast cancer in the women with osteoporosis, compared with the placebo [19].

CORE. Only a subset of patients at US sites had BMD assessments during CORE. In addition, based on the significant 72% reduction of the incidence of invasive breast cancer in postmenopausal women with osteoporosis during the 4 years of treatment with raloxifene compared with the placebo in the MORE trial [27], the CORE trial (4011 women continuing from the MORE trial, with a mean age of 65.8) was designed to evaluate the efficacy of an additional 4 years of raloxifene therapy in reduction in risk of invasive breast cancer in women who participated in the MORE trial [21].

RUTH. Because of the significant beneficial effects on bone and reduction in risk of breast cancer, and the possible benefits for the cardiovascular system in postmenopausal women taking raloxifene, the RUTH trial (10,101 postmenopausal women, with a mean age of 67.5 years) was designed to assess the risks and benefits of treatment with raloxifene in women with, or at increased risk of, coronary heart disease, with the primary aim of determining the effects on coronary outcomes and invasive breast cancer [23,28].

STAR. The National Surgical Adjuvant Breast and Bowel Project (NSABP) protocol P-2, the Study of Tamoxifen and Raloxifene (STAR), directly compared tamoxifen with raloxifene in 19,747 healthy postmenopausal women at an increased risk for development of breast cancer. STAR was a two-arm, randomized, double-blinded trial of tamoxifen versus raloxifene for the reduction of breast cancer incidence; participants and their physicians were unaware of the treatment that was being administered until the trial was unblinded in April 2006 [24]. The update report is based on a cutoff date of 31 March 2009, providing a median follow-up of 81 months in patients who had stopped their study drug [9].

2.6.1 *Efficacy of raloxifene on osteoporosis*

2.6.1.1 *Preventing bone loss*

There are some results from clinical trials and observational studies which suggest that raloxifene is less potent on the skeleton than estrogen [29,30] (**Table 2**). Nevertheless, raloxifene was effective in preventing postmenopausal bone loss over a 3-year period in the MORE trial [18]. The BMD gains after 3 years were 2.1% in the spine and 2.6% in the femur. Concomitantly, significant decreases were noted for osteocalcin (-26.3 vs -8.6% in the placebo group) and urinary crosslinked N-telopeptides of type I collagen (-34 vs -8.1% in the placebo group). BMD gains after 4 years were 2.6% in the spine and 2.1% in the femur. BMD increases were significant during the third year, but not during the fourth year [20]. Of the 386 women who took no other drugs known to affect bone during the 8-year study, 259 continued on raloxifene during the CORE trial and experienced maintenance of their BMD

values in the spine and proximal femur [22]. After 7 years of treatment (4 years in the MORE trial and 3 years in the CORE trial), BMD was higher in the raloxifene group than in the placebo group by 2.2% in the spine and 3% in the total hip ($p < 0.01$) [22]. Raloxifene discontinuation after 5 years was followed by significant declines in BMD at the lumbar spine and femur (-2.4%) within the first year [31]. The discontinuation was actually between the 4-year MORE study and initiation of CORE study. The gap between the studies was on average about 1 year. However, with resumption of study drug in CORE, BMD differences between raloxifene and placebo were maintained.

Taken together, raloxifene was proved to be effective in decreasing bone turnover, with a resultant increase in BMD. Therefore, in the prevention trials, it was not surprising to find that fewer women in the raloxifene treatment group progressed from normal to osteopenia and from osteopenia to osteoporosis [32]. Because raloxifene has a significant effect on preventing bone loss, the question remains as to how long patients should take raloxifene for postmenopausal osteoporosis. No data are available on the fracture risk after raloxifene discontinuation [33]. However, raloxifene is available for indefinite treatment use for the prevention and treatment of osteoporosis.

The efficacy of raloxifene in osteoporosis prevention and treatment has been proved not only in populations in Western countries (the US and Europe), but also in Asian countries [34,35]. The population in one study included 968 healthy postmenopausal Asian women (mean age, 57 years) from Australia, Hong Kong, India, Indonesia, Malaysia, Pakistan, Philippines, Singapore, Taiwan and Thailand. Consistent with the MORE and CORE studies [18,20,22], raloxifene significantly decreased osteocalcin and N-telopeptide by medians of 15.9 and 14.6%, respectively, compared with placebo, and increased mean lumbar spine BMD (1.9%), compared with placebo at 1 year ($p < 0.001$) [34]. Compared with baseline, women taking raloxifene had significant increases in lumbar spine (L2-L4) BMD at 24 weeks (+ 3.3%, $p < 0.001$) through 52 weeks (+ 3.5%, $p < 0.001$) of therapy [34].

2.6.1.2 Bone health

Evaluation of bone collagen maturation may provide additional information when we discuss anti-fracture efficacy, because besides a concomitant increase in BMD during anti-resorptive therapy, bone quality is also important for anti-fracture efficacy. In addition, anti-fracture efficacy cannot simply be explained by an increase in BMD during anti-resorptive therapy. Bone collagen maturation was measured as the ratio between the degradation products (non-isomerized ααC-telopeptides of type I collagen (CTX) of newly synthesized and mature isomerized ββCTX) [36]. There were two main findings: i) treatment with bisphosphonates, HRT or raloxifenewas associated with a statistically highly significant suppression of bone resorption of both newly synthesized (ααCTX) and mature (ββCTX) collagen type I degradation, with the most pronounced suppression observed in the bisphosphonates groups, and ii) treatment with bisphosphonates induced a lower ratio between ααCTX and ββCTX compared with that of HRT and raloxifene (a reduction in the ratio between the two CTX isoforms was 52% with alendronate, 38% with ibandronate, 3% with HRT and 15% with raloxifene) [36]. In addition to BMD, this finding is worthy of further investigation, especially with regard to the different anti-resorptive therapies [36].

2.6.1.3 Anti-fracture efficacy

The anti-fracture efficacy of raloxifene has been well established by the MORE trial [18,20]. Raloxifene was efficacious (with a vertebral fracture reduction of 30% in women with and 55% in women without prevalent fractures over 3 years) [18], sustainable (with a 50% reduction in the fourth year vs a 55% reduction in years 0 – 3) [20], fast-acting (with 68% reduction, $p = 0.01$, in a 1-year *post hoc* analysis, and 90% reduction, $p = 0.01$, in a 6-month *post hoc* analysis) [37,38] and very fast-acting (with an 80% reduction, $p = 0.034$, in a 3-month *post hoc* analysis) [38]. In another *post hoc* analysis of postmenopausal women without baseline vertebral fractures who were osteopenic at the total hip, using NHANES III (the Third National Health and Nutrition Examination Survey) criteria, treatment with raloxifene significantly reduced the risk of new vertebral fractures (47% reduction) and new clinical vertebral fractures (75% reduction) [39]. The RUTH trial clearly demonstrates the benefits of raloxifene in the prevention of clinical vertebral fracture (35% reduction, $p = 0.007$) [23]. Taken together, raloxifene has a definite anti-fracture efficacy.

Raloxifene not only offers benefits in the absolute reduction of the risk of vertebral fractures, but also ameliorates the severity of future vertebral fracture [40]. First, raloxifene treatment can decrease the severity of all vertebral fractures. Raloxifene decreases the risk of at least one new moderate/severe vertebral fracture by 61% in women without prevalent vertebral fractures (relative risk (RR) = 0.39, 95% CI, 0.17 – 0.69), and by 37% in women with prevalent vertebral fractures (RR = 0.63, 95% CI, 0.49 – 0.83) at 3 years. Second, raloxifene treatment can decrease the absolute number of vertebral fractures. The cumulative RRs of multiple (≥ 2) new vertebral fractures over 4 years were 0.54 (95% CI, 0.38 – 0.77) with raloxifene compared with a placebo [41].

The risk reduction for non-vertebral fractures in the overall MORE population was not significant, but a reduction of 47% ($p = 0.04$) was noted in a *post hoc* analysis of patients with severe (semi-quantitative grade 3) prevalent vertebral fractures [41]. In the CORE study, the risk of at least one new non-vertebral fracture was similar in the placebo (22.9%) and raloxifene (22.8%) groups (hazard ratio (HR) = 1; Bonferroni-adjusted CI, 0.82 – 1.21) [22]. The incidence of at least one new non-vertebral fracture at six major sites (clavicle, humerus, wrist, pelvis, hip and lower leg) was 17.5% in both groups. *Post hoc* Poisson analyses, which

account for multiple events, showed no overall effect on non-vertebral fracture risk; however, a decreased risk (a reduction of 22%) was found at six major non-vertebral sites in women with prevalent vertebral fractures (HR = 0.78; 95% CI, 0.63 – 0.96, p = 0.017) and with severe (baseline SQ grade 3) vertebral fractures (HR = 0.64; 95% CI, 0.44 – 0.92, p < 0.05) [22]. The RUTH trial also showed that raloxifene was not sufficient for preventing non-vertebral fractures because there was no difference in non-vertebral fractures between the raloxifene treatment and placebo groups [23]. A meta-analysis of seven randomized placebo-controlled trials of raloxifene found that BMD increased by 2.51% (p < 0.01) at the lumbar spine and 2.11% at the total hip (p < 0.01), and there was evidence for the reduction of vertebral fractures (40% reduction; p = 0.01), but not for non-vertebral fractures (p = 0.24) [42]. One explanation for this apparent absence of a non-vertebral effect is that the weaker anti-resorptive effects of raloxifene can return high bone turnover to normal and prevent micro-architectural deterioration in trabecular bone, but the reduction of fracture risk at sites of cortical bone, such as the hip, requires more potent anti-resorptive effects [43].

2.6.2 Reduction of breast cancer incidence with raloxifene

Raloxifene is approved by the FDA for treating and preventing osteoporosis in postmenopausal women and reducing the risk of invasive breast cancer in postmenopausal women at increased risk of breast cancer. Raloxifene is not recommended for reducing the risk of breast cancer in premenopausal, high risk women. Tamoxifen is the medicine of choice. Raloxifene does not have acceptable activity against ER-positive metastatic breast cancer, and raloxifene should not be used to treat breast cancer or prevent its recurrence [44].

An increase in mammographic density should be regarded as an unwanted side effect of HRT, because increased breast density can impair the interpretation of mammograms, thus increasing the failure rate of breast cancer screening programs [45]. In fact, the WHI report showed that combination HRT did indeed increase the risk of the incidence of breast cancers [3]. Therefore, because raloxifene does not increase mammographic breast density [46] and can reduce breast cancer proliferative indices [47], these factors may play a protective role in decreasing the incidence of invasive breast cancer.

A decrease in breast cancer incidence in the MORE trial was observed as a secondary end point in participants taking raloxifene (**Table 3**). During 40 months of follow-up, 54 total cases of breast cancer were confirmed, 22 (0.42%) in the raloxifene group and 32 (1.24%) in the placebo group, with a risk reduction of 65% (RR = 0.35) [19]. Among the 40 invasive breast cancers, the risk reduction of 76% (RR = 0.24; 27 with the placebo vs 13 with raloxifene) was even more striking. The risk reduction was similar for both doses of raloxifene and was limited to ER-positive tumors (RR = 0.10), with no risk reduction occurring in ER-negative tumors (RR = 0.88) [19].

Continued follow-up of MORE participants using additional annual mammograms at 4 years showed an ongoing breast cancer risk reduction in postmenopausal women treated with raloxifene (**Table 3**) [27]. Among 61 invasive breast cancers reported as of November 1999, the risk reduction was 72% (RR = 0.28), with 39 (1.51%) using a placebo versus 22 (0.43%) using raloxifene. It was more striking to find that the risk reduction was 84% (RR = 0.16) of the ER-positive breast cancers, including 31 (1.20%) patients using a placebo versus 10 (0.20%) using raloxifene. No difference between the treatment groups was observed regarding the incidence of ER-negative tumors. These observations are consistent with a model in which raloxifene antagonizes estrogen activity at the ER in the breast [48].

Following on from the significant effect of raloxifene in decreasing the incidence of invasive breast cancer observed in the MORE study, the CORE trial provided even stronger evidence to support the benefits of raloxifene in the reduction in risk of invasive breast cancer in postmenopausal women with osteoporosis (**Table 3**) [21]. CORE participants had 5-year breast cancer risk assessed at study entry with the Gail model [49]. During the 4 years of the CORE trial, 61 cases of breast cancer (30 using a placebo vs 31 using raloxifene) were reported and confirmed by adjudication. Of the 61 breast cancer cases, 52 were invasive, and there was a 59% reduction in the incidence of invasive breast cancer in those using raloxifene versus a placebo (2.1 vs 5.2 cases/1000 woman-years; HR = 0.41, 95% CI, 0.24 – 0.71, p < 0.001). For ER-positive invasive breast cancers (78% of invasive breast cancers), a 66% reduction was found in those using raloxifene versus a placebo (1.3 vs 3.9 cases/1000 woman-years; HR = 0.34, 95% CI, 0.18 – 0.66, p < 0.001). However, for the prevention of either invasive ER-negative breast cancer or non-invasive breast cancer, the effect of raloxifene seemed to be uncertain, because no statistical difference was noted between the treatment group and the placebo group (0.55 vs 0.61/1000 woman-years; HR = 1.13, 95% CI, 0.29 – 4.35; p = 0.86, HR = 1.78, 95% CI, 0.37 – 8.61; p = 0.47, respectively). The overall incidence of breast cancer, regardless of invasiveness, was reduced by 50% in the raloxifene group compared with the placebo group (2.7 vs 5.5 cases/1000 woman-years; HR = 0.50, 95% CI, 0.30 – 0.82, p < 0.001) [21].

During the 8 years of the MORE and CORE trials, 40 invasive breast cancers were reported in the raloxifene group and 58 in the placebo group, with a 66% reduction in the incidence of invasive breast cancer with raloxifene versus a placebo (1.4 vs 4.2 cases/1000 woman-years; HR = 0.34, 95% CI, 0.22 – 0.50, p < 0.001). For ER-positive invasive breast cancers (75% of invasive breast cancers), a 76% reduction was found in those using raloxifene versus placebo (0.8 vs 3.2 cases/1000 woman-years; HR = 0.24, 95% CI, 0.15 – 0.40, p < 0.001). There was no statistical difference in the incidence of either invasive ER-negative breast cancer or non-invasive breast cancer between the treatment group and the placebo group (0.53 vs 0.51/1000 woman-years;

HR = 1.06; 95% CI, 0.43 – 2.59; p = 0.90, 16 patients on raloxifene vs 7 on a placebo, HR = 1.12, 95% CI, 0.46 – 2.73; p = 0.80). The overall incidence of breast cancer, regardless of invasiveness, was reduced by 58% in the raloxifene group compared with the placebo group (1.96 vs 4.9 cases/1000 woman years; HR = 0.42, 95% CI, 0.29 – 0.60; p = 0.001) [21].

The RUTH trial further confirmed the chemoprotective role of raloxifene in preventing the development of ER-positive invasive breast cancers (**Table 3**). Raloxifene reduced the incidence of the primary outcome of invasive breast cancer (HR = 0.56; 95% CI, 0.38 – 0.83; p = 0.003), principally because of a reduction in ER-positive invasive breast cancer [23,50]. The absolute risk (AR) reduction/1000 women treated with raloxifene for 1 year was 1.2 cases of invasive breast cancer and 1.2 cases of ER-positive invasive breast cancer. The results of the as-treated analysis for invasive breast cancer were similar (HR = 0.61; 95% CI, 0.39 – 0.95; p = 0.03). There was no significant difference between the treatment groups regarding the incidence of ER-negative invasive breast cancer.

In the STAR trial, the incidence of invasive breast cancer in the tamoxifen and raloxifene groups was not significantly different [24] (Data is not shown). There were 168 of 9745 women on raloxifene diagnosed with invasive breast cancer compared with 163 of 9726 women on tamoxifen (4.41/1000 women on raloxifene per year compared with 4.30/1000 women on tamoxifen per year; RR = 1.02; 95% CI, 0.82 – 1.28). There were more non-invasive breast cancers in the raloxifene (n = 80) group than in the tamoxifen (n = 57) group (RR = 1.40; 95% CI, 0.98 – 2), but the difference was not statistically significant. Findings were also comparable for women diagnosed with ER-positive tumors (109 women in the raloxifene group vs 115 women in the tamoxifen group; RR = 0.94; 95% CI, 0.72 – 1.24). FDA approval of raloxifene for breast cancer risk reduction following its demonstrated effectiveness in reduction of invasive breast cancer risk was mainly based on the results from this trial.

Table 4 presents the results from the update STAR trial [9], comparing raloxifene and tamoxifen. In this report, updated analysis was presented with an 81-month median follow-up, that is, well after treatment was stopped at 60 months. The RR (raloxifene:tamoxifen) for invasive breast cancer was 1.24 (95% CI, 1.05 – 1.47) and for non-invasive disease, 1.22 (95% CI, 0.95 – 1.59). Compared with initial results [24], the RRs widened for invasive and narrowed for non-invasive breast cancer. As stated in the recent STAR trial update [9], raloxifene may need to be given indefinitely to maintain control and reduce the risk of invasive breast cancer.

The American Society of Clinical Oncology (ASCO) first published a technology assessment for the use of chemoprevention agents for breast cancer risk reduction in 1999 [51]. ASCO guidelines are updated periodically by a subset of the original expert panel, and in 2002 the first update and in 2009 the second update to the breast cancer risk reduction technology assessment were published [10,52]. For postmenopausal women at increased risk for breast cancer, raloxifene (60 mg/day) for 5 years may be offered as another option to reduce the risk of ER-positive invasive breast cancer. Raloxifene may be used for longer than 5 years in women with osteoporosis in whom breast cancer risk reduction is an additional potential benefit. Raloxifene is not recommended in premenopausal women or in women with a previous history of deep vein thrombosis (DVT), pulmonary embolism (PE), stroke or transient ischemic attack.

2.6.2.1 Bisphosphonate to reduce the risk of breast cancer

Bisphosphonate therapy has become the pharmacologic treatment of choice for preventing bone loss and fractures in postmenopausal women with osteoporosis [53,54]. This is primarily because bisphosphonates have proven efficacy for treating bone loss, relative low cost, ease of use and low risk of adverse effects versus HRT, which have been associated with increased risk of breast cancer and cardiovascular disease [55]. In addition, several recent clinical trials demonstrated the efficacy of bisphosphonates for preventing cancer treatment-induced bone loss in pre- and postmenopausal women with early-stage breast cancer [56-58].

Their classical mechanism of action of bisphosphonates is through inhibition of osteoclast-mediated bone resorption and reduction in the release of calcium and other minerals into the blood stream [59]. Beyond preventing osteoclast-mediated bone resorption, bisphosphonates have also demonstrated anticancer activity in a variety of preclinical and clinical studies [60]. There is also evidence for anticancer synergy between cytotoxic chemotherapy agents and zoledronic acid, a finding that was recently confirmed in women receiving neoadjuvant therapy for breast cancer [61]. Furthermore, adding adjuvant zoledronic acid in large, randomized clinical trials produced significant reductions in disease recurrence in women with breast cancer, and suggests that bisphosphonates have a beneficial effect on the microenvironment in which dormant tumor stem cells survive in early disease [62]. Based on these important findings, several recent population-based studies examined whether long-term use of oral bisphosphonates in women with postmenopausal osteoporosis may be associated with a reduced risk of breast cancer.

Chlebowski *et al.* [63] report on an analysis of longitudinal data from the Women's Health Initiative Observational Study (WHI-OS) that included 154,768 women. In summary, their multivariate analysis revealed that women who received bisphosphonates for osteoporosis had a 32% relative reduction in the overall risk of breast cancer compared with those who did not receive bisphosphonates (HR = 0.68; 95% CI, 0.52 – 0.88). Rennert *et al.* [64] also reported a 28% reduced risk of breast cancer (odds ratio (OR) = 0.72; 95% CI, 0.57 – 0.90) among postmenopausal women receiving bisphosphonates for > 1 year in a similar analysis, this time using the Breast Cancer in Northern Israel Study (BCINIS) database (n = 4039).

A recent population-based, case-controlled study in Wisconsin (n = 5911) from Newcomb *et al.* [65] found that current bisphosphonate use was associated with a comparable 33% reduction in the risk of breast cancer (OR = 0.67; 95% CI, 0.51 – 0.89). Important factors such as body mass index and HRT were considered. Although it was a small study, this represents an additional, independent report of the correlation between bisphosphonate use and decreased breast cancer risk. It is interesting to note that the relative breast cancer risk reduction is ~ 30% across all three studies.

Potential anticancer effects of bisphosphonates (clodronate [66,67], pamidronate [68], Zoledronate [57]), such as reduction of breast cancer recurrence and prolongation of survival have also been reported in pre- and postmenopausal women with early-stage breast cancer. The reduction in disease recurrence with adjuvant bisphosphonate therapy may result, in part, from modification of the bone marrow microenvironment, making this niche less receptive to tumor stem cells [69,70]. Bisphosphonates have also demonstrated direct and indirect anticancer effects on cancer cells including inducing cancer cell apoptosis; inhibiting cancer cell adhesion and extravasation, anticancer synergy with endocrine therapy and cytotoxic chemotherapy; deterring angiogenesis; and activating immune cells with anticancer activity among others [60].

In summary, we present the observational and preliminary results of the efficacy of bisphosphonates or anticancer agents for scientific completeness. A direct comparison with raloxifene is not appropriate as no large prospective clinical trials of risk reduction for breast cancer have been completed with bisphosphonates.

2.7 Safety and tolerability

There are several adverse events and side effect of using raloxifene. Two major concerns noted in the RUTH study are the increased risks of venous thromboembolism (RR = 44%, 103 vs placebo 71 events; HR, 1.44; 95% CI, 1.06 – 1.95; AR, 1.2/1000 woman-years) and fatal stroke (RR = 49%, 59 vs placebo 39 events; HR, 1.49; 95% CI, 1.00 – 2.24; AR, 0.7/1000 woman-years) while taking raloxifene [23]. But, there was no significant difference in the rates of death from any cause or total stroke according to group assignment. These observations are consistent with earlier reports [19,20]. The increased risk of thromboembolism should not be too surprising. Almost all, if not all, hormones or related agents contribute to an increased risk of thromboembolism to a significant, but different, degree. HRT in the WHI study has shown a significantly increased incidence of thromboembolism [3]. Furthermore, tamoxifen also contributed to a significantly increased incidence of thromboembolism [9,24]. Besides thromboembolism, tamoxifen also demonstrated other adverse events, such as stroke, cataract and endometrial lesions, all of which have contributed to significant morbidity and mortality [9,24]. Although there have been many adverse events associated with tamoxifen use for preventing and treating breast cancer, it remains the antihormonal treatment of choice for premenopausal women with ER-positive breast cancer and for risk reduction in premenopausal women who are at a high risk of developing breast cancer [71]. Tamoxifen does not increase endometrial cancer or clots in the premenopausal population [72].

In view of this consideration, the question is raised regarding the possibility of using raloxifene in place of tamoxifen, because the efficacy of raloxifene in reduction in risk of breast cancer is clear [9,19,21-25]. According to the results of a 20,000 women head-to-head comparison of tamoxifen and raloxifene for breast cancer risk reduction in the STAR trial (Tables 1 and 4) [9,24,25], raloxifene appears superior compared with tamoxifen, because although raloxifene showed an efficacy equal to tamoxifen in the reduction of invasive breast cancer risk, women taking raloxifene had fewer instances of thromboembolic events, fewer cataracts, fewer cataract surgeries, fewer endometrial hyperplasia events with atypia or without atypia, fewer requests for hysterectomy and fewer endometrial cancer. There was no statistically significant increase in uterine cancer when raloxifene was compared with placebo in the MORE, CORE or RUTH trials. In the STAR trial [9], a significant decrease in uterine cancer was observed in women taking raloxifene compared with tamoxifen (RR = 0.55; 95% CI, 0.36 – 0.83). In a previous report [24], the difference between treatment groups for the rate of invasive uterine cancer was not statistically significant. However, the average annual incidence rate of uterine hyperplasia, the majority of which was hyperplasia without atypia, was 5 times higher in the tamoxifen group (4.40/1000) than in the raloxifene group (0.84/1000; RR = 0.19; 95% CI, 0.12 – 0.29). The number of hysterectomies performed in the tamoxifen group (349), including those done for benign disease, was more than double that performed in the raloxifene group (162; RR = 0.45; 95% CI, 0.37 – 0.54) [9].

There was less mean symptom severity for the gynecological problems of the treated women (0.29 vs 0.19, $p < 0.001$) and for their vasomotor symptoms (0.96 vs 0.85, $p < 0.001$), and fewer leg cramps (1.10 vs 0.91, $p < 0.001$) and bladder control symptoms (0.88 vs 0.73, $p < 0.001$) with raloxifene, although women taking tamoxifen may benefit from some parameters, such as better sexual functioning and lower mean symptom severity of musculoskeletal problems, less dyspareunia and less weight gain. However, based on the superior side effect profile of raloxifene, primary care physicians may be more willing, given their experience with raloxifene, to prescribe it for breast cancer chemoprevention than they have been to prescribe tamoxifen [73].

Although the risk of thromboembolism in women gave rise to concern about the use of raloxifene in the MORE and CORE trials, the application of these data to Asian populations may not be appropriate, because the previous data were derived from populations in the US and Europe. Thromboembolism, an adverse event associated with taking oral pills, whether hormones or similar drugs, is extremely rare in Asian populations [34,74]. This finding was also noted in Asian populations taking HRT or undergoing major pelvic

surgeries [75]. By contrast, gastrointestinal tract problems occurred more frequently in Asian populations [76]. Taken together, raloxifene may be a better choice for the prevention and management of osteoporosis and reduction of breast cancer risk in Asian postmenopausal women.

Finally, the AR rather than the RR with regard to the positive effects and adverse events associated with raloxifene use in postmenopausal women with osteoporosis can be used as a reference when making a decision. An important question raised by the raloxifene trials is how to balance the substantial relative reductions in the risks of invasive breast cancer and clinical vertebral fractures with the increased risk of thromboembolism. The same model of a 'global index', including coronary heart disease, stroke, PE, invasive breast cancer, endometrial cancer, colorectal cancer, hip fracture and death from other causes, proposed in the WHI trial [3], was applied to the participants in the MORE trial, and the results suggested a favorable risk–benefit safety profile for raloxifene, even though the risk of hip fractures was not significantly reduced [77].

A recent review that showed the efficacy of raloxifene in the prevention of osteoporotic vertebral and non-vertebral fractures or hip fractures compared with that of bisphosphonates, calcitonin and teriparatide, provides some comparative insights [78]. There is good evidence that shows alendronate, etidronate, ibandronate, risedronate, zoledronic acid, estrogen, parathyroid hormone[1-34] and raloxifene can prevent vertebral fractures effectively compared with a placebo, and that alendronate, risedronate and estrogen can prevent hip fractures effectively compared with a placebo. For vertebral fracture prevention, the evidence for calcitonin was only fair. For hip fracture prevention, the evidence for zoledronic acid is again fair [79,80].

The potential adverse effects (safety profile) of each drug may be relevant as compliance is essential for efficiency. Gastrointestinal tract problems are frequently noted in women taking alendronate [26]. Alendronate and other bisphosphonates may cause oversuppression of bone turnover; therefore, an important potential side effect of taking alendronate is osteonecrosis of the jaw (ONJ) [81,82], This concern has uncertain outcomes because of low incidence [83,84]. Recently, there was an attempt to estimate the frequency of ONJ and describe the clinical characteristics of patients diagnosed with bisphosphonate-associated ONJ of the jaws [85]. The results showed that the frequency of ONJ in osteoporotic patients mainly taking weekly oral alendronate was 1 in 2260 – 8470 (0.01 – 0.04%), and if extractions were carried out, the calculated frequency was 1 in 296 – 1130 cases (0.09 – 0.34%) [85]. The study reported that the total dose of oral alendronate at the onset of ONJ was 9060 (± 7269) mg, and that the median time to onset of ONJ was 12 months for zoledronate, 24 months for pamidronate and 24 months for alendronate [85].

The results from a study on compliance with raloxifene and bisphosphonate in an Asian population showed that compliance with raloxifene is better than that with bisphosphonates [76]. Asian women showed lower discontinuation rates and higher treatment satisfaction with raloxifene than with bisphosphonates [76]. Postmenopausal women with osteoporosis, who have poor compliance when taking alendronate, can be switched to raloxifene, because they can still see benefits in BMD and bone turnover with raloxifene after discontinuing alendronate therapy [86].

2.8 Regulatory affairs

Based on data generated in prospective randomized clinical trials, raloxifene has been FDA approved in the US for the treatment and prevention of osteoporosis since 1998 and for the reduction of breast cancer risk since 2004. Raloxifene has been approved and available in the EU since 1999 and in numerous other the countries around the world for the treatment and prevention of osteoporosis.

3. Conclusion

Based on these observations (MORE, CORE and RUTH trials), the efficacy of raloxifene in the prevention and management of osteoporosis, the decreased incidence of fracture and the decreased incidence of invasive breast cancer has been proved. The updated STAR trial results reported here demonstrate that after a median follow-up of 81 months, which represents 60 months of treatment plus an additional 21 months of follow-up, raloxifene no longer appears to be as effective as tamoxifen in preventing primary invasive breast cancer [9]. Raloxifene does appear, however, to retain ~ 76% of tamoxifen's effectiveness, which represents as much as a 38% reduction in invasive breast cancer (compared with an untreated group).

It must be stressed that these data derived from the updated STAR trial [9] are after the 5 years of planned treatment was stopped and data evaluated 21 months later. Tamoxifen retains a consistent long lasting antitumor effect after therapy stops but raloxifene does not. Raloxifene must, therefore, be given indefinitely and this strategy is permitted for the treatment of osteoporosis. A study of the accumulative incidence of invasive breast cancer during MORE/CORE demonstrates an effective long-term antitumor effect of raloxifene out of 8 years of treatment [87].

The potential risk of thromboembolism has also been noted. A recent meta-analysis to evaluate the effect of raloxifene on the risk of DVT and PE showed that therapy with raloxifene was associated with a 62% increase in the odds of either DVT or PE (OR = 1.62; 95% CI, 1.25 – 2.09; $p < 0.001$). Similarly, raloxifene therapy was associated with a 54% increase in the odds of DVT (OR = 1.54; 95% CI, 1.13 – 2.11; $p = 0.006$) and a 91% increase in the odds of PE alone (OR = 1.91; 95% CI, 1.05 – 3.47; $p = 0.03$) [88], although raloxifene is probably not associated with an increased risk of arterial thromboembolism [88]. In addition, raloxifene may improve platelet metabolism in healthy postmenopausal women through an increase in the

bioavailability of platelet NO by a reduction of iNOS and the beneficial effects on lipid metabolism [89]. By contrast, other side effects, such as the higher frequency of hot flushes, cramps of the lower limbs and fluid retention may be a reason for halting raloxifene use in menopausal women [87]. Efficacy of raloxifene depends on compliance and so the issue of quality of life is critical.

However, based on the concept of the choice of tamoxifen for the chemoprevention of invasive breast cancer, and the long-term tolerance to a lot of the adverse events relating to tamoxifen, such as cataracts, endometrial cancer, stroke and so on, raloxifene is a better alternative, because the STAR trial clearly demonstrated the superiority of raloxifene to tamoxifen during treatment, not only for equal efficacy in the reduction of invasive breast cancer risk, but also for the fewer serious adverse events, including thromboembolism. Therefore, because postmenopausal women > 60 years of age with osteoporosis also have an elevated risk of breast cancer, raloxifene may then be considered in this specific population. Additionally, based on the low risk of thromboembolism and the high incidence of gastrointestinal tract problems, it is rational to use raloxifene in Asian postmenopausal women with osteoporosis [34,74,76].

Because there is no miracle cure that can reduce the risks of major health problems related to estrogen deprivation during aging without introducing other potentially serious health concerns [90], raloxifene remains a good choice for postmenopausal women with osteoporosis. As in the case of other hormonal preparations, such as thyroid replacement therapy or insulin treatment [91], raloxifene can be prescribed for clear indications, including the prevention of osteoporosis and its related fractures and the reduction in risk of invasive breast cancer. Raloxifene can be monitored carefully for potential risks, such as thromboembolism. Therefore, it offers the best benefits for a specific population: climacteric symptom-free postmenopausal women who need osteoporosis therapy, fracture prevention and breast cancer risk reduction, but are at a low risk of thromboembolism.

4. Expert opinion

Since the initial publication of the WHI [3], the actual medical value of the HRT in the management of postmenopausal women has become clear. Subsequent analyses have identified numerous problems including increases in breast cancer incidence, enhanced malignancies of breast cancer, and no positive effects on coronary heart disease and Alzheimer's disease and so on. In contrast, control of menopausal symptoms and decreases in fracture rate are benefits of HRT. As a result of no overall benefit for HRT, major efforts have been made to identify target specific alternatives. The recognition and description of selective modulation of estrogen target tissues by non-steroidal 'antiestrogens' suggested an appropriate rationale for the development of SERMs to target multiple diseases associated with the menopausal diseases [11]. It was clear that by targeting major diseases such as osteoporosis or atherosclerosis with SERMs, one could anticipate a reduction in breast cancer incidence [92]. Although we still need to find the 'ideal' SERM, progress is being made with raloxifene that is approved for both the prevention of osteoporosis and the reduction of breast cancer risk. The next generation SERM, lasofoxifene [93], is an advance because it reduces osteoporosis, breast cancer risk, coronary heart disease and strokes and, as with, raloxifene, no increase in endometrial cancer. Also, like raloxifene, there is a small elevation in thromboses. However, lasofoxifene is only approved outside of the US (the EU) and the drug has not been launched. An advantage of a SERM of the future would be a reduction of menopausal symptoms. One current approach is the use of a SERM (bazedoxifene) and conjugated estrogen [94]. Apparently, the estrogen still reduces hot flashes, but the SERM protects the uterus and breast from carcinogenesis. Although limited data are currently available with regard to the next generation SERMs, the challenge for the future is to assess SERMs adequately in Phase III clinical trials. The time and financial investment are too great at this time. Each clinical end point must be evaluated individually, and conclusions about any particular SERM can only be established through multiple clinical trials over a decade.

One interesting clinical observation with the drug tibolone, currently used in Europe for the prevention of osteoporosis and as a hormone replacement therapy, emerges from the recent clinical trial published by Cummings *et al.* [95]. The randomized trial assigned 4538 older postmenopausal women to placebo or tibolone (1.5 mg/day) for a median of 34 months of treatment. Tibolone increased BMD and significantly decreased the risk of non-vertebral fractures. However, there was also a significant and somewhat paradoxical decrease in the incidence of invasive breast cancer. On the face of it, this clinical result would appear to not have been supported by the fact that tibolone is known to have estrogenic properties, producing a modest increase in the risk of breast cancer in the Million Women Study in the UK [96] and stimulating the proliferation of human MCF-7 breast cancer cells in the laboratory [97]. Nevertheless, it is known that long-term estrogen deprivation of breast cancer cells can sensitize them to the apoptotic actions of physiological concentrations of estrogen [98]. This is a topic of considerable academic interest and some clinical studies in the literature have applied the concepts to treat metastatic breast cancer [99]. Indeed, the estrogen alone arm of the WHI in postmenopausal women with the median age of 63 [100] actually produced a decrease in the incidence of breast cancer. Thus, it would not be unreasonable to suggest that the weak estrogen-like activity of tibolone used in the Cummings study [95] in a population of older postmenopausal women, median age of 68, is actually causing apoptosis, rather than growth. This hypothesis, should it be proven correct, would obviously limit the use of tibolone in the postmenopausal population.

Thus, it is clear from prospective randomized clinical trials that it is possible to reduce the risk of invasive breast cancer in both high and low risk postmenopausal women. There are clinical reports of risk reductions with ERT [100], tibolone [95], and prospective randomized studies and observational information with bisphophonates [63-65], but no prospective randomized trials with breast cancer incidence as the primary end point. However, the extensive clinical evaluation of raloxifene in pivotal clinical trials to treat osteoporosis or reduce the risk of developing invasive breast cancer in high risk postmenopausal women remains definitive. The pharmacological innovations of SERM action of raloxifene to be anti-estrogenic in the breast to prevent the development of invasive breast cancer as long as treatment is continued is a benchmark and remains consistent with laboratory research findings used for the recommendations in the STAR trial update [9].

Acknowledgments

This work (VCJ) was supported by the Department of Defense Breast Program under Award number BC050277 Center of Excellence; subcontract under the SU2C (AACR) Grant number SU2C-AACR-DT0409; the Susan G Komen For The Cure Foundation under Award number SAC100009 and the Lombardi Comprehensive Cancer Center Support Grant (CCSG) Core Grant NIH P30 CA051008. The views and opinions of the author(s) do not reflect those of the US Army or the Department of Defense.

Declaration of interest

The authors state no conflict of interest and have received no payment in preparation of this manuscript.

Bibliography

1. Riggs BL, Khosla S, Melton LJ III. Sex steroids and the construction and conservation of the adult skeleton. Endocr Rev 2002;23:279-302
2. National Osteoporosis Foundation. America's Bone Health: The State of Osteoporosis and Low Bone Mass.; Available from: http://www.nof.org/advocacy/prevalence/index.htm [Cited 13 Augest 2010]
3. Rossouw JE, Anderson GL, Prentice RL, et al. Risks and benefits of estrogen plus progestin in healthy postmenopausal women: principal results From the Women's Health Initiative randomized controlled trial. JAMA 2002;288:321-33
4. Chlebowski RT, Anderson GL, Gass M, et al. Estrogen plus progestin and breast cancer incidence and mortality in postmenopausal women. JAMA 2010;304:1684-92
5. Yager JD, Davidson NE. Estrogen carcinogenesis in breast cancer. N Engl J Med 2006;354:270-82
6. Riggs BL, Hartmann LC. Selective estrogen-receptor modulators - mechanisms of action and application to clinical practice. N Engl J Med 2003;348:618-29
7. Jordan VC. SERMs: meeting the promise of multifunctional medicines. J Natl Cancer Inst 2007;99:350-6
8. Jordan VC. Chemoprevention of breast cancer with selective oestrogen-receptor modulators. Nat Rev Cancer 2007;7:46-53
9. Vogel VG, Costantino JP, Wickerham DL, et al. Update of the National Surgical Adjuvant Breast and Bowel Project Study of Tamoxifen and Raloxifene (STAR) P-2 Trial: preventing breast cancer. Cancer Prev Res (Phila Pa) 2010;3:696-706
10. Visvanathan K, Chlebowski RT, Hurley P, et al. American society of clinical oncology clinical practice guideline update on the use of pharmacologic interventions including tamoxifen, raloxifene, and aromatase inhibition for breast cancer risk reduction. J Clin Oncol 2009;27:3235-58
11. Jordan VC. Selective estrogen receptor modulation: a personal perspective. Cancer Res 2001;61:5683-7
12. Jensen EV, Greene GL, Closs LE, et al. Receptors reconsidered: a 20-year perspective. Recent Prog Horm Res 1982;38:1-40
13. Bryant HU. Mechanism of action and preclinical profile of raloxifene, a selective estrogen receptor modulation. Rev Endocr Metab Disord 2001;2:129-38
14. Chen Z, Yuhanna IS, Galcheva-Gargova Z, et al. Estrogen receptor alpha mediates the nongenomic activation of endothelial nitric oxide synthase by estrogen. J Clin Invest 1999;103:401-6
15. Kuiper GG, Carlsson B, Grandien K, et al. Comparison of the ligand binding specificity and transcript tissue distribution of estrogen receptors alpha and beta. Endocrinology 1997;138:863-70
16. Wijayaratne AL, Nagel SC, Paige LA, et al. Comparative analyses of mechanistic differences among antiestrogens. Endocrinology 1999;140:5828-40
17. Messalli EM, Mainini G, Scaffa C, et al. Raloxifene therapy interacts with serum osteoprotegerin in postmenopausal women. Maturitas 2007;56:38-44
18. Ettinger B, Black DM, Mitlak BH, et al. Reduction of vertebral fracture risk in postmenopausal women with osteoporosis treated with raloxifene: results from a 3-year randomized clinical trial. Multiple Outcomes of Raloxifene Evaluation (MORE) Investigators. JAMA 1999;282:637-45
19. Cummings SR, Eckert S, Krueger KA, et al. The effect of raloxifene on risk of breast cancer in postmenopausal women: results from the MORE randomized trial. Multiple Outcomes of Raloxifene Evaluation. JAMA 1999;281:2189-97
20. Delmas PD, Ensrud KE, Adachi JD, et al. Efficacy of raloxifene on vertebral fracture risk reduction in postmenopausal women with osteoporosis: four-year results from a randomized clinical trial. J Clin Endocrinol Metab 2002;87:3609-17
21. Martino S, Cauley JA, Barrett-Connor E, et al. Continuing outcomes relevant to Evista: breast cancer incidence in

postmenopausal osteoporotic women in a randomized trial of raloxifene. J Natl Cancer Inst 2004;96:1751-61

22. Siris ES, Harris ST, Eastell R, et al. Skeletal effects of raloxifene after 8 years: results from the continuing outcomes relevant to Evista (CORE) study. J Bone Miner Res 2005;20:1514-24
23. Barrett-Connor E, Mosca L, Collins P, et al. Effects of raloxifene on cardiovascular events and breast cancer in postmenopausal women. N Engl J Med 2006;355:125-37
24. Vogel VG, Costantino JP, Wickerham DL, et al. Effects of tamoxifen vs raloxifene on the risk of developing invasive breast cancer and other disease outcomes: the NSABP Study of Tamoxifen and Raloxifene (STAR) P-2 trial. JAMA 2006;295:2727-41
25. Land SR, Wickerham DL, Costantino JP, et al. Patient-reported symptoms and quality of life during treatment with tamoxifen or raloxifene for breast cancer prevention: the NSABP Study of Tamoxifen and Raloxifene (STAR) P-2 trial. JAMA 2006;295:2742-51
26. Recker RR, Kendler D, Recknor CP, et al. Comparative effects of raloxifene and alendronate on fracture outcomes in postmenopausal women with low bone mass. Bone 2007;40:843-51
27. Cauley JA, Norton L, Lippman ME, et al. Continued breast cancer risk reduction in postmenopausal women treated with raloxifene: 4-year results from the MORE trial. Multiple outcomes of raloxifene evaluation. Breast Cancer Res Treat 2001;65:125-34
28. Barrett-Connor E, Wenger NK, Grady D, et al. Coronary heart disease in women, randomized clinical trials, HERS and RUTH. Maturitas 1998;31:1-7
29. Prestwood KM, Gunness M, Muchmore DB, et al. A comparison of the effects of raloxifene and estrogen on bone in postmenopausal women. J Clin Endocrinol Metab 2000;85:2197-202
30. Weinstein RS, Parfitt AM, Marcus R, et al. Effects of raloxifene, hormone replacement therapy, and placebo on bone turnover in postmenopausal women. Osteoporos Int 2003;14:814-22
31. Neele SJ, Evertz R, De Valk-De Roo G, et al. Effect of 1 year of discontinuation of raloxifene or estrogen therapy on bone mineral density after 5 years of treatment in healthy postmenopausal women. Bone 2002;30:599-603
32. Jolly EE, Bjarnason NH, Neven P, et al. Prevention of osteoporosis and uterine effects in postmenopausal women taking raloxifene for 5 years. Menopause 2003;10:337-44
33. Briot K, Tremollieres F, Thomas T, Roux C. How long should patients take medications for postmenopausal osteoporosis? Joint Bone Spine 2007;74:24-31
34. Kung AW, Chao HT, Huang KE, et al. Efficacy and safety of raloxifene 60 milligrams/day in postmenopausal Asian women. J Clin Endocrinol Metab 2003;88:3130-6
35. Morii H, Ohashi Y, Taketani Y, et al. Effect of raloxifene on bone mineral density and biochemical markers of bone turnover in Japanese postmenopausal women with osteoporosis: results from a randomized placebo-controlled trial. Osteoporos Int 2003;14:793-800
36. Byrjalsen I, Leeming DJ, Qvist P, et al. Bone turnover and bone collagen maturation in osteoporosis: effects of antiresorptive therapies. Osteoporos Int 2008;19:339-48
37. Maricic M, Adachi JD, Sarkar S, et al. Early effects of raloxifene on clinical vertebral fractures at 12 months in postmenopausal women with osteoporosis. Arch Intern Med 2002;162:1140-3
38. Qu Y, Wong M, Thiebaud D, Stock JL. The effect of raloxifene therapy on the risk of new clinical vertebral fractures at three and six months: a secondary analysis of the MORE trial. Curr Med Res Opin 2005;21:1955-9
39. Kanis JA, Johnell O, Black DM, et al. Effect of raloxifene on the risk of new vertebral fracture in postmenopausal women with osteopenia or osteoporosis: a reanalysis of the Multiple Outcomes of Raloxifene Evaluation trial. Bone 2003;33:293-300
40. Siris E, Adachi JD, Lu Y, et al. Effects of raloxifene on fracture severity in postmenopausal women with osteoporosis: results from the MORE study. Multiple Outcomes of Raloxifene Evaluation. Osteoporos Int 2002;13:907-13
41. Delmas PD, Genant HK, Crans GG, et al. Severity of prevalent vertebral fractures and the risk of subsequent vertebral and nonvertebral fractures: results from the MORE trial. Bone 2003;33:522-32
42. Brown JP, Fortier M, Frame H, et al. Canadian consensus conference on osteoporosis, 2006 update. J Obstet Gynaecol Can 2006;28:S95-112
43. Riggs BL, Melton LJ III. Bone turnover matters: the raloxifene treatment paradox of dramatic decreases in vertebral fractures without commensurate increases in bone density. J Bone Miner Res 2002;17:11-14
44. Gradishar W, Glusman J, Lu Y, et al. Effects of high dose raloxifene in selected patients with advanced breast carcinoma. Cancer 2000;88:2047-53
45. Lundstrom E, Christow A, Kersemaekers W, et al. Effects of tibolone and continuous combined hormone replacement therapy on mammographic breast density. Am J Obstet Gynecol 2002;186:717-22
46. Freedman M, San Martin J, O'Gorman J, et al. Digitized mammography: a clinical trial of postmenopausal women randomly assigned to receive raloxifene, estrogen, or placebo. J Natl Cancer Inst 2001;93:51-6
47. Dowsett M, Bundred NJ, Decensi A, et al. Effect of raloxifene on breast cancer cell Ki67 and apoptosis: a double-blind, placebo-controlled, randomized clinical trial in postmenopausal patients. Cancer Epidemiol Biomarkers Prev 2001;10:961-6
48. Dunn BK, Wickerham DL, Ford LG. Prevention of hormone-related cancers: breast cancer. J Clin Oncol 2005;23:357-67
49. Gail MH, Costantino JP, Bryant J, et al. Weighing the risks and benefits of tamoxifen treatment for preventing breast cancer. J Natl Cancer Inst 1999;91:1829-46
50. Wenger NK, Barrett-Connor E, Collins P, et al. Baseline characteristics of participants in the Raloxifene Use for

The Heart (RUTH) trial. Am J Cardiol 2002;90:1204-10

51. Chlebowski RT, Collyar DE, Somerfield MR, Pfister DG. American Society of Clinical Oncology technology assessment on breast cancer risk reduction strategies: tamoxifen and raloxifene. J Clin Oncol 1999;17:1939-55
52. Chlebowski RT, Col N, Winer EP, et al. American Society of Clinical Oncology technology assessment of pharmacologic interventions for breast cancer risk reduction including tamoxifen, raloxifene, and aromatase inhibition. J Clin Oncol 2002;20:3328-43
53. National Osteoporosis Foundation. Clinician's Guide to Prevention and Treatment of Osteoporosis. National Osteoporosis Foundation, Washington, DC; 2010
54. World Health Organization. Prevention and management of osteoporosis. World Health Organ Tech Rep Ser 2003;921:1-164
55. Stevenson JC. Hormone replacement therapy and cardiovascular disease revisited. Menopause Int 2009;15:55-7
56. Brufsky AM, Bosserman LD, Caradonna RR, et al. Zoledronic acid effectively prevents aromatase inhibitor-associated bone loss in postmenopausal women with early breast cancer receiving adjuvant letrozole: Z-FAST study 36-month follow-up results. Clin Breast Cancer 2009;9:77-85
57. Eidtmann H, de Boer R, Bundred N, et al. Efficacy of zoledronic acid in postmenopausal women with early breast cancer receiving adjuvant letrozole: 36-month results of the ZO-FAST Study. Ann Oncol 2010;21:2188-94
58. Van Poznak C, Hannon RA, Mackey JR, et al. Prevention of aromatase inhibitor-induced bone loss using risedronate: the SABRE trial. J Clin Oncol 2010;28:967-75
59. Russell RG, Watts NB, Ebetino FH, Rogers MJ. Mechanisms of action of bisphosphonates: similarities and differences and their potential influence on clinical efficacy. Osteoporos Int 2008;19:733-59
60. Winter MC, Holen I, Coleman RE. Exploring the anti-tumour activity of bisphosphonates in early breast cancer. Cancer Treat Rev 2008;34:453-75
61. Coleman RE, Winter MC, Cameron D, et al. The effects of adding zoledronic acid to neoadjuvant chemotherapy on tumour response: exploratory evidence for direct anti-tumour activity in breast cancer. Br J Cancer 2010;102:1099-105
62. Gnant M. Bisphosphonates in the prevention of disease recurrence: current results and ongoing trials. Curr Cancer Drug Targets 2009;9:824-33
63. Chlebowski RT, Chen Z, Cauley JA, et al. Oral bisphosphonate use and breast cancer incidence in postmenopausal women. J Clin Oncol 2010;28:3582-90
64. Rennert G, Pinchev M, Rennert HS. Use of bisphosphonates and risk of postmenopausal breast cancer. J Clin Oncol 2010;28:3577-81
65. Newcomb PA, Trentham-Dietz A, Hampton JM. Bisphosphonates for osteoporosis treatment are associated with reduced breast cancer risk. Br J Cancer 2010;102:799-802
66. Diel IJ, Jaschke A, Solomayer EF, et al. Adjuvant oral clodronate improves the overall survival of primary breast cancer patients with micrometastases to the bone marrow: a long-term follow-up. Ann Oncol 2008;19:2007-11
67. Powles T, Paterson A, McCloskey E, et al. Reduction in bone relapse and improved survival with oral clodronate for adjuvant treatment of operable breast cancer [ISRCTN83688026]. Breast Cancer Res 2006;8:R13
68. Kristensen B, Ejlertsen B, Mouridsen HT, et al. Bisphosphonate treatment in primary breast cancer: results from a randomised comparison of oral pamidronate versus no pamidronate in patients with primary breast cancer. Acta Oncol 2008;47:740-6
69. Aft R, Naughton M, Trinkaus K, et al. Effect of zoledronic acid on disseminated tumour cells in women with locally advanced breast cancer: an open label, randomised, phase 2 trial. Lancet Oncol 2010;11:421-8
70. Rack B, Juckstock J, Genss EM, et al. Effect of zoledronate on persisting isolated tumour cells in patients with early breast cancer. Anticancer Res 2010;30:1807-13
71. Swaby RF, Sharma CG, Jordan VC. SERMs for the treatment and prevention of breast cancer. Rev Endocr Metab Disord 2007;8:229-39
72. Fisher B, Costantino JP, Wickerham DL, et al. Tamoxifen for the prevention of breast cancer: current status of the National Surgical Adjuvant Breast and Bowel Project P-1 study. J Natl Cancer Inst 2005;97:1652-62
73. Vastag B. Raloxifene prevails in STAR trial, may face easier road to acceptance than previous drugs. J Natl Cancer Inst 2006;98:733-5
74. Morii H. Safety profile of raloxifene. Clin Calcium 2004;14:100-4
75. Gelber RP, Seto TB. Patient ethnicity and use of venous thromboembolism prophylaxis. Int J Qual Health Care 2006;18:23-9
76. Pasion EG, Sivananthan SK, Kung AW, et al. Comparison of raloxifene and bisphosphonates based on adherence and treatment satisfaction in postmenopausal Asian women. J Bone Miner Metab 2007;25:105-13
77. Barrett-Connor E, Cauley JA, Kulkarni PM, et al. Risk-benefit profile for raloxifene: 4-year data From the Multiple Outcomes of Raloxifene Evaluation (MORE) randomized trial. J Bone Miner Res 2004;19:1270-5
78. MacLean C, Newberry S, Maglione M, et al. Systematic review: comparative effectiveness of treatments to prevent fractures in men and women with low bone density or osteoporosis. Ann Intern Med 2008;148:197-213
79. Black DM, Delmas PD, Eastell R, et al. Once-yearly zoledronic acid for treatment of postmenopausal osteoporosis. N Engl J Med 2007;356:1809-22
80. Lyles KW, Colon-Emeric CS, Magaziner JS, et al. Zoledronic acid and clinical fractures and mortality after hip fracture. N Engl J Med 2007;357:1799-809
81. Woo SB, Hellstein JW, Kalmar JR. Narrative [corrected] review: bisphosphonates and osteonecrosis of the jaws. Ann Intern Med 2006;144:753-61
82. Odvina CV, Zerwekh JE, Rao DS, et al. Severely suppressed bone turnover: a potential complication of alendronate

therapy. J Clin Endocrinol Metab 2005;90:1294-301

83. Grey A, Cundy T. Bisphosphonates and osteonecrosis of the jaw [author reply 92]. Ann Intern Med 2006;145:791
84. Watts NB, Harris ST, McClung MR, et al. Bisphosphonates and osteonecrosis of the jaw [author reply 92]. Ann Intern Med 2006;145:791-2
85. Mavrokokki T, Cheng A, Stein B, Goss A. Nature and frequency of bisphosphonate-associated osteonecrosis of the jaws in Australia. J Oral Maxillofac Surg 2007;65:415-23
86. Michalska D, Stepan JJ, Basson BR, Pavo I. The effect of raloxifene after discontinuation of long-term alendronate treatment of postmenopausal osteoporosis. J Clin Endocrinol Metab 2006;91:870-7
87. Martino S, Disch D, Dowsett SA, et al. Safety assessment of raloxifene over eight years in a clinical trial setting. Curr Med Res Opin 2005;21:1441-52
88. Blumenthal RS, Baranowski B, Dowsett SA. Cardiovascular effects of raloxifene: the arterial and venous systems. Am Heart J 2004;147:783-9
89. Nanetti L, Camilletti A, Francucci CM, et al. Role of raloxifene on platelet metabolism and plasma lipids. Eur J Clin Invest 2008;38:117-25
90. Stefanick ML. Risk-benefit profiles of raloxifene for women. N Engl J Med 2006;355:190-2
91. Pines A. Postmenopausal hormone therapy: the way ahead. Maturitas 2007;57:3-5
92. Jordan VC. Chemosuppression of breast cancer with tamoxifen: laboratory evidence and future clinical investigations. Cancer Invest 1988;6:589-95
93. Cummings SR, Ensrud K, Delmas PD, et al. Lasofoxifene in postmenopausal women with osteoporosis. N Engl J Med 2010;362:686-96
94. Pinkerton JV, Stovall DW. Bazedoxifene when paired with conjugated estrogens is a new paradigm for treatment of postmenopausal women. Expert Opin Investig Drugs 2010;19:1613-21
95. Cummings SR, Ettinger B, Delmas PD, et al. The effects of tibolone in older postmenopausal women. N Engl J Med 2008;359:697-708
96. Beral V. Breast cancer and hormone-replacement therapy in the Million Women Study. Lancet 2003;362:419-27
97. Mueck AO, Lippert C, Seeger H, Wallwiener D. Effects of tibolone on human breast cancer cells and human vascular coronary cells. Arch Gynecol Obstet 2003;267:139-44
98. Lewis JS, Meeke K, Osipo C, et al. Intrinsic mechanism of estradiol-induced apoptosis in breast cancer cells resistant to estrogen deprivation. J Natl Cancer Inst 2005;97:1746-59
99. Jordan VC, Lewis-Wambi JS, Patel RR, et al. New hypotheses and opportunities in endocrine therapy: amplification of oestrogen-induced apoptosis. Breast 2009;18(Suppl 3):S10-17
100. Anderson GL, Limacher M, Assaf AR, et al. Effects of conjugated equine estrogen in postmenopausal women with hysterectomy: the Women's Health Initiative randomized controlled trial. JAMA 2004;291:1701-12

Affiliation

Seung Sang Ko[1,2] MD PhD &
V Craig Jordan[†3] OBE PhD DSc FMedSci
[†]Author for correspondence
[1]Visiting professor,
Georgetown University Medical Center,
Lombardi Comprehensive Cancer Center,
Department of Oncology,
3970 Reservoir Rd NW.,
Research Building,
Suite E204 A,
Washington, DC 20057, USA
[2]Associate professor,
Kwandong University College of Medicine,
Cheil General Hospital,
Department of Surgery,
1-19 Mukjeong-dong Jung-gu
Seoul (Seoul 100-380 Korea)
[3]Scientific Director,
Lombardi Comprehensive Cancer Center,
Georgetown University Medical Center,
Vincent T. Lombardi Chair of Translational Cancer Research,
Vice Chair of Department of Oncology,
Professor of Oncology and Pharmacology,
3970 Reservoir Rd NW.,
Research Building, Suite E501,
Washington, DC 20057, USA
Tel: +1 202.687.2897; Fax: +1 202.687.6402;
E-mail: vcj2@georgetown.edu

Chapter 26

Omics-Based Molecular Target and Biomarker Identification

Zhang-Zhi Hu, Hongzhan Huang, Cathy H. Wu, Mira Jung, Anatoly Dritschilo, Anna T. Riegel, and Anton Wellstein

Abstract

Genomic, proteomic, and other omic-based approaches are now broadly used in biomedical research to facilitate the understanding of disease mechanisms and identification of molecular targets and biomarkers for therapeutic and diagnostic development. While the Omics technologies and bioinformatics tools for analyzing Omics data are rapidly advancing, the functional analysis and interpretation of the data remain challenging due to the inherent nature of the generally long workflows of Omics experiments. We adopt a strategy that emphasizes the use of curated knowledge resources coupled with expert-guided examination and interpretation of Omics data for the selection of potential molecular targets. We describe a downstream workflow and procedures for functional analysis that focus on biological pathways, from which molecular targets can be derived and proposed for experimental validation.

Key words: Proteomics, Genomics, Bioinformatics, Biological pathways, Cell signaling, Databases, Molecular targets, Biomarkers

1. Introduction

Biomarkers are referred to as biological entities or characteristics that can be used to indicate the states of healthy or diseased cells, tissues, or individuals. Nowadays, biomarkers are mostly molecular makers, such as genes, proteins, metabolites, glycans, and other molecules, that can be used for disease diagnosis, prognosis, prediction of therapeutic responses, as well as therapeutic development (1–3). Over the past decade, high-throughput technologies, such as genomic microarrays, proteomic and metabolomic mass spectrometry, have been used to generate large amount of data from single experiments that allow for global comparison of changes in molecular profiles that underlie particular cellular phenotypes. As a result, the omics-based approaches,

Bernd Mayer (ed.), *Bioinformatics for Omics Data: Methods and Protocols*, Methods in Molecular Biology, vol. 719,
DOI 10.1007/978-1-61779-027-0_26, © Springer Science+Business Media, LLC 2011

coupled with computational and bioinformatics methods, provide unprecedented opportunities to speed up the biomarker discovery and now are widely used to facilitate diagnostic and therapeutic developments for many diseases and particularly in cancers (4–10). Potential biomarkers have been identified at various molecular levels, including genetic, mRNA, protein/peptide, as well as epigenetic (11), miRNA (12), glycans (13), and metabolites (4). For example, using DIGE-based proteomics potential biomarkers (e.g., PPA2 and Ezrin) were identified to be useful for the diagnosis of metastatic prostate cancer (14), and a proteolytic fragment of alpha1-antitrypsin (BF5) was identified as a potential diagnostic and prognostic marker for inflammatory breast cancer as well as a target for potential therapeutic intervention (15, 16). Epigenetic marker, such as PITX2 DNA methylation, is reported as a robust assay for paraffin-embedded tissue for outcome prediction in early breast cancer patients treated by adjuvant tamoxifen therapy (11). In addition, microRNAs, such as miR-500, were identified as a potential diagnostic marker for hepatic cell carcinoma (17).

Increasingly, pathway and network-based analyses are applied to Omics data to gain more insight into the underlying biological function and processes, such as cell signaling and metabolic pathways and gene regulatory networks (18, 19). For example, 12 core signaling pathways were shown to be altered in human pancreatic cancers through genomic analyses (18). Network modeling linked breast cancer susceptibility to the centrosome dysfunction (20), and led to the identification of a proliferation/differentiation switch in cellular networks of multicellular organisms (21). These approaches have led to a new trend in identifying biomarkers in recent years, namely, pathway and network-based biomarker discovery, which identify panels of, instead of single, biomarkers for practical use in diagnostic and therapeutic developments (22–24). Protein networks have been shown to provide a powerful source of information for disease classification and to help in predicting disease causing genes (25, 26). Network approaches have also been used for improving the prediction of cancer outcome (27, 28), providing novel hypotheses for pathways involved in tumor progression (28), and exploring cancer-associated genes (29).

In this chapter, we focus on the methodology for the identification of molecular targets through functional Omics data analysis particularly of biological pathways, which can provide more mechanistic insights into the underlying phenotypes and may facilitate therapeutics development. We adopt a strategy that emphasizes the use of curated knowledge resources, and describe a workflow and procedures, coupled with expert-guided analysis and interpretation, for the selection of potential molecular targets.

2. Materials

Despite the rapid advancement of the high-throughput technologies and the bioinformatics tools, the functional analysis and interpretation of Omics data remain challenging due to high variation, low reproducibility, and noise of the data. Although many algorithms and tools have been developed to address these challenges, much is inherent to the long workflows of the Omics experiments, e.g., from sample preparation and raw data acquisition, to data processing and analysis. Many statistical and machine learning methods have been developed for better partitioning or clustering of genes (30–33), however, understanding of the biological meaning and functional interpretation of the group of genes/proteins are critical downstream steps in the Omics workflow, and are necessary for the design of therapeutic strategies. This downstream functional analysis relies heavily on existing knowledge annotated for genes or proteins and frequently requires expert-guided analysis for appropriate interpretation.

2.1. Bioinformatics Databases

Annotations of genes and proteins integrated from multiple bioinformatics databases are the basis for functional analysis and interpretation of Omics data (34). Numerous gene and protein databases, varying in size and scope, have been developed to provide functional annotations for genes and gene products, as archived for the past decade, e.g., in the "Molecular Biology Database Collection" in the journal *Nucleic Acids Research* (35). The number of databases and database entries is rapidly growing, e.g., in 2009 the journal archived a total of 1,170 databases, nearly 100 more than in 2008. These databases are divided into 14 general categories, including databases of DNA, RNA and protein sequences, structure, genomics, proteomics, metabolic, and signaling pathways. Databases most relevant to Omics data analyses include: (1) Gene and protein databases, such as UniProt (36) for protein-based annotations, Entrez Gene (37) and model organism databases (e.g., Mouse Genome Database) (38) for gene-based annotations; (2) GO annotations, such as GOA for annotation of gene products with Gene Ontology (GO) terms (39); (3) Biological pathways, such as KEGG (40) and Pathway Interaction Database (PID) (41) for annotations of proteins involved in metabolic and signaling pathways; Pathway Commons has been developed as a single point of access for diverse pathway databases; and (4) Protein–protein interaction (PPI) databases, such as IntAct (42) and MINT (43) for annotations of proteins involved in physical interaction of proteins.

2.2. Data Mapping and Integration Tools

Mapping different Omics data types (e.g., gene, mRNA, peptide/protein, metabolite) to the common biological entities (e.g., proteins) is an essential step for deriving comprehensive

annotations for functional Omics data analysis (34). Omics data mapping is accomplished most commonly by ID (database entry identifier) mapping that allows different but related biological entities to be mapped to the IDs of common entities (e.g., proteins). One of the most common issues in protein mapping is that the relation between different types of biological entity could be one-to-one (e.g., one gene ID to one protein ID) or one-to-many (e.g., one gene ID to two or more protein IDs), and this is not only caused by the difference between genes and proteins (e.g., one gene encodes several protein isoforms), but can also result from database redundancy (see Note 1). UniProt Knowledgebase (UniProtKB) is the main section of UniProt with comprehensive and high-quality protein sequence annotations (44), and iProClass is an integrated database for all UniProt protein sequences with value-added annotations integrated from over 100 other databases (45). The UniProt and iProClass databases thus serve as the underlying infrastructure for protein ID mapping (different IDs mapped to UniProtKB protein IDs) and data integration for experimental Omics data. ID mapping based on the two databases allows ~32 commonly used, heterogeneous IDs to be converted from each other and the ID mapping services are available online both at the Protein Information Resource (PIR) (http://pir.georgetown.edu) and UniProt (http://www.uniprot.org). ID mapping data files are also available at PIR for download to perform data mapping offline. Other ID mapping tools include DAVID gene ID conversion tool (http://david.abcc.ncifcrf.gov/conversion.jsp) (46) and Protein Identifier Cross-Reference Service (PICR, http://www.ebi.ac.uk/Tools/picr) (47).

2.3. Functional Profiling and Pathway Analysis Tools

Various bioinformatics tools are available for functional profiling of Omics data based on annotations of genes and proteins, such as PIR batch retrieval and functional categorization tool (http://pir.georgetown.edu/pirwww/search/batch.shtml), iProXpress (http://pir.georgetown.edu/iproxpress) (34), DAVID (48), and BABELOMICS (http://babelomics.bioinfo.cipf.es) (49). Annotations used for profiling by these tools include GO terms, pathways, keywords, sequence features, and families, among which GO terms and pathways are the most commonly used: GO has become a common annotation standard, and pathways provide more insightful biological meaning for the data. Moreover, many concepts in other annotations, such as keywords, have been covered by GO terms. While most of these tools allow profiling of single gene/protein list or two for comparison, iProXpress provides comparative profiling of multiple data sets (or data groups) for cross-data sets comparison, a very useful feature that accommodates many real-world data analysis issues.

For pathway analysis, mapping experimental data to metabolic and signaling pathways is a key for functional interpretation of the Omics data. Curated canonical pathway maps are available in many pathway databases, however, few public Omics analysis tools integrate the maps into their systems to allow experimental data superimposed onto the pathway maps. Several commercial pathway analysis systems are available, such as Ingenuity IPA (http://www.ingenuity.com) and GeneGO MetaCore (http://www.genego.com). Although these tools differ in features, such as visualization of canonical pathways and presentation of experimental data mapped onto the pathways, they all have one feature in common, i.e., integration of additional pathway and functional association data manually curated from literature into the systems in addition to the publicly available data in pathway databases, such as KEGG and PID.

2.4. Literature Text Mining Tools

Despite the extensive use of annotations from current knowledgebase for functional analysis of Omics data, annotations of genes and proteins lag far behind the rapid growth of literature due to the ever-expanding sequence data and the laborious nature of manual curation. In nearly all Omics experiments, varying numbers of identified genes or proteins lack sufficient annotations in databases to be functionally analyzed, and in such cases literature becomes the critical source for deriving functional information. Although literature data have been used solely or combined with other Omics data to generate gene/protein association networks (50–52), currently no literature mining tools have been integrated into any pipelined Omics system in a fashion that computationally extracted data are directly used as annotations for functional data analysis. Nonetheless, literature text mining is an important component of the data analysis workflow, and has been used to assist pathway analysis, such as ResNet of Pathway Studio (53) (http://www.ariadnegenomics.com/products/databases/ariadne-resnet). A variety of text mining tools are available to assist in mining relevant gene or protein data from literature, and this coupled with manual search of PubMed are often necessary for functional Omics data analyses (see Note 2).

3. Methods

The pathway and network-based Omics data analysis approach aims to delineate molecular maps that underlie the changes in biological samples under investigation, and to aid in discovery of molecular targets and biomarkers for diagnostic and therapeutic developments. Below we describe practical procedures applied to analyses of Omics data related to cell signaling and metabolic pathways, as well as organelle biogenesis.

3.1. Omics Data Analysis Workflow

We focus on downstream analytical steps of the Omics workflow leading to functional interpretation of Omics data. The workflow begins with a list of gene or protein identifiers or peptide sequences as results from upstream data processing and analysis, e.g., gene clusters or differentially expressed genes or proteins and follows steps 1–6 depicted in Fig. 1: The genes or proteins in the list are then mapped to UniProtKB protein identifiers (step 1). Next, functional annotations are derived for the list of genes or proteins (step 2) based on integrated data from multiple bioinformatics databases (step 4), including text mining of literature for information that has not yet been annotated in databases (step 5). Steps 4 and 5 make maximal use of public knowledge resources. Functional analyses are often conducted using several approaches (step 3) based on different types of knowledge annotated in bioinformatics databases, i.e., GO profiling, molecular networks, and biological pathways. Among them, GO profiling, while revealing limited biological insights into Omics data, usually covers most of the genes/proteins under analysis (see Note 3). By contrast, while

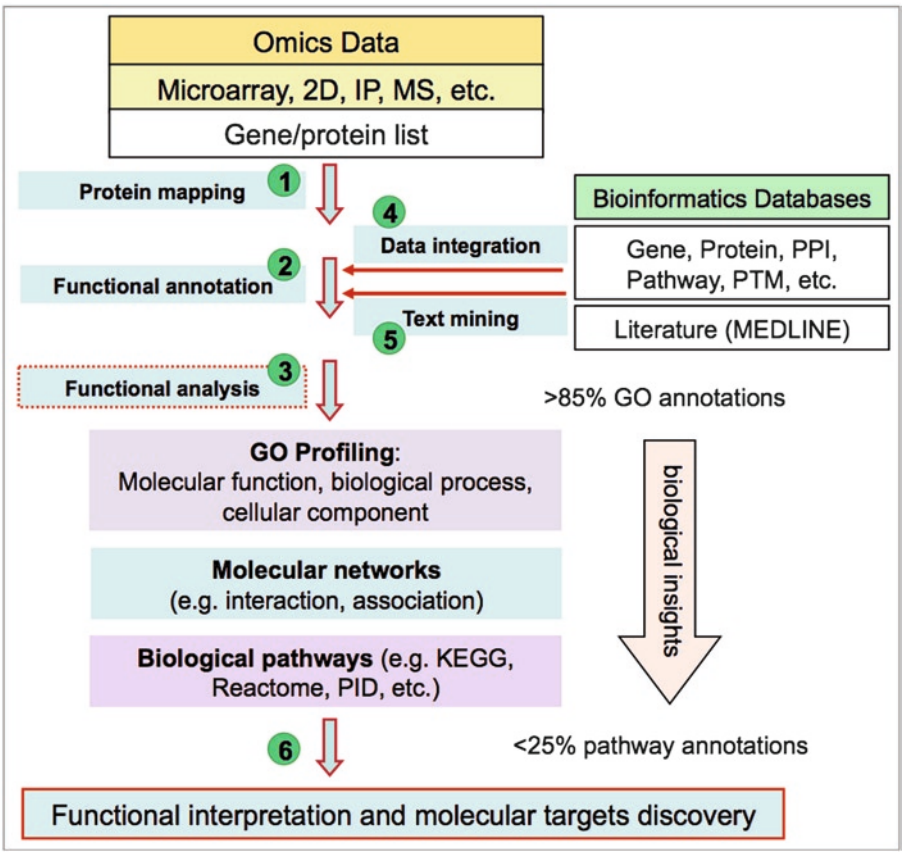


Fig. 1. A downstream functional analysis workflow for molecular target and biomarker discovery from Omics data.

giving more biological insights, pathway analysis is limited by low coverage of proteins annotated in known canonical pathways (see Note 4). In between the GO profiling and pathway mapping is molecular network analysis of interactions or functional associations between genes or proteins. Finally, molecular targets are inferred from the functional analysis (step 6).

3.2. Omics Data Grouping

Omics experiments are often carried out under various experimental conditions, from which differential patterns of gene or protein expressions are to be analyzed and potential molecular targets are sought. To assist the subsequent bioinformatics analysis, genes or proteins associated with different experimental conditions are divided into appropriate data groups and assigned with proper notations (Table 1). Although there is no fixed scheme for assignment, the notations usually clearly distinguish the key conditions under which each experiment is carried out and/or data are collected for given studies. There are additional considerations in Omics data grouping in the case of proteomic data (see Note 5).

Table 1
Proteomics data grouping based on experimental design and methods

	Common types	Examples
Experimental group	Treatment	−/+ Radiation; −/+ Estrogen (E2)
	Time course	One time point or multiple (30 m, 1 h, 3 h, 9 h…)
	Cell types	ATCL8 and AT5BIVA (Ref. 54); MCF-7 and MCF-7:5C (Ref. 59)
	Immunoprecipitation (IP)	Phosphotyrosine (pY) IP; AIB1 IP
	Sample separation	1D or 2D gel electrophoresis
	Mass spectrometry (MS)	Single MS; tandem MS (MS/MS)
	Data type	Proteomics; mRNA expression microarray
	Changes	Increased or decreased
Notations for groups		*A_8_3h_increase* – Increased on 2D-gel at 3h postradiation in ATCL8 cells *MS2AIB1_A* – Identified in lane A using anti-AIB1 IP and MS/MS (MS2) in MCF-7 cells (−) E2
Experimental notes		"ATCL8 6.413, 8-pep, 3 h" – Increased by 6.413-fold on 2D-gel and identified with 8 peptides, at 3 h in ATCL8 cells "B11 30K 24K 100 CI90" – Identified in lane B of 1D-gel, band 11 of MW 30 kDa, calculated MW 24 kDa, a score 100 and CI > 90%

3.3. Omics Data Mapping and Integration

Since the UniProt and iProClass databases are the data warehouse of the iProXpress system and serving as the underlying infrastructure for Omics data mapping and integration, the list of genes or proteins from Omics data are mapped to UniProtKB protein entries, referred to as *protein mapping*, to obtain functional annotations. Protein mapping is primarily based on gene/protein identifiers. For gene expression microarray data, commonly used gene identifiers include Entrez Gene ID, NCBI gi number, and Refseq ID. For mass spectrometry (MS) proteomic data, depending on the database selected for protein identification by the search engine (e.g., MASCOT), the commonly used identifiers include UniProtKB, IPI, NCBI nr, Refseq, etc. Gene and protein IDs are mapped to UniProtKB entries based on comprehensive ID mapping tools available at PIR or UniProt, which converts commonly used gene and protein IDs (such as NCBI's gi number and Entrez Gene ID) to UniProtKB IDs and vice versa. After protein mapping, all gene or protein IDs from one or more data sets or experimental groups are integrated into a master list of UniProtKB identifiers (ACs or IDs), each associated with corresponding experimental groups and notes (Table 1). This master list of proteins is the basis for the subsequent functional annotation and analysis using the iProXpress system.

Frequently, UniProtKB entry matches are not found for a fraction of input gene or protein identifiers, resulting from updates of database identifiers or deletion of entries occurring to most databases, especially when analyzing legacy data in which mixed database identifiers are often used. In such cases, the mapping can be based on sequence comparison or name mapping if the sequence is not available. For genes, the sequence identity and taxonomy information may be used to map the gi numbers to UniProtKB IDs in addition to the mapping bridged by EMBL/GenBank protein accessions (34). For MS proteomic data, peptide sequences are matched against all sequences in UniProtKB (see Note 6).

When gene microarray and MS proteomic experiments are conducted on the same biological samples under identical or similar conditions, the two Omics data sets are compared after data being merged through protein mapping. Direct comparison of expression at both mRNA and protein levels can provide stronger evidences for the underlying changes. For example, the 2D-gel/MS proteomics study identified 412 and 771 proteins that potentially changed in response to radiation treatment in ATM (Ataxia Telangiectasia Mutated) mutated (ATM^-) and wild type (ATM^+) cells, respectively, while the gene microarray study identified 103 and 131 significantly changed genes in the two cells, respectively (54). Among those genes/proteins, only 13 were commonly identified, including RRM2, the catalytic subunit of ribonucleoside-diphosphate reductase (RR), a rate-limiting

enzyme required for synthesis of dNDP and thus of DNA synthesis in human (55). However, care should be taken in mapping data from genes to proteins due to one-to-many relations and redundancy existing in the UniProt database (see Note 1).

3.4. The Omics Data Annotation and Functional Profiling

3.4.1. Metadata Annotation

As discussed above, the experimental groups in which the genes or proteins are identified, as well as additional experimental information are annotated for all proteins with proper notations. The annotated data groups are used for direct comparative analysis between selected groups of interest, such as cell types, treatment types and time course, as well as Omics data types. The metadata annotation can also be used for limiting functional profiling to proteins in selected groups using the iProXpress interface (see below).

3.4.2. Functional Annotation

After protein mapping, rich annotations are described for given Omics data sets in the so-called protein information matrix (Table 2) that captures salient features of proteins, such as functions, pathways, and protein–protein interactions, derived from

Table 2
Major categories of a protein information matrix

Major category	Example data sources[a]
General information	
Protein name	UniProtKB, RefSeq
Taxonomy	NCBI Taxon
Gene name	UniProtKB
Keywords	UniProtKB
Function	UniProtKB
Subunit	UniProtKB
Tissue specificity	UniProtKB
Bibliography	UniProtKB, SGD, GeneRIF
Gene-related information	
Genome/gene	GenBank, Entrez Gene, MGI
Gene expression	GEO, CleanEx
Genetic variation/disease	HapMap, OMIM
Gene regulation	ISG
Protein function-related information	
Ontology	GOA
Enzyme/function	KEGG, BRENDA, MetaCyc
Pathway	KEGG, EcoCyc, PID, Reactome
Complex/interaction	IntAct, DIP
Protein expression	Swiss-2DPAGE, PMG
Structure	PDB, SCOP, CATH
Feature and posttranslational modifications	UniProtKB, RESID, PhosphoSite
Protein family	PIRSF, Pfam, COG, InterPro

[a] Detailed data sources are available at http://pir.georgetown.edu/cgi-bin/iproclass_stat

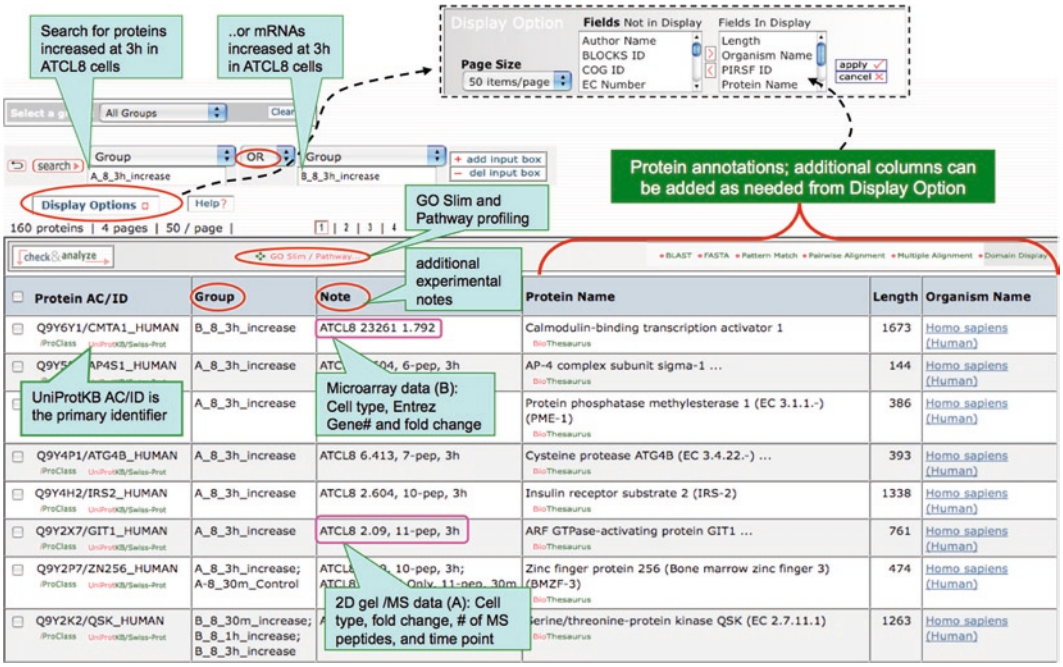


Fig. 2. iProXpress interface for browsing, searching, and functional profiling of Omics data. As an example, the interface displays the proteomic data sets derived from 2D gel and mass spectrometry as well as the gene expression microarray data sets from ATM⁻ (AT5BIVA) and ATM⁺ (ATCL8) human fibroblast cells (54).

comprehensive protein annotations integrated into the UniProt and iProClass databases. The matrix allows for browsing and search of rich protein information through the iProXpress Web interface, which facilitates detailed examination of the Omics data (Fig. 2). Among protein annotations, GO terms, including *molecular function, biological process and cellular component*, and pathways, such as KEGG, are most commonly used for functional profiling.

3.4.3. GO Profiling

Gene Ontology profiling is primarily based on GO slim, a cut-down version of GO terms at high levels of GO hierarchy (http://www.geneontology.org/GO.slims). GO slims are usually derived from terms at second and third levels of the GO hierarchy, though varying from sources to sources in the selection of additional terms from deeper levels. GO profiling provides a general view of biology underlying the Omics data and can suggest significant functional categories of genes or proteins that can be further investigated. For example, 26 genes are found upregulated in ionizing radiation treated ATM⁺ cells, which were identified from gene expression microarray data and were profiled using GO *biological process* (Fig. 3). The profile shows high representation of proteins in GO categories, such as "cell communication,"

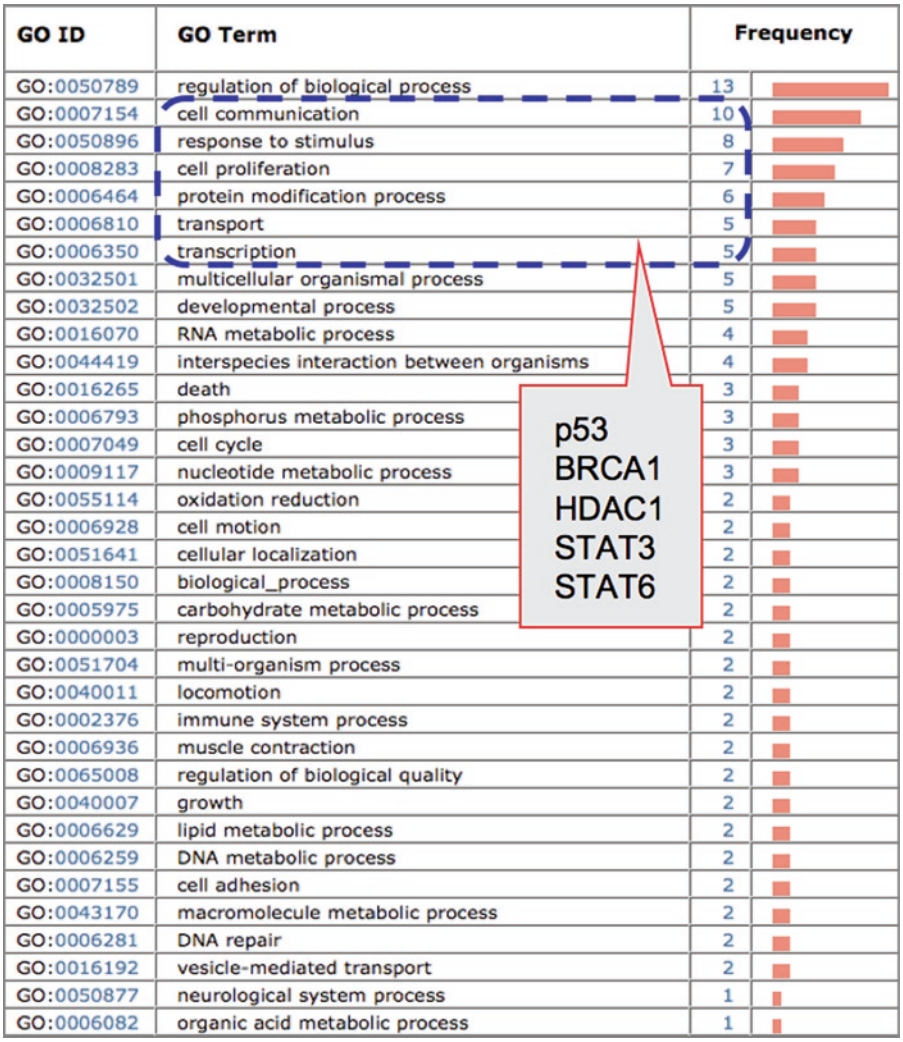


Fig. 3. GO *biological process* profiling of upregulated genes in ATCL8 cells (ATM^+) at 30 min postirradiation. A total of 26 differentially expressed genes are profiled and the GO categories are ranked based on the number of proteins annotated with the corresponding GO terms (frequency); categories with only one protein are partially displayed at the *bottom*. *Encircled* in *dashed line* are top six categories of GO terms that cover 77% of the proteins (20/26), e.g., five genes appearing in three to five GO categories (in the *box*).

"response to stimulus," and "cell proliferation," in which several proteins are known to be involved in radiation-induced responses, e.g., BRCA1, p53, HDAC1, and STAT3. Because GO slims are terms of high level, genes/proteins profiled under given GO categories often overlap to varying degrees, e.g., the above mentioned proteins are common in three or more of the top five GO categories (Fig. 3). However, some terms are too broad, such as "regulation of biological process" or "biological regulation" to reveal meaningful biological information (see Note 7).

3.4.4. Pathway Profiling

Due to the overall low coverage of pathway annotations for a given organism, relatively large numbers of proteins are usually missed in pathway profiling for any Omics data set. Nonetheless, it could provide significant insights into the underlying biology, particularly when used for cross-data set comparative profiling. For example, in our previous study, comparison of nine organelle proteomes, including mitochondria, endoplasmic reticulum (ER), and seven other lysosome-related organelles (56), the pathway profiles based on KEGG pathways show that "oxidative phosphorylation pathway" is prevalent in mitochondria while "N-glycan biosynthesis pathway" is in the ER (Fig. 4), which are consistent with the well-established functions of the two organelles. Pathway profiling also led to the identification of "purine metabolism pathway" that showed notable differences between radiation-treated vs. untreated ATM$^-$ and ATM$^+$ cells (Fig. 5a) (54).

KEGG Pathway Statistics

ER

Mit

Show Selected

Pathway ID	Pathway Term	ED	ER	EX	LY	ME	MI	NG	PL	SY	All
PATH:hsa00010	Glycolysis / Gluconeogenesis			1		2	1			2	4
PATH:hsa00020	Citrate cycle (TCA cycle)	1	1	4		4	17		6	4	19
PATH:hsa00030	Pentose phosphate pathway	1	2	4		7	3		2	2	10
PATH:hsa00031	Inositol metabolism						1				1
PATH:hsa00040	Pentose and glucuronate interconversions	1		3	1	3	2				5
PATH:hsa00051	Fructose and mannose metabolism								1		1
PATH:hsa00061	Fatty acid biosynthesis						1				1
PATH:hsa00062	Fatty acid elongation in mitochondria		1		2	1	3	1	1		5
PATH:hsa00071	Fatty acid metabolism						2				2
PATH:hsa00100	Biosynthesis of steroids		5			4	1				7
PATH:hsa00120	Bile acid biosynthesis		2								2
PATH:hsa00130	Ubiquinone biosynthesis						8				8
PATH:hsa00140	C21-Steroid hormone metabolism		2				1				3
PATH:hsa00150	Androgen and estrogen metabolism	3	6		1		4				8
PATH:hsa00190	Oxidative phosphorylation		8		1	12	65		2	1	67
PATH:hsa00193	ATP synthesis	2	4		7	17	16	7	4	3	27
PATH:hsa00220	Urea cycle and metabolism of amino groups			1			1				2
PATH:hsa00230	Purine metabolism	5	1	1	1	7	8		7	2	24
PATH:hsa00240	Pyrimidine metabolism					3	5			1	8

Mit

…pathways partially omitted …

PATH:hsa00362	Benzoate degradation via hydroxylation	1	2				1				2
PATH:hsa00380	Tryptophan metabolism	1	2								2
PATH:hsa00400	Phenylalanine, tyrosine and tryptophan biosynthesis			1		3	1		1	2	3
PATH:hsa00440	Aminophosphonate metabolism		1								1
PATH:hsa00450	Selenoamino acid metabolism	1									1
PATH:hsa00500	Starch and sucrose metabolism				1	1		1			2
PATH:hsa00510	N-Glycan biosynthesis		14	1	3	8		1	3		17
PATH:hsa00530	Aminosugars metabolism	1	3		2	3	3		3		11
PATH:hsa00534	Heparan sulfate biosynthesis		5		1						6
PATH:hsa00561	Glycerolipid metabolism		1			1				1	2
PATH:hsa00562	Inositol phosphate metabolism	2	2			1	1	1	2		5
PATH:hsa00563	Glycosylphosphatidylinositol(GPI)-anchor biosynthesis		1								1
PATH:hsa00564	Glycerophospholipid metabolism				1	2	3		1		6
PATH:hsa00565	Ether lipid metabolism		2			2					4
PATH:hsa00590	Arachidonic acid metabolism	4	12		2	2	3	1	1		19
PATH:hsa00600	Sphingolipid metabolism	1	7		4	6		2			14

ER

Fig. 4. Comparative profiling of organellar proteomes using KEGG pathways. Proteomes of nine organelles (56) are profiled using KEGG pathways. Although only a small portion of the proteome is covered by the KEGG pathways, the profiles show striking contrast between organelles, e.g., endoplasmic reticulum (ER) and mitochondria (Mit) enriched for "oxidative phosphorylation" and "N-Glycan biosynthesis" pathways (*encircled* on the *left*), respectively.

a

KEGG Pathway Statistics

Pathway ID	Pathway Term	ATM⁻ cell down	ATM⁻ cell up	ATM⁺ cell down	ATM⁺ cell up	All
PATH:hsa00010	Glycolysis / Gluconeogenesis	1	1	1	2	5
PATH:hsa00020	Citrate cycle (TCA cycle)				1	1
PATH:hsa00030	Pentose phosphate pathway		1			1
PATH:hsa00040	Pentose and glucuronate interconversions				1	1
PATH:hsa00051	Fructose and mannose metabolism			2	1	3
PATH:hsa00052	Galactose metabolism			1	1	2
PATH:hsa00053	Ascorbate and aldarate metabolism				1	1
PATH:hsa00061	Fatty acid biosynthesis				1	1
PATH:hsa00062	Fatty acid elongation in mitochondria	1				1
PATH:hsa00071	Fatty acid metabolism	1				1
PATH:hsa00072	Synthesis and degradation of ketone bodies				1	1
PATH:hsa00120	Bile acid biosynthesis				1	1
PATH:hsa00150	Androgen and estrogen metabolism				1	1
PATH:hsa00190	Oxidative phosphorylation			1		1
PATH:hsa00220	Urea cycle and metabolism of amino groups			1		1
PATH:hsa00230	Purine metabolism	4	2		4	10
PATH:hsa00240	Pyrimidine metabolism	2	1	1	2	6
PATH:hsa00251	Glutamate metabolism				1	1
PATH:hsa00252	Alanine and aspartate metabolism		1		1	1
PATH:hsa00260	Glycine, serine and threonine metabolism			1	1	2
PATH:hsa00271	Methionine metabolism		1			1
PATH:hsa00272	Cysteine metabolism	1				1

b

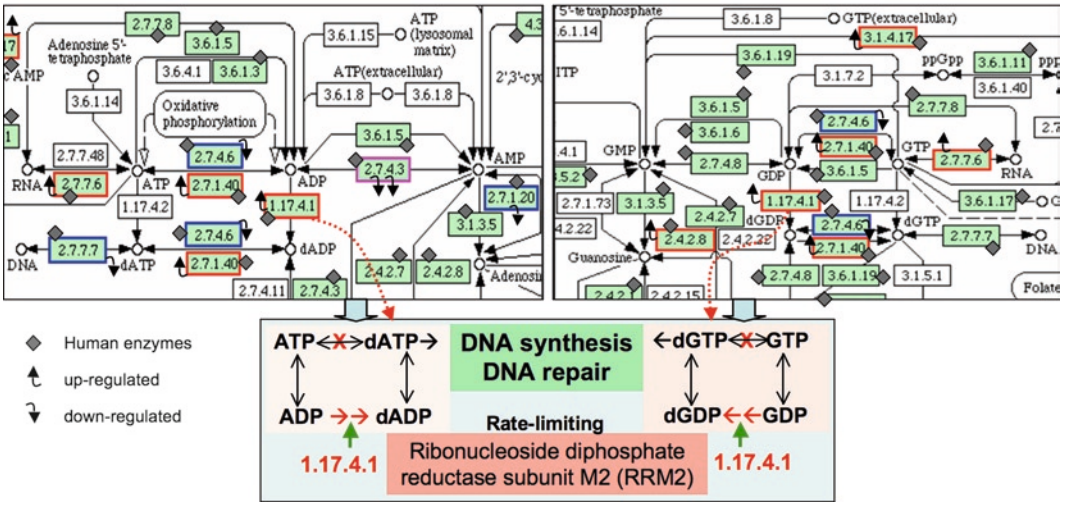


Fig. 5. (**a**) KEGG pathway profiling of radiation-induced protein expression changes in ATM mutated (ATM⁻) and ATM wild type (ATM⁺) cells at 3 h postirradiation. The "purine metabolism" pathway is *encircled* and it shows that the most differentially changed proteins (up- or downregulated in response to radiation in the two cells) is found in this pathway. This profile is a partial display, with the rest having small number of proteins and no striking differences between groups. The figure is adapted from Hu et al. (54). (**b**) Mapping of radiation-induced protein changes onto the purine metabolic pathway. Enzymes in the KEGG reference map are represented using Enzyme Commission numbers (EC#, e.g., 1.17.4.1). Enzymes labeled with a *diamond shape* are those identified in human, and all others without such a label are those known to be absent in human. Enzymes with *up-tilted arrows*, upregulated in ATM⁺ cells; those with *down-tilted arrows*, downregulated in ATM⁻ cells; the enzyme with *double down-tilted arrows* are downregulated in both cells. *Upper left*, biochemical steps surrounding dADP/dATP; *upper right*, biochemical steps surrounding dGDP/dGTP; *bottom*, illustration of the rate-limiting step in dATP or dGTP synthesis from the reduction of ADP or GDP, respectively, catalyzed by RRM2 in human.

3.5. Pathway Mapping and Visualization

One key step in functional Omics data analysis is pathway mapping, a process that maps genes/proteins detected by Omics experiments to corresponding proteins annotated in canonical pathways. Various software tools are available for pathway mapping, including iProXpress, DAVID, and commercial tools, such as IPA (http://www.ingenuity.com) and MetaCore (http://www.genego.com). Visualization of the mapped pathways greatly facilitates the comparative analysis and understanding of the underlying differences across experimental groups, thus being critical for identifying potential molecular targets. Visualization of mapped pathways is provided as part of several software systems, e.g., mapped proteins in canonical pathways are highlighted by a distinct color (for one experimental condition as in IPA) or labeled with experimental conditions under which they were detected (as in MetaCore). Recently, KEGG developed a standalone tool, KegArray, for mapping gene expression profiles to pathways and genomes (57).

Different pathway tools should be used to maximize the identification of potential pathway-based targets because pathways annotated in different databases vary in their contents and boundaries (see Note 8). We used iProXpress, KEGG, IPA, and MetaCore pathway tools for mapping and/or visualization of metabolic and signaling pathways in several proteomic and functional genomic studies, including those on organelle biogenesis (58), radiation-induced DNA damage repair (54), and estrogen-induced apoptosis in breast cancer cells (59). Pathway mapping could lead to the identification of specific steps in which the proteins participate and the roles they may play.

3.6. Literature Mining

For genes or proteins of interest that were derived from the Omics data based on differential expression and/or functional profiling, but do not have annotated pathway information, literature mining is used to uncover their potential associations with or pathways for the underlying phenotypes. Various text mining tools are available to assist literature mining (see Note 2).

3.7. Practical Applications

3.7.1. Examples

We use the functional analysis of Omics data generated from radiation-treated ATM$^-$ and ATM$^+$ cells (54) as an example to illustrate the Omics workflow described above. ATM, a serine–threonine protein kinase, plays critical roles in stress-induced responses, such as DNA damage repair and cell cycle regulation. Using human fibroblast cell lines expressing mutated ATM gene (AT5BIVA cell, ATM$^-$) or wild type ATM (ATCL8 cell, ATM$^+$), the study aims to better understand ATM-mediated pathways in response to ionizing radiation, which could facilitate identification of molecular targets for therapeutic interventions, such as increasing radiation or drug sensitivities of cancers. The two cell lines are subjected to global expression profiling using gene

microarray and 2D-gel and MS proteomics. Below are the steps used for the analysis.

1. Proteins identified from the MASCOT search engine (http://www.matrixscience.com) output files are compiled into one protein list and annotated with corresponding experimental groups (e.g., cells and time points). The database searched by MASCOT is SwissProt (a manually annotated portion of the UniProtKB). The differentially changed genes (up- or down-regulated genes from the microarray) are mapped to UniProtKB accessions (ACs) from Entrez Gene IDs.
2. Some UniProtKB ACs in the protein list from the MASCOT output might need replacement by new ACs (but usually still identify the same protein sequence) if the bioinformatics analysis is conducted at a time later than MS when UniProtKB has newer releases, in which protein sequences may be updated/corrected or redundant sequences be merged. Updated ID mapping files can be downloaded at ftp://ftp.pir.georgetown.edu/databases/idmapping/idmapping.tb.gz and used to obtain an updated experimental protein list. Alternatively, online ID mapping is available at PIR (http://pir.georgetown.edu) or UniProt (http://www.uniprot.org).
3. Functional annotations of the protein list are derived from the iProClass database containing comprehensive annotations, which is available for download at ftp://ftp.pir.georgetown.edu/databases/iproclass/iproclass.xml.gz. An output data file that contains all identified proteins, corresponding groups and experimental notes, as well as functional annotations is generated.
4. The data file is browsed, searched, and profiled using the iProXpress interface: http://pir.georgetown.edu/iproxpress (data set: http://pir.georgetown.edu/cgi-bin/textsearch_iprox.pl?data=gu1). Boolean searches (AND, OR, NOT) can be used to display specific experimental groups or proteins pertinent to certain annotations, e.g., using "A_8_3h_increase" OR "B_8_3h_increase" as "group" query displays proteins that are increased at protein (2D-gel/MS) or mRNA (microarray) level 3 h after radiation in ATCL8 cells (ATM+), resulting in 160 proteins (Fig. 2). While providing many analytic functions, the interface mainly provides functionalities for profiling the list of proteins using GO Slims and KEGG pathways.
5. The GO or pathway profiles are examined and compared across experimental groups for the entire or selected proteins from the list, and most differential GO categories or pathways are examined. Comparison could also be made on merged or de-merged groups using the interface, e.g., experimental

repeats could be merged as a single group based on experimental conditions. GO and pathway profiles can also be generated for single list of proteins/genes using PIR batch retrieval at http://pir.georgetown.edu/pirwww/search/batch.shtml, but without metadata annotations (Fig. 3).

6. The iProXpress interface is used for pathway profiling and shows that the purine metabolism pathway is significantly and differentially represented in radiation treated or untreated ATM^-/ATM^+ cells (Fig. 5a). Pathway mapping using KEGG is conducted at http://www.genome.jp/kegg/tool/color_pathway.html, which allows to input enzymes of interests (using EC numbers, e.g., *1.17.4.1*) and to generate pathway maps with input enzymes highlighted in colors corresponding to different experimental groups (Fig. 5b).
7. For pathway analysis using Ingenuity IPA, the entire protein list from this study is loaded and "my list" of genes/proteins is created for specific experimental groups. Pathway profiles are examined, and pathway maps are analyzed regarding the positions and relations of specific genes/proteins of interest (e.g., certain experimental groups) in the pathway, e.g., p53, BRCA1, and Chk1, increased in ATM^+ cell after irradiation, are mapped to the G2/M DNA damage check point regulation pathway (Fig. 6a). Since one protein could appear in multiple canonical pathways, the pathway maps should be examined carefully with expert guidance. In addition to canonical pathways, gene/protein networks could be generated based on functional associations annotated in the knowledgebase of Ingenuity IPA (Fig. 6b), which provides further evidence for the ATM-mediated radiation response pathways that involve p53, BRCA1, HDAC1, and RRM2.

In summary, through functional profiling and pathway mapping, this example shows that purine metabolism is significantly represented and differentially changed in the ATM^- and ATM^+ cells in response to radiation. The increased expression of RRM2 at both mRNA and protein levels, and of p53, BRCA1, HDAC1, and Chk1 at the mRNA level in ATM^+ but not in ATM^- cells, strongly suggest that RRM2 is a downstream target of the ATM-mediated radiation response pathways and is required for radiation-induced DNA repair. This is supported by a recent report that upregulation of RRM2 transcription in response to DNA damage in human involves ATR/ATM-Chk1-E2F1 pathway (60). RRM2 is also known to play roles in cell proliferation, tumorigenicity, metastasis, and drug resistance (61). Increased expression of RRM2 has been linked to increased drug resistance, and its decrease in expression is linked to the reversal of drug-resistance in cancer cells (61, 62). RRM2 is a potential

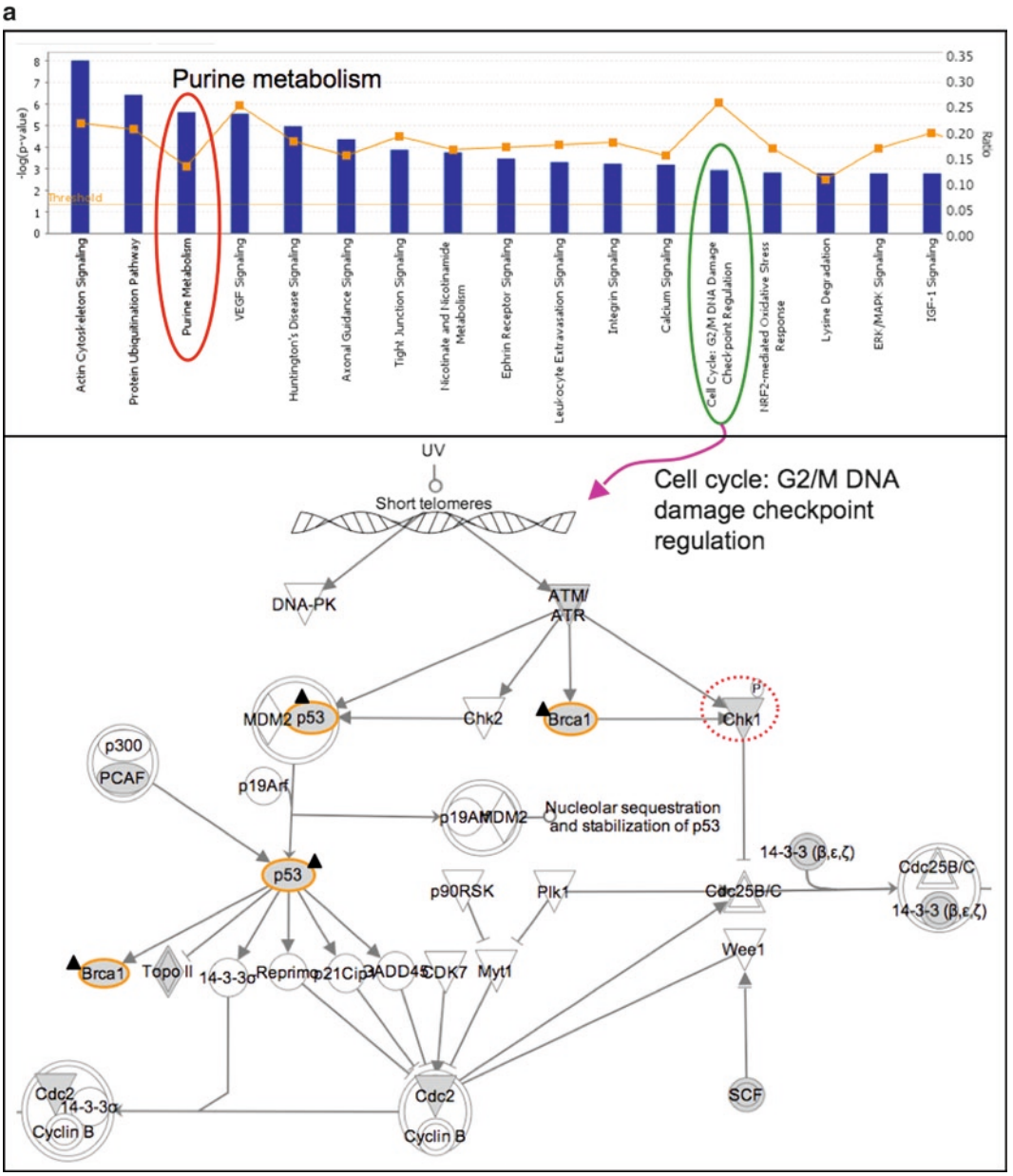


Fig. 6. (**a**) Ingenuity pathway profiling and mapping of genes/proteins from ATM^{-}/ATM^{+} cells with or without ionizing radiation treatment. The analysis is performed using Ingenuity IPA. *Top*, top-ranked pathway profiles (well above the threshold *p*-value), in which the ratio of genes/proteins detected in the experiment over the total number of proteins annotated in the pathway, is given as *gray squares*. Purine metabolism (*encircled* on the *left*) is shown as the third top pathway in the study. *Bottom*, pathway map of cell cycle G2/M DNA damage check point regulation. BRCA1 and p53 are upregulated at mRNA level 30 min after irradiation in ATCL8 cells (labeled with a *dark triangle shape*). Chk1, identified from 2D gel/MS, was increased at 3 h after irradiation in ATCL8 cells (*encircled* with a *dashed line*). (**b**) Gene networks linking RRM2 with DNA damage repair pathway proteins. Functional networks showing RRM2 connected to other major DNA repair and cell cycle proteins, such as p53, BRCA1, and HDAC1. Networks are generated using the Ingenuity IPA tool, and are merged from three subnetworks, one containing RRM2 and HDAC1, one with p53, and the third with BRCA1.

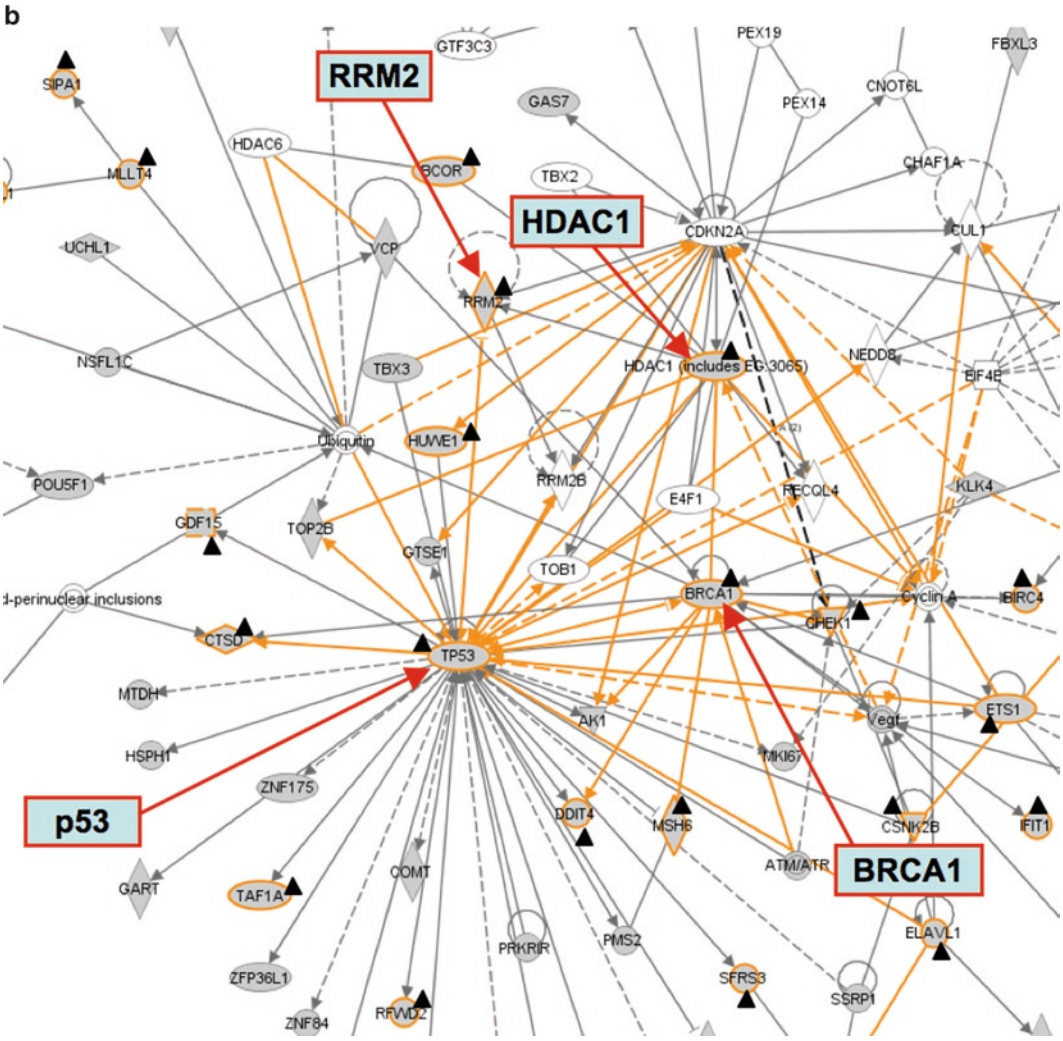


Fig. 6. (continued) The protein or gene nodes labeled with a *dark triangle shape* are those differentially expressed in the study. The *lines* (edges) connecting nodes indicate associations between proteins or genes, which encompass interaction, binding, activation, inhibition, etc. *Solid lines* (edges) are for direct and *dashed ones* for indirect associations. The figure is adapted from Hu et al. (54).

therapeutic target for cancers, e.g., targeting RRM2 for sensitizing cancer cells to drug effects through enhancing camptothecin (CPT)-induced DNA damage in breast cancer cells (60).

3.7.2. Pitfalls

Omics-based molecular target and biomarker identifications remain challenging, and many limitations exist, e.g., see review in ref. 63.

1. Proteomics data coverage bias. Missing (or false negative) identifications are common to mass spectrometry-based proteomics, thus experimental repeats including those at the level of sample preparation often improve the protein

identification rate. The coverage bias also partially accounts for the relatively small percentage of overlaps between proteomics and gene expression microarray data from identical biological samples (54, 64).

2. Limitations of knowledgebases. Although our approach heavily relies on the annotations in knowledgebases, these curated databases have several limitations. Common shortcomings that might affect the analysis include database entry redundancy, insufficient annotations, and high proportion of electronically derived annotations. For example, database entry redundancy can cause ambiguous ID mapping (see Note 1), and insufficient annotations can limit the power of functional interpretation of Omics data. In the case of GO annotation, the vast majority of GO terms (~90%) annotated for gene products are inferred from electronic annotation (IEA) (see http://www.geneontology.org/GO.current.annotations.shtml), thus cautions should be exercised when using GO slim profiling.
3. Lack of tissue and/or isoform specificity in pathway annotations. A potential bias in interpretation of pathway mapping results could come from the fact that pathway annotations currently take little consideration of tissue specificities of genes or proteins in the pathway. Thus, specific steps of a pathway may not be actually active in given tissues/cells from which the Omics data may be generated. In some cases, this may occur because protein isoforms or splice variants have been annotated as a protein class or a canonical protein sequence, respectively, in the pathway while they may be expressed differentially in different tissues/cells.
4. Variations in pathway annotations. Because biological pathways are inherently complex and dynamic, pathway annotations in different pathway databases vary significantly in pathway models and in a number of other aspects, e.g., specific protein forms, dynamic complex formation, subcellular locations, and pathway cross talks (pathway boundaries, also see Note 8). Pathway Commons is an effort to provide a link between the disparate pathway databases.

4. Notes

1. Gene IDs such as Entrez Gene numbers are often mapped to multiple UniProt protein entries, some of which result from protein isoforms that need to be merged under the entry of the same protein precursor, but most result from sequence redundancy in the database. For example, UniProtKB has two

sections, UniProtKB/Swiss-Prot and UniProtKB/TrEMBL; the former is manually annotated with minimal redundancy and the latter is computationally annotated with more redundancy, including fragments of the same gene products. If the complete proteome annotation is available for an organism (e.g., human), in most cases one can limit the ID mapping to UniProtKB/Swiss-Prot and check any remaining unmapped IDs. Redundant sequence entries can be resolved using UniRef100 and/or UniRef90, which cluster sequences of 100 or 90% identity into one group for the selection of the appropriate entries (http://www.uniprot.org/help/uniref).

2. Although PubMed is the primary tool to access literature citation, some literature mining tools are available to help mining relevant protein data, such as PPI (e.g., MetaServer, http://bcms.bioinfo.cnio.es) and protein phosphorylation (e.g., RLIMS-P, http://pir.georgetown.edu/pirwww/iprolink/rlimsp.shtml). In addition, gene or protein synonyms can be identified using BioThesaurus (http://pir.georgetown.edu/iprolink/biothesaurus), which help identify more relevant literature from PubMed for a given gene/protein.
3. GO annotations have high coverage for a given genome, e.g., currently >88% of human proteins in UniProtKB/Swiss-Prot are annotated with GO terms (Table 3). Overall, the vast majority of GO terms (~90%) are annotated based on computational inference (evidence code *IEA*, Inferred from Electronic Annotation: http://www.geneontology.org/GO.evidence.shtml). Manual annotation of GO remains laborious.

Table 3
Numbers of UniProtKB/Swiss-Prot entries with functional annotations

Organism (Taxon ID)	# Total entry	Ontology	Pathway			PPI
		GO[b]	KEGG	PID	Reactome	IntAct
Mammal (40674)	64,813	59,865	14,289	1,652	3,834	8,281
Human[a] (9606)	20,328	18,049 (88.8)[c]	4,925 (24.2)	1,649 (8.1)	3,790 (18.6)	6,423 (31.6)
Mouse[a] (10090)	16,204	14,955 (92.3)	3,685 (22.7)	N/A	N/A	1,467 (9.1)
Rat (10116)	7,449	7,060	2,415	N/A	N/A	304

All numbers are derived from iProClass database as of November 24, 2009

[a] Complete human proteome has been annotated in UniProtKB/Swiss-Prot (Human Proteome Initiative project), and the mouse proteome also has high coverage when compared to rat and other mammals. *N/A* not applicable because only human proteins and pathways are annotated in PID and the Reactome pathway databases

[b] GO annotations are with all evidence codes, including IEA

[c] Numbers in parenthesis are the percentage of proteins annotated in the categories over the total number of entries for the corresponding species. *GO* gene ontology, *PPI* protein–protein interaction

4. In general, only a small percentage of a proteome has been annotated with pathways, thus depending on the data sets being analyzed, the coverage of pathways for the given Omics data vary. For human, currently only about one quarter of proteins are covered by pathway databases, including KEGG, PID, and Reactome (Table 3). Although integrated into Pathway Commons (http://www.pathwaycommons.org), PPI data are not part of annotated pathways, but can be used to generate protein interaction networks.
5. Another aspect of dividing experimental data relates to dividing proteins identified from mass spectrometry, such as MALDI-TOF into groups of proteins identified with high (>90%) or low (<90%) confidence intervals (CI) assigned from statistical processing of MASCOT search results by software, e.g., GPS Explorer™, to increase the probability of true target identifications. The low CI values could result from factors, such as the size of database for the search engine, protein abundance, and the type of mass spectrometry instruments. Furthermore, MS proteomic data often require additional filtering for appropriate analysis. For example, a number of proteins that are deemed to be nonspecific (e.g., keratins) are frequently detected for the underlying experiment, which could be caused by factors such as sample contamination and/or detection bias toward high abundant proteins, thus often are removed from analysis. For proteins identified from 1D gel that migrate at apparent molecular weight (MW) highly deviating from the calculated MW could be removed, albeit with caveats that protein degradation or aggregation may have occurred at or before gel electrophoresis. These practices are currently applied to an ongoing study on investigating E2-induced cell apoptosis pathways in breast cancer cells (59).
6. A two-step procedure is generally used for the peptide mapping: direct sequence mapping and reducing redundancy using UniRef90 clusters (http://www.uniprot.org/help/uniref) (65). Sequences in UniProtKB with 90% or more sequence identity are grouped in a UniRef90 cluster. Proteins within a UniRef90 cluster are more likely to have the same function. For the peptide matched to more than one UniProtKB sequences, if the matching sequences are in the same UniRef90 cluster, then the peptide is mapped to the representative sequence of the cluster.
7. Some GO terms nearly always appear in high frequencies for any given list of proteins, such as "GO:0065007: biological regulation," thus reveal little specific functions for the list of proteins being profiled. Statistical testing is provided in such cases to obtain functional enrichment of GO terms by tools, such as DAVID (http://david.abcc.ncifcrf.gov/summary.jsp).

In some cases, a pie chart using GO terms is used to depict the functional categories of the list of proteins. This should be interpreted with caution because the GO categories are not mutually exclusive, especially with regard to the molecular functions and biological processes. A list of proteins can be categorized also based on keywords, functions, and other information from literature, as well as guided by experts.

8. Biological pathways are inherently complex and cross talk between pathways is frequent. Pathways are often annotated using different models in different pathway databases. Among the differences, the pathway boundary for the same core pathway differs most notably in different databases, depending on what additional proteins to be included that are known to interact with the core pathway. For example, 62 proteins are included in TGF beta signaling in PID database (http://pid.nci.nih.gov), while 40 are found in Reactome (http://reactome.org). Thus, the combined pathway data from different databases have better coverage on proteins to be analyzed even when they share the same core pathways.

Acknowledgments

The work has been supported in part by Federal funds from the National Cancer Institute (NCI), National Institutes of Health (NIH), under Contract No. HHSN261200800001E (Z.Z.H.), by NCI grant P01CA074175 (A.D.), by NIH grant U01-HG02712 (C.W.), and by the Department of Defense Breast Cancer Research Program W81XWH-06-10590 Center of Excellence Grant (A.W., A.T.R.). The content of this publication does not necessarily reflect the views or policies of the Department of Health and Human Services, nor does mention of trade names, commercial products, or organizations imply endorsement by the US Government.

References

1. Ransohoff, D.F. (2003). Cancer. Developing molecular biomarkers for cancer *Science* **299**, 1679–80.
2. Riesterer, O., Milas, L., and Ang, K.K. (2007) Use of molecular biomarkers for predicting the response to radiotherapy with or without chemotherapy *J Clin Oncol* **25**, 4075–83.
3. Kim, Y.S., Maruvada, P., and Milner, J.A. (2008) Metabolomics in biomarker discovery: future uses for cancer prevention *Future Oncol* **4**, 93–102.
4. Tainsky, M.A. (2009) Genomic and proteomic biomarkers for cancer: a multitude of opportunities *Biochim Biophys Acta* **1796**, 176–93.
5. Hanash, S. (2004) Integrated global profiling of cancer *Nat Rev Cancer* **4**, 638–44.
6. Souchelnytskyi, S. (2005) Proteomics of TGF-beta signaling and its impact on breast cancer *Expert Rev Proteomics* **2**, 925–35.
7. Walgren, J.L., and Thompson, D.C. (2004) Application of proteomic technologies in the

drug development process *Toxicol Lett* **149**, 377–85.

8. Tugwood, J.D., Hollins, L.E., and Cockerill, M.J. (2003) Genomics and the search for novel biomarkers in toxicology *Biomarkers* **8**, 79–92.
9. Merrick, B.A., and Bruno, M.E. (2004) Genomic and proteomic profiling for biomarkers and signature profiles of toxicity *Curr Opin Mol Ther* **6**, 600–7.
10. Sreekumar, A., Poisson, L.M., Rajendiran, T.M., Khan, A.P., Cao, Q., Yu, J., Laxman, B., Mehra, R., Lonigro, R.J., Li, Y., Nyati, M.K., Ahsan, A., Kalyana-Sundaram, S., Han, B., Cao, X., Byun, J., Omenn, G.S., Ghosh, D., Pennathur, S., Alexander, D.C., Berger, A., Shuster, J.R., Wei, J.T., Varambally, S., Beecher, C., and Chinnaiyan, A.M. (2009) Metabolomic profiles delineate potential role for sarcosine in prostate cancer progression *Nature* **457**, 910–4.
11. Martens, J.W., Margossian, A.L., Schmitt, M., Foekens, J., and Harbeck, N. (2009) DNA methylation as a biomarker in breast cancer *Future Oncol* **5**, 1245–56.
12. Ruan, K., Fang, X., and Ouyang, G. (2009) MicroRNAs: novel regulators in the hallmarks of human cancer *Cancer Lett* **285**, 116–26.
13. Brooks, S.A. (2009) Strategies for analysis of the glycosylation of proteins: current status and future perspectives *Mol Biotechnol* **43**, 76–88.
14. Pang, J., Liu, W.P., Liu, X.P., Li, L.Y., Fang, Y.Q., Sun, Q.P., Liu, S.J., Li, M.T., Su, Z.L., and Gao, X. (2010) Profiling protein markers associated with lymph node metastasis in prostate cancer by DIGE-based proteomics analysis *J Proteome Res* **9(1)**, 216–26.
15. Li, J., Zhao, J., Yu, X., Lange, J., Kuerer, H., Krishnamurthy, S., Schilling, E., Khan, S.A., Sukumar, S., and Chan, D.W. (2005) Identification of biomarkers for breast cancer in nipple aspiration and ductal lavage fluid *Clin Cancer Res* **11**, 8312–20.
16. Zhou, J., Trock, B., Tsangaris, T.N., Friedman, N.B., Shapiro, D., Brotzman, M., Chan-Li, Y., Chan, D.W., and Li, J. (2010) A unique proteolytic fragment of alpha1-antitrypsin is elevated in ductal fluid of breast cancer patient *Breast Cancer Res Treat* **123(1)**, 73–86.
17. Yamamoto, Y., Kosaka, N., Tanaka, M., Koizumi, F., Kanai, Y., Mizutani, T., Murakami, Y., Kuroda, M., Miyajima, A., Kato, T., and Ochiya, T. (2009) MicroRNA-500 as a potential diagnostic marker for hepatocellular carcinoma *Biomarkers* **14**, 529–38.
18. Jones, S., Zhang, X., Parsons, D.W., Lin, J.C., Leary, R.J., Angenendt, P., Mankoo, P., Carter, H., Kamiyama, H., Jimeno, A., Hong, S.M., Fu, B., Lin, M.T., Calhoun, E.S., Kamiyama, M., Walter, K., Nikolskaya, T., Nikolsky, Y., Hartigan, J., Smith, D.R., Hidalgo, M., Leach, S.D., Klein, A.P., Jaffee, E.M., Goggins, M., Maitra, A., Iacobuzio-Donahue, C., Eshleman, J.R., Kern, S.E., Hruban, R.H., Karchin, R., Papadopoulos, N., Parmigiani, G., Vogelstein, B., Velculescu, V.E., and Kinzler, K.W. (2008) Core signaling pathways in human pancreatic cancers revealed by global genomic analyses *Science* **321**, 1801–6.
19. Zhu, X., Gerstein, M., and Snyder, M. (2007) Getting connected: analysis and principles of biological networks *Genes Dev* **21**, 1010–24.
20. Pujana, M.A., Han, J.D., Starita, L.M., Stevens, K.N., Tewari, M., Ahn, J.S., Rennert, G., Moreno, V., Kirchhoff, T., Gold, B., Assmann, V., Elshamy, W.M., Rual, J.F., Levine, D., Rozek, L.S., Gelman, R.S., Gunsalus, K.C., Greenberg, R.A., Sobhian, B., Bertin, N., Venkatesan, K., Ayivi-Guedehoussou, N., Solé, X., Hernández, P., Lázaro, C., Nathanson, K.L., Weber, B.L., Cusick, M.E., Hill, D.E., Offit, K., Livingston, D.M., Gruber, S.B., Parvin, J.D., and Vidal, M. (2007) Network modeling links breast cancer susceptibility and centrosome dysfunction *Nat Genet* **39**, 1338–49.
21. Xia, K., Xue, H., Dong, D., Zhu, S., Wang, J., Zhang, Q., Hou, L., Chen, H., Tao, R., Huang, Z., Fu, Z., Chen, Y.G., and Han, J.D. (2006) Identification of the proliferation/differentiation switch in the cellular network of multicellular organisms *PLoS Comput Biol* **2**, e145.
22. Bertagnolli, M.M. (2009) The forest and the trees: pathways and proteins as colorectal cancer biomarkers *J Clin Oncol* **27(35)**, 5866–7.
23. Zhang, D.Y., Ye, F., Gao, L., Liu, X., Zhao, X., Che, Y., Wang, H., Wang, L., Wu, J., Song, D., Liu, W., Xu, H., Jiang, B., Zhang, W., Wang, J., and Lee, P. (2009) Proteomics, pathway array and signaling network-based medicine in cancer *Cell Div* **4**, 20.
24. Ptitsyn, A.A., Weil, M.M., and Thamm, D.H. (2008) Systems biology approach to identification of biomarkers for metastatic progression in cancer *BMC Bioinformatics* **9 Suppl 9**, S8.
25. Ideker, T., and Sharan, R. (2008) Protein networks in disease *Genome Res* **18**, 644–52.
26. Loscalzo, J., Kohane, I., and Barabasi, A.L. (2007) Human disease classification in the postgenomic era: a complex systems approach to human pathobiology *Mol Syst Biol* **3**, 124.

27. Auffray, C. (2007) Protein subnetwork markers improve prediction of cancer outcome *Mol Syst Biol* **3**, 141
28. Chuang, H.Y., Lee, E., Liu, Y.T., Lee, D., and Ideker, T. (2007) Network-based classification of breast cancer metastasis *Mol Syst Biol* **3**, 140.
29. Wang, E., Lenferink, A., and O'Connor-McCourt, M. (2007) Cancer systems biology: exploring cancer-associated genes on cellular networks *Cell Mol Life Sci* **64**, 1752–62.
30. Do, J.H., and Choi, D.K. (2008) Clustering approaches to identifying gene expression patterns from DNA microarray data *Mol Cells* **25**, 279–88.
31. Kerr, G., Ruskin, H.J., Crane, M., and Doolan, P. (2008) Techniques for clustering gene expression data *Comput Biol Med* **38**, 283–93.
32. Weeraratna, A.T., and Taub, D.D. (2007) Microarray data analysis: an overview of design, methodology, and analysis *Methods Mol Biol* **377**, 1–16.
33. Handl, J., Knowles, J., and Kell, D.B. (2005) Computational cluster validation in post-genomic data analysis *Bioinformatics* **21**, 3201–12.
34. Huang, H., Hu, Z.Z., Arighi, C.N., and Wu, C.H. (2007) Integration of bioinformatics resources for functional analysis of gene expression and proteomic data *Front Biosci* **12**, 5071–88.
35. Galperin, M.Y., and Cochrane, G.R. (2009) Nucleic Acids Research annual Database Issue and the NAR online Molecular Biology Database Collection in 2009 *Nucleic Acids Res* **37(Database issue)**, D1–4.
36. UniProt Consortium. (2009) The Universal Protein Resource (UniProt) 2009 *Nucleic Acids Res* **37(Database issue)**, D169–74.
37. Maglott, D., Ostell, J., Pruitt, K.D., and Tatusova, T. (2005) Entrez Gene: gene-centered information at NCBI *Nucleic Acids Res* **33(Database issue)**, D54–8.
38. Bult, C.J., Kadin, J.A., Richardson, J.E., Blake, J.A., and Eppig, J.T. The Mouse Genome Database Group. (2010) The Mouse Genome Database: enhancements and updates *Nucleic Acids Res* **38(Database issue)**, D586–92.
39. Barrell, D., Dimmer, E., Huntley, R.P., Binns, D., O'Donovan, C., and Apweiler, R. (2009) The GOA database in 2009 – an integrated Gene Ontology Annotation resource *Nucleic Acids Res* **37(Database issue)**, D396–403.
40. Kanehisa, M., Araki, M., Goto, S., Hattori, M., Hirakawa, M., Itoh, M., Katayama, T., Kawashima, S., Okuda, S., Tokimatsu, T., and Yamanishi, Y. (2008) KEGG for linking genomes to life and the environment *Nucleic Acids Res.* **36(Database issue)**, D480–4.
41. Schaefer, C.F., Anthony, K., Krupa, S., Buchoff, J., Day, M., Hannay, T., and Buetow, K.H. (2009) PID: the Pathway Interaction Database *Nucleic Acids Res* **37(Database issue)**, D674–9.
42. Aranda, B., Achuthan, P., Alam-Faruque, Y., Armean, I., Bridge, A., Derow, C., Feuermann, M., Ghanbarian, A.T., Kerrien, S., Khadake, J., Kerssemakers, J., Leroy, C., Menden, M., Michaut, M., Montecchi-Palazzi, L., Neuhauser, S.N., Orchard, S., Perreau, V., Roechert, B., van Eijk, K., and Hermjakob, H. (2010) The IntAct molecular interaction database in 2010 *Nucleic Acids Res* **38(Database issue)**, D525–31.
43. Ceol, A., Chatr Aryamontri, A., Licata, L., Peluso, D., Briganti, L., Perfetto, L., Castagnoli, L., and Cesareni, G. (2010) MINT, the molecular interaction database: 2009 update *Nucleic Acids Res* **38(Database issue)**, D532–9.
44. Apweiler, R., Bairoch, A., Wu, C.H., Barker, W.C., Boeckmann, B., Ferro, S., Gasteiger, E., Huang, H., Lopez, R., Magrane, M., Martin, M.J., Natale, D.A., O'Donovan, C., Redaschi, N., and Yeh, L.S. (2004) UniProt: the Universal Protein knowledgebase *Nucleic Acids Res* **32**, D115–9.
45. Wu, C.H., Huang, H., Nikolskaya, A., Hu, Z., and Barker, W.C. (2004) The iProClass integrated database for protein functional analysis *Comput Biol Chem* **28**, 87–96.
46. Huang, da W., Sherman, B.T., Stephens, R., Baseler, M.W., Lane, H.C., and Lempicki, R.A. (2008) DAVID gene ID conversion tool *Bioinformation* **2**, 428–30.
47. Côté, R.G., Jones, P., Martens, L., Kerrien, S., Reisinger, F., Lin, Q., Leinonen, R., Apweiler, R., and Hermjakob, H. (2007) The Protein Identifier Cross-Referencing (PICR) service: reconciling protein identifiers across multiple source databases *BMC Bioinformatics* **8**, 401.
48. Sherman, B.T., Huang, da W., Tan, Q., Guo, Y., Bour, S., Liu, D., Stephens, R., Baseler, M.W., Lane, H.C., and Lempicki, R.A. (2007) DAVID Knowledgebase: a gene-centered database integrating heterogeneous gene annotation resources to facilitate high-throughput gene functional analysis *BMC Bioinformatics* **8**, 426.
49. Al-Shahrour, F., Carbonell, J., Minguez, P., Goetz, S., Conesa, A., Tárraga, J., Medina, I., Alloza, E., Montaner, D., and Dopazo, J.

(2008) Babelomics: advanced functional profiling of transcriptomics, proteomics and genomics experiments *Nucleic Acids Res* **36(Web Server issue)**, W341–6.

50. Li, Y., and Agarwal, P. (2009) A pathway-based view of human diseases and disease relationships *PLoS One* **4**, e4346.
51. Ozgür, A., Vu, T., Erkan, G., and Radev, D.R. (2008) Identifying gene-disease associations using centrality on a literature mined gene-interaction network *Bioinformatics* **24**, i277–85.
52. Li, S., Wu, L., and Zhang, Z. (2006) Constructing biological networks through combined literature mining and microarray analysis: a LMMA approach *Bioinformatics* **22**, 2143–50.
53. Nikitin, A., Egorov, S., Daraselia, N., and Mazo, I. (2003) Pathway studio – the analysis and navigation of molecular networks *Bioinformatics* **19**, 2155–7.
54. Hu, Z.Z., Huang, H., Cheema, A., Jung, M., Dritschilo, A., and Wu, C.H. (2008) Integrated bioinformatics for radiation-induced pathway analysis from proteomics and microarray data *J Proteomics Bioinform* **1**, 47–60.
55. Nordlund, P., and Reichard, P. (2006) Ribonucleotide reductases *Annu Rev Biochem* **75**, 681–706.
56. Hu, Z.Z., Valencia, J.C., Huang, H., Chi, A., Shabanowitz, J., Hearing, V.J., Appella, E., and Wu, C.H. (2007) Comparative bioinformatics analyses and profiling of lysosome-related organelle proteomes *Int J Mass Spectrom* **259**, 147–60.
57. Wheelock, C.E., Wheelock, A.M., Kawashima, S., Diez, D., Kanehisa, M., van Erk, M., Kleemann, R., Haeggström, J.Z., and Goto, S. (2009) Systems biology approaches and pathway tools for investigating cardiovascular disease *Mol Biosyst* **5**, 588–602.
58. Chi, A., Valencia, J.C., Hu, Z.Z., Watabe, H., Yamaguchi, H., Mangini, N.J., Huang, H., Canfield, V.A., Cheng, K.C., Yang, F., Abe, R., Yamagishi, S., Shabanowitz, J., Hearing, V.J., Wu, C., Appella, E., and Hunt, D.F. (2006) Proteomic and bioinformatic characterization of the biogenesis and function of melanosomes *J Proteome Res* **5**, 3135–44.
59. Hu, Z.Z., Kagan, B., Huang, H., Liu, H., Jordan, V.C., Riegel, A., Wellstein, A., and Wu, C. (2009) Pathway and Network Analysis of E2-Induced Apoptosis in Breast Cancer Cells *100th AACR Conference*, Denver, CO, April 18–22, Abstract #3285.
60. Zhang, Y.W., Jones, T.L., Martin, S.E., Caplen, N.J., and Pommier, Y. (2009) Implication of checkpoint kinase-dependent up-regulation of ribonucleotide reductase R2 in DNA damage response *J Biol Chem* **284**, 18085–95.
61. Zhou, B., and Yen, Y. (2001) Characterization of the human ribonucleotide reductase M2 subunit gene; genomic structure and promoter analyses *Cytogenet Cell Genet* **95**, 52–59.
62. Zhou, B., Tsai, P., Ker, R., Tsai, J., Ho, R., Yu, J., Shih, J., and Yen, Y. (1998) Overexpression of transfected human ribonucleotide reductase M2 subunit in human cancer cells enhances their invasive potential *Clin Exp Metastasis* **16**, 43–9.
63. Ransohoff, D.F. (2009). Promises and limitations of biomarkers *Recent Results Cancer Res* **181**, 55–9.
64. Waters, K.M., Pounds, J.G., and Thrall, B.D. (2006) Data merging for integrated microarray and proteomic analysis *Brief Funct Genomic Proteomic* **5**, 261–72.
65. Wu, C.H., Apweiler, R., Bairoch, A., Natale, D.A., Barker, W.C., Boeckmann, B., Ferro, S., Gasteiger, E., Huang, H., Lopez, R., Magrane, M., Martin, M.J., Mazumder, R., O'Donovan, C., Redaschi, N., Suzek, B. (2006) The Universal Protein Resource (UniProt): an expanding universe of protein information *Nucleic Acids Res* **34(Database issue)**, D187–91.

ehp ENVIRONMENTAL HEALTH PERSPECTIVES

ehponline.org

Most Plastic Products Release Estrogenic Chemicals: A Potential Health Problem That Can Be Solved

Chun Z. Yang, Stuart I. Yaniger, V. Craig Jordan, Daniel J. Klein, George D. Bittner

doi: 10.1289/ehp.1003220 (available at http://dx.doi.org/)
Online 2 March 2011



NIEHS
National Institute of Environmental Health Sciences

National Institutes of Health
U.S. Department of Health and Human Services

Most Plastic Products Release Estrogenic Chemicals: A Potential Health Problem That Can Be Solved

Chun Z. Yang[1], Stuart I. Yaniger[2], V. Craig Jordan[3], Daniel J. Klein[2], and George D. Bittner[1,2,4 *]

Affiliations:

[1] CertiChem, Inc., 11212 Metric Blvd, Suite 500, Austin, TX 78758

[2] PlastiPure, Inc., 11212 Metric Blvd, Suite 600, Austin, TX 78758

[3] Lombardi Comprehensive Cancer Center, Georgetown University Medical Center, Washington, D.C. 20057

[4] Neurobiology Section, School of Biology, The University of Texas, Austin, TX 78712

***Corresponding author**:

George D. Bittner

CertiChem, Inc.

11212 Metric Blvd, Suite 500

Austin, TX 78758

gbittner@certichem.com

512-339-0550 X 201 (Office), 512-339-0551 (FAX); 512-923-3735 (Cell)

Acknowledgments: This work was supported by the following NIH grants R44 ES011469, 01-03 and 1R43/44 ES014806, 01-03 to CZY, R44 ES016964, 01-03 to SIY and P30 CA051008 to VCJ.

Competing interests/financial declaration: CZY is employed by, and owns stock in, CertiChem (CCi) and PlastiPure (PPi). SIY and DJK are employed by PPi. VCJ has no financial interests in CCi or PPi. He was PI for a subcontract at Northwestern Medical School to help develop the MCF-7 assay on NIH grant# P30 CA051008 awarded to CCi. GDB owns stock in, and is a consultant CEO of CCi and a consultant CSO of PPi. All authors had freedom to design, conduct, interpret, and publish research uncompromised by any controlling sponsor.

Running Title: Most Plastic Products Release Estrogenic Chemicals

Key words: bisphenol-A, endocrine disruptor chemical, estrogen receptor binding, estrogenic activity, plastic

List of abbreviations and their definitions:

anti-EA: anti-estrogenic activity

BHA: butylated hydroxyanisole

BHT: butylated hydroxytoluene

BPA: bisphenol-A

E2: 17β-estradiol

EA: estrogenic activity

EA-free: no detectable estrogenic activity

ER: estrogen receptor

EtOH: ethanol

COC: cyclic olefin copolymer

COP: cyclic olefin polymer

Co-PET: Copolymer using polyethylene terephthalate

HC: hard and clear (plastic)

HDPE: high density polyethylene

LDPE: Low density polyethylene

nM: nanomolar [10^{-9}M]

PC: polycarbonate

PE: polyethylene

PES: polyethersulfone

PET: polyethylene terephthalate

PETG: glycol-modified polyethylene terephthalate

PLA: polylactic acid

pM: picomolar [10^{-12}M]

PP: polypropylene

PPCO: polypropylene copolymer

PS: polystyrene

UV: ultraviolet

ABSTRACT

Background: Chemicals having estrogenic activity (EA) reportedly cause many adverse health effects, especially at low (pM-nM) doses in fetal and juvenile mammals.

Objectives: To determine whether commercially available plastic resins and products, including baby bottles and other products advertised as BPA-free, release chemicals having EA.

Materials and Methods: We used a very sensitive, accurate, repeatable, roboticized MCF-7 cell proliferation assay to quantify the EA of chemicals leached into saline or ethanol extracts of many types of commercially available plastic materials, some exposed to common-use stresses (microwaving, UV radiation, and/or autoclaving).

Results: Almost all commercially available plastic products we sampled, independent of the type of resin, product, or retail source, leached chemicals having reliably-detectable EA, including those advertised as BPA-free. In some cases, BPA-free products released chemicals having more EA than BPA-containing products.

Conclusions: Many plastic products are mischaracterized as being EA-free if extracted with only one solvent and not exposed to common-use stresses. However, we can identify existing, or have developed, monomers, additives or processing agents that have no detectable EA and similar costs. Hence, our data suggest that EA-free plastic products exposed to common-use stresses and extracted by saline and ethanol solvents could be cost-effectively made on a commercial scale, and thereby eliminate a potential health risk posed by most currently-available plastic products that leach chemicals having EA into food products.

INTRODUCTION

Chemicals that mimic or antagonize the actions of naturally occurring estrogens are defined as having estrogenic activity (EA), which is the most common form of endocrine disruptor activity (ICCVAM 2003, 2006; National Research Council 1999). Chemicals having EA typically interact with one or more of the classical nuclear estrogen receptor (ER) subtypes ERα, β, non-classical membrane, or ER-related (ERR) subtypes (Hewitt et al. 2005; Matsushima et al. 2008; National Research Council 1999). Chemicals having EA in mammals can produce many health-related problems, such as early puberty in females, reduced sperm counts, altered functions of reproductive organs, obesity, altered sex-specific behaviors, and increased rates of some breast, ovarian, testicular, and prostate cancers (Della Seta et al. 2006; Gray 2008; Kabuto et al. 2004; National Research Council 1999; Newbold et al. 2008; Patisaul et al. 2006, 2009). Fetal, newborn, and juvenile mammals are especially sensitive to very low doses (sometimes pM-nM) of chemicals having EA (Gray 2008; vom Saal et al. 2005). Many of these effects observed in mammals would also be expected to be produced in humans, since basic endocrine mechanisms have been highly conserved across all classes of vertebrates (Kavlock et al. 1996; National Research Council 1999).

Thermoplastics used for many items that contain food are made by polymerizing a specific monomer or monomers in the presence of catalysts into a high molecular weight chain known as a thermoplastic polymer (see Supplemental Material, Figure 1). The resulting polymer is mixed with small quantities of various additives (antioxidants, plasticizers, clarifiers, etc) and melted, mixed, extruded, and pelletized to form a base thermoplastic resin. Base resins are either used as-is [e.g., bisphenol-A (BPA)-based polycarbonate (PC), non-BPA-based polypropylene copolymer (PPCO), and non-BPA-based polypropylene homopolymer (PPHO)] or, more commonly, mixed with other resins, additives, colorants, and/or extenders to form plastic compounds (e.g., polymer blends and pre-colored polymers). Plastic products are then made by

using one or more plastic compounds or resins to form a finished plastic part that can be subjected to finishing processes that may utilize inks, adhesives, etc., to make a finished product.

As previously described (Begley et al. 1990, 2005; De Meulenaer and Huyghebaert 2004), plastic resins and manufacturing protocols (see Supplemental Material, Figure 1) collectively use many monomers and additives that may exhibit EA because they have physicochemical properties, often an insufficiently-hindered phenol group, that enable them to bind to ERs (see Supplemental Material, Table 1). Because polymerization of monomers is rarely complete and additives are not chemically part of the polymeric structure, chemicals having EA can leach from plastic products at very low (e.g., nM –pM) concentrations that individually or in combination can produce adverse effects, especially in fetal to juvenile mammals. This leaching of monomers and additives from a plastic item into its contents is often accelerated if the product is exposed to common-use stresses such as UV radiation in sunlight, microwave radiation, and/or moist heat via boiling or dishwashing. The exact chemical composition of almost any commercially available plastic part is proprietary and not known. A single part may consist of 5-30 chemicals, and a plastic item containing many parts (e.g., a baby bottle) may consist of 100 or more chemicals, almost all of which can leach from the product, especially when stressed. Unless the selection of chemicals is carefully controlled, some of those chemicals will almost certainly have EA, and even when using all materials that initially test EA-free, the stresses of manufacturing can change chemical structures or create chemical reactions to convert an EA-free chemical into one with EA.

Very few studies (Soto et al. 1991; Till et al. 1982) have examined the extent to which plastics that presumably do not contain BPA nevertheless release other chemicals having detectable EA. For example, a recent comprehensive review (table on page 72 in Gray 2008) describes polyethylene (PE), polypropylene (PP), and polyethylene terephthalate (PET) plastics as being "'OK' for use with respect to release of chemicals exhibiting EA."

We report herein that most of the over 500 commercially available plastic products that we sampled, even those that are presumably BPA-free, release chemicals having detectable EA -- especially if assayed by more-polar and less-polar solvents and exposed to common-use stresses. That is, to reliably detect such leachable chemicals having EA, we show that unstressed or stressed plastic resins or products should be extracted with more-polar (e.g., saline) and less-polar (e.g., ethanol) solutions and exposed to common-use stresses (boiling water, microwaving, and UV radiation).

MATERIALS AND METHODS

We developed a sensitive and accurate roboticized version of the MCF-7 cell proliferation assay (E-screen assay) that has been used for decades to reliably assess EA and anti-EA (Leusch et al. 2010; Soto et al. 1995) and is currently undergoing validation for international use by ICCVAM/NICEATM. Chemicals with EA bind to ERs (either α, β, or ERRs) and activate the transcription of estrogen-responsive genes, which leads to proliferation of MCF-7 cells.

Detailed methods for the MCF-7 assay are provided in Supplemental Materials. In brief, plastic resins or products are extracted using saline, a more polar solvent, or EtOH, a less polar solvent. Aliquots of the extracts are then diluted 4-8 times to produce up to 8 test concentrations. Each test chemical or extract at each concentration is added in triplicate or quadruplicate to 96-well plates containing MCF-7 cells in EA-free culture media. After 6 days of exposure, the amount of DNA/well, an indication of cell proliferation, is assayed using a microplate modification of the Burton diphenylamine assay (Burton 1956; Natarajan 1994).

The effect of a test chemical or extract on proliferation is expressed as the %E2, a percentage of the maximum DNA/well produced by the maximum response to 17β-estradiol (E2,

positive control) corrected by the DNA response to the vehicle (negative) control (see Supplemental Material, Equation 1). For estrogenic test chemicals, the concentration needed to obtain half-maximum stimulation of cell proliferation (EC50, in M, a measure of binding affinity) is calculated from best fits to dose-response data that meet a well-defined set of criteria by Michaelis-Menton kinetics. The estrogenicity of extracts is calculated as the relative maximum %E2 (%RME2, a measure of response amplitude), a percentage of the maximum DNA/well produced by an extract at any dilution with respect to the maximum DNA/well produced by E2 at any dilution, corrected by the DNA response to the vehicle (negative) control (see Supplemental Material, Equation 2). If a test chemical has a positive response > 15%RME2, but an EC50 cannot be calculated because all criteria are not met, then the estrogenicity of the test chemical is simply characterized as EA positive or by its %RME2.

The EA of a test chemical or extract is considered detectable if it produces cell proliferation that is greater than 15% of the maximum response to E2 (> 15%RME2), which is greater than three standard deviations from the historic control baseline response (about 10^{-15}M), i.e. a rather conservative measure of EA detectability. Stimulation of MCF-7 proliferation induced by the test chemical or extract is confirmed to be estrogenic (versus non-specific) in an EA confirmation study: If the stimulation of MCF-7 proliferation by a test chemical or extract is suppressed by co-incubation with a strong anti-estrogen (ICI 182,780 at 10^{-7} - 10^{-8}M), the estrogenic activity of the test chemical or extract is confirmed. Therefore, a test chemical or extract is classified as not having detectable EA if it does not induce MCF-7 cell proliferation, or it induces proliferation that cannot be inhibited by ICI 182,780.

Panels A-F of Figure 1, respectively, show typical MCF-7 responses plotted as %E2 to some test chemicals: E2 (positive control), BPA, and butylated hydroxyanisole (BHA: a common antioxidant) and test extracts of plastic food bags, polycarbonate (PC) bottles and BPA-free baby bottles plotted as %RME2 -- and their ICI-suppressed responses confirming their EA. Some

chemicals or products were also analyzed for anti-EA (see Supplemental Material pages 7-8 for details).

Purchase and analyses of plastic products in survey studies

For Tables 1 and 2, we purchased 455 plastic products used to contain foodstuffs from various commercial retailers from 2005-2008. The relative frequency of products having detectable EA did not change with later, compared to earlier, purchases. In some cases, we instructed undergraduate students or other employees to purchase a mix of plastic items used to contain foodstuffs from a given large retailer (Albertsons, HEB, Randalls, Target, Wal-Mart, Trader Joe's, and Whole Foods) mainly in the Austin, TX, or Boston, MA areas, some marketing many "organic" products. In other cases, we purchased products of a particular plastic type (e.g., PE or PP-based containers). We recorded the retailer, resin type [high density PE (HDPE), PET, polycarbonate (PC), PP, polystyrene (PS), polylactic acid (PLA)] and product type (flexible packaging, food wrap, rigid packaging, baby bottle component, deli containers, plastic bags). In addition, since the contents of some plastic items might have added or extracted chemicals having EA from the plastic container before we purchased and tested the product (Sax 2010), we recorded whether the plastic items had contents or did not have contents when purchased. For any plastic container having "contents", the contents were thoroughly washed out with distilled water before testing the plastic of the container. Except for PC-based items, none of these products were known to have BPA. [Plastic products typically do not list their chemical composition, which is proprietary to the manufacturer.] Samples were chosen in product areas where adverse health effects might occur if the samples leached chemicals having EA. Samples from each retailer generally included most of the product types listed above. In addition to surveying commercially available products, we tested plastic resins (e.g., PC, PET, PETG) that were purchased from M. Holland Company (Northbrook, IL) and individual chemicals used to

manufacture plastic products (e.g., BPA, BHA, BHT, dimethyl terephthalate, etc) that were purchased in their purest form from Sigma-Aldrich (St. Louis, MO).

Many plastic products have more than one plastic part. For example, baby bottles have 3-10 different plastic parts in various combinations: bottle, nipple, anti-colic item(s), sealing ring(s), liner bag, cap, etc -- each part typically having different and rather unique combinations of 5-30 chemicals. Over the course of this entire study, we assayed over 100 component parts from more than 20 different baby bottles, including many advertised as BPA-free. Only some (13) of these component parts were purchased for the initial survey study (Tables 1-2).

Most of the samples (338 of 455) in the survey study (Tables 1-2) were extracted using only one extraction protocol. For the remaining samples (n = 102), both saline and ethanol extractions were used so that the efficacy of each protocol could be directly compared. A paired Student's t-test was used to test whether differences between pairs of samples were statistically significant ($p < 0.05$).

Protocols for common-use stresses of some plastic items

Given that common-use stresses can alter the complex chemical composition of plastics and/or increase the rate of leaching (Begley et al. 1990, 2005; De Meulenaer and Huyghebaert 2004), for some resins or products, we examined how leaching of chemicals having EA might be affected by exposure to microwave radiation, autoclaving (moist heat), and UV light. Additional plastic items, some of which are described in Figure 2 and Table 3, were purchased in 2008-2010 and subjected to common-use stresses. In addition, we tested a variety of resins (including PE and PP-based resins, see Table 3), antioxidants (see Supplemental Material, Table 3) and other additives or processing agents (see Supplemental Material, Table 4) identified by our laboratory

as being free of detectable EA and hence possibly suitable for use to produce final products that would be EA-free even after exposure to common use stresses.

The stresses used were as follows:

a. UV light (radiation stress) by placing samples about two feet from a 254nm fluorescent fixture for 24 hours, simulating repeated UV stress by sunlight (e.g., water bottles) or UV sterilizers (e.g., baby bottles and medical items).

b. Autoclave (heat and moisture stress) by autoclaving at 134°C for 8 minutes, simulating moist heat stress in an automatic dishwasher.

c. Microwave (heat and radiation stress) by microwaving 10 times for 2 minutes each, using a 1000W kitchen microwave oven set to “high”, simulating microwave heat stress experienced by reusable food containers.

RESULTS

Release of chemicals having EA from unstressed plastics

The percent of samples in each category that had reliably-detectable EA (>15%RME2) in our survey of 455 commercially available plastic products is presented in Tables 1 and 2. For the %RME2 and content-status of individual samples and the average %RME2 for products classified by resins (HDPE, PP, PET, PS, PLA, PC), product type (flexible packaging, food wrap, rigid packaging, baby bottle components, plastic bags), and retailer (large retailers 1-5 and large organic retailers 1 and 2) see Supplemental Material, Tables 5A-T. For example, 9 of 13 HDPE plastic products extracted by our standard EtOH protocol (69%) had detectable EA (Table 1), with a mean %RME2 of 66% ± 25% (see Supplemental Material Table 5A). For PET products extracted by saline, 26 of 34 (76%) had detectable EA (Table 1) with a mean %RME2 of 64% ± 41% (see Supplemental Material Table 5C). There was no consistent correlation

between the percentage of items in a product type with detectable EA and their mean %RME2 (data not shown).

There was no significant difference ($p > 0.05$) in the percentage of items with detectable EA between those that had contents and those with no contents (76%, n=160) at the time of purchase based on the standard EtOH extraction protocol (67% versus 70%, Supplemental Material Table 2A), the standard saline protocol (62% versus 75%, Supplemental Material Table 2C), or all extraction protocols combined (69% versus 76%). Most importantly, items without contents in all categories exhibited detectable EA in at least one protocol (see Supplemental Material, Tables 2A-C and 5A-T), including 78% of items made from HDPE (n=18), 57% from PP (n=14), and 100% from PET (n=6). Given all these results, we present the data for all items tested in Tables 1 and 2 without regard to their content status.

Using different solvents increases the probability of detecting EA

Most (71%) unstressed plastic items released chemicals with reliably-detectable EA in one or more extraction protocols, independent of resin type, product type, or retailer (Table 1). Results often differed between saline and EtOH extracts of the same ***unstressed*** plastic item, and EA was reliably detected most frequently (92% of all items in Table 2) when analyzed using both saline (more polar) and EtOH (less polar) extracts. For example, 15% of unstressed HDPE plastic items leached chemicals with detectable EA into both EtOH and saline extracts, 15% leached only into EtOH and 31% only into saline (Table 2). That is, the leaching of a chemical with EA was significantly ($p < 0.01$) more likely to be detected if both polar and non-polar solvents were used (61%) than if only one solvent were used (30% for EtOH only or 45% for saline only). We obtained similar results for all types of plastic products (data not shown).

Assays of over 100 component parts from more than 20 different baby bottles, including many advertised as BPA-free, indicated that extracts of at least one bottle component of each

baby bottle always had EA based on at least one assay (some data shown in Table 2 and Figure 2) – as did at least one other component part (data not shown)..

Stresses increase the release of chemicals having EA

Leaching of chemicals with EA was increased by common stresses. For example, one unstressed sample of an HDPE resin (P5 in Table 3) that had no detectable EA (i.e., RME2 < 15%) in two saline extracts and two EtOH extracts released chemicals with EA equivalent to 47% RME2 when extracted using EtOH after the resin was stressed with UV light. Similarly, two samples of low-density polyethylene resins (LDPE Resins 1 and 2) and glycol-modified polyethylene terephthalate (PETG) resins (PETG Baby Bottle and PETG Resin 1) that had no detectable EA before stressing, subsequently exhibited EA when stressed, especially by UV (Table 3). Samples (n > 10) of products made from PETG resins advertised as BPA-free all released detectable EA when stressed, especially by UV light. Similarly, 25% of unstressed samples of PET and 50% of unstressed polystyrene (PS) products surveyed did not have detectable EA in assays of EtOH and/or saline extracts (Table 1). However, when stressed and assayed using both saline and EtOH extracts, all PET (n > 10) and PS (n > 10) products all released chemicals having detectable EA in at least one extracting solvent (Table 3).

EA-containing and EA-free monomers

Polymerization of monomers is rarely complete, and unpolymerized monomers are almost always released from polymer resins (Begley et al. 1990, 2005; De Meulenaer and Huyghebaert 2004). PE and PP polymers are often used to manufacture flexible and/or non-transparent rigid products (Figure 3). MCF-7 assays (n=6) consistently showed that extracts of “barefoot” (no additives) polymers (e.g. LDPE P1 in Table 3) were EA-free, even when stressed. [PP-based polymers require antioxidants to prevent severe degradation during their use in

manufacturing plastic products.] Furthermore, PE and PP-based resins containing appropriate additives to produce fit-for-use products could be constructed that remained EA-free (n > 100 assays of > 10 resins), even when exposed to common-use stresses. Representative data from several such resins (LDPE P1, HDPE P2, PPHO P3, PPCO P4) are given in Table 3.

Figure 3 also shows other monomers and polymers that can or can not be used to make hard-and-clear (HC) plastics. For example, HC PC plastics (n > 10) all released chemicals having EA (e.g. PC baby bottle B_1 and PC water bottle W_1 in Figure 2), almost certainly phenolics such as BPA (Fig. 1B). The dimethyl terephthalate monomer used to make PET and PETG plastics exhibited anti-EA (n = 3 assays; data not shown. see Supplemental Material for anti-EA assay protocol). Furthermore, breakdown products of dimethyl terephthalate, PET, and PETG resins probably contain and release phenolic moieties that have EA that account for some of the data for PET products in Tables 1-2. Polyethersulfone (PES) HC products also consistently released chemicals having EA or anti-EA, especially when stressed with UV light (data not shown) -- possibly from unreacted phenolic monomer residues or phenolic stress-degradation products. In contrast, some HC cyclic olefin polymer (COP)/cyclic olefin copolymer (COC) polymers produced from saturated cyclic olefin monomers contained no phenolics, and did not release chemicals having detectable EA, even when stressed (Table 3).

Polymers which can be made EA-free have a similar cost compared with polymers made from monomers that have EA. For example, at the time of the writing of this paper, clarified PP having no additives that exhibit EA (even when stressed) that is suitable for molding bottles costs approximately $1.20 per pound. PP resins containing additives that have EA also cost about $1.20 per pound. Commodity resins such as PET, which are made from monomers having EA and are suitable for molding bottles, are priced at approximately $1.28 per pound (Plastics News 2011).

EA-containing and EA-free additives

Many additives are physically, but not chemically, bound to a polymeric structure --- and hence can almost always leach from the polymer, especially when stressed (Begley et al. 1990, 2005; De Meulenaer and Huyghebaert 2004). Antioxidants are the most critical class of additives because they prevent or minimize plastic degradation due to oxidation that breaks polymer chains (chain scission) and/or causes cross-links (Kattas et al. 2000). The oldest and most common antioxidants deemed suitable for food contact belong to a chemical class known as hindered phenols, such as butylated hydroxytoluene (BHT) and BHA, in large part because both are inexpensive and assumed to be non-toxic. However, BHT (n=4 assays) had reliably-detectable EA, as did BHA (n=3 assays). [The EC50 of BHT and BHA (Figure 1C) could not be accurately calculated because both also exhibited cellular toxicity at higher (10^{-5}M) concentrations.] Other commonly used hindered phenolic antioxidants (n= 4/5) and organophosphines (n=6/7) also exhibited reliably-detectable EA, especially when exposed to moist heat, which presumably causes hydrolysis (data not shown). For example, proprietary antioxidants Phos OX 1 and HP AOX 2 had no detectable EA whereas HP AOX 1 and Ph AOX 1 had reliably-detectable EA (see Supplemental Material, Table 3).

Many other additives (n > 50) with a phenolic group had reliably-detectable EA such as agents found in many base resins (tris(nonylphenyl) phosphite, octylphenol, nonylphenol, butylbenzene phthalate), colorants (especially blues or greens with phthalocyanine groups), polystyrene-based purge compounds, and mold-release agents (see Supplemental Material, Table 4). In contrast, many metal-oxide-based inorganic pigments did not exhibit EA. However, these EA-free pigments are often mixed with dispersing agents and carrier resins that have EA to produce colorant masterbatch concentrates. Nevertheless, we have identified resins, dispersants, pigments, and antioxidants that are FDA-approved for direct food contact (see Supplemental Material, Tables 3 and 4) to create colorant masterbatch concentrates (n > 100) that produce even

colorant dispersion into a plastic and that have no detectable EA, cellular toxicity, or adverse processing effects, even when stressed.

Because additives comprise a small fraction (typically 0.1-1% by weight) of plastic resins and compounds, and because plastic resins and compounds using EA-free additives are processed during manufacture in a nearly identical manner as conventional resins and compounds containing chemicals with EA, the replacement of additives having EA with EA-free additives should have very little impact on the cost of the final product. Furthermore, EA-free additives have only a slightly higher or no additional cost compared to additives with EA, so that their cost impact is very small or non-existent.

Products currently marketed as BPA-free are not EA-free

In response to market and regulatory pressures to eliminate BPA in HC plastics, BPA-free HC materials have recently been introduced as replacements for PC resins. PET and PETG are two such resins, but HC plastic products made from these resins leached chemicals that had detectable EA (Tables 1-3 and Figures 2-3), often in the absence of exposure to common-use stresses. Two popular brands of water bottles made from a PETG resin now marketed as an HC BPA-free replacement also released chemicals having significant EA (Table 3 and Figures 2-3), as did uncompounded PETG resins (Table 3). Most PE/PP-based plastic products were presumably BPA-free, but nevertheless had readily detectable EA (Tables 1-2), almost certainly due to one or more additives having EA. Many components of BPA-free baby bottles had reliably-detectable EA (22%-95%RME2) when extracted in either saline or ethanol, including the bottle, nipple, anti-colic, and liner (data not shown).

In fact, all BPA-replacement resins or products tested to date ($n > 25$) released chemicals having reliably-detectable EA (data not shown), including PES or PETG, sometimes having more total EA measured as %RME2 than many PC products when stressed. For example, the %RME2 released by various BPA-free baby and water bottle component parts extracted by

saline or EtOH solutions and exposed to one or more common-use stresses can be greater than PC products under the same conditions (Figure 2). UV stress, in particular, often leads to the release of chemicals having greater EA than BPA-containing HC plastics currently sold. For example, saline extracts of BPA-free baby bottle B_3 (Figure 2) after exposure to UV showed greater EA than any of the PC baby bottle extracts after any of the stresses. Saline extracts from BPA-free baby bottle B_1 after any of the stresses (microwave, autoclave, and UV) showed greater EA than the saline extracts from PC baby bottle B_2 after any of the stresses. Ethanol extracts from BPA-free baby bottle B_1 after UV stress show greater EA than extracts from PC baby bottle B_1. Saline extracts from BPA-free baby bottle B_2 after microwave or autoclave stresses showed greater EA than saline extracts from PC baby bottles B_1 or B_2 following any of the stresses. Note also in Figure 2 that multiple extracts of the same product using the same solvent/stress combination typically give rather similar %RME2 data, but different solvent/stress combinations can give very different results from very high EA to non-detectable EA. For example, ethanol extracts from PC baby bottle B_2 show very high EA under all stress conditions, whereas saline extracts of the same bottle under the same stress conditions show no detectable EA. Hence, to reliably detect EA, plastic resins or products must be extracted with both polar and non-polar solvents — and exposed to common-use stresses.

DISCUSSION

Most plastic products release chemicals having EA

Our data show that both more-polar (e.g., saline) and less-polar (e.g., EtOH) solvents should be used to extract chemicals from plastics because the use of only one solvent significantly reduces the probability of detecting chemicals having EA. The ability to detect more-polar and less-polar chemicals having EA is important because plastic containers may hold either type of liquid or a liquid that is a mixture of more-polar and less-polar solvents (e.g.,

milk). When both more-polar and less-polar solvents are used, most newly purchased and unstressed plastic products release chemicals having reliably-detectable EA independent of the type of resin used in their manufacture, type of product, processing method, retail source, and whether the product had contents prior to testing. However, we wish to emphasize that the lack of significant difference in average percentage having detectable EA between plastic items with and without contents does not imply that the contents do not affect the total EA or specific chemicals having EA released by individual plastic items.

Our data show that most monomers and additives used to make many commercially available plastic items exhibit EA. Even when a “barefoot” polymer such as PE or PVC does not exhibit EA, commercial resins and products from these polymers often release chemicals (almost certainly additives) having EA.

Our data show that exposure to one or more common-use stresses often increases the leaching of chemicals having EA. In fact, our data suggest that almost all commercially available plastic items would leach detectable amounts of chemicals having EA once such items are exposed to boiling water, sunlight (UV), and/or microwaving. Our data are also consistent with recently published reports that PET products release chemicals having EA (Wagner and Oehlmann 2009), and that different PET products leach different amounts of EA. For example (see Supplemental Material, Table 5C), different PET products release different amounts of EA measured as %E2 or %RME2, almost certainly because different PET copolymer manufacturers choose different monomers, additive packages, and synthetic processes to produce PET copolymer resins.

Our data are consistent with the hypotheses that the presence of a phenolic moiety is the best predictor of whether a chemical exhibits EA, and that benzene moieties often probably convert to phenolic moieties when the monomer and/or polymer is exposed to one or more manufacturing or common-use stresses. For example, although in theory most organophosphites

(antioxidants commonly used with hindered phenols to provide synergistic oxidation protection), in their unaltered state should not bind to ERs (see Supplemental Material, Table 1), organophosphites are hydrolytically unstable and often produce phenols when exposed to water (Kattas et al. 2000). Most organophosphite antioxidants we tested exhibited detectable EA (data not shown).

Likewise, various additives that are high molecular weight hindered phenolics do not have EA, but if exposed to moist heat they can undergo hydrolysis and produce lower molecular weight phenolics that have EA. Therefore, antioxidants and other additives should be tested for EA in both their original, unstressed form and after stressing. We can identify monomers and additives (antioxidants, clarifiers, slip agents, colorants, inks, etc) having no detectable EA for use at all stages of manufacturing processes to make flexible nontransparent or HC plastic items that are EA-free, even after exposure to common-use stresses. All our data suggest that, when both are manufactured in comparable quantities, carefully formulated EA-free plastic products could have all the fit-for-use properties of current EA-releasing products at minimal additional cost.

BPA-free is not EA-free

Although most items listed in Tables 1-3 would not be expected to contain BPA, nevertheless almost all stressed plastic items tested leached chemicals having reliably-detectable EA measured as %RME2 if extracted with both more-polar and less-polar solvents. In response to market and regulatory pressures, BPA-free PET or PETG resins and products have recently been introduced as replacements for PC resins. However, all such replacement resins and products tested to date release chemicals having EA (measured as %RME2), sometimes having more EA than BPA-containing PC resins or products, especially when stressed by UV light (Figure 2 and Table 3). Monomer or polymer breakdown products that have EA account for some of this EA, but the rest of the measured EA is almost certainly due to release of additives

having EA in BPA-free products — including the bottle and many component parts of baby bottles advertised as BPA-free.

Avoiding a potential health problem

We recognize that we quantitatively measure EA relative to E2 (EC50 or %RME2) using sensitive assay/extraction protocols. Furthermore, it is almost impossible to gauge how much EA anyone is exposed to, given such unknowns as the number of chemicals having EA, their relative EA, their release rate under different conditions, and their metabolic degradation products or half-lives ***in vivo***. Also unknown at present are the appropriate levels of EA in males ***versus*** females at different life stages. Nevertheless (**1) *In vitro*** data overwhelmingly show that exposures to chemicals having EA (often in very low doses) change the structure and function of many human cell types (Gray 2008); (**2**) Many ***in vitro and in vivo*** studies document in detail cellular/molecular/systemic mechanisms by which chemicals having EA produce changes in various cells, organs and behaviors (Gray 2008); **(3)** Recent epidemiological studies (Gray 2008; Koch and Calafat 2009; Meeker et al. 2009; Swan et al. 2005; Talsness et al. 2009; Thompson et al. 2009) strongly suggest that chemicals having EA produce measurable changes in the health of various human populations, e.g., on the offspring of mothers given diethylstilbesterol, or sperm counts in Danish males and other groups correlated with BPA levels in body tissues.

Many scientists believe that it is not appropriate to bet our health and that of future generations on an assumption that known cellular effects of chemicals having EA released from most plastics will have no severe adverse health effects (Gray 2008; Talsness et al. 2009; Thompson et al. 2009). Since we can identify existing, relatively-inexpensive monomers and additives that do not exhibit estrogenic activity, even when stressed, we believe that plastics having comparable physical properties but that do not release chemicals having detectable EA could be produced at minimal additional cost.

REFERENCES

Begley T, Castle L, Feigenbaum A, Franz R, Hinrichs K, Lickly T, et al. 2005. Evaluation of migration models that might be used in support of regulations for food-contact plastics. Food Addit Contam 22:73-90.

Begley, TH, Dennison, JL, Hollifield, HC. 1990. Migration into food of polyethylene terephthalate (PET) cyclic oligomers from PET microwave packaging. Food Addit Contam 7:797-803.

Burton K. 1956. A study of the conditions and mechanism of the diphenylamine reaction for the colorimetric estimation of deoxyribonucleic acid. Biochem J 62:315-323.

Della Seta D, Minder I, Belloni V, Aloisi AM, Dessi-Fulgheri F, Farabollini F. 2006. Pubertal exposure to estrogenic chemicals affects behavior in juvenile and adult male rats. Horm Behav 50:301-307.

De Meulenaer B, Huyghebaert A. 2004. Packaging and other food contact material residues. In: Handbook of Food Analysis, Vol. 2, 2nd Ed. (Nollet LML, ed) New York:Marcel Dekker, 1297-1330.

Gray J, ed. 2008. State of the Evidence: The Connection Between Breast Cancer and the Environment. 5th ed. Breast Cancer Fund. Available: http://www.niehs.nih.gov/health/docs/breast-cancer-enviro.pdf [accessed 3 November 2010].

Hewitt SC, Deroo BJ, Korach KS. 2005. Signal Transduction: A new mediator for an old hormone? Science 307:1572-1573.

ICCVAM. 2003. ICCVAM Evaluation of ***In Vitro*** Test Methods for Detecting Potential Endocrine Disruptors: Estrogen Receptor and Androgen Receptor Binding and Transcriptional Activation Assays. May, 2003. NIH Pub 03-4503. Available: http://iccvam.niehs.nih.gov/docs/endo_docs/edfinalrpt0503/edfinrpt.pdf [accessed 3 November 2010].

ICCVAM. 2006. Addendum to ICCVAM Evaluation of ***In Vitro*** Test Methods for Detecting Potential Endocrine Disruptors: Estrogen Receptor and Androgen Receptor Binding and Transcriptional

Activation Assays. September, 2006. NIH Pub 03-4503, addendum. Available: http://iccvam.niehs.nih.gov/docs/endo_docs/EDAddendFinal.pdf [accessed 3 November 2010].

Kabuto H, Amakawa M, Shishibori T. 2004. Exposure to bisphenol A during embryonic/fetal life and infancy increases oxidative injury and causes underdevelopment of the brain and testis in mice. Life Sci 74:2931-40.

Kattas L, Gastrock F, Levin I, Cacciatore A. 2000. Plastics additives. In: Modern Plastics Handbook. 1st Ed. (Harper CA, ed) New York:McGraw-Hill, 4.1-4.69.

Kavlock RJ, Daston GP, DeRosa C, Fenner-Crisp P, Gray LE, Kaattari S, et al. 1996. Research needs for the risk assessment of health and environmental effects of endocrine disruptors: A US EPA-Sponsored Workshop. Environ Health Perspect Suppl 104:715-740.

Koch MK and Calafat AM. 2009. Human body burdens of chemicals used in plastics manufacture. Phil Trans R Soc B 364:2063-2078.

Leusch FDL, de Jager C, Levi Y, Lim R, Puijker L, Sacher F, et al. 2010. Comparison of five in vitro bioassays to measure estrogenic activity in environmental waters. Environ Sci Technol 44:3853-3860.

Matsushima A, Teramoto T, Okada H, Liu X, Tokunaga T, Kakuta Y, et al. 2008. ERRγ tethers strongly bisphenol A and 4-α-cumylphenol in an induced-fit manner. Biochem Biophys Res Commun. 373(3):408-13.

Meeker JD, Sathyanarayana S, Swan SH. 2009. Phthalates and other additives in plastics: human exposure and associated health outcomes. Phil Trans R Soc B 364:2097-2113.

Natarajan N, Shambaugh GE, III, Elseth KM, Haines GK, Radosevich JA. 1994. Adaptation of the diphenylamine (DPA) assay to a 96-well plate tissue culture format and comparison with the MTT assay. BioTechniques 17:166-171.

National Research Council. 1999. Hormonally active agents in the environment. Washington, D.C.: National Academies Press.

Newbold RR, Jefferson WN, Padilla-Banks E, Haseman J. 2004. Developmental exposure to diethylstilbestrol (DES) alters uterine response to estrogens in prepubescent mice: low versus high dose effects. Reprod Toxicol 18:399-406.

Patisaul HB, Fortino AE, Polston EK. 2006. Neonatal genistein or bisphenol-A exposure alters sexual differentiation of the AVPV. Neurotoxicol Teratol 28:111-118.

Patisaul HB, Todd KL, Mickens JA, Adewale HB. 2009. Impact of neonatal exposure to the ERα agonist PPT, bisphenol-A or phytoestrogens on hypothalamic kisspeptin fiber density in male and female rats. Neurotoxicology 30:350-357.

Plastics News. 2011. Resin Pricing Chart. 21 February: 21-22.

Sax L. 2010. Polyethylene terephthalate may yield endocrine disruptors. Environ Health Perspect 118:445-448.

Soto AM, Justicia H, Wray JW, Sonnenschein C. 1991. ***p***-Nonyl-phenol: an estrogenic xenobiotic released from "modified" polystyrene. Environ. Health Perspect. 92:167-173.

Soto AM, Sonnenschein C, Chung, KL, Fernandez MF, Olea N, Serrano FO. 1995. The E-SCREEN assay as a tool to identify estrogens: an update on estrogenic environmental pollutants. Environ Health Perspect 103:113-122.

Swan SH, Main KM, Liu F, Stewart SL, Kruse RL, Calafat AM, et al. 2005. Decrease in anogenital distance among male infants with prenatal phthalate exposure. Environ Health Perspect 113:1056-1061.

Talsness CE, Andrade AJ, Kuriyama SN, Taylor JA, vom Saal FS. 2009. Components of plastic: experimental studies in animals and relevance for human health. Phil Trans R Soc B 364:2079-2096

Thompson RC, Swan SH, Moore CJ, vom Saal FS. 2009. Our plastic age. Phil Trans R Soc B 364:1973-1976.

Till DE, Ehntholt DJ, Reid RC, Schwartz PS, Sidman KR, Schwope AD, et al. 1982. Migration of BHT antioxidant from high density polyethylene to foods and food simulants. Ind Eng Chem Prod Res Dev 21:106-113.

vom Saal FS, Nagel SC, Timms BG, Welshons WV. 2005. Implications for human health of the extensive bisphenol A literature showing adverse effects at low doses. Toxicology 212:244-252.

Wagner M, Oehlmann J. 2009. Endocrine disruptors in bottled mineral water: total estrogenic burden and migration from plastic bottles. Environ Sci Pollut Res 16:278-286.

Table 1. Percent of unstressed plastic products having EA in at least one extract.

Extract Solution	EtOH		Conc EtOH		Saline		Any Extract	
	N	**%D**	**N**	**%D**	**N**	**%D**	**N**	**%D**
Resin Type								
HDPE	13	69%	11	55%	18	56%	30	70%
PP	23	52%	6	33%	16	81%	37	68%
PET	30	40%	17	94%	34	76%	57	75%
PS	13	62%	--	--	16	38%	28	50%
PLA	10	70%	1	100%	8	100%	11	91%
PC	1	0%	1	100%	2	100%	2	100%
Product Type								
Flexible Packaging	82	66%	6	33%	35	74%	121	67%
Food Wrap	9	100%	--	--	9	78%	9	100%
Rigid Packaging	57	56%	18	67%	31	45%	83	64%
Baby Bottle Comp	13	69%	--	--	16	94%	19	89%
Deli Containers	11	36%	--	--	7	7%	16	44%
Plastic Bags	33	97%	1	100%	23	96%	43	98%
Product Retailer								
Large Retailer 1	31	81%	2	100%	4	75%	36	81%
Large Retailer 2	4	50%	4	0%	50	54%	53	53%
Large Retailer 3	18	83%	2	100%	7	29%	25	72%
Large Retailer 4	37	51%	--	--	--	--	37	51%
Large Retailer 5	20	50%	3	100%	4	100%	23	70%
Organic Retailer 1	28	71%	5	60%	5	80%	32	81%
Organic Retailer 2	33	88%	1	100%	10	80%	35	89%
Total for extract	**308**	**68%**	**51**	**73%**	**214**	**69%**	**455**	**72%**

Percent (%) of samples (N = total number of samples purchased) for which EA was detected (D) using a standard or concentrated EtOH (Conc. EtOH) extract, a saline extract (Saline) or one or more such extract (Any Extract). EA in an extract in this table and in all other tables or figures was defined as detectable (D) if the extract produced cell proliferation that was greater than 15%RME2 (see Methods). Note that N for Any Extract must be is less than the sum of N's for individual extracts if some items are tested by more than one extraction protocol. Some individual items are listed in two or three categories (e.g., PET and baby bottles), but only counted once for the tally of "Total for extract." Baby Bottle Comp means baby bottle component, of which 11 were the bottle itself and 2 sealant ring components.

Table 2. Percent of unstressed plastic products having detectable EA in two extracts.

Category	N	only in EtOH	only in S	in both EtOH & S	in either EtOH or S
HDPE	13	15	31	15	61
PET	21	19	29	52	100
PP	4	0	25	75	100
PLA	7	0	14	86	100
Bottles	38	13	34	42	89
Baby Bottles	11	0	36	64	100
Rigid Packaging	10	30	20	40	90
Food Wrap	8	25	0	75	100
All Products	**102**	**17**	**21**	**54**	**92**

Percent (%) of unstressed plastic items (N) having detectable EA (>15%RME2) only in an EtOH extract (and not in a saline (S) extract), only in a standard saline extract (only in S), in both EtOH & S extracts or in either EtOH or S extracts. Note that this last measure (column) is the sum of the three previous measures (columns). “All Products” gives the total for each column when each product (N = 102) is only counted once (some products are listed in two categories). The standard EtOH extract was used for most (N=81) products and the concentrated EtOH extract for the remainder (N = 21).

If EA was detected in a saline or standard EtOH extract in survey studies such as those reported in Table 1, other extracts were often not performed. A concentrated EtOH extract was usually performed to generate the data in Tables 1 and 2 only if EA was ***not*** detected in a saline or standard EtOH extract. That is, samples listed for concentrated EtOH in Table 1 and EtOH in Table 2 had a selection bias for ***not*** having detectable EA.

Table 3. Representative %RME2 values for stressed resins or parts made from flexible or hard and clear polymers.

Sample Type	Stress and Extraction Solvent					
	Microwave		UV		Autoclave	
	Saline	EtOH	Saline	EtOH	Saline	EtOH
Flexible Polymers						
LDPE Resin 1	5	7	0	4	4	30[a]
LDPE Resin 2	3	7	26[a]	3	-1	27[a]
PET Water Bottle	100[a]	3	31[a]	2	47[a]	1
LDPE Resin P1	2	3	0	0	4	5
HDPE Resin P2	6	-4	2	-2	-1	-3
PPHO Resin P3	0	-4	3	2	-6	-3
PPCO Resin P4	3	7	-7	-6	-9	-3
HDPE Resin P5	--[b]	--[b]	--[b]	47[a]	--[b]	--[b]
Hard and Clear Polymers						
Water Bottle 1.1	3	23[a]	71[a]	17[a]	-1	19[a]
Water Bottle 1.2	4	21[a]	57[a], 69[a], 98[a]	48[a], 39[a]	8	23[a]
Water Bottle 2.1	-7	-5	81[a]	22[a]	0	4
Water Bottle 2.2	34[a]	-2	80[a]	12	-1	1
PETG Baby Bottle	0	-2	122[a]	44[a]	0	1
PETG Resin 1	-8	17[a]	61[a]	111[a]	0	15[a]
Polystyrene 1	4	3	17[a]	45[a]	76[a]	0
COC 3	9	7	20[a]	20[a]	0	6
COC Resin P18	4	1	9	11	1	-2
COC Resin P19	6	2	6	-2	4	2

Numerical values: %RME2 response of extract for several different baby bottle and other component parts. Resins designated with P (e.g., P1, P2, P3, and P4) are EA-free formulations developed at PlastiPure. Resin P5 exhibited EA when stressed.
[a] Plastic items leaching chemicals having detectable EA > 15%RME2.
[b] not determined

Figure Legends

Figure 1. **Percent E2 Dilution Response Curves for E2, BPA, BHA and Extracts.**

Dilution ***versus*** %E2 response curves for (**A**) E2, (**B**) BPA, (**C**) BHA, extracts of (**D**) plastic bags, (E) PC bottle, and (F) BPA-free bottle made from PETG. Dotted lines in A-F represent three standard deviations from the vehicle control response. Extract conditions given by text defining symbols in each panel. [E2] = 10^{-9}M is the positive control diluted as indicated in **C-F**; negative control is 1% EtOH or saline plotted as 0%E2 in **B-F**. VC: vehicle control.

A. MCF-7 assay of E2 dissolved in EtOH (standard extract, red squares) or concentrated 10x and re-diluted (black triangles) to show that the EtOH concentration protocol has very little effect on the EC50 of E2 (50%E2). EC50 of E2 is ~$1.3x10^{-13}$M and threshold of detection (15%E2) is ~10^{-15}M. The maximum E2 response was attained at 10^{-11}M and remained constant at higher E2 concentrations. Each point plotted is the average of three or four replicates for each concentration whose standard deviation is very small and falls within the space taken up by each data point symbol in all panels of Figure 1.

B. EC50 of E2 (as above) and BPA = ~$6.6x10^{-8}$M, threshold detection = ~10^{-9}M, all suppressed by 10^{-8}M ICI.

C. BHA does not meet criteria needed for accurate calculation of EC50 (see pages 5-7 of Supplemental Material). EA is positive, its maximum response is about 50%E2 (i.e., 50%RME2) and is suppressed by 10^{-8}M ICI.

D Commercially available plastic bags extracted by 100% EtOH or different extracts of a PC bottle (**E**) or BPA-free bottle (**F**).

Figure 2. Total EA Released By Some PC and BPA-free Water and Baby Bottles.

Materials: BPA-free water bottles W_1, W_2, W_3, and W_4 are PETG. BPA-free water bottle W_5 is PET. BPA-free baby bottles B_1 and B_2 are PES. BPA-free baby bottle B_3 is PETG. BPA-free baby bottles B_4 and B_5 are PP.

The leaching of chemicals having EA (measured as %RME2) from PC or BPA-free baby (B) or water (W) bottles (excluding caps, nipples, and other components) extracted using saline or ethanol as solvents and exposed to autoclaving, microwaving, and/or UV light (see Methods). Orange bars indicate the data set for each individual product. The %RME2 for saline extracts is represented by solid black lines and EtOH as solid red lines. The %RME2 of chemicals released by each assay of a product after an autoclaving stress is indicated by (□), microwaving by (●), and UV light by (**x**). The dotted horizontal line at 15%RME2 is the rather conservative value below which EA was considered non-detectable (ND) for any assay. For some products shown (e.g., PC B_1, BPA-free B_4), if one solvent and/or stress condition showed reliably-detectable EA, other solvents and stress conditions were not subsequently tested. Some values plotted as 0%RME2 actually had slightly negative %RME2 values (-1%RME2 to -7%RME2) due to cellular toxicity.

Figure 3. Properties of Monomers and Polymers Used to Make Common Resins.

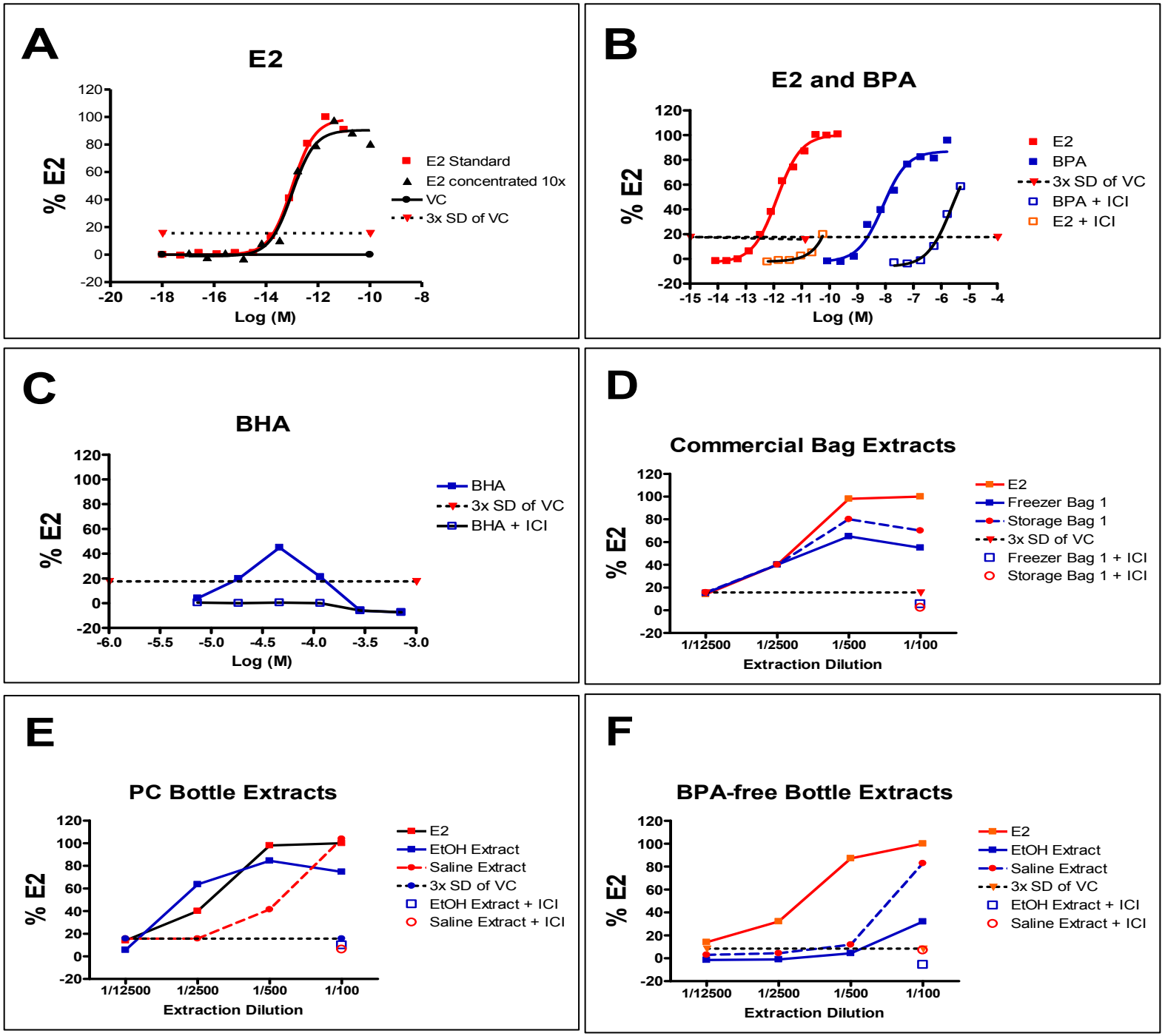
[a] Polymer exhibits other toxic effects (e.g. cellular damage or carcinogenicity) or toxic chemicals (e.g. phosgene and acrylonitrile) are used or produced during polymerization.

[b] "Hard and Clear" (HC) polymers generally have limited or no ability to crystallize and a glass transition temperature (T_g) above room temperature.

[c] Monomer has anti-EA in MCF-7 assays

[d] Under certain conditions, degradation products exhibit EA

[e] Monomer has EA in MCF-7 assays


A
E2
% E2
Log (M)
E2 Standard
E2 concentrated 10x
VC
3x SD of VC
B
E2 and BPA
% E2
Log (M)
E2
BPA
3x SD of VC
BPA + ICI
E2 + ICI
C
BHA
% E2
Log (M)
BHA
3x SD of VC
BHA + ICI
D
Commercial Bag Extracts
% E2
Extraction Dilution
E2
Freezer Bag 1
Storage Bag 1
3x SD of VC
Freezer Bag 1 + ICI
Storage Bag 1 + ICI
E
PC Bottle Extracts
% E2
Extraction Dilution
E2
EtOH Extract
Saline Extract
3x SD of VC
EtOH Extract + ICI
Saline Extract + ICI
F
BPA-free Bottle Extracts
% E2
Extraction Dilution
E2
EtOH Extract
Saline Extract
3x SD of VC
EtOH Extract + ICI
Saline Extract + ICI

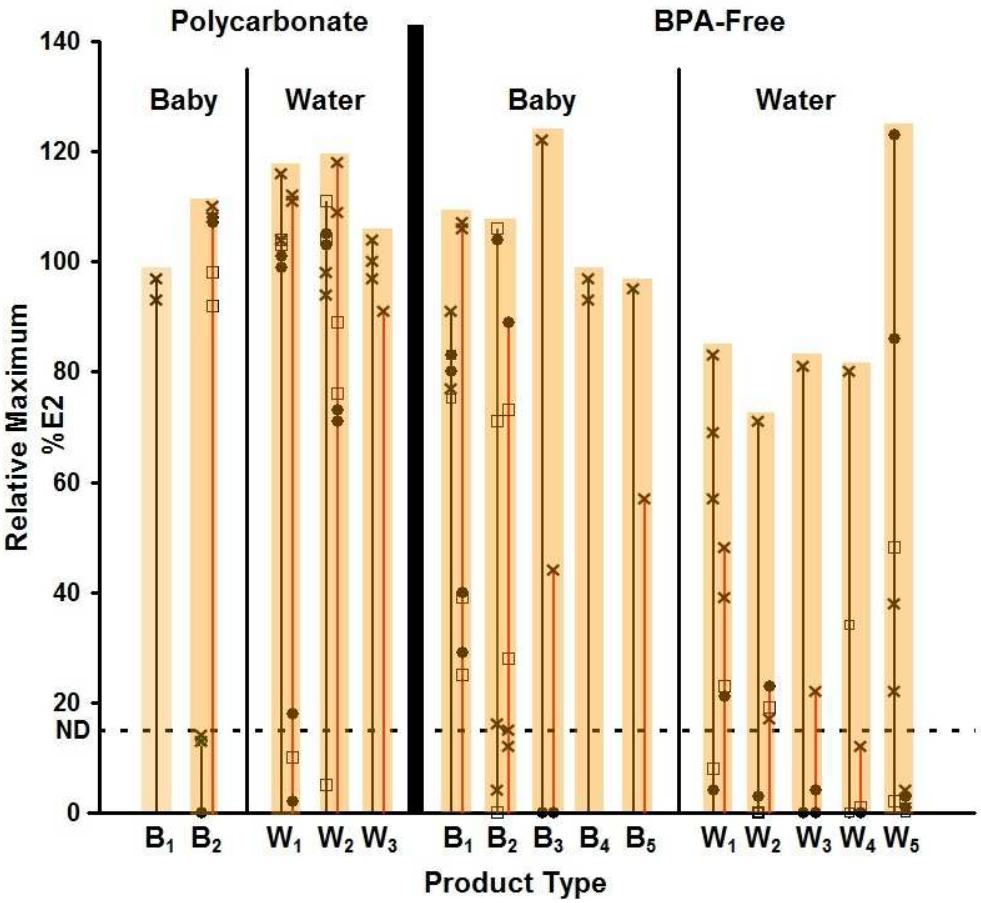
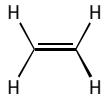
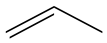
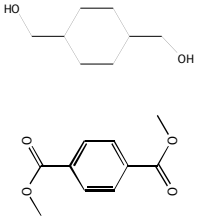
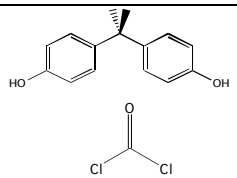
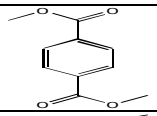
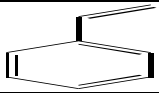
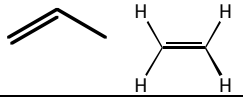
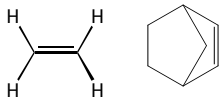
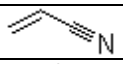
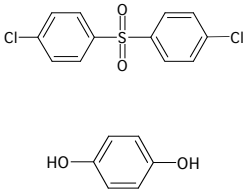


Figure 2. Total EA Released By Some PC and BPA-free Water and Baby Bottles
169x153mm (120 x 120 DPI)

Figure 3. Properties of monomers and polymers used to make common resins

Flexible Polymers	Monomer	Structure	EA	Toxicity[a]
Low-Density Polyethylene (LDPE) Linear Low-Density Polyethylene (LLDPE) High Density Polyethylene (HDPE)	Ethylene		No	No
Polypropylene Homopolymer (PPHO)	Propylene		No	No
Hard and Clear Polymers[b]				
Copolymer using terephthalate PETG	1,4 cyclohexanedimethanol, Dimethyl terephthalate[c]		Yes[d]	No
Polycarbonate (PC)	Bisphenol A[e], phosgene		Yes	Yes
Polyethylene terephthalate (PET)	Dimethyl terephthalate[e]		Yes[d]	No
Polystyrene (PS)	Styrene		Yes[d]	No
Polypropylene Copolymer (PPCO)	Propylene, Ethylene		No	No
Cyclic olefin polymer (COP) Cyclic olefin copolymer (COC)	Ethylene, norbornene		No	No
Polyacrylonitrile (PAN)	Acrylonitrile		No	Yes
Polyethersulfone (PES)	1,4-Bis(4-chlorophenyl) sulfone, 1,4-dihydroxybenzene[e]		Yes[d]	No

Published OnlineFirst April 10, 2011; DOI:10.1158/1940-6207.CAPR-11-0185

Cancer Prevention Research

Paradoxical Clinical Effect of Estrogen on Breast Cancer Risk: A "New" Biology of Estrogen-induced Apoptosis

V. Craig Jordan and Leslie G. Ford

Cancer Prev Res 2011;4:633-637. Published OnlineFirst April 10, 2011.

Updated Version	Access the most recent version of this article at: doi:10.1158/1940-6207.CAPR-11-0185
Supplementary Material	Access the most recent supplemental material at: http://cancerpreventionresearch.aacrjournals.org/content/suppl/2011/04/08/1940-6207.CAPR-11-0185.DC1.html

Cited Articles	This article cites 28 articles, 16 of which you can access for free at: http://cancerpreventionresearch.aacrjournals.org/content/4/5/633.full.html#ref-list-1

E-mail alerts	Sign up to receive free email-alerts related to this article or journal.
Reprints and Subscriptions	To order reprints of this article or to subscribe to the journal, contact the AACR Publications Department at pubs@aacr.org.
Permissions	To request permission to re-use all or part of this article, contact the AACR Publications Department at permissions@aacr.org.

Downloaded from cancerpreventionresearch.aacrjournals.org on May 24, 2011
Copyright © 2011 American Association for Cancer Research

Published OnlineFirst April 10, 2011; DOI:10.1158/1940-6207.CAPR-11-0185

Cancer Prevention Research

Insight

Paradoxical Clinical Effect of Estrogen on Breast Cancer Risk: A "New" Biology of Estrogen-induced Apoptosis

V. Craig Jordan[1] and Leslie G. Ford[2]

Abstract

Administration of estrogen replacement therapy (ERT) decreases the incidence of breast cancer, as shown in a double-blind, placebo-controlled randomized trial of the *Women's Health Initiative* (WHI) in 10,739 postmenopausal women with a prior hysterectomy. Although paradoxical because estrogen is recognized to stimulate breast cancer growth, laboratory data support a mechanism of estrogen-induced apoptosis under the correct environmental circumstances. Long-term antiestrogen treatment or estrogen deprivation causes the eventual development and evolution of antihormone resistance. Cell populations emerge with a vulnerability, as estrogen is no longer a survival signal but is an apoptotic trigger. The antitumor effect of ERT in estrogen-deprived postmenopausal women is consistent with laboratory models. *Cancer Prev Res; 4(5); 633–7. ©2011 AACR.*

Introduction

It is widely held that estrogen can be carcinogenic in breast tissue (1) and is the "fuel for the fire" to stimulate the growth of estrogen receptor (ER)-positive breast cancer cells (2). This knowledge, supported by an enormous body of laboratory data, provides the conceptual basis for the successful development of antihormonal strategies to treat breast cancer (3). Selective ER modulators (SERMs), for example, tamoxifen, block estrogen-stimulated tumor growth at the ER, and aromatase inhibitors prevent peripheral estrogen synthesis in postmenopausal patients, thereby creating estrogen deprivation to stop tumor growth (3). The successful treatment strategy for breast cancer with SERMs was subsequently translated into reducing the risk of breast cancer in high-risk women. SERMs are available to reduce the incidence of breast cancer in pre- and postmenopausal (tamoxifen) or postmenopausal (raloxifene) women (4–6). As predicted by the mechanism of action of SERMs as anticancer agents, only ER-positive breast cancer is reduced. In practice, preventing estrogen action prevents breast tumor initiation and growth. Paradoxically, the recent analysis of estrogen replacement therapy (ERT) in the *Women's Health Initiative* (WHI) double-blind, placebo-controlled randomized trial in 10,739 postmenopausal women with a prior hysterectomy (ages 50–79; ref. 7) actually showed a decrease in invasive breast cancer, which was sustained for 5 years after ERT was stopped. This result seems to run counter to the perceived wisdom of the role of estrogen in breast carcinogenesis, was significant in women of all ages, and was similar in every age group.

When the WHI was initiated in 1993, their present clinical result of a reduction in breast cancer was unanticipated (7) but is consistent nevertheless with parallel laboratory studies completed over the past 20 years. Estrogen-induced apoptosis is a plausible molecular mechanism to support an antitumor action of physiologic estrogen (8). The key to our understanding of estrogen-induced apoptosis is the finding that breast cancer cell populations adapt to estrogen deprivation, but these populations are dynamic, and resistance to estrogen deprivation evolves over time (5 years). This evolution of resistance to estrogen deprivation causes a reconfiguration of cellular survival pathways, which in turn exposes a vulnerability of breast cancer cell survival. Physiologic estrogen causes apoptosis and does not act as a survival signal (8).

We will weigh the laboratory and clinical evidence to support the proposition that physiologic estrogen can cause apoptosis in breast cancer cells following long-term estrogen deprivation. Our objective is to make a case based on scientific observations to support our proposition that nascent breast cancer cells could have the same apoptotic response to ERT after estrogen deprivation caused by menopause. We will present the evidence in chronological order (Box 1).

Evidence from the Historical Use of Estrogens to Treat Metastatic Breast Cancer

The application of high-dose estrogen therapy for the treatment of metastatic breast cancer was the first use of a chemical therapy to treat any cancer successfully (9). Estrogen therapy became the standard of care to treat metastatic breast cancer in postmenopausal patients until

Authors' Affiliations: [1]Georgetown Lombardi Comprehensive Cancer Center, Georgetown University Medical Center, Washington, District of Columbia; and [2]Division of Cancer Prevention, National Cancer Institute, National Institutes of Health, Bethesda, Maryland

Corresponding Author: V. Craig Jordan, Georgetown University Medical Center, 3970 Reservoir Rd NW, Research Building, Suite E501, Washington, DC 20057. Phone: 202-687-2897; Fax: 202-687-6402; E-mail: vcj2@georgetown.edu

doi: 10.1158/1940-6207.CAPR-11-0185

©2011 American Association for Cancer Research.

Downloaded from cancerpreventionresearch.aacrjournals.org on May 24, 2011
Copyright © 2011 American Association for Cancer Research

Published OnlineFirst April 10, 2011; DOI:10.1158/1940-6207.CAPR-11-0185

BOX 1. Cumulative evidence to support low dose estrogen-induced apoptosis in long-term estrogen-deprived nascent breast cancer?

1. Historical use of estrogens to treat breast cancer.
2. Physiologic estrogen as an antitumor agent in SERM-resistant breast cancer models *in vivo*.
3. Estrogen-induced apoptosis in estrogen-deprived ER-positive cell lines *in vitro*.
4. A current evaluation of estrogen to treat acquired antihormone resistance in metastatic breast cancer.
5. The extrapolation of the concept that physiologic estrogen kills breast cancer cells to adjuvant antihormone therapy.

the introduction of tamoxifen (late 1970s in the United States), a nonsteroidal antiestrogen (10). Tamoxifen became the "gold standard" for the treatment of ER-positive (estrogen stimulated) breast cancer for the next 20 years. Estrogen was all but abandoned as a treatment option, but Ingle and colleagues completed a provocative trial of tamoxifen versus the synthetic estrogen diethylstilbestrol (DES; high-dose) in metastatic breast cancer (11). Responses were equivalent with fewer side effects with tamoxifen, but a re-analysis years later demonstrated that survival was significantly improved with DES (12).

Towards the end of his distinguished career, Professor Sir Alexander Haddow FRS reflected (during the inaugural Karnofsky Memorial Lecture; ref. 13) on the remarkable responses noted with estrogen in some tumors, often when treatment was more than a decade past menopause: "*The extraordinary extent of tumour regression observed in perhaps 1% of post-menopausal cases (with oestrogen) has always been regarded as of major theoretical importance, and it is a matter for some disappointment that so much of the underlying mechanisms continues to elude us.*"

Although laboratory research to address Haddow's estrogen paradox essentially ceased for the next 20 years, at least 1 animal model transplanted with a human breast tumor replicated the antitumor action of high-dose estrogen therapy for breast cancer (14, 15). The question could have been addressed. However, the breakthrough in our understanding of a mechanism for estrogen-induced apoptosis came with a study of continuous long-term SERM treatment in transplantable SERM-resistant breast cancer in athymic mice. As often happens in science, a discovery in an apparently unrelated area becomes the required breakthrough to create transparency in nature.

Physiologic Estrogen Is an Antitumor Agent in SERM-Resistant Breast Cancer *In Vivo*

In the 1980s, the first athymic animal models of tamoxifen-induced antihormone resistance were reported, but the acquired resistance surfaced within 2 years as tamoxifen-stimulated growth (2). This replicated the use of tamoxifen in the treatment of metastatic ER-positive breast cancer but did not explain the astonishing success of 5 years of adjuvant tamoxifen therapy in reducing recurrences by 50% and mortality by 30%. Most important, the gains obtained during therapy are maintained (and mortality further reduced) for the next 15 years. We were missing a vital clue about the evolution of antihormone resistance in micrometastatic breast cancer.

Five years of re-transplantation of tumors into tamoxifen-treated athymic mice revealed a vulnerability in breast cancer that would subsequently be exploited in clinical trial. Physiologic estradiol does not promote tumor growth, but small tumors undergo rapid and complete regression (16). It was suggested (16) that following the cessation of adjuvant tamoxifen, a woman's own estrogen would exert an antitumor action and enhance survivorship. Further studies (17) subsequently demonstrated that following tumor regression with physiologic estradiol, any remaining tumor that re-grows in the estrogen environment is again responsive to tamoxifen as an antitumor agent. Continuing studies demonstrated that the principle of physiological estrogen therapy causing apoptosis in SERM-resistant disease was also true for raloxifene (18, 19). These data provided a scientific rationale for subsequent clinical studies.

Estrogen Induces Apoptosis in Estrogen-deprived ER-positive Breast Cancer Cell Lines

Song and colleagues (20) first showed in cell culture that high concentrations of estrogen could induce cellular apoptosis directly through a FAS/FASL pathway. However, the discovery that physiologic concentrations of estradiol could induce apoptosis (21) in both cell culture and animal models was the advance pertinent to the clinical observation that ERT reduces the incidence of breast cancer in postmenopausal women (7). This is now a consistent experimental observation with new knowledge emerging about the molecular mechanisms of estrogen-induced apoptosis. Figure 1 summarizes much of the current data on molecular mechanisms of estrogen-induced apoptosis, the topic of a forthcoming mini-review in *Cancer Prevention Research* later this year.

Despite the significant body of laboratory data to support the proposition that physiologic estrogen can induce apoptosis in long-term estrogen-deprived breast cancer cells, only the translation to patients tests the veracity of the experimental approach as a conversation with nature and a general principle.

Current Evaluation of Estrogen to Treat Acquired Antihormone Resistance in Metastatic Breast Cancer

Lonning and colleagues (22) studied the efficacy of high dose of DES on the responsiveness of metastatic breast

Downloaded from cancerpreventionresearch.aacrjournals.org on May 24, 2011
Copyright © 2011 American Association for Cancer Research

Published OnlineFirst April 10, 2011; DOI:10.1158/1940-6207.CAPR-11-0185

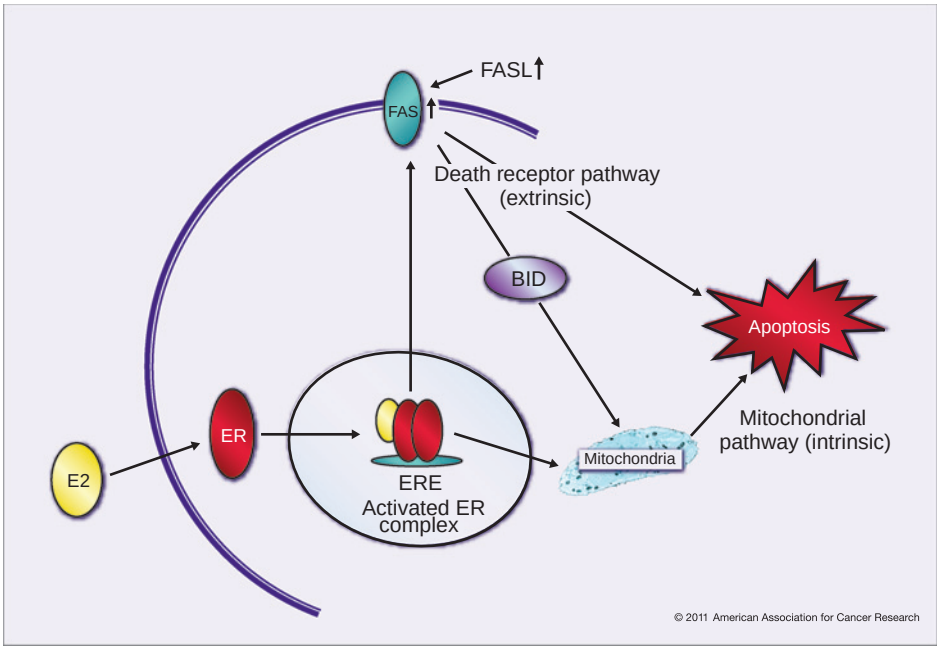


Figure 1. The 2 main pathways involved in estrogen-induced apoptosis regulation. This apoptosis can be triggered either through the extrinsic death-receptor pathway with an increase in Fas ligand (20) or Fas (27) or via the intrinsic pathway of mitochondrial disruption and release of cytochrome *C* (28). E2, estradiol (the most potent estrogen in women); ERE, estrogen response element; BID, Bcl-2–interacting domain.

cancer following exhaustive treatment with antihormone therapies (tamoxifen, aromatase inhibitors, etcetera). A remarkable 4 of 32 patients had complete responses (22), and 1 patient, who was treated for 5 years, had no recurrence of her disease 6 years after stopping DES (23). The question, however, is whether physiologic estrogen has efficacy as an antitumor agent in the appropriately prepared estrogen-deprived breast tumor. Ellis and colleagues (24) addressed this question and found an equivalent clinical benefit for high (30 mg daily) and low (6 mg daily) dose of estradiol in metastatic breast cancer patients who had failed aromatase inhibitor therapy, that is, long-term estrogen deprivation. Their clinical advance was that low-dose estrogen was as efficacious as high-dose estrogen for antitumor therapy in breast cancer (for the appropriate tumor that had been estrogen deprived), but there were fewer side effects with low-dose therapy. The target, estrogen-deprived breast cancer, is vulnerable to physiologic estrogen.

The Extrapolation of the Concept that Physiologic Estrogen Kills Breast Cancer to Adjuvant Antihormone Therapy

The result from the WHI Trial of ERT in hysterectomized women (7), which showed a sustained reduction in the incidence of breast cancer, provides additional evidence that the strategy to decipher the mechanism of physiologic estrogen to induce apoptosis (8, 25, 26) has significance for both treatment and prevention. Indeed, the idea that a woman's own estrogen was responsible for enhanced survivorship by causing apoptosis of the appropriately prepared and vulnerable micrometastases (16) followed the completion of long-term adjuvant tamoxifen therapy and now is incorporated into the Study of Letrozole Extension (SOLE) Trial. This extended adjuvant antihormone treatment study (Fig. 2) is addressing the question of whether regular drug holidays will decrease recurrence rates compared with continuous therapy. For initial safety reasons, a women's own estrogen during the drug holiday is hypothesized to be adequate as an apoptotic trigger because rigorous prior antihormone therapy will have selected vulnerable cell populations as the waiting target. Subsequent trials may have to use ERT for a few weeks to trigger apoptosis.

We have presented an integrated approach to support the proposition that ERT could induce apoptosis and reduce the incidence of breast cancer. The important issue for the decision of breast cancer cells to survive or die in response to estradiol depends entirely on the cell populations present in an estrogenized environment or following estrogen deprivation. Based on laboratory data, the decision is survival or death, respectively. The role of estrogen deprivation, either pharmacologic with antihormones or physiologic with menopause, is to select populations of cells that can survive without physiologic estrogen. These cells choose to die through a natural process when re-exposed to pharmacologic or physiologic estrogen. The genetics are the same, but different epigenetic events based on the well-established property of cancer cells to be able to adapt to any environment and survive remains true. As the WHI study of ERT shows (7), physiologic estrogen has delivered what the scientific database would now predict.

Downloaded from cancerpreventionresearch.aacrjournals.org on May 24, 2011
Copyright © 2011 American Association for Cancer Research

Published OnlineFirst April 10, 2011; DOI:10.1158/1940-6207.CAPR-11-0185

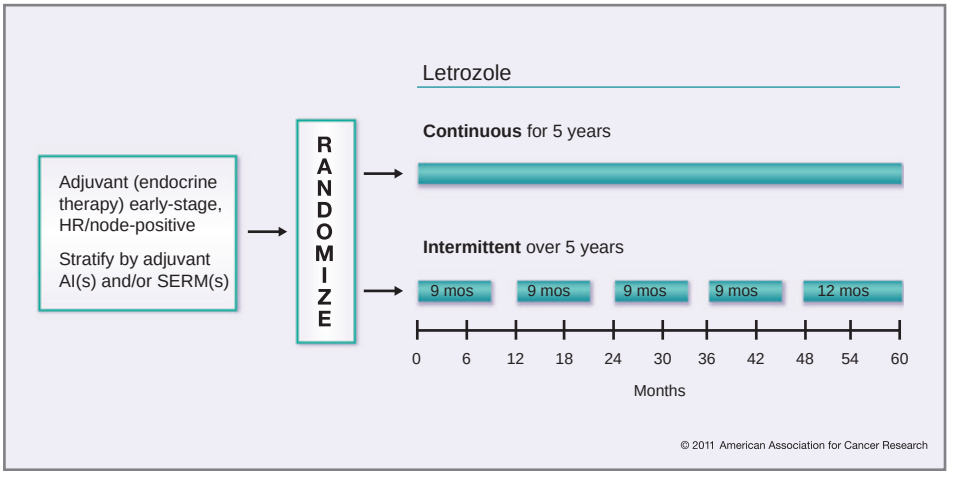


Figure 2. Schema for the Study of Letrozole Extension (SOLE; IBCSG 35-07) conducted by the International Breast Cancer Study Group (IBCSG). Upon completing 4 to 6 years of prior adjuvant endocrine therapy with a SERM(s) and/or aromatase inhibitor(s) (AI), patients were randomly assigned to continuous or intermittent letrozole (3-month drug holidays per year) for 5 years. The rationale for this approach was that the woman's own estrogen in the intermittent arm would trigger apoptosis in long-term estrogen-deprived breast cancer and reduce recurrence rates. Adapted from *International Breast Cancer Study Group* - Study of Letrozole Extension (www.ibcsg.org).

Disclosure of Potential Conflicts of Interest

The content is solely the responsibility of the authors and does not necessarily represent the official views of the National Cancer Institute or the NIH. The views and opinions of the author(s) do not reflect those of the U.S. Army or the Department of Defense. No conflicts of interest were reported.

Grant Support

This work was supported by the following grants of VC Jordan: Department of Defense Breast Program under Award number BC050277 Center of Excellence (this interdisciplinary research grant supports research into estrogen-induced apoptosis in breast cancer); subcontract under the SU2C (AACR) grant number SU2C-AACR-DT0409); the Susan G. Komen for the Cure Foundation under Award number SAC100009 and the Lombardi Comprehensive Cancer Center Support Grant (CCSG) Core Grant NIH P30 CA051008 from the National Cancer Institute.

Received April 8, 2011; accepted April 8, 2011; published OnlineFirst April 10, 2011.

References

1. Yager JD, Davidson NE. Estrogen carcinogenesis in breast cancer. N Engl J Med 2006;354:270–82.
2. Levenson AS, Jordan VC. MCF-7: the first hormone-responsive breast cancer cell line. Cancer Res 1997;57:3071–8.
3. Jordan VC. A century of deciphering the control mechanisms of sex steroid action in breast and prostate cancer: the origins of targeted therapy and chemoprevention. Cancer Res 2009;69:1243–54.
4. Fisher B, Costantino JP, Wickerham DL, Cecchini RS, Cronin WM, Robidoux A, et al. Tamoxifen for the prevention of breast cancer: current status of the National Surgical Adjuvant Breast and Bowel Project P-1 study. J Natl Cancer Inst 2005;97:1652–62.
5. Vogel VG, Costantino JP, Wickerham DL, Cronin WM, Cecchini RS, Atkins JN, et al. Effects of tamoxifen vs raloxifene on the risk of developing invasive breast cancer and other disease outcomes: the NSABP Study of Tamoxifen and Raloxifene (STAR) P-2 trial. JAMA 2006;295:2727–41.
6. Vogel VG, Costantino JP, Wickerham DL, Cronin WM, Cecchini RS, Atkins JN, et al. Update of the National Surgical Adjuvant Breast and Bowel Project Study of Tamoxifen and Raloxifene (STAR) P-2 Trial: preventing breast cancer. Cancer Prev Res 2010;3:696–706.
7. La Croix AZ, Chlebowski RT, Manson JE, Aragaki AK, Johnson KC, Martin L, et al. Health outcomes after stopping conjugated equine estrogens among postmenopausal women with prior hysterectomy: a randomized controlled trial. JAMA 2011;305:1305–14.
8. Jordan VC. The 38th David A. Karnofsky Lecture: the paradoxical actions of estrogen in breast cancer—survival or death? J Clin Oncol 2008;26:3073–82.
9. Haddow A, Watkinson JM, Paterson E, Koller PC. Influence of synthetic oestrogens on advanced malignant disease. Br Med J 1944;2:393–8.
10. Lerner LJ, Jordan VC. Development of antiestrogens and their use in breast cancer: Eighth Cain Memorial Award Lecture. Cancer Res 1990;50:4177–89.
11. Ingle JN, Ahmann DL, Green SJ, Edmonson JH, Bisel HF, Kvols LK, et al. Randomized clinical trial of diethylstilbestrol versus tamoxifen in postmenopausal women with advanced breast cancer. N Engl J Med 1981;304:16–21.
12. Peethambaram PP, Ingle JN, Suman VJ, Hartmann LC, Loprinzi CL. Randomized trial of diethylstilbestrol vs. tamoxifen in postmenopausal women with metastatic breast cancer. An updated analysis. Breast Cancer Res Treat 1999;54:117–22.
13. Haddow A, David A. Karnofsky memorial lecture. Thoughts on chemical therapy. Cancer 1970;26:737–54.
14. Brunner N, Spang-Thomsen M, Vindelov L, Nielsen A. Effect of 17 beta-oestradiol on growth curves and flow cytometric DNA distribution of two human breast carcinomas grown in nude mice. Br J Cancer 1983;47:641–7.
15. Brunner N, Bastert GB, Poulsen HS, Spang-Thomsen M, Engelholm SA, Vindelov L, et al. Characterization of the T61 human breast carcinoma established in nude mice. Eur J Cancer Clin Oncol 1985;21:833–43.
16. Wolf DM, Jordan VC. A laboratory model to explain the survival advantage observed in patients taking adjuvant tamoxifen therapy. Recent Results Cancer Res 1993;127:23–33.

Downloaded from cancerpreventionresearch.aacrjournals.org on May 24, 2011
Copyright © 2011 American Association for Cancer Research

Published OnlineFirst April 10, 2011; DOI:10.1158/1940-6207.CAPR-11-0185

17. Yao K, Lee ES, Bentrem DJ, England G, Schafer JI, O'Regan RM, et al. Antitumor action of physiological estradiol on tamoxifen-stimulated breast tumors grown in athymic mice. Clin Cancer Res 2000;6:2028–36.
18. Liu H, Lee ES, Gajdos C, Pearce ST, Chen B, Osipo C, et al. Apoptotic action of 17beta-estradiol in raloxifene-resistant MCF-7 cells in vitro and in vivo. J Natl Cancer Inst 2003;95:1586–97.
19. Balaburski GM, Dardes RC, Johnson M, Haddad B, Zhu F, Ross EA, et al. Raloxifene-stimulated experimental breast cancer with the paradoxical actions of estrogen to promote or prevent tumor growth: a unifying concept in anti-hormone resistance. Int J Oncol 2010;37:387–98.
20. Song RX, Mor G, Naftolin F, McPherson RA, Song J, Zhang Z, et al. Effect of long-term estrogen deprivation on apoptotic responses of breast cancer cells to 17beta-estradiol. J Natl Cancer Inst 2001;93:1714–23.
21. Jordan VC, Liu H, Dardes R. Re: Effect of long-term estrogen deprivation on apoptotic responses of breast cancer cells to 17 beta-estradiol and the two faces of Janus: sex steroids as mediators of both cell proliferation and cell death. J Natl Cancer Inst 2002;94:1173–5.
22. Lonning PE, Taylor PD, Anker G, Iddon J, Wie L, Jorgensen LM, et al. High-dose estrogen treatment in postmenopausal breast cancer patients heavily exposed to endocrine therapy. Breast Cancer Res Treat 2001;67:111–6.
23. Lonning PE. Additive endocrine therapy for advanced breast cancer—back to the future. Acta Oncol 2009;48:1092–101.
24. Ellis MJ, Gao F, Dehdashti F, Jeffe DB, Marcom PK, Carey LA, et al. Lower-dose vs high-dose oral estradiol therapy of hormone receptor-positive, aromatase inhibitor-resistant advanced breast cancer: a phase 2 randomized study. JAMA 2009;302:774–80.
25. Maximov PY, Lewis-Wambi JS, Jordan VC. The paradox of oestradiol-induced breast cancer cell growth and apoptosis. Curr Signal Transduct Ther 2009;4:88–102.
26. Lewis-Wambi JS, Jordan VC. Estrogen regulation of apoptosis: how can one hormone stimulate and inhibit? Breast Cancer Res 2009;11:206.
27. Osipo C, Gajdos C, Liu H, Chen B, Jordan VC. Paradoxical action of fulvestrant in estradiol-induced regression of tamoxifen-stimulated breast cancer. J Natl Cancer Inst 2003;95:1597–608.
28. Lewis JS, Meeke K, Osipo C, Ross EA, Kidawi N, Li T, et al. Intrinsic mechanism of estradiol-induced apoptosis in breast cancer cells resistant to estrogen deprivation. J Natl Cancer Inst 2005;97:1746–59.

Downloaded from cancerpreventionresearch.aacrjournals.org on May 24, 2011
Copyright © 2011 American Association for Cancer Research

Estrogen Receptor (ER)

Lizie Sweeney[1] and V. Craig Jordan[2] OBE, PhD, DSc, FMedSci

[1]Lombardi Comprehensive Cancer Center, Georgetown University Medical Center
[2]Scientific Director Lombardi Comprehensive Cancer Center, Vincent T. Lombardi Chair of Translational Cancer Research, Vice Chair of Department of Oncology, Professor of Oncology and Pharmacology, Georgetown University Medical Center

Target

The estrogen receptor (ER) is a nuclear receptor whose primary activating ligand is estrogen. The ER comprises five regions: the activating region, DNA binding domain, hinge domain, ligand-binding domain, and the C-terminus region (Figure 1). There exist two isoforms of ER, ERα and ERβ, which are encoded by different genes, on different chromosomes, which have different primary structures. The ERα gene is located on chromosome 6, and encodes a 595 amino acid protein with a molecular mass of about 66 kD (Couse and Korach 1999). The two isoforms also seem to have distinct functions; ERα generally promotes growth while ERβ can inhibit growth in some tissues (Deroo and Korach 2006) (Figure 1). The ratio of isoforms differs in tissues and can confer tissue-specific actions of ER (Deroo and Korach 2006). This ER isoform ratio indicates a general trend in growth of tumor cells; that is, a high ERα/ERβ ratio is associated with strong proliferation, while the inverse ratio correlates with low levels of cellular proliferation (Deroo and Korach 2006). ERα was the first isoform to be discovered, and is the one to be discussed in this article, as it mediates most of the physiological responses investigated in the laboratory (Couse and Korach 1999).

Biology of the target

Belonging to the nuclear receptor superfamily, the ER resides in the nucleus to bind and retain estrogens that have diffused through the cell from the bloodstream (Jordan 2009). The inactive ER is bound to heat shock proteins that dissociate once the ligand binds, allowing an active conformational change to occur (Couse and Korach 1999). When the estrogen and receptor complex is formed, it binds

to estrogen response elements (EREs), and coregulators are recruited to the ER complex tethered to the promotor region of a target gene. Tissues possess unique levels of the 258 known nuclear receptor coregulators (Jordan and O'Malley 2007). Nuclear receptor coregulator recruitment is considered the rate-limiting factor of transcription in mammals, making the arrival of coactivators and/or corepressors at the DNA an integral step in the regulation or control of ER activity (Jordan and O'Malley 2007).

When a ligand binds to the ER, a conformational change occurs to the receptor, depending on the nature of the ligand. X-ray crystallography has offered a detailed look into the structures of ligand-bound ER. An antagonistic or antiestrogenic complex will prop the "jaws" (Helix 12) of the ER open, while a planar steroidal estrogen or estrogenic molecule permit the "jaws" of the receptor to close. Estrogen response elements (EREs) can also influence ER conformation, thereby causing varied recruitment of coregulators and therefore gene function (Jordan and O'Malley 2007).

ER bound with either an estrogen or antiestrogen causes coregulator binding based on the ligand-receptor complex shape. Many varied ligands can bind to the ER, as many varied responses can occur; that is, gradient levels of estrogenicity or antiestrogenicity develop due to recruitment of coactivators or corepressors based on receptor-ligand conformation (Jordan 2008). Figure 1 summarizes the activation of the ER through its signal transduction pathway (Jordan 2006).

Target assessment

The ER was discovered through the injection of [^{3}H]estradiol into immature rats, followed by analysis of radioactivity in specific tissues. It was found that the uterus and vagina, estrogen target tissues, bound and retained the [^{3}H]estradiol, while organs such as the kidney and liver, estrogen nontarget tissues, washed out the radioactive marker (Jensen and Jordan 2003). This generated the notion that perhaps a receptor was present in the target tissues, allowing the ligand to induce estrogen-associated cellular function and activity. X-ray crystallography was subsequently used to visualize ligand binding to the purified ER protein (Jensen and Jordan 2003).

Clinically, when a patient presents with breast cancer, a biopsy of the breast tissue is taken and observed under a microscope. The tissue can then be evaluated for the presence and status of the ER by staining with a monocolonal antibody against the ER linked to a fluorescent or radioactive marker.

This immunohistochemistry allows the pathologist or clinician to visualize and quantify the ER level in patients' tumors, a critical step in choosing a treatment process that will be effective for that certain tumor phenotype. If the biopsied cells do not present ER, the tumor is termed ER-negative; if they do, they are termed ER-positive. Immunohistochemistry is also used to evaluate other hormone receptor levels applicable in breast cancer, such as HER2 and progesterone receptor (PR).

High level overview

The ER became the first successful major target for cancer therapy (Jordan 2007), but its role in cancer treatment began as a marker in a diagnostic test to predict whether endocrine ablation, such as oophorectomy, would be of value to the patient (McGuire 1973). The assay indicated whether the patient's tumor was ER-positive, therefore likely responsive to estrogen withdrawal (Deroo and Korach 2006; Jensen and Jordan 2003; Jordan 2009). ER-negative breast cancer tumors do not respond to hormonal therapy because there is no ER present by which cellular functions and replication can be modulated (McGuire 1973).

The ER is considered the first drug target for the treatment of breast cancer. Although physiologic estrogen has been shown to stimulate growth of breast cancer, counterintuitively, high-dose estrogen therapy was successfully used as the first chemical cancer therapy (Haddow et al. 1944). Because the ER has the capacity to be modulated, selective estrogen receptor modulators (SERMs) such as raloxifene and tamoxifen were recognized to be useful in the clinic for targeted ER agonism and antagonism. By targeting the ER with drugs like tamoxifen, patients gain a survival advantage from breast cancer. This ER-directed therapy increases the likelihood of survival, thus demonstrating the efficacy of ER as a major therapeutic target in the breast tumor.

Diagnostic, prognostic, predictive

The ER is used in clinical diagnostics to determine what breast cancer phenotype the patient presents. An ER-positive breast tumor indicates the presence of ER in the tissue, and is one facet used

to describe and diagnose the disease. Further, ER-positive tumors generally represent a better prognosis since it is predicted, reasoned, and demonstrated that ER-positive tumors will respond to hormone therapy.

Therapeutics

Many therapeutics have been proposed and developed based on the mechanism of blocking ER action in breast cancer cells. Since the fate of the ER-mediated gene expression relies on the recruitment of coactivators and/or corepressors, it follows that the ER action can be altered by the presence or absence of coregulators. SERMs catalyze the tissue-specific modulation of the ER (Jordan 2004). SERMs bind to the ER, causing a conformational change in the receptor, thereby influencing what coregulators are recruited to the DNA. This process also depends on the presence and level of coactivators and corepressors in the tissue of interest, and the response elements to which the ligand-bound ER complex binds (Deroo and Korach 2006). Figure 2 details an ideal SERM (Jordan 2004).

SERMs are neither purely antagonists or agonists, but a mixed complex generating partial agonism and partial antagonism when ER-bound. In other words, the conformation the receptor forms when bound to a SERM has mixed affinity for coactivators and corepressors. With that thought, it is logical that concentrations of the coregulators in the physical context of the receptor is of critical importance in determining gene function (Jordan and O'Malley 2007). Tissue-specific SERM actions are not only regulated by coregulators, but also other elements include receptor isoform subtypes, ERE DNA sequences, and the turnover of the ER complex (Jordan and O'Malley 2007) (Figure 1).

Pre-clinical summary

Initial pre-clinical animal studies, as early as 1900, investigated ER knock-out mice to investigate endocrine ablation therapy (Couse and Korach 1999). These studies began to illustrate the effects and actions which require genomic ER function. Other pre-clinical studies illustrated the correlation between breast tumorigenesis and duration of lifetime estrogen exposure (Couse and Korach 1999).

Important present pre-clinical investigation focuses on the resistance that can occur with the current clinical therapy. Acquired resistance is considered to be a major concern that limits the effectiveness of long-term antihormonal therapy. Athymic mouse (immune deficient) studies show that ER-positive PR-positive tumors treated at length with tamoxifen will eventually grow when treated with either estradiol or tamoxifen. Long-term SERM therapy induces a profound change in the signal transduction of breast cancer cells from estrogen-stimulated growth to SERM-stimulated growth (Jordan 2008). After extended antihormone therapy for many years, estrogen, once a breast cancer tumor growth enhancer, remarkably becomes an apoptotic trigger. This clinical and laboratory observation is seemingly counterintuitive, since it is established that oophorectomy can prevent tumors and estrogen can enhance tumor growth in the laboratory (Jordan 2004). The "estrogen paradox" is under intense investigation in the laboratory to facilitate effective translation to clinical practice (Jordan 2008). It had been established in 1944 that high-dose estrogen therapy could cause regression of some breast tumors in post-menopausal patients, a then perplexing paradox (Haddow et al. 1944). This pioneering use of high-dose estrogen, the first clinical therapy to treat any cancer, could not be explained at the time but now supports the principle behind the "estrogen paradox." In normal physiological pre-menopausal breast cancer environment, the ligand-bound ER promotes tumor growth. When this environment is deprived of estrogen for a prolonged period of time, whether it be through use of SERMs or decades after menopause, drug resistance develops, and estrogen eventually triggers cellular apoptosis in the long-term surviving estrogen-deprived tumor cells (Jordan 2008). Pre-clinical laboratory investigation continues to focus on elucidation of acquired SERM resistance and estrogen-induced apoptosis.

Clinical summary

Though radiation and chemotherapy are also widely used in the clinic, hormonal therapy is the treatment most relevant to the ER. ER-positive breast cancer accounts for about 70% of all breast tumors (Masood 1992). Studies show that estrogen causes growth and proliferation of ER-positive breast cancer cells. Tamoxifen, a SERM, acts as an antagonist of the ER in breast tissue, allowing it to block estrogenic action in breast cancer cells, therefore providing effective therapy. Tamoxifen exhibits

estrogen-like (agonist action) in bone and the uterus (Deroo and Korach 2006). Nevertheless, tamoxifen has had widespread and pioneering success, saving hundreds of thousands of lives by treating breast cancer and becoming the pioneering medicine for the prevention of any cancer (Jordan and O'Malley 2007). Long-term adjuvant therapy targeted the breast ER specifically, and tamoxifen became the first drug approved to successfully treat high-risk pre- and post-menopausal patients. Tamoxifen was also found to inhibit the formation of contralateral primary breast cancer. However, this medicine started life as a failed contraceptive that was reinvented as the "gold standard" for the treatment of breast cancer. Unfortunately, the SERM effect of tamoxifen is evidenced by a small but significant increase in the incidence of endometrial cancer in post-menopausal women. This is an estrogen-like effect in the uterus which limits its use as a chemopreventive for breast cancer in post-menopausal women at high-risk.

In order to carry out its functions, tamoxifen must be converted, by the CYP2D6 enzyme system, to endoxifen. If any component of the enzyme system is mutated or functionally inactivated, tamoxifen resistance can occur. Further, some ER-positive breast cancer cells are intrinsically resistant to tamoxifen, perhaps dependent on the presence or absence of other receptors, such as progesterone receptor (PR) or HER-2/neu (Jordan and O'Malley 2007).

Selective serotonin reuptake inhibitors (SSRIs) are used to lessen menopausal symptoms such as hot flashes that can occur during treatment with tamoxifen. However, paroxetine and fluoxetine, two SSRIs, block tamoxifen's conversion to its active metabolite, endoxifen, thereby nullifying the drug. Fortunately, venlafaxine, a serotonin-norepinephrine reuptake inhibitor (SNRI), does not block CYP2D6 from metabolizing tamoxifen to endoxifen and can be taken simultaneously with tamoxifen to prevent hot flashes (Jordan 2009).

Raloxifene, previously known as keoxifene or LY126758, is another SERM structurally similar to tamoxifen. It began development as a potential breast cancer drug but because of its low bioavailability and cross-resistance with tamoxifen was subsequently found to be better suited for reduction of osteoporosis incidence with the prevention of breast cancer as a beneficial side effect (Jordan 2009). Raloxifene became an effective long-term drug therapy for treatment and prevention of osteoporosis for women at risk with the benefit of reducing the incidence of breast cancer (Cummings et al. 1999). Additionally, raloxifene is available with FDA approval to reduce breast cancer incidence in post-

menopausal women at risk for developing the disease (Vogel et al. 2010). Raloxifene does not increase the incidence of endometrial cancer. A new SERM, lasofoxifene, is 100x more potent than raloxifene for the treatment and prevention of osteoporosis. Its beneficial side effects are a reduction of strokes, breast cancer, endometrial cancer, and coronary heart disease (Cummings et al. 2010).

Other than SERMs, another way that the ER activity can be modified is by limiting the availability of the activating ligand, estrogen. Aromatase inhibitors block the aromatase enzyme either competitively or as suicide inhibitors. This prevents the conversion of androgen to estrogen, therefore blocking estrogen production (Deroo and Korach 2006).

Patients with ER-positive breast cancer respond effectively to treatment with SERMs and aromatase inhibitors; these therapies are used routinely in the clinic. ICI 182,780, also known as fulvestrant, is a pure antiestrogen that enhances ER protein destruction and is used as a second-line therapy after acquired resistance occurs with tamoxifen or aromatase inhibitors (Jordan 2009).

Long-term treatment of ER-positive breast cancer patients with tamoxifen is the standard-of-care for pre-menopausal women. Alternatively, the majority of post-menopausal patients receive aromatase inhibitors instead of tamoxifen since it causes fewer side effects while still preventing estrogenic action (Jordan 2008).

Anticipated high-impact results (bullet points of anticipated data)

- Personalized targeted therapy for ER+ breast tumors
- Elucidation of mechanism of SERM resistance
- Therapy to prevent resistance to SERMs
- Therapy to exploit estrogen-induced apoptosis

The application of the ER as a cancer therapeutic target continues to offer promise in laboratory science and for the benefit of patients worldwide. Past scientific discoveries involving ER modulation have laid the foundation for other hormonal receptors and their applicable cancer therapy and/or prevention. The defining principles drawn from the targeting in breast cancers are already being applied to the androgen receptor (AR) and the treatment of prostate cancer (Chen et al. 2005). In the future, the

therapeutic targeting of the hormone receptor superfamily will have profound impact on cancer medicine. Investigation continues in this field to optimally exploit the expressed biology in breast tumors.

Cross-references

DNA, PR, AR

(insert Figure1 here)

Figure 1. The potential decision network in estrogen target tissues that could program a ligand receptor complex to activate estrogenic or antiestrogenic responses. There are two distinct estrogen receptors (ERs) (alpha and beta) that are differentially distributed throughout the body. The shape of the ligand can change the shape of the receptor complex. This is turn preprograms the complex to bind either a co-activator or co-repressor protein to enhance the intrinsic activity of the complex for estrogenic responses or reduces intrinsic activity for antiestrogenic responses, respectively. The final decision point is to activate or suppress genes directly at DNA estrogen response elements (ERE) or tether the AP-1 sites to increase gene transcription. Overall, a tissue can modify the decision network through cell surface receptor tyrosine kinases (RTK) enhancing the phosphorylation cascade. This in turn can increase phosphorylation of coactivators or the ER. The balance of decision outcomes modulates the response of a particular tissue.

Reprinted from British Journal of Pharmacology, Volume 147, V. Craig Jordan, Tamoxifen (ICI46,474) as a targeted therapy to treat and prevent breast cancer, p. S269-S276, Copyright (2006), with permission from John Wiley and Sons.

(insert Figure2 here)

Figure 2. Progress toward an ideal SERM. The overall good or bad aspects of administering hormone replacement therapy to postmenopausal women compared with the observed site-specific actions of the selective estrogen receptor modulators (SERMs) tamoxifen and raloxifene. The known beneficial or negative actions of SERMs have opened the door for drug discovery to create the ideal SERM or targeted SERMs to either improve quality of life or prevent diseases associated with aging in women.

Reprinted from Cancer Cell, Vol 5, Issue 3, V. Craig Jordan, Selective estrogen receptor modulation: Concept and consequences in cancer, p. 207-213, Copyright (2004), with permission from Elsevier.

References

Chen J, Kim J, Dalton JT. Discovery and therapeutic promise of selective androgen receptor modulators. Molecular Interventions 2005;5:173–88.

Couse JF, Korach KS. Estrogen receptor null mice: What have we learned and where will they lead us? Endocrine Reviews 1999;20(3):358-417.

Cummings SR, et al. The effect of raloxifene on risk of breast cancer in postmenopausal women: results from the MORE randomized trial. Multiple Outcomes of Raloxifene Evaluation. Journal of American Medical Association 1999;281:2189–97.

Cummings SR, et al. Lasofoxifene in postmenopausal women with osteoporosis. New England Journal of Medicine 2010;362:686-696.

Deroo BJ, Korach KS. Estrogen receptors and human disease. Journal of Clinical Investigation 2006;116(3):561-570.

Haddow A, Watkinson JM, Paterson E. Influence of synthetic oestrogens upon advanced malignant disease. British Medical Journal 1944;2:393–8.

Masood S. Estrogen and progesterone receptors in cytology: a comprehensive review. Diagnostic Cytopathology 1992;8:475–491.

McGuire WL. Estrogen receptors in human breast cancer. Journal of Clinical Investigation 1973;52(1):73-77.

Jensen EV, Jordan VC. The estrogen receptor: a model for molecular medicine. The Dorothy P. Landon AACR Prize for Translational Research. Clinical Cancer Res 2003;9:1980–9.

Jordan VC. Selective estrogen receptor modulation: Concept and consequences in cancer. Cancer Cell 2004;5(3):207-213.

Jordan VC. Tamoxifen (ICI46,474) as a targeted therapy to treat and prevent breast cancer. British Journal of Pharmacology 2006;147(S1):S269-S276.

Jordan VC. Tamoxifen: Catalyst of the change to targeted therapy. European Journal of Cancer 2007;44(1):30-38.

Jordan VC. The 38th David A. Karnofsky lecture: The paradoxical actions of estrogen in breast cancer -- survival or death? Journal of Clinical Oncology 2008;26(18):3073-3082.

Jordan VC. A century of deciphering the control mechanisms of sex steroid action in breast and prostate cancer: The origins of targeted therapy and chemoprevention. Cancer Research 2009;69:1243.

Jordan VC, O'Malley BW. Selective estrogen receptor modulators and antihormonal resistance in breast cancer. Journal of Clinical Oncology 2007;25(36):5815-5824.

Vogel VG, et al. Update of the national surgical adjuvant breast and bowel project study of tamoxifen and raloxifene (STAR) P-2 trial: Preventing breast cancer. Cancer Prevention Research 2010;3:696-706.

Figure 1

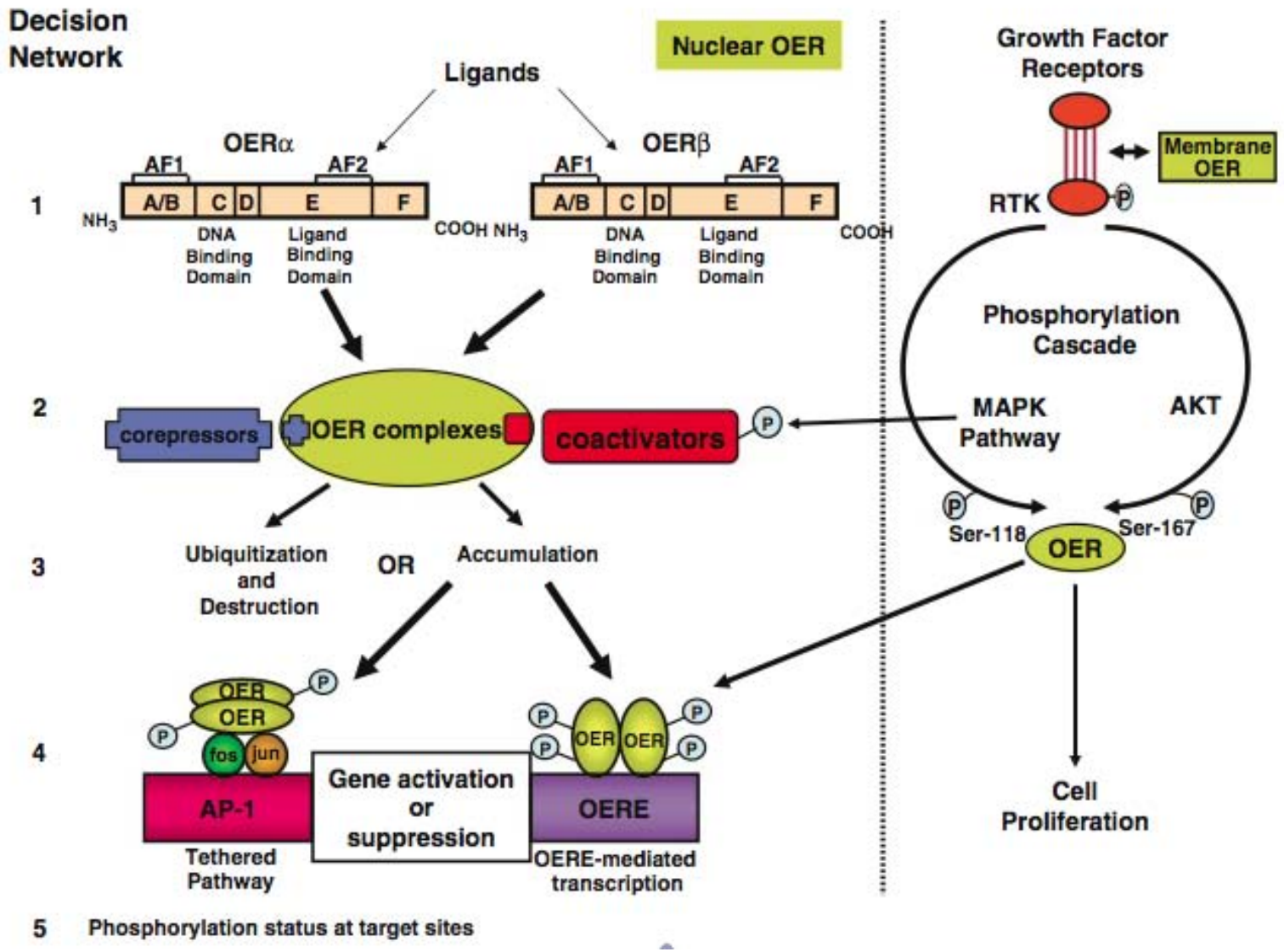
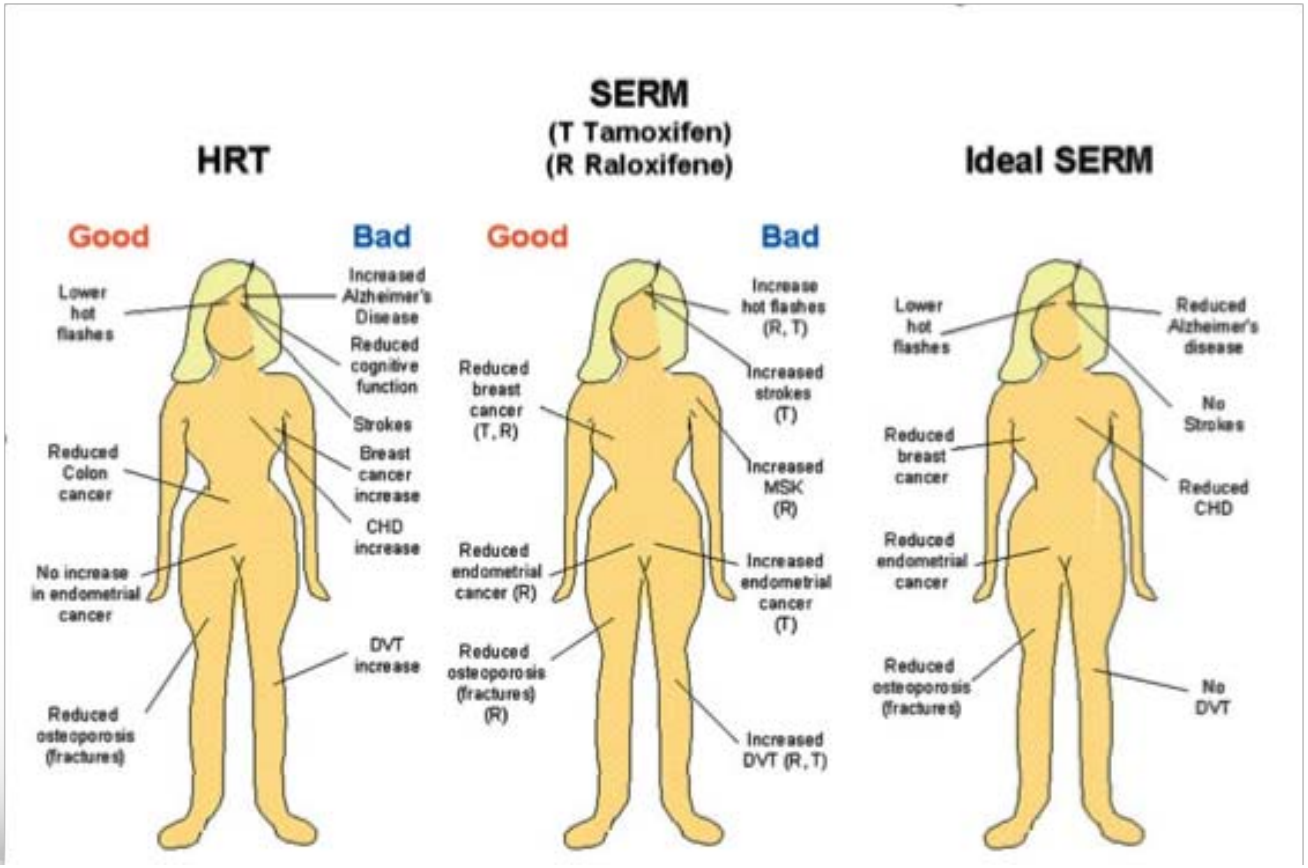

Decision Network
Nuclear OER
Ligands
Growth Factor Receptors
Membrane OER
RTK
OERα
OERβ
AF1
AF2
A/B
C
D
E
F
NH3
COOH
DNA Binding Domain
Ligand Binding Domain
1
2
corepressors
OER complexes
coactivators
Phosphorylation Cascade
MAPK Pathway
AKT
Ser-118
Ser-167
OER
3
Ubiquitization and Destruction
OR
Accumulation
4
fos
jun
AP-1
Tethered Pathway
Gene activation or suppression
OERE
OERE-mediated transcription
Cell Proliferation
5
Phosphorylation status at target sites

Figure 2


HRT
Good
Bad
Lower hot flashes
Increased Alzheimer's Disease
Reduced cognitive function
Strokes
Reduced Colon cancer
Breast cancer increase
CHD increase
No increase in endometrial cancer
DVT increase
Reduced osteoporosis (fractures)
SERM
(T Tamoxifen)
(R Raloxifene)
Good
Bad
Increase hot flashes (R, T)
Reduced breast cancer (T, R)
Increased strokes (T)
Increased MSK (R)
Reduced endometrial cancer (R)
Increased endometrial cancer (T)
Reduced osteoporosis (fractures) (R)
Increased DVT (R, T)
Ideal SERM
Lower hot flashes
Reduced Alzheimer's disease
No Strokes
Reduced breast cancer
Reduced CHD
Reduced endometrial cancer
Reduced osteoporosis (fractures)
No DVT

Evolution of Long-Term Adjuvant Anti-hormone Therapy:

Consequences and Opportunities.

The St. Gallen Prize Lecture.

V. Craig Jordan[1], Ifeyinwa Obiorah[1], Ping Fan[1], Helen R. Kim[1], Eric Ariazi[2], Heather Cunliffe[3] and Hiltrud Brauch[4]

1. Lombardi Comprehensive Cancer Center, Georgetown University, Washington, D.C. 20057, USA
2. Fox Chase Cancer Center, Philadelphia, PA, 19111, USA
3. Translational Genomics, Phoenix, AZ, 85004, USA
4. Dr. Margarete Fischer-Bosch-Institute of Clinical Pharmacology, Stuttgart, Germany

Short title: St. Gallen Prize Lecture

Key words: tamoxifen, selective oestrogen receptor modulators (SERMs), raloxifene, apoptosis, oestrogen, acquired drug resistance, chemoprevention

Address correspondence and enquires to: V. Craig Jordan, OBE, PhD, DSc, F.MedSci
Scientific Director
Lombardi Comprehensive Cancer Center
Georgetown University
3970 Reservoir Road NW, Research Building E-501
Washington, D.C. 20057, USA
vcj2@georgetown.edu

ABSTRACT

The successful translation of the scientific principles of targeting the breast tumour oestrogen receptor (ER) with the nonsteroidal anti-oestrogen tamoxifen and using extended durations (at least 5-years) of adjuvant therapy, dramatically increased patient survivorship and significantly enhanced a drop in national mortality rates from breast cancer. The principles are the same for the validation of aromatase inhibitors to treat post-menopausal patients but tamoxifen remains a cheap, life-saving medicine for the pre-menopausal patient. Results from the Oxford Overview Analysis illustrate the scientific principle of "longer is better" for adjuvant therapy in pre-menopausal patients. One-year of adjuvant therapy is ineffective at preventing disease recurrence or reducing mortality, whereas five-years of adjuvant tamoxifen reduces recurrence by 50% which is maintained for a further ten-years after treatment stops. Mortality is reduced but the magnitude continues to increase to 30% over a 15-year period. With this clinical database, it is now possible to implement simple solutions to enhance survivorship. Compliance with long-term anti-hormone adjuvant therapy is critical. In this regard, the use of selective serotonin reuptake inhibitors (SSRIs) to reduce severe menopausal side effects may be inappropriate. It is known that SSRIs block the CYP2D6 enzyme that metabolically activates tamoxifen to its potent anti-oestrogenic metabolite, endoxifen. The selective nor-epinephrine reuptake inhibitor, venlafaxine, does not block CYP2D6, and may be a better choice. Nevertheless, even with perfect compliance, the relentless drive of the breast cancer cell to acquire resistance to therapy persists. The clinical application of long-term anti-hormonal therapy for the early treatment and prevention of breast cancer, focused laboratory research on the discovery of mechanisms involved in acquired anti-hormone resistance. Decades of laboratory study to reproduce clinical experience described not only the unique mechanism of SERM-stimulated breast cancer growth, but also a new apoptotic biology of oestradiol action in

breast cancer, following 5-years of anti-hormonal treatment. Oestradiol-induced apoptotic therapy is currently shown to be successful for the short-term treatment of metastatic ER positive breast cancer following exhaustive treatment with anti-hormones. The "oestrogen purge" concept is now being integrated into trials of long-term adjuvant anti-hormone therapy. The Study of Letrazole Extension (SOLE) trial employs "anti-hormonal drug holidays" so that a woman's own oestrogen may periodically purge and kill the nascent sensitized breast cancer cells that are developing. This is the translation of an idea first proposed at the 1992 St. Gallen Conference. Although tamoxifen is the first successful targeted therapy in cancer, the pioneering medicine is more than that. A study of the pharmacology of tamoxifen opened the door for a pioneering application in cancer chemoprevention and created a new drug group: the Selective ER Modulators (SERMs) with group members (raloxifene and lasofoxifene) approved for the treatment and prevention of osteoporosis with a simultaneous reduction of breast cancer risk. Thus, the combined strategies of long-term anti-hormone adjuvant therapy, targeted to the breast tumour ER, coupled with the expanding use of SERMs to prevent osteoporosis and prevent breast cancer as a beneficial side effect have advanced patient survivorship significantly and promises to reduce breast cancer incidence.

INTRODUCTION

Professor Hans-Joerg Senn asked me to cast light on future opportunities for improving adjuvant anti-hormone therapy that can be implemented or tested in clinical trial. This I will do, but first I will preface my remarks with a quote from Patrick Henry, the first elected Governor of Virginia, who said it best: *"I have but one lamp by which my feet are guided, and that is the lamp of experience. I know no way of judging of the future, but by the past."* In 1969, when I started my research on the pharmacology of non-steroidal anti-oestrogen, there was no tamoxifen

(Fig 1), only ICI 46,474, an effective anti-fertility agent in rats[1]. The compound had anti-oestrogenic properties, so I proposed[2] to enhance its clinical application from an orphaned drug, with modest efficacy in metastatic breast cancer, to a targeted anti-cancer agent for adjuvant therapy and chemoprevention. Tamoxifen became my lamp, and subsequent laboratory research results shed light on the future of successful and safe adjuvant anti-hormone therapy, a new drug group of selected estrogen receptor modulation (SERMs)[3], a lead compound in the SERMs raloxifene for clinical applications, the promise of multi-functional medicines, the unique qualities of acquired anti-hormone drug resistance and a new apoptotic biology of oestrogen in breast cancer (Fig 1, Table 1)[4]. Tamoxifen, a failed contraceptive in women, is now a pioneering medicine in oncology [1] and is listed as an essential medicine by the World Health Organization.

The clinical validation[5, 6] of the laboratory principles of targeting the breast tumour oestrogen-receptor (ER)[7] with long-term adjuvant antihormonal therapy (tamoxifen and oestrogen withdrawal)[8, 9] using a long acting anti-oestrogen, metabolically activated to potent hydroxylated metabolites[9-12], established a treatment strategy that continues to enhance the survivorship of millions of women world-wide. The key to success was the application of the first effective medicine to target the tumour through blocking oestrogen-stimulated growth at the ER, but coupled with the application of the counter-intuitive laboratory finding, that long-term adjuvant therapy would be superior to short-term therapy to control recurrence. The strategy succeeded, despite initial clinical findings that the tumour response to tamoxifen was not strongly correlated to ER status[13, 14] and the legitimate concern that long-term therapy would precipitate early drug resistance. This concern was based on the fact that tamoxifen was only an effective treatment in unselected metastatic disease for about a year or two[15], so why would

extended or indefinite adjuvant tamoxifen treatment be effective at preventing recurrence in the adjuvant setting?

Clinical trials finally demonstrated that the laboratory principle of "longer was more effective at controlling recurrence" was correct[5, 6]. The subsequent development of the aromatase (AIs)[16] expanded post-menopausal patient treatment options and reduced "oestrogen-like" side effects associated with tamoxifen, such as endometrial cancer and thromboembolic disorders[17]. There was also a modest improvement of disease-free survival compared with tamoxifen. The widespread acceptance of long-term antihormonal therapy as the standard of care and the intense and exhaustive examination of patient population databases, now permit questions to be addressed to improve patient survivorship. At a time of shrinking resources for biomedical research but expanding menus of purported targeted drugs to close one pathway or another, it is time to apply simple, basic rules that will make an impact immediately on enhancing survivorship. Only then, is it prudent to fine tune the results from a position of strength, by interrogating the tumour biology with blockers of survival pathways.

SIMPLE SOLUTIONS TO ENHANCE SURVIVAL

It seems obvious but it must be stated. The past 30-years of successful translational research is without value if an infrastructure does not exist to ensure that a patient's treatment is maintained when the medicine has proven value to aid survival from breast cancer. A medical team is available to support a patient's needs but there must be a refocus of the team to relearn basic principles: chronic therapy that requires years to provide benefit is worthless if the patients will not follow the regimen. This act will **dramatically** reduce their potential for survival. The fashion over the past four decades, for evidence based medicine, requires effective delivery.

Significantly, delivery is a minor commitment compared to the effort behind discovering and proving the efficiency of a medicine in prospective clinical trials.

Based on the published evidence, several general principles are emerging about compliance. A recent analysis of anti-hormone therapy conducted in patients enrolled in the Kaiser Permanente of Northern California health system[18], revealed that approximately 30% of all patients discontinued either AI or tamoxifen early but of those who did continue, 70% were fully adherent for up to 5-years. Thus, only 49% overall are adherent for the full course of adjuvant anti-hormonal therapy. Predictors of non-adherence were African-American race, lumpectomy, unknown tumour site, lymph node involvement and other co-morbidities. Adherence was associated with Asian/Pacific Island ethnicity, married, earlier years of diagnosis (tamoxifen era), prior chemotherapy, radiation therapy and longer prescription refills. These and similar findings[19, 20] describe the extent of the problem but noncompliance with effective therapeutic agents also increases recurrence and mortality[21-23].

Another significant finding of the Hershman study[18] was that young women under 40-years old were more likely to discontinue anti-hormone therapy. This group would be prescribed tamoxifen but reasons for stopping could be because the women chose to start a family or the menopausal side effects were too severe. In regard to the latter, many women have been routinely prescribed selective serotonin reuptake inhibitors (SSRIs) over the past decade to reduce menopausal side effects. Members of this drug group block the CYP2D6 enzyme that metabolically activates tamoxifen to the potent anti-oestrogen endoxifen thereby (Fig. 2) impairing full drug benefit (Fig. 3)[24]. However, it must be stressed that not all SSRIs have the same ability to block tamoxifen metabolism and as a result, studies that group all SSRIs together are not uniformly consistent with the hypothesis[25, 26]. Nevertheless, the recent Canadian study of

co-prescription of various SSRIs and the selective nor-epinephrine reuptake inhibitor (SNRI) venlafaxine does implicate paroxitene as increasing mortality during tamoxifen treatment and venlafaxine decreases mortality[27]. Overall, enhancing compliance and avoiding SSRIs that block CYP26D will significantly increase the chances of patient survival. That being said, the next issue to address is anti-hormone drug resistance.

Anti-hormonal drug resistance can be manifest in two forms for the ER positive tumour: intrinsic resistance where the tumour does not respond at all to anti-hormone therapy, despite being ER positive and acquired anti-hormone therapy where the tumour initially responds to anti-hormone therapy but then grows despite the continuing treatment. Much effort has focused on an understanding of the molecular mechanism of intrinsic anti-hormone resistance and it seems that cross-talk between growth factor receptors and the low levels of ER have essentially made the ER irrelevant for cell survival. No scientific advance has yet reversed intrinsic resistance and aided patients. In contrast, there have been significant advances in understanding acquired anti-hormone resistance in the laboratory and these emerging data have been translated to clinical practice.

THE CHALLENGE: ACQUIRED DRUG RESISTANCE

Clinical experience with the successful application of long-term tamoxifen as an adjuvant therapy produced a clear survival advantage for patients[28]. Unselected patients treated for 5-years with adjuvant tamoxifen lived longer than patients in the non-treatment (placebo) arm but who were treated with tamoxifen at first recurrence as they had metastatic breast cancer. The clinical results with successful adjuvant tamoxifen therapy demonstrated[28] that our understanding of the development of drug resistance to tamoxifen treatment in ER positive disease were incorrect on July 25, 1987 (the publication date of the Scottish MRC trial), but supported the

principle of early treatment of micrometastatic disease. Also, it highlights the fact that resistance to tamoxifen for the treatment of metastatic disease occurs rapidly within 2-years, and this biology did not apply to an adjuvant application of tamoxifen. Despite the fact that the rat mammary carcinoma model demonstrates that earlier, longer treatment with an anti-oestrogen was a suitable clinical strategy[8], there was no model of human diseases to test this hypothesis. However, in the mid-1980s, this was about to change. The ER positive breast cancer cell line MCF-7[29] exhibits oestradiol-stimulated tumor growth when transplanted into ovariectomized athymic mice. Tamoxifen blocks oestradiol-stimulated tumor growth but cannot maintain growth inhibition as ER positive tumors eventually grow despite tamoxifen treatment[30]. However, it seems that SERM and antihormonal resistance in breast cancer evolves and exposes a vulnerability in breast cancer that can be exploited in the clinic[31].

The first transplantable model of tamoxifen resistance in breast cancer demonstrated that drug resistance to tamoxifen was unique[32]. Although tamoxifen can initially block oestradiol-stimulated growth of MCF-7 cells, resistant ER positive tumors can use either oestradiol or tamoxifen to *stimulate* tumor growth (Fig. 4). Tumours do not grow unless treated with tamoxifen or oestradiol so in the ovariectomized mouse, this is equivalent to the "non-oestrogen state" created by aromatase inhibitors. Tumours also do not grow if treated with the pure anti-oestrogen fulvestrant that destroys the ER[33, 34]. This laboratory model replicates clinical experience with drug resistance to tamoxifen in metastatic breast cancer and explains why aromatase inhibitors or fulvestrant are effective second line treatments[35, 36]. So, how does a study of the drug resistance to tamoxifen in the laboratory explain the effectiveness of 5-years of adjuvant tamoxifen to reduce recurrence rates in ER positive breast cancer to tamoxifen by fifty-percent and continue to reduce mortality a decade after tamoxifen treatment is stopped? The

answer is the evolution and reconfiguration of cell survival pathways that occurs in micrometastatic breast cancer during years of treatment.

Continuous retransplantation of successive generations of tamoxifen-stimulated MCF-7 tumor lines into athymic mice for more than 5-years results in a derived tumor line that does not respond to physiologic oestradiol with growth but rapid tumor regression through apoptotic cell death (Fig. 5)[37, 38]. These data were first presented at the St. Gallen meeting in 1992[37]. The concept offered at the time was that the ultimate and long lasting value of adjuvant tamoxifen therapy derives from stopping adjuvant tamoxifen when the woman's own oestrogen can now destroy the micrometastases that have been sensitized to oestrogen-induced apoptosis. The initial laboratory observations on low dose oestradiol-induced tumour regression were subsequently confirmed[38], expanded[39-42] and translated successfully to clinical trial[43, 44]. As a result, it is now possible to define the evolution of acquired anti-hormone therapy into a Treatment Phase where the anti-hormone blocks oestradiol stimulated tumour growth, Phase I when a SERM or oestradiol stimulates growth (or an aromatase inhibitor creates oestrogens independent growth) and Phase II when a SERM stimulates growth but physiological oestrogen provokes apoptosis either after stopping a SERM or after stopping an aromatase inhibitor (Fig. 6).

Thus, over the past four decades, general scientific principles have emerged and translated to clinical care for patients. The application of these principles of endocrine adjuvant therapy have benefited, and continued to benefit, millions of women worldwide, through a simple and cheap therapeutic intervention. We will now consider how emerging laboratory knowledge may reverse or at least hold Phase II resistance to enhance the longevity of the patient. We will, however then, revisit the clinical reality that increased tumour burden is a poor

indicator of patient survival, so that the founding principles of our initial work, i.e. early treatment targeting the ER with long-term therapy[2] must be embraced by the clinical community.

Oestradiol-Induced Apoptosis under Laboratory Conditions

The administrations of physiologic oestradiol to athymic mice implanted with phase II SERM (tamoxifen or raloxifene) resistant ER positive MCF-7 tumours[38, 40, 41, 45] causes tumours to stop growing and/or rapidly regress. Similarly, the long-term oestrogen deprived clinical cell line MCF-7:5C[42, 46] rapidly undergoes oestrogen-induced apoptosis both *in vitro* and *in vivo*. These laboratory observations are reminiscent of the pioneering studies of Sir Alexander Haddow FRS with his application of the first Chemical Therapy to successfully treat any cancer – high dose synthetic oestrogens to treat metastatic breast cancer[47, 48]. He observed a 25% response rate but these were short-lasting[47]. The observation was made that no responses were observed close to menopausal but often dramatic responses occurred in women in their late 60s and 70s. By 1970, during the presentation of the Inaugural Karnofsky Award Lecture at the American Society of Clinical Oncology (ASCO)[48] (incidentally, when I was starting my PhD in Pharmacology at Leeds University) he stated: *"…the extraordinary extent of tumour regression observed in perhaps 1% of post-menopausal cases (with oestrogen) has always been regarded as of major theoretical importance, and it is a matter for some disappointment that so much of the underlying mechanisms continues to elude us…"*

Now we know that the responses Haddow observed occur because of oestrogen deprivation following the menopause. Longer oestrogen withdrawal after menopause was more effective at creating Phase II resistance in select patients, but high dose oestrogen therapy was necessary. Based on laboratory studies and clinical correlations, anti-hormone therapy does a better job in driving the rapid evolution to Phase II resistance and as a result, only physiological oestrogen is

necessary to trigger apoptosis. Haddow's paradox that stood for 40-years now has clarity and we can start to offer treatment options to exploit the concept further.

Cell culture models provide a vehicle to examine, over time, oestrogen-induced apoptosis with the aim of pharmacologic modulation and the discovery of mechanisms that may have relevance for patient care. Through a knowledge of mechanisms, the elegant oestrogen trigger for naturally initiating tumour cell death may subsequently be exploited to other treatment scenarios. If we can decipher the process of ER-induced apoptosis from its current obscurity, this knowledge could be applied with the discovery of new drugs to trigger the mechanism without the involvement of ER. The ER is our current guide and light to find a new drug group.

We have undertaken an extensive examination of the actions of oestradiol on the growth (MCF-7), immediate apoptosis (MCF-7:5C) and delayed apoptosis (MCF-7:2A)[49] of our model cells using a 2-week time course of gene activity documented through mRNA analysis, creation of cDNA libraries and competitive hybridization with a cDNA library from no treatment controls using Agilent Gene Arrays. These studies were conducted in collaboration with Dr. Eric Ariazi and Dr. Heather Cunliffe. We extensively analyzed the gene time course, and completed gene segregation based on hierarchical pathway analysis. We found that MCF-7 and MCF-7:2A, our control cells remained quiescent during the initial few days of oestradiol treatment (1nM) whereas the pre-apoptotic MCF-7:5C cells responded with a massive rise in the activation of inflammatory genes. Analysis of the sequence of events during the first few days of gene activation, we propose that apoptosis occurs in MCF-7:5C cells by the exploitation of the non-canonical pathway for NF-κB signal transduction (Fig. 7). Furthermore, we have mapped out the time-course activation of each caspase (except caspase 3 that is absent in MCF-7) and determined that caspase 4 is the first and controlling executioner to provoke programmed cell

death. We have interrogated the apoptotic process with purported inhibitors of individual activated caspases to confirm our conclusion of the role of caspase 4. Blockade of caspase 4, blocks oestrogen-induced apoptosis.

Most importantly, the activation of inflammatory genes suggests that oestradiol-induced apoptosis could be inhibited or at least modulated by glucocorticoids. We have subsequently established that dexamethazone inhibits oestrogen-induced apoptosis in a concentration related manner. This novel observation may have important implications for the application of oestradiol-induced apoptosis for individualized patient care. It is possible that the inadvertent administration of glucocorticoids during patient care could block oestrogen-induced apoptosis or that a patient's own glucocorticoids may also inhibit apoptosis, if patients are challenged with oestrogen following exhaustive anti-hormone therapy? The anti-glucocorticoid mifipristone (RU486) could potentially be used with oestrogen to block glucocorticoid action temporarily for a few weeks during low dose oestrogen administration to enhance apoptosis.

Examination of the Agilent gene array data confirmed our previous work[49] that elevated synthesis of glutathione, is protecting MCF-7:2A cells from immediate apoptosis in response to oestrogen. Apoptosis appears to be retarded in MCF-7:2A cells but an activation of autophagy heralds an enhanced transcription of caspase 4 and then triggers oestrogen-induced apoptosis during the second week of oestradiol treatment. We have previously successfully used pharmacological inhibitors to test our hypothesis. Buthionine sulfoximine (BSO), an inhibitor of glutathione synthesis[49] enhances oestradiol-induced apoptosis from a slow event lasting 2-weeks to an immediate event. Unfortunately, BSO, though used extensively in clinical trial a decade or more ago, is no longer available to examine whether it is possible to enhance oestrogen-induced apoptosis in patients with select tumours.

Thus far, our studies have described what happens, but the real question is how does the oestradiol/ER complex triggers apoptosis? Are there clues about the actual shape or structure of the oestrogen ER complex that can be modulated and investigated further? The MCF-7:5C cells depend on a functioning ER for oestradiol-induced apoptosis. The pure anti-oestrogen fulvestrant binds to the ER and causes the rapid destruction of the protein complex. As a result, fulvestrant blocks oestradiol-induced apoptosis in a concentration related manner. Interestingly enough, the tamoxifen metabolites 4-hydroxytamoxifen (4OHTam) and endoxifen do not block or affect the autonomous growth of MCF-7:5C cells but do block the initiation of oestradiol-induced apoptosis. Herein lies a clue to the mechanism that triggers oestradiol-induced apoptosis (Fig. 8). X-Ray crystallographic studies of the ER ligand binding domain and the oestrogens, oestradiol and diethylstilboestrol (DES) and the SERMs 4OHTam[50] and raloxifene[51] provide a fascinating insight into oestrogen and anti-oestrogen action. The solution of the crystal structures demonstrate that the planar oestrogens are sealed within the ligand binding domain by helix 12 which then allows co-activators to bind to the activating function (AF)-2 site on the complex. This event amplifies oestrogen action through gene transcription. In contrast, the bulky side chain of the triphenylethylene 4OHTam and the benzothiophene raloxifene prevent helix 12 from sealing the hydrophobic ligand binding domain which prevents coactivator binding to AF-2. The promiscuous oestrogen-like activity of 4OHTam is explained by the inability of the anti-oestrogenic side chain to neutralize and shield the exposed aspartate at position 351 at the surface of the ligand binding domain. This exposed carboxylic acid communicates with AF-1 to induced oestrogen-like actions. Raloxifene completely blocks and neutralizes the aspartate at 351 and the raloxifene ER complex does not activate AF-1. This hypothesis has been successfully interrogated with changes in the ligand and the aspartate at 351 to modulate the

activation of a model oestrogen target gene Transforming Growth Factor α[52-55]. Overall, we concluded that activation of AF-1 by an exposed surface aspartate 351 confirms that helix 12 is not sealing the ligand binding domain so it can, therefore, communicate a signal to AFI to induce oestrogen-like gene activation. If aspartate 351 is masked under helix 12 with a planar oestrogen than AF-2 is activated and the communication between AF-1 and aspartate 351 is mute. These data and conclusions subsequently resulted in a reclassification of oestrogens into class 1 (planar) and class 2 (non-planar)[56] using a simple assay to determine whether helix 12 was locking the ligand into the hydrophobic ligand binding domain or not. However, the biological significance of this molecular insight was not apparent until recently.

Based on the fact that 4OHTam blocks oestradiol induced apoptosis at the ER and the statement that the "bulky side chain" of 4OHTam altered the conformation of the ER preventing helix 12 from sealing the ligand binding domain[50], we advanced the hypothesis that the "bulky side chain" of 4OHTam was the phenyl ring of the oestrogenic triphenylbut-l-ene not just the *para*-dimethylaminoethoxy group traditionally associated with anti-oestrogen action. Perhaps the phenyl ring of the triphenylbut-l-ene anti-oestrogen was stopping helix 12 from sealing the binding site? A series of triphenylethylenes (TPEs), previously known to be classified exclusively as oestrogens in rodent uterine weight and vagina cornification assays, was used to establish oestrogenic activity in MCF-7 breast cancer cells. All compounds were found to be full oestrogens in growth assays compared with oestradiol and DES and fully-activate an ERE luciferase report ER gene system in MCF-7 cells[57]. In contrast, while oestradiol and DES will trigger apoptosis and cell death in MCF-7:5C cells within a week, the synthetic TPE "oestrogens" do not provoke massive apoptosis and indeed block oestradiol-induced apoptosis. Studies using the CHIP assay at the ERE site in the promoter region of the oestrogen responsive

pS_2 gene demonstrate that whereas oestradiol E_2ER complex is recruited with the co-activator SRC3 in AF-2 neither 4OHTam nor the TPE ER complexes are recruited to the promoter[58].

Overall, these data demonstrate that oestrogen-induced apoptosis is governed and programmed by the shape of the ER complex. As a consequence, shape governs coactivator binding at AF-2 and these events subsequently trigger apoptosis. A recent study by[59] advances our initial oestrogen reclassification paper[56] and confirmed, using a phage display library, that the shape of the ligand programs the external shaped of the ER complex. A precise evaluation of the immediate early genes involved in the apoptotic response will describe the mechanism of the oestrogenic trigger for cell death. Exploitation of this knowledge may find applications in other disease states.

OESTROGEN TREATMENT: CURRENT CLINICAL FINDINGS AND TRANSLATION TO ADJUVANT THERAPY

The laboratory finding[37-39] that acquired resistance to anti-hormone therapy evolves and exposes a vulnerability of breast cancer cells to the apoptotic actions of physiological oestrogen, provides an important insight into potential therapeutic applications. As previously noted in this paper, the anti-tumour effect of physiological oestrogen is reminiscent of the early therapeutic use of high dose oestrogen therapy for the treatment of metastatic breast cancer in post-menopausal women[47]. It was noted that the further from menopause patients were, the more likely there was to be a tumour response, but these responses never exceeded 30% in any given population.

It is now clear that the acute oestrogen deprivation caused by anti-hormones speeds up the molecular adaptation and reconfiguration of vulnerable survival pathways. The surviving

populations of susceptible breast cancer cells also have increased sensitivity to oestrogen-induced apoptosis. Low dose oestrogen therapy now becomes a clinically viable strategy with the prospect of reducing oestrogen associated side effects.

The laboratory data generated and published in the 1990s proposed the clinical strategy of using low-dose oestrogen therapy to "purge" breast cancer cells with Phase II –acquired anti-hormone resistance, but then the re-introduction of anti-hormone therapy would control oestradiol-stimulated tumour growth[37, 38]. Nevertheless, a European trial lead by Dr. Per Lonning[43] recruited patients with metastatic breast cancer following exhaustive anti-hormone therapy were treated with standard high-dose DES (5mg tid). Results are summarized in Table 2a. Select patients responded well with one patient subsequently reported[60] being disease-free more than 10-years after first initiating a high dose oestrogen "purge" therapy. *"…the extraordinary extent of tumour regression observed in perhaps 1% post-menopausal cases (with oestrogen) has always been regarded as of major theoretical importance, and it is a matter for some disappointment that so much of the underlying mechanisms continues to elude us…"*

In a follow-up study, Ellis[44] compared and contrasted high dose (10mg tid) and low dose (1mg tid) oestradiol therapy in patients who relapsed during adjuvant aromatase inhibitor therapy. Results are summarized in Table 2b. Results were not as impressive as the Lonning study probably because patients did not receive "exhaustive" endocrine therapy prior to an oestrogen "purge". Nevertheless, the clinical trial confirms that low dose oestrogen can produce similar clinical benefit when compared with high-dose oestrogen treatment but with fewer, serious side effects.

Finally, there is further clinical evidence from the Women's Health Initiative (WHI) that oestrogen replacement therapy (ERT) alone causes a decrease rather than increase in the incidence of breast cancer[61] and a recent report from the Million Women Study in the UK demonstrates that oestrogen alone increases breast cancer incidence immediately following the menopause but if ERT is used more than 5-years after oestrogen exposure, oestrogen replacement therapy does not cause a rise in breast cancer incidences[62]. An overarching explanation for these apparently confusing clinical observations is clarified by our evolving molecular model to exploiting the role of oestradiol in the life and death of breast cancer cells[63, 64]. We interpret these clinical findings based on the evolution of anti-hormone resistance as follows: breast cancer cells in an environment of oestrogen only grow in response to exogenous oestrogen, but following long-term oestrogen depriving surviving breast cancer cells either die or at least do not develop into tumours.

The clinical and laboratory database also provides continuing support for the ongoing adjuvant Study of Letrozole Extension (SOLE) trial (Fig. 9). Patients who have completed 5-years of adjuvant therapy with tamoxifen, an AI or any sequence are then randomized to an AI continuously for 5-years or an AI with a drug holiday for 3-months a year. The trial seeks to exploit the hypothesis, advanced at the 1992 St. Gallen Meeting, that a woman's own oestrogen may act as an anti-tumour agent after adjuvant anti-hormone therapy is stopped. The SOLE trial proposes a rigorous test of the hypothesis under controlled conditions that promises to create a practical advantage for patients following drug holidays. Results from this trial coupled with the expanding molecular database concerning the modulation of oestrogen-induced apoptosis may result in the proposition of regularly purging patients for a week or two with ERT if decades of

anti-hormone therapy are to become common place in order that the disease is held in check and prevented from recurring. The question is now – at what point is oestrogen intervention too late?

FIGHTING OVERWHELMING CANCER CELL FLEXIBILITY

The enemy is us, Haddow[48] in the Inaugural Karnofsky Lecture reasoned that it would not be possible to develop a cancer specific therapy in the same way Ehrlich had for syphilis, as cancer was our own cells. What he did not know was that the situation is worse than that. The replicative fidelity of normal cells replace exactly what is lost, but in its own special place. Cytotoxic chemotherapy kills the patient by indiscriminately killing normal differentiated cells, and perhaps stem cells, so life saving repopulation for the host organism is impossible or too late. In contrast, human populations eventually adapt to external destructive forces such as fatal infectious diseases (plague, small pox, etc.) but individuals only survive through their preprogrammed nimble immunology. The survivors repopulate. And so it is with cancer at the cellular level within the body. However, immunology has not yet been proven to be of significance for breast cancer prevention. Haddow was right there – the enemy is us. The tumour at diagnosis has hundreds of mutations compared to the (purportedly) normal human genome[65, 66]. This and activated oncogenes, or loss of tumour suppression genes, provides the random survival flexibility within the cancer cell population to adapt and eventually thrive in a hostile (cytotoxic) environment within a few months. The principle is a microscopic adaptation of simple Darwinian evolution that has played out over the millennia by animals on earth. Random mutations create a preferred trait that permits survival, while the non-adaptive species or population dies out. The situation with cancer only becomes worse through adaptive survival responses preprogrammed in the cancer stem cell. These cellular “spores” seek to expand and prepare for massive repopulation in an enforced anoxic environment. The clinician is confronted

with a perverted microcosm of the struggle for life by cancer cells programmed to create infinite candidates in the quest for survival. The patient is overwhelmed by sheer numbers in the wrong places. This is the challenge of targeted molecular therapeutics but how to build rationally on the advances in survivorship achieved over the past 40-years in breast cancer?

The path to progress in drug development has not changed significantly during this time, despite our new knowledge of the disease. The administrative plan for drug evaluation is in place to protect citizens and provide safe and therapeutically proven medicines for clinical care. To market a new drug to treat breast cancer, a precise system must be followed to obtain government approval. Phase I clinical trials must offer the hope of potentially effective treatment to patients who have received all possible therapeutic options. The goal is to document dose limiting toxicities and at this stage of the disease, responses are a major bonus. Phase II trials focus on a cancer type of interest based on reasonable data from preclinical studies or an unanticipated response in Phase I trials. If a candidate is successful in Phase II trials, the drug is evaluated against or with the current standard of care. It should be emphasized that therapeutic results from Phase II trials with tamoxifen were not very dramatic, but Phase I data on toxicity for the patient was excellent compared with other therapies available. Only by targeting the ER in the tumour and applying long-term adjuvant therapy did patient survivorship increase. A discarded contraceptive became the "gold standard" for breast cancer therapy over a 30-year journey[1].

With this background, how do we build on success? Today there are dozens of good potential targets and dozens of plausible candidates for each target. However, unlike the ER which was, it is turned out, the principle messenger to stimulate breast tumour growth in about 30% of tumours, other candidate targets are proving to be not the star but part of the chorus. In

late stage disease, one pathway is blocked but others now compensate. Pathways to preserve cellular life can be essential in all cells, but a cancer cell specific pathway is the only key to success in cancer therapeutics.

Based on our current work investigating oestradiol-induced apoptosis of breast cancer cells with long-term acquired resistance, we purposed a hypothesis: can we block breast cancer cell survival mechanisms and enhance the chances that the cell must undergo apoptosis in response to oestradiol?

c-Src was the first identified oncogene in cancer and is said to be present in more than 70% of breast cancer[67]. It controls AKT and MAPK phosphorylation cascades as the intermediary from growth factor receptor activation. It would appear to be an ideal target to subvert cell survival; almost as good as the ER! We posed the question, that if we blocked c-Src in breast cancer cells resistant to aromatase inhibitors would we then enhance apoptosis? In other words, would we generate value for the cancer patient by increasing cell kill as we have previously found that c-Src inhibitors were completely ineffective in affecting growth of oestrogen stimulated MCF-7 cells, but had significant efficiency in blocking the growth of ER-negative MDA-MB-231 and oestrogen stimulated ER-positive T47D cells. More importantly, long-term oestrogen-deprived MCF-7 cells have elevated pSrc. As most ER-positive cancers are exhaustively treated with antihormones before Phase I/II testing and we were building on a known efficacy of estrogen therapy, the proposition appeared sound. Our model cell, MCF-7:5C, had elevated phospho c-Src and are targeted inhibitor PP2 completely blocked phosphorylation. However, a 2 month course of treatment of MCF-7:5C cells with physiological oestrogen levels (1nM) that would be present in a postmenopausal patient plus the c-Src inhibitor (5 microMolar), resulted in the blockade of oestrogen-induced apoptosis and the reversion of the cell population

to Phase I drug resistance (Fig. 10), i.e. estrogen or SERM-stimulated for growth. Within 2 months, the flexibility of cell populations had created no real advance that could realistically aid the patient.

Thus, as an illustration of the challenge, we face for the application of logical targeted therapy, one could conclude the following: an expanding menu of targeted medicines is available for testing, but only select populations will respond. Testing a c-Src inhibitor in the incorrect stage of antihormone resistance or patient populations cannot be successful. This is the problem: the testing populations for registration may be inappropriate for a drug candidate that is magnificent in a neoadjuvant therapy naïve disease study. However, does this enhance registration? Unfortunately not.

We need practical strategies to aid communities to hold the development and death from breast cancer while we attempt to decipher the enormous complexity of pathways and permutations of targeted therapies. This conclusion brings us back to the second piece of translational research started in our laboratory in the 1970's – chemoprevention. Remarkably, the lamp of tamoxifen shed light on an alternative strategy to reduce cancer incidence and preempt the aforementioned Gordian Knot. Unfortunately, the initial strategy for the clinical application of chemoprevention requires the identification of high-risk populations to be treated with the pioneer tamoxifen. This approach is flawed. However, a public health strategy for an aging population that creates wellness for as long as possible is a laudable goal now within our grasp.

TAMOXIFEN IS ALSO ABOUT PROGRESS IN CHEMOPREVENTION

An extensive study of the pharmacology of tamoxifen[68] identified its ability to modulate oestrogen target tissues around the body; tamoxifen is anti-oestrogenic in the breast and

oestrogen-like in bone and lowers circulating cholesterol[69-72]. Translational research also first identified the potential of tamoxifen to increase the risk of developing endometrial cancer during extended treatment schedules[73-75]. Tamoxifen blocks breast tumour growth and development but enhances endometrial cancer growth. As a result, new procedures were introduced for the gynecological monitoring of post-menopausal patients receiving long-term tamoxifen therapy. New agents, without endometrial problems, were needed for investigation. Knowledge of selective ER modulation by tamoxifen and also the pharmacology of the structurally-related failed breast cancer drug, raloxifene, led to the creation of a new drug group, the Selective ER Modulators (SERMs)[76], with the potential to treat and prevent multiple diseases in women ***and*** prevent breast cancer at the same time. The fact that raloxifene was less oestrogen-like than tamoxifen in the rodent uterus and less likely to increase the incidence of the endometrial cancer in patients[77, 78] meant that safer compounds could be identified as chemopreventives for breast cancer but a new strategy to achieve the goal was essential. Benefits for a tiny, unidentifiable minority is unacceptable if the vast majority of women in a high risk population have side effects, some life-threatening. The road map for the pharmaceutical industry was clearly stated in 1990[79]. *Is this the end of the possible applications for anti-oestrogens? Certainly not! We have obtained valuable clinical information about this group of drugs that can be applied in other disease states. Research does not travel in straight lines and observations in one field of science often become major discoveries in another. Important clues have been garnered about the effects of tamoxifen on bone and lipids so it is possible that derivatives could find targeted applications to retard osteoporosis or atherosclerosis. The ubiquitous application of novel compounds to prevent diseases associated with the progressive changes after menopause may, as a side effect, significantly retard the development of breast cancer. The target population would*

be postmenopausal women in general, thereby avoiding the requirement to select a high risk group to prevent breast cancer.

Raloxifene pioneered the concept in the clinic confirming the prediction that the prevention of breast cancer would occur during the treatment and prevention of osteoporosis in high risk post-menopausal women[80] with no increase in endometrial cancer. Today, the prediction that SERMs could control multiple diseases in women following the menopause is poised to become a reality. Lasofoxifene (Fig. 1) is approved in the European Union for the prevention and treatment of osteoporosis which simultaneously decreases the incidence of breast cancer, strokes and myocardial infarction, but without increasing endometrial cancer risk[81]. Lasofoxifene is more than one hundred times more potent than raloxifene and the aforementioned strategy[79] to improve women's health in aging populations is the new face of chemoprevention in breast cancer - treat the majority of women for major diseases like osteoporosis and coronary heart disease and prevent breast cancer as a beneficial side effect. The saving in health care costs by **not** paying for the treatment of breast cancer in tens of thousands of women **without** breast cancer will be considerable, but admittedly hard to quantitate.

Raloxifene is not only available in the United States of America for the treatment and prevention of osteoporosis but also for reduction of the incidence for breast cancer in post-menopausal, high-risk women[82]. However, the SERM must be given indefinitely to remain effective in both diseases[83]. In contrast, tamoxifen remains effective for decades after the limited treatment period of 5-years is stopped[84, 85]. As mentioned previously, the key to understanding this fact probably resides in the laboratory study of drug resistance to SERMs and aromatase inhibitors and the development of a cellular susceptibility to oestrogen-induced apoptosis. The fact that the same tumour responsiveness to raloxifene appears to be retarded in clinical practice

suggests that the known poor pharmacokinetics and bioavailability of raloxifene is not able to rapidly produce an "anti-oestrogenic" state around the nascent tumour like tamoxifen. This may explain the reduced performance of raloxifene against tamoxifen in the STAR trial, following the cessation of 5-years of treatment[83].

SUMMARY AND CLOSING THOUGHTS

Over the past 40-years, we have witnessed, a dramatic improvement in the survivorship of the majority of patients with a diagnosis of ER positive breast cancer. The SERM tamoxifen pioneered the process. Translational research has added further cheap and effective targeted anti-hormonal therapies to the physician's armamentarium that are proven to be of benefit in randomized adjuvant clinical trials world-wide. Not only has therapy been improved substantially over the past 40-years, from the time in the early 1970s when there was stated to be little prospect of successful survival advances with "endocrine therapy", but also the parallel path of chemoprevention has been pioneered successfully with the same SERM tamoxifen. This SERM heralded a new era of general medicine where a family of SERMs would allow women to expect to reduce their risk of fractures but prevent breast cancer at the same time. This was only a laboratory concept 20-years ago[79, 86] but it seems obvious that with an aging population that seeks to remain active for as long as possible, that the SERMs will play their part in reducing the incidence of breast cancer if used wisely in the post-menopausal population.

The lessons learned with the lamp-light of the pioneer tamoxifen are now established principles in cancer therapeutics. The principles are: aim at the target (ER), start therapy as early as possible (i.e. as few lymph nodes as possible involved), long therapy is preferable to shorter therapy, compliance with the medicine is essential and drug interaction with SSRIs to stop

menopausal side effect in a few should be avoided. Conforming to these principles aids patients' survival. The light from the lamp also taught us what we did not know. Firstly tamoxifen is a selective modulator of ER action around a woman's body and heralded a new drug group (the SERMs) that prevent osteoporosis and prevent breast cancer as a beneficial side effect. This avoids the need to find the exact women who would benefit from chemoprevention using the Gail Model[87]. Secondly, drug resistance evolves so that oestradiol becomes an apoptotic trigger. Further studies solved the concern expressed by Haddow in 1970 that the mechanism of oestrogen-induced apoptosis was a mystery. Now oestrogen therapy has a niche application in patient care.

During the past 40-years, the mosaic of endocrine adjuvant therapy and chemoprevention with SERMs has been clarified by effective translational research[4, 88]. The next challenge for a generation of "omic" scientists is to prioritize the opportunities in molecular therapeutics based on this solid start, so as to advance and individualize treatment.

ACKNOWLEDGEMENTS

Acknowledgements: We would like to thank Julia Jessup Tijerina and Russell E. McDaniel for their administrative support in preparing this manuscript.

Competing interests: None.

Funding: This work (VCJ) was supported by the Department of Defense Breast Program under Award number BC050277 Center of Excellence; subcontract under the SU2C (AACR) Grant number SU2C-AACR-DT0409; the Susan G Komen for the Cure Foundation under Award number SAC100009 and the Lombardi Comprehensive Cancer Center Support Grant (CCSG) Core Grant NIH P30 CA051008. The project described was supported by Award Number P30

CA051008 from the National Cancer Institute. The content is solely the responsibility of the authors and does not necessarily represent the official views of the National Cancer Institute or the National Institutes of Health. The views and opinions of the author(s) do not reflect those of the US Army or the Department of Defense.

REFERENCES

1. Jordan VC. Tamoxifen: a most unlikely pioneering medicine. *Nat Rev Drug Discov* 2003;**2**:205-13.
2. Jordan VC. Tamoxifen: catalyst for the change to targeted therapy. *Eur J Cancer* 2008;**44**:30-8.
3. Jordan VC. Selective estrogen receptor modulation: a personal perspective. *Cancer Res* 2001;**61**:5683-7.
4. Jordan VC. The 38th David A. Karnofsky lecture: the paradoxical actions of estrogen in breast cancer--survival or death? *J Clin Oncol* 2008;**26**:3073-82.
5. EBCTCG. Tamoxifen for early breast cancer: an overview of the randomised trials. . *Lancet* 1998;**351**:1451-67.
6. EBCTCG. Effects of chemotherapy and hormonal therapy for early breast cancer on recurrence and 15-year survival: an overview of the randomised trials. *Lancet* 2005;**365**:1687-717.
7. Jordan VC, Koerner S. Tamoxifen (ICI 46,474) and the human carcinoma 8S oestrogen receptor. *Eur J Cancer* 1975;**11**:205-6.
8. Jordan V, Dix CJ, Allen KE. The effectiveness of long term tamoxifen treatment in a laboratory model for adjuvant hormone therapy of breast cancer. *Adjuvant Ther Cancer* 1979;**2**:19-26.
9. Jordan VC, Allen KE. Evaluation of the antitumour activity of the non-steroidal antioestrogen monohydroxytamoxifen in the DMBA-induced rat mammary carcinoma model. *Eur J Cancer* 1980;**16**:239-51.
10. Jordan VC, Collins MM, Rowsby L, Prestwich G. A monohydroxylated metabolite of tamoxifen with potent antioestrogenic activity. *J Endocrinol* 1977;**75**:305-16.
11. Jordan VC, Dix CJ, Naylor KE, Prestwich G, Rowsby L. Nonsteroidal antiestrogens: their biological effects and potential mechanisms of action. *J Toxicol Environ Health* 1978;**4**:363-90.
12. Allen KE, Clark ER, Jordan VC. Evidence for the metabolic activation of non-steroidal antioestrogens: a study of structure-activity relationships. *Br J Pharmacol* 1980;**71**:83-91.
13. NATO. Controlled trial of tamoxifen as adjuvant agent in management of early breast cancer. Interim analysis at four years by Nolvadex Adjuvant Trial Organisation. *Lancet* 1983;**1**:257-61.
14. NATO. Controlled trial of tamoxifen as single adjuvant agent in management of early breast cancer. Analysis at six years by Nolvadex Adjuvant Trial Organisation. *Lancet* 1985;**1**:836-40.
15. Cole MP, Jones CT, Todd ID. A new anti-oestrogenic agent in late breast cancer. An early clinical appraisal of ICI46474. *Br J Cancer* 1971;**25**:270-5.
16. Jordan VC, Brodie AM. Development and evolution of therapies targeted to the estrogen receptor for the treatment and prevention of breast cancer. *Steroids* 2007;**72**:7-25.
17. Howell A, Cuzick J, Baum M, Buzdar A, Dowsett M, Forbes JF, et al. Results of the ATAC (Arimidex, Tamoxifen, Alone or in Combination) trial after completion of 5 years' adjuvant treatment for breast cancer. *Lancet* 2005;**365**:60-2.

18. Hershman DL, Kushi LH, Shao T, Buono D, Kershenbaum A, Tsai WY, et al. Early discontinuation and nonadherence to adjuvant hormonal therapy in a cohort of 8,769 early-stage breast cancer patients. *J Clin Oncol* 2010;**28**:4120-8.
19. Partridge AH, LaFountain A, Mayer E, Taylor BS, Winer E, Asnis-Alibozek A. Adherence to initial adjuvant anastrozole therapy among women with early-stage breast cancer. *J Clin Oncol* 2008;**26**:556-62.
20. Lash TL, Fox MP, Westrup JL, Fink AK, Silliman RA. Adherence to tamoxifen over the five-year course. *Breast Cancer Res Treat* 2006;**99**:215-20.
21. McCowan C, Shearer J, Donnan PT, Dewar JA, Crilly M, Thompson AM, et al. Cohort study examining tamoxifen adherence and its relationship to mortality in women with breast cancer. *Br J Cancer* 2008;**99**:1763-8.
22. Geiger AM, Thwin SS, Lash TL, Buist DS, Prout MN, Wei F, et al. Recurrences and second primary breast cancers in older women with initial early-stage disease. *Cancer* 2007;**109**:966-74.
23. Yood MU, Owusu C, Buist DS, Geiger AM, Field TS, Thwin SS, et al. Mortality impact of less-than-standard therapy in older breast cancer patients. *J Am Coll Surg* 2008;**206**:66-75.
24. Brauch H, Jordan VC. Targeting of tamoxifen to enhance antitumour action for the treatment and prevention of breast cancer: the 'personalised' approach? *Eur J Cancer* 2009;**45**:2274-83.
25. Dezentje VO, van Blijderveen NJ, Gelderblom H, Putter H, van Herk-Sukel MP, Casparie MK, et al. Effect of concomitant CYP2D6 inhibitor use and tamoxifen adherence on breast cancer recurrence in early-stage breast cancer. *J Clin Oncol* 2010;**28**:2423-9.
26. Lash TL, Cronin-Fenton D, Ahern TP, Rosenberg CL, Lunetta KL, Silliman RA, et al. Breast cancer recurrence risk related to concurrent use of SSRI antidepressants and tamoxifen. *Acta Oncol* 2010;**49**:305-12.
27. Kelly CM, Juurlink DN, Gomes T, Duong-Hua M, Pritchard KI, Austin PC, et al. Selective serotonin reuptake inhibitors and breast cancer mortality in women receiving tamoxifen: a population based cohort study. *BMJ* 2010;**340**:c693.
28. SCTO. Adjuvant tamoxifen in the management of operable breast cancer: the Scottish Trial. Report from the Breast Cancer Trials Committee, Scottish Cancer Trials Office (MRC), Edinburgh. *Lancet* 1987;**2**:171-5.
29. Levenson AS, Jordan VC. MCF-7: the first hormone-responsive breast cancer cell line. *Cancer Res* 1997;**57**:3071-8.
30. Osborne CK, Coronado EB, Robinson JP. Human breast cancer in the athymic nude mouse: cytostatic effects of long-term antiestrogen therapy. *Eur J Cancer Clin Oncol* 1987;**23**:1189-96.
31. Jordan VC. Selective estrogen receptor modulation: concept and consequences in cancer. *Cancer Cell* 2004;**5**:207-13.
32. Gottardis MM, Jordan VC. Development of tamoxifen-stimulated growth of MCF-7 tumors in athymic mice after long-term antiestrogen administration. *Cancer Res* 1988;**48**:5183-7.
33. Gottardis MM, Jiang SY, Jeng MH, Jordan VC. Inhibition of tamoxifen-stimulated growth of an MCF-7 tumor variant in athymic mice by novel steroidal antiestrogens. *Cancer Res* 1989;**49**:4090-3.
34. Wakeling AE, Dukes M, Bowler J. A potent specific pure antiestrogen with clinical potential. *Cancer Res* 1991;**51**:3867-73.
35. Osborne CK, Pippen J, Jones SE, Parker LM, Ellis M, Come S, et al. Double-blind, randomized trial comparing the efficacy and tolerability of fulvestrant versus anastrozole in postmenopausal women with advanced breast cancer progressing on prior endocrine therapy: results of a North American trial. *J Clin Oncol* 2002;**20**:3386-95.
36. Howell A, Robertson JF, Quaresma Albano J, Aschermannova A, Mauriac L, Kleeberg UR, et al. Fulvestrant, formerly ICI 182,780, is as effective as anastrozole in postmenopausal women with advanced breast cancer progressing after prior endocrine treatment. *J Clin Oncol* 2002;**20**:3396-403.

37. Wolf DM, Jordan VC. A laboratory model to explain the survival advantage observed in patients taking adjuvant tamoxifen therapy. *Recent Results Cancer Res* 1993;**127**:23-33.
38. Yao K, Lee ES, Bentrem DJ, England G, Schafer JI, O'Regan RM, et al. Antitumor action of physiological estradiol on tamoxifen-stimulated breast tumors grown in athymic mice. *Clin Cancer Res* 2000;**6**:2028-36.
39. Song RX, Mor G, Naftolin F, McPherson RA, Song J, Zhang Z, et al. Effect of long-term estrogen deprivation on apoptotic responses of breast cancer cells to 17beta-estradiol. *J Natl Cancer Inst* 2001;**93**:1714-23.
40. Liu H, Lee ES, Gajdos C, Pearce ST, Chen B, Osipo C, et al. Apoptotic action of 17beta-estradiol in raloxifene-resistant MCF-7 cells in vitro and in vivo. *J Natl Cancer Inst* 2003;**95**:1586-97.
41. Osipo C, Gajdos C, Liu H, Chen B, Jordan VC. Paradoxical action of fulvestrant in estradiol-induced regression of tamoxifen-stimulated breast cancer. *J Natl Cancer Inst* 2003;**95**:1597-608.
42. Lewis JS, Meeke K, Osipo C, Ross EA, Kidawi N, Li T, et al. Intrinsic mechanism of estradiol-induced apoptosis in breast cancer cells resistant to estrogen deprivation. *J Natl Cancer Inst* 2005;**97**:1746-59.
43. Lonning PE, Taylor PD, Anker G, Iddon J, Wie L, Jorgensen LM, et al. High-dose estrogen treatment in postmenopausal breast cancer patients heavily exposed to endocrine therapy. *Breast Cancer Res Treat* 2001;**67**:111-6.
44. Ellis MJ, Gao F, Dehdashti F, Jeffe DB, Marcom PK, Carey LA, et al. Lower-dose vs high-dose oral estradiol therapy of hormone receptor-positive, aromatase inhibitor-resistant advanced breast cancer: a phase 2 randomized study. *JAMA* 2009;**302**:774-80.
45. Balaburski GM, Dardes RC, Johnson M, Haddad B, Zhu F, Ross EA, et al. Raloxifene-stimulated experimental breast cancer with the paradoxical actions of estrogen to promote or prevent tumor growth: a unifying concept in anti-hormone resistance. *Int J Oncol* 2010;**37**:387-98.
46. Lewis JS, Osipo C, Meeke K, Jordan VC. Estrogen-induced apoptosis in a breast cancer model resistant to long-term estrogen withdrawal. *J Steroid Biochem Mol Biol* 2005;**94**:131-41.
47. Haddow A, Watkinson JM, Paterson E, Koller PC. Influence of Synthetic Oestrogens on Advanced Malignant Disease. *Br Med J* 1944;**2**:393-8.
48. Haddow A. David A. Karnofsky memorial lecture. Thoughts on chemical therapy. *Cancer* 1970;**26**:737-54.
49. Lewis-Wambi JS, Kim HR, Wambi C, Patel R, Pyle JR, Klein-Szanto AJ, et al. Buthionine sulfoximine sensitizes antihormone-resistant human breast cancer cells to estrogen-induced apoptosis. *Breast Cancer Res* 2008;**10**:R104.
50. Shiau AK, Barstad D, Loria PM, Cheng L, Kushner PJ, Agard DA, et al. The structural basis of estrogen receptor/coactivator recognition and the antagonism of this interaction by tamoxifen. *Cell* 1998;**95**:927-37.
51. Brzozowski AM, Pike AC, Dauter Z, Hubbard RE, Bonn T, Engstrom O, et al. Molecular basis of agonism and antagonism in the oestrogen receptor. *Nature* 1997;**389**:753-8.
52. Levenson AS, Jordan VC. The key to the antiestrogenic mechanism of raloxifene is amino acid 351 (aspartate) in the estrogen receptor. *Cancer Res* 1998;**58**:1872-5.
53. MacGregor Schafer J, Liu H, Bentrem DJ, Zapf JW, Jordan VC. Allosteric silencing of activating function 1 in the 4-hydroxytamoxifen estrogen receptor complex is induced by substituting glycine for aspartate at amino acid 351. *Cancer Res* 2000;**60**:5097-105.
54. Liu H, Lee ES, Deb Los Reyes A, Zapf JW, Jordan VC. Silencing and reactivation of the selective estrogen receptor modulator-estrogen receptor alpha complex. *Cancer Res* 2001;**61**:3632-9.
55. Liu H, Park WC, Bentrem DJ, McKian KP, Reyes Ade L, Loweth JA, et al. Structure-function relationships of the raloxifene-estrogen receptor-alpha complex for regulating transforming growth factor-alpha expression in breast cancer cells. *J Biol Chem* 2002;**277**:9189-98.

56. Jordan VC, Schafer JM, Levenson AS, Liu H, Pease KM, Simons LA, et al. Molecular classification of estrogens. *Cancer Res* 2001;**61**:6619-23.
57. Maximov PY, Myers CB, Curpan RF, Lewis-Wambi JS, Jordan VC. Structure-function relationships of estrogenic triphenylethylenes related to endoxifen and 4-hydroxytamoxifen. *J Med Chem* 2010;**53**:3273-83.
58. Sengupta S, Sharma CG, Jordan VC. Estrogen regulation of X-box binding protein-1 and its role in estrogen induced growth of breast and endometrial cancer cells. *Horm Mol Biol Clin Investig* 2010;**2**:235-43.
59. Bourgoin-Voillard S, Gallo D, Laios I, Cleeren A, Bali LE, Jacquot Y, et al. Capacity of type I and II ligands to confer to estrogen receptor alpha an appropriate conformation for the recruitment of coactivators containing a LxxLL motif-Relationship with the regulation of receptor level and ERE-dependent transcription in MCF-7 cells. *Biochem Pharmacol* 2010;**79**:746-57.
60. Lonning PE. Additive endocrine therapy for advanced breast cancer - back to the future. *Acta Oncol* 2009;**48**:1092-101.
61. Stefanick ML, Anderson GL, Margolis KL, Hendrix SL, Rodabough RJ, Paskett ED, et al. Effects of conjugated equine estrogens on breast cancer and mammography screening in postmenopausal women with hysterectomy. *JAMA* 2006;**295**:1647-57.
62. Beral V, Reeves G, Bull D, Green J. Breast Cancer Risk in Relation to the Interval Between Menopause and Starting Hormone Therapy. *J Natl Cancer Inst* 2011;**103**:296-305.
63. Lewis-Wambi JS, Jordan VC. Estrogen regulation of apoptosis: how can one hormone stimulate and inhibit? *Breast Cancer Res* 2009;**11**:206.
64. Maximov PY, Lewis-Wambi JS, Jordan VC. The Paradox of Oestradiol-Induced Breast Cancer Cell Growth and Apoptosis. *Curr Signal Transduct Ther* 2009;**4**:88-102.
65. Berger MF, Lawrence MS, Demichelis F, Drier Y, Cibulskis K, Sivachenko AY, et al. The genomic complexity of primary human prostate cancer. *Nature* 2011;**470**:214-20.
66. Pfeifer GP, Hainaut P. Next-generation sequencing: emerging lessons on the origins of human cancer. *Curr Opin Oncol* 2011;**23**:62-8.
67. Ottenhoff-Kalff AE, Rijksen G, van Beurden EA, Hennipman A, Michels AA, Staal GE. Characterization of protein tyrosine kinases from human breast cancer: involvement of the c-src oncogene product. *Cancer Res* 1992;**52**:4773-8.
68. Jordan VC. Tamoxifen (ICI46,474) as a targeted therapy to treat and prevent breast cancer. *Br J Pharmacol* 2006;**147 Suppl 1**:S269-76.
69. Jordan VC, Robinson SP. Species-specific pharmacology of antiestrogens: role of metabolism. *Fed Proc* 1987;**46**:1870-4.
70. Jordan VC, Phelps E, Lindgren JU. Effects of anti-estrogens on bone in castrated and intact female rats. *Breast Cancer Res Treat* 1987;**10**:31-5.
71. Love RR, Mazess RB, Barden HS, Epstein S, Newcomb PA, Jordan VC, et al. Effects of tamoxifen on bone mineral density in postmenopausal women with breast cancer. *N Engl J Med* 1992;**326**:852-6.
72. Love RR, Wiebe DA, Newcomb PA, Cameron L, Leventhal H, Jordan VC, et al. Effects of tamoxifen on cardiovascular risk factors in postmenopausal women. *Ann Intern Med* 1991;**115**:860-4.
73. Gottardis MM, Robinson SP, Satyaswaroop PG, Jordan VC. Contrasting actions of tamoxifen on endometrial and breast tumor growth in the athymic mouse. *Cancer Res* 1988;**48**:812-5.
74. Fornander T, Cedermark B, Mattsson A, Skoog L, Theve T, Askergren J, et al. Adjuvant Tamoxifen in Early Breast-Cancer - Occurrence of New Primary Cancers. *Lancet* 1989;**1**:117-20.
75. Fisher B, Costantino JP, Wickerham DL, Redmond CK, Kavanah M, Cronin WM, et al. Tamoxifen for prevention of breast cancer: report of the National Surgical Adjuvant Breast and Bowel Project P-1 Study. *J Natl Cancer Inst* 1998;**90**:1371-88.

76. Smith CL, O'Malley BW. Coregulator function: a key to understanding tissue specificity of selective receptor modulators. *Endocr Rev* 2004;**25**:45-71.
77. Black LJ, Jones CD, Falcone JF. Antagonism of estrogen action with a new benzothiophene derived antiestrogen. *Life Sci* 1983;**32**:1031-6.
78. Gottardis MM, Ricchio ME, Satyaswaroop PG, Jordan VC. Effect of steroidal and nonsteroidal antiestrogens on the growth of a tamoxifen-stimulated human endometrial carcinoma (EnCa101) in athymic mice. *Cancer Res* 1990;**50**:3189-92.
79. Lerner LJ, Jordan VC. Development of antiestrogens and their use in breast cancer: eighth Cain memorial award lecture. *Cancer Res* 1990;**50**:4177-89.
80. Cummings SR, Eckert S, Krueger KA, Grady D, Powles TJ, Cauley JA, et al. The effect of raloxifene on risk of breast cancer in postmenopausal women: results from the MORE randomized trial. Multiple Outcomes of Raloxifene Evaluation. *JAMA* 1999;**281**:2189-97.
81. Cummings SR, Ensrud K, Delmas PD, LaCroix AZ, Vukicevic S, Reid DM, et al. Lasofoxifene in postmenopausal women with osteoporosis. *N Engl J Med* 2010;**362**:686-96.
82. Vogel VG, Costantino JP, Wickerham DL, Cronin WM, Cecchini RS, Atkins JN, et al. Effects of tamoxifen vs raloxifene on the risk of developing invasive breast cancer and other disease outcomes: the NSABP Study of Tamoxifen and Raloxifene (STAR) P-2 trial. *JAMA* 2006;**295**:2727-41.
83. Vogel VG, Costantino JP, Wickerham DL, Cronin WM, Cecchini RS, Atkins JN, et al. Update of the National Surgical Adjuvant Breast and Bowel Project Study of Tamoxifen and Raloxifene (STAR) P-2 Trial: Preventing breast cancer. *Cancer Prev Res (Phila)* 2010;**3**:696-706.
84. Fisher B, Costantino JP, Wickerham DL, Cecchini RS, Cronin WM, Robidoux A, et al. Tamoxifen for the prevention of breast cancer: current status of the National Surgical Adjuvant Breast and Bowel Project P-1 study. *J Natl Cancer Inst* 2005;**97**:1652-62.
85. Powles TJ, Ashley S, Tidy A, Smith IE, Dowsett M. Twenty-year follow-up of the Royal Marsden randomized, double-blinded tamoxifen breast cancer prevention trial. *J Natl Cancer Inst* 2007;**99**:283-90.
86. Jordan VC. Chemosuppression of breast cancer with tamoxifen: laboratory evidence and future clinical investigations. *Cancer Invest* 1988;**6**:589-95.
87. Gail MH, Brinton LA, Byar DP, Corle DK, Green SB, Schairer C, et al. Projecting individualized probabilities of developing breast cancer for white females who are being examined annually. *J Natl Cancer Inst* 1989;**81**:1879-86.
88. Jordan VC. A century of deciphering the control mechanisms of sex steroid action in breast and prostate cancer: the origins of targeted therapy and chemoprevention. *Cancer Res* 2009;**69**:1243-54.

FIGURE LEGENDS:

Fig. 1. The structure of medicines and compounds mentioned in the text. Oestradiol and diethylstilboestrol are oestrogens, whereas all others are selective oestrogen receptor modulators (SERMs) used in medicine for the treatment and chemoprevention of breast cancer (tamoxifen), treatment and prevention of osteoporosis and the chemoprevention of breast cancer (raloxifene). The new SERM, lasofoxifene, is approved for the treatment and prevention of osteoporosis in the European Union.

Fig. 2. The metabolic activation of tamoxifen with a low affinity to the tumour oestrogen receptor by the P_{450} enzyme CYP2D6 enzyme to endoxifen with a high affinity for the tumour oestrogen receptor.

Fig. 3. The metabolism of tamoxifen to 4-hydroxytamoxifen, a metabolite with a high affinity for the oestrogen receptor. Tamoxifen's major metabolite is N-desmethyltamoxifen that has a similar binding affinity to the oestrogen receptors as tamoxifen. However, N-desmethyltamoxifen is metabolically activated to endoxifen, with a high binding affinity for the oestrogen receptor. The selective serotonin re-uptake inhibitors (SSRIs), paroxetine and fluoxetine block the metabolic activation of tamoxifen by blocking CYP2D6. Venlafaxine, a selective norepinephrine re-uptake inhibitor (SNRI), does not affect tamoxifen's metabolic activation, and therefore is the preferred choice to treat menopausal symptoms experienced with tamoxifen.

Fig. 4. The development of acquired antihormone resistance to selective oestrogen receptor modulators (SERMs) (tamoxifen or raloxifene). The unique feature of Phase I antihormone resistance is that oestrogen receptor positive breast tumours grow in response to either physiological oestradiol or the SERM. In the clinical setting (and laboratory models), an aromatase inhibitor (no oestrogen) or the pure anti-oestrogen, fulvestrant, that destroys the oestrogen receptor, stops the growth of Phase I resistant tumours to tamoxifen.[31]

Fig. 5. Diagrammatic representation of the actions of physiologic oestradiol (E2) on the growth of small phase II MCF-7 tamoxifen resistant tumors in ovariectomized athymic mice. A larger tumour will regress with oestradiol treatment but will eventually display oestrogen-stimulated growth. If tumours are re-transplanted into a new generation of ovariectomized athymic mice and treated with oestradiol, tamoxifen will block oestrogen-stimulated tumour growth.[38] First presented in St. Gallen, 1993. [37]

Fig. 6. The evolution of drug resistance to SERMs. Acquired resistance occurs during long-term treatment with a SERM and is evidenced by SERM-stimulated breast tumour growth. Tumours also continue to exploit oestrogen for growth when the SERM is stopped, so a dual signal

transduction process develops. The aromatase inhibitors prevent tumour growth in SERM-resistant disease and fulvestrant that destroys the ER is also effective. This phase of drug resistance is referred to as Phase I resistance. Continued exposure to a SERM results in continued SERM-stimulated growth (Phase II), but eventually autonomous growth occurs that is unresponsive to fulvestrant or aromatase inhibitors. The event that distinguishes Phase I from Phase II acquired resistance is a remarkable switching mechanism that now causes apoptosis, rather than growth, with physiologic levels of oestrogen. A similar evolution occurs with aromatase inhibitor resistance from oestrogen independent growth with a transition to oestrogen-induced apoptosis. These distinct phases of laboratory drug resistance have their clinical parallels and this new knowledge is being integrated into the treatment plan.

Fig. 7. The non-canonical pathway results in the activation of IKKα by NIK and phosphorylation of the NF-κB subunit. This process results in the conversion of p100 to p52. It is the p52-RelB heterodimers that target distinct κB elements on DNA. ANK (ankyrin-repeat motifs). NIK (NF-κB kinase). RelB (NF-κB family member). RHD (Rel-homology domain). TAD (transcriptional activation domain).

Fig. 8. The reversal of oestradiol-induced apoptosis (1 nM) by increasing concentrations of 4-hydroxytamoxifen or endoxifen. This nonsteroidal antioestrogen effect highlights the ER dependence for oestradiol-induced apoptosis.

Fig. 9. The Schema for the Study of Letrozole Extension (SOLE) conducted by the International Breast Cancer Study Group (IBCSG 35-07). Patients randomized following five years of adjuvant antihormone therapy to letrozole continuously or intermittent letrozole (3 month drug holidays per year for 5 years). The rationale is that the woman's own oestrogen in the intermittent arm will trigger apoptosis in aromatase inhibitor resistant cells and reduce recurrence rates.

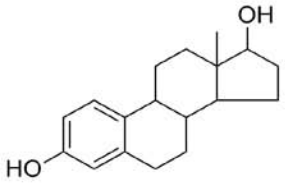
Fig. 10. The evolution of drug resistance and rapid alterations in cell populations if a c-Src inhibitor PP2 (5 μM) is incubated with MCF-7:5C cells in the presence of 1 nM oestradiol for two months to mimic a clinical scenario of a postmenopausal woman who fails an aromatase inhibitor to block growth. Apoptosis from oestrogen is blocked and the cells revert to Phase I resistance, i.e. oestrogen and SERM-stimulated growth.

TABLE LEGENDS

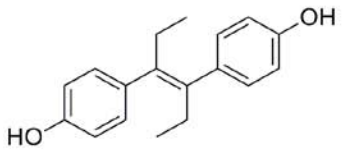
Table 1. Decades of discovery. The development of scientific principles in the laboratory were translated to clinical trials ten years later and subsequently became the standards for clinic care for the treatment or chemoprevention of breast cancer, or in the case of the SERM, raloxifene, a treatment option for the treatment and prevention of osteoporosis with the prevention of breast carcinogenesis as a beneficial side effect.

Table 2. The proof of principle for a) high dose oestrogen (DES, 15 mg daily) triggering tumour responses in patients with metastatic breast cancer following exhaustive antihormone therapy[43] or b) a comparison of high dose oestrogen (oestradiol, 30 mg daily) or low dose oestrogen (oestradiol, 6 mg daily), producing similar clinical benefit rates following the failure of therapy with an aromatase inhibitor.[44]

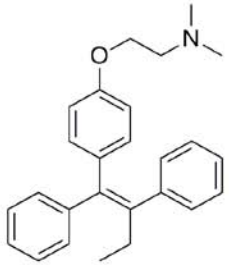
Figure 1



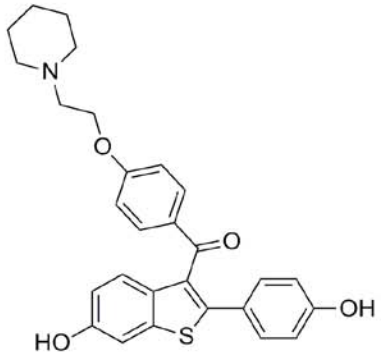
oestradiol-17β



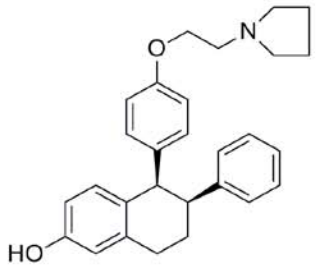
diethylstilboestrol



tamoxifen (ICI 46,474)



raloxifene



lasofoxifene

Figure 2

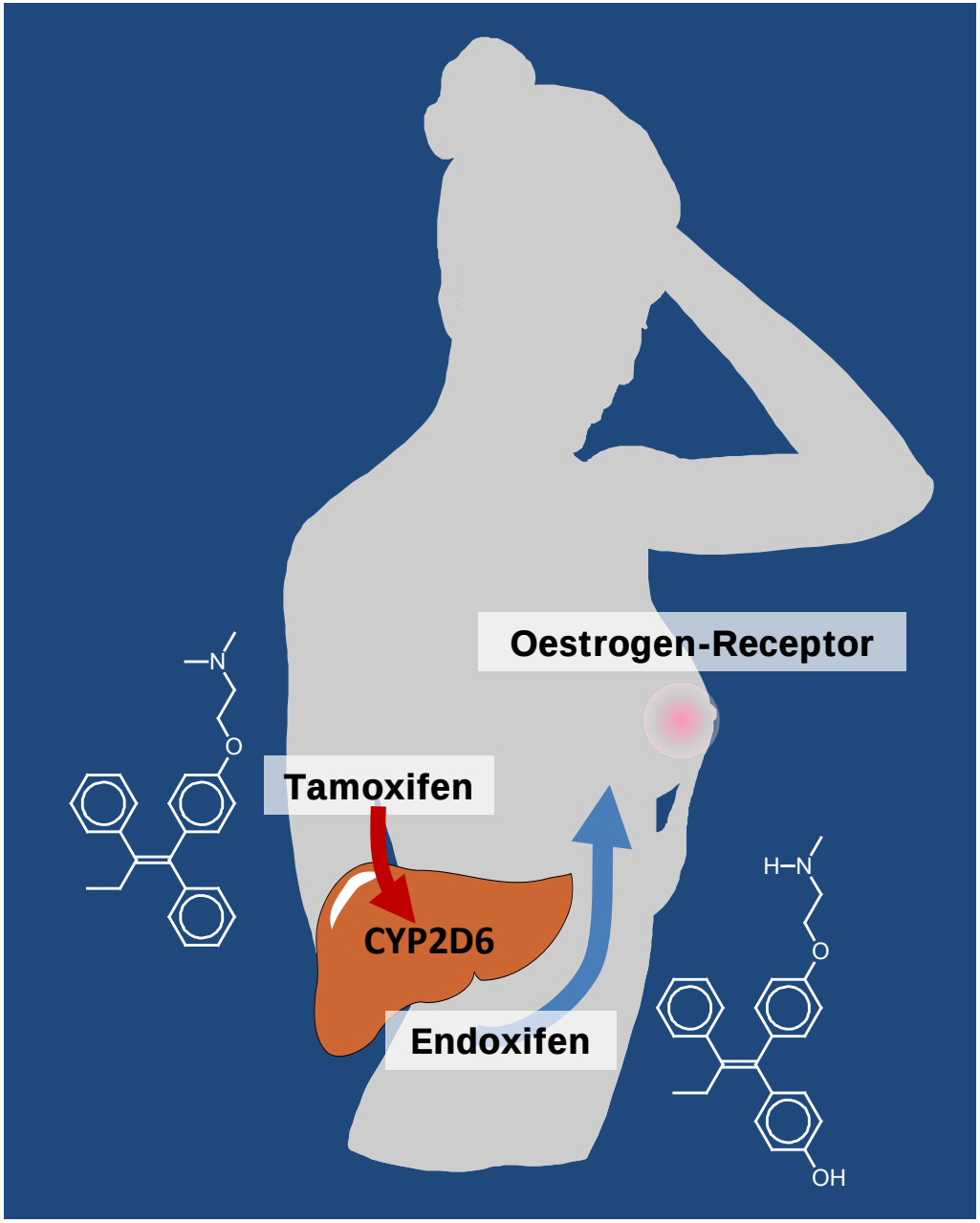


Figure 3

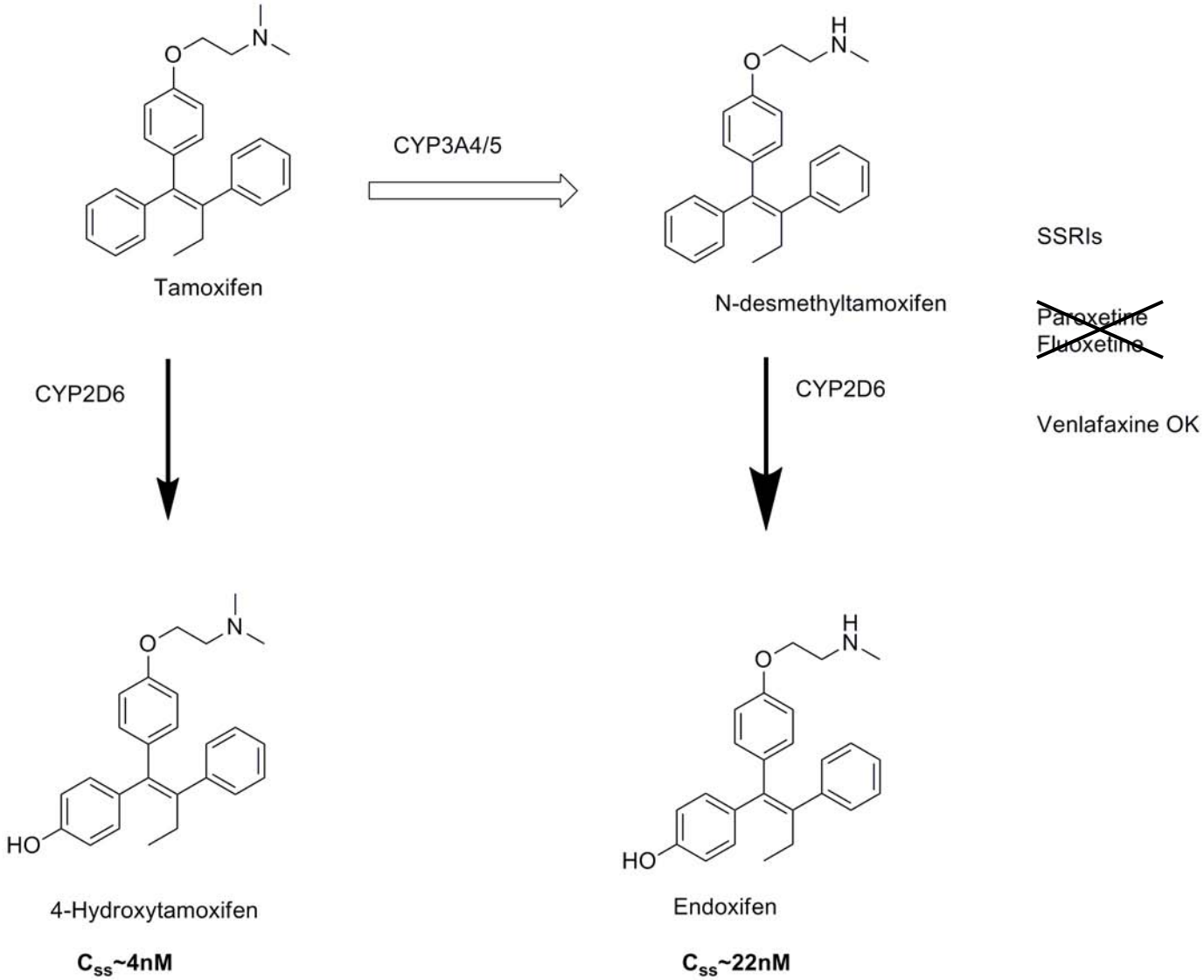
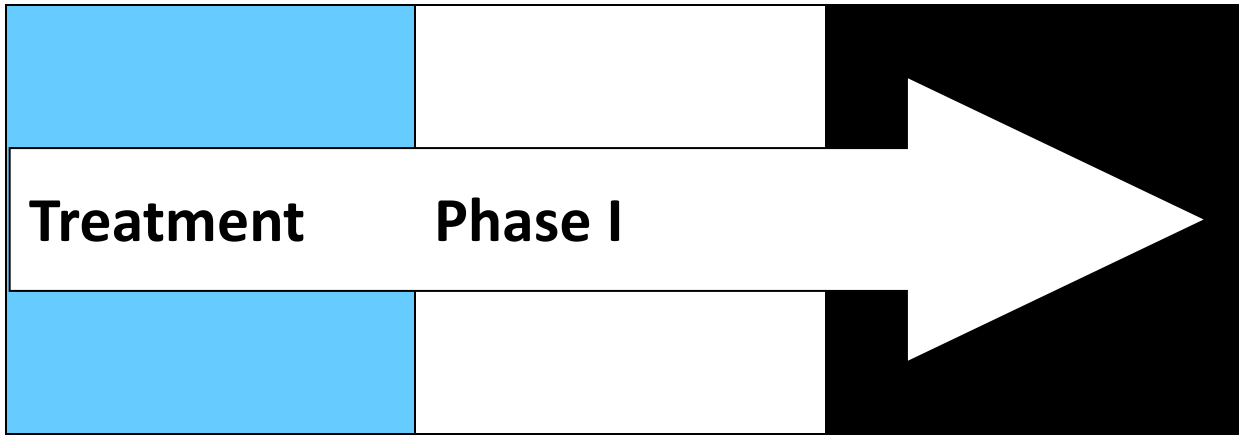

CYP3A4/5
Tamoxifen
N-desmethyltamoxifen
SSRIs
Paroxetine
Fluoxetine
Venlafaxine OK
CYP2D6
CYP2D6
4-Hydroxytamoxifen
C_{ss}~4nM
Endoxifen
C_{ss}~22nM
Active Metabolites

Figure 4

EVOLUTION OF SERM RESISTANCE



Antioestrogen action of SERMs

E_2 or SERM-stimulated

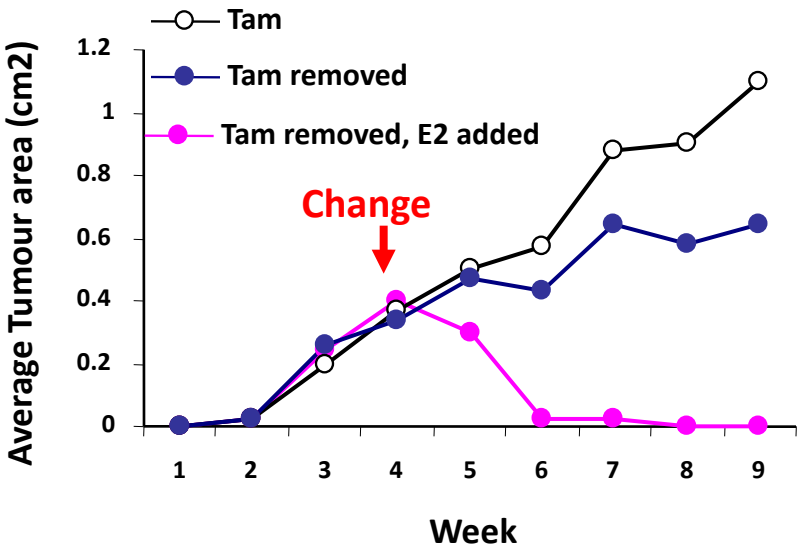
This is why aromatase inhibitor or fulvestrant work as 2nd line therapies after tamoxifen failure

Current Clinical applications

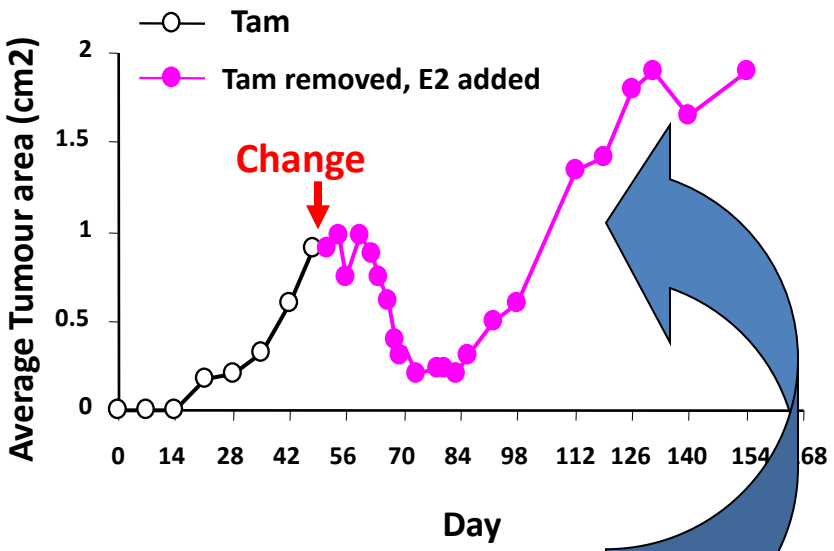
Figure 5

St. Gallen 1992

Regression of MCF-7 Tamoxifen stimulated tumours after administration of oestradiol



Regression and regrowth of Tamoxifen stimulated tumours during oestradiol treatment



Tumour regains antihormonal sensitivity

Loss of drug resistance

Figure 6

NEW CONCEPT
EVOLUTION OF SERM RESISTANCE

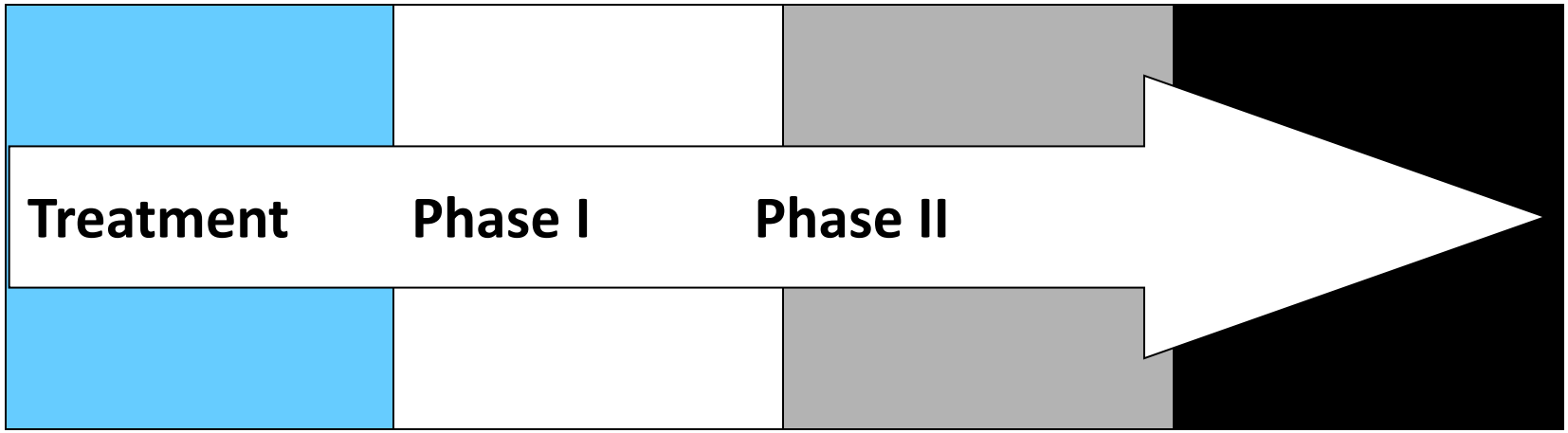


Figure 7

NF-κB Non-canonical Pathway

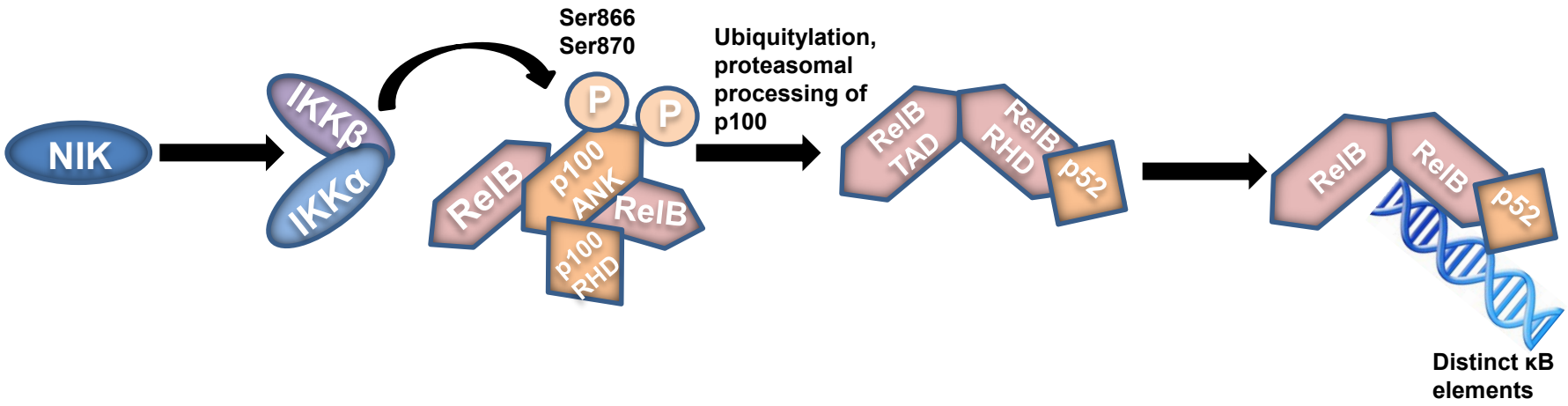


Figure 8

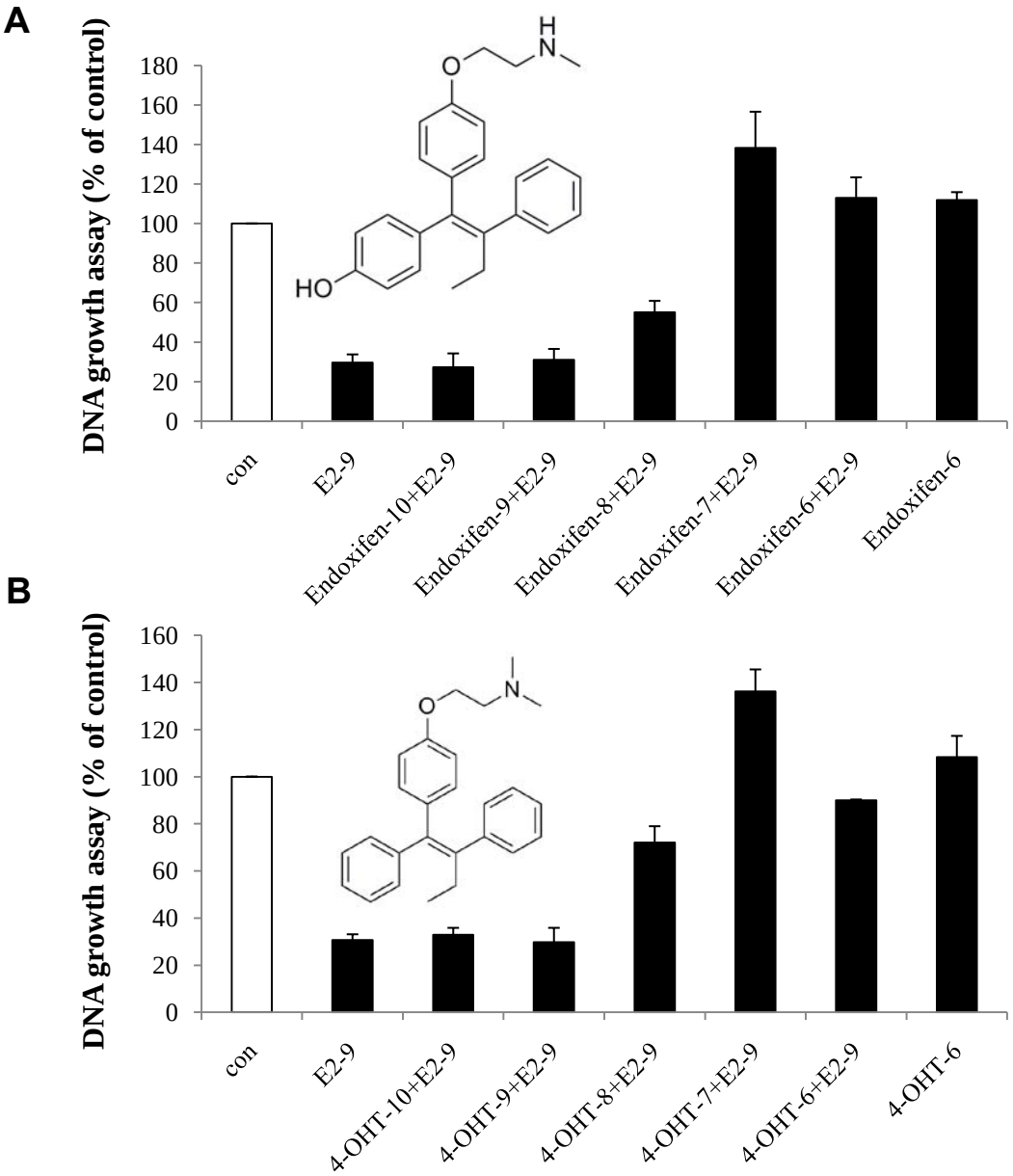

A
DNA growth assay (% of control)
180
160
140
120
100
80
60
40
20
0
H
N
O
HO
con
E2-9
Endoxifen-10+E2-9
Endoxifen-9+E2-9
Endoxifen-8+E2-9
Endoxifen-7+E2-9
Endoxifen-6+E2-9
Endoxifen-6
B
DNA growth assay (% of control)
160
140
120
100
80
60
40
20
0
N
O
con
E2-9
4-OHT-10+E2-9
4-OHT-9+E2-9
4-OHT-8+E2-9
4-OHT-7+E2-9
4-OHT-6+E2-9
4-OHT-6

Figure 9

International Breast Cancer Study Group (IBCSG)

IBCSG 35-07 - Study Of Letrozole Extension (SOLE)

At completion of 4 to 6 years of prior adjuvant SERM/AI endocrine therapy, patients will be randomized to one of two treatment groups:

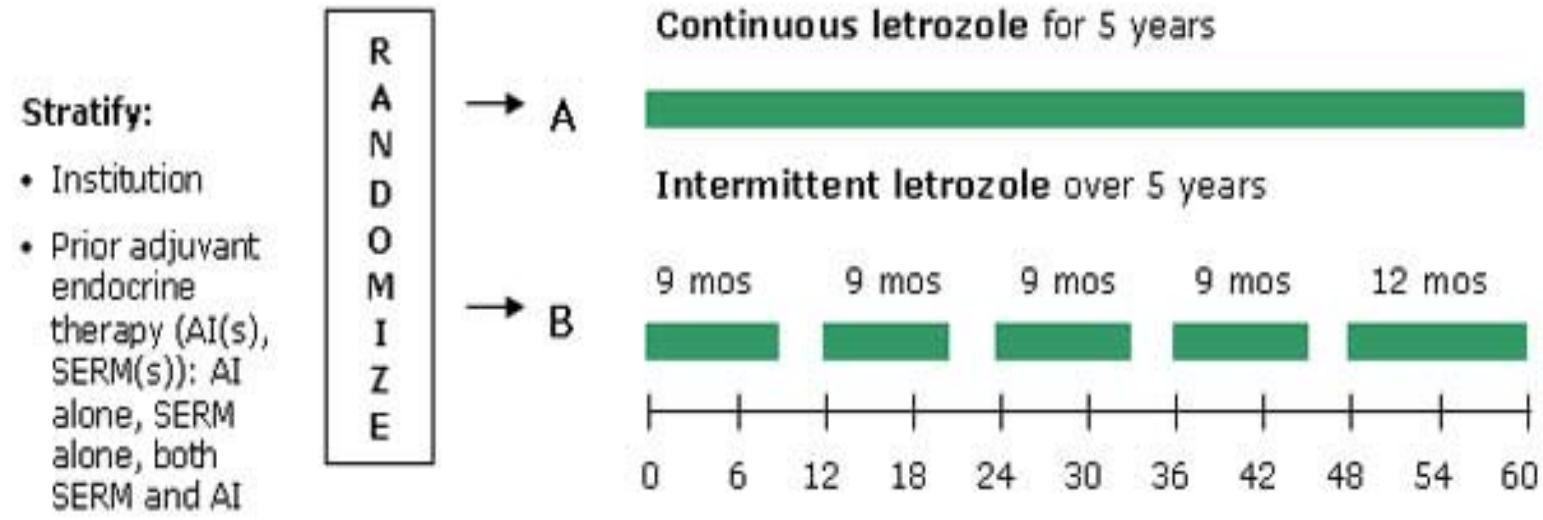
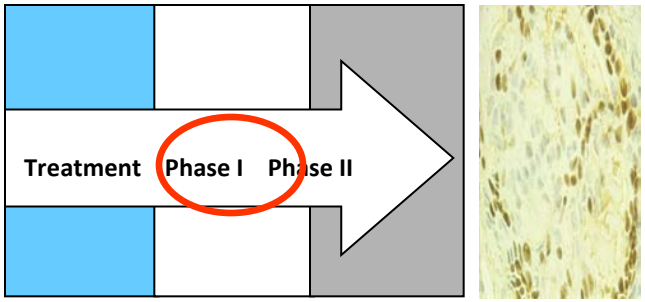


Figure 10

PLAN FOR POSTMENOPAUSAL WOMEN:

i.e. with a background of physiologic oestrogen



c-Src inhibitor

2 month treatment regimen

Tumour cells rapidly revert to Phase I Resistance

CONCLUSION: c-Src inhibitor blocks oestrogen-induced apoptosis, a result that undermines the anti-tumour actions of these compounds in patients treated exhaustively with antihormones

Table 1

Decades of Translational Discovery

DECADE	SCIENTIFIC PRINCIPLE	CLINICAL BENEFIT
1970s	Long-term adjuvant tamoxifen therapy targeted to ER	----------
	Foundation of chemoprevention with tamoxifen	----------
1980s	Selective ER modulation	Survival benefits for long-term adjuvant tamoxifen
1990s	Evolution of drug resistance to hormones	Chemoprevention with SERMs, tamoxifen and raloxifene
	Anti-tumour actions of physiologic oestrogens	
2000s	Oestrogen-induced apoptosis	Clinical translation of oestrogen-induced apoptosis

Table 2

A

Response		
COMPLETE	PARTIAL	SD
4[a]/32	6/32	2/32

[a]One patient remains disease-free 10 years and six months after commencing DES treatment."

B

Dose	# patients	Response	Clinical benefit
6 mg	34	10/34	29%
30 mg	32	9/32	28%

Decades of Discovery: The Selective Estrogen Receptor Modulator (SERM) Story: The St. Gallen Prize

V. Craig Jordan

Short title: Decades of Discovery

"*I have but one lamp by which my feet are guided, and that is the lamp of experience. I know no way of judging of the future but by the past*." (Patrick Henry, the First Elected Governor of Virginia, 1775)

Authors' Affiliations: [1]Georgetown Lombardi Comprehensive Cancer Center, Georgetown University Medical Center, Washington, DC 20057

Corresponding Author:
V. Craig Jordan
Georgetown University Medical Center
3970 Reservoir Rd NW
Research Building, Suite E501
Washington, DC 20057
Tel: 202.687.2897
Fax: 202.687.6402
E-mail: vcj2@georgetown.edu

Selective Estrogen Receptor Modulators (SERMs) are a well-established drug group in medicine. The SERMs are also unique, as their mechanisms depend on differentially switching on and switching off target sites around a woman's body--selectively [1]! Tamoxifen is the pioneering SERM [2] and the first medicine to be tested and approved for the reduction of risk of any cancer [3]. The problem to be solved was how to identify and treat the appropriate high risk women to reduce or eliminate their risk of developing breast cancer. The population based models [4] could focus down on a few thousand high risk women, but breast carcinogenesis would only be subverted in a few dozen. These lucky few did not know who they were, amongst the thousands who were treated and who would never get breast cancer. Unfortunately, the strategy to apply the pioneering SERM, tamoxifen, for population based chemoprevention was flawed at the outset, as laboratory and clinical evidence predicted that there was an elevated risk of an increase in endometrial cancer for postmenopausal women [5, 6]. This was a slight, but significant risk. Women worried. A range of other side effects (e.g. blood clots, cataracts, menopausal symptoms) would also be experienced by the many to benefit the few. The situation changed dramatically with the discovery that the two "lead" SERMs, tamoxifen and raloxifene, maintained bone density in laboratory animals, but also prevented mammary carcinogenesis [7, 8]. Raloxifene was also less uterotrophic than tamoxifen. Would there be no endometrial risk? With the recognition of SERMs in the 1980's, a unique public health strategy was possible.

The new strategy was stated (twice) in the literature, which provided a simple roadmap for the pharmaceutical industry to follow (eventually!). *Are we looking in the wrong place? The majority of breast cancer occurs unexpectedly and from unknown origin. Great efforts are being focused upon the identification of a population of high-risk women to test "chemopreventive" agents. But are resources being used less than optimally? The problem is much greater than the*

current horizon. Indeed, even if we had the best chemopreventive for a minority of selected women, the overall impact on the disease might be negligible. An alternative would be to seize upon the developing clues provided by an extensive clinical investigation of available antiestrogens. Could analogs be developed to treat osteoporosis or even retard the development of atherosclerosis? If this proved to be true, then a majority of women in general could be treated for these conditions as soon as menopause occurred. Should the agent also retain antibreast tumor actions, then it might be expected to act as a chemosuppressive on all developing breast cancers if these have an evolution from hormone-dependent to hormone-independent disease. A bold commitment to drug discovery and clinical pharmacology will potentially place us in a key position to prevent the development of breast cancer by the end of this century [9].

And subsequently: *Is this the end of the possible applications for anti-estrogens? Certainly not! We have obtained valuable clinical information about this group of drugs that can be applied in other disease states. Research does not travel in straight lines and observations in one field of science often become major discoveries in another. Important clues have been garnered about the effects of tamoxifen on bone and lipids so it is possible that derivatives could find targeted applications to retard osteoporosis or atherosclerosis. The ubiquitous application of novel compounds to prevent diseases associated with the progressive changes after menopause may, as a side effect, significantly retard the development of breast cancer. The target population would be postmenopausal women in general, thereby avoiding the requirement to select a high risk group to prevent breast cancer* [10].

Today, new SERMs hold the promise of fulfilling the stated prediction from two decades ago. Lasofoxifene [11] for example, is approved in the E.U. for the prevention of osteoporosis in

osteopenic women, but at the same time, lasofoxifene reduces the incidence of breast cancer, coronary heart events, strokes and endometrial cancer. Raloxifene, the pioneering SERM to prevent both breast cancer and osteoporosis [12, 13] is not as robust in its SERM pharmacology (there is no effect on coronary events or strokes) as lasofoxifene. Remarkably, lasofoxifene is 100 times more potent as a SERM; raloxifene is recommended at 60 mg daily but lasofoxifene is effective at 0.5 mg daily!

With this background of the current success of SERMs, my goal is to guide the reader through an evolution of ideas. History is often written as the achievement of Dynasties. But as with Dynasties, the dogma of the preceding Dynasty in medicine must be overcome, not by sudden force, but by unrelenting pressure and the reason of evidence. Only tenacity can change medicine through ideas as the standard of care is maintained and jealously guarded by the Dynasty.

My early catalytic role in the evolution of our story is well-documented in the refereed literature [2, 14]. Suffice to say as a pharmacologist, I had a passion to develop drugs to treat cancer. But where to start? By a series of accidents, I met the right people at the right time, but the career choice to study the pharmacology of nonsteroidal antiestrogen for my Ph.D. was then seen as a dead end. They were failed contraceptives and of only academic interest. But this was the point of a Ph.D. in Britain—training in research method with a Medical Research Scholarship. Thus, we enter the first of our 4 decades.

The 1970's: The re-invention of tamoxifen as the "gold standard" for the treatment and prevention of breast cancer

The Dynasty to be defeated in the opening years of the 1970's was combination cytotoxic chemotherapy. Chemotherapy was king, fresh from the victory over childhood leukemia and poised to "MOPP" up Hodgkin's Disease. It was reasoned by the Dynasty, if only the right combination of agents could be found in the lexicon of options, a cure was assured. No one was advocating antihormone (or as it was described, "hormone therapy"!) research and treatment.

I saw an opportunity to develop a failed contraceptive, ICI 46,474, further than was believed originally it could go. In 1972, ICI 46,474 was abandoned by the pharmaceutical industry for continuing clinical testing because there was no profit to be made. Nevertheless, the meeting between me and the Head of the Fertility Control Program, Arthur Walpole (or "Walop" as he was affectionately known), proved to be critical to our story. He examined my Ph.D. at Leeds University, but ensured I had the resources at the Worcester Foundation in Shrewsbury, MA, USA and Leeds University, to create a clinical strategy for this orphan drug. He ensured it was put on the market, now tell us how to use it! The strategy I conceived and implemented is in **Figure 1**.

The strategy was based on 3 principles:

1) Target the tumor ER with tamoxifen
2) Give long term adjuvant tamoxifen therapy
3) Plan for chemoprevention

All these principles were unpopular at the outset, but persistence and hundreds of evidence-based lectures around the world to my clinical colleagues slowly defeated the Dynasty of combination cytotoxic chemotherapy to cure breast cancer. "Antihormone therapy" became the treatment of

choice with long term adjuvant tamoxifen therapy targeted to the tumor ER (the first targeted therapy).

How bad was the first Decade of Discovery? If I may be so bold at this point to tell a story of my friend and colleague, Steven E. Jones, M.D. When I started my international journey to advocate my principles for adjuvant antihormone therapy, Steven was in Arizona, the co-Director of the Adjuvant Therapy of Cancer Meeting in the 1970's. I was setting up a Ludwig Institute in Bern, Switzerland and was invited to present my new ideas about the use of tamoxifen at their 1979 m eeting. There I was, sandwiched between the greats of cyotoxic chemotherapy, Vince DeVita and Bernie Fisher. I, in contrast, was advocating a stealth attack on breast cancer with tamoxifen that by comparison had no s ide effects. Little hope, one would think, but the plan succeeded. Two decades later, Steven Jones rose at a meeting in Washington and started his talk by declaring, "Craig Jordan was correct." Through the clinical trials mechanism, it is now proven that long term (5 years) adjuvant tamoxifen treatment targeted to the tumor ER has enhanced the survival of millions of women worldwide [15]. An orphan drug that is cheap and easy to administer has and continues to save hundreds of thousands of lives annually.

Now our story changes to the second decade with the "new" fashion in oncology—chemoprevention.

The 1980's: SERMs surface

The idea of preventing cancer became popular in the 1980's. This is a noble goal and one of the primary goals of cancer research, but the goal has proved hard to address. The idea as applied to breast cancer has its origin with the French Scientist, Professor Antoine Lacassagne,

who stated, at his lecture at the Annual Meeting of the American Association for Cancer Research in Boston (1936): "*If one accepts the consideration of adenocarcinoma of the breast as a consequence of a special hereditary sensibility to the proliferative action of oestrone, one is led to imagine a therapeutic preventive for subjects predisposed by their heredity to this cancer…*" [16]. However, Lacassagne's evidence was based on oophorectomy of mice from strains that develop a high incidence of mammary cancer and there were no mechanisms or compounds to advance and address the question. This would have to wait another quarter century with the serendipitous discovery of the nonsteroidal antiestrogens [10].

Tamoxifen was advanced for testing as a potential chemopreventive for breast cancer in the early 1980's based on three facts:

1) There was laboratory evidence that tamoxifen would prevent rat mammary carcinogenesis [17-19].
2) Tamoxifen was becoming widely used in medicine to treat breast cancer so, it was argued that side effects were known and anticipated. This was not really true, as it took translational research [5] to draw the attention of the clinical community of the small risk of endometrial cancer [6].
3) Tamoxifen, when used as an adjuvant therapy reduced the incidence of contralateral breast cancer [20].

Nevertheless, there was a major toxicological (and ethical issue) with treating well women with a drug classified as a "nonsteroidal antiestrogen" [21]. If, as was believed at the time, estrogen was good to build bone and to reduce the risk of coronary heart disease, what would be the value of the chemoprevention strategy that prevents breast cancer but condemns women to an elevated risk of crushing osteoporosis or fatal coronary heart disease. To address the concern,

laboratory studies were initiated to evaluate the pharmacology of tamoxifen on estrogen target tissues.

Studies in rats demonstrated that both tamoxifen and the failed and discontinued breast cancer drug, raloxifene (then known as keoxifene) [22], both maintained bone density in ovariectomized rats [7] and prevented rat mammary carcinogenesis [8]. However, raloxifene was not as effective as tamoxifen, probably because of poor pharmacodynamics, i.e. raloxifene does not accumulate, is rapidly excreted and there is only 2% bioavailability by the oral route of administration [23]. This pharmacological fact was to recur clinically following clinical trials 20 years later (see next section).

A pattern was emerging in the mid 1980's concerning the pharmacology of the nonsteroidal antiestrogens clomiphene, tamoxifen and raloxifene. The facts that lead to the SERM concept being described in my laboratory can now be summarized.

1) Clomiphene, a mixture of estrogenic *cis* and antiestrogenic *trans* geometric isomers, has bone preserving properties in the ovariectomized rat [24]. Clomiphene had been tested as a breast cancer drug in patients [25], but the manufacturer declined to advance development based on potential problems with cholesterol metabolism and a concern about cataracts. The drug remained the gold standard for the induction of ovulation where only give day courses were given [26].
2) The fact that clomiphene was an impure mixture of estrogenic and antiestrogenic isomers made the bone preserving effects uncertain. The estrogenic isomer might have been the favored pharmacologic agent at bone. In contrast, tamoxifen is the pure antiestrogenic trans isomer that preserves bone [7] and raloxifene is a fixed ring structure that is

exclusively antiestrogenic (very weakly estrogenic) in the uterus, but estrogenic in bone [7].

3) Both tamoxifen and raloxifene are antitumor agents in rat mammary carcinogenesis [8].
4) Tamoxifen stimulates endometrial cancer growth (and mouse uterine growth) but blocks estradiol-stimulated growth of breast cancer transplanted in the same immune deficient animal [5, 27]. This experiment demonstrates target site specificity.
5) Tamoxifen lowers circulating cholesterol in the rat [28] and this property was included in the initial patent application which read: "*The alkene derivatives of the invention are useful for the modification of the endocrine status in man and animals and they may be useful for the control of hormone-dependent tumours or for the management of the sexual cycle and aberrations thereof. They also have useful hypocholesterolaemic activity*" [2].

The claims as a breast cancer drug were denied and required to be omitted in the United States until eventually a patent was awarded in 1985 in the Court of Appeals. In other words, tamoxifen was tested and marketed in America initially without patent protection for a dozen years. But, nobody cared, as there was little possibility of success, either as a therapy or commercially (or so everybody thought!).

Thus, based on all these data, primarily from my laboratory, the SERM concept surfaced and the roadmap for clinical development started as noted previously [9, 10]. These data were the scientific basis of the Wisconsin Tamoxifen Study initiated in the late 1980's to evaluate the pharmacology of tamoxifen on bone density and circulating cholesterol. It was the proven clinical translation of the tamoxifen (SERM) concept to preserve bone density [29] and lower circulating cholesterol [30, 31] that awakened the sleeping pharmaceutical industry to develop raloxifene to prevent and treat osteoporosis in postmenopausal women. This started with the

"magical" patenting in 1992 of raloxifene for this indication [22] and the publication of laboratory studies confirming my work on the SERM actions of raloxifene in rats [32].

The 1990's: Raloxifene's Promise is a Reality

During the 1990's, I transitioned from my focus on laboratory investigations with SERMs to a role of "scientific resource" for major clinical trials. I was invited by Eli Lilly to chair their Oncology Advisory Committee, which had responsibilities to adjudicate breast cancer detection in their initial osteoporosis trial, Multiple Outcomes with Raloxifene Evaluation (MORE). Subsequently, Dr. Norman Wolmark would invite me to be the scientific chair of the largest breast chemoprevention study—the Study of Tamoxifen and Raloxifene (STAR).

The MORE trial recruited 7,705 postmenopausal women with osteoporosis to be randomized to placebo, 60 or 120 mg raloxifene daily. Raloxifene reduced fractures of the spine by 40% over the initial 3 year evaluation period [12]. In our parallel evaluation of the incidence of breast cancer, there was a significant decrease in the incidence of ER-positive breast cancer by 70% with no increase in endometrial cancer [12]. The laboratory concept of SERMs [10] translated to the clinic. Women being treated for osteoporosis would develop less breast cancer if they took raloxifene. But here was an important pharmacological point--it was proved that they must keep taking raloxifene to obtain benefit. This laboratory principle noted with rapidly excreted SERMs in the 1980's [8, 18] was to emerge as a clinical fact from the STAR trial after treatment stopped (see later).

What happened to tamoxifen in chemoprevention, Professor Trevor Powles initiated the first pilot toxicity study of tamoxifen in high risk women in the early 1980's [33], but it was Dr. Bernard Fisher who successfully conducted the first randomized placebo controlled clinical

chemoprevention trial of tamoxifen in women at high risk for breast cancer. All preclinical predictors were confirmed—tamoxifen reduced the incidence of breast cancer, increased the incidence of endometrial in postmenopausal women and there was a decrease, though not significant in fracture rate [3, 34]. Unanticipated information (though prior clinical studies suggested an effect) was an increase in operations for cataracts. The other fact consistent with the overview analysis of clinical trial for adjuvant therapeutic tamoxifen [15] was that tamoxifen alone caused a long term beneficial effect to suppress the development of breast cancer more than a decade after tamoxifen therapy stopped [35]. We will return to the science behind this observation later. The fact, as we noted, that tamoxifen increased endometrial cancer in postmenopausal women, now caused a turn to raloxifene, that had no increased endometrial cancer in MORE [12].

The STAR Trial pitted tamoxifen 20 mg daily against raloxifene 60 mg daily for 5 years to compare and contrast efficacy and side effects for the reduction of breast cancer incidence in high risk postmenopausal women. As an aside, I was often asked how I would feel if raloxifene was found to be superior to tamoxifen. Happy—as the science of both drugs came from my laboratory and both drugs had to be reinvented as useful medicine after being essentially discarded by industry: tamoxifen, a failed contraceptive and raloxifene, a failed breast cancer drug. The first analysis of the STAR Trial showed equivalent efficacy to reduce the incidence of breast cancer by 50% [13]. However, side effects were reduced with raloxifene. In particular, there was less endometrial hyperplasia with raloxifene and fewer hysterectomies. Operations for cataracts were lower on raloxifene. This analysis was conducted during raloxifene therapy [13], but the subsequent analysis conducted after therapy had stopped [36] demonstrated tamoxifen

had a sustained antitumor action whereas there was a reduced (75%) efficacy for raloxifene. The drugs were different with their pharmacology and raloxifene must be given indefinitely.

We conclude that the fact that raloxifene is a drug with low bioavailability and therefore the pharmacodynamics to concentrate at the target site—the effect on the breast tissue is reduced. If sustained, local concentrations of tamoxifen and raloxifene are different and the elevated concentrations of tamoxifen drive cell population to evolve differently than those exposed to low levels of raloxifene, there will be, therefore, consequences for tumorigenesis and the evolution of drug resistance. We hypothesize that the low levels of raloxifene remain therapeutically "antiestrogenic" for the duration of therapy, but the endogenous estrogen from the woman's own body causes nascent tumor regrowth.

In contrast, the sustained high concentrations of tamoxifen locally in the breast causes a change in the evolution of the breast cancer cell population that in some way leaves an "antitumor memory" for years after therapy stops—but how? This leads us to the final decade of discovery: estrogen-induced apoptosis.

The 2000's: Estrogen-induced apoptosis?

The first chemical therapy to treat any cancer successfully was the use of high dose estrogen therapy to treat metastatic breast cancer in postmenopausal patients [37]. High dose estrogen therapy became the standard of care until the introduction of tamoxifen in the 1970's [10, 38]. At the end of his career, Sir Alexander Haddow FRS, presented the inaugural Karnofsky Lecture, where he expressed his disappointment about the lack of progress in understanding mechanisms: "*…the extraordinary extent of tumour regression observed in perhaps 1% of post-menopausal cases (with oestrogen) has always been regarded as of major*

theoretical importance ,and it is a matter for some disappointment that so much of the underlying mechanisms continues to elude us…" [39]. What was known was that the high dose estrogen therapy was more effective as a breast cancer treatment the further away the patient was from the menopause, but why?

The advance in our understanding was to await an examination of model systems in the laboratory to decipher the mechanisms of antihormone drug resistance (**Figure 2**). The whole topic has recently been summarized [40], but the facts must be stated to illustrate how transparency in nature can occur through unanticipated results in another area of research.

The first transplantable model of resistance to long term tamoxifen therapy demonstrated unique qualities. Acquired resistance is evidenced by tamoxifen-stimulated (actually SERM-stimulated as it turns out) growth. Tumors grow because of tamoxifen, not in spite of tamoxifen, as occurs with all other anticancer agents. What was even more surprising was the fact that when tamoxifen treatment is stopped, then estrogen again can stimulate growth. This model replicates tamoxifen resistance during the treatment of ER-positive metastatic breast cancer: resistance occurs within a couple of years, estrogen or tamoxifen is required for continued growth and estrogen withdrawal or fulvestrant (the pure antiestrogen that causes destruction of the ER) is an appropriate second line therapy. What the model of acquired resistance did not do was explain how it was possible to use 5 years of adjuvant tamoxifen therapy to treat patients selectively. If the laboratory model was correct, and had been available at the time long term adjuvant therapy was planned as a treatment strategy, then no one would consider treatment longer than a year for adjuvant antihormone therapy. It would obviously be dangerous for patients. The same argument was used in the 1970's by the clinical community. Tamoxifen cannot control metastatic breast cancer on average, more than 2 years, so one cannot give long term (greater than 5 years)

adjuvant tamoxifen. We were missing something fundamental about the biology of micrometastatic breast cancer exposed to long term tamoxifen therapy.

The breakthrough in understanding came through serendipity and as always, with outstanding graduate students with exceptional laboratory skills. The model of acquired resistance to tamoxifen could only only be maintained by serial transplantation in successive generations of tamoxifen-treated athymic mice. We were unable to transfer the tumors to cell culture for study, so the expense of preserving the only naturally developed model of resistance to tamoxifen had to be born. That, as it turned out, was the good, new and an opportunity for future discovery.

The acquired drug resistance to tamoxifen evolves in an environment of tamoxifen (**Figure 2**). Retransplantation of tumor into further tamoxifen treated mice causes adapted cell populations to develop rather than rely entirely on tamoxifen for growth (Phase I), but as the survival networks become reconfigured, a vulnerability emerges (Phase II). After 5 years of exposure to tamoxifen, the resulting tumor no longer sees estrogen as a survival signal, but as an apoptotic trigger (Phase II).

In 1992, these data were presented for the first time at the St. Gallen Breast Cancer Conference [41]. The hypothesis advanced was that the termination of tamoxifen, at the correct time, was important for the woman's own estrogen to destroy the microfoci of appropriately prepared target cells. This new biology of physiologic estrogen causing apoptosis was the reason for the enhanced survivorship of patients treated with a full 5 years of tamoxifen. As a result, a shift in thinking occurred and the clinical trials community subsequently exploited the concept, now published in the refereed literature [42], that therapeutic estrogen or indeed "physiologic estrogen" in the form of low dose estrogen replacement therapy (ERT) could cause the correctly

configured tumors with acquired antihormone resistance to regress [43, 44]. The Estrogen Dynasty originally deposed, struck back. Nature answered as well. Today, there is much interest in the paradoxical actions of physiologic estradiol in breast cancer [45, 46]. Recent results from the Women's Health Initiative demonstrate a reduction in the incidence of breast cancer for hysterectomized, postmenopausal women who take long term estrogen replacement therapy [47]. Like our tamoxifen story, the effects persist for years following stopping ERT [48]. Practical advances, not only in the therapy of cancer, but preemptively in "natural" chemoprevention may result from these findings in the future.

In summary, I have mapped out the Decades of Discovery that emerged from a single quest some 40 years ago—to develop a drug useful for the treatment and prevention of breast cancer. At the time, I could count on the fingers of one hand, the people who were interested in the quest. No one cared, and it was not going to happen. But science is not like that; as in politics, ideas have their time but it is really about people and a passion to keep the flame of truth alight. I am immensely grateful to Professor Hans-Jörg Senn and his Committee for selecting me to receive the St. Gallen Prize for Advances in Breast Cancer Research. Thanks also go to my friends and colleagues Aron Goldhirsch and Richard Gelber. We all started our personal journeys together in Bern, Switzerland in the late 1970's and we remain older friends and colleagues to this day. Most importantly, I thank the 40 years of "Tamoxifen Teams" that worked and trained with me in my laboratories in Leeds University (UK), WFEB (US), Ludwig Institute for Cancer Research, Bern (Switzerland), University of Wisconsin (Madison), Northwestern University (Chicago), Fox Chase Cancer Center (Philadelphia) and the Lombardi Comprehensive Cancer

Center (Washington, DC). I had the privilege to guide their lives and they turned the ideas we conceived into lives saved around the world.

The quotation in the heading of this Editorial was the one I used to open my Prize Lecture in St. Gallen, 16 March 2011: "*I have but one lamp by which my feet are guided, and that is the lamp of experience. I know no way of judging of the future but by the past*" (Patrick Henry, the First Elected Governor of Virginia, 1775). My lamp was tamoxifen. However, this journey, as I hope I have illustrated, is so much more than the successful development of tamoxifen for the adjuvant treatment of breast cancer. It is about a way of constructing a conversation with nature with the goal of defeating a powerful enemy within us—cancer.

Acknowledgement:

Grant support (to VCJ): This work (VCJ) was supported by the Department of Defense Breast Program under Award number BC050277 Center of Excellence (this interdisciplinary research grant supports research into estrogen-induced apoptosis in breast cancer); subcontract under the SU2C (AACR) Grant number SU2C-AACR-DT0409; the Susan G Komen for the Cure Foundation under Award number SAC100009 and the Lombardi Comprehensive Cancer Center Support Grant (CCSG) Core Grant NIH P30 CA051008 from the National Cancer Institute. The content is solely the responsibility of the authors and does not necessarily represent the official views of the National Cancer Institute or the National Institutes of Health. The views and opinions of the author(s) do not reflect those of the US Army or the Department of Defense.

References

1. Jordan VC (2001) Selective estrogen receptor modulation: a personal perspective. Cancer Res 61: 5683-7.
2. Jordan VC (2003) Tamoxifen: a most unlikely pioneering medicine. Nat Rev Drug Discov 2: 205-13.
3. Fisher B, Costantino JP, Wickerham DL, Redmond CK, Kavanah M, Cronin WM, Vogel V, Robidoux A, Dimitrov N, Atkins J, Daly M, Wieand S, Tan-Chiu E, Ford L, Wolmark N (1998) Tamoxifen for prevention of breast cancer: report of the National Surgical Adjuvant Breast and Bowel Project P-1 Study. J Natl Cancer Inst 90: 1371-88.
4. Gail MH, Brinton LA, Byar DP, Corle DK, Green SB, Schairer C, Mulvihill JJ (1989) Projecting individualized probabilities of developing breast cancer for white females who are being examined annually. J Natl Cancer Inst 81: 1879-86.
5. Gottardis MM, Robinson SP, Satyaswaroop PG, Jordan VC (1988) Contrasting actions of tamoxifen on endometrial and breast tumor growth in the athymic mouse. Cancer Res 48: 812-5.
6. Fornander T, Rutqvist LE, Cedermark B, Glas U, Mattsson A, Silfversward C, Skoog L, Somell A, Theve T, Wilking N, et al. (1989) Adjuvant tamoxifen in early breast cancer: occurrence of new primary cancers. Lancet 1: 117-20.
7. Jordan VC, Phelps E, Lindgren JU (1987) Effects of anti-estrogens on bone in castrated and intact female rats. Breast Cancer Res Treat 10: 31-5.
8. Gottardis MM, Jordan VC (1987) Antitumor actions of keoxifene and tamoxifen in the N-nitrosomethylurea-induced rat mammary carcinoma model. Cancer Res 47: 4020-4.
9. Jordan VC (1988) Chemosuppression of breast cancer with tamoxifen: laboratory evidence and future clinical investigations. Cancer Invest 6: 589-95.
10. Lerner LJ, Jordan VC (1990) Development of antiestrogens and their use in breast cancer: eighth Cain memorial award lecture. Cancer Res 50: 4177-89.
11. Cummings SR, Ensrud K, Delmas PD, LaCroix AZ, Vukicevic S, Reid DM, Goldstein S, Sriram U, Lee A, Thompson J, Armstrong RA, Thompson DD, Powles T, Zanchetta J, Kendler D, Neven P, Eastell R (2010) Lasofoxifene in postmenopausal women with osteoporosis. N Engl J Med 362: 686-96.
12. Cummings SR, Eckert S, Krueger KA, Grady D, Powles TJ, Cauley JA, Norton L, Nickelsen T, Bjarnason NH, Morrow M, Lippman ME, Black D, Glusman JE, Costa A, Jordan VC (1999) The effect of raloxifene on risk of breast cancer in postmenopausal women: results from the MORE randomized trial. Multiple Outcomes of Raloxifene Evaluation. JAMA 281: 2189-97.
13. Vogel VG, Costantino JP, Wickerham DL, Cronin WM, Cecchini RS, Atkins JN, Bevers TB, Fehrenbacher L, Pajon ER, Jr., Wade JL, 3rd, Robidoux A, Margolese RG, James J, Lippman SM, Runowicz CD, Ganz PA, Reis SE, McCaskill-Stevens W, Ford LG, Jordan VC, Wolmark N (2006) Effects of tamoxifen vs raloxifene on the risk of developing invasive breast cancer and other disease outcomes: the NSABP Study of Tamoxifen and Raloxifene (STAR) P-2 trial. JAMA 295: 2727-41.
14. Jordan VC (2006) Tamoxifen (ICI46,474) as a targeted therapy to treat and prevent breast cancer. Br J Pharmacol 147 Suppl 1: S269-76.
15. EBCTCG (2005) Effects of chemotherapy and hormonal therapy for early breast cancer on recurrence and 15-year survival: an overview of the randomised trials. Lancet 365: 1687-717.

16. Lacassagne A (1936) Hormonal pathogenesis of adenocarcinoma of the breast. Am J Cancer 27: 217-25.
17. Jordan VC (1976) Effect of tamoxifen (ICI 46,474) on initiation and growth of DMBA-induced rat mammary carcinomata. Eur J Cancer 12: 419-24.
18. Jordan VC, Allen KE (1980) Evaluation of the antitumour activity of the non-steroidal antioestrogen monohydroxytamoxifen in the DMBA-induced rat mammary carcinoma model. Eur J Cancer 16: 239-51.
19. Jordan VC, Allen KE, Dix CJ (1980) Pharmacology of tamoxifen in laboratory animals. Cancer Treat Rep 64: 745-59.
20. Cuzick J, Baum M (1985) Tamoxifen and contralateral breast cancer. Lancet 2: 282.
21. Jordan VC (1984) Biochemical pharmacology of antiestrogen action. Pharmacol Rev 36: 245-76.
22. Lewis JS, Jordan VC (2006) Case Histories: Raloxifene. Comprehensive Medicinal Chemistry II 8: 103-21.
23. Snyder KR, Sparano N, Malinowski JM (2000) Raloxifene hydrochloride. Am J Health Syst Pharm 57: 1669-75; quiz 76-8.
24. Beall PT, Misra LK, Young RL, Spjut HJ, Evans HJ, LeBlanc A (1984) Clomiphene protects against osteoporosis in the mature ovariectomized rat. Calcif Tissue Int 36: 123-5.
25. Herbst AL, Griffiths CT, Kistner RW (1964) Clomiphene Citrate (Nsc-35770) in Disseminated Mammary Carcinoma. Cancer Chemother Rep 43: 39-41.
26. ASRM PC (2006) Use of clomiphene citrate in women. Fertil Steril 86: S187-93.
27. Jordan VC, Robinson SP (1987) Species-specific pharmacology of antiestrogens: role of metabolism. Fed Proc 46: 1870-4.
28. Harper MJ, Walpole AL (1967) A new derivative of triphenylethylene: effect on implantation and mode of action in rats. J Reprod Fertil 13: 101-19.
29. Love RR, Mazess RB, Barden HS, Epstein S, Newcomb PA, Jordan VC, Carbone PP, DeMets DL (1992) Effects of tamoxifen on bone mineral density in postmenopausal women with breast cancer. N Engl J Med 326: 852-6.
30. Love RR, Wiebe DA, Newcomb PA, Cameron L, Leventhal H, Jordan VC, Feyzi J, DeMets DL (1991) Effects of tamoxifen on cardiovascular risk factors in postmenopausal women. Ann Intern Med 115: 860-4.
31. Love RR, Newcomb PA, Wiebe DA, Surawicz TS, Jordan VC, Carbone PP, DeMets DL (1990) Effects of tamoxifen therapy on lipid and lipoprotein levels in postmenopausal patients with node-negative breast cancer. J Natl Cancer Inst 82: 1327-32.
32. Black LJ, Sato M, Rowley ER, Magee DE, Bekele A, Williams DC, Cullinan GJ, Bendele R, Kauffman RF, Bensch WR, et al. (1994) Raloxifene (LY139481 HCI) prevents bone loss and reduces serum cholesterol without causing uterine hypertrophy in ovariectomized rats. J Clin Invest 93: 63-9.
33. Powles TJ, Hardy JR, Ashley SE, Farrington GM, Cosgrove D, Davey JB, Dowsett M, McKinna JA, Nash AG, Sinnett HD, et al. (1989) A pilot trial to evaluate the acute toxicity and feasibility of tamoxifen for prevention of breast cancer. Br J Cancer 60: 126-31.
34. Fisher B, Costantino JP, Wickerham DL, Cecchini RS, Cronin WM, Robidoux A, Bevers TB, Kavanah MT, Atkins JN, Margolese RG, Runowicz CD, James JM, Ford LG, Wolmark N (2005) Tamoxifen for the prevention of breast cancer: current status of the National Surgical Adjuvant Breast and Bowel Project P-1 study. J Natl Cancer Inst 97: 1652-62.

35. Powles TJ, Ashley S, Tidy A, Smith IE, Dowsett M (2007) Twenty-year follow-up of the Royal Marsden randomized, double-blinded tamoxifen breast cancer prevention trial. J Natl Cancer Inst 99: 283-90.
36. Vogel VG, Costantino JP, Wickerham DL, Cronin WM, Cecchini RS, Atkins JN, Bevers TB, Fehrenbacher L, Pajon ER, Wade JL, 3rd, Robidoux A, Margolese RG, James J, Runowicz CD, Ganz PA, Reis SE, McCaskill-Stevens W, Ford LG, Jordan VC, Wolmark N (2010) Update of the National Surgical Adjuvant Breast and Bowel Project Study of Tamoxifen and Raloxifene (STAR) P-2 Trial: Preventing breast cancer. Cancer Prev Res (Phila) 3: 696-706.
37. Haddow A, Watkinson JM, Paterson E, Koller PC (1944) Influence of Synthetic Oestrogens on Advanced Malignant Disease. Br Med J 2: 393-8.
38. Jordan VC (2009) A century of deciphering the control mechanisms of sex steroid action in breast and prostate cancer: the origins of targeted therapy and chemoprevention. Cancer Res 69: 1243-54.
39. Haddow A (1970) Thoughts on Chemical Therapy. Cancer 26: 737-54.
40. Jordan VC, Ford LG (2011) Paradoxical Clinical Effect of Estrogen on Breast Cancer Risk: A "New" Biology of Estrogen-Induced Apoptosis. Cancer Prev Res (Phila): Epub (Ahead of print).
41. Wolf DM, Jordan VC (1993) A laboratory model to explain the survival advantage observed in patients taking adjuvant tamoxifen therapy. Recent Results Cancer Res 127: 23-33.
42. Yao K, Lee ES, Bentrem DJ, England G, Schafer JI, O'Regan RM, Jordan VC (2000) Antitumor action of physiological estradiol on tamoxifen-stimulated breast tumors grown in athymic mice. Clin Cancer Res 6: 2028-36.
43. Lonning PE, Taylor PD, Anker G, Iddon J, Wie L, Jorgensen LM, Mella O, Howell A (2001) High-dose estrogen treatment in postmenopausal breast cancer patients heavily exposed to endocrine therapy. Breast Cancer Res Treat 67: 111-6.
44. Ellis MJ, Gao F, Dehdashti F, Jeffe DB, Marcom PK, Carey LA, Dickler MN, Silverman P, Fleming GF, Kommareddy A, Jamalabadi-Majidi S, Crowder R, Siegel BA (2009) Lower-dose vs high-dose oral estradiol therapy of hormone receptor-positive, aromatase inhibitor-resistant advanced breast cancer: a phase 2 randomized study. JAMA 302: 774-80.
45. Lewis-Wambi JS, Jordan VC (2009) Estrogen regulation of apoptosis: how can one hormone stimulate and inhibit? Breast Cancer Res 11: 206.
46. Maximov PY, Lewis-Wambi JS, Jordan VC (2009) The Paradox of Oestradiol-Induced Breast Cancer Cell Growth and Apoptosis. Curr Signal Transduct Ther 4: 88-102.
47. Stefanick ML, Anderson GL, Margolis KL, Hendrix SL, Rodabough RJ, Paskett ED, Lane DS, Hubbell FA, Assaf AR, Sarto GE, Schenken RS, Yasmeen S, Lessin L, Chlebowski RT (2006) Effects of conjugated equine estrogens on breast cancer and mammography screening in postmenopausal women with hysterectomy. JAMA 295: 1647-57.
48. LaCroix AZ, Chlebowski RT, Manson JE, Aragaki AK, Johnson KC, Martin L, Margolis KL, Stefanick ML, Brzyski R, Curb JD, Howard BV, Lewis CE, Wactawski-Wende J (2011) Health outcomes after stopping conjugated equine estrogens among postmenopausal women with prior hysterectomy: a randomized controlled trial. JAMA 305: 1305-14.

Figure Legends:

Figure 1:

The translational development of tamoxifen for breast cancer. Tamoxifen, was originally a failed oral contraceptive, ICI 46,474, that was abandoned by the pharmaceutical industry in 1972. The successful development of tamoxifen required three key components: 1) target the tumor ER with tamoxifen 2) give long term adjuvant tamoxifen therapy 3) plan for chemoprevention. As a result of targeting the tumor ER with tamoxifen, antihormone therapy became the treatment of choice for long term adjuvant tamoxifen therapy. This has been successfully validated through clinical trials [15] and in turn has saved the lives of millions of women around the world.

Figure 2:

The evolution of drug resistance to SERMs. Acquired resistance occurs during long-term treatment with a SERM and is evidenced by SERM-stimulated breast tumor growth. Tumors also continue to exploit estrogen for growth when the SERM is stopped, so a dual signal transduction process develops. The pure antiestrogen, fulvestrant, destroys the ER and prevents tumor growth in SERM-resistant disease. This phase of drug resistance is referred to as Phase I resistance. Continued exposure to a SERM results in continued SERM-stimulated growth (Phase II), but eventually autonomous growth occurs that is unresponsive to fulvestrant or aromatase inhibitors. The event that distinguishes Phase I from Phase II acquired resistance is a remarkable switching mechanism that now causes apoptosis, rather than growth, with physiologic levels of estrogen. These distinct phases of laboratory drug resistance have their clinical parallels and this new knowledge is being integrated into the treatment plan.

Figure 1

TAMOXIFEN

(A FAILED CONTRACEPTIVE FROM THE 1960s)

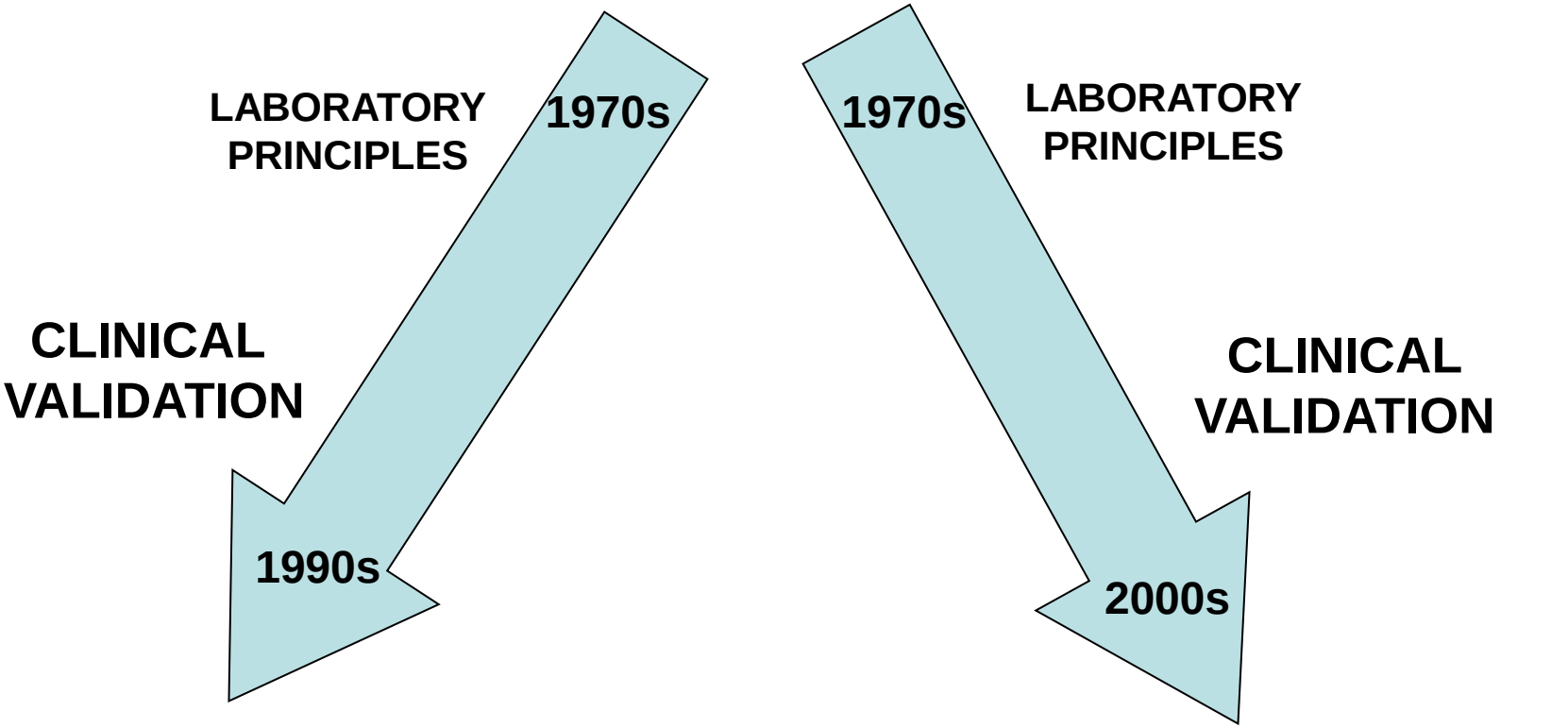


Figure 2

NEW CONCEPT
EVOLUTION OF SERM RESISTANCE

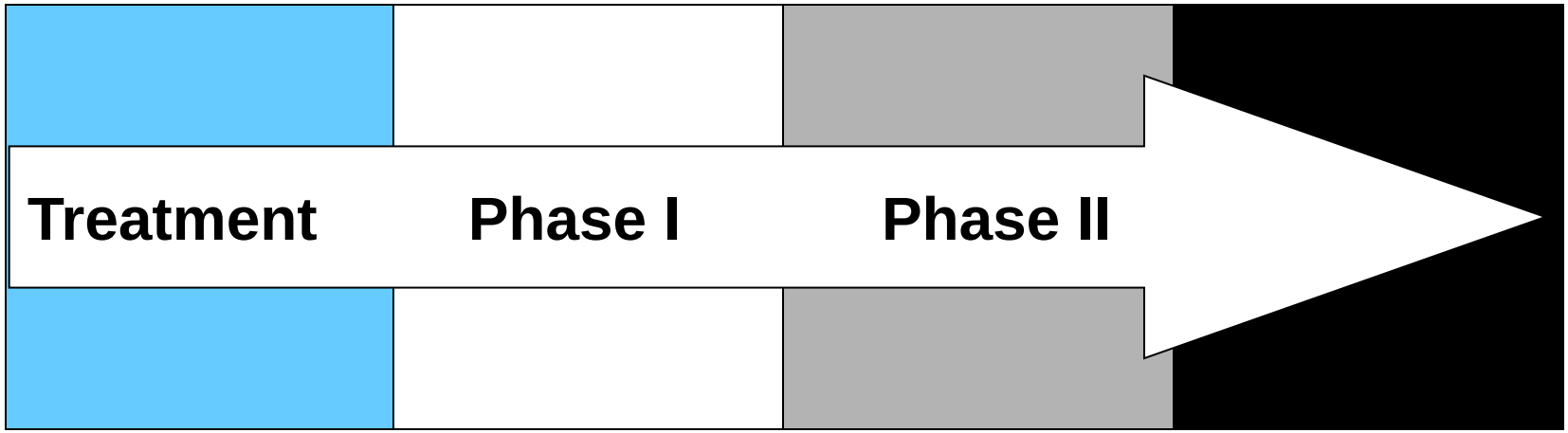


Table 1

Table 1.
Decades of Discovery

- The 1970's: The re-invention of tamoxifen as the "gold standard" for the treatment and prevention of breast cancer
- The 1980's: SERMs surface
- The 1990's: Raloxifene's Promise is a Reality
- The 2000's: Estrogen-induced apoptosis?

*Manuscript
Click here to download Manuscript: Hu_PloS_One revised MS with Legend Suppl Figs.doc

Proteomic analysis of pathways involved in estrogen-induced growth and apoptosis of breast cancer cells

Zhang-Zhi Hu[a,b,1], Benjamin L. Kagan[a,1], Eric A. Ariazi[c], Dean S. Rosenthal[a], Lihua Zhang[a], Jordan V. Li, Hongzhan Huang[b], Cathy Wu[b], V. Craig Jordan,[a] Anna T. Riegel[a], and Anton Wellstein[a,2]

[a]Lombardi Cancer Center and [b]Protein Information Resource Georgetown University, Washington, DC 20057; [c]Fox Chase Cancer Center, Philadelphia, PA 19111

[1]Z.Z.H. and B.L.K. contributed equally to this work.

[2]E-mail: wellstea@georgetown.edu

Running title: Estrogen-induced growth and apoptosis

Funding: This work was supported by Department of Defense Breast Program W81XWH-06-10590 Center of Excellence Grant (V.C.J., P.I.; A.W., P.I. Proteomics), NIH/NCI R01 CA113477 (A.T.R.) and P30 CA051008. Views and opinions of, and endorsements by the author(s) do not reflect those of the US Army or the Department of Defense. The funders had no role in study design, data collection and analysis, decision to publish, or preparation of the manuscript.

Competing Interests: The authors have declared that no competing interests exist.

Abstract

Background: Estrogen is a known growth promoter for estrogen receptor (ER)-positive breast cancer cells. Paradoxically, in breast cancer cells that have been chronically deprived of estrogen stimulation, re-introduction of the hormone can induce apoptosis.

Methodology/Principal Findings: Here, we sought to identify signaling networks that are triggered by 17ß-estradiol (E2) in isogenic MCF-7 breast cancer cells that undergo apoptosis (MCF-7:5C) versus cells that proliferate upon exposure to E2 (MCF-7). The nuclear receptor co-activator AIB1 (Amplified in Breast Cancer-1) is known to be rate-limiting for E2-induced cell survival responses in MCF-7 cells and was found here to also be required for the induction of apoptosis by E2 in the MCF-7:5C cells. Proteins that interact with AIB1 as well as complexes that contain tyrosine phosphorylated proteins were isolated by immunoprecipitation and identified by mass spectrometry (MS) at baseline and after a brief exposure to E2 for two hours. Bioinformatic network analyses of the identified protein interactions were then used to analyze E2 signaling pathways that trigger apoptosis versus survival. Comparison of MS data with a computationally-predicted AIB1 interaction network showed that 26 proteins identified in this study are within this network, and are involved in signal transduction, transcription, cell cycle regulation and protein degradation.

Conclusions: G-protein-coupled receptors, PI3 kinase, Wnt and Notch signaling pathways were most strongly associated with E2-induced proliferation or apoptosis and are integrated here into a global AIB1 signaling network that controls qualitatively distinct responses to estrogen.

Introduction

Estrogen induces proliferation of estrogen receptor (ER)-positive breast cancer cells [1]. This response is consistent with the finding that antihormone therapies, such as tamoxifen or aromatase inhibitors, can enhance survivorship and reduce recurrence in patients with ER-positive breast cancers [2,3]. However, the majority of tumors eventually become unresponsive to antihormone treatments [4,5] and molecular mechanisms and markers of antihormone resistance have been described [6,7]. Once patients have failed on antihormone therapy, one treatment option has been the use of pharmacologic doses of estrogens [8,9] based on well-established findings that some breast cancers shrink during high dose estrogen treatment [10,11,12]. This phenomenon has also been observed in laboratory models of ER-positive breast cancer with acquired anti-hormone resistance that regress and undergo apoptosis in the presence of physiologic concentrations of estrogen [13,14] and was reviewed recently for its potential clinical implications [15].

Estrogen exerts diverse effects including genomic and non-genomic effects through multiple signaling pathways, that are significantly altered in anti-hormone resistant ER positive breast cancer cells. In antihormone resistant cells, for example, there is a general increase in EGFR and IGFR tyrosine kinase signaling [16,17], accompanied by increased ligand-independent phosphorylation of ER [18] and nuclear receptor co-activators such as AIB1/SRC3 (Amplified in Breast Cancer 1/Steroid Receptor Co-activator3) [19]. Overexpression and activation of AIB1 is associated with endocrine resistance in human breast cancer [20,21,22] and has been shown to be rate-limiting for estrogen-induced growth of breast cancer cells [23,24]. Beyond its role in these effects of estrogen, AIB1 was also shown to be rate-limiting for the growth of estrogen-insensitive breast cancer cells [25] as well as prostate cancer [26], pancreatic cancer [27] and lymphoma cells [28]. Furthermore, in AIB1 knockout mice, responses to hormones [29] as well as growth factor signaling [30] are blunted whereas overexpression of an AIB1 transgene leads to increased estrogen and growth factor responses

resulting in hyperplasia and neoplasia of mammary glands [31,32,33]. Thus, a large body of data support a crucial role for AIB1 in estrogen and growth factor signaling [reviewed in Refs 34,35] and provides the rationale for the experimental paradigm used here.

To identify pathways that initiate estrogen-induced apoptosis versus growth, we used a combined proteomics and systems biology approach to elucidate triggering events and associated signaling pathways. We focused on changes of AIB1 interacting proteins, because of its central role in estrogen control of phenotypic behavior of breast cancer cells outlined above. AIB1 also coactivates IGF1R, EGFR and HER2 through modulation of tyrosine phosphorylation of these transmembrane receptors and phosphorylation of their subsequent signaling intermediaries [27,30,33,34]. Thus, to complement the analysis of direct AIB1 interacting proteins, we also monitored changes of phosphotyrosine (pY)-containing protein complexes, that are most likely regulated by growth factor signaling, as a means of discovering global intersecting pathways. As a model system, we used MCF-7 cells that proliferate in response to E2 [1], but also respond to EGF and heregulin [36] and have high levels of AIB1 protein due to gene amplification [37]. Wild-type MCF-7 cells were compared with MCF-7:5C cells that had been isolated under estrogen-free growth conditions [38,39]. MCF-7:5C cells were derived following long-term culture of MCF-7 cells in phenol red-free media. MCF-7:5C cells are ER-positive and undergo apoptosis after exposure to physiological concentrations of E2. In contrast, wild-type parental MCF-7 cells proliferate in the presence of the same concentration range of E2 [38,39]. The MCF-7:5C cells represent many of the characteristics of Phase II SERM resistant cells [40]. A parallel analysis after estrogen stimulation of these isogenic breast cancer cell lines served as a basis for the comparisons of signaling responses.

Here, we show that RNAi-mediated depletion of AIB1 reduces E2-induced growth of MCF-7 cells, and reverses the estrogen-induced apoptosis in MCF-7:5C cells. AIB1-interacting and pY-containing protein complexes were immunoprecipitated from short-term E2-treated cells, and the complexed proteins were identified by mass spectrometry (MS) analysis (Fig. 1A).

From a comparison of the data sets obtained with MCF-7 versus MCF-7:5C cells treated with or without E2, and from a computationally-derived global AIB1-interacting network prediction, we identified pathways that participate in the differential response to E2 in these breast cancer cells. We found that a limited number of major cellular signaling pathways i.e. GPCR, PI3 kinase, Wnt, Notch and their associated molecules were involved in the control of estrogen induced proliferative or apoptotic responses. This information will be useful for determining appropriate targets to induce apoptosis in endocrine resistant human breast cancer.

Results and Discussion

Impact of AIB1 depletion on E2-induced growth effects in MCF-7 and MCF-7:5C cells

To determine the role of AIB1 in the E2-induced, distinct growth phenotypes of MCF-7:5C and wild-type MCF-7 cells, both cell lines were infected with lentiviral vectors that express control or two distinct AIB1-targeted shRNAs, and selected in puromycin for stable integrants. Both MCF-7 and MCF-7:5C cells were depleted of AIB1 protein, compared to uninfected and control shRNA infected cells with either of the shRNAs (Fig. 1B). Treatment with E2 significantly induced growth of control shRNA-infected MCF-7 cells and reduced the growth of MCF-7:5C cells (Fig. 1C, black symbols). In contrast to this, in AIB1-depleted, wild-type MCF-7 cells, E2 did not stimulate growth significantly above baseline and in AIB1 depleted MCF-7:5C, E2 lost its apoptosis-inducing effect (Fig. 1C, red symbols). These data suggest that AIB1 is a significant control hub of the E2-controlled growth phenotype in these ER-positive breast cancer cells.

Global analysis of AIB1- and phosphotyrosine-complexed proteins

Because AIB1 is rate-limiting for the E2-induced changes in the growth phenotype of MCF-7 and MCF-7:5C cells, we performed AIB1-specific immunoprecipitations of lysates from untreated and E2-treated (2 hrs) MCF-7 and MCF-7:5C cells to fractionate the respective proteome. Immunoprecipitation of phosphotyrosine-containing protein complexes was also performed to complement the AIB1-specific proteome fractionation (Fig. 1A). The immunoprecipitates were released from the beads, separated by denaturing gel electrophoreses (SDS-PAGE) and followed by Coomassie Blue staining of proteins in the gels (Fig. S7). Visible bands and the same region in parallel gel lanes were harvested and proteins present identified by mass spectrometry (MS). Stringent filtering of the initial proteomic data resulted in a subset of 101 proteins that either interacted with AIB1 (n=58, Table S1) or are present in pY-protein complexes (n=56, Table S2), with 13 proteins common to both.

The analytical approach emphasizes reliable identification of proteins by correlating mass spectrometry ID with the apparent molecular mass obtained from the SDS-PAGE (Fig. S7). This approach mimics Western blotting without having to rely on the availablility of antibodies, appropriate sensitivity, suitability for Western blotting and specificity. Still, we used Western blotting of some proteins identified by MS and show two examples in Fig. S8 (see below). To validate the mass spectrometry findings, separate experiments with independent mass spectrometry analyses were run. We found 48% of the proteins reported here in two and 16% in three or more independent experiments. This compares favorably with a recent HUPO study where only 7 of 27 laboratories identified all 20 proteins present at equimolar concentrations in a test sample [41]. In our experiments, the abundance of individual endogenous proteins captured in the immunoprecipitates covers a wide range (see Fig. S7). Thus, we expected that lower abundance proteins may drop below detection in repeat experiments. A combination of bioinformatics and mass spectrometry analysis was thus applied to meet this challenge as also described elsewhere [42,43].

The Venn diagrams of proteins pulled down with anti-AIB1 or anti-pY (Fig. 2) show the distribution of proteins between E2-treated and untreated, as well as wild-type MCF-7 versus MCF-7:5C cells (A and B), or between E2-treated and untreated cells regardless of cell type (C, *top*; and D, *top*), or between MCF-7 and MCF-7:5C cells regardless of treatment (C, *bottom*; and D, *bottom*). The number of pY-complexed proteins identified was affected very little by E2 treatment (18 vs. 25 proteins) with 13 proteins in either treatment group (Fig. 2D). In contrast, there was a significant, 4-fold higher number of AIB1-interacting proteins in the E2-treatment group (8 vs. 33 proteins; $p<0.05$, chi-square test; Fig. 2C) with 17 proteins not impacted in their interaction with AIB1. This suggests that AIB1-mediated protein-protein interactions are more responsive to E2 treatment, and new protein complexes are induced by E2 (Fig. 2A,C). In addition, the total number of proteins in complexes with AIB1 that overlap between MCF-7 and MCF-7:5C cells was not altered by the treatment, although the fraction of proteins per cell line that overlap decreases by 1/2 with E2-treatment (31% to 16%; Fig. 2A). Finally, while pathways activated by E2 gave rise to different sets of pY-containing protein complexes in both MCF-7 and MCF-7:5C cells, the percentage of proteins that overlap between cell lines remain almost constant regardless of treatment (4 vs. 5 in Fig. 2B).

Figure 3 shows the functional categories ascribed to the AIB1-associated (top) and pY-complexed (bottom) proteins. Tables S1 and S2 identify the proteins in each of these categories, cell lines (MCF-7 versus MCF-7:5C), and conditions (+/- E2) under which they were identified. Nearly half of the AIB1-interacting proteins fall into four categories, i.e. cytoskeleton and structural proteins, metabolism, transcription regulation, and signal transduction. Most of the pY-complexed proteins fall into four major functional categories: cytoskeleton and structural proteins, transcription regulation, signal transduction, and protein transport and vesicle trafficking. Thirteen proteins were found to be both AIB1-interacting and pY-complexed in MCF-7 and MCF-7:5C cells (Table S1).

Distinct profiles were observed for metabolism-related proteins between AIB1- and pY-complexed proteins, where the AIB1 complexes contained eight different enzymes in contrast to only one in the anti-pY group. This is consistent with studies demonstrating that AIB1 plays a role in the control of basal metabolic processes [44,45] that resulted in growth retardation and reduced hormonal responses in AIB1 knock-out mice [46]. Quite strikingly, all of these proteins were identified in E2 treated cells (e.g. 5-oxoprolinase in MCF-7:5C and fatty acid synthase in MCF-7 cells), whereas only three were identified in untreated as well as E2 treated cells. Seven AIB1-interacting proteins were detected in the categories of transcriptional regulation and chromatin complex, consistent with the role of AIB1 as a transcriptional coactivator. Interestingly, several proteins were found with pY immunoprecipitation that were unique to E2-treated MCF-7:5C cells, one of which was FAK1 (PTK2; Table S2). FAK1 is known to complex with EGFR as well as with an isoform of AIB1 and thus contribute to cellular signaling in breast cancer cells [47]. The MS based identification of FAK1 in the anti-pY immunoprecipitates was also seen by Western blot (Fig. S8A).

AIB1-containing protein complexes in E2-treated MCF-7:5C cells

We identified 18 proteins (CI >95%) that interact with AIB1 in E2-treated but not in untreated MCF-7:5C cells, 10 of which are also unique to MCF-7:5C cells (Table S1; Fig. 2A). These E2-induced AIB1-interacting proteins in MCF-7:5C cells mainly segregate in the category “transcriptional regulation” (6 of 18), several of which are also known to be involved in the control of apoptosis. For example, PRDM5, a PR domain and zinc-finger transcriptional regulator is a putative tumor suppressor and has been linked to cancer cell apoptosis [48]. TLE3, a transcriptional corepressor that binds to a number of transcription factors [49], can form a transcriptional repressor complex with RUNX3 [50], a known tumor suppressor that has been shown to be involved in apoptosis in gastric and colon cancer [51]. TLE3 has also been associated with the development of anti-estrogen resistance [52]. The MS identification of the

83 kDa TLE3 in AIB1 immunoprecipitations (IP) by was also seen by Western blot analysis (Fig. S8B). IASPP was identified in complex with AIB1 in both E2-treated MCF-7 and MCF-7:5C cells, but not in untreated cells. IASPP, a member of ASPP family of proteins, exerts anti-apoptosis effects through modulation of p53 [53,54,55]. Interestingly PRPF6, identified here as AIB1-interacting, is an U5 snRNP-associated protein involved in pre-mRNA splicing and has been shown to be a coactivator of the androgen receptor and mediates its ligand-independent AF-1 activation [56]. TLE3, PRDM5 and PRPF6 were all uniquely identified in E2-treated MCF-7:5C cells.

Potential pathways involved in E2-induced growth and apoptosis

To increase the potential of identifying pathways participating in E2-induced growth and apoptosis from the MS data sets, we not only analyzed proteins identified from MS with high confidence (CI ≥95%), but also took a global approach to include all proteins identified at various CI levels (see http://pir.georgetown.edu/iproxpress/coe2) by MS before filtering for pathway mapping with the Ingenuity™ and GeneGO™ pathway tools [43]. We hypothesized that if proteins identified at lower-level confidence by MS are found in known pathways that are consistent with the cellular phenotypes, they may provide valuable mechanistic insights. Also, supporting this approach are data from a recent study [57] with immunoprecipitation of nuclear extracts from MCF-7 cells that identified 13 of the 15 proteins we had seen at CI values in the lower range of 42-90%. The canonical pathway mapping analyses of all identified proteins suggest that several pathways are significantly represented both for proteins immunoprecipitated with anti-AIB1 and for those with anti-pY, including GPCRs, apoptosis, PI3K/AKT, and Wnt/β-catenin and Notch signaling pathways (Fig. S1-S4):

GPCR and growth factor signaling. Figure S1 depicts the GPCR-induced cell growth pathway, in which a number of proteins were identified in both AIB1 and pY-associated

complexes. Gα(o) (GNAO2, IP-pY) and Rap1GAP (IP-AIB1) (Table S3), for example were identified exclusively in E2-treated MCF-7:5C cells. Gα(o) has been shown to directly bind to Rap1GAP resulting in the inhibition of the Ras-MAPK proliferation pathway [58]. In E2-treated MCF-7 cells, Gα(s) (GAS, GNAS) and CALM1 were coimmunoprecipitated with AIB1, while IP3R (ITPR3) was coimmunoprecipitated with AIB1 in both E2 treated MCF-7 and MCF-7:5C cells (Table S3). Each of these proteins is found downstream of GPCRs, and could lead to MAPK pathway activation and cell proliferation.

GPCRs and growth factors (IGF-1 and EGF) act via phosphorylation of the proapoptotic Bcl-2 family member BAD to regulate mitochondrial-mediated apoptosis (Fig. S2). BAD has been shown to be phosphorylated by Cdc2 (CDK1) at S128 [59] and Cdc2 was identified by anti-pY immunoprecipitation in E2-treated MCF-7:5C cells (Table S2). Also, two phosphatases, PP2B (PPP3CB) and PP2C (WIP1; Table S3, Fig. S2), associated with AIB1 only in MCF-7 cells. Both phosphatases can dephosphorylate BAD and thus modulate apoptosis [60]. In addition, RSK1 and RSK2, identified only in E2-treated cells (Table S3, Fig. S2), are also known to modulate cell survival [61,62].

Growth factors and cytokines can induce cellular growth and proliferation through PI3K-AKT signaling. A number of proteins complexed with AIB1 were identified in this pathway under different conditions (Fig. S3 and Table S3). The non-receptor tyrosine kinase TYK2 was detected in both MCF-7 and MCF-7:5C cells with or without E2 treatment. Both PI3K catalytic (p110) and regulatory (p85) subunits were pulled down only in E2-treated, not in untreated MCF-7 cells (Fig. S3C). PI3K/p110 was detected, additionally, in untreated but not treated MCF-7:5C cells (Fig. S3B). Thus, PI3K/p110 was isolated only under conditions that promoted proliferation in both cell lines. GSK3β, identified in AIB1 immunoprecipitates in E2-treated MCF-7 cells (Fig. S3C), can be activated by PI3K/AKT, and has also been shown to be a regulator of Wnt signaling (see below). Finally, BCL3, a member of the I-kappa-B family that regulates

NFκB-mediated transcription [63,64], was only identified in E2-treated MCF-7 cells.

Wnt/β-catenin and Notch signaling. Our data indicate that Wnt/β-catenin, and Notch signaling pathways participate in E2 responses in both MCF-7 and MCF-7:5C cells (Fig. S4). Several key proteins in the pathway, such as Wnt ligands, cadherin, β-catenin, casein kinases and GSK3β were identified in distinct AIB1- and pY-containing complexes, amongst different cells and treatments (Fig. S4A, B and C). For example, in MCF-7:5C cells, Frizzled-7 (FZD7) and cadherin 22 (CDH22) were identified in pY-containing complexes after E2 treatment, while β-catenin associated with AIB1 regardless of E2 treatment (Table S3). In MCF-7 cells, the Wnt ligand Wnt-7a, CK1δ, and GSK3β were identified in AIB1 immunoprecipitates (Table S3). CK1δ was recently reported to modulate the transcriptional activity of ERα in an estrogen-dependent manner and regulates ER-AIB1 interactions [65]. An additional protein, δ-catenin, or $p120^{ctn}$, a member of armadillo/β-catenin superfamily [66], was identified in the AIB1 immunoprecipitates of E2-treated MCF-7 cells (Table S1).

Our results suggest that multiple proteins found in AIB1 associated complexes, that function in Wnt signaling, also crosstalk with Notch and growth factor-induced signaling in response to E2 treatment in breast cancer cells. TLE3 was detected only in E2-treated MCF-7:5C cells, and Notch1, Notch3, and Numb-like protein were identified only in E2-treated MCF-7 cells (Table S3). TLE3, the mammalian homolog of Gro [67], is a global corepressor mediating transcriptional repression targeted by a number of signal pathways. As shown in Fig. S4D, TLE3 connects the Notch and Wnt pathways [68,69]. In addition to the apoptosis related proteins discussed above (TLE3, PRDM5, CDK1), DBC1 was isolated from anti-pY immunoprecipitates in E2 treated MCF-7:5C cells (Table S2). Interestingly, DBC1 was recently reported to increase p53 mediated apoptosis in breast cancer cells [70]. Taken together, proteins from GPCR and PI3K/AKT-mediated growth signaling pathways were more prevalent in E2-stimulated MCF-7 cells, whereas proteins related to apoptosis pathways were more prevalent in E2-stimulated

MCF-7:5C cells. The respective connectivity of the pathways is depicted in Figure 4.

Global AIB1 interaction networks

To extract further information from these experimental data, they were linked with an AIB1 interaction network generated from published data [43]. A computational global AIB1 protein interaction network can be constructed from 91 AIB1 interaction partners (first neighbors) based on the literature published since AIB1 was first described in 1997 [37]. These 91 proteins belong to several major functional categories that include transcription, cell communication, developmental processes and cell cycle regulation. The initial network was expanded to secondary interaction neighbors, based on protein-protein interaction data in the public domain. At this level, the network is composed of 1150 proteins, including 21 highly connected nodes that form major hubs (Fig. 5). These hubs include p53, BRCA1, BCL2, ABL1, CDK2, CDK4, EGFR, ER (=ESR1), p38, and MYC (Fig. 5 and S5). Closely related subnetworks of AIB1 (=NCOA3) shown in Figure S5 (*lower panel*), contain four hub proteins: BRCA1, MYC, CDK2 and PSME3. In the present study we identified 26 proteins that are part of the global AIB1 interaction network and function in signal transduction, transcriptional regulation, the cytoskeleton, and the heat shock response.

Eighteen of the proteins experimentally associated with tyrosine-phosphorylated protein complexes are also part of the global AIB1-interaction network. Of these, seven were identified as interacting with AIB1, including CALM1, ACTB, ACTG1, TUBGCP2, MYH9, HSPA1B, and HSPA9. These proteins correspond to interacting hubs, such as CDK4, MYC, PSME3 and CHUK. We conclude that these hubs may participate in the differential cellular responses to E2.

Connection of E2 transcriptome and proteome effects

An interesting question is to what extent the proteomic pathway mapping parallels mRNA expression profiling in MCF-7 and MCF-7:5C cells. Baseline mRNA expression profiles of these cell lines have been posted earlier (GSE10879; ncbi.nlm.nih.gov/). An analysis of mRNA expression regulation after 48 hrs of E2 treatment of the cells was analyzed and published recently [71]. In MCF-7 cells Bcl-2, a major anti-apoptosis gene, was found upregulated by E2 treatment whereas no change of bcl-2 was seen in MCF-7:5C cells. In our analysis Bcl-2 is one of the major hubs in the AIB1 interaction networks (Fig. 5 and S5). On the other hand, the pro-apototic Bcl-2 antagonists Bak, Bax and Bim mRNAs were found upregulated 2- to 7-fold after E2 treatment of MCF-7:5C cells whereas no mRNA expression change was seen in the MCF-7 cells. Our analysis shows that upstream regulators of the canonical intrinsic mitochondrial pathway such as RSKs, were identified in the proteomics approach (Fig. 4 and S2).

The most differentially regulated mRNA after E2 treatment was Gadd45beta that was found up-regulated 5-fold in MCF-7:5C cells but down-regulated 5-fold in MCF-7 cells [71]. Gadd45beta was described earlier as a hub of the MAP kinase signaling cascade and connects to relA, the NFkappaB p65 subunit (see e.g. Ref. [72]) as well as cell survival in apoptosis resistant cells [73]. We isolated components of GPCR signaling in our proteomics analysis (Fig. 4 and S1) that can connect to these downstream effectors and can thus serve as trigger mechanisms. Interestingly, GPR30 mRNA was found upregulated in MCF-7:5C cells after estradiol treatment [40] and GPR30 was shown to rapidly transmit non-genomic effects of E2 in breast cancer cells [74]. Overall, the mRNA expression analyses and proteomics data show some interesting convergences especially in apoptotic regulatory pathways which may be

functionally relevant as initiators of estradiol–induced apoptosis or cell survival.

Conclusions

The estrogen induced apoptotic response is most strongly associated with early signaling changes in G-protein coupled receptors, PI3 kinase, Wnt and Notch signaling and are integrated here into a global AIB1 signaling network that controls qualitatively distinct responses to estrogen.

Materials and Methods

The overall experimental design

We used combined proteomics and bioinformatics approaches [43] to identify the E2 induced signaling pathways and networks that are associated with AIB1 and/or tyrosine phosphorylated proteins and that differentiate the MCF-7 from MCF-7:5C cells in responses to E2 treatment (Fig. 1A). A single early time point after E2 treatment (2 hrs) was examined to capture signaling events that drive apoptosis or proliferation in these cells. Repeat independent proteomic experiments for each of the 4 experimental conditions and the two different immunoprecipitations were run.

Cell culture

MCF-7 (ATCC) human breast cancer cells and the MCF-7 variant MCF-7:5C [75] , which is a clonal variant of MCF-7 derived after longterm estrogen deprivation, were cultured in RPMI-1640 without Phenol Red (Invitrogen) supplemented with 10% FBS, or in RPMI-1640 supplemented with 10% charcoal/dextran-stripped FBS (Hyclone) and other supplements, respectively, as described previously [38]. MCF-7 or MCF-7:5C cells deprived of steroid

hormones for 2 days were plated at a density of 2,000 and 3,000 cells per well, respectively, in 96-well cell culture plates. One day after plating, cells were treated with E2 (in ethanol) or vehicle (ethanol). To monitor the portion of viable cells after 6 days of growth, the CellTiter-Glo luminescent cell viability assay (Promega) or WST1 colorimetric cell proliferation assay (Roche) were used. Typical readings of baseline growth without E2 were $2.0x10^5$ RLU (CellTiter-Glo) or an OD450 of 0.5 (WST1). Data are shown relative to the baseline.

Infection of MCF-7 and MCF-7:5C with lentiviral shRNA expression vectors

Prior to infection, MCF-7 and MCF-7:5C cells were plated at a density of $3X10^5$ cells on 10 cm tissue culture dishes. 24 hrs later, cells were infected with lentiviral particles expressing control or AIB1-targeting shRNAs (in pLKO.1). The AIB1(1) shRNA was derived from an siRNA for AIB1 previously described [25], and the AIB1(2) shRNA was from Sigma (TRCN0000019703). The control shRNA used in the experiments is a scrambled sequence described previously [76]. Briefly, 1 ml of lentivirus-containing supernatant was added to 9 ml of growth medium and 8 ng/ml polybrene, and then added to cells for 24 hrs. Medium containing lentivirus was then replaced with growth medium without lentivirus. After two days, cells were treated for 48 hours with 5 μg/ml puromycin for the selection of lentiviral shRNA expression.

Western blot analysis, immunoprecipitation and protein isolation

Western blot analyses were done as previously described [25], using a monoclonal antibody for AIB1 (SRC3; clone 5E11, Cell Signaling). For the mass spectrometry analysis, protein lysates from cells treated for 2 hours with E2 or vehicle were subjected to immunoprecipitation using gamma-bind G-Sepharose beads and an anti-AIB1 monoclonal antibody (BD Biosciences) as described [77] or an anti-phosphotyrosine monoclonal antibody (4G-10, Millipore). The amount of protein input for immunoprecipitations ranged between 7 mg and 14 mg for each of the

experimental conditions with bovine serum albumin used as the standard. It is noteworthy that over a 24 hour period of E2 treatment of cells the AIB1 protein expression levels varied less than 2-fold as illustrated in Figure S6. The immunoprecipitated proteins were separated by denaturing SDS-PAGE on 4-12% Nu-PAGE gels (Invitrogen). After electrophoresis, gels were stained with Coomassie blue overnight and washed with ddH2O overnight to remove background staining. Stained gels were imaged using a color scanner and visible bands were cut from the gels. The corresponding segments of lanes from the different treatments were also cut for analyses and served as controls. Figure S7 shows a representative set of stained gels with an overlay of the grid of segments harvested for the mass spectrometry analyses.

Mass spectrometry analysis

SDS-PAGE gel slices were subjected to tryptic digest and followed by MS and MS/MS on an ABI MALDI-TOF-TOF. Proteins in the MS or MS/MS analysis were identified based on searches of the Swiss-Prot database using the search engine Mascot 2.0. The Swiss-Prot database searched was based on its 9/24/2007 release (287,050 sequences). The database search parameters used were: 1) enzyme specificity considered, trypsin; 2) number of missed cleavages permitted, 1; 3) fixed modification(s), carbamidomethyl (C); 4) variable modification(s), oxidation (M); 5) mass tolerance for precursor ions, 75ppm; and 6) mass tolerance for fragment ions, 0.3 Da. Trypsin autolysis peaks were excluded from the peak list. GPS Explorer (Version 3.0) with default parameter setting was used to generate the peak list from raw data which were submitted to database searches using Mascot. The confidence interval (CI) for the peptide identification was calculated by GPS Explorer. A CI of ≥95% (or expectation value ≤0.05) was used as a cut off for the high CI proteins.

Bioinformatics Analysis

Protein data filtering: Proteins identified from mass spectrometry were subjected to extensive bioinformatics analysis, including protein data filtering, functional profiling and pathway mapping as described previously [78]. Protein identities from different experimental groups were assigned levels of identification confidence based on statistical processing by GPS Explorer™ of the MASCOT search results. It is commonly known that false negative identification is generated because low-scored proteins may result from factors such as database size, protein abundance and the type of mass spectrometry instrumentation. Therefore, in addition to analyzing the proteomic data based on the prioritized list of proteins with high Confidence Interval (CI; Tables S1, S2), we also used a global approach for pathway mapping on proteins identified at all confidence levels. We provide the identity, CI and spectra of those proteins as well as the reference to the respective pathway figures in Table S3.

We used the following criteria to filter the protein lists. (i) Proteins with MS confidence interval (CI) values smaller than 95% were removed to reduce false-positive results; (ii) Proteins described to be non-specific interactors e.g. HSPA5 and Desmoplakin [79] were removed; (iii) High abundant, non-specific proteins e.g. keratins were removed; (iv) Proteins migrating at an apparent mass in the SDS-PAGE that was different from the calculated mass or the experimentally described mass or the predicted mass were removed. A representative set of Coomassie stained gels after immunoprecipitations is shown in Fig. S7 to illustrate this latter consideration.

Protein annotation, profiling and pathway analysis: The iProXpress bioinformatics system (http://pir.georgetown.edu/iproxpress) was used for protein annotation, function and pathway profiling of the proteomics data. The experimental group(s) in which the proteins were identified was annotated for all proteins and integrated into the iProXpress system for direct functional comparison between selected groups, such as cell types, E2 treatment, and experimental repeats. The procedure of using iProXpress system has been described recently

[43,78]. The data sets are accessible at http://pir.georgetown.edu/iproxpress/coe2/. Pathway mapping and network visualization are assisted with Ingenuity Pathways Analysis (IPA) (www.ingenuity.com) and GeneGO MetaCore (www.GeneGO.com) software tools.

Data mining for known AIB1 interactors: The global AIB1 interaction network refers to a network of genes or proteins that directly or indirectly interact or are functionally associated with AIB1 regardless of cell/tissue types or species in which the interaction occurs. The network is was computationally generated based on two sources of data, i.e. the published literature (PubMed) and protein-protein interactions (PPI) available from public databases. A list of AIB1 synonyms included as query terms “AIB1 OR AIB-1 OR NCOA3 OR NCOA-3 OR SRC3 OR SRC-3 OR TRAM1 OR ACTR OR pCIP” to search PubMed and retrieved a total of about 650 papers related to AIB1. Of these papers about 250 papers that contain AIB1 interaction or functional association information were curated, and a total of 91 AIB1 interaction partners were thus obtained. The interaction types in the literature included physical interactions, such as "*binding*", "*complex*", "*interact*", "*phosphorylation*", etc., and functional associations, such as *"activation"*, "*correlated expression*", "*lead to degradation*", "*modulate*", "*promoter binding*", "*suppression*", etc. These interacting proteins/genes reported for human as well as other species from mouse to *Xenopus*, were mapped to corresponding human orthologs based on UniProtKB database.

The protein/protein interaction (PPI) data annotated in bioinformatics databases were obtained from IntAct database [80], which contains high throughput PPI data from Y2H and IP in addition to literature data. The AIB1 interaction network was constructed based on the binary interactions of the curated 91 AIB1-interacting proteins and those from the PPI database. The network was clustered and filtered, and major hubs were selected using a cutoff of a node degree of 20. Cytoscape open source software was used to display the network for visual examinations.

Acknowledgements. We thank Helen Kim and Drs. Annabell Oh, Tyler Lahusen (Georgetown U), and Joan Lewis-Wambi (FCCC) for experimental assistance and Dr. Michael Johnson (Georgetown U) for advice.

References

1. Lippman ME, Bolan G (1975) Oestrogen-responsive human breast cancer in long term tissue culture. Nature 256: 592-593.

2. EBCTCG (2005) Effects of chemotherapy and hormonal therapy for early breast cancer on recurrence and 15-year survival: an overview of the randomised trials. The Lancet 365: 1687-1717.

3. Howell A, Cuzick J, Baum M, Buzdar A, Dowsett M, et al. (2005) Results of the ATAC (Arimidex, Tamoxifen, Alone or in Combination) trial after completion of 5 years' adjuvant treatment for breast cancer. Lancet 365: 60-62.

4. Nicholson RI, Johnston SR (2005) Endocrine therapy--current benefits and limitations. Breast Cancer Res Treat 93 Suppl 1: S3-10.

5. Brauch H, Jordan VC (2009) Targeting of tamoxifen to enhance antitumour action for the treatment and prevention of breast cancer: the 'personalised' approach? Eur J Cancer 45: 2274-2283.

6. Fichtner I, Becker M, Zeisig R, Sommer A (2004) In vivo models for endocrine-dependent breast carcinomas: special considerations of clinical relevance. Eur J Cancer 40: 845-851.

7. Ariazi EA, Lewis-Wambi JS, Gill SD, Pyle JR, Ariazi JL, et al. (2006) Emerging principles for the development of resistance to antihormonal therapy: Implications for the clinical utility of fulvestrant. The Journal of Steroid Biochemistry and Molecular Biology 102: 128-138.

8. Lønning PE, Taylor PD, Anker G, Iddon J, Wie L, et al. (2001) High-dose estrogen treatment in postmenopausal breast cancer patients heavily exposed to endocrine therapy. Breast Cancer Res Treat 67: 111-116.

9. Ellis MJ, Gao F, Dehdashti F, Jeffe DB, Marcom PK, et al. (2009) Lower-dose vs high-dose oral estradiol therapy of hormone receptor-positive, aromatase inhibitor-resistant advanced breast cancer: a phase 2 randomized study. JAMA 302: 774-780.

10. Dodds EC, Goldberg L, Lawson W, Robinson R (1938) Estrogenic activity of certain synthetic compounds. Nature 141: 247-248.

11. Haddow A, Watkinson J, Paterson E (1944) Influence of synthetic oestrogens upon advanced malignant disease. BMJ 2: 393 - 398.

12. Carter AC, Sedransk N, Kelley RM, Ansfield FJ, Ravdin RG, et al. (1977) Diethylstilbestrol: recommended dosages for different categories of breast cancer patients. Report of the Cooperative Breast Cancer Group. JAMA 237: 2079-2078.

13. Jordan VC, Lewis JS, Osipo C, Cheng D (2005) The apoptotic action of estrogen following exhaustive antihormonal therapy: a new clinical treatment strategy. Breast 14: 624-630.

14. Song RX, Mor G, Naftolin F, McPherson RA, Song J, et al. (2001) Effect of long-term estrogen deprivation on apoptotic responses of breast cancer cells to 17beta-estradiol. J Natl Cancer Inst 93: 1714-1723.

15. Jordan VC, Ford LG (2011) Paradoxical Clinical Effect of Estrogen on Breast Cancer Risk: A "New" Biology of Estrogen-Induced Apoptosis. Cancer prevention research (Philadelphia, Pa).

16. Macedo LF, Sabnis G, Brodie A (2009) Aromatase inhibitors and breast cancer. Ann N Y Acad Sci 1155: 162-173.

17. Musgrove EA, Sutherland RL (2009) Biological determinants of endocrine resistance in breast cancer. Nat Rev Cancer 9: 631-643.

18. Arpino G, Wiechmann L, Osborne C, Schiff R (2008) Crosstalk between the estrogen receptor and the HER tyrosine kinase receptor family: molecular mechanism and clinical implications for endocrine therapy resistance. Endocr Rev 29: 217 - 233.

19. Lahusen T, Henke R, Kagan B, Wellstein A, Riegel A (2009) The role and regulation of the nuclear receptor co-activator AIB1 in breast cancer. Breast Cancer Research and Treatment 116: 225-237.

20. Zhao W, Zhang Q, Kang X, Jin S, Lou C (2009) AIB1 is required for the acquisition of epithelial growth factor receptor-mediated tamoxifen resistance in breast cancer cells. Biochem Biophys Res Commun 380: 699-704.

21. Osborne CK, Bardou V, Hopp TA, Chamness GC, Hilsenbeck SG, et al. (2003) Role of the estrogen receptor coactivator AIB1 (SRC-3) and HER-2/neu in tamoxifen resistance in breast cancer. J Natl Cancer Inst 95: 353-361.

22. Schiff R, Massarweh S, Shou J, Osborne CK (2003) Breast cancer endocrine resistance: how growth factor signaling and estrogen receptor coregulators modulate response. Clin Cancer Res 9: 447S-454S.

23. List HJ, Lauritsen KJ, Reiter R, Powers C, Wellstein A, et al. (2001) Ribozyme targeting demonstrates that the nuclear receptor coactivator AIB1 is a rate-limiting factor for estrogen-dependent growth of human MCF-7 breast cancer cells. J Biol Chem 276: 23763-23768.

24. Font de Mora J, Brown M (2000) AIB1 is a conduit for kinase-mediated growth factor signaling to the estrogen receptor. Mol Cell Biol 20: 5041-5047.

25. Oh A, List HJ, Reiter R, Mani A, Zhang Y, et al. (2004) The nuclear receptor coactivator AIB1 mediates insulin-like growth factor I-induced phenotypic changes in human breast cancer cells. Cancer Res 64: 8299-8308.

26. Zhou G, Hashimoto Y, Kwak I, Tsai SY, Tsai MJ (2003) Role of the steroid receptor coactivator SRC-3 in cell growth. Mol Cell Biol 23: 7742-7755.

27. Lahusen T, Fereshteh M, Oh A, Wellstein A, Riegel AT (2007) Epidermal growth factor receptor tyrosine phosphorylation and signaling controlled by a nuclear receptor coactivator, amplified in breast cancer 1. Cancer Res 67: 7256-7265.

28. Coste A, Antal M, Chan S, Kastner P, Mark M, et al. (2006) Absence of the steroid receptor coactivator-3 induces B-cell lymphoma. EMBO J 25: 2453-2464.

29. Xu J, Liao L, Ning G, Yoshida-Komiya H, Deng C, et al. (2000) The steroid receptor coactivator SRC-3 (p/CIP/RAC3/AIB1/ACTR/TRAM-1) is required for normal growth, puberty, female reproductive function, and mammary gland development. Proc Natl Acad Sci U S A 97: 6379-6384.

30. Fereshteh MP, Tilli MT, Kim SE, Xu J, O'Malley BW, et al. (2008) The nuclear receptor coactivator amplified in breast cancer-1 is required for Neu (ErbB2/HER2) activation, signaling, and mammary tumorigenesis in mice. Cancer Res 68: 3697-3706.

31. Torres-Arzayus MI, De Mora JF, Yuan J, Vazquez F, Bronson R, et al. (2004) High tumor incidence and activation of the PI3K/AKT pathway in transgenic mice define AIB1 as an oncogene. Cancer Cell 6: 263-274.

32. Torres-Arzayus MI, Yuan J, DellaGatta JL, Lane H, Kung AL, et al. (2006) Targeting the AIB1 oncogene through mammalian target of rapamycin inhibition in the mammary gland. Cancer Res 66: 11381-11388.

33. Tilli MT, Reiter R, Oh AS, Henke RT, McDonnell K, et al. (2005) Overexpression of an N-terminally truncated isoform of the nuclear receptor coactivator amplified in breast cancer 1 leads to altered proliferation of mammary epithelial cells in transgenic mice. Mol Endocrinol 19: 644-656.

34. Lahusen T, Henke RT, Kagan BL, Wellstein A, Riegel AT (2009) The role and regulation of the nuclear receptor co-activator AIB1 in breast cancer. Breast Cancer Res Treat 116: 225-237.

35. Xu J, Wu R-C, O'Malley BW (2009) Normal and cancer-related functions of the p160 steroid receptor co-activator (SRC) family. Nat Rev Cancer 9: 615-630.

36. Konecny GE, Pegram MD, Venkatesan N, Finn R, Yang G, et al. (2006) Activity of the dual kinase inhibitor lapatinib (GW572016) against HER-2-overexpressing and trastuzumab-treated breast cancer cells. Cancer Res 66: 1630-1639.

37. Anzick SL, Kononen J, Walker RL, Azorsa DO, Tanner MM, et al. (1997) AIB1, a steroid receptor coactivator amplified in breast and ovarian cancer. Science 277: 965-968.

38. Lewis JS, Osipo C, Meeke K, Jordan VC (2005) Estrogen-induced apoptosis in a breast cancer model resistant to long-term estrogen withdrawal. J Steroid Biochem Mol Biol 94: 131-141.

39. Lewis JS, Meeke K, Osipo C, Ross EA, Kidawi N, et al. (2005) Intrinsic mechanism of estradiol-induced apoptosis in breast cancer cells resistant to estrogen deprivation. J Natl Cancer Inst 97: 1746-1759.

40. Jordan VC, Lewis-Wambi J, Kim H, Cunliffe H, Ariazi E, et al. (2007) Exploiting the apoptotic actions of oestrogen to reverse antihormonal drug resistance in oestrogen receptor positive breast cancer patients. Breast 16 Suppl 2: S105-113.

41. Bell AW, Deutsch EW, Au CE, Kearney RE, Beavis R, et al. (2009) A HUPO test sample study reveals common problems in mass spectrometry-based proteomics. Nat Methods 6: 423-430.

42. Aebersold R (2009) A stress test for mass spectrometry-based proteomics. Nat Methods 6: 411-412.

43. Hu Z-Z, Huang H, Wu CH, Jung M, Dritschilo A, et al. (2011) Omics-based molecular target and biomarker identification. Methods Mol Biol 719: 547-571.

44. Louet JF, Coste A, Amazit L, Tannour-Louet M, Wu RC, et al. (2006) Oncogenic steroid receptor coactivator-3 is a key regulator of the white adipogenic program. Proc Natl Acad Sci U S A 103: 17868-17873.

45. Coste A, Louet JF, Lagouge M, Lerin C, Antal MC, et al. (2008) The genetic ablation of SRC-3 protects against obesity and improves insulin sensitivity by reducing the acetylation of PGC-1{alpha}. Proc Natl Acad Sci U S A 105: 17187-17192.

46. Xu J, Liao L, Ning G, Yoshida-Komiya H, Deng C, et al. (2000) The steroid receptor coactivator SRC-3 (p/CIP/RAC3/AIB1/ACTR/TRAM-1) is required for normal growth, puberty, female reproductive function, and mammary gland development. Proc Natl Acad Sci USA 97: 6379-6384.

47. Long W, Yi P, Amazit L, Lamarca HL, Ashcroft F, et al. (2010) SRC-3Delta4 Mediates the Interaction of EGFR with FAK to Promote Cell Migration. Molecular Cell 37: 321-332.

48. Deng Q, Huang S (2004) PRDM5 is silenced in human cancers and has growth suppressive activities. Oncogene 23: 4903-4910.

49. Brinkmeier ML, Potok MA, Cha KB, Gridley T, Stifani S, et al. (2003) TCF and Groucho-related genes influence pituitary growth and development. Mol Endocrinol 17: 2152-2161.

50. Nagahama Y, Ishimaru M, Osaki M, Inoue T, Maeda A, et al. (2008) Apoptotic pathway induced by transduction of RUNX3 in the human gastric carcinoma cell line MKN-1. Cancer Sci 99: 23-30.

51. Tong DD, Jiang Y, Li M, Kong D, Meng XN, et al. (2009) RUNX3 inhibits cell proliferation and induces apoptosis by TGF-beta-dependent and -independent mechanisms in human colon carcinoma cells. Pathobiology 76: 163-169.

52. van Agthoven T, Sieuwerts AM, Meijer-van Gelder ME, Look MP, Smid M, et al. (2009) Relevance of breast cancer antiestrogen resistance genes in human breast cancer progression and tamoxifen resistance. J Clin Oncol 27: 542-549.

53. Ahn J, Byeon IJ, Byeon CH, Gronenborn AM (2009) Insight into the structural basis of pro- and antiapoptotic p53 modulation by ASPP proteins. J Biol Chem 284: 13812-13822.

54. Liu ZJ, Cai Y, Hou L, Gao X, Xin HM, et al. (2008) Effect of RNA interference of iASPP on the apoptosis in MCF-7 breast cancer cells. Cancer Invest 26: 878-882.

55. Sullivan A, Lu X (2007) ASPP: a new family of oncogenes and tumour suppressor genes. Br J Cancer 96: 196-200.

56. Zhao Y, Goto K, Saitoh M, Yanase T, Nomura M, et al. (2002) Activation function-1 domain of androgen receptor contributes to the interaction between subnuclear splicing factor compartment and nuclear receptor compartment. Identification of the p102 U5 small nuclear ribonucleoprotein particle-binding protein as a coactivator for the receptor. J Biol Chem 277: 30031-30039.

57. Lanz RB, Bulynko Y, Malovannaya A, Labhart P, Wang L, et al. (2010) Global characterization of transcriptional impact of the SRC-3 coregulator. Mol Endocrinol 24: 859-872.

58. Jordan JD, Carey KD, Stork PJ, Iyengar R (1999) Modulation of rap activity by direct interaction of Galpha(o) with Rap1 GTPase-activating protein. J Biol Chem 274: 21507-21510.

59. Zhang J, Liu J, Yu C, Lin A (2005) BAD Ser128 is not phosphorylated by c-Jun NH2-terminal kinase for promoting apoptosis. Cancer Res 65: 8372-8378.

60. Klumpp S, Krieglstein J (2002) Serine/threonine protein phosphatases in apoptosis. Curr Opin Pharmacol 2: 458-462.

61. Fernando RI, Wimalasena J (2004) Estradiol abrogates apoptosis in breast cancer cells through inactivation of BAD: Ras-dependent nongenomic pathways requiring signaling through ERK and Akt. Mol Biol Cell 15: 3266-3284.

62. Roux PP, Richards SA, Blenis J (2003) Phosphorylation of p90 ribosomal S6 kinase (RSK) regulates extracellular signal-regulated kinase docking and RSK activity. Mol Cell Biol 23: 4796-4804.

63. Bundy DL, McKeithan TW (1997) Diverse effects of BCL3 phosphorylation on its modulation of NF-kappaB p52 homodimer binding to DNA. J Biol Chem 272: 33132-33139.

64. Mathas S, Johrens K, Joos S, Lietz A, Hummel F, et al. (2005) Elevated NF-kappaB p50 complex formation and Bcl-3 expression in classical Hodgkin, anaplastic large-cell, and other peripheral T-cell lymphomas. Blood 106: 4287-4293.

65. Castellano L, Giamas G, Jacob J, Coombes RC, Lucchesi W, et al. (2009) The estrogen receptor-alpha-induced microRNA signature regulates itself and its transcriptional response. Proc Natl Acad Sci USA 106: 15732-15737.

66. Zimmer A, Reynolds K (1994) Gene targeting constructs: effects of vector topology on co-expression efficiency of positive and negative selectable marker genes. Biochem Biophys Res Commun 201: 943-949.

67. Hoffman BG, Zavaglia B, Beach M, Helgason CD (2008) Expression of Groucho/TLE proteins during pancreas development. BMC Dev Biol 8: 81.

68. Liu Y, Dehni G, Purcell KJ, Sokolow J, Carcangiu ML, et al. (1996) Epithelial expression and chromosomal location of human TLE genes: implications for notch signaling and neoplasia. Genomics 31: 58-64.

69. Cuevas IC, Slocum AL, Jun P, Costello JF, Bollen AW, et al. (2005) Meningioma transcript profiles reveal deregulated Notch signaling pathway. Cancer Res 65: 5070-5075.

70. Hiraike H, Wada-Hiraike O, Nakagawa S, Koyama S, Miyamoto Y, et al. (2010) Identification of DBC1 as a transcriptional repressor for BRCA1. Br J Cancer 102: 1061-1067.

71. Lewis-Wambi JS, Jordan VC (2009) Estrogen regulation of apoptosis: how can one hormone stimulate and inhibit? Breast Cancer Res 11: 206.

72. Papa S, Zazzeroni F, Bubici C, Jayawardena S, Alvarez K, et al. (2004) Gadd45β mediates the NF-κB suppression of JNK signalling by targeting MKK7/JNKK2. Nat Cell Biol 6: 146-153.

73. Engelmann A, Speidel D, Bornkamm GW, Deppert W, Stocking C (2008) Gadd45 beta is a pro-survival factor associated with stress-resistant tumors. Oncogene 27: 1429-1438.

74. Ariazi EA, Brailoiu E, Yerrum S, Shupp HA, Slifker MJ, et al. (2010) The G protein-coupled receptor GPR30 inhibits proliferation of estrogen receptor-positive breast cancer cells. Cancer Res 70: 1184-1194.

75. Jiang SY, Wolf DM, Yingling JM, Chang C, Jordan VC (1992) An estrogen receptor positive MCF-7 clone that is resistant to antiestrogens and estradiol. Mol Cell Endocrinol 90: 77-86.

76. Sarbassov DD, Guertin DA, Ali SM, Sabatini DM (2005) Phosphorylation and regulation of Akt/PKB by the rictor-mTOR complex. Science 307: 1098-1101.

77. Oh AS, Lahusen JT, Chien CD, Fereshteh MP, Zhang X, et al. (2008) Tyrosine phosphorylation of the nuclear receptor coactivator AIB1/SRC-3 is enhanced by Abl kinase and is required for its activity in cancer cells. Mol Cell Biol 28: 6580-6593.

78. Hu Z-Z, Huang H, Cheema A, Jung M, Dritschilo A, et al. (2008) Integrated Bioinformatics for Radiation-Induced Pathway Analysis from Proteomics and Microarray Data. Journal of proteomics & bioinformatics 1: 47-60.

79. Han SJ, Jung SY, Malovannaya A, Kim T, Lanz RB, et al. (2006) A scoring system for the follow up study of nuclear receptor coactivator complexes. Nucl Recept Signal 4: e014.

80. Kerrien S, Alam-Faruque Y, Aranda B, Bancarz I, Bridge A, et al. (2007) IntAct--open source resource for molecular interaction data. Nucleic Acids Res 35: D561-565.

Figure Legends

Figure 1. Phenotypic impact of AIB1 depletion on estradiol (E2) growth response in MCF-7 or MCF-7:5C cells (*A*) The experimental paradigm. The differential responses to estradiol (E2) treatment of MCF-7 (cell growth) and long-term estrogen deprived MCF-7:5C cells (apoptosis) are indicated. Proteomics profiles of the two cell lines at baseline and after a brief (2 h) E2 treatment were generated using immunoprecipitations (IP). Proteins interacting with AIB1 or phosphotyrosine containing protein complexes were isolated by IP followed by mass spectrometry. Data were then subjected to an integrated bioinformatics analysis of signaling pathways and protein networks. (*B,C*) Reversal of E2-dependent effects on MCF-7 and MCF-7:5C after depletion of endogenous AIB1 protein using two different lentiviral shRNAs. MCF-7 or MCF-7:5C cells were infected with lentiviral particles expressing control or AIB1-targeting shRNAs. *(B)* RNAi-mediated knockdown was assayed by Western blot analysis for AIB1 relative to an actin loading control. *(C)* Cell growth was assayed 6 days after plating without or with E2. The E2 effect is shown relative to the respective untreated controls (mean $\pm$S.E.M.). Closed circles: control shRNA; Open circles (red): AIB1 shRNA. #, $p<0.05$ E2 treatment effect vs. no treatment in control shRNA cells; *, $p<0.05$ E2 treatment effect in control shRNA cells vs. E2 treatment in AIB1 depleted cells. Representative data from one of at least three independent experiments are shown.

Figure 2. Summary of proteins identified under different conditions. Venn diagrams of proteins identified from anti-AIB1 (*A,C*) or anti-pY IP (*B,D*) experimental groups. (*C,D*) Proteins in combined AIB1-IP or pY-IP data sets. Individual proteins and subgroups are shown in Tables S1 & S2.

Figure 3. Functional categories of anti-AIB1 (upper) and anti-pY immunoprecipitated proteins (lower) from MCF-7 and MCF-7:5C breast cancer cells. Numbers in parenthesis are the number of proteins belonging to the respective category. Proteins profiled are those with CI values ≥95% from mass spectrometry.

Figure 4. Pathway overview map of proteins involved in E2-induced cell growth or apoptosis in MCF-7 versus MCF-7:5C breast cancer cells. The thick grey line in the middle provides an arbitrary boundary between the pathways. Anti-AIB1 immunoprecipitated (AIB1-IPed) and anti-pY-immunoprecipitated proteins (pY-IPed) are indicated by red or green circles respectively (keys at the bottom). The blue circled proteins are AIB1-IPed proteins from MCF-7 (CALM1) or MCF-7:5C cells (β-catenin) under both E2- treated and untreated conditions; the purple circled one (ITPR3) is an AIB1-IPed protein from both cells only under E2 treated condition, while the yellow circled one (TYK2) is an AIB1-IPed protein from both cells under both E2 treated and untreated conditions. Proteins circled in grey are from known canonical pathways (e.g. ERK in cell growth or BAD in apoptosis) but not identified here. Solid line arrows indicate direct interactions (e.g. CDK1 phosphorylates Rap1GAP) or translocations (e.g. catenins) of proteins, while dashed arrows indicate indirect actions of proteins (e.g. AKT activate MEK through several steps). Hammer-ended lines indicate inhibitory effects on the target. Detailled pathways are shown in Fig. S1 - S4.

Figure 5. A global AIB1 interaction network showing the major hub proteins. Twenty-one hubs were identified using a cutoff of 20 node degrees. The full names of the respective gene symbols are provided in Table S8. Detailed nodes in the network are shown in Fig. S5.

Supplemental Figure Legends

Figure S1. **Proteins identified in GPCR signaling pathways**. Canonical cell growth pathways initiated by GCPR signaling are depicted based on the MetaCore pathway tool of GeneGO. The AIB1- and pY-IPed proteins identified from the study were mapped to the pathway using MetaCore, which were manually re-annotated in the red-lined white boxes with black arrows pointing to the specific protein depictions. The corresponding experimental conditions under which the proteins were identified are indicated at the bottom. Proteins were AIB1-IPed under conditions indicated as A-D, or pY-IPed indicated by “p”.

Figure S2. Proteins identified in apoptosis pathways. The canonical intrinsic mitochondrial apoptosis pathway is depicted based the MetaCore pathway tool of GeneGO. Similar to Fig. S3, the anti-AIB1- and pY-IPed proteins identified from the study were mapped to the pathway and were manually re-annotated with red-lined white boxes with the specific protein identified here.

Figure S3. Proteins identified in the PI3K/AKT pathway. The canonical PI3K/AKT pathway is depicted based on the Ingenuity pathway tool. AIB1-IPed proteins that were mapped to the canonical pathway are shown as orange-colored shapes in four panels, each representing the same PI3K/AKT pathway with different mapped proteins that were identified from untreated MCF-7 (A) or MCF-7:5C (B) and E2-treated MCF-7 (C) or MCF-7:5C (D) cells. Some proteins in the pathway were manually re-annotated with green-colored box to indicate the specific protein forms identified in this study that correspond to the protein classes represented in the canonical pathway, e.g. JAK refers to the non-receptor type tyrosine kinases, such as TYK2 here.

Figure S4. Proteins identified in the Wnt/β-catenin pathway. The canonical Wnt/β-catenin pathway is depicted based on the Ingenuity pathway tool. AIB1-IPed proteins that can be mapped to the canonical pathway are shown as orange-colored shapes in four panels, each representing the same Wnt/β-catenin pathway with different mapped proteins that were identified from untreated MCF-7 (A) or MCF-7:5C (B) and E2-treated MCF-7 (C) or MCF-7:5C (D) cells. Some proteins in the pathway were manually re-annotated with green-colored box to indicate the specific protein forms identified in the experiment that correspond to the classes represented in the canonical pathway, e.g. Wnt refers to class of Wnt ligands, such as Wnt-4 and Wnt-7a. Some proteins manually labeled with a "P" in red indicate that they were identified as pY-IPed.

Figure S5. AIB1 interaction network. A global AIB1 interaction network (upper) and the selected sub-networks (lower) are shown. The overall topology of the network is displayed with Spring-embedded layout using Cytoscape network visualization software before network clustering (image can be zoomed in to view individual node). Proteins that are identified with high confidence in this study are colored as green (AIB1-IPed), yellow (pY-IPed) or dark brown (both AIB1- and pY-IPed) nodes. Hub proteins that are subsequently clustered with AIB1 in several subnetworks are indicated with arrows (*upper*). Individual nodes in AIB1-clustered subnetworks are shown in the lower panel, with major functional categories labeled for the hub proteins.

Figure S6. Western blot analysis for AIB1. Cells treated with E2 for different times were harvested and Western blot analysis for AIB1 was performed as described in Materials and Methods.

Figure S7. Coomassie stained protein gels after anti-AIB1 or -pY immunoprecipitation (IP). MCF-7 and MCF-7:5C cells were treated or not with E2 for 2 hours, and proteins were extracted for IP. The immunoprecipitated proteins were separated by 4-12% Nu-PAGE, stained, washed with ddH20 and imaged using a color scanner. The images were magnified and analyzed visually on a screen. After identification, bands were cut from the gels and great care was taken to isolate the same segment of all lanes from the different treatments for a parallel MS analysis. Representative stained gels with the segments to be cut for analysis are indicated. Slices numbered 1-10 or 1-13 were cut from the gels for each segment that showed at least one distinctly regulated protein. Molecular masses of marker proteins are indicated (10 – 250 kDa).

Figure. S8. Western blot analysis confirms that FAK1 and TLE3 are immunoprecipitated from E2 treated MCF7:5C cells. MCF-7:5C cells were treated or not with E2 for 2 hours, and proteins were extracted for IP/Western analysis A) Tyrosine-phosphorylated endogenous proteins were immunoprecipitated with anti-phosphotyrosine monoclonal antibody (4G-10, Millipore) and the immunoprecipitate was resolved on SDS-PAGE followed by Western analysis. The input is 5% of the amount of total cell lysates for IP. FAK1 was detected on the blot with an anti-FAK1 antibody (A-17, Santa Cruz). B) AIB1 interacting proteins were immunoprecipitated using an anti-AIB1 monoclonal antibody (BD Biosciences). The input is 5% of the amount of total cell lysates for IP. TLE3 was detected on the blot with a TLE3 antibody (Abcam).

Figure 1

Click here to download Figure: Hu_Fig 1A_C.eps

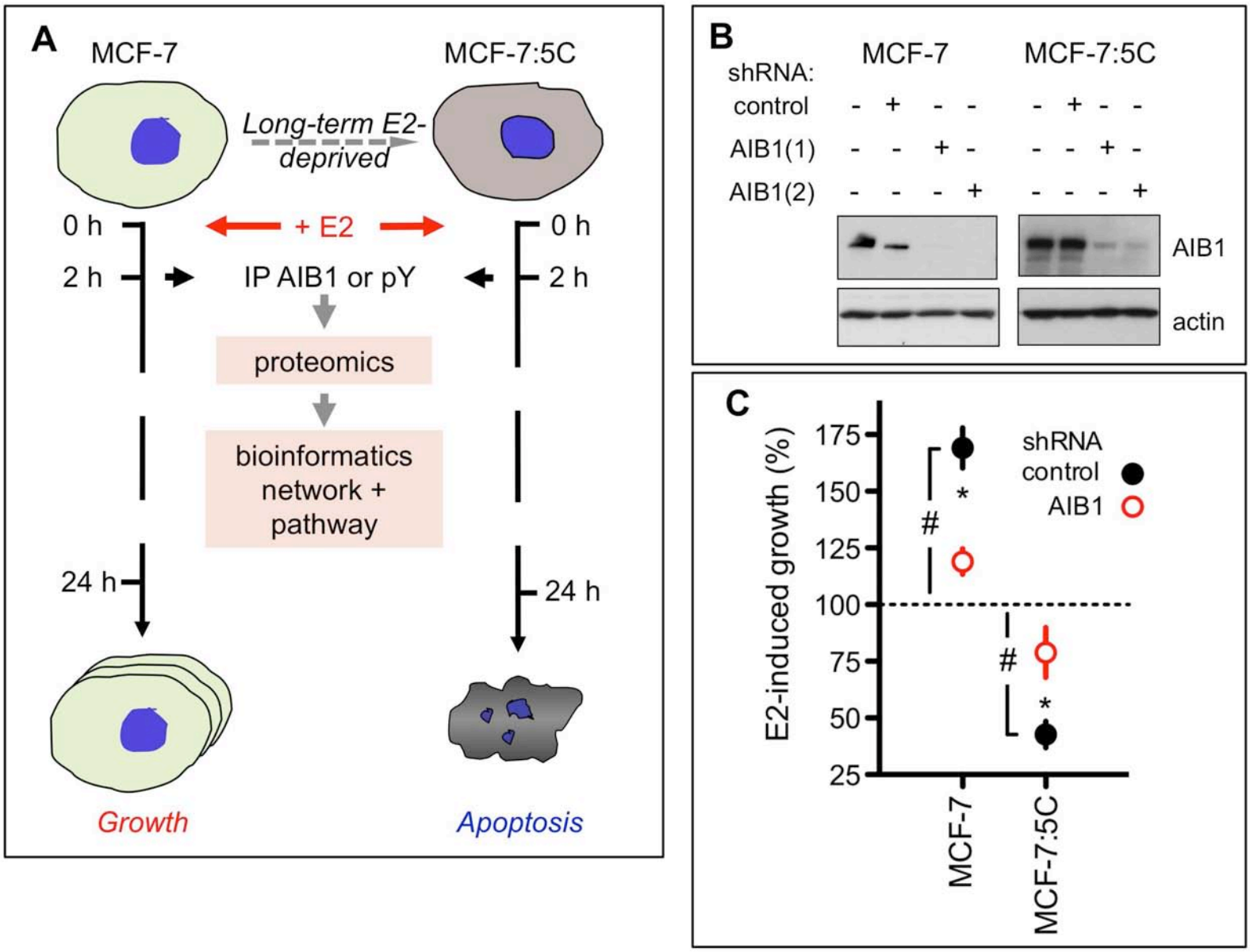


Figure 2

Click here to download Figure: Hu_Fig 2.eps

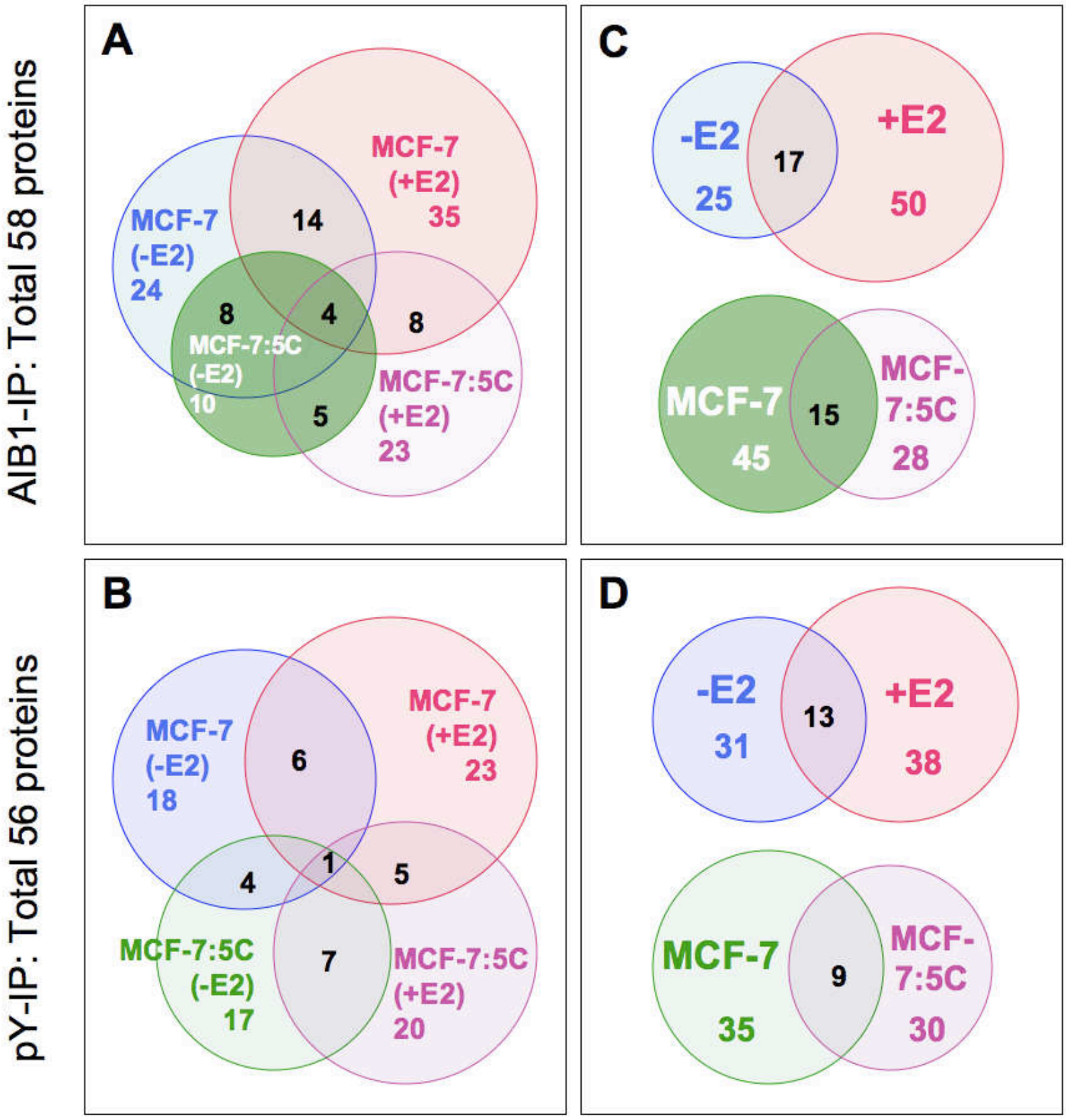


Figure 3

Click here to download Figure: Hu_Fig 3.eps

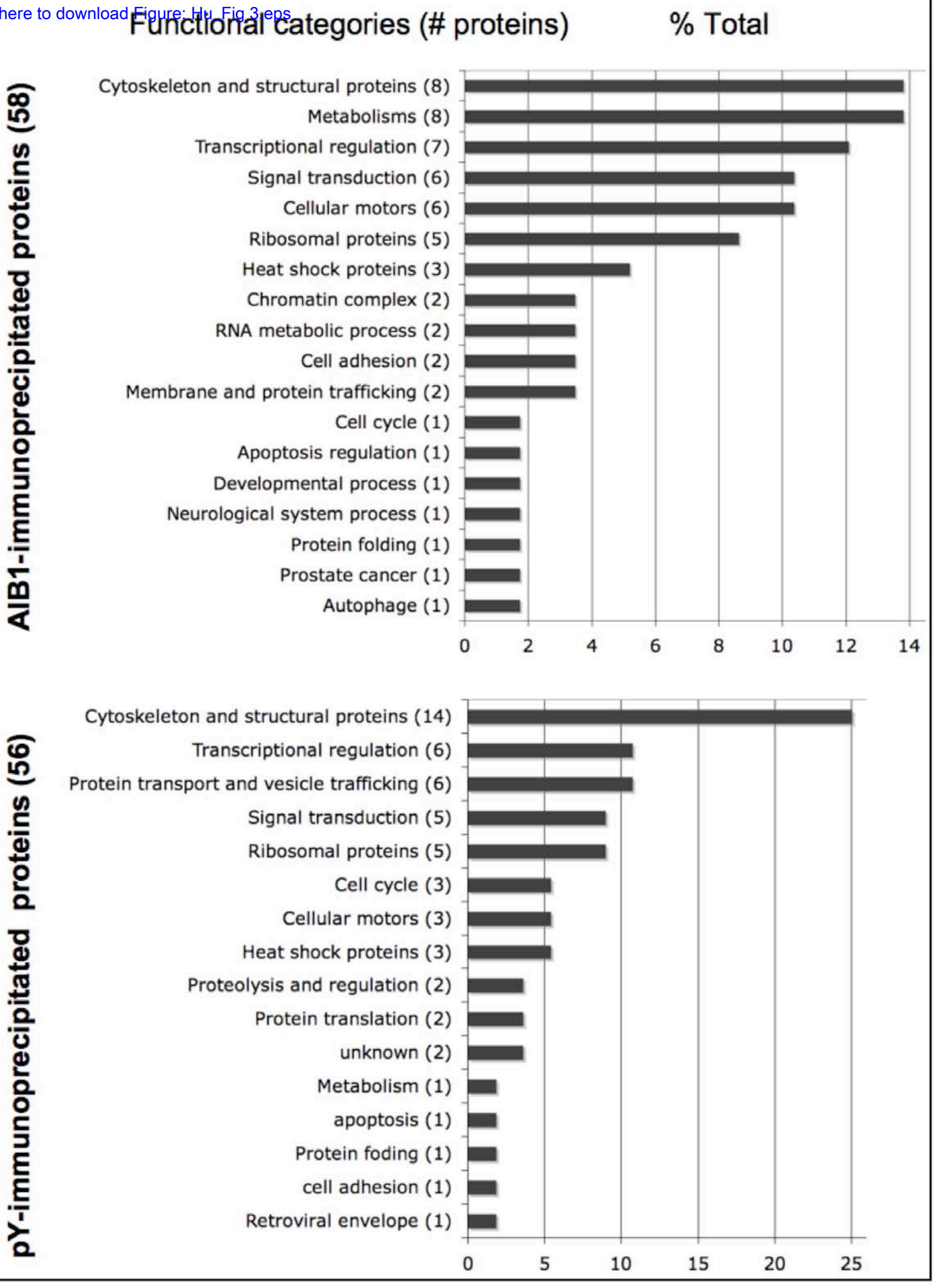


Figure 4

Click here to download Figure: Hu_Fig 4.eps

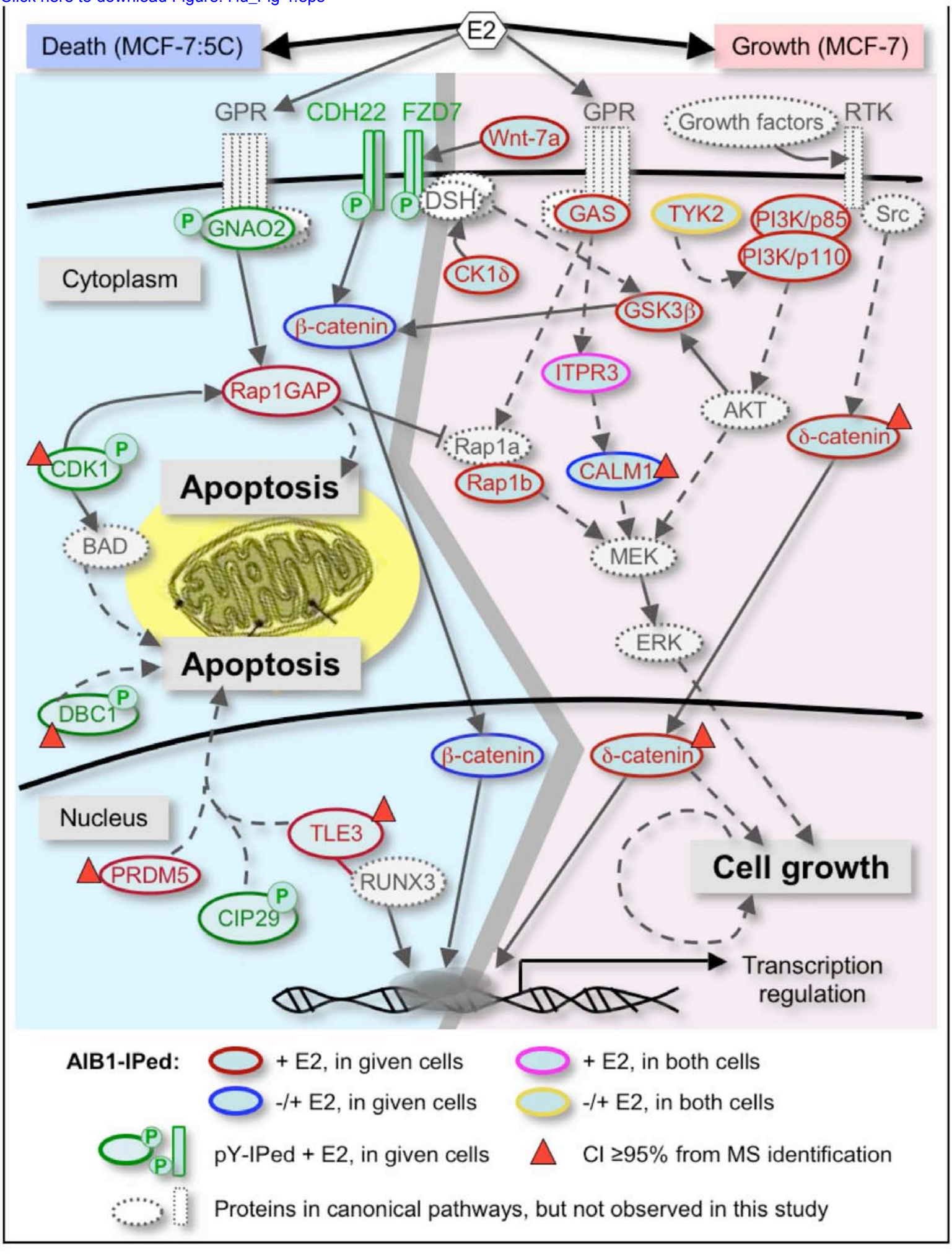
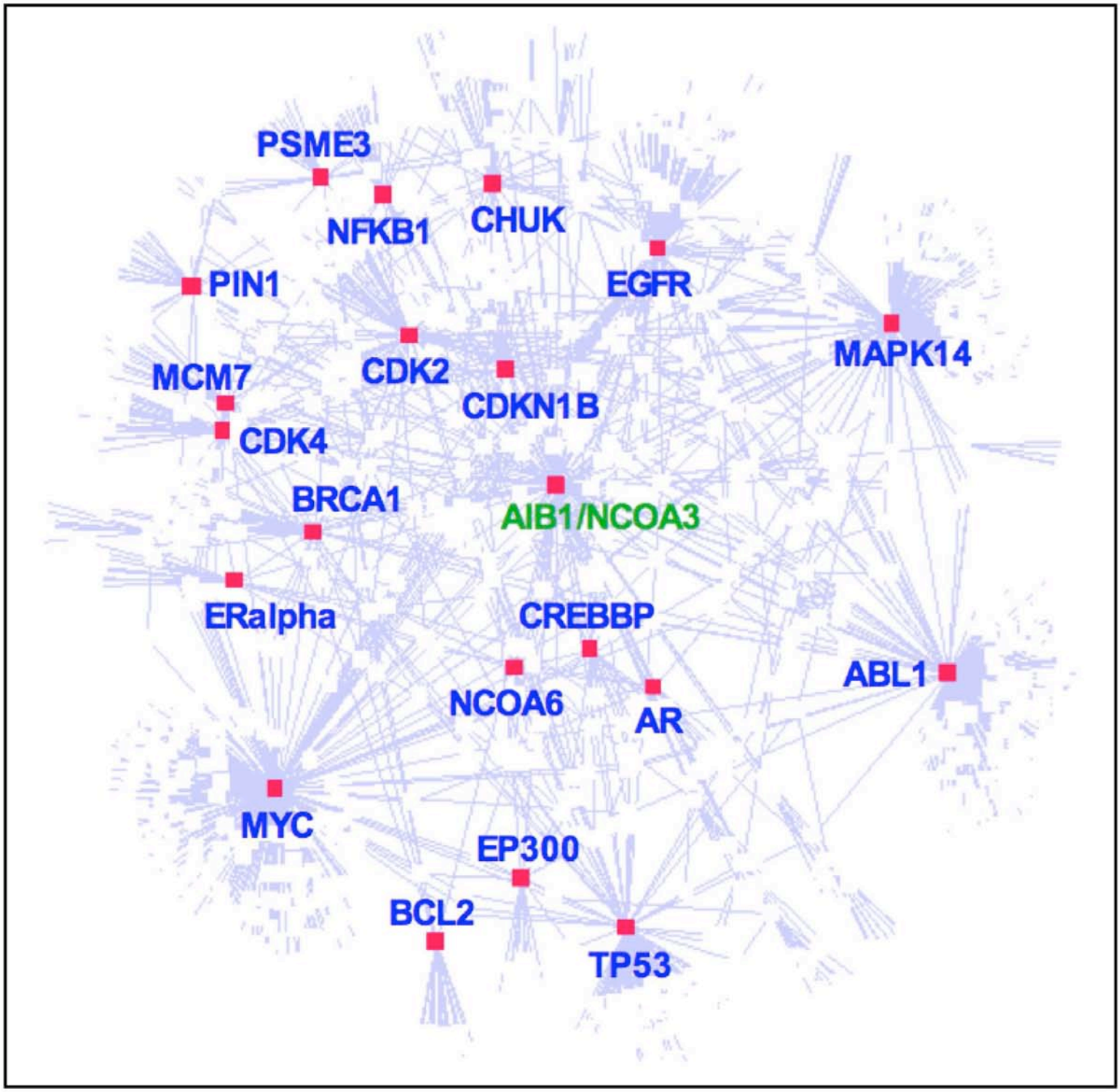


Figure 5

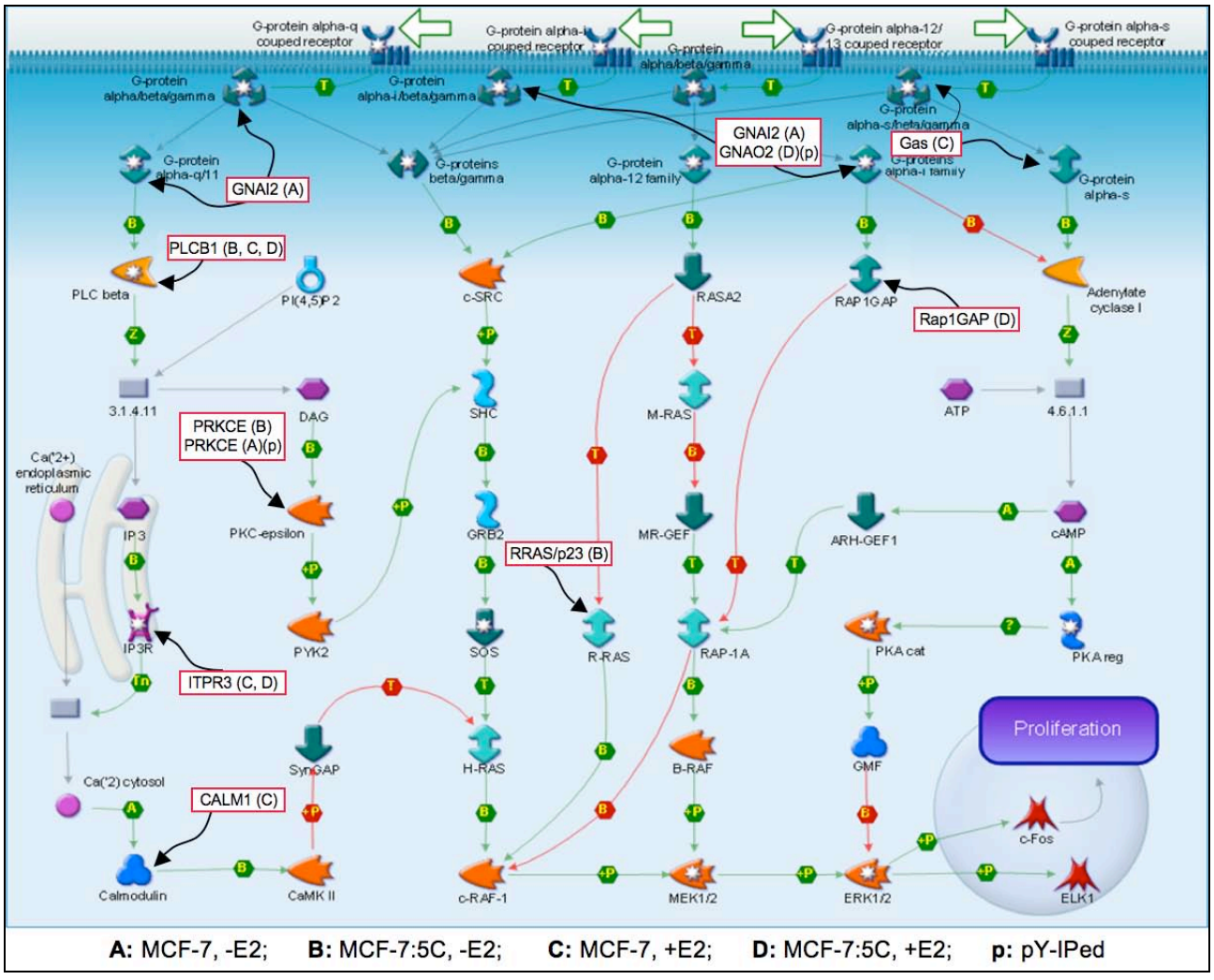
Click here to download Figure: Hu_Fig 5.eps



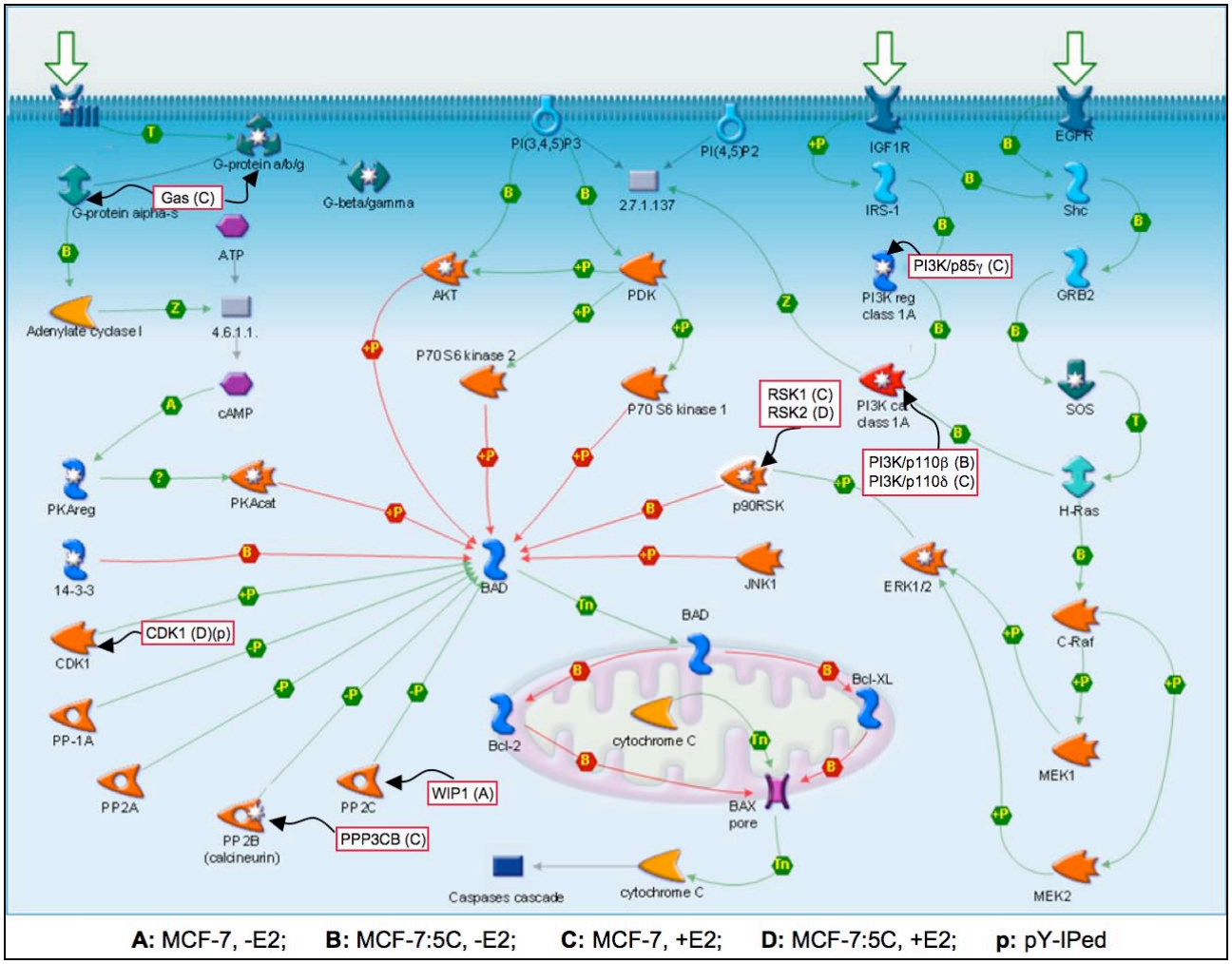
PROTEOMIC ANALYSIS OF PATHWAYS INVOLVED IN ESTRADIOL-INDUCED GROWTH AND APOPTOSIS IN BREAST CANCER CELLS

Hu, Kagan et al.

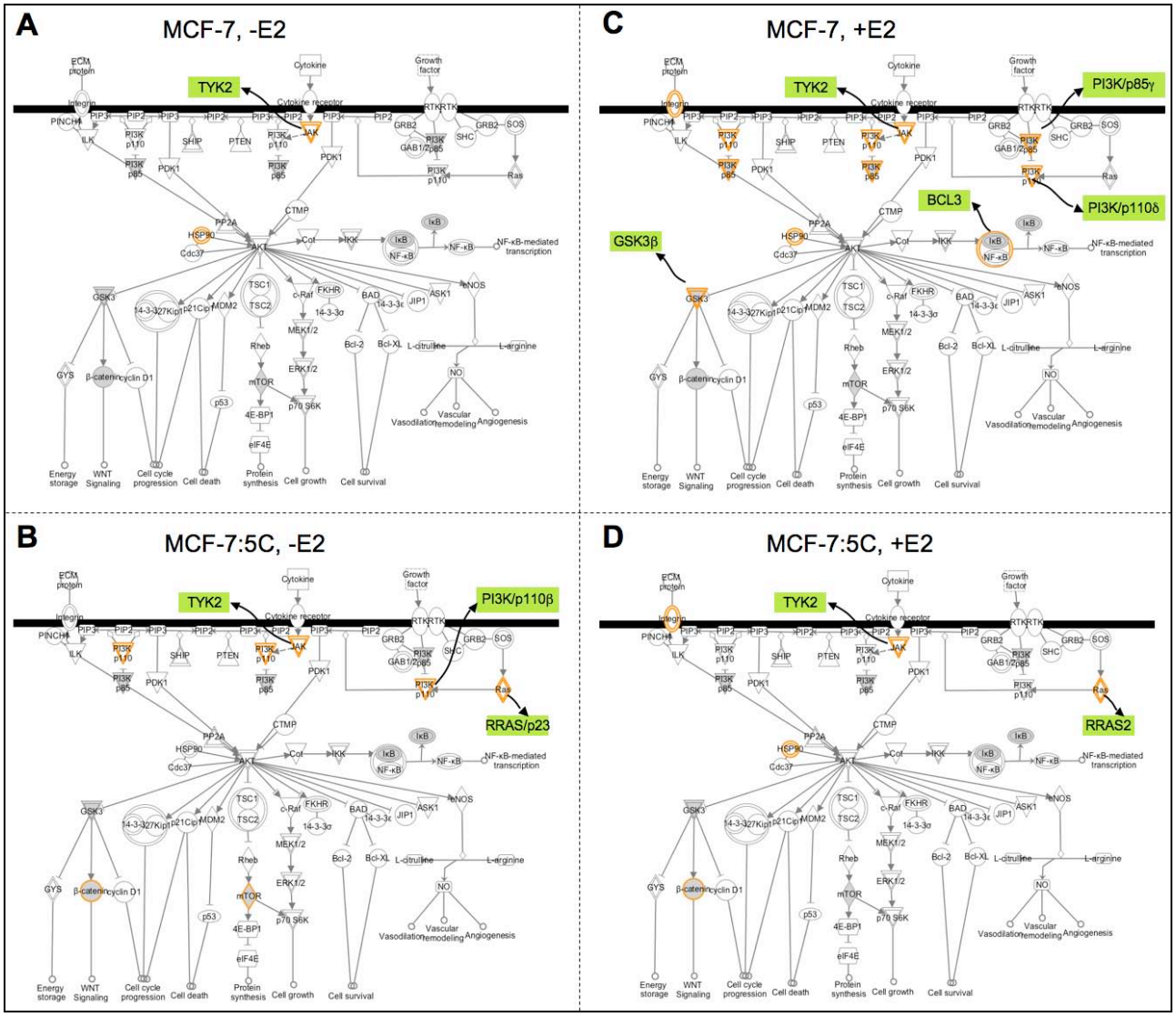
Supplemental Figures S1 – S8



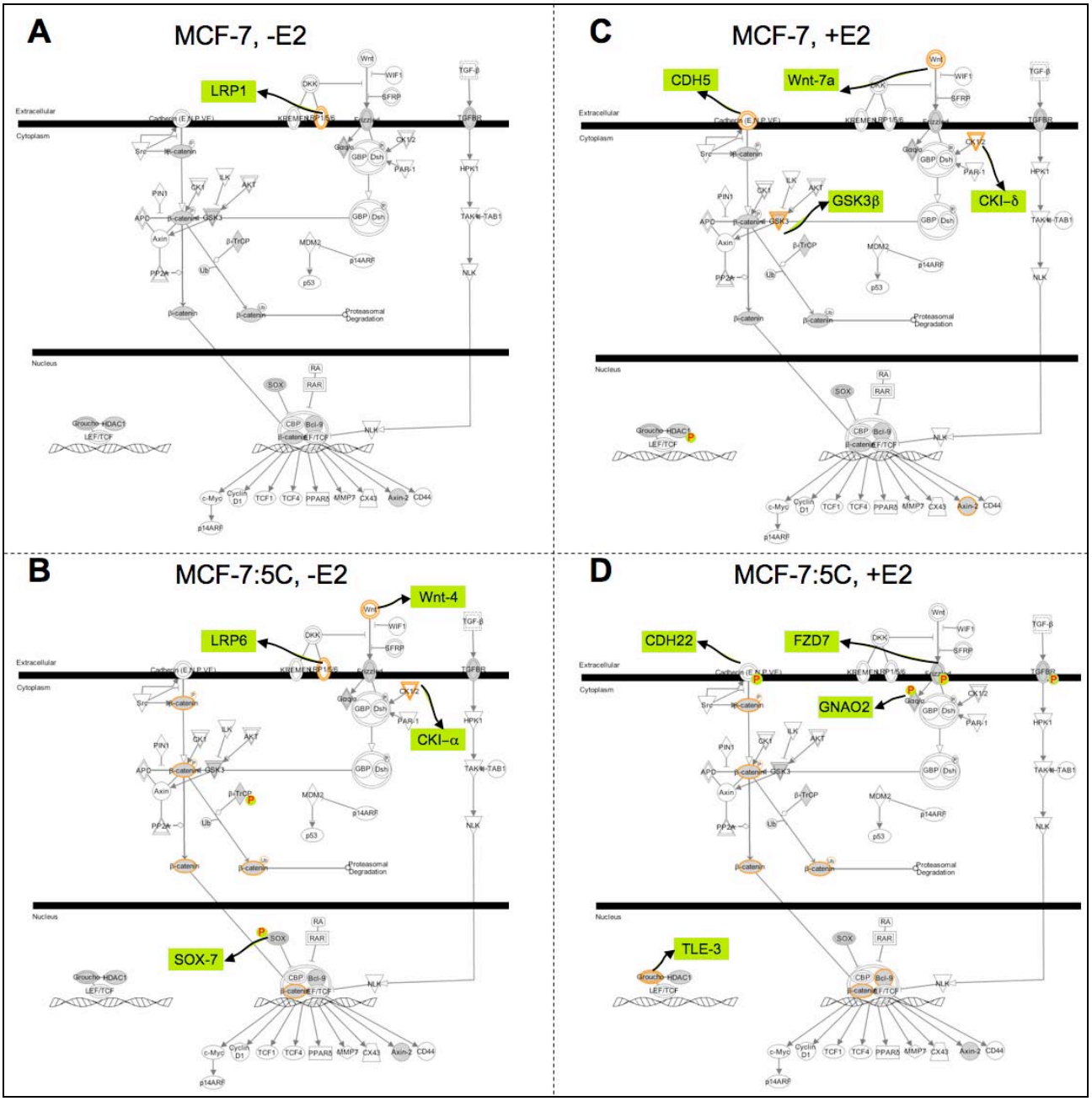
Hu et al., Fig. S1



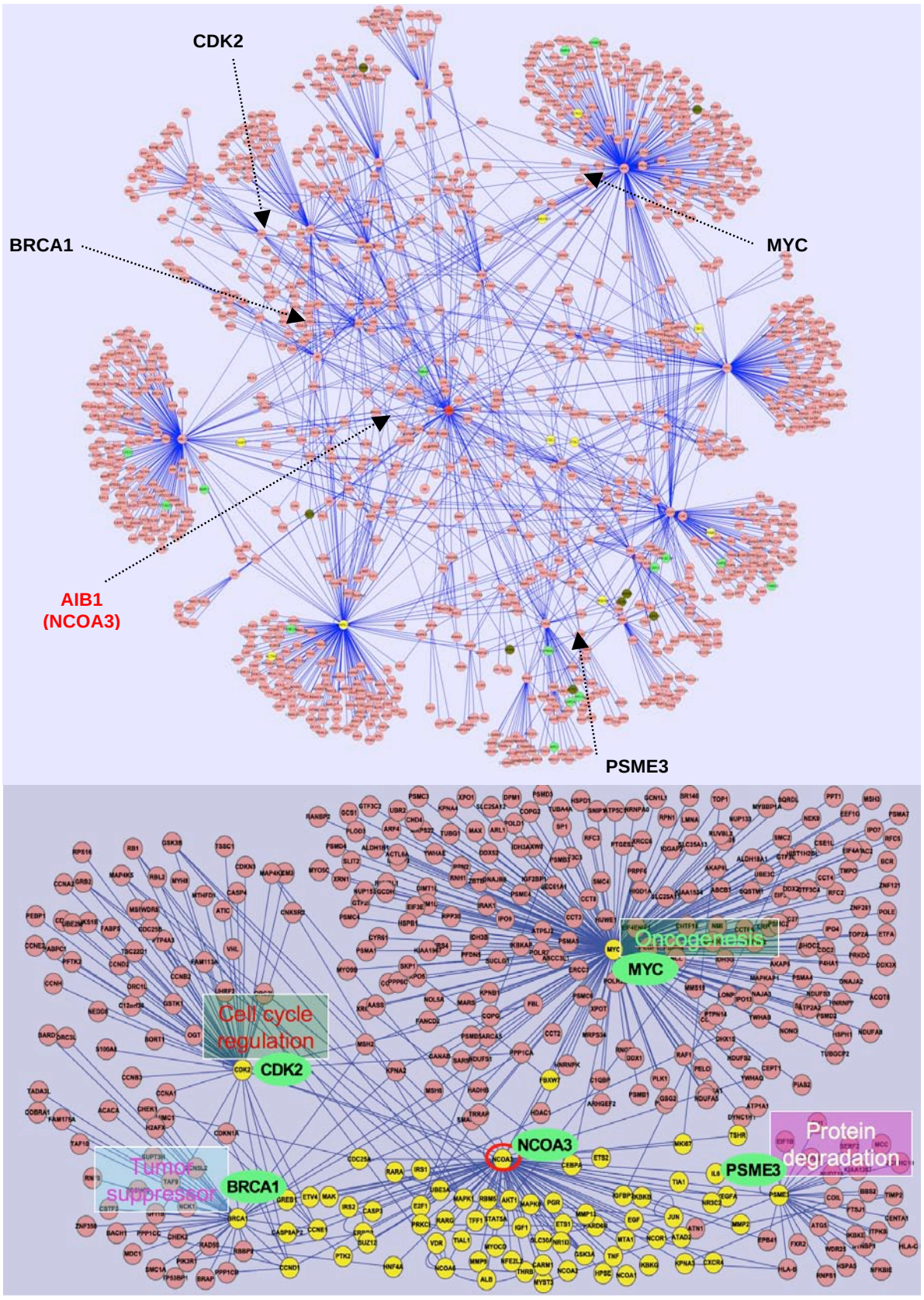
Hu et al., Fig. S2



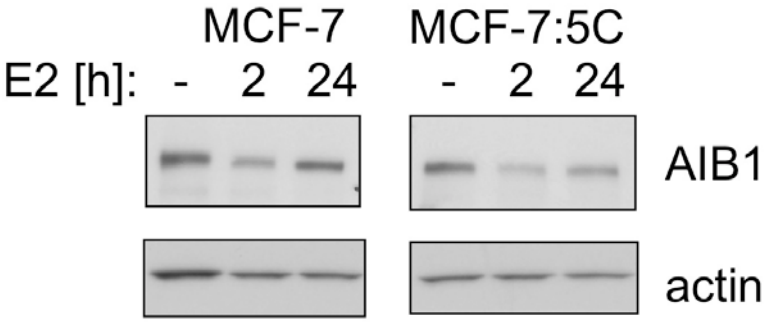
Hu et al., Fig. S3



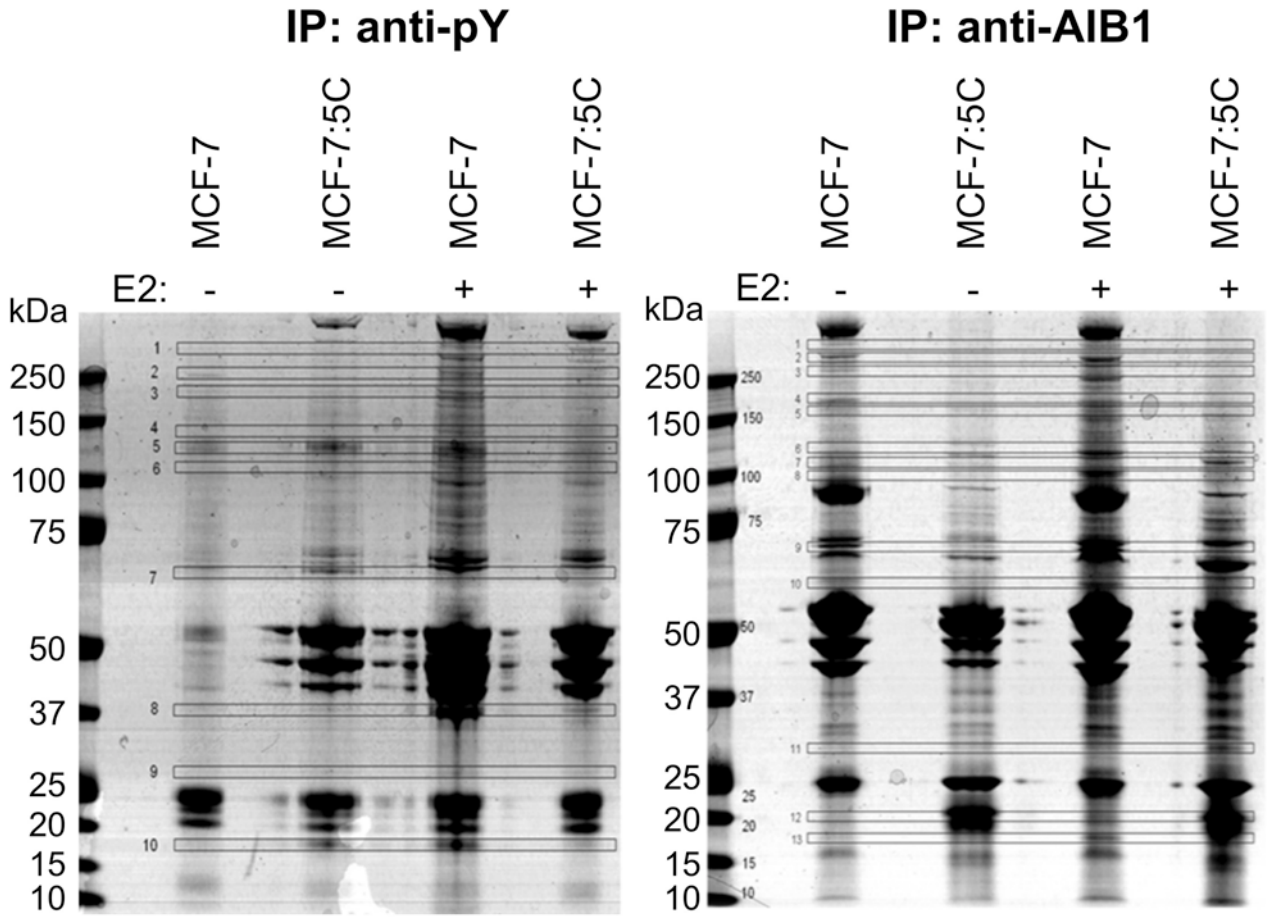
Hu et al., Fig. S4



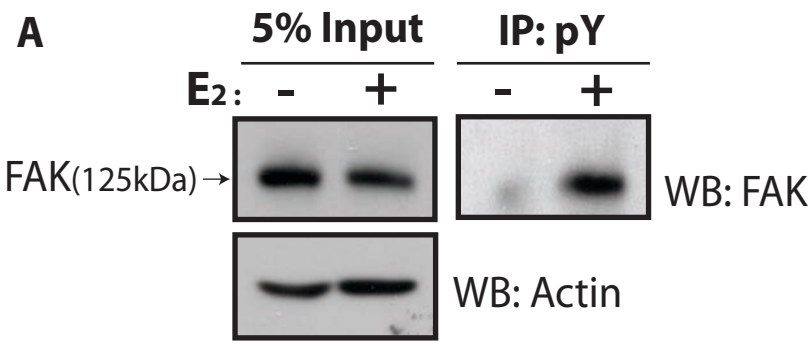
Hu et al., Fig. S5

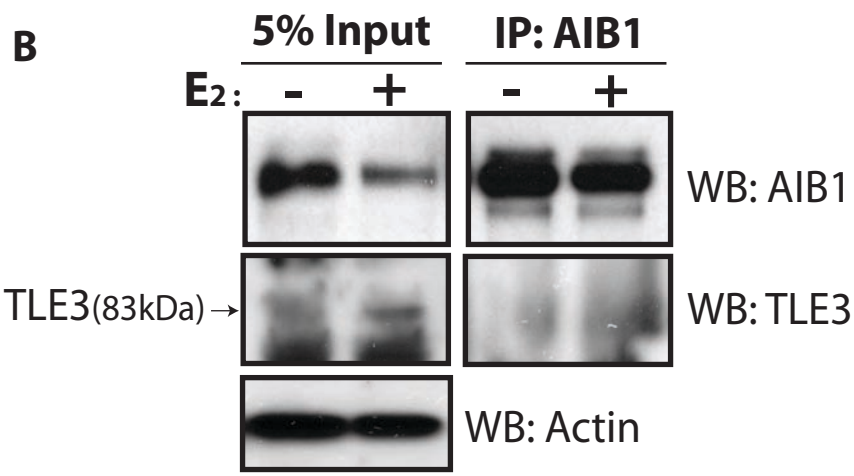


Hu et al., Fig. S6



Hu et al., Fig. S7





Hu et al., Fig. S8

Role of the Nuclear Receptor Coactivator AIB1-Δ4 in the Control of Gene Transcription

Christopher D. Chien, Alexander Kirilyuk, Jordan V. Li, Wentao Zhang, Tyler Lahusen, Marcel O. Schmidt, Annabell S. Oh, Anton Wellstein, and Anna T. Riegel
From the Departments of Oncology and Pharmacology, Lombardi Cancer Center, Georgetown University Medical Center, Washington, D. C. 20007
Running Title: AIB1-Δ4 and transcription control
Address correspondence to: Anna T. Riegel Tel.: 202-687-1479;
Fax: 202-687-4821; E-mail: ariege01@georgetown.edu.

Abstract

The oncogene Amplified in Breast Cancer 1 (AIB1) is a nuclear receptor coactivator that plays a major role in the progression of various cancers. We previously identified a splice variant of AIB1 called AIB1-Δ4 that is overexpressed in breast cancer. Using mass spectrometry, we define the translation initiation of AIB1-Δ4 at M_{224} of the full-length AIB1 sequence and have raised an antibody to a peptide representing the acetylated N-terminus. We show that AIB1-Δ4 is predominantly localized in the cytoplasm, although leptomycin B nuclear export inhibition demonstrates that AIB1-Δ4 can enter and traffic through the nucleus. Our data indicate an import mechanism enhanced by other coactivators such as p300/CBP. We report that the endogenously and exogenously expressed AIB1-Δ4 is recruited as efficiently as full-length AIB1 to estrogen response elements of genes, and enhances estrogen-dependent transcription more effectively than AIB1. Expression of an N-terminal AIB1 protein fragment, that is lost in the AIB1-Δ4 isoform, potentiates AIB1 as a coactivator. This suggests a model whereby the transcriptional activity of AIB1 is squelched by a repressive mechanism utilizing the N-terminal domain and that the increased coactivator function of AIB1-Δ4 is due to the loss of this inhibitory domain. Finally we show, using Scorpion primer technology, that AIB1-Δ4 expression is correlated with metastatic capability of human cancer cell lines.

Introduction

Gene transcription in eukaryotes is a complex and highly regulated process. One of the major controls of gene transcription is exerted by the coregulator family of proteins. These include both corepressors, which dampen transcription, and coactivators, which potentiate transcription. A subgroup of coactivators has been shown to be critical for the malignant progression of cancer and is known as the p160 steroid receptor coactivators (1). One member in particular was identified to be amplified in breast cancer. Amplified in Breast Cancer 1 (AIB1, SRC-3, NCOA3, ACTR, TRAM-1, pCIP, RAC3) has been shown to be gene amplified in breast cancer (2) and is also overexpressed at the mRNA and protein level in various cancers (1,3,4). Its role in tumorigenesis is attributed to its ability to coactivate both steroid hormone and growth factor dependent transcription (3,5-7). In several oncogene driven mouse models (8-11) reduction of AIB1 levels lead to a decrease in tumorigenesis and overexpression of AIB1 lead to the formation of various tumors (12). Clinically, AIB1 expression in breast cancer cases is correlated with high HER2 levels, larger tumor size, higher tumor grade and shorter disease free survival (13-15). Also, high levels of AIB1 in conjunction with high HER2 levels coincide with reduced disease free survival in patients treated with tamoxifen, suggesting a role for AIB1 in tamoxifen resistance (16).

We had previously identified a splice variant of AIB1, where exon 3 was spliced from the mature mRNA and was named AIB1-Δ3 (17). More recently, an additional 5' exon 81,164 bases upstream of the known 5'UTR was identified. Thus the deleted exon is now exon 4 and we now refer to the splice variant as AIB1-Δ4. We had reported that AIB1-Δ4 mRNA results in an N-

terminally truncated isoform of the AIB1 protein that was found to be a more potent coactivator of steroid dependent transcription on a per mole basis when compared with the full-length AIB1 protein. AIB1-Δ4 mRNA expression was elevated in breast tumor tissue relative to normal breast tissue (17). It was also shown to increase the efficacy of estrogenic compounds and the agonist effects of the selective estrogen receptor modulator tamoxifen in breast and endometrial tumor cells (17,18). Overexpression of AIB1-Δ4 in mice leads to ductal ectasia in the mammary gland with an increased expression of proliferative markers such as PCNA, phospho-histone H3, and Cyclin D1 (19) as well as increased cross talk with ERα in epithelial and stromal responses (20). More recently, AIB1-Δ4 was shown to act as a molecular bridge between Epidermal Growth Factor Receptor (EGFR) and Focal Adhesion Kinase (FAK) in the cytoplasm and its overexpression increased the invasiveness of the MDA-MB-231 metastatic breast cancer cell line (21).

Since AIB1-Δ4 lacks a nuclear localization sequence (NLS) any function for this protein in cancer to date has been attributed predominantly to its role in the cytoplasm (21). We now show that AIB1-Δ4 can enter the nucleus by a non-canonical nuclear import mechanism. AIB1-Δ4 is recruited to estrogen response elements of endogenous estrogen-regulated genes and increases their expression. We also determined that the N-terminal region absent from the AIB1-Δ4 protein contains an inhibitory domain. Through the use of Scorpion primer technology, we have created the first quantitative assay for the AIB1-Δ4 transcript and found a correlation between AIB1-Δ4 expression and the metastatic phenotype of human cancer cell lines. These data suggest that the nuclear activities of AIB1-Δ4 can contribute to its function in malignancy.

Experimental Procedures

Plasmids- p300-HA and ERα constructs were provided by Dr. Maria L. Avantaggiati (Georgetown University) and from Dr. Pierre Chambon (INSERM, Strassbourg) respectively. AIB1, AIB1-Δ4, FLAG AIB1, and FLAG AIB1-Δ4 were described previously (17,22). A C-terminal FLAG was added to the AIB1-Δ4 cDNA by deletion of the stop codon in AIB1-Δ4 and addition of FLAG peptide sequence by site-directed mutagenesis (Stratagene). HA AIB1 was generated by PCR amplification of the AIB1 sequence from pcDNA3-AIB1 and cloned into phCMV2. The AIB1 N term construct was created by PCR amplification of the ACTR/AIB1 cDNA (184 bp to 777bp) to add a new 5' NotI site and 3'BglII site. The PCR product was then cloned into p3XFLAG-CMV-10 (Sigma).

Cell lines and transient transfection- MDA231-BrM2 were kindly provided by Dr. Joan Massagué (Sloan Kettering Institute), 4175-TR and SCP2-TR cells by Yibin Kang (Princeton University), AIB1 KO/SRC-3$^{-/-}$ mouse embryonic fibroblasts (MEFs) by Dr. Jiangming Xu (Baylor College of Medicine), T47D A1-2 cells by Dr. Steve Nordeen (University of Colorado), and COLO SL and COLO PL cells by Dr. John M. Jessup (Georgetown University). Chinese Hamster Ovary (23), COLO 357 were purchased from ATCC. HEK293, HEK293T, COS-7, MCF-7, and MDA-MB-231 were obtained from the Tissue Culture Shared Resource at Georgetown University. The Human mammary epithelial cells (HMEC) were purchased and cultured in commercially supplied medium (BulletKit, Lonza). HEK293T, COS-7, COLO 357, COLO SL, and COLO PL, MDA-MB-231, MDA231-BrM2 (brain), 4175-TR (lung), SCP2-TR (bone), and AIB1 KO MEFs were grown in Dulbecco modified Eagle medium (DMEM, Invitrogen) with 10% FBS. CHO cells were grown in DMEM F12 (Invitrogen) with 10% FBS. HEK293 cells were grown in phenol red free Iscove's modified Eagle medium (IMEM, Invitrogen) with 10% Charcoal stripped serum (CCS). T47D A1-2 and MCF-7 cells were grown in phenol red free IMEM+5%CCS. HEK293, HEK293T, CHO, COS-7, and T47D A1-2 cells were transiently transfected with FuGENE 6 (Roche).

Identification of N-terminus of AIB1-Δ4- HEK293T cells grown to 80% confluence were transiently transfected with 18 μg C-terminal FLAG AIB1-Δ4 cDNA. 24 hours later whole cell lysates were prepared and subjected to

immunoprecipitation using Anti-FLAG M2 affinity gel (Sigma). After washing AIB1-Δ4 protein was recovered by heating the affinity gel to 95°C and the sample was subjected to SDS-PAGE. A band corresponding to AIB1-Δ4 protein was isolated and trypsinized using a conventional in-gel digestion protocol where cysteines were reduced with DTT and alkylated by iodoacetamide. Extracted tryptic peptides were analyzed using the MIDAS-MS based algorithm on an LC-ESI-MS 4000QTRAP instrument (AB SCIEX, Framingham, MA). In silico predicted peptides and corresponding collision energy settings were generated using recommended settings in MRMpilot software (AB SCIEX, Framingham, MA). The list of predicted precursors includes the potential variable modification of methionine oxidation and the fixed modification of cysteine alkylation. A final MS method was created for detection of the tryptic peptides produced from the full-length AIB1 protein. This approach allows detecting only tryptic peptides that overlaps with the spliced version of AIB1 and was tested on endogenous AIB1 protein isolated by immunoprecipitation followed by SDS-PAGE. In silico predictions for tryptic peptides with methionine as an initial amino acid residue were applied to data for identification of the N-terminus. More detailed methods are provided in the supplemental material.

Generation of affinity purified AIB1-Δ4 antibodies and characterization- Rabbit polyclonal antibodies were generated against the identified N-terminus using a N-acetylated peptide MQCFALSQPRK and detection of AIB1-Δ4 reactive antibodies was monitored through ELISA by Abgent. Anti-AIB1-Δ4 serum was then subjected to positive and negative selection with N-acetylated AIB1-Δ4 N terminal peptide and non-acetylated AIB1-Δ4 N terminal peptide respectively. The resultant affinity purified antibodies reactive against N-acetylated AIB1-Δ4 were used in experiments.

Endogenous and transfected AIB1-Δ4 were detected after pulldown with AIB1-Δ4 specific antibody and detected with an AIB1 antibody that detects both full-length AIB1 and AIB1-Δ4 in MCF-7 and HEK293T cells respectively. HEK293T cells were transfected with C-terminal FLAG tagged AIB1-Δ4 used to determine the N-terminus of AIB1-Δ4. For both experiments, AIB1-Δ4 containing lysates were immunoprecipitated with 10μg of polyclonal antibody/1mg of lysate overnight.

Peptide competition assays to validate the affinity purified AIB1-Δ4 antibodies were performed by adding 1μg of either N-acetylated or non-acetylated MQCFALSQPRK peptide to 1 mg of MCF-7 cell lysate with 10μg of affinity purified AIB1-Δ4 antibodies.

Western blot (WB) analysis and Immunoprecipitation (IP)- Western blotting was done with the following antibodies: AIB1 (5E11, Cell Signaling), FLAG M2 (Sigma), HA (Cell Signaling), ERα (Ab-10, Neomarkers), ERα (G-20, Santa Cruz), human Actin (Millipore). (i) Interaction of AIB1 with AIB1-Δ4. HEK293T cells were transfected with 6μg of either FLAG AIB1, AIB1-Δ4, or FLAG AIB1 and AIB1-Δ4 together. After washing with cold 1X PBS whole cell lysates were prepared by adding 1% NP-40 lysis buffer containing 1mM NaO_3VO_4 and 1x Complete protease inhibitor tablet (Roche). IP was performed with Anti-FLAG M2 affinity gel as described previously (6) and samples were subjected to SDS-PAGE. (ii) Interaction of AIB1 and AIB1-Δ4 with p300-HA. HEK293T cells were transfected with either FLAG AIB1, FLAG AIB1-Δ4, or p300-HA. Whole cell lysates were prepared as in section (i). Equal amounts of FLAG AIB1 and FLAG AIB1-Δ4 were added to equal amounts of p300-HA lysate. After immunoprecipitation using HA antibody (Cell Signaling) the amounts of FLAG AIB1 or FLAG AIB1-Δ4 were detected with FLAG M2 antibody (Sigma). Densitometry was performed by using Adobe Photoshop 7.0 normalizing AIB1-Δ4 bands to AIB1 bands for both input and IP. (iii) Immunoprecipitation with AIB1-Δ4 antibody. 500 μg of lysate from MCF-7 or HEK293T transfected with C-terminal FLAG tagged AIB1-Δ4 were subjected to IP with 5μg AIB1-Δ4 antibody. AIB1 or AIB1-Δ4 proteins were detected with AIB1 antibody (5E11, Cell Signaling).

Nuclear Cytoplasmic fractionation- Fractionation of lysates was carried out as per the protocol

recommended by the NE-PER Nuclear and Cytoplasmic extraction reagents (78833, Pierce). Endogenous or transfected AIB1-Δ4 was detected by either AIB1 (5E11) or FLAGM2 antibody. Controls use for nuclear and cytoplasmic fractions were HDAC1 (#2062, Cell Signaling) and HSP90 (05-594, Upstate).

Immunofluorescence and leptomycin B treatment- CHO cells were plated on glass coverslips and transfected with 500ng of either FLAG AIB1 or FLAG AIB1-Δ4. 24 hours later cells were fixed with 3.7% paraformaldehyde in PBS for 10 minutes at 25°C. Cells were then washed three times with 1x PBS and permeabolized with 1x PBS containing 0.2% Triton X-100 for 5 minutes 25°C. Cells were then washed with three times with 1xPBS. Coverslips with cells were then blocked for 30 minutes with 1%BSA in PBS. Cells were then incubated with FLAG M2 antibody (1:500, Sigma) and HA antibody (1:500, Abcam ab9110) for 20 minutes. After three 5 minute washes with 1xPBS, cells were incubated with anti-mouse IgG AlexaFluor488 (1:1000, Invitrogen) and anti-rabbit AlexaFluor594 (1:1000, Invitrogen) for 20 minutes. Coverslips were then washed three times with 1x PBS and mounted with ProLong Gold antifade reagent with DAPI (Invitrogen) on to glass slides. 50 nM leptomycin B was added into the culture medium 4 hours before fixation. 200 cells were counted and the percentage of nuclear, nuclear/cytoplasmic, and cytoplasmic stained cells was quantified from 3 different experiments. Nuclear staining was defined as protein specific signal that overlaid with the DAPI signal only. Nuclear/cytoplasmic was defined as protein specific staining that overlaid with the DAPI signal but also showed staining in the cytoplasmic compartment. Cytoplasmic staining was defined as protein specific staining that did not overlay with the DAPI staining of the nucleus. Imaging of stained CHO cells was performed on a Nikon E600 Fluorescence Digital Microscope System and analyzed with Nuance multi-spectral imaging system and software (Cambridge Research & Instrumentation).

Chromatin immunoprecipitation assays (ChIP)- HEK293 cells in a 10 cm dish were transfected with 5μg ERα and either 6μg FLAG AIB1 or 3 μg FLAG AIB1-Δ4 in phenol red free IMEM+10%CCS. 24 hours later cells were treated with Estrogen (E2) for 0, 15, 30, 45, or 60 minutes. Cells were fixed with formaldehyde fixation solution (3.7% formaldehyde, 100 mM NaCl, 50 mM Tris/HCl pH 8.0, 1 mM EDTA, 0.5 mM EGTA) for 10 minutes at 37°C and stopped with 0.125 M Glycine in 1x PBS for 5 minutes at 25°C. Cells were washed three times 1xPBS and resuspended in SDS lysis buffer (50 mM Tris pH 8.0, 10 mM EDTA pH 8.0, 1% SDS). Cells were sonicated and resuspended in ChIP dilution buffer (20 mM Tris pH8.0, 2 mM EDTA pH 8.0, 150mM NaCl, 1% Triton-X-100) and pre-cleared with 30 μl of protein G agarose/salmon sperm DNA (Millipore) for 1 hour. 500 μg of total protein was immunoprecipitated with 2 μl FLAG M2 antibody (Sigma) 16 hours and immunoprecipitated with 30 μl protein G agarose/salmon sperm DNA for 2 hours. Agarose was washed with once with low salt buffer (20 mM Tris pH 8.0, 2 mM EDTA pH 8.0, NaCl 150 mM, 0.1% SDS, 1% Triton-X-100), twice with high salt buffer (20 mM Tris pH 8.0, 2 mM EDTA pH 8.0, 500 mM NaCl, 0.1% SDS, 1% Triton-X-100), once with LiCl salt buffer (10 mM Tris pH 8.0, 1 mM EDTA pH 8.0, 250 mM LiCl, 1% Na deoxycholate, 1% NP-40), and twice with TE buffer (10 mM Tris pH 8.0, 1mM EDTA, pH 8.0). Samples were eluted with elution buffer (1%SDS, 0.1M $NaHCO_3$) for 15 minutes on rotator and 10 minutes on vortexer. Crosslinks were removed with 200mM NaCl for 6 hours at 65°C and proteins digested with 1 μg proteinase K for 1 hour at 45°C. DNA was purified using GENECLEAN Turbo kit (Q-Biogene). Samples were analyzed by real time PCR to examine the ERE recruitment of FLAG AIB1 or FLAG AIB1-Δ4 with the following primers: pS2 ERE s: 5'GGCCATCTCTCACTATGAATCACTTC, pS2 ERE as: 5'-GGCAGGCTCTGTTTGCTTAAAGAGCG-3', hC3 ERE s: 5'-GAGAAAGGTCTGTGTTCACCAGG-3' hC3 ERE as: 5'-TGCAGGGTCAGAGGGACAGA-3', HER2 ERE s: 5'-GTTCCTCCCTCCTGTTCC TC-3', HER2 ERE as: 5'-CCACAAACTGGTGGTCTCCT-3'. Cycling conditions for real time PCR using iCycler were 95°C 3 minutes followed by 40 cycles of 95°C 20 sec, 57°C 30 sec, 72°C 40 sec for hC3 ERE and

pS2 ERE. For HER2 ERE cycling conditions were 95°C 3 minutes followed by 40 cycles of 95°C 20 sec, 65°C 30 sec, 72°C 40 sec. The percentage of the input for each time point is plotted on the graphs and normalized time 0 for each transfection.

For ChIP assays with endogenous AIB1-Δ4, MCF-7 cells were plated in 15 cm dishes in phenol red free IMEM+5%CCS. Fresh IMEM+5%CCS was added for three days. Cells were treated as the HEK293 cells except they were subjected to immunoprecipitation with either 4 μg affinity purified AIB1-Δ4 antibodies (Abgent), 2μg AIB1 (C-20, Santa Cruz), or 2μg ER antibody (HC-20, Santa Cruz). After immunoprecipitation the ChIP procedure for HEK293 cells was then followed. All primers were synthesized by Integrated DNA Technologies (IDT).

Real time PCR analysis- HEK293 cells were transfected with FLAG AIB1 or FLAG AIB1-Δ4 at levels that give equal amounts of transfected protein in IMEM +10% CCS. 16 hours later cells were stimulated with E2 for 0, 4, 8, and 24 hours. Total RNA was harvested using RNeasy mini kit (Qiagen) and reverse transcribed with iScript cDNA synthesis kit (Bio-Rad) using 1 μg of total RNA. Samples were analyzed by real time PCR (iCycler, Bio-Rad) using the following conditions: 95°C 3 min, 40 cycles of 95°C 20 sec 56°C 30 sec 72°C 40 sec. Primer sequences used were: pS2 s: 5'-CCCCGTGAAAGACAGAATTGT-3', pS2 as: 5'-GGTGTCGTCGAAACAGCAG-3', hC3 s: 5'-CTGTCCACGACTTCCCAGG-3', hC3 as: 5'-CCCTTTTCTGACTTGAACTCCC, HER2 s: 5'-AAAGGCCCAAGACTCTCTCC, HER2 as: 5'-CAAGTACTCGGGGTTCTCCA-3', human actin s: 5'-CCTGGCACCCAGCACAAT-3', human actin as: 5'-GCCGATCCACACGGAGTACT-3'. All primers were synthesized by IDT. Expression level for each gene is normalized to actin expression and multiplied by either 1000 or 100,000 to obtain whole value numbers.

Quantitation of AIB1-Δ4 and AIB1 mRNA levels using Scorpion primer based quantitative RT-PCR- A total of 2 x 10^6 cells were plated for each cell line. 24 hours later total RNA was extracted with RNeasy mini kit (Qiagen) and reverse transcribed with iScript cDNA Synthesis Kit (Bio-Rad) using 1μg of total RNA. Real-time PCR was performed using IQ SYBR Green Supermix (Bio-Rad) with AIB1Δ4-scorpion primer and human actin primers. Cycling conditions for the AIB1-Δ4-scorpion primer consist of an initial denaturing step at 94°C (2 min), and 50 cycles (20 seconds at 94°C, 15 seconds at 55.5°C and 20 seconds at 72°C). Unlike SYBR green real time PCR analysis where data is collected during the extension step, data for the Scorpion primer reactions were collected during the 55.5°C annealing step (iCycler; Bio-Rad). Cycling conditions for the human actin primers include a denaturing step at 94°C (2 min), and 45 cycles (20 seconds at 94°C, 30 seconds at 58°C and 40 seconds at 72°C). Primer sequences for the AIB1-Δ4 Scorpion reaction: 5'FAMCCCGCGCTTGGAAATAGTTTTTCCCTTGTCCGCGCGGG-BHQ1HEG-CGCAAATTGCCATGTGATAC. AIB1-Δ4 reverse primer: 5'-CCATCCAATGCCTGAAGTAA-3'. The expression level of AIB1-Δ4 is normalized to actin expression levels and multiplied by either 10,000 or 100,000 to obtain whole number values.

For AIB1 Scorpion primer detection the same procedures were followed except the primer sequence of the AIB1 Scorpion primer was as follows: 5'HEXCCCGCGCGTTTTTCACCACTGCAGGTAAGAGCGCGGG-BHQ1HEG-GCCATGTGATACTCCAGGA. AIB1 reverse primer: 5'-ACGTATCTGTCTTACTGTTTCC- 3'. The AIB1 and AIB1-Δ4 scorpion primers were custom designed and synthesized by Sigma-Aldrich.

Luciferase assay- 25,000 COS-7 cells per well in a 24 well dish were transfected in DMEM without serum with 100 ng MMTV luciferase, 25 ng Progesterone receptor (PR), 5 ng Thymidine Kinase (TK) Renilla luciferase, and either 500 ng pcDNA3, 500 ng FLAG AIB1, 500 ng FLAG N term, or 125, 500, and 750 ng of FLAG N term with 500 ng FLAG AIB1. 24 hours later cells were treated with 10 nM R5020 or an equivalent volume of ethanol. 24 hours after stimulation cells were lysed and luciferase values were measured using the Dual-Luciferase Reporter Assay System (Promega). Firefly luciferase values were

normalized to Renilla luciferase values and averaged for each transfection condition plated in triplicate.

Results

Identification of the N-terminus of AIB1-Δ4

As we have previously identified, AIB1-Δ4 is a splice variant of the nuclear receptor coactivator AIB1 (17) which results in the translation of an N-terminally truncated isoform of the full-length AIB1 protein with a molecular weight of approximately 130 kDa. The translation start site of AIB1-Δ4 was predicted to be at the methionine at position 199 in the full-length AIB1 protein since this was the next in frame methionine residue, however the translation start site was not identified experimentally. There is a cluster of methionines at positions 199, 201, 217, 224, 235, 236, 246, and 289 of full-length AIB1 sequence from which initiation of translation could result in an approximately 130 kDa protein (Fig. 1a). To determine which of these 8 methionines is the translation start site of the AIB1-Δ4 protein we used mass spectrometry. We isolated AIB1-Δ4 protein from HEK293T cells transfected with a C-terminal FLAG AIB1-Δ4 cDNA construct. After immunoprecipitation with FLAG antibody, we isolated AIB1-Δ4 from a Coomassie stained SDS-PAGE gel and subjected the tryptic peptides to mass spectrometric analysis. Through an initial protein identification we detected an AIB1 related protein based on the initial analysis of the peptides. A search for the peptide **TPHDILEDINASPEM$_{217}$R** (boxed in Fig. 1a) was employed because it is an easily detectable fragment present in the full-length AIB1 protein in previous studies (22). This peptide was not found in the analysis of the tryptic fragments from AIB1-Δ4. This eliminated the possibility of the translation start site at M_{199} and M_{201}. The most N-terminal peptide identified from the AIB1-Δ4 protein was **AM$_{235}$M$_{236}$EEGEDLQSCM$_{246}$ICVAR** (underlined in Fig. 1a). This ruled out the M_{235}, M_{236}, M_{246}, and M_{289} methionines as possible translation start sites and limited the possibilities to the M_{217} and M_{224} methionine residues. As a next step we tested these methionines using in silico predictions for tryptic peptides with an initial methionine as the first amino acid residue. We also included predicted precursors that could appear as a result of cotranslational modifications such as N-terminal acetylation. In eukaryotes, 80% of all proteins have been described with an acetyl moiety added to the N-terminus (24,25). Interestingly, we observed only one predicted peptide **M$_{224}$QCFALSQPR** that retained an initiator methionine, which was M_{224}. This peptide harbored N-terminal acetylation and double charge state of this peptide defines an m/z value of 640.3 (Fig. 1b). Due to chemical oxidation of methionines, the precursor ions are split between the m/z ratio of 640.3 and an m/z shift of +8 amu to 648.3. Fragmentation analysis of both precursors matched to corresponding peptides with different oxidation states of methionine and with Mascot scores assigned of 45 and 65 respectively where scores above 23 indicate peptide identity. Therefore, we define the N-terminus of AIB1-Δ4 to be at the M_{224} residue of full-length AIB1. To further verify that this was the correct N-terminus of AIB1-Δ4, we used the N-terminal acetylated sequence **M$_{224}$QCFALSQPR** determined by mass spectrometry to generate polyclonal antibodies that detect the AIB1-Δ4 with little or no detectable cross reaction with full length AIB1. Immunoprecipitations with the affinity purified antibodies for AIB1-Δ4 detected both endogenous and transfected AIB1-Δ4 in MCF-7 and HEK293T cells respectively (Fig. 1c i and ii). The immunoprecipitated AIB1-Δ4 is competed by the N-acetylated peptide but not by the non-acetylated peptide, which also suggests that, the unique acetylation present at the M_{224} provides an epitope not present in full-length AIB1 (Fig. 1c iii).

The full-length and alternatively spliced AIB1 mRNAs and proteins derived from these data are depicted schematically in Fig. 1d. The full-length human AIB1 transcript has 23 exons coding for a 1424 amino acid protein of 155 kDa. Translation of AIB1 is initiated in exon 3 and continues until the stop codon in exon 23. The AIB1-Δ4 transcript lacks exon 4 due to alternative splicing. Translation of the AIB1-Δ4 isoform is initiated in exon 7 and the resultant protein lacks the N-terminal 223 amino acids of the full-length protein. Due to the loss of exon 4 in the AIB1-Δ4 transcript, the NLS, basic helix loop helix (bHLH),

and PAS A domain are lost from the AIB1-Δ4 protein. Thus, we now define AIB1-Δ4 as a 130 kDa protein of 1201 amino acids.

AIB1-Δ4 is a predominantly cytoplasmic protein that enters the nucleus

It has not been determined if the phenotypic effects of AIB1-Δ4 are only due to its cytoplasmic function or if there are additional direct transcriptional effects of this protein in the nucleus. Others have published the presence of a bipartite NLS in the N-terminus of the AIB1 protein at amino acids 16-19 and 35-38 (26-28) indicating that AIB1-Δ4 lacks this NLS sequence. Initially we examined the subcellular distribution of endogenous AIB1-Δ4 in fractionated MCF-7 cell extracts. Using an AIB1 antibody that detects both full-length AIB1 and AIB1-Δ4, we determined that both AIB1 isoforms were detected in the cytoplasmic and nuclear extracts from MCF-7 cells (Fig. 2a). AIB1-Δ4 is present in the nuclear extracts, although at levels considerably less than in the cytoplasm (68% cytoplasmic vs. 32% nuclear).

We next examined the dynamics of the subcellular distribution of AIB1-Δ4 by immunofluorescence. We utilized a transfected FLAG tagged construct of AIB1-Δ4 (22) to determine its cellular localization since the AIB1-Δ4 affinity purified antibodies signal in immunofluorescence for endogenous protein is very weak and not quantifiable. This transfected FLAG AIB1-Δ4 protein was detected in both nucleus and cytoplasm after subcellular fractionation and the distribution was 77% cytoplasmic vs. 23% nuclear (Fig. 2b). Chinese Hamster Ovary cells (CHO) were transfected with either FLAG AIB1 or FLAG AIB1-Δ4 in media with 10% FBS and the number of nuclear, nuclear/cytoplasmic, and cytoplasmic stained cells were quantified. CHO cells were chosen because their endogenous AIB1 is not detected by available AIB1 antibodies (17). We confirmed the fractionation result that the majority of AIB1-Δ4 resides in the cytoplasm (Fig. 2c). CHO cells transfected with AIB1 showed nuclear and nuclear/cytoplasmic staining in 75% and 25% of the cells respectively. Cells transfected with AIB1-Δ4 showed nuclear, nuclear/cytoplasmic, and cytoplasmic staining in 1.5%, 41.3%, and 57.2% of cells respectively. Large field images of staining for AIB1 and AIB1-Δ4 as well as typical staining for nuclear, nuclear/cytoplasmic, and cytoplasmic stained cells are shown.

Since we detected some nuclear and nuclear/cytoplasmic staining for AIB1-Δ4, we wanted to determine if AIB1-Δ4 traffics through the nucleus. We took advantage of the nuclear export inhibitor leptomycin B, which inhibits CRM1 dependent nuclear export of proteins that contain a nuclear export sequence (NES). Both AIB1 and AIB1-Δ4 contain the NES that is in the C-terminal half of the proteins (Fig. 1d) (27) so we hypothesized that if we blocked nuclear export that AIB1-Δ4 protein would accumulate in the nucleus if it is imported into the nucleus. CHO cells were transfected with FLAG AIB1-Δ4 in media with 10% FBS and were either treated with vehicle or leptomycin B. Cells were fixed, stained, and the localization was quantified as before (Fig. 2d). We observed the same distribution of staining in the transfected CHO cells treated with vehicle, however we saw an increase in the number of cells showing nuclear staining for AIB1-Δ4. CHO cells transfected with AIB1-Δ4 and treated with leptomycin B showed staining in the nuclear, nuclear/cytoplasmic, and the cytoplasmic compartments in 18%, 60%, and 22% of cells respectively. The increase in the number of nuclear stained cells after leptomycin B treatment suggests that AIB1-Δ4 is imported into the nucleus however, lack of a canonical NLS and this present data suggests that nuclear import of AIB1-Δ4 is an inefficient process, which contributes to the lower steady state levels of nuclear staining of the protein.

Nuclear import of AIB1-Δ4 can be facilitated by other NLS containing proteins

Various proteins involved in signaling have been shown to be imported into the nucleus in an NLS independent manner (29-34). To study if the localization of AIB1-Δ4 could be altered by other NLS containing proteins, CHO cells were transfected with FLAG AIB1-Δ4 in the presence of HA AIB1 (Fig. 3a). We observed a statistically significant increase in nuclear staining of AIB1-Δ4 after transfection with HA AIB1. CHO cells transfected with AIB1-Δ4 alone showed 67±3.6% and 33±3.6% of cells staining in cytoplasm and

nucleus respectively. After co-transfection of AIB1-Δ4 with HA AIB1, cells stained the nuclear, nuclear/cytoplasmic, and cytoplasmic staining patterns in 2.7±1.5%, 63.3±1.5%, and 34±1% of cells. To determine that this effect was not cell line specific, we confirmed that AIB1 expression increased AIB1-Δ4 nuclear levels in mouse embryonic fibroblasts derived from AIB1 knockout mice (Sup Fig 1). The pattern of staining of AIB1-Δ4 that was cytoplasmic, nuclear/cytoplasmic, or nuclear was 86±1%, 14±1%, and 0% respectively and shifted to 70.3±3.5%, 29.3±4%, and 0.3±0.6% with expression of full-length AIB1.

We next investigated possible mechanisms whereby AIB1 could enhance AIB1-Δ4 nuclear localization. It has been shown that the PAS B domain is sufficient for heterodimerization and homodimerization of p160 SRC family members (35). Since AIB1 and AIB1-Δ4 both contain PAS B domains, we set out to determine if AIB1-Δ4 could interact with full-length AIB1 and piggyback into the nucleus with AIB1. HEK293T cells were transfected with FLAG AIB1 alone, AIB1-Δ4 alone, or FLAG AIB1 and AIB1-Δ4 together. After immunoprecipitation with FLAG antibody to pulldown AIB1, Western blotting with a pan AIB1 antibody showed that AIB1-Δ4 immunoprecipitates with AIB1 (Fig. 3c, lane 6, top panel). There is also a detectable amount of endogenous AIB1-Δ4 protein in HEK293T cells and immunoprecipitation with FLAG AIB1 is able to pulldown endogenous AIB1-Δ4 protein as well (Fig. 3c, lane 4, bottom panel). When no FLAG AIB1 is present, we do not detect any AIB1-Δ4 present after immunoprecipitation (Fig. 3c, lane 5, top and bottom panels). However, it should be noted that we have been unable to detect full-length AIB1 in AIB1-Δ4 immunoprecipitates with a variety of tags (not shown) or with immunoprecipitation using AIB1-Δ4 affinity purified antibodies (Fig. 1d). Thus the AIB1 interaction with AIB1-Δ4 is most likely weak and we conclude that most of the full-length and AIB1-Δ4 are not heterodimerized with each other in the cells we have examined. This suggests that AIB1 may increase nuclear import of AIB1-Δ4 through a non-dimerization mediated mechanism.

The interaction of AIB1 with other proteins involved in transcription is well characterized (7). One of these proteins is p300/CBP (36) and we show that AIB1-Δ4 interacts with p300 by immunoprecipitation (Fig. 4a). HEK293T cells were transfected with either p300-HA, FLAG AIB1, or FLAG AIB1-Δ4 and cell lysates were harvested. After normalization for protein content, equal amounts of either FLAG AIB1 or FLAG AIB1-Δ4 were added to p300-HA cell lysate. The amount of FLAG AIB1 and FLAG AIB1-Δ4 proteins were observed after immunoprecipitation with p300-HA. We found that both AIB1 and AIB1-Δ4 are associated with p300. However, with equal amounts of FLAG AIB1 or FLAG AIB1-Δ4 in the lysate we found twice as much AIB1-Δ4 associated with p300 as compared to AIB1. This suggests that AIB1-Δ4 may be able to preferentially complex with p300 in active transcriptional complexes.

Consistent with this data, we see in CHO cells transfected with AIB1-Δ4 and p300-HA an increase in AIB1-Δ4 staining in the nucleus relative to cells transfected with AIB1-Δ4 alone (Fig. 4b). CHO cells transfected with FLAG AIB1-Δ4 alone showed staining in the nuclear/cytoplasmic and cytoplasmic compartments in 32.3±1.5% and 67.7±1.5% respectively, which shifted to 56±5.3% and 44±5.3%. The induction of AIB1-Δ4 nuclear transport by p300 was not cell line specific as we also replicated this finding in AIB1 KO MEFs transfected with FLAG AIB1-Δ4 and p300-HA. The pattern of staining of AIB1-Δ4 that was nuclear, nuclear/cytoplasmic, or cytoplasmic was 0%, 14±1%, and 86±1% respectively and shifted to 13.3±2.3%, 63±4.6%, and 23.7±2.5% (Fig. 4c). Overall the data suggest that AIB1-Δ4 may interact with other NLS containing proteins to traffic into the nucleus.

AIB1-Δ4 is recruited to active transcriptional complexes and coactivates estrogen responsive genes

Since it is known that both AIB1 and AIB1-Δ4 coactivate estrogen dependent transcription we decided to examine whether or not AIB1-Δ4 is recruited to known transcriptional targets of estrogen receptor. To examine the recruitment of AIB1-Δ4 to estrogen responsive elements (ERE), we transfected HEK293 cells

with ER and either FLAG AIB1 or FLAG AIB1-Δ4 and performed Chromatin Immunoprecipitation (ChIP) analysis (Fig. 5a). Cells were treated with estrogen for 15, 30, 45, and 60 minutes to observe the recruitment of AIB1 or AIB1-Δ4 over time. Both AIB1 and AIB1-Δ4 were recruited to the three different estrogen response elements in pS2, hC3, and HER2 (23,37,38) known to be binding sites for ERα (confirmed in Sup Fig 3a). Maximal recruitment of FLAG AIB1 was at 15 minutes to 8.7%, 4.3%, and 5.0% of the EREs in the pS2, hC3, and HER2 genes respectively. In contrast, maximal recruitment of FLAG AIB1-Δ4 was at 30 minutes to 3.5%, 4.2%, and 3.1% of the EREs in the pS2, hC3, and HER2 genes respectively. Thus, both AIB1 and AIB1-Δ4 are recruited to these EREs confirming that AIB1-Δ4 is found in the nucleus and found at active sites of transcription. The corresponding protein levels are shown by Western blot for all the different times of estrogen stimulation. Interestingly, the kinetics of AIB1-Δ4 recruitment is delayed which is possibly due to inefficient or altered nuclear transport because of lack of the NLS. Alternatively, this time delay could be an artifact generated by driving transcription with transiently transfected proteins. To determine if this was the case we also examined the dynamics of endogenous AIB1-Δ4 on estrogen responsive genes using IP with the affinity purified AIB1-Δ4 antibodies in MCF-7 cells (Fig. 5b). ChIP assays with this antibody confirmed that AIB1-Δ4 binds to ERE in estrogen responsive genes and consistent with the transfected AIB1-Δ4 protein the peak of binding for AIB1-Δ4 was delayed relative to the peak binding for full-length AIB1 for the ERE in pS2 and HER2. Of note is that recruitment of AIB1-Δ4 is not exclusive to estrogen regulated genes since we also observed its recruitment to a progesterone response element in T47D A1-2 cells that have a stable integration of the MMTV luciferase construct (39) (Sup Fig. 3b).

To confirm that recruitment of AIB1-Δ4 leads to an increase in these estrogen-regulated genes, we looked at the levels of expression of the pS2, hC3, and HER2 after estrogen stimulation. HEK293 cells were transfected with ER and either FLAG AIB1 or FLAG AIB1-Δ4 and stimulated with estrogen for 4, 8, and 24 hours. RNA was harvested from the cells and the gene expression examined by real time PCR. We found maximal gene expression in AIB1-Δ4 transfected cells at 8 hours for HER2 and at 24 hours for pS2 and hC3. Interestingly, significant differences in gene expression were only observed in the AIB1-Δ4 transfected cells suggesting that estrogen responsive genes are more sensitive to changes in AIB1-Δ4 levels than full-length AIB1.

The region deleted from AIB1-Δ4 contains an inhibitory domain

A possible hypothesis explaining the more potent coactivator function of AIB1-Δ4 could be its lack of repression by an endogenous factor that is able to bind to the full-length AIB1 protein (Fig. 6a). One prediction of this model is that expression of an N-terminal fragment that bound this repressor could relieve repression of full-length AIB1. To test this hypothesis we created a FLAG tagged N-terminal AIB1 construct (AIB1 N term) which contains the bHLH and PAS A domains not present in the AIB1-Δ4 protein (Fig. 1c). This construct should have no coactivator function since it lacks the C-terminal activation domain responsible for binding to nuclear receptors and molecules that affect transcription such as p300/CBP and CARM1. For this experiment we used progesterone induced transcription in COS-7 cells as a read out of AIB1 activity since this has consistently given the strongest dose-response coactivator readout for AIB1 (17). We transfected COS-7 cells with progesterone receptor and AIB1 with increasing amounts of AIB1 N term and monitored the coactivator function of AIB1 on a progesterone inducible MMTV luciferase reporter construct (Fig. 6b). As expected, AIB1 is able to coactivate transcription of the luciferase reporter relative to empty vector transfected cells (AIB1 0 vs. 500). Co-transfection of AIB1 with AIB1 N term significantly increased the amount of transcription from the luciferase reporter. This effect was increased with the amount of AIB1 N term co-transfected with AIB1 (AIB1 co-transfection with AIB1 N term 125, 500, 750). A relief of repression on endogenous AIB1 coactivator activity due to co-expression of the AIB1 N term construct alone was also apparent (AIB1 N term 0 vs. 500). The levels of AIB1 and AIB1 N term

protein are shown by Western blot and there is no increase in the AIB1 protein with co-transfection of higher levels of AIB1 N term (Fig. 6b). These data suggest a suppressor role of the N-terminal region of AIB1 in the regulation of the coactivator function of AIB1. This region is the most highly conserved region among steroid receptor coactivator proteins and has been suggested to contain an inhibitory function for AIB1 also in the cytoplasm (21).

AIB1-Δ4 expression is correlated with metastatic potential

We have shown previously that the mRNA expression of AIB1-Δ4 transcript was increased in breast tumor tissue relative to normal breast tissue and was higher in the MCF-7 breast cancer cell line relative to non-transformed breast cell lines (17). However, the only method we had previously to detect AIB1-Δ4 transcript was by semi-quantitative hybridization of a radioactive DNA probe to total RNA isolated from cells, thus making accurate quantification difficult. We therefore designed a quantitative assay to measure AIB1-Δ4 mRNA levels through the use of Scorpion primer technology (40,41). We designed a Scorpion primer with a primer sequence complimentary to a sequence in exon 3 and a probe sequence complimentary to the unique sequence generated by the splicing of exon 3 and exon 5 (Fig. 7a). This scorpion primer specifically recognizes the AIB1-Δ4 transcript and not the AIB1 transcript due to the fact that after amplification of AIB1 transcript, the probe sequence is not complimentary to any sequence generated in the full-length AIB1 transcript. In addition we designed an AIB1 specific Scorpion primer with a primer sequence in exon 3 and a probe sequence complimentary to exon 4, which is not contained in the splice variant AIB1-Δ4 transcript. We subjected plasmids containing either AIB1 or AIB1-Δ4 cDNA to an analysis by real time PCR with the AIB1 and AIB1-Δ4 scorpion primers (Sup Fig. 4a and b). We show that the AIB1-Δ4 scorpion primer specifically identifies AIB1-Δ4 cDNA and not full-length AIB1 cDNA and vice versa for the AIB1 scorpion primer. To confirm the increased expression of AIB1-Δ4 in breast cancer cell lines, total RNA was harvested from human mammary epithelial cells (HMEC), parental MDA-MB-231, and three tissue specific metastatic variants of MDA-MB-231 cells. The three tissue specific variants home either to the brain, bone, or lung after intravenous or intracardiac injection (42-44). After reverse transcription, cDNA generated from these RNAs was subjected to real time PCR analysis with Scorpion primers for AIB1 or AIB1-Δ4 (Fig. 7b). Expression of AIB1-Δ4 mRNA relative to AIB1 was higher in the parental and three tissue specific metastatic variants of MDA-MB-231 cells relative to HMECs confirming increased expression of AIB1-Δ4 with malignant phenotype.

We also examined if AIB1-Δ4 expression is also correlated with metastatic potential in another cancer metastasis model. We used parental COLO 357 pancreatic cancer cells and two metastatic derivative cell lines, which were in vivo selected to metastasize from the pancreas to liver or spleen to liver (COLO PL and COLO SL) (45). The expression of AIB1-Δ4 was found increased in the more metastatic variants of the COLO 357 cell line (Fig. 7c) suggesting a correlation between increased metastatic capability and AIB1-Δ4 expression.

Discussion

We show in this study that AIB1-Δ4 enters the nucleus and has a nuclear function. In accordance with previous data that the NLS is contained in the N-terminus of AIB1 (26-28), we found that the majority of AIB1-Δ4, which lacks a NLS, is predominantly in the cytoplasm at steady state levels. This is in contrast to the localization of AIB1, which resides mostly in the nucleus. Coactivation occurs in the nucleus, which raised the question how the mainly cytoplasmic AIB1-Δ4 had such potent effects on transcription. The first question to address was if AIB1-Δ4 enters the nucleus. We observed that AIB1-Δ4 accumulated in the nucleus after blockade of nuclear export suggesting that it was indeed being imported into the nucleus. The next question to address was whether AIB1-Δ4 had a functional role in the nucleus. We saw that AIB1-Δ4 was recruited as efficiently as AIB1 to ERE in estrogen-regulated genes in the nucleus despite significantly lower steady-state nuclear levels of AIB1-Δ4. The mainly cytoplasmic location of AIB1-Δ4 is

potentially due to either an inefficient nuclear import mechanism or through a rapid nuclear export mechanism. We argue for the former scenario given that AIB1-Δ4 lacks the N-terminal NLS and there is no alteration in the nuclear export sequence of AIB1-Δ4. It is known that molecules larger than 40 kDa have to be actively transported through the nuclear pore complex through interaction of the NLS with nuclear importins (46). Another potential mechanism for nuclear import termed "piggybacking" was demonstrated for various proteins such as eIF4E, IκBα and Cdk2, and BRCA1 (47-52). BRCA1 has a naturally occurring splice variant that lacks an NLS and it is able to localize to the nucleus through interaction with another protein BARD1, which contains a canonical NLS. We propose that AIB1-Δ4 is able to similarly piggyback onto p300/CBP and/or other NLS containing proteins and thus enter the nucleus. Alternatively NLS containing coactivators could upregulate genes involved in Ran-independent nuclear import mechanisms such as via calmodulin (53). Whatever the mechanism it appears to be an inefficient process likely accounting for the largely cytoplasmic distribution of AIB1-Δ4 in the cell. Also consistent with this hypothesis is the difference in the kinetics of recruitment of AIB1 and AIB1-Δ4. We saw a delay in the recruitment of AIB1-Δ4 to the ERE relative to AIB1 suggesting that the mechanism of nuclear import of AIB1-Δ4 is less efficient than that of AIB1.

The fact that we saw more effective coactivation by AIB1-Δ4 despite having much more AIB1 in the nucleus than AIB1-Δ4 suggests that there is a regulation of AIB1 coactivator activity that does not exist for AIB1-Δ4. Since we observed that the levels of AIB1-Δ4 interacting with p300 was higher than the levels of AIB1 associated with p300 (Fig. 4a) and p300 is generally found in active transcriptional complexes, we believe that AIB1-Δ4 is highly recruited to sites of active transcription. The increased coactivator activity of AIB1-Δ4 was confirmed by a higher increase in endogenous estrogen regulated gene expression in cells transfected with AIB1-Δ4. This data suggests that the large amount of AIB1 that resides in the nucleus is not in active transcriptional complexes and the reason why AIB1-Δ4 is a more potent coactivator than AIB1 can best be explained by the presence of an inhibitory domain in the N-terminal 223 amino acids of AIB1. Alternatively loss of the N-terminus could cause steric changes that increase the affinity for other coactivators. We conjectured that this N-terminal fragment containing the bHLH and PAS A domains would be able to bind N-terminal repressors of AIB1. We found that the N-terminal fragment containing the bHLH and PAS A domains of AIB1 when co-transfected with AIB1 is able to relieve repression of the coactivator function of the AIB1 protein. This effect was dose dependent and the more AIB1 N-terminal fragment added to the cells the less repression there was on the AIB1 protein. Interestingly, transfection of the fragment alone showed an increase in luciferase activity, which is probably not due to an inherent coactivator function of this fragment since most of the transcriptional activity of the AIB1 and AIB1-Δ4 proteins reside in their recruitment of p300/CBP in the C-terminus (36). This increase in transcription is most likely due to a relief of repression of the endogenous AIB1 in the COS-7 cells since we are able to detect endogenous AIB1 protein by Western blot (17). Previous studies from our group and others have suggested that the N-terminal region containing the bHLH and PAS A domains contain an inhibitory domain that represses activity in both the nucleus and cytoplasm (17,18,21,26,36). Our studies and those from Chen et al (36) have shown that the loss of the N-terminal region leads to potent coactivation of nuclear hormone receptor mediated transcription. Expression of AIB1-Δ4 (loss of amino acids 1-223 of AIB1) or ACTR38 (loss of amino acids 1-447 of AIB1) leads to potent coactivation of nuclear receptor dependent transcription from estrogen, progesterone, retinoic acid, thyroid, glucocorticoid, vitamin D, and retinoid X receptors. Interestingly, data from Li et al (26) showed expression of AIB1 constructs containing mutations in either or both NLS (NLS amino acids 16-19 and 35-38 of AIB1) or with the bHLH domain deleted (amino acids 16-88 of AIB1) had no coactivator activity presumably because of lack of import into the nucleus. The other possibility is that they still retained amino acids 88 through 224, which would support the evidence that there is an inhibitory domain in this region. Loss of these amino acids in AIB1-Δ4 and

ACTR38 allows these proteins to be potent coactivators. A number of proteins have been shown to bind to the bHLH PAS domain of p160 SRC family members. These have been described as having coactivator, corepressor and phosphatase activity (54-59) depending on the context in which they are examined. It remains to be determined if these proteins play a role in repression or loss of activation of AIB1 on endogenous genes or conversely whether they have lost affinity or changed interaction with AIB1-Δ4.

Both AIB1 and AIB1-Δ4 have been shown to have effects in the Epidermal Growth Factor (EGF) signaling. Data from our lab has shown that loss of both AIB1 and AIB1-Δ4 protein together can lead to a decrease in EGF receptor (EGFR) phosphorylation (6) and AIB1-Δ4 is able to potently coactivate EGF stimulated transcription (17). Long et al (21) have shown that AIB1-Δ4 acts as a bridging molecule between EGFR and FAK and this interaction facilitates the motility and metastatic capability of MDA-MB-231 breast cancer cells. They also show that AIB1-Δ4 is phosphorylated by p21-activated kinase (PAK1), which increases the association of AIB1-Δ4 with EGFR and FAK. Intriguingly in this latter study the N-terminal region of AIB1 inhibited the interaction of AIB1 with FAK and therefore was unable to stimulate the EGF induced migration of cancer cells, suggesting that even in the cytoplasm the N-terminal region of AIB1 was repressive. Expression of a NLS mutant of AIB1, which resides predominantly in the cytoplasm showed much weaker interaction with FAK in cells. Another recent publication from Cai et al (60) shows in non-small cell lung cancer (NSCLC) that AIB1 expression is correlated with poor prognosis and knockdown of AIB1 in NSCLC cell line resistant to gefitinib treatment restored sensitivity to EGFR inhibition by gefitinib. Taken together these data indicate that there is a signaling loop existing between AIB1/AIB1-Δ4 and EGFR where EGFR can affect AIB1-Δ4 through PAK1 activation and AIB1/AIB1-Δ4 can affect EGFR signaling and transcription as well. It is unclear if the siRNA used to target AIB1 in the gefitinib study also targeted AIB1-Δ4 as well so the effects of AIB1-Δ4 on EGFR signaling are not currently known. Overall the contribution of nuclear versus cytoplasmic function of AIB1-Δ4 to steroid and growth factor signaling needs to be further explored.

Given that we have found that the expression of AIB1-Δ4 at the protein level is higher in breast and pancreatic cancer cells (17,61), we were interested to investigate if AIB1-Δ4 is regulated at the protein level. We have previously shown that AIB1 protein levels are greatly reduced in response to growth of cells at high confluence and the removal of growth factors (62). Interestingly we found that the AIB1-Δ4 isoform is not regulated in the same fashion as AIB1 protein (Sup Fig. 5). AIB1-Δ4 is resistant to proteasomal degradation induced by high confluence. This is probably due to loss of a site of regulation in the N-terminal 223 amino acids. The proteasomal regulation of AIB1 has been well characterized (57,62,63). Interestingly, regulation of a phospho-degron at S102 by protein phosphatase 1 (PP1) was shown to be important for regulating the activity of AIB1. PP1 overexpression was able to inhibit the reporter activity as well as the cell proliferative ability of AIB1. The S102 site is also a site of regulation by the ubiquitin ligase SPOP (64). This site is lost in AIB1-Δ4 and could explain the high coactivator activity and stability of the AIB1-Δ4 protein.

A major question that arises from these studies on AIB1-Δ4 is whether there are distinct biological functions for this isoform. To begin to investigate this, we took advantage of the unique splice junction sequence that exists in the AIB1-Δ4 transcript to develop a new technique to specifically measure the amounts of AIB1-Δ4 mRNA independent of AIB1 transcript. By utilizing Scorpion primer technology we see higher expression of AIB1-Δ4 in cancer cell lines relative to normal cell lines and higher expression in more metastatic cancer cell lines. Observations on the role of AIB1 in disease do not make the distinction between the relative contribution of AIB1 or AIB1-Δ4 to the phenotype. Studies that analyze mRNA expression of AIB1 utilize primers that detect both AIB1 and AIB1-Δ4. We believe that it will be important to dissect out the contribution to phenotypes attributed to AIB1-Δ4 independent of AIB1 and vice versa in future clinical studies. We have also developed affinity purified antibodies based on the knowledge of the unique N-acetylated N-terminal sequence of

AIB1-Δ4 which will serve as another resource to determine the expression of AIB1-Δ4 at the protein level at various stages of tumorigenesis.

The precise role of AIB1-Δ4 in tumorigenesis is not known. It is intriguing that AIB1-Δ4 is not degraded under conditions of low growth (e.g. high confluence) whereas full-length AIB1 is rapidly lost. AIB1-Δ4 protein expression may provide a selective advantage for a cancer cell to continue to grow in conditions unfavorable for proliferation for both its metastatic and transcriptional function. Therefore further studies into the regulation and possible targets of AIB1-Δ4 in tumorigenesis need to be pursued.

References

1. Xu, J., Wu, R. C., and O'Malley, B. W. (2009) *Nat Rev Cancer* **9**, 615-630
2. Anzick, A. L., Kononen, J., Walker, R. L., Azorsa, D. O., Tanner, M. M., Guan, X.-Y., Sauter, G., Kallioniemi, O.-P., Trent, J. M., and Meltzer, P. S. (1997) *Science* **277**, 965-968
3. Lahusen, T., Henke, R. T., Kagan, B. L., Wellstein, A., and Riegel, A. T. (2009) *Breast Cancer Res Treat* **116**, 225-237
4. List, H. J., Reiter, R., Singh, B., Wellstein, A., and Riegel, A. T. (2001) *Breast Cancer Res Treat* **68**, 21-28
5. Oh, A., List, H. J., Reiter, R., Mani, A., Zhang, Y., Gehan, E., Wellstein, A., and Riegel, A. T. (2004) *Cancer Res* **64**, 8299-8308
6. Lahusen, T., Fereshteh, M., Oh, A., Wellstein, A., and Riegel, A. T. (2007) *Cancer Res* **67**, 7256-7265
7. York, B., and O'Malley, B. W. (2010) *J Biol Chem* **285**, 38743-38750
8. Fereshteh, M. P., Tilli, M. T., Kim, S. E., Xu, J., O'Malley, B. W., Wellstein, A., Furth, P. A., and Riegel, A. T. (2008) *Cancer Res* **68**, 3697-3706
9. Kuang, S. Q., Liao, L., Wang, S., Medina, D., O'Malley, B. W., and Xu, J. (2005) *Cancer Res* **65**, 7993-8002
10. Kuang, S. Q., Liao, L., Zhang, H., Lee, A. V., O'Malley, B. W., and Xu, J. (2004) *Cancer Res* **64**, 1875-1885
11. Qin, L., Liao, L., Redmond, A., Young, L., Yuan, Y., Chen, H., O'Malley, B. W., and Xu, J. (2008) *Mol Cell Biol* **28**, 5937-5950
12. Torres-Arzayus, M. I., Font de Mora, J., Yuan, J., Vazquez, F., Bronson, R., Rue, M., Sellers, W. R., and Brown, M. (2004) *Cancer Cell* **6**, 263-274
13. Bautista, S., Valles, H., Walker, R. L., Anzick, S., Zeillinger, R., Meltzer, P., and Theillet, C. (1998) *Clin Cancer Res* **4**, 2925-2929
14. Harigopal, M., Heymann, J., Ghosh, S., Anagnostou, V., Camp, R. L., and Rimm, D. L. (2009) *Breast Cancer Res Treat* **115**, 77-85
15. Thorat, M. A., Turbin, D., Morimiya, A., Leung, S., Zhang, Q., Jeng, M. H., Huntsman, D. G., Nakshatri, H., and Badve, S. (2008) *Histopathology* **53**, 634-641
16. Osborne, C. K., Bardou, V., Hopp, T. A., Chamness, G. C., Hilsenbeck, S. G., Fuqua, S. A., Wong, J., Allred, D. C., Clark, G. M., and Schiff, R. (2003) *J Natl Cancer Inst* **95**, 353-361
17. Reiter, R., Wellstein, A., and Riegel, A. T. (2001) *J Biol Chem* **276**, 39736-39741
18. Reiter, R., Oh, A. S., Wellstein, A., and Riegel, A. T. (2004) *Oncogene* **23**, 403-409
19. Tilli, M. T., Reiter, R., Oh, A. S., Henke, R. T., McDonnell, K., Gallicano, G. I., Furth, P. A., and Riegel, A. T. (2005) *Mol Endocrinol* **19**, 644-656
20. Nakles, R. E., Shiffert, M. T., Diaz-Cruz, E. S., Cabrera, M. C., Alotaiby, M., Miermont, A. M., Riegel, A. T., and Furth, P. A. (2011) *Mol Endocrinol* **25**, 549-563
21. Long, W., Yi, P., Amazit, L., LaMarca, H. L., Ashcroft, F., Kumar, R., Mancini, M. A., Tsai, S. Y., Tsai, M. J., and O'Malley, B. W. (2010) *Mol Cell* **37**, 321-332
22. Oh, A. S., Lahusen, J. T., Chien, C. D., Fereshteh, M. P., Zhang, X., Dakshanamurthy, S., Xu, J., Kagan, B. L., Wellstein, A., and Riegel, A. T. (2008) *Mol Cell Biol* **28**, 6580-6593
23. Hurtado, A., Holmes, K. A., Geistlinger, T. R., Hutcheson, I. R., Nicholson, R. I., Brown, M., Jiang, J., Howat, W. J., Ali, S., and Carroll, J. S. (2008) *Nature* **456**, 663-666
24. Driessen, H. P., de Jong, W. W., Tesser, G. I., and Bloemendal, H. (1985) *CRC Crit Rev Biochem* **18**, 281-325
25. Polevoda, B., and Sherman, F. (2002) *Genome Biol* **3**, reviews0006
26. Li, C., Wu, R. C., Amazit, L., Tsai, S. Y., Tsai, M. J., and O'Malley, B. W. (2007) *Mol Cell Biol* **27**, 1296-1308

27. Qutob, M. S., Bhattacharjee, R. N., Pollari, E., Yee, S. P., and Torchia, J. (2002) *Mol Cell Biol* **22**, 6611-6626
28. Yeung, P. L., Zhang, A., and Chen, J. D. (2006) *Biochem Biophys Res Commun* **348**, 13-24
29. Fagotto, F., Gluck, U., and Gumbiner, B. M. (1998) *Curr Biol* **8**, 181-190
30. Matsubayashi, Y., Fukuda, M., and Nishida, E. (2001) *J Biol Chem* **276**, 41755-41760
31. Whitehurst, A. W., Wilsbacher, J. L., You, Y., Luby-Phelps, K., Moore, M. S., and Cobb, M. H. (2002) *Proc Natl Acad Sci U S A* **99**, 7496-7501
32. Xu, L., Chen, Y. G., and Massague, J. (2000) *Nat Cell Biol* **2**, 559-562
33. Xu, L., and Massague, J. (2004) *Nat Rev Mol Cell Biol* **5**, 209-219
34. Yokoya, F., Imamoto, N., Tachibana, T., and Yoneda, Y. (1999) *Mol Biol Cell* **10**, 1119-1131
35. Lodrini, M., Munz, T., Coudevylle, N., Griesinger, C., Becker, S., and Pfitzner, E. (2008) *Nucleic Acids Res* **36**, 1847-1860
36. Chen, H., Lin, R. J., Schiltz, R. L., Chakravarti, D., Nash, A., Nagy, L., Privalsky, M. L., Nakatani, Y., and Evans, R. M. (1997) *Cell* **90**, 569-580
37. Masiakowski, P., Breathnach, R., Bloch, J., Gannon, F., Krust, A., and Chambon, P. (1982) *Nucleic Acids Res* **10**, 7895-7903
38. Sundstrom, S. A., Komm, B. S., Ponce-de-Leon, H., Yi, Z., Teuscher, C., and Lyttle, C. R. (1989) *J Biol Chem* **264**, 16941-16947
39. Nordeen, S. K., Kuhnel, B., Lawler-Heavner, J., Barber, D. A., and Edwards, D. P. (1989) *Mol Endocrinol* **3**, 1270-1278
40. Taveau, M., Stockholm, D., Spencer, M., and Richard, I. (2002) *Anal Biochem* **305**, 227-235
41. Thelwell, N., Millington, S., Solinas, A., Booth, J., and Brown, T. (2000) *Nucleic Acids Res* **28**, 3752-3761
42. Bos, P. D., Zhang, X. H., Nadal, C., Shu, W., Gomis, R. R., Nguyen, D. X., Minn, A. J., van de Vijver, M. J., Gerald, W. L., Foekens, J. A., and Massague, J. (2009) *Nature* **459**, 1005-1009
43. Kang, Y., Siegel, P. M., Shu, W., Drobnjak, M., Kakonen, S. M., Cordon-Cardo, C., Guise, T. A., and Massague, J. (2003) *Cancer Cell* **3**, 537-549
44. Minn, A. J., Gupta, G. P., Siegel, P. M., Bos, P. D., Shu, W., Giri, D. D., Viale, A., Olshen, A. B., Gerald, W. L., and Massague, J. (2005) *Nature* **436**, 518-524
45. Bruns, C. J., Harbison, M. T., Kuniyasu, H., Eue, I., and Fidler, I. J. (1999) *Neoplasia* **1**, 50-62
46. Stewart, M. (2007) *Nat Rev Mol Cell Biol* **8**, 195-208
47. Dostie, J., Ferraiuolo, M., Pause, A., Adam, S. A., and Sonenberg, N. (2000) *EMBO J* **19**, 3142-3156
48. Fabbro, M., Rodriguez, J. A., Baer, R., and Henderson, B. R. (2002) *J Biol Chem* **277**, 21315-21324
49. Jans, D. A., and Hubner, S. (1996) *Physiol Rev* **76**, 651-685
50. Moore, J. D., Yang, J., Truant, R., and Kornbluth, S. (1999) *J Cell Biol* **144**, 213-224
51. Thompson, M. E. (2010) *FEBS J* **277**, 3072-3078
52. Turpin, P., Hay, R. T., and Dargemont, C. (1999) *J Biol Chem* **274**, 6804-6812
53. Hanover, J. A., Love, D. C., and Prinz, W. A. (2009) *J Biol Chem* **284**, 12593-12597
54. Belandia, B., and Parker, M. G. (2000) *J Biol Chem* **275**, 30801-30805
55. Goel, A., and Janknecht, R. (2004) *J Biol Chem* **279**, 14909-14916
56. Kim, J. H., Li, H., and Stallcup, M. R. (2003) *Mol Cell* **12**, 1537-1549
57. Li, C., Liang, Y. Y., Feng, X. H., Tsai, S. Y., Tsai, M. J., and O'Malley, B. W. (2008) *Mol Cell* **31**, 835-849
58. Wu, X., Li, H., and Chen, J. D. (2001) *J Biol Chem* **276**, 23962-23968
59. Zhang, A., Yeung, P. L., Li, C. W., Tsai, S. C., Dinh, G. K., Wu, X., Li, H., and Chen, J. D. (2004) *J Biol Chem* **279**, 33799-33805
60. Cai, D., Shames, D. S., Raso, M. G., Xie, Y., Kim, Y. H., Pollack, J. R., Girard, L., Sullivan, J. P., Gao, B., Peyton, M., Nanjundan, M., Byers, L., Heymach, J., Mills, G., Gazdar, A. F., Wistuba, I., Kodadek, T., and Minna, J. D. (2010) *Cancer Res* **70**, 6477-6485

61. Henke, R. T., Haddad, B. R., Kim, S. E., Rone, J. D., Mani, A., Jessup, J. M., Wellstein, A., Maitra, A., and Riegel, A. T. (2004) *Clin Cancer Res* **10**, 6134-6142
62. Mani, A., Oh, A. S., Bowden, E. T., Lahusen, T., Lorick, K. L., Weissman, A. M., Schlegel, R., Wellstein, A., and Riegel, A. T. (2006) *Cancer Res* **66**, 8680-8686
63. Li, X., Lonard, D. M., Jung, S. Y., Malovannaya, A., Feng, Q., Qin, J., Tsai, S. Y., Tsai, M. J., and O'Malley, B. W. (2006) *Cell* **124**, 381-392
64. Li, C., Ao, J., Fu, J., Lee, D. F., Xu, J., Lonard, D., and O'Malley, B. W. (2011) *Oncogene*

Footnotes

Grant Support: This work was supported by grants from the Department of Defense Breast Cancer Research Program BC083320 (C.D. Chien), NIH/NCI R01 CA113477 (A.T.R.), Department of Defense Breast Cancer Research Program W81XWH-06-10590 Center of Excellence Grant (PI V.C. Jordan, A.W., A.T.R.). Mass spectrometric analysis was performed in the Proteomics & Metabolomics Shared Resource and microscopy was performed in the Microscopy & Imaging Shared Resource which are partially supported by NIH/NCI grant P30-CA051008.

We also thank Geoffrey Storchan for his help with Chromatin Immunoprecipitation experimental design.

Figure Legends

Figure 1. **Identification of the translation start site of AIB1-Δ4 and characterization of affinity purified AIB1-Δ4 antibodies. a,** After overexpression of a C-terminal FLAG AIB1-Δ4 construct in HEK293T cells, we determined by mass spectrometric analysis that the AIB1-Δ4 transcript initiates translation at the methionine at position 224 in the full-length AIB1 protein. The TPHDILEDINASPEMR peptide was not identified in AIB1-Δ4 (boxed) and the AMMEEGEDLQSCMICVAR peptide was identified (underlined) by mass spectrometric analysis. The MQCFALSQPR peptide identified through further mass spectrometry analysis containing the translation start site is shown in bold. **b,** The annotated fragmentation spectra of the MQCFALSQPR peptide are shown. This tryptic peptide is bearing acetylation of the initial methionine as a result of cotranslational modification. The left spectrum shows collision induced dissociation (CID) fragmentation of the double charged peptide with a non-oxidized methionine and m/z ratio of 640.3. The right spectrum depicts fragmentation of the double charged peptide with m/z ratio of 648.3 due to a mass shift caused by oxidation of the initial methionine. Stars indicate the position of parental ions in the MS/MS spectra. Based on the analysis of the CID fragmentation acetylation was assigned to the initial methionine residue. **c,** (i) IP of endogenous AIB1-Δ4 in MCF-7 cells using AIB1-Δ4 specific antibody and detection with AIB1 (5E11) antibody which detects both isoforms of AIB1. (ii) IP of transfected C-terminal FLAG AIB1-Δ4 in HEK293T cells. (iii) Peptide competition assay during IP of AIB1-Δ4 from MCF-7 cells using both a N-acetylated and non-acetylated MQCFALSQPRK peptide. IP was performed as in (i) except 1μg of peptides was added during immunoprecipitation. **d,** The full-length human AIB1 transcript consists of 23 exons. This leads to the creation of a 155 kDa protein consisting of 1424 amino acids. The AIB1-Δ4 transcript lacks exon 4 due to alternative splicing and the resultant protein lacks the N-terminal 223 amino acids of the full-length protein. This results in a 130 kDa protein consisting of 1201 amino acids.

Figure 2. **AIB1-Δ4 is found predominantly in the cytoplasm but can be detected in the nucleus. a,** The distribution of AIB1-Δ4 in nuclear and cytoplasmic fractions from MCF-7 cells was determined with AIB1 (5E11) antibody. HSP90 was used as a cytoplasmic fraction control and HDAC1 as a nuclear

fraction control. **b,** FLAG AIB1-Δ4 localization in the HEK293T cells was determined as in Fig 2a using FLAG M2 antibody for Western blotting. **c,** Chinese Hamster Ovary cells were grown in DMEM F12+10%FBS and transfected with FLAG AIB1 or FLAG AIB1-Δ4. Cells were fixed and stained for FLAG peptide and DAPI and visualized by indirect immunofluorescence. FLAG staining is shown in the left panels (green), DAPI staining DNA in the nucleus is shown in the middle panels (blue), and merge images in the right panels. Typical nuclear, nuclear/cytoplasmic, and cytoplasmic staining is shown in the smaller panels below the larger images. Red, yellow, and blue arrowheads note the nuclear, nuclear/cytoplasmic, and cytoplasmic stained cells shown in the insets below the large field images. The percentage of nuclear, nuclear/cytoplasmic, and cytoplasmic staining cells is graphed. 200 cells were counted per transfection and cell compartment staining was quantified for three separate experiments. Nuclear, nuclear/cytoplasmic, and cytoplasmic stained cells are represented by the black, gray, and white bars respectively. **d,** CHO cells were transfected with FLAG AIB1-Δ4 and treated as in panel c. 24 hours after transfection, either the carrier EtOH or 50 nM leptomycin B (LMB in EtOH) was added to the culture media for 4 hours before fixing and staining cells. The percentage of nuclear, nuclear/cytoplasmic, and cytoplasmic staining cells is shown in the absence and presence of LMB. Cells were quantified as in panel c. Nuclear, nuclear/cytoplasmic, and cytoplasmic stained cells are represented by the black, gray, and white bars respectively. Red arrowheads note the nuclear stained cells in the field of FLAG AIB1-Δ4 transfected cells.

Figure 3. **Overexpression of AIB1 localizes AIB1-Δ4 to the nucleus. a,** CHO cells were transfected with FLAG AIB1-Δ4 alone or with an equal amount of HA-AIB1 and plated on glass cover slips in DMEM F12+10% FBS. Cells were fixed and permeabolized 24 hours after plating and stained for FLAG containing proteins (green), HA tagged proteins (red) and nuclei stained with DAPI (blue). Cells were then analyzed by indirect immunofluorescence. **b,** The number of nuclear, nuclear/cytoplasmic, and cytoplasmic staining cells was quantified for three experiments as in Fig 2c. Data were analyzed by t-test. ***=$p<0.001$ when compared to AIB1-Δ4 transfection alone. **c,** HEK293T cells grown in DMEM+10%FBS were transfected with either FLAG AIB1 alone, AIB1-Δ4 alone, or FLAG AIB1 and AIB1-Δ4 together and lysates were immunoprecipitated using FLAG antibody to pulldown FLAG AIB1 and any interacting proteins.

Figure 4. **Overexpression of p300 localizes AIB1-Δ4 to the nucleus. a,** HEK293T cells were transfected with either p300-HA, FLAG AIB1, or FLAG AIB1-Δ4. Equal amounts of FLAG AIB1 or FLAG AIB1-Δ4 protein were incubated with equal amounts of p300-HA. After immunoprecipitation with HA antibody to pull down p300 and associated proteins, a FLAG Western blot was performed to determine how much AIB1 and AIB1-Δ4 immunoprecipitated with p300. **b,** CHO cells were transfected with FLAG AIB1-Δ4 alone or with an equal amount of p300-HA and plated on glass cover slips in DMEM F12+10% FBS. Cells were fixed and permeabolized 24 hours after plating and stained for DAPI (blue), FLAG (green), and HA (red) containing proteins as in Fig 3b. Cells were then analyzed by indirect immunofluorescence. **c,** The number of nuclear, nuclear/cytoplasmic, and cytoplasmic staining cells was quantified as in Fig 2a. The percentage of nuclear, nuclear/cytoplasmic, and cytoplasmic stained cells is shown in the black, gray, and white bars respectively for three experiments is shown. Data were analyzed by t-test. **=$p<0.01$ when compared to AIB1-Δ4 transfection alone.

Figure 5. **AIB1-Δ4, like AIB1, is recruited to ERE in the nucleus. a,** HEK293 cells grown in phenol red free IMEM + 10% charcoal stripped serum were transfected with either FLAG AIB1 or FLAG AIB1-Δ4 and ERα. 24 hours later cells were stimulated with estrogen and harvested at 0, 15, 30, 45, and 60 minutes after estrogen stimulation. These lysates were subjected to a quantitative ChIP analysis using a FLAG antibody. The percentage of the input recovered after immunoprecipitation for each ERE in pS2, hC3, or HER2 was determined. Data is representative of three independent experiments. The relative amount of transfected proteins and actin after transfection for each time point is shown by Western blot.

b, MCF-7 cells were grown in phenol red free IMEM + 10% charcoal stripped serum for three days before stimulation with 10 nM estrogen. Quantitative ChIP analysis was performed as in a except the immunoprecipitation was carried out with AIB1 antibody or AIB1-Δ4 affinity purified antibodies. Data is representative of two independent experiments. **c,** HEK293 cells were grown as in panel a and total RNA was harvested from cells at 0, 4, 8, and 24 hours after estrogen treatment to determine the relative gene expression for pS2, hC3, and HER2. Data were analyzed by two way ANOVA with Bonferroni post test where *=$p<0.05$ **=$p<0.01$ ***=$p<0.001$ relative to time 0. None of the time points for AIB1 were significantly different. The relative amount of proteins after transfection for each time point is shown by the Western blot.

Figure 6. **The N-terminus of AIB1 contains an inhibitory domain that is lost in AIB1-Δ4. a,** Proposed mechanism of repression of the full-length AIB1 protein. An inhibitor that binds to the N-terminus of AIB1, ordinarily represses its coactivator function. Overexpression of a N-terminal fragment of AIB1 lost in AIB1-Δ4 may bind to the squelching factor, which normally regulates the coactivator function of AIB1 thereby relieving repression on the full-length AIB1 protein. **b,** COS-7 cells were transfected with human progesterone receptor B (25 ng), MMTV luciferase (100 ng), and either pcDNA3 or FLAG AIB1 (500 ng) with increasing amounts of FLAG AIB1 N term (125, 500, 750 ng). 24 hours later cells were treated with 10 nM R5020 for 24 hours before reporter activity was determined. Luciferase values were normalized to TK Renilla (10 ng) reporter activity. The assay was plated in triplicate and a representative graph is shown from three separate experiments. Data were analyzed by one way ANOVA with Tukey's multiple comparison post test. **=$p<0.01$, ***=$p<0.001$ when compared to FLAG AIB1 transfection alone. **c,** The relative amount of FLAG proteins in the COS-7 cells is shown by Western blot.

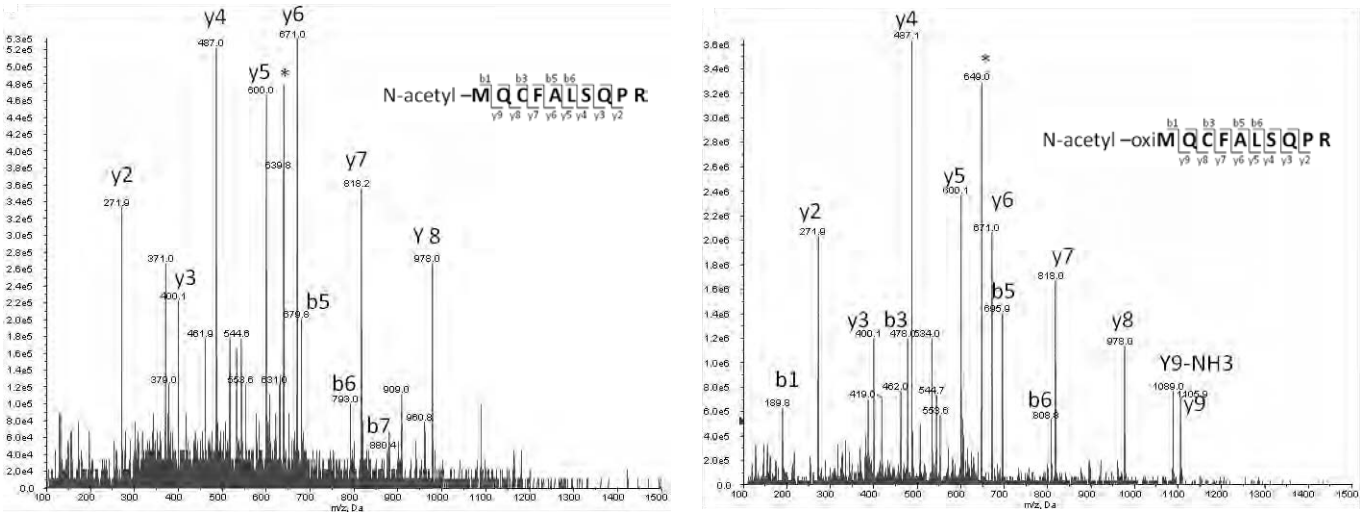
Figure 7. **AIB1-Δ4 expression is increased in metastatic cancer cell lines. a,** A scorpion primer was designed to specifically recognize the unique splice junction of exon 3 and exon 5. The scorpion primer consists of primer (black half arrow), blocker (blue jagged line), quencher (purple octagon), probe (red - exon3, light blue - exon 5), stem (black attached lines), and reporter (green ball). The stem region will only be dissociated when a target sequence is created during the process of PCR. In the case of AIB1, no appropriate target is generated so the preferred conformation is to remain in the stem loop with the reporter quenched. For the AIB1-Δ4 transcript an appropriate target is generated and the probe can then bind its target sequence allowing the reporter to fluoresce. Scorpion primers specific for AIB1-Δ4 transcript had a probe sequence complimentary to the splice junction of exon 3 and 5. Scorpion primers for AIB1 had a probe sequence complimentary to exon 4. **b,** Scorpion primers were used to quantitate the amount of AIB1 and AIB1-Δ4 transcript from the RNA of human mammary epithelial cells (HMEC), parental MDA-MB-231 breast cancer cells and three tissue specific metastatic variants of MDA-MB-231 cells. The Ct values were normalized to actin expression as a control. The ratio of AIB1-Δ4 to AIB1 is shown. Data were analyzed by one way ANOVA with Bonferroni post test. *=$p<0.05$, ***=$p<0.001$ when compared to HMEC. **c,** Scorpion primers were used as in panel b to analyze RNA from parental COLO 357 pancreatic cancer cells and two metastatic variants which metastasized from pancreas to liver (COLO PL) or from spleen to liver (COLO SL). Ct values were normalized to actin expression as a control. The ratio of AIB1-Δ4 to AIB1 is shown. Data were analyzed by one way ANOVA with Newman-Keuls post test. *=$p<0.05$ when compared to parental COLO 357 cells.

Figure 1

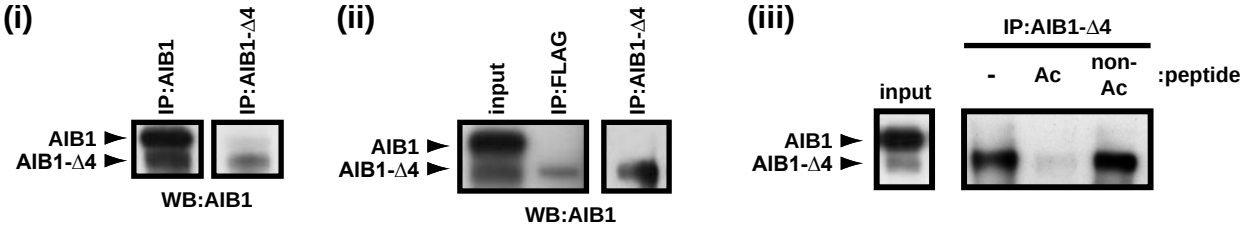
a

MSGLGENLDPLASDSRKRKLPCDTPGQGLTCSGEKRRREQESKYIEELAEL
ISANLSDIDNFNVKPDKCAILKETVRQIRQIKEQGKTISNDDDVQKADVSS
TGQGVIDKDSLGPLLLQALDGFLFVVNRDGNIVFVSENVTQYLQYKQEDLV
NTSVYNILHEEDRKDFLKNLPKSTVNGVSWTNETQRQKSHTFNCRM$_{199}$LM$_{201}$
KTPHDILEDINASPEM$_{217}$RQRYETM$_{224}$QCFALSQPRAM$_{235}$M$_{236}$EEGEDLQSC
M$_{246}$ICVARRITTGERTFPSNPESFITRHDLSGKVVNIDTNSLRSSM$_{289}$RPGF
EDIIRRCIQRFFSLNDGQSWSQKRHYQEAYLNGHAETPVYRFSLADGTIVT
AQTKSKLFRNPVTNDRHGFVSTHFLQREQNGYRPNPNPVGQGIRPPMAGCN
SSVGGMSMSPNQGLQ

b



c



d

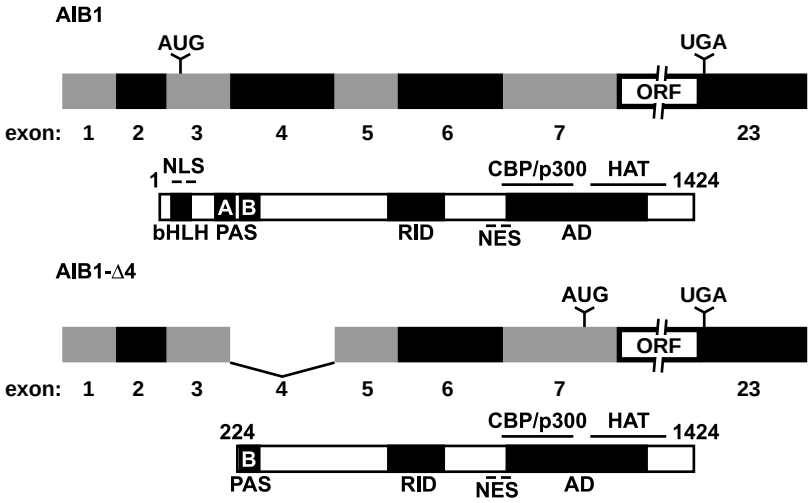


Figure 2

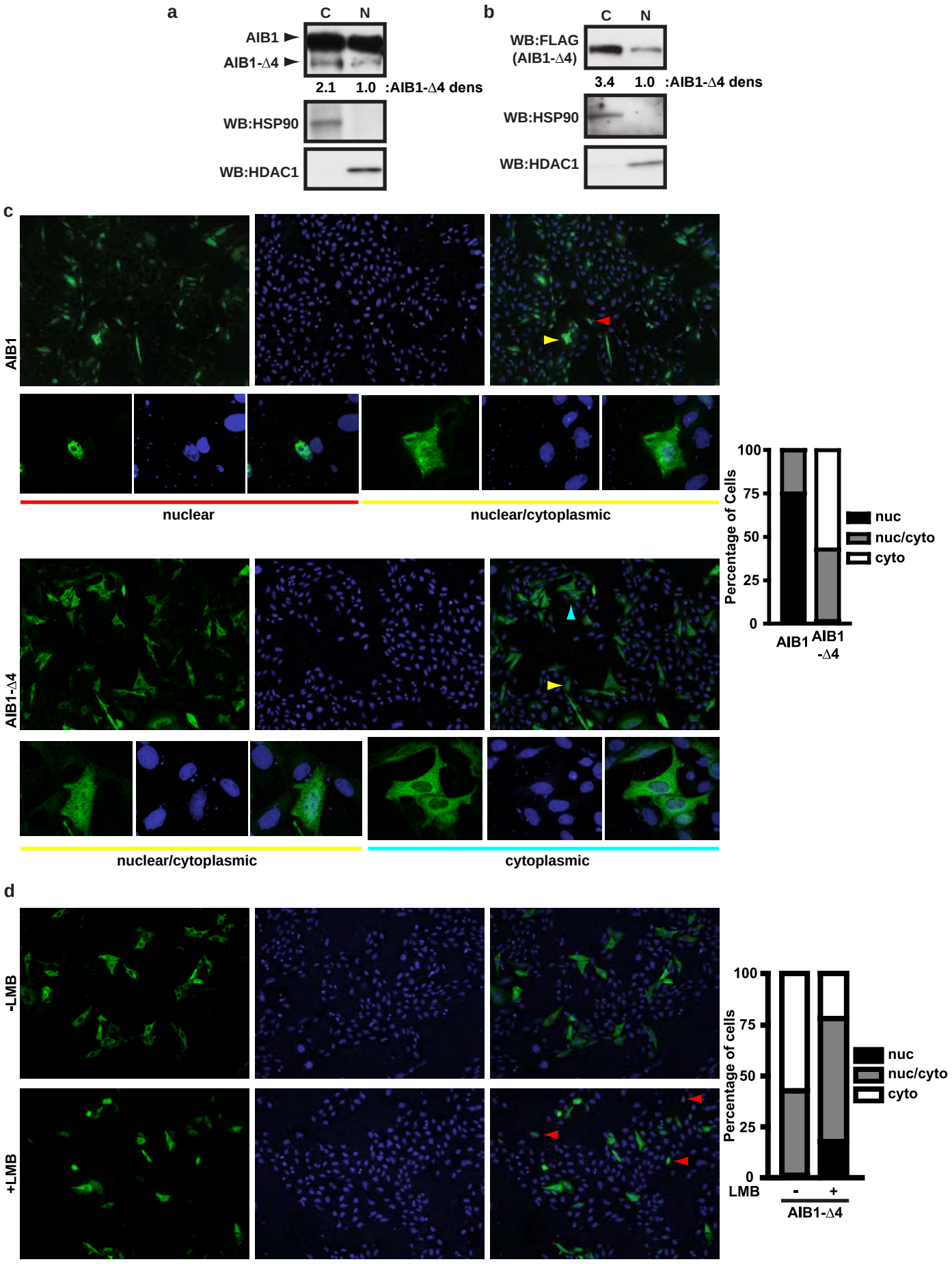
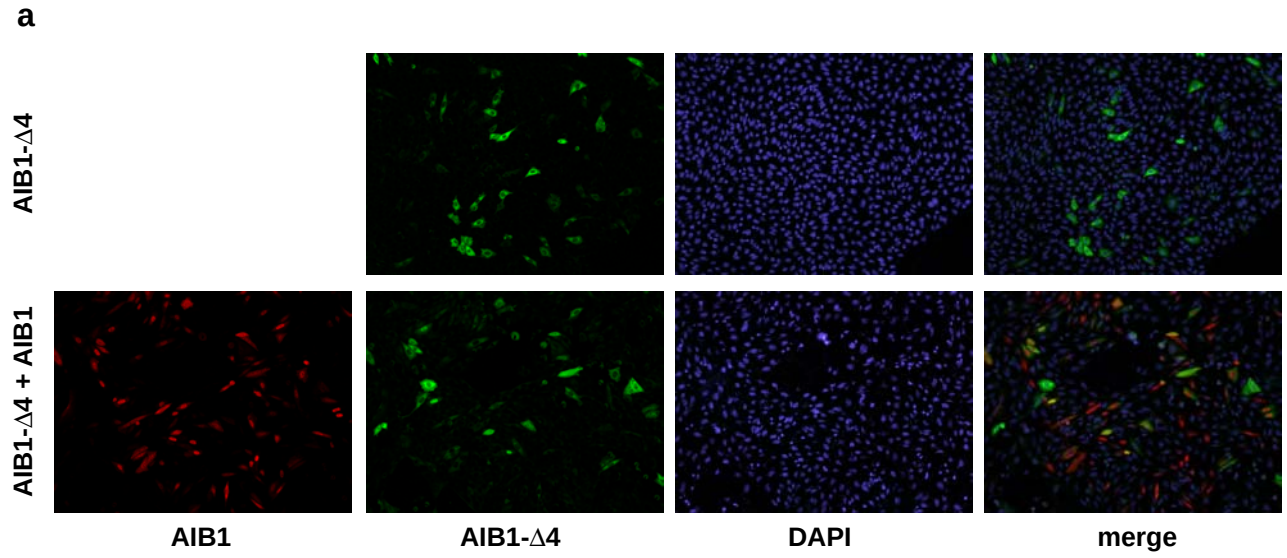
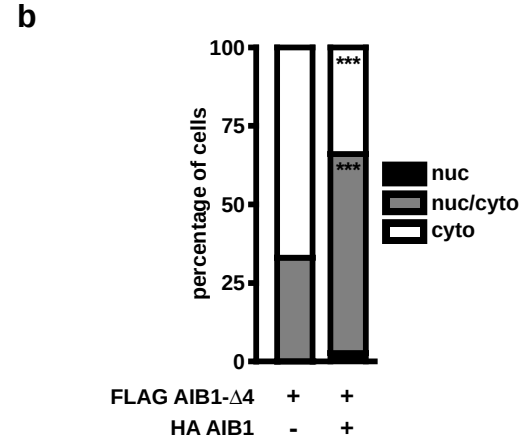

a
C
N
AIB1
AIB1-Δ4
2.1
1.0
:AIB1-Δ4 dens
WB:HSP90
WB:HDAC1
b
C
N
WB:FLAG
(AIB1-Δ4)
3.4
1.0
:AIB1-Δ4 dens
WB:HSP90
WB:HDAC1
c
AIB1
nuclear
nuclear/cytoplasmic
AIB1-Δ4
nuclear/cytoplasmic
cytoplasmic
Percentage of Cells
100
75
50
25
0
AIB1
AIB1 -Δ4
nuc
nuc/cyto
cyto
d
-LMB
+LMB
Percentage of cells
100
75
50
25
0
LMB
-
+
AIB1-Δ4
nuc
nuc/cyto
cyto

Figure 3


a
AIB1-Δ4
AIB1-Δ4 + AIB1
AIB1
AIB1-Δ4
DAPI
merge


b
100
75
50
25
0
percentage of cells
***
***
nuc
nuc/cyto
cyto
FLAG AIB1-Δ4 + +
HA AIB1 - +

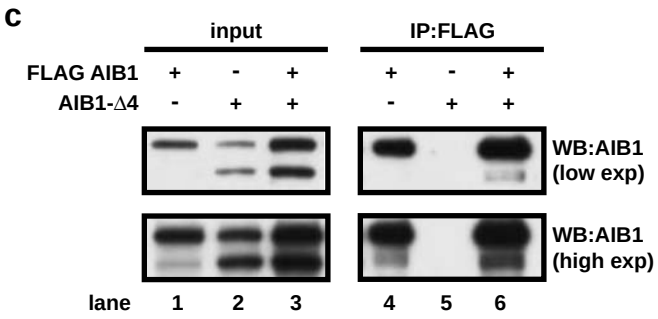

c
input
IP:FLAG
FLAG AIB1 + - + + - +
AIB1-Δ4 - + + - + +
WB:AIB1
(low exp)
WB:AIB1
(high exp)
lane 1 2 3 4 5 6

Figure 4

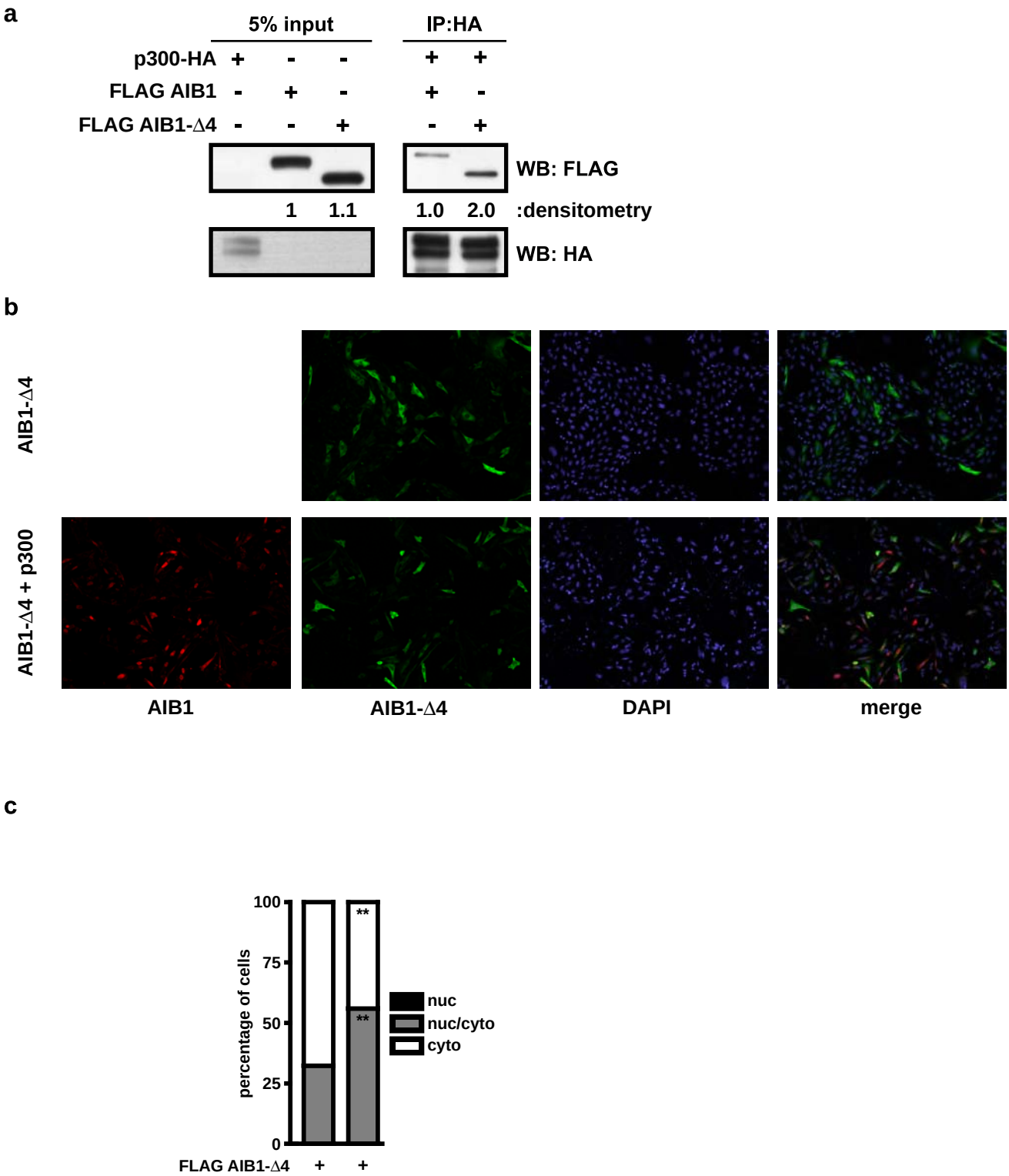

a
5% input
IP:HA
p300-HA + - - + +
FLAG AIB1 - + - + -
FLAG AIB1-Δ4 - - + - +
WB: FLAG
1 1.1 1.0 2.0 :densitometry
WB: HA
b
AIB1-Δ4
AIB1-Δ4 + p300
AIB1
AIB1-Δ4
DAPI
merge
c
100
75
50
25
0
percentage of cells
**
**
nuc
nuc/cyto
cyto
FLAG AIB1-Δ4 + +
p300-HA - +

Figure 5

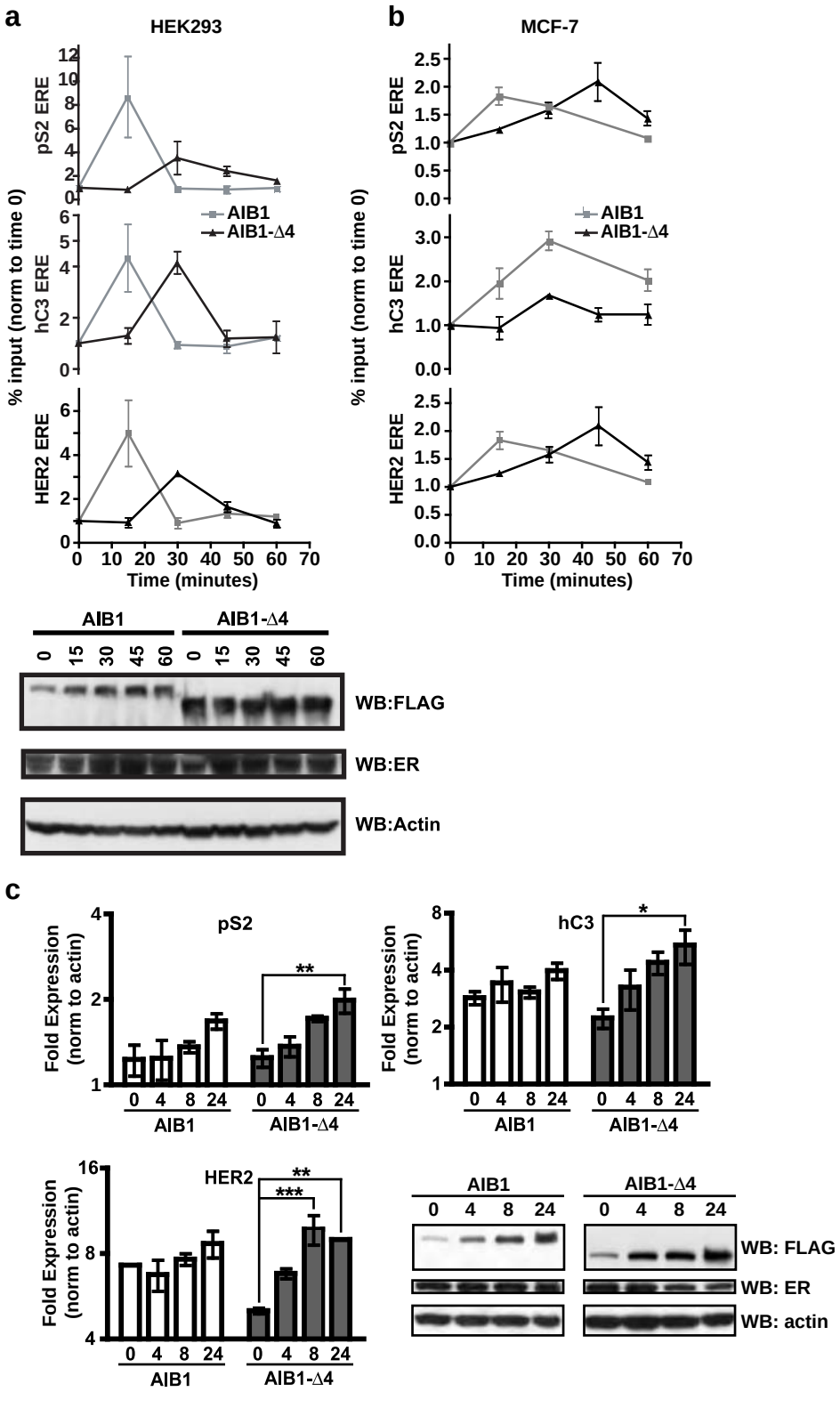
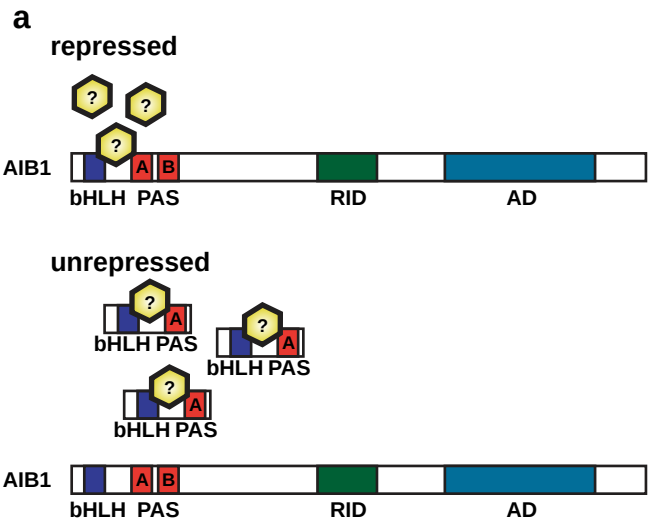
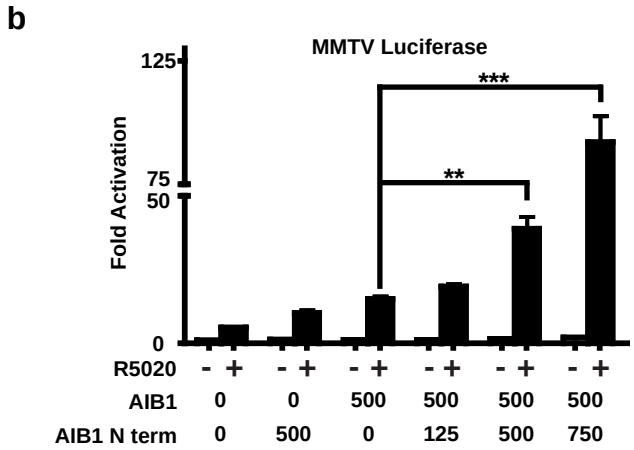

a
HEK293
pS2 ERE
hC3 ERE
HER2 ERE
% input (norm to time 0)
AIB1
AIB1-Δ4
Time (minutes)
b
MCF-7
AIB1
AIB1-Δ4
0 15 30 45 60 0 15 30 45 60
WB:FLAG
WB:ER
WB:Actin
c
pS2
hC3
HER2
Fold Expression (norm to actin)
0 4 8 24 0 4 8 24
AIB1
AIB1-Δ4
WB: FLAG
WB: ER
WB: actin

Figure 6


a
repressed
?
?
?
AIB1
A
B
bHLH PAS
RID
AD
unrepressed
?
A
bHLH PAS
?
A
bHLH PAS
?
A
bHLH PAS
AIB1
A
B
bHLH PAS
RID
AD


b
MMTV Luciferase
125
75
50
0
Fold Activation
***
**
R5020 - + - + - + - + - + - +
AIB1 0 0 500 500 500 500
AIB1 N term 0 500 0 125 500 750

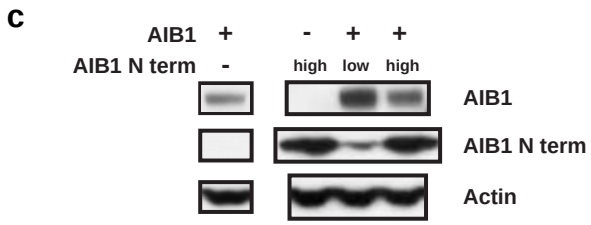
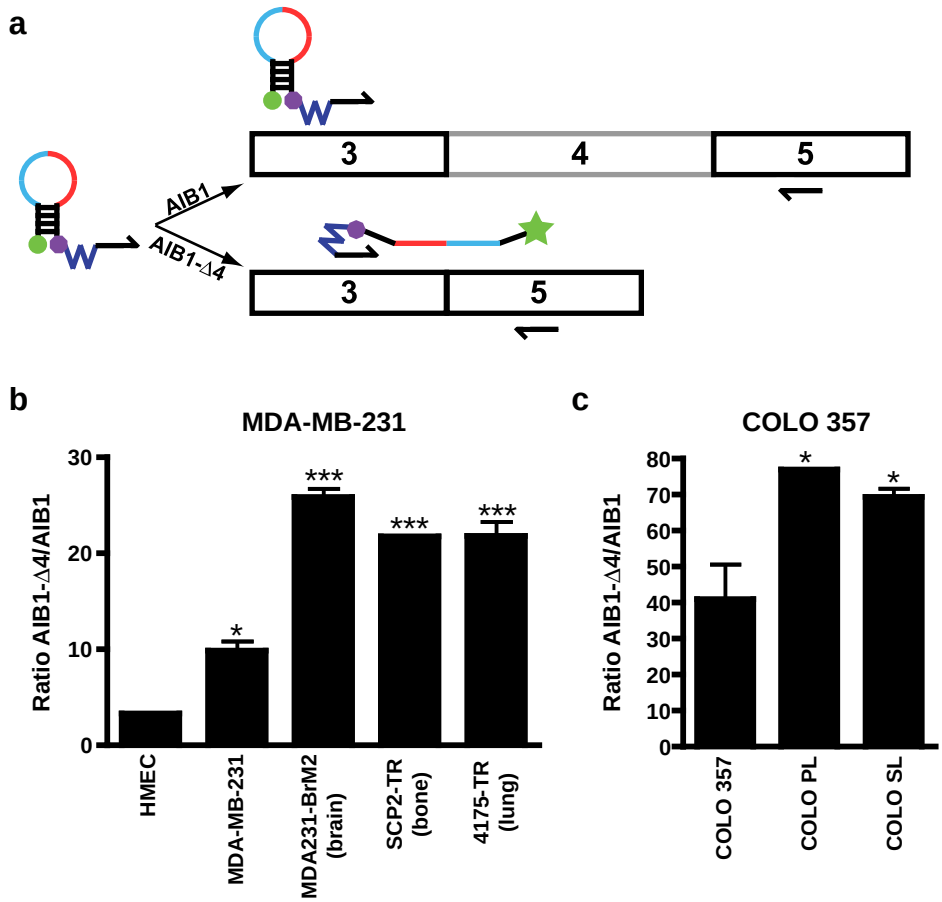

c
AIB1 + - + +
AIB1 N term - high low high
AIB1
AIB1 N term
Actin

Figure 7


a
3
4
5
AIB1
AIB1-Δ4
3
5
b
MDA-MB-231
Ratio AIB1-Δ4/AIB1
30
20
10
0
*
***
***
***
HMEC
MDA-MB-231
MDA231-BrM2 (brain)
SCP2-TR (bone)
4175-TR (lung)
c
COLO 357
Ratio AIB1-Δ4/AIB1
80
70
60
50
40
30
20
10
0
*
*
COLO 357
COLO PL
COLO SL

The New Selective Estrogen Receptor Modulator Bazedoxifene Inhibits Hormone-Independent Breast Cancer Cell Growth and Downregulates Estrogen Receptor α and Cyclin D1

Joan S Lewis-Wambi, Helen Kim, Ramona Curpan, Ronald Grigg, Mohammed A. Sarker, and V. Craig Jordan

Authors' Affiliations: *Women's Cancer Program, Fox Chase Cancer Center, Philadelphia, Pennsylvania (J.S.L.W.); Lombardi Comprehensive Cancer Center, Georgetown University, Washington, DC (V.C.J., H.K.); Institute of Chemistry, Romanian Academy, Timisoara, Romania (R.C.); School of Chemistry, University of Leeds, Leeds, UK (R.G., M.A.S.)*

a) Running Title: **Bazedoxifene inhibits endocrine-resistant breast cancer**

b) Address correspondence to: Dr. Joan Lewis-Wambi, Women's Cancer Program, Fox Chase Cancer Center, 333 Cottman Ave, Philadelphia, PA 19111. Phone: 215-728-4094; Fax: 215-728-4333. Email: joan.lewis@fccc.edu

c) Number of text pages: 22

Number of Tables: 0

Number of Figures: 5

Number of references: 40

Abstract word count: 246

Introduction word count: 607

Discussion word count: 1453

d) ABBREVIATIONS: ERα, estrogen receptor alpha; ERβ, estrogen receptor beta; SERM, selective estrogen receptor modulator; BZA, bazedoxifene acetate; TAM, tamoxifen; RAL, raloxifene; E2, 17β-E2; FUL, fulvestrant; siRNA, small interfering RNA; 4OHT, 4-hydroxytamoxifen; ENDOX, endoxifen; PgR, progesterone receptor; FBS, fetal bovine serum; Luc, luciferase; ERE, estrogen response element; pRT-PCR, quantitative reverse transcriptase-PCR; DMSO, dimethyl sulfoxide; CHX, cycloheximide

Abstract

Bazedoxifene (BZA) is a third generation selective estrogen receptor modulator (SERM) that was recently approved for the prevention and treatment of postmenopausal osteoporosis. It has antitumor activity; however, its mechanism of action remains largely unclear. In the present study, we characterized the effects of BZA and several other SERMs on the proliferation of hormone-dependent MCF-7 and T47D breast cancer cells and hormone-independent MCF-7:5C and MCF-7:2A cells and examined their mechanism of action in these cells. We found that all of the SERMs inhibited the growth of MCF-7 and T47D cells, however, BZA was the only SERM that inhibited the growth of hormone-independent MCF-7:5C and MCF-7:2A cells. Consistent with these growth results, we found that BZA induced G1 blockade in MCF-7:5C and MCF-7:2A cells and it significantly downregulated ERα and cyclin D1 which were constitutively overexpressed in these cells. In addition, siRNA knockdown of ERα and/or cyclin D1 significantly reduced the inhibitory effect of BZA in MCF-7:5C cells. Further analysis revealed that BZA downregulated ERα protein by increasing its degradation and it suppressed cyclin D1 protein and promoter activity in MCF-7:5C cells. Lastly, molecular modeling studies demonstrated that BZA bound to ERα in an orientation similar to raloxifene and had the tendency to form the same contacts with the aminoacids lining the binding cavity. Together, these findings indicate that BZA is distinct from raloxifene and tamoxifen in its ability to inhibit hormone-independent breast cancer cells and its antagonist activity is ERα-dependent and involves down-regulation of cyclin D1.

Introduction

Bazedoxifene acetate (BZA) is a new third generation selective estrogen receptor modulator (SERM) (Silverman et al., 2008) that is approved in Europe and is under regulatory review in the United States for the prevention and treatment of postmenopausal osteoporosis. In phase III clinical trials (Archer et al., 2009; Miller et al., 2008; Pinkerton et al., 2009a) BZA (20 or 40 mg/daily) has been shown to prevent bone loss and to reduce bone turnover in postmenopausal women at risk for osteoporosis, with a favorable endometrial, ovarian, and breast safety profile. BZA also significantly reduces the risk of new vertebral fractures in postmenopausal women with osteoporosis compared to placebo (Silverman et al., 2008). In addition, recent studies indicate that BZA combined with conjugated estrogens relieves hot flashes and improves vulvovaginal atrophy and its symptoms (Kagan et al., 2010).

BZA is an indole-based ER ligand with unique structural characteristics with respect to tamoxifen (TAM) and raloxifene (RAL). It was assembled by using RAL as a template and substituting an indole ring for the benzothiophene core (Komm et al., 2005; Miller et al., 2001). BZA binds to both ER alpha (ERα) and ER beta (ERβ), with a slight higher affinity for ERα, however, it is less ERα selective than RAL, with an affinity for ERα that is about 10-fold lower than 17β-estradiol (E2) (Miller et al., 2001). ERα is a well studied member of the steroid/nuclear receptor family of transcription regulators. ERα acts in the nucleus to regulate gene expression by binding to estrogen response elements (EREs) and related DNA sequences and through association with transcription factors bound at SP1 and AP-1 DNA binding sites. In response to high affinity estrogen binding, ERα dimerizes, binds to ERE DNAs, and undergoes a conformational change in the ligand binding domain that facilitates the recruitment of coactivators. In contrast, antagonist-occupied ERα recruits corepressors. While previous studies

have reported that BZA antagonizes E2-dependent MCF-7 breast cancer cell proliferation *in vitro* (Komm et al., 2005), little is known about the actions of BZA on ERα expression and functionality. Also not known is whether BZA has antitumor activity in breast cancer cells that have acquired resistance to endocrine therapies.

We have previously reported the development of two ERα-positive human breast cancer cell lines; MCF-7:5C (Jiang et al., 1992; Lewis et al., 2005a) and MCF-7:2A (Lewis-Wambi et al., 2008b; Pink et al., 1995) which were clonally selected from hormone-dependent MCF-7 breast cancer cells following long term (> 1 year) estrogen deprivation. An interesting phenotype of MCF-7:5C and MCF-7:2A cells is that, unlike MCF-7 cells which require estrogen to grow and are inhibited by antiestrogens, they do not require estrogen to grow and they undergo apoptosis when exposed to physiologic levels of E2 (Jordan, 2008; Lewis-Wambi et al., 2008b; Lewis et al., 2005a). However, the effects of SERMs on MCF-7:5C and MCF-7:2A cells have not been fully examined. In this study, we investigated the effects of BZA, 4-hydroxytamoxifen (4OHT), endoxifen, raloxifene, and the pure antiestrogen fulvestrant (ICI 182,780) on the growth of MCF-7:5C and MCF-7:2A breast cancer cells and determined the mechanism of action of BZA in these cells. We found that all of the SERMs inhibited E2-stimulated MCF-7 and T47D breast cancer cell growth, however, only BZA significantly inhibited the hormone-independent growth of MCF-7:5C and MCF-7:2A cells. The inhibitory effect of BZA was associated with cell cycle arrest and ERα and cyclin D1 downregulation which was completely reversed by ERα or cyclin D1 suppression. Together, these data show that BZA is distinct from the other members of the SERM family in its ability to inhibit the growth of breast cancer cells that are resistant to long-term estrogen deprivation.

Materials and Methods

Reagents and cell culture. E2, 4-hydroxytamoxifen (4OHT; the active metabolite of TAM), and MG132 were purchased from Sigma Chemical Co. Fulvestrant (ICI 182,780, Faslodex) was a generous gift from Dr. A. E. Wakeling (Zeneca Pharmaceuticals, Macclesfield, United Kingdom). Endoxifen (ENDOX) was a kind gift from Dr James Ingle of the Mayo Clinic (Rochester, Minnesota). Raloxifene (RAL) was a generous gift from Lilly Research Laboratories (Indianapolis, IN). Bazedoxifene acetate (BZA) was synthesized by Drs Ron Grigg and Mohammed Sarker of Leeds University using a previously described protocol (Miller et al., 2001). All of the compounds were dissolved in 100% ethanol except MG132 which was dissolved in dimethyl sulfoxide (DMSO). The compounds were added to the medium such that the total solvent concentration was never higher than 0.1%. An untreated group served as a control. The chemical structures of all of the compounds used in this study are shown in Supplemental Fig. S1.

MCF-7:WS8 and T47D:A18 human mammary carcinoma cells, clonally selected from their parental counterparts for sensitivity to growth stimulation by E2 (Pink and Jordan, 1996), were used in all experiments indicating MCF-7 and T47D cells. Cells were maintained in estrogenized medium [phenol red RPMI 1640 plus 10% fetal bovine serum], but 3 days before all experiments, were cultured in steroid-free media as previously described (Lewis et al., 2005a; Lewis et al., 2005b; Pink and Jordan, 1996). MCF-7:5C (Jiang et al., 1992; Lewis et al., 2005a; Lewis et al., 2005b) and MCF-7:2A cells (Lewis-Wambi et al., 2008b; Pink and Jordan, 1996) were derived from the MCF-7 line by growth in estrogen-free media and two rounds of limiting dilution cloning and were maintained in phenol red-free RPMI 1640 medium containing 10% 3X dextran-coated charcoal treated FBS. MC2 cells were derived by stably transfecting ER-negative

MDA-MB-231 breast cancer cells with the wild-type ERα (Jiang and Jordan, 1992) and these cells were grown in phenol red-free MEM supplemented with 5% 3× dextran-coated charcoal-treated calf serum, 0.5 mg/ml Geneticin. All cell culture reagents were from Invitrogen (Carlsbad, CA).

Cell proliferation assay. These procedures have been previously reported (Lewis et al., 2005; Lewis-Wambi et al., 2008). Briefly, MCF-7 and T47D cells were grown in fully estrogenized medium whereas MCF-7:5C and MCF-7:2A cells were grown in non-estrogenized media. Cells were seeded in 24-well plates (30,000/well) and after overnight incubation cells were treated with various concentrations of the tested compounds for 7 days. Media was changed on days 3 and 5 and the experiment was ended on day 7 and the DNA content of the cells was determined as previously described (Labarca and Paigen, 1980) using a Fluorescent DNA Quantitation kit (Bio-Rad Laboratories, Hercules, CA). Cell proliferation was also determined by cell counting using a hemocytometer.

Western blot analyses. Immunoblotting was performed using 30 μg protein per well as previously described (Lewis et al., 2005a). Membranes were probed with primary antibodies against ERα, PgR, cyclin A, cyclin B1 or cyclin D1 (Santa Cruz Biotechnology) with β-actin (AC-15; Sigma Chemical Co.) used to standardize loading. The appropriate secondary antibody conjugated to horseradish peroxidase (Santa Cruz Biotechnology) was used to visualize the stained bands with an enhanced chemiluminescence (ECL) visualization kit (Amersham, Arlington Heights, IL). Bands were quantitated by densitometry using Molecular Dynamics Software (ImageQuant) and densitometric values were corrected for loading control.

Cell cycle analyses. MCF-7 and MCF-7:5C cells were treated with E2 or BZA for 24 and 48 hours and then fixed using ice-cold 70% ethanol. Cell cycle distribution was determined by

propidium idodide staining using a fluorescence-activated cell sorter (FACS; Becton Dickinson) as previously described (Ariazi et al., 2010). Data was analyzed using FlowJo 7.2.5 for Windows (Tree Star).

Knockdown of ERα and cyclin D1 by siRNA. MCF-7:5C cells were seeded at 1 x 10^5 per well in a 24-well plate and, 24 h later, cells were transfected with nonspecific, ERα, or cyclin D1 (50 nmol/L) small interfering RNA (siRNA; Dharmacon) using Lipofectomine 2000 (Invitrogen), as previously described (Lewis et al., 2005a) Cells were harvested at 48 h for Western blot analysis or at 120 h for cell counting.

Quantitative real-time PCR. The detail procedures have been previously reported (Lewis et al., 2005). MCF-7 and MCF-7:5C cells were treated with either E2 (10^{-9} mol/L) or BZA (10^{-7} mol/L) for 48 h and total RNA was isolated and then reverse transcribed to cDNA using the SuperScript II RNase H-reverse transcriptase system (Invitrogen, Life Technologies, Carlsbad, CA). Aliquots of the cDNA were combined with the SYBR green kit (Superarray) and primers, and assayed in triplicate by quantitative PCR over 40 cycles using a GeneAmp® 5700 Sequence detection system (Applied Biosystems), as previously described (Lewis et al., 2005a). Quantitation was done using the comparative CT method with 18S rRNA as the normalization gene, as previously described (Lewis-Wambi et al., 2008a). PCR primer sequences used were as follow : ERα forward 5'–GGAGGGCAGGGGTGAA–3', ERα reverse 5'–GGCCAGGCTGTTCTTC TTAGA–3'; cyclin D1 forward 5'–TCCTGTGCTGCGA AGTGGAAAC–3', cyclin D1 reverse 5'–AAATCGTGCGGGGTCATTGC; pS2 forward 5–GAGGCCCAGACAGAGACGTG–3, pS2 reverse 5–CCCTGCAGAAGTGTCTAAAATTCA–3.

Transient transfections and luciferase assays. Cells were cultured in estrogen-free RPMI 1640 media for 48 h prior to transfection. On the day of the experiment, cells were seeded in estrogen-free media at a density of 1.5 x 10^5 cells per well in 24-well plates. After 24h, cells were transfected with the firefly luciferase reporter plasmid pERE(5x)TA-ffLuc (containing 5 copies of a consensus ERE and a TATA-box driving firefly luciferase) and the pTA-srLuc Renilla luciferase plasmid (containing a TATA-box element driving renilla luciferase) (Promega) using LT1 (Mirus) transfection reagent, according to the manufacturer's protocol. After 24 hours, transfection reagents were removed and fresh media was added. Cells were then treated with ethanol (vehicle), 10^{-9} M E2, 10^{-8} M BZA, or E2 + BZA combined for 24 h. At the indicated time point, cells were washed, lysed, and ERE luciferase activity was determined using the Dual-Luciferase Reporter Assay System (Promega, Madison, WI) according to the manufacturer's recommendations. Samples were then read on a Mithras MB540 luminometer (Berthold Technologies, Oak Ridge, TN).

For the cyclin D1 promoter assay, MCF-7:5C cells were transiently transfected with the full length cyclin D1 promoter plasmid (-1745CD1-LUC) as previously described (Lewis et al., 2005c; Lewis et al., 2005d). The full length cyclin D1 plasmid (-1745CD1-LUC) (Albanese et al., 1995) was a gift from Dr Richard Pestell.

Molecular Modeling. The molecular modeling performed in this study has previously been described (Maximov et al., 2010). Briefly, the coordinates for the agonist and antagonist conformations of human ERα ligand binding domain co-crystallized with E2 (E2), raloxifene (RAL) and 4-hydroxytamoxifen (4OHT) were extracted from the RCSB Protein Data Bank (PDB) (Berman et al., 2000) Entries 1gwr for E2 (Warnmark et al., 2002), 1err for RAL (Brzozowski et al., 1997) and 3ert for 4OHT (Shiau et al., 1998) were selected for further

modeling and these structures were prepared for docking using the Protein Preparation Workflow (Schrödinger, LLC, New York, NY, 2008) implemented in Schrödinger suite and accessible from within the Maestro 8.5 program (Schrödinger, LLC, New York, NY, 2008). To study the molecular basis of interaction of bazedoxifene in the antagonist conformation of ERα, the ligands were docked into the binding site of the receptor co-crystallized with RAL (PDB code 1err). For comparison reasons, RAL was also docked in its native protein structure.

The input geometries of the ligands were generated with CORINA (online demo, http://www.molecular-networks.com/online_demos/corina_demo) and were further prepared for docking using the LigPrep2.2 utility (LigPrep, version 2.2, Schrödinger, LLC, New York, NY, 2008). The prepared structure of ERα co-crystallized with RAL was used to generate the scoring grid for docking simulations. A grid box of 26 x 26 x 26 $Å^3$ centered on the ligand was created, using the default parameters and without constraints.

Flexible ligand docking simulations were carried out with Glide 5.0 (Glide, version 5, Schrödinger, LLC, New York, NY, 2008) using the default settings and the best 10 poses for each ligand were evaluated using Glide in Standard-Precision (GlideSP) and Extra-Precision (GlideXP) mode. The results obtained from the docking runs were compared and GlideXP docking poses were selected for analysis.

Statistical Analysis. All quantitative experiments were performed in triplicate and/or repeated three times. Data were expressed as mean ± S.D. Statistical significances between vehicle treatment versus drug-treatment were determined by one-way analysis of variance and the Student's *t* test. A value of $p < 0.05$ was considered statistically significant.

Results

BZA Inhibits the Growth of Hormone-Independent MCF-7:5C and MCF-7:2A Breast Cancer Cells. We first compared the growth characteristics of hormone-dependent MCF-7 and T47D breast cancer cells to those of long-term estrogen deprived MCF-7:5C and MCF-7:2A cells in the presence of E2. Cells were grown in estrogen-free media and then treated with 10^{-14} M to 10^{-8} M E2 for 7 days and cellular DNA was measure as an index of growth. In parallel, cells were also treated with 10^{-9} M E2 for 2 to 12 days and then harvested and counted using a hemocytometer. Fig. 1A shows that E2 treatment stimulated the growth of MCF-7 and T47D cells in a concentration-dependent (top panel) and time-dependent manner (bottom panel) with maximum stimulation at 10^{-9} M, however, in MCF-7:5C and MCF-7:2A cells, E2 treatment at similar concentrations had the opposite effect causing either complete growth inhibition in MCF-7:5C cells or partial growth inhibition in MCF-7:2A cells. This current finding is consistent with our previously published work (Lewis-Wambi et al., 2008b; Lewis et al., 2005a) which showed that physiologic concentrations of E2 induced programmed cell death (apoptosis) in MCF-7:5C and MCF-7:2A cells through activation of the mitochondrial death pathway.

Next, we determined the inhibitory effects of BZA and other SERMs (see Supplemental Fig. S1 for chemical structures) on MCF-7, T47D, MCF-7:5C, and MCF-7:2A cells. For experiments, MCF-7 and T47D cells were grown in fully estrogenized media and MCF-7:5C and MCF-7:2A cells were grown in estrogen-free media and then treated with 10^{-12} M to 10^{-6} M BZA, RAL, FUL, 4OHT, or ENDOX for 7 days and cellular DNA was measured as an index of growth. Fig. 1B shows that all of the tested SERMs along with the pure antiestrogen FUL inhibited E2-stimulated growth in MCF-7 and T47D cells and hormone-independent growth in MCF-7:2A cells in a concentration-dependent manner, however, in MCF-7:5C cells, only BZA and FUL

inhibited the growth of these cells with no effects observed with RAL, 4OHT, and ENDOX. BZA reduced the growth of MCF-7:5C cells in a concentration dependent manner causing an 80% reduction at 10^{-8} M whereas FUL reduced the growth by 55% at similar concentration.

BZA Downregulates ERα Protein in MCF-7:5C and MCF-7:2A Cells. Since BZA dramatically reduced the growth of MCF-7:5C cells, we next determined whether BZA had actions similar to that of 4OHT or FUL at the level of ERα stability/degradation. We treated MCF-7:5C, MCF-7:2A, MCF-7, and T47D cells with 10^{-9} M E2 or 10^{-7} M FUL, 4OHT, RAL, or BZA for 24 hours and monitored ERα protein level. As shown in Fig. 2A, ERα protein was highly expressed in MCF-7:5C and MCF-7:2A cells compared to MCF-7 and T47D cells and treatment with BZA dramatically downregulated ERα protein in MCF-7:5C and MCF-7:2A cells however it did not significantly reduce ERα levels in MCF-7 and T47D cells. The ability of BZA to downregulate ERα protein in MCF-7:5C and MCF-7:2A cells was greater than that of RAL and almost comparable to that of the pure antiestrogen ICI 182780 (FUL) which completely downregulated ERα in all of the cell lines. E2 treatment also markedly down-regulated ERα protein in MCF-7:5C cells and the other cell lines (Fig. 2A), however, 4OHT stabilized ERα against degradation in MCF-7 and T47D cells (Fig. 2A), which is consistent with previous studies (Pink and Jordan, 1996). We also examined the effect of the tamoxifen metabolite, endoxifen, on ERα expression in the different cell lines and found that endoxifen failed to down-regulate ERα in all of the tested cell lines (Supplemental Fig. S2). Our finding differs from that of Wu and coworkers (2009) who reported that endoxifen downregulated ERα in breast cancer cells.

We also performed dose response and time response studies in MCF-7:5C and MCF-7 cells to determine the concentration and time of BZA treatment that optimally downregulated ERα protein. Fig. 2B showed that BZA reduced ERα protein levels in MCF-7:5C cells in a concentration dependent manner with maximum inhibition at 10^{-6} M and this down-regulation was observed as early as 4 hours after treatment (Fig. 2C, top). BZA also downregulated ERα mRNA levels in MCF-7:5C cells compared to control and this level of inhibition was comparable to that of fulvestrant (Fig. 2C, bottom). To show that the decreased ERα protein by BZA was due to protein degradation, we used MG132 to inhibit the proteosome in MCF-7:5C and MCF-7 cells. We found that inhibition of proteosome activity completely blocked ERα degradation in response to BZA and E2 with partial reversal with fulvestrant (Fig. 2D). We further determined whether BZA might affect ERα protein expression by inhibiting its synthesis. We treated MCF-7:5C cells with 0.5 to 5.0 μM cycloheximide (CHX) for 4 h to address this question. The impact of CHX on ERα protein expression was much less dramatic than that of BZA (data not shown), which suggest that BZA-induced down-regulation of ERα protein is not likely to involve protein synthesis inhibition. Together, these data show that BZA downregulates ERα and that it differs from other SERMs in its ability to regulate cell growth and ERα protein expression.

BZA Inhibits ERα Transcriptional Activity in MCF-7:5C Cells. To determine whether BZA blocks ERα function, we next examined the transcriptional activation of an estrogen response element (ERE) in MCF-7, T47D, 5C, and 2A cells. For experiment, cells were transiently transfected with an ERE-luciferase reporter plasmid and treated for 24 h with 10^{-10} M E2 or 10^{-8} M BZA either alone or in combination with E2. The results of these studies showed that the ERE was activated maximally by E2 in all of the cell lines with T47D showing the most robust E2

response (Fig. 3A). BZA, as an individual treatment, reduced basal ERE luciferase activity in MCF-7:5C and MCF-7:2A cells and in combination with E2 was able to completely block E2-induced ERE activity in these cells (Fig. 3A).

To further test whether BZA is able to block E2 activation of endogenous genes, we analyzed the expression level of pS2 mRNA in MCF-7:5C cells using qRT-PCR. The pS2 gene is often used as a prognostic marker in breast cancer cells and is frequently used in studies of ER action. Furthermore, it is suggested that estrogen regulates the expression of pS2 through an imperfect ERE in the pS2 promoter (Berry et al., 1989). Our results showed that basal pS2 mRNA level was ~3.5-fold higher in MCF-7:5C cells compared to wild-type MCF-7 cells and E2 treatment further increased basal pS2 mRNA level in MCF-7 and MCF-7:5C cells which was completely blocked by BZA (Fig. 3B). Notably, we also found that siRNA knockdown of ERα (Fig. 3C) significantly reduced the basal proliferation of MCF-7:5C cells and markedly reduced the responsiveness of these cells to BZA (Fig. 3C, bottom). Suppression of ERα also significantly reduced cyclin D1 protein levels in MCF-7:5C cells. Overall, these results show that BZA is a potent antiestrogen capable of blocking ERα-mediated transcriptional activation in hormone-independent breast cancer cells and that its inhibitory effect is ERα-dependent.

BZA blocks cell cycle progression in MCF-7:5C cells and downregulates cyclin D1. Since BZA significantly reduced the growth of MCF-7:5C cells, we next examined its effect on cell cycle progression. For experiment, MCF-7 and MCF-7:5C cells were treated with 10^{-9} M E2, 10^{-8} M BZA, or E2 plus BZA for 48 h followed by propidium iodide staining and flow cytometric analysis. The results showed that in MCF-7:5C cells, BZA treatment increased the proportion of cells in G0/G1 phase from 60% (control) to 81% at 48 h and it reduced the proportion of S phase cells from 33% to 9%, however, in MCF-7 cells, E2 treatment increased the proportion of S-

phase cells from 19% to 42% at 48 h with no effect observed with BZA alone (Fig. 4A). Notably, the inhibitory effect of BZA on cell cycle in MCF-7:5C cells was almost comparable to that of fulvestrant; however, none of the other SERMs induced G1 arrest in these cells (data not shown).

The G-1–induced cell cycle block in MCF-7:5C cells was further investigated by measuring protein expression of G_1-phase–specific cyclin D1. MCF-7 and MCF-7:5C cells were treated with E2, BZA, RAL, 4OHT or FUL and then collected at 24 h for immunoblotting analysis. Fig. 4B shows that in parental MCF-7 cells, treatment with E2 increased cyclin D1 protein ~5-fold above control with significant induction with 4OHT and BZA, however, in MCF-7:5C cells, cyclin D1 protein was constitutively overexpressed and treatment with BZA dramatically reduced basal cyclin D1 protein to an almost undetectable level. Notably, none of the other tested compounds including the pure antiestrogen fulvestrant had any significant affect on cyclin D1 protein in MCF-7:5C cells (Fig. 4B, bottom). Further analysis showed that the inhibitory effect of BZA on cyclin D1 occurred as early as 2 h and persisted up to 24 hours (Fig. 4C, top left). BZA also completely reduced constitutive cyclin D1 mRNA level (Fig. 4C, bottom) and cyclin D1 promoter activity (Fig. 4C, top right) in MCF-7:5C cells compared to parental MCF-7 cells and it completely blocked cyclin D1 induction by E2 in these cells. Lastly, we found that siRNA knockdown of cyclin D1 significantly reduced the basal growth of MCF-7:5C cells and it significantly reduced the inhibitory effect of BZA in these cells (Fig. 4D). It should be noted that cyclin D1 protein was also significantly reduced in MCF-7:5C cells due to ERα knockdown (Fig. 3D), thus suggesting an important collaboration between cyclin D1 and ERα in mediating the growth inhibitory effect of BZA in MCF-7:5C cells.

Molecular modeling and docking of BZA into the ligand binding site of ERα. Molecular modeling and docking studies were carried out in an attempt to predict the bioactive

conformation of BZA and to understand the molecular basis of interaction of this ligand with ERα. Therefore, using the available X-ray crystallographic data, the flexible docking of BZA into the ligand binding domain (LBD) of ERα co-crystallized with RAL was performed and for comparison reasons, FUL and RAL were also docked in their native protein structure. The superimposition of the docked solution and experimental structure of RAL shows that the docking model recapitulates the orientation of the native ligand in the active site and the same interactions with the key aminoacids of the binding cavity are formed (ligand RMSD of 0.362 when compared with the crystal structure; Supplemental Fig. S3A–upper left panel). The experimental structure of ERα co-crystallized with E2 (PDB code 1gwr), the agonist conformation of the receptor, is displayed in Fig. 5A, while the experimental antagonist conformations of ERα bound to 4OHT and RAL are superimposed and also presented in Fig. 5B, to emphasize the differences between these agonist and antagonist conformations of ERα. The docking results analysis demonstrates that BZA binds to ERα in an orientation similar with RAL (Fig. 5C), i.e. to the antagonist conformation of the receptor and has the tendency to form the same hydrophobic contacts with the aminoacids lining the binding cavity. Also, the same complex H-bond network is formed with D351, E353, R394, H524 and a highly ordered water molecule, located in the vicinity of residues E353 and R394 (Fig. 5C). Additionally, the docked structure of BZA was compared with the binding mode of 4OHT to ERα (Fig. 5B) and it was superimposed in the binding site of 4OHT-ERα complex (Fig. 5D). It is interesting to note that for the 4OHT bound receptor (Fig. 5B), the H-bond between BZA and H524 is missing (Fig. 5D) due to the different orientation of this aminoacid in the binding site compared with the RAL-ERα complex (Fig. 5B). When FUL was docked to RAL-ERα complex, the H-bond network was recapitulated with one exception, the interaction with D351 is missing, while the flexible side

chain of FUL fills the groove between helix 3 and helix 12 (Supplemental Fig. S3B and Fig. S3C). It can be concluded that BZA binds to the antagonist conformation of ERα LBD, in a similar alignment with RAL not 4OHT or FUL, and forms, basically, the same favorable hydrophobic and hydrophilic interactions with the key aminoacids of ERα binding site.

Discussion

While TAM (Cuzick et al., 2003; Fisher et al., 1998) and RAL (Vogel et al., 2010) are the best known of the SERMs, promising results have been observed with the targeted development of newer and more tissue-specific SERMs, many of which are under investigation for postmenopausal osteoporosis. Of the newer SERMs in development, Phase 3 clinical data have shown that BZA is effective in preventing and treating postmenopausal osteoporosis, without adverse effects on the endometrium or breast (Archer et al., 2009). BZA in combination with conjugated estrogens has also been shown to relieve hot flashes and improve vulvovaginal atrophy and its symptoms (Kagan et al., 2010; Pinkerton et al., 2009b). In the present study, we report for the first time that BZA, in addition to inhibiting the growth of hormone-dependent MCF-7 and T47D breast cancer cells, also inhibits the growth of breast cancer cells that have acquired resistance to long-term estrogen deprivation (i.e. hormone-independent/aromatase inhibitor resistant). Specifically, we found that BZA at 10^{-8} M inhibited the growth of hormone-independent MCF-7:5C breast cancer cells by ~75-85% and this inhibitory effect was associated with G1 arrest and cyclin D1 and ERα down-regulation. BZA also completely blocked E2-induced ERE luciferase activity and reduced basal pS2 mRNA levels in MCF-7:5C and MCF-7:2A cells. BZA was the only SERM capable of inhibiting hormone-independent growth of MCF-7:5C cells with no effects observed with 4OHT, endoxifen, or RAL (Fig. 1B). Notably, our molecular modeling studies indicated that BZA bound the ligand binding domain of ERα in an antagonist orientation similar to RAL (Fig. 5C), but distinct from 4OHT (Fig. 5D) and fulvestrant (Supplemental Fig. S3B and Fig. S3C), and it formed the same network of H-bond contacts as RAL with the aminoacids lining the binding cavity of the receptor. It should be noted that BZA and RAL are similar in structure (Supplemental Fig. S1), however, despite their

similarities, there are reported structural differences between them (Komm et al., 2005; Miller et al., 2001). In particular, BZA possesses a core binding domain that consists of a 2-phenyl-3-methyl indole whereas RAL has a benzothiophene core and TAM has a trans-stilbene core. Additionally, the side chain affecter region of BZA is connected to the core binding region via a methylene hinge, whereas RAL has its side chain connected via a carbonyl hinge and TAM has its side chain directly connected to its core binding region and. Finally, BZA contains a hexamethylenamine ring at the side chain terminus whereas RAL and TAM contain a piperidine ring and dimethylamine, respectively (Miller et al., 2001). These structural differences are thought to explain the 10-fold lower binding affinity of BZA for ERα compared to RAL (IC_{50} of 26 nM versus 2.4 nM), however, these differences do not appear to affect the potency of BZA as an antagonist in breast cancer cells, as demonstrated in this study. Indeed, these findings help to further distinguish BZA from the other SERMs such as TAM and RAL and they support the concept that subtle but moderate structural differentiation can dramatically impact the ability of a ligand to regulate cell proliferation.

Previous research has indicated that deregulation of ERα expression is a driving force in the initiation and progression of estrogen-sensitive breast tumors (Garcia-Closas and Chanock, 2008; Garcia-Closas et al., 2008). Indeed, it has been suggested that alterations in pathways leading to ERα synthesis and/or degradation underlie the deregulation of ERα and its consequent manifestations, including enhanced proliferation in breast tumors (Sommer and Fuqua, 2001). ERα is the predominant receptor isoform expressed in breast cancer cells, and increased numbers of ERα-expressing cells as well as increased individual cell ERα content can be observed at the earliest stages of breast tumorigenesis. Previously, we have shown that ERα mRNA and protein levels are significantly elevated in breast cancer cells that have been adapted to grow in an

estrogen-depleted environment (Lewis et al., 2005a; Murphy et al., 1990; Pink et al., 1996). This particular type of regulation in which ERα levels are increased following estrogen deprivation has been described as a Model I response (Pink and Jordan, 1996). A Model I response is characterized by an ERα that is expressed at high levels in the absence of estrogen and is subsequently down-regulated following estrogen binding, primarily through repression of the steady-state level of the mRNA. In the present study, we found that basal ERα protein levels were upregulated greater than 2-fold in hormone-independent MCF-7:5C and MCF-7:2A breast cancer cells compared to MCF-7 cells and treatment with BZA (10^{-8} M) induced proteasome-mediated degradation of ERα in these cells which was reversed by the broad spectrum proteasome inhibitor MG132. The ability of BZA to degrade ERα in MCF-7:5C cells was rapid and robust occurring as early as 4 h after treatment with maximum degradation at 24 h and it was comparable to the pure antiestrogen fulvestrant which also completely degraded ERα. Notably, BZA and fulvestrant were the only compounds that markedly reduced the growth of both MCF-7:5C and MCF-7:2A breast cancer cells and blocking BZA-induced ERα degradation with MG132 dramatically reduced its growth inhibitory effects on these cells (data not shown). The importance of ERα in mediating the antagonist effects of BZA in hormone-independent MCF-7:5C cells was further confirmed by siRNA knockdown experiments which showed a 60% reduction in the ability of BZA to inhibit the growth of these cells. Suppression of ERα also significantly reduced the basal growth of MCF-7:5C cells and E2-induced growth in wild-type MCF-7 cells, which is consistent with recent findings by Ariazi and coworkers (Ariazi et al., 2010). It should be noted; however, that degradation or suppression of ERα is not the only mechanism by which an antagonist can inhibit cell proliferation. For example, TAM has been shown to stabilize ERα protein against degradation in breast cancer cells (Murphy et al., 1990;

Pink et al., 1996; Pink et al., 1995; Pink and Jordan, 1996), however, it is a potent antagonist in the breast with the ability to block E2-stimulated proliferation and E2-induced ERE activity in these cells. Based on these findings, we speculate that, in the absence of estrogen, the unliganded ERα drives the proliferation of hormone-independent breast cancer cells; however, in the presence of BZA, the ability to inhibit cell proliferation is dependent on receptor degradation.

Apart from ERα, BZA also significantly reduced cyclin D1 expression in MCF-7:5C breast cancer cells. Specifically, we found that cyclin D1 protein was constitutively overexpressed by 3-to 5-fold in hormone-independent MCF-7:5C cells compared to wild-type MCF-7 cells and treatment with BZA completely reduced it to an undetectable level. In addition, we found that suppression of cyclin D1 reduced the basal growth of MCF-7:5C cells and it significantly reduced the inhibitory effect of BZA in these cells. Suppression of cyclin D1 also significantly reduced ERα protein levels in MCF-7:5C cells with similar effects observed following ERα suppression, thus suggesting a link between cyclin D1 and ERα in these cells. Cyclin D1 is a breast cancer oncogene whose overexpression has been linked to poor prognosis in ERα and PgR-positive breast cancers (Lammie and Peters, 1991). It is a multifunctional G_1-phase cyclin whose regulatory effects are particularly important in breast development and cancer (Sutherland and Musgrove, 2004). Cyclin D1 is regulated by estrogen and progesterone (Said et al., 1997) and it contributes to poor treatment response of ER-positive tumors by acting downstream to promote hormone agonist- and antagonist-independent proliferation (Wilcken et al., 1997). There is also evidence that cyclin D1 can interact with ER coactivators to activate estrogen response element (ERE) in a ligand-independent manner (Zwijsen et al., 1997) and this interaction is not inhibited by antiestrogens (Zwijsen et al., 1997). Notably, we found that BZA not only reduced basal cyclin D1 protein and mRNA levels but also completely reduced its promoter activity in

hormone-independent MCF-7:5C cells and these changes were associated with decreased cell proliferation. In contrast, RAL, 4OHT, endoxifen, and FUL failed to inhibit cyclin D1 expression in MCF-7:5C cells, and these compounds, with the exception of fulvestrant, did not have any growth inhibitory effect in MCF-7:5C cells.

In conclusion, it is clear from clinical data that BZA in combination with conjugated estrogens represents a new form of therapeutic agents for the treatment of postmenopausal symptoms and prevention of postmenopausal osteoporosis. The fact that it does not stimulate the breast or endometrium and is very effective at inhibiting the proliferation of endocrine-resistant breast cancer cells highlights its widespread therapeutic potential and demonstrates that not all SERMs are alike. Our data also suggest that the overexpression of ERα and cyclin D1 in MCF-7:5C cells might be driving the hormone-independent growth of these cells and that the ability of BZA to down-regulate ERα and cyclin D1 is critical to treat and possibly reverse antihormone resistance in breast cancer.

Acknowledgments

We thank Dr James Ingle for the endoxifen compound and Drs Richard Pestell and Chris Albanese for the full-length cyclin D1 promoter plasmid.

Authorship Contributions

Participated in research design: Lewis-Wambi and Jordan.

Conducted experiments: Lewis-Wambi and Kim.

Performed data analysis: Lewis-Wambi.

Wrote or contributed to the writing of the manuscript: Lewis-Wambi and Jordan.

Other: Grigg and Sarker synthesized the Bazedoxifene compound and Curpan performed the molecular modeling studies.

References

Albanese C, Johnson J, Watanabe G, Eklund N, Vu D, Arnold A and Pestell RG (1995) Transforming p21ras mutants and c-Ets-2 activate the cyclin D1 promoter through distinguishable regions. *J Biol Chem* **270**:23589-23597.

Archer DF, Pinkerton JV, Utian WH, Menegoci JC, de Villiers TJ, Yuen CK, Levine AB, Chines AA and Constantine GD (2009) Bazedoxifene, a selective estrogen receptor modulator: effects on the endometrium, ovaries, and breast from a randomized controlled trial in osteoporotic postmenopausal women. *Menopause* **16**:1109-1115.

Ariazi EA, Brailoiu E, Yerrum S, Shupp HA, Slifker MJ, Cunliffe HE, Black MA, Donato AL, Arterburn JB, Oprea TI, Prossnitz ER, Dun NJ and Jordan VC (2010) The G protein-coupled receptor GPR30 inhibits proliferation of estrogen receptor-positive breast cancer cells. *Cancer Res* **70**:1184-1194.

Berman HM, Westbrook J, Feng Z, Gilliland G, Bhat TN, Weissig H, Shindyalov IN and Bourne PE (2000) The Protein Data Bank. *Nucleic Acids Res* **28**:235-242.

Berry M, Nunez AM and Chambon P (1989) Estrogen-responsive element of the human pS2 gene is an imperfectly palindromic sequence. *Proc Natl Acad Sci U S A* **86**:1218-1222.

Brzozowski AM, Pike AC, Dauter Z, Hubbard RE, Bonn T, Engstrom O, Ohman L, Greene GL, Gustafsson JA and Carlquist M (1997) Molecular basis of agonism and antagonism in the oestrogen receptor. *Nature* **389**:753-758.

Cuzick J, Powles T, Veronesi U, Forbes J, Edwards R, Ashley S and Boyle P (2003) Overview of the main outcomes in breast-cancer prevention trials. *Lancet* **361**:296-300.

Fisher B, Costantino JP, Wickerham DL, Redmond CK, Kavanah M, Cronin WM, Vogel V, Robidoux A, Dimitrov N, Atkins J, Daly M, Wieand S, Tan-Chiu E, Ford L and Wolmark N (1998) Tamoxifen for prevention of breast cancer: report of the National Surgical Adjuvant Breast and Bowel Project P-1 Study. *J Natl Cancer Inst* **90**:1371-1388.

Garcia-Closas M and Chanock S (2008) Genetic susceptibility loci for breast cancer by estrogen receptor status. *Clin Cancer Res* **14**:8000-8009.

Garcia-Closas M, Hall P, Nevanlinna H, Pooley K, Morrison J, Richesson DA, Bojesen SE, Nordestgaard BG, Axelsson CK, Arias JI, et al. (2008) Heterogeneity of breast cancer associations with five susceptibility loci by clinical and pathological characteristics. *PLoS Genet* **4**:e1000054.

Jiang SY and Jordan VC (1992) Growth regulation of estrogen receptor-negative breast cancer cells transfected with complementary DNAs for estrogen receptor. *J Natl Cancer Inst* **84**:580-591.

Jiang SY, Wolf DM, Yingling JM, Chang C and Jordan VC (1992) An estrogen receptor positive MCF-7 clone that is resistant to antiestrogens and estradiol. *Mol Cell Endocrinol* **90**:77-86.

Jordan VC (2008) The 38th David A. Karnofsky lecture: the paradoxical actions of estrogen in breast cancer--survival or death? *J Clin Oncol* **26**:3073-3082.

Kagan R, Williams RS, Pan K, Mirkin S and Pickar JH (2010) A randomized, placebo- and active-controlled trial of bazedoxifene/conjugated estrogens for treatment of moderate to severe vulvar/vaginal atrophy in postmenopausal women. *Menopause* **17**:281-289.

Komm BS, Kharode YP, Bodine PV, Harris HA, Miller CP and Lyttle CR (2005) Bazedoxifene acetate: a selective estrogen receptor modulator with improved selectivity. *Endocrinology* **146**:3999-4008.

Labarca C and Paigen K (1980) A simple, rapid, and sensitive DNA assay procedure. *Anal Biochem* **102**:344-352.

Lammie GA and Peters G (1991) Chromosome 11q13 abnormalities in human cancer. *Cancer Cells* **3**:413-420.

Lewis-Wambi JS, Cunliffe HE, Kim HR, Willis AL and Jordan VC (2008a) Overexpression of CEACAM6 promotes migration and invasion of oestrogen-deprived breast cancer cells. *Eur J Cancer* **44**:1770-1779.

Lewis-Wambi JS, Kim HR, Wambi C, Patel R, Pyle JR, Klein-Szanto AJ and Jordan VC (2008b) Buthionine sulfoximine sensitizes antihormone-resistant human breast cancer cells to estrogen-induced apoptosis. *Breast Cancer Res* **10**:R104.

Lewis JS, Meeke K, Osipo C, Ross EA, Kidawi N, Li T, Bell E, Chandel NS and Jordan VC (2005a) Intrinsic mechanism of estradiol-induced apoptosis in breast cancer cells resistant to estrogen deprivation. *J Natl Cancer Inst* **97**:1746-1759.

Lewis JS, Osipo C, Meeke K and Jordan VC (2005b) Estrogen-induced apoptosis in a breast cancer model resistant to long-term estrogen withdrawal. *J Steroid Biochem Mol Biol* **94**:131-141.

Lewis JS, Thomas TJ, Pestell RG, Albanese C, Gallo MA and Thomas T (2005c) Differential effects of 16alpha-hydroxyestrone and 2-methoxyestradiol on cyclin D1 involving the transcription factor ATF-2 in MCF-7 breast cancer cells. *J Mol Endocrinol* **34**:91-105.

Lewis JS, Vijayanathan V, Thomas TJ, Pestell RG, Albanese C, Gallo MA and Thomas T (2005d) Activation of cyclin D1 by estradiol and spermine in MCF-7 breast cancer cells: a mechanism involving the p38 MAP kinase and phosphorylation of ATF-2. *Oncol Res* **15**:113-128.

Maximov PY, Myers CB, Curpan RF, Lewis-Wambi JS and Jordan VC (2010) Structure-function relationships of estrogenic triphenylethylenes related to endoxifen and 4-hydroxytamoxifen. *J Med Chem* **53**:3273-3283.

Miller CP, Collini MD, Tran BD, Harris HA, Kharode YP, Marzolf JT, Moran RA, Henderson RA, Bender RH, Unwalla RJ, Greenberger LM, Yardley JP, Abou-Gharbia MA, Lyttle CR and Komm BS (2001) Design, synthesis, and preclinical characterization of novel, highly selective indole estrogens. *J Med Chem* **44**:1654-1657.

Miller PD, Chines AA, Christiansen C, Hoeck HC, Kendler DL, Lewiecki EM, Woodson G, Levine AB, Constantine G and Delmas PD (2008) Effects of bazedoxifene on BMD and bone turnover in postmenopausal women: 2-yr results of a randomized, double-blind, placebo-, and active-controlled study. *J Bone Miner Res* **23**:525-535.

Murphy CS, Pink JJ and Jordan VC (1990) Characterization of a receptor-negative, hormone-nonresponsive clone derived from a T47D human breast cancer cell line kept under estrogen-free conditions. *Cancer Res* **50**:7285-7292.

Pink JJ, Bilimoria MM, Assikis J and Jordan VC (1996) Irreversible loss of the oestrogen receptor in T47D breast cancer cells following prolonged oestrogen deprivation. *Br J Cancer* **74**:1227-1236.

Pink JJ, Jiang SY, Fritsch M and Jordan VC (1995) An estrogen-independent MCF-7 breast cancer cell line which contains a novel 80-kilodalton estrogen receptor-related protein. *Cancer Res* **55**:2583-2590.

Pink JJ and Jordan VC (1996) Models of estrogen receptor regulation by estrogens and antiestrogens in breast cancer cell lines. *Cancer Res* **56**:2321-2330.

Pinkerton JV, Archer DF, Utian WH, Menegoci JC, Levine AB, Chines AA and Constantine GD (2009a) Bazedoxifene effects on the reproductive tract in postmenopausal women at risk for osteoporosis. *Menopause* **16**:1102-1108.

Pinkerton JV, Utian WH, Constantine GD, Olivier S and Pickar JH (2009b) Relief of vasomotor symptoms with the tissue-selective estrogen complex containing bazedoxifene/conjugated estrogens: a randomized, controlled trial. *Menopause* **16**:1116-1124.

Said TK, Conneely OM, Medina D, O'Malley BW and Lydon JP (1997) Progesterone, in addition to estrogen, induces cyclin D1 expression in the murine mammary epithelial cell, in vivo. *Endocrinology* **138**:3933-3939.

Shiau AK, Barstad D, Loria PM, Cheng L, Kushner PJ, Agard DA and Greene GL (1998) The structural basis of estrogen receptor/coactivator recognition and the antagonism of this interaction by tamoxifen. *Cell* **95**:927-937.

Silverman SL, Christiansen C, Genant HK, Vukicevic S, Zanchetta JR, de Villiers TJ, Constantine GD and Chines AA (2008) Efficacy of bazedoxifene in reducing new vertebral fracture risk in postmenopausal women with osteoporosis: results from a 3-year, randomized, placebo-, and active-controlled clinical trial. *J Bone Miner Res* **23**:1923-1934.

Sutherland RL and Musgrove EA (2004) Cyclins and breast cancer. *J Mammary Gland Biol Neoplasia* **9**:95-104.

Vogel VG, Costantino JP, Wickerham DL, Cronin WM, Cecchini RS, Atkins JN, Bevers TB, Fehrenbacher L, Pajon ER, Wade JL, 3rd, Robidoux A, Margolese RG, James J, Runowicz CD, Ganz PA, Reis SE, McCaskill-Stevens W, Ford LG, Jordan VC and Wolmark N (2010) Update of the National Surgical Adjuvant Breast and Bowel Project Study of Tamoxifen and Raloxifene (STAR) P-2 Trial: Preventing breast cancer. *Cancer Prev Res (Phila Pa)* **3**:696-706.

Warnmark A, Treuter E, Gustafsson JA, Hubbard RE, Brzozowski AM and Pike AC (2002) Interaction of transcriptional intermediary factor 2 nuclear receptor box peptides with the coactivator binding site of estrogen receptor alpha. *J Biol Chem* **277**:21862-21868.

Wilcken NR, Prall OW, Musgrove EA and Sutherland RL (1997) Inducible overexpression of cyclin D1 in breast cancer cells reverses the growth-inhibitory effects of antiestrogens. *Clin Cancer Res* **3**:849-854.

Zwijsen RM, Wientjens E, Klompmaker R, van der Sman J, Bernards R and Michalides RJ (1997) CDK-independent activation of estrogen receptor by cyclin D1. *Cell* **88**:405-415.

Footnote

This work was supported by the National Institutes of Health National Cancer Institute [Grants K01CA120051 01A2, P30CA006927], the American Cancer Society [Grant IRG-9202714], the Department of Defense [Grant BC050277], and the National University Research Council of Romania-CNCSIS-UEFISCU [Grant PN-II-PCE-ID1268].

Figure legends

Fig. 1. Effects of E2 and SERMs on the growth of hormone-dependent MCF-7 and T47D cells versus hormone-independent MCF-7:5C and MCF-7:2A cells. A, MCF-7 and T47D cells were grown in phenol red-free RPMI medium supplemented with 10% charcoal stripped FBS for 3 days prior to the start of the experiment. On the day of the experiment, all cell lines were seeded in phenol red-free RPMI medium supplemented with 10% charcoal stripped FBS at 30,000 per well in 24-well dishes and after 24 h were treated with 10^{-14} to 10^{-8} M E2 for 7 days, with retreatment every other day. At the conclusion of the experiment, cells were harvested and proliferation was assessed as cellular DNA mass (μg/well) using a DNA quantitation kit. The effect of E2 on proliferation of the different cell lines over a 12-day period was also determined by cell counting. B, the effects of antihormones at inhibiting E2-stimulated growth in MCF-7 and T47D cells and hormone-independent growth in MCF-7:5C and MCF-7:2A cells. Cells were seeded as described above except MCF-7 and T47D cells were grown in fully estrogenized media and then treated with 10^{-12} M to 10^{-6} M fulvestrant (FUL), bazedoxifene (BZA), raloxifene (RAL), 4-hydroxytamoxifen (4OHT), or endoxifen (ENDOX) for 7 days with retreatment on alternate days. Proliferation was assessed as cellular DNA mass (μg/well) as described in the methods section. C, effects of SERMs on reversing E2-induced growth inhibition of hormone-independent MCF-7:5C cells. Cells were seeded as described above and then treated with 10^{-9} M E2 alone or E2 combined with increasing concentrations (10^{-12} M to 10^{-6} M) of BZA, RAL, 4OHT, or ENDOX for 7 days and processed as described above. All data are presented as the mean from three different experiments in triplicate.

Fig. 2. Effects of SERMs on ERα expression and stability in hormone-dependent MCF-7 and T47D cells and hormone-independent MCF-7:5C and MCF-7:2A cells. A, Western blot analysis of ERα protein levels in MCF-7, T47D, MCF-7:5C, and MCF-7:2A cells in response to 24-h treatment with 10^{-9} M E2 or 10^{-7} M FUL, 4OHT, RAL or BZA. β-actin was used as a loading control. B, Western blot analysis of ERα protein levels in MCF-7:5C and MCF-7 cells following treatment with 10^{-9} M to 10^{-6} M for 24 h. For comparison, cells were also treated with 10^{-9} M E2 or 10^{-8} M FUL. C, Western blot analysis of ERα protein levels in MCF-7:5C cells in response to 10^{-8} M BZA treatment over a 24h time period. Quantitated protein levels were normalized to β-actin. Densitometric quantitation relative to the control is shown on the bottom of the immunoreactive bands. Also shown is ERα mRNA levels in MCF-7:5C cells treated with 10^{-9} M E2, 10^{-8} M BZA, or the combination of E2 plus BZA for 24 hours. The amount of ERα mRNA was determined by real-time RT-PCR and normalized to the internal control 18S rRNA. Each data point represents the average of four biological replicates from three independent experiments. D, Western blot analysis of ERα protein levels in MCF-7 and MCF-7:5C cells pretreated with the proteosome inhibitor MG132 (4 μmol/L) for 4 hours and then treated as indicated for 8 h. β-actin levels are shown as protein loading controls. All experiments were repeated three times and the same results were obtained.

Fig. 3. BZA inhibits constitutive ERα transcriptional activity and expression of endogenous ER-regulated genes in hormone-independent and hormone-dependent breast cancer cells. A, ERE luciferase activity in hormone-dependent MCF-7 and T47D cells and hormone-independent MCF-7:5C and MCF-7:2A cells. For experiment, cells were transiently transfected with an ERE-luciferase reporter construct and treated with 10^{-9} M E2, 10^{-7} M BZA, or E2+BZA for 24 h.

Luciferase values are reported as relative fold change compared to control (untreated cells). *, significance at the $p < 0.001$ level (ANOVA) compared with control. #, significance at the $p < 0.01$ compared with E2 treatment. B, real time RT-PCR analysis of pS2 mRNA gene expression in MCF-7 and MCF-7:5C cells after indicated treatments for 24 h. Each data point represents the average of four biological replicates. *, significance at the $p < 0.001$ level compared with control. #, significance at the $p < 0.05$ level compared with MCF-7:5C control. C, MCF-7:5C cells were transfected with nontarget (control) or ERα siRNAs for 48 h. Transfected cells were then harvested for Western blot analysis (top panel) or treated with 10^{-7} M BZA for an additional 4 days followed by cell counting using a hemocytometer (bottom panel). Data shown are representative of three independent experiments with duplicate (*, $p < 0.01$ versus nontarget transfected cells).

Fig. 4. Effects of BZA on cell cycle progression and cyclin D1 regulation in MCF-7 and MCF-7:5C cells. A, cell cycle distribution was determined by propidium iodide staining of DNA content and flow cytometry. Cells were treated with 10^{-9} M E2, 10^{-7} M BZA, or E2 plus BZA for 24 and 48h. Thirty-thousand cells per sample and three replicates per group were collected. Representative histograms are shown. B, Western blot analysis of cyclin D1 expression level in MCF-7 and MCF-7:5C cells following treatment with BZA and other SERMs. Prior to experiment, MCF-7 cells were switched from fully estrogenized media to estrogen-free media for 3 days and then treated with ethanol vehicle (control), 10^{-9} M E2 alone, or 10^{-9} M E2 plus FUL (10^{-7} M), RAL (10^{-7} M), 4OHT (10^{-7} M), or BZA (10^{-7} M) for 24 h. MCF-7:5C cells, however, did not require a media switch since they are hormone-independent and are routinely grown in estrogen-free media. MCF-7:5C cells were treated as described above for MCF-7 cells.

Quantitated protein levels normalized to β-actin are indicated. C, BZA regulation of cyclin D expression and promoter activity in MCF-7:5C cells. Cells were treated with 10^{-7} M BZA for the indicated time points. Cyclin D1 protein and mRNA levels were determined by Western blot and quantitative RT-PCR, respectively with β-actin and 18S rRNA as internal controls. For cyclin D1 promoter activity experiment, MCF-7 and MCF-7:5C cells were cotransfected with a full-length cyclin D1 promoter plasmid (-1745CDLUC) and Renilla luciferase control plasmid overnight and then treated with 10^{-9} M E2, 10^{-8} M BZA, or E2 + BZA for 24 h. Luciferase activity was measured as described in materials and methods. D, proliferation of MCF-7:5C cells transfected with the nontarget or cyclin D1 siRNA. Cells were transfected and then seeded at 15,000 per well in 24-well dishes. Medium was replenished the day after seeding on day 0 and every other day thereafter. Cells were collected on day 5 and counted using a hemocytometer. All data are presented as the mean from three independent experiments with duplicate (*, $p <$ 0.01 versus nontarget transfected cells).

Fig. 5. Molecular modeling of ERα binding site with various ligands. A, agonist conformation of ERα co-crystallized with E2 (PDB code 1gwr); helix 12 is depicted in orange and lies over the binding site sealing the ligand inside it. The antagonist conformations of the receptor are shown in panels B, C, and D. B, the superimposed X-ray structures of ERα co-crystallized with 4OHT and raloxifene. C, bazedoxifene docked into the ERα-raloxifene crystal structure. D, Bazedoxifene superimposed in the binding site of ERα co-crystallized with 4OHT. Helix 12 is depicted in magenta for 4OHT bound conformation and yellow for raloxifene and bazedoxifene. Also the key aminoacids lining the binding site are displayed and the network of hydrogen bonds in which they are involved with the ligands is shown in black dashed lines. Carbon atoms are

colored in yellow for E2, orange for 4OHT, cyan for raloxifene and pink for bazedoxifene. These images point out the differences between the agonist (A) and antagonist conformation (B) of ERα and present the alignment of bazedoxifene in the binding site of ERα which is very similar to raloxifene's orientation showing the same interactions with the key aminoacids of the binding cavity (C).

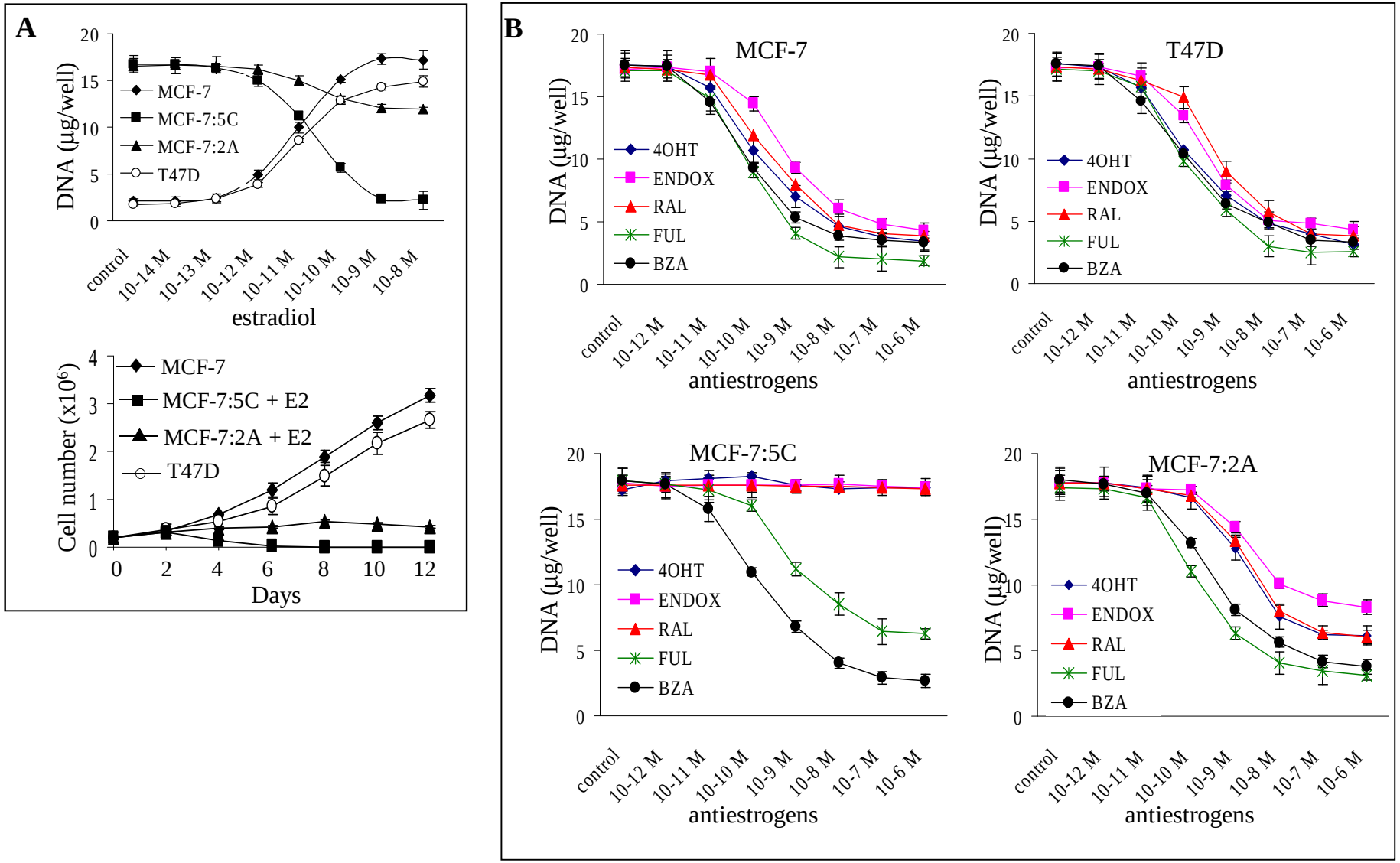
Supplemental Figure Legends

Supplemental Fig. S1. The chemical structures of the compounds used in this study. The agonist 17β-estradiol (E2) is shown, along with the pure antiestrogen fulvestrant (ICI 182,780), the hydroxylated metabolites of tamoxifen; 4-hydroxytamoxifen (4OHT) and endoxifen, and the related SERMs raloxifene (RAL) and bazedoxifene (BZA).

Supplemental Fig. S2. Effect of endoxifen on ERα protein expression in MCF-7:5C cells. Western blot analysis of ERα protein levels in MCF-7:5C cells in response to 24 h of treatment with different concentrations of endoxifen. Also shown are the effects of 1 μM treatment of BZA, FUL, and 4OHT on ERα expression in MCF-7:5C, MCF-7, T47D, and MCF-7:2A cells. Quantitated protein levels were normalized to β-actin.

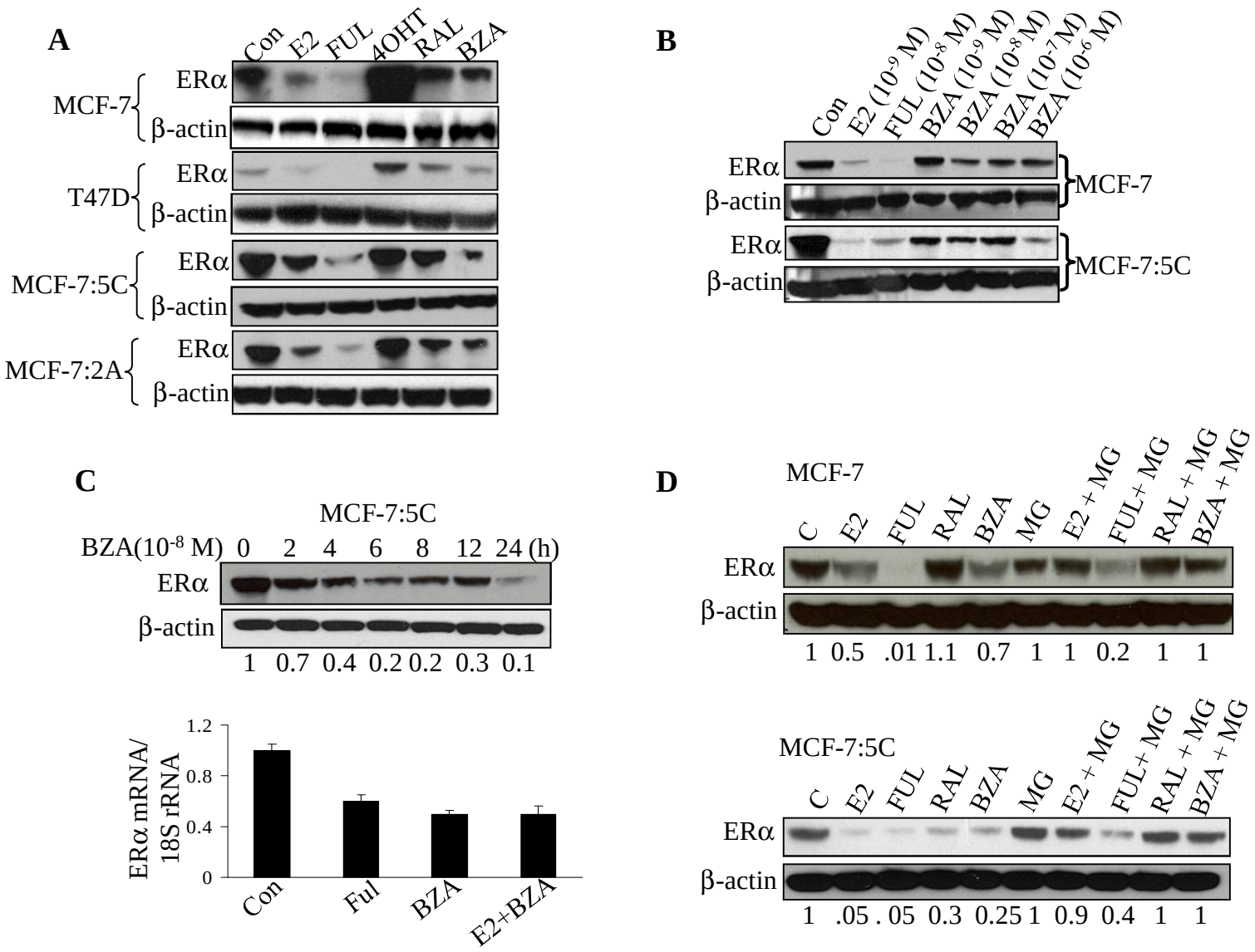
Supplemental Fig. S3. A, comparison between the experimental (yellow sticks) and top ranked docking pose (cyan sticks) of raloxifene (RAL) to ERα binding site. The docking pose recapitulates very well the alignment of the co-crystallized ligand in the receptor binding site having a ligand RMSD of 0.36 Å. B, cartoon representation of the ERα binding site with the best docking pose for fulvestrant (FUL, purple sticks). For comparison, the native ligand (RAL) is also displayed (cyan sticks). C, surface representation of ERα binding site accommodating FUL. Hydrophobic areas are mapped in purple while the hydrophilic parts are colored in light yellow-green. The binding site accommodates very well the ligand which forms the H-bond contacts with the same aminoacids like E2 or RAL, while the aliphatic side chain protrudes out of the

binding site and lies in the groove between helix 3 (orange cartoon) and helix 12 (purple cartoon). Only the key amino acids underlying the binding site are shown.



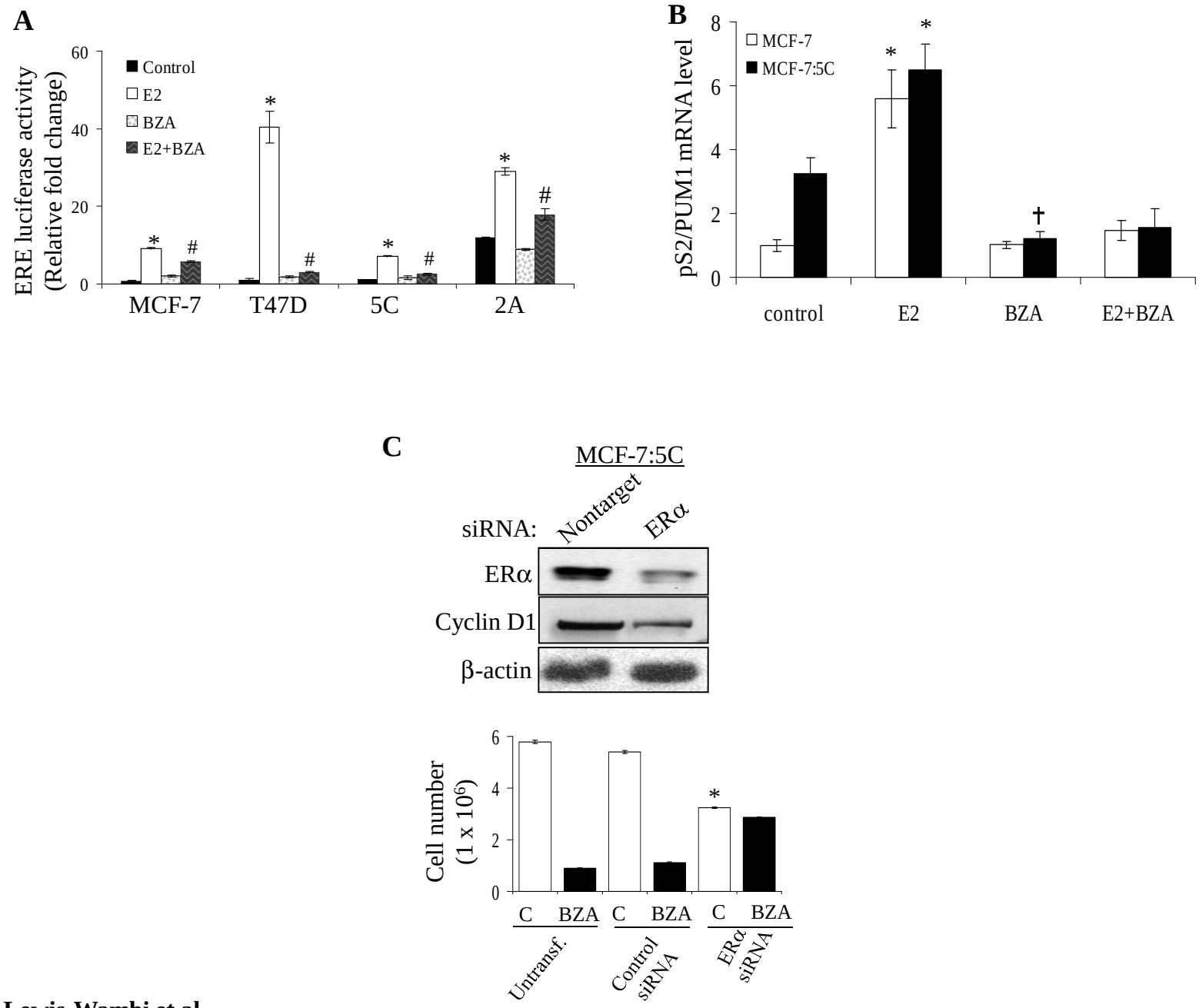
Lewis-Wambi et al.

Fig. 1



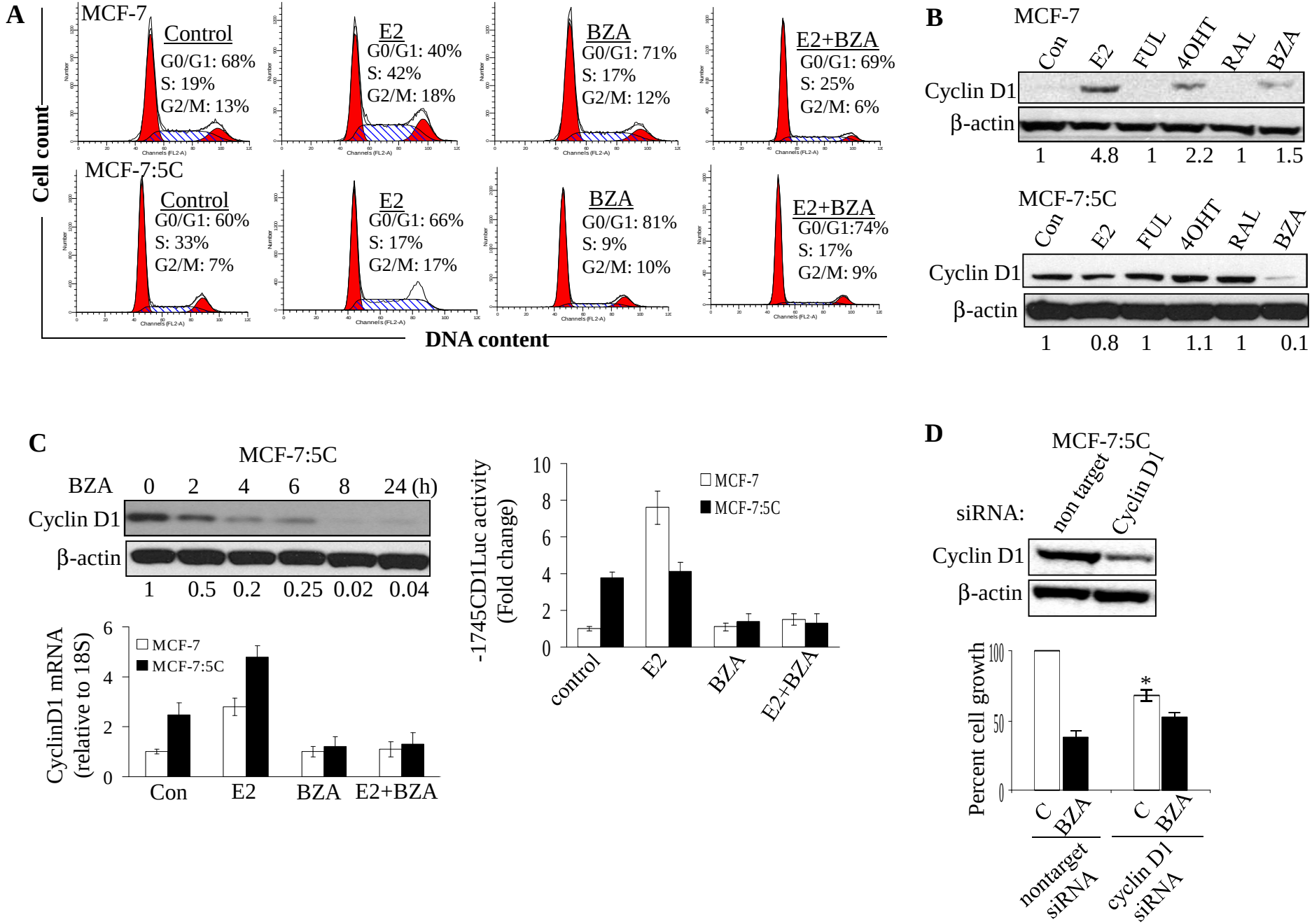
Lewis-Wambi et al.

Fig. 2



Lewis-Wambi et al.

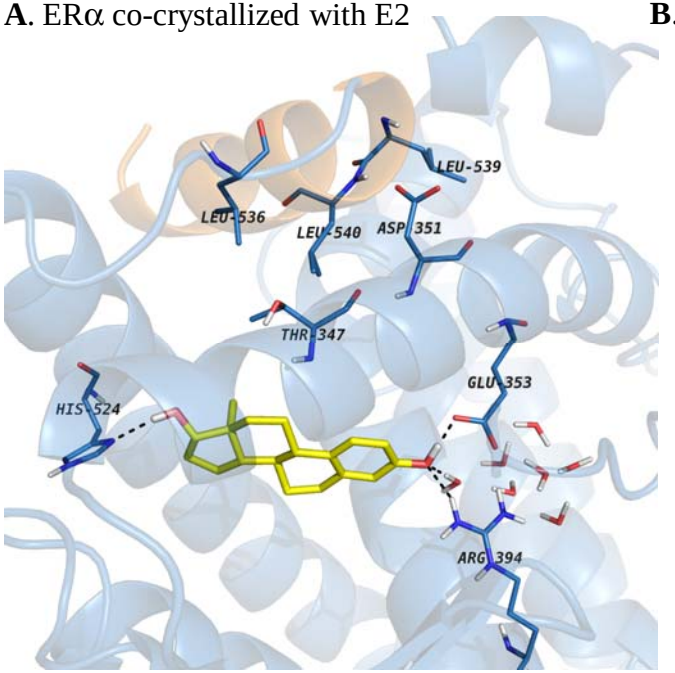
Fig. 3



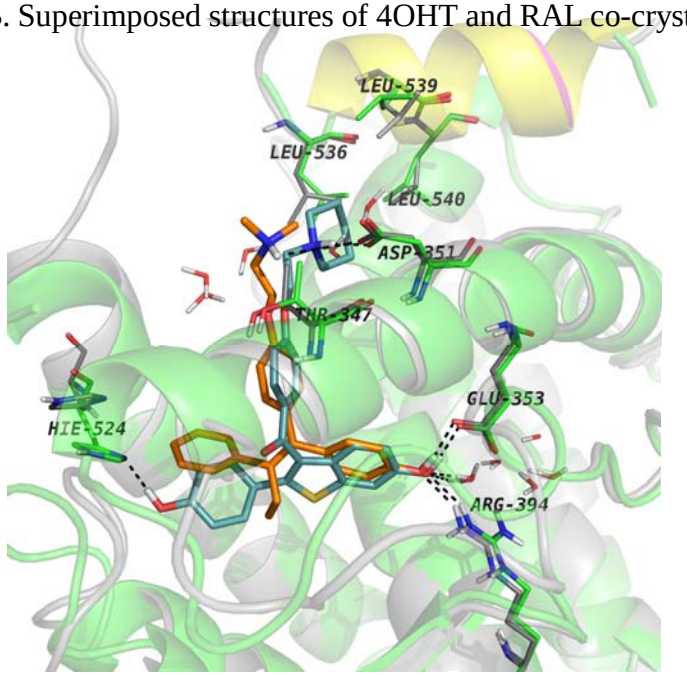
Lewis-Wambi et al.

Fig. 4

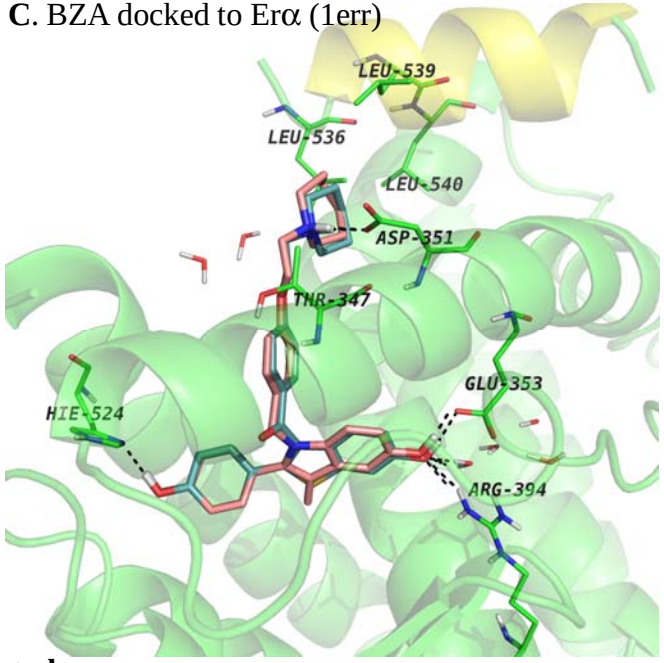
A. ERα co-crystallized with E2



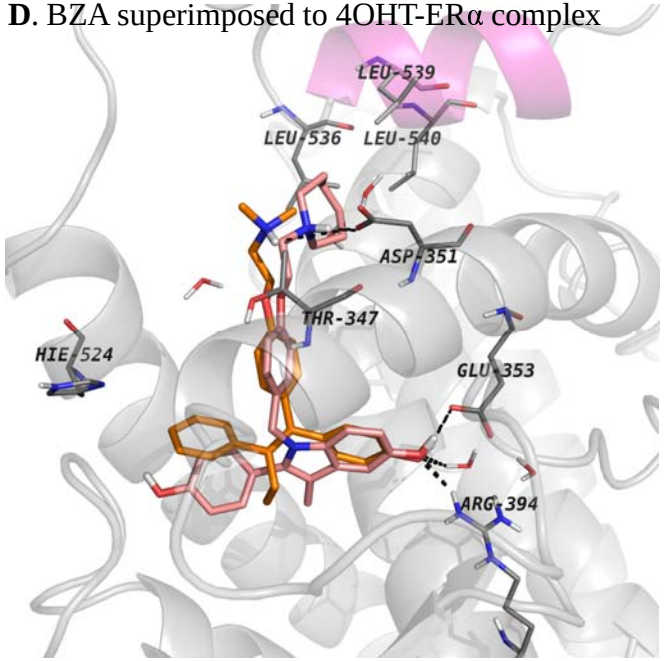
B. Superimposed structures of 4OHT and RAL co-crystallized with ERα



C. BZA docked to Erα (1err)



D. BZA superimposed to 4OHT-ERα complex



Lewis-Wambi et al. **Fig. 5**